Stars and stellar evolution

Veronika Schaffenroth

WS 2021/22

Master of Science Astrophysics - Module 750

Institute for Physics and Astronomy
Email: `schaffenroth@astro.physik.uni-potsdam.de`
Haus 28, Room: 2.118

Structure

Structure

Two sessions from 14:15-15:45 and 16:15-17:45 on Wednesday

Blocks of lectures, exercises and seminar according to the detailed schedule

Exercises: Two groups

- first group: 12:00-15:00, tutor: Judy Chebly
- second group: 15:00-18:00, tutor: Harry Dawson
- (third group: 12:00-15:00 online, Judy Chebly)

27.10.21	Lecture: group 1	05.01.21	Exercises
03.11.21	Lecture: group 2	12.01.21	Exercises
10.11.21	Lecture: group 1	19.01.21	Lecture: group 2
17.11.21	Lecture: online	26.01.21	Lecture: group 1
24.11.21	Exercises	02.02.21	Exercises
01.12.21	Exercises	09.02.21	Seminar: group 1
08.12.21	Lecture: group 2	16.02.21	Seminar: group 2
15.12.21	Lecture: group 1	23.02.21	Exam: 13:30-14:30: 2.27.0.01

Structure

Requirements to reach the final exam

- Hand in the exercises in time and reach more than 50% of the points (groups of two persons)
- Give a talk about a modern topic related to stellar astrophysics in the seminar and actively contribute to the discussion

Final exam

- written exam of **one hour** duration on Wednesday 23.02.2020?, 13:30-14:30
- Grade on this exam combined with part II will be grade of Modul 750

Seminar topics

Based on recent review papers on modern topics. Up to two speakers per topic, about 20 minutes per individual talk

- Stellar Dynamics and Stellar Phenomena Near a Massive Black Hole
- Near-Field Cosmology with Extremely Metal-Poor Stars
- Hypervelocity Stars
- Hot Subluminous Stars
- Observational Clues to the Progenitors of Type Ia Supernovae
- Multiple Stellar Populations in Globular Clusters
- Red Clump Stars
- Asteroseismology of Solar-Type and Red-Giant Stars
- Mass Loss: Its Effect on the Evolution and Fate of High-Mass Stars
- The Most Luminous Supernovae
- Masses, Radii, and the Equation of State of Neutron Stars
- Microarcsecond Astrometry: Science Highlights from Gaia
- Evolution and Mass Loss of Cool Aging Stars: A Daedalean Story
- Astrochemistry During the Formation of Stars
- Probing the interior physics of stars through asteroseismology

Seminar talks

Audience: Members of the class

→ Basics can be expected, but no in-depth knowledge about details

Talk should be as simple and easy to understand as possible!

→ Of course not all topics are simple ... this is the challenge here

Stay in time!

→ Talk must be practised several times before delivering it in class

Use material from the review papers, references therein, textbooks, the internet (always with proper citations)

Papers can be downloaded using a UP account from the SAO/NASA Astrophysics Data System (ADS) webpage

http://adsabs.harvard.edu/abstract_service.htm

Using the HTML version allows to download all the images and plots in high-resolution

Seminar talks

Basic structure:

- **Introduction** should be sufficient for the audience to get the context (about one third of the time)
- **Methods** should be described in a general way avoiding too many details
- **Results** must be clearly summarized and put into context $\rightarrow$ the abstract and conclusions session of a paper are very helpful here, also press releases related to the articles

Each talk needs to tell a story, which is self-contained!

Seminar talks

Common mistakes

- Too many details – People who really get interested in the topic of their talk sometimes forget who is listening
- Showing off – Some people think, they can impress the lecturer and the other students with an extra complicated talk (lots of formulae, unexplained jargon etc.)
- Trying to show off – See above, but for the reason that they don't understand the topic and try to hide that. **This never works!**
- Underestimating the effort – Compared to other tasks, giving such a talk might look easy and doable within a day or so. It is not and requires preparation and practice!

Literature

- Kippenhahn, R., Weigert, D., & Weiss, A., Stellar Structure and Evolution, 2012
- de Boer, K. S., & Seggewiss, W., Stars and Stellar Evolution, 2008
- Prialnik, D., An Introduction to the Theory of Stellar Structure and Evolution, 2010

Slides of the lecture, seminar topics and exercise sheet and solution can be found on Moodle.UP

Introduction

Why study stars?

Gravitational waves

NASA/SXS

Cosmology

NASA, Harvard CfA, Illustris Collaboration

Exoplanet

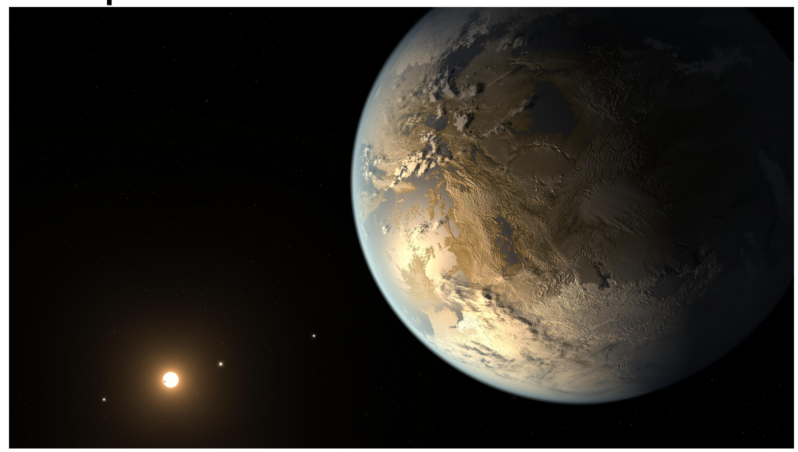

NASA Ames/SETI Institute/JPL-Caltech

Nucleosynthesis

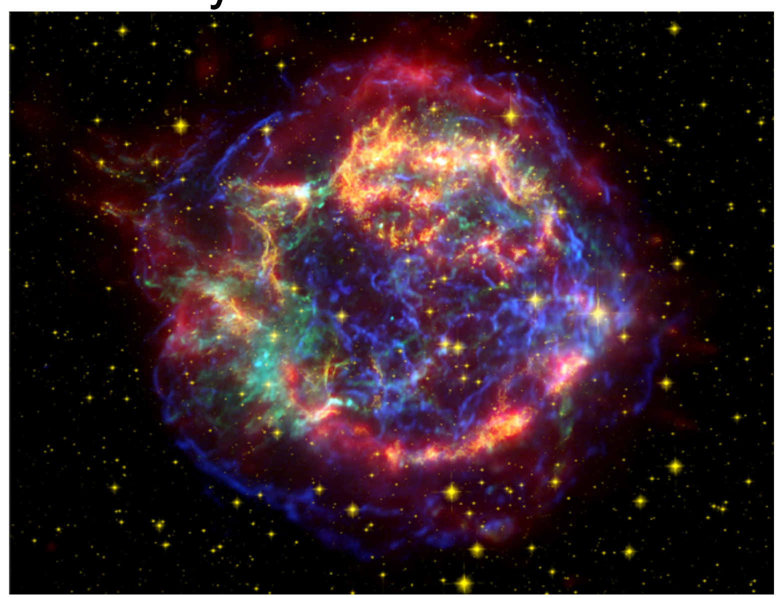

NASA/CXC/SAO/STScI/JPL-Caltech

Why study stars?

Massive binary star progenitors

ESO

Studied by effects on host stars

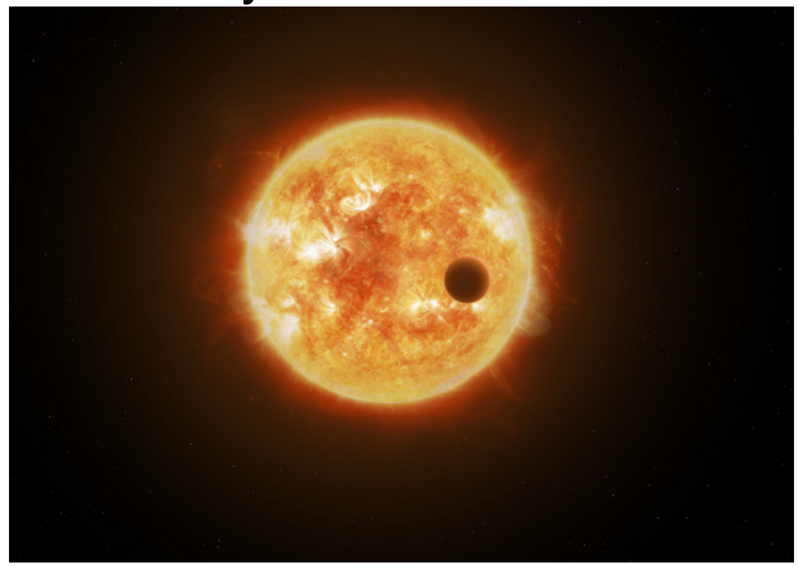

ESA/ATG medialab

Stars needed to understand galaxies

ESO

nuclear processes, stellar evolution

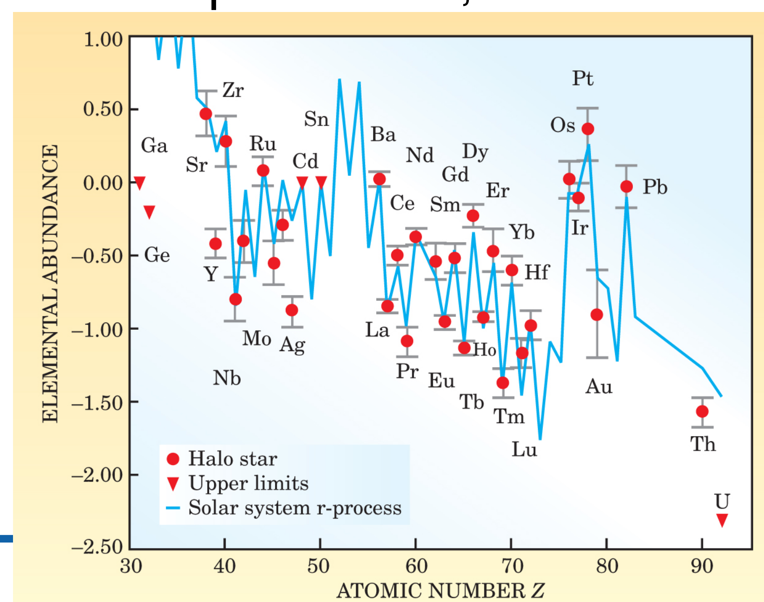

adapted from Sneden et al. 2003

Relevance for astrophysics

- Stars are an important constituent of visible matter in the universe
  $\rightarrow$ 10^{11} stars per galaxy $\times 10^{10}$ galaxies in the observable universe
  $\rightarrow$ 0.5% of the mass of the universe
- Stars synthesise all heavy elements
- Stars are well-studied and can be used to calibrate distance and to unravel structures
- Stars host planetary systems and dominate their evolution
  $\rightarrow$ Sun is crucial for life on Earth
- Stars are laboratories to study all kinds of physics
  $\rightarrow$ Thermodynamics, general relativity, nuclear and particle physics

Relevance for astrophysics

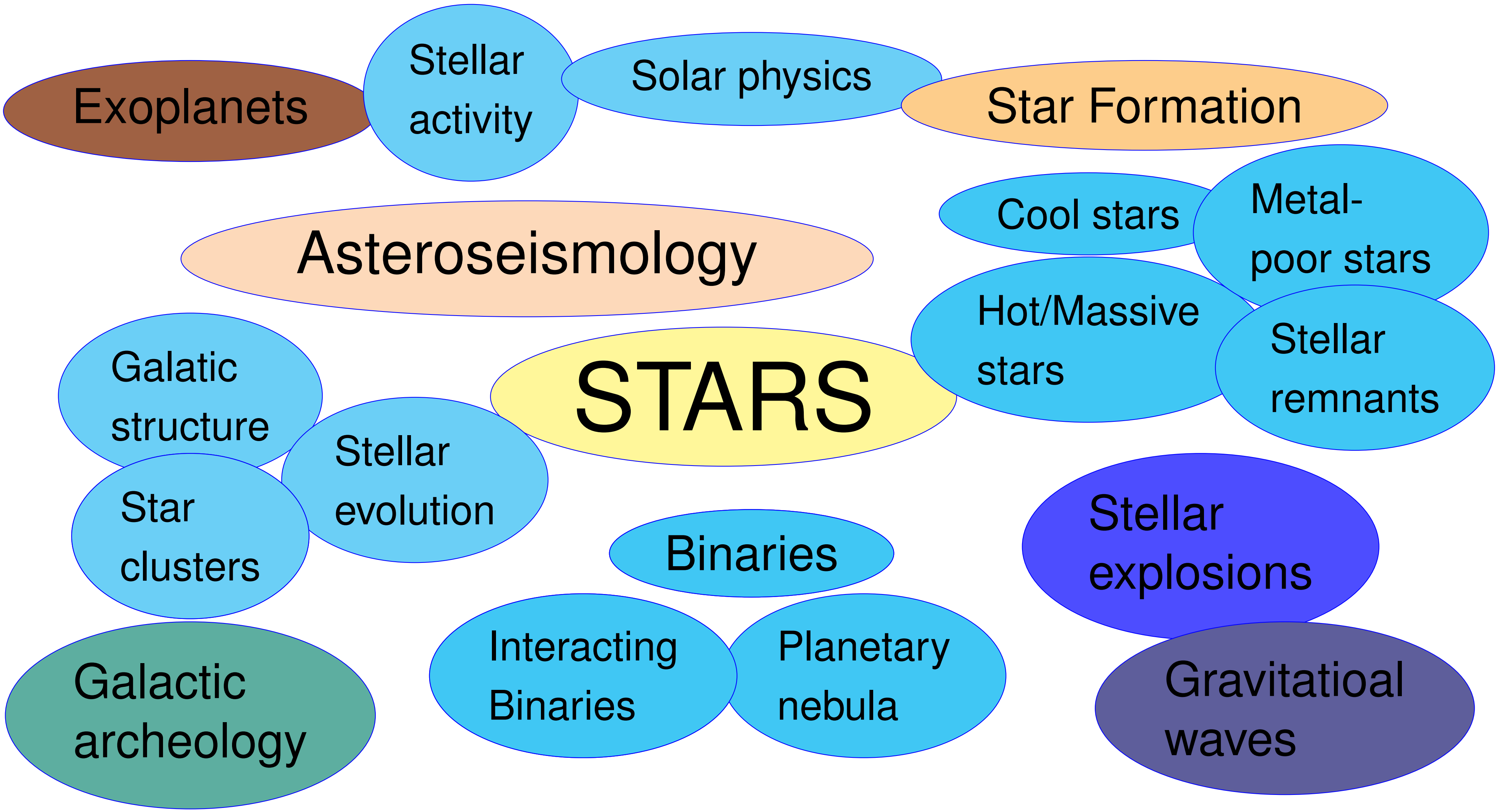

What is a star?

A star can be defined as a body that satisfies two conditions:

- It is bound by self-gravity.
- It radiates energy supplied by an internal source.

There is a certain range of masses stars can have:

- Objects below $\sim 0.08\,\mathrm{M}_\odot$ are no longer stars but brown dwarfs or planets because they shine (mostly) by reflection of stellar light instead of radiating it on their own.
- Stars with more than several hundred $M_\odot$ are not possible because their strong radiation-driven stellar winds prevent them from accumulating more material.

Parameters of the sun

Our sun $\odot$ as reference star

radius	$R_\odot$	696 000 km
mass	$M_\odot$	1.989×10^{30} kg
luminosity	$L_\odot$	3.86×10^{26} W
effective temperature	T_{eff}	5780 K
central temperature	T_c	15×10^6 K
age	$t_\odot$	4.5×10^9 yr

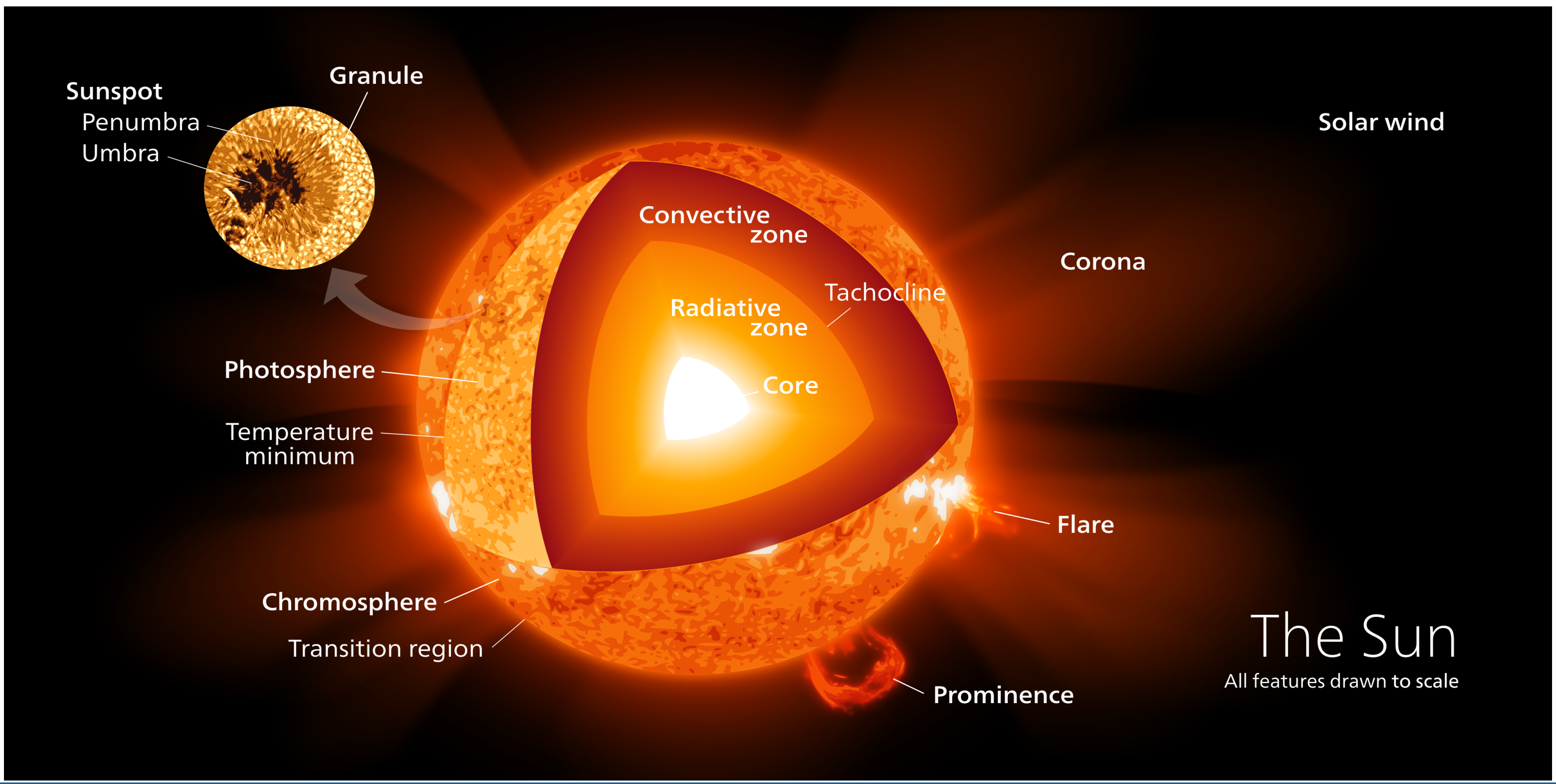

Historical overview

History

Ancient times	E.g., Anaxagoras, Aristotle: Stars are "flaming stones"
1600	Heliocentric models identify the Sun as gigantic heat source in space
1695	Christiaan Huygens compared the brightness of stars with the Sun to calculate their distances
$\sim$ 1800	William Herschel speculated, that the Sun might be inhabitated under a thick mat of clouds
1814	Joseph von Fraunhofer discovers absorption lines in the Sun and some stars $\rightarrow$ Spectral classification in the early 20th century
1838	Friedrich Bessel, Friedrich Struve and Thomas Henderson measure the first parallax distances of stars $\rightarrow$ Distinction between giant and dwarf stars
Pre-1848	E.g., Kant, Laplace: Stars are "fire balls"

History

1842/43	Julius Robert Mayer (surgeon!) and James Prescott Joule propose conservation of energy as physical law (thermodynamics)
1848	Mayer: First proposal of a specific heat mechanism for the power supply of stars, namely the infall of meteors
1854 + 1861	Helmholtz & Kelvin: Power supply by contraction (gravity) $\rightarrow$ Lifetime of less than 100 million years $\leftrightarrow$ Charles Darwin and geologists (billions of years)
1861	Lane: Stars get hotter as they radiate and shrink ("Lane's law")
1865	Herve Faye suggested that sunspots are regions, where the glowing surface is blown aside
1869	Lane: Theory of polytropic gas spheres
1878	Ritter: First theory of stellar evolution based on Lane's law
$\sim$ 1880	Assuming that stars derive energy from contraction, A. Ritter calculated the lifetime of the Sun to less than 6 million years, after which contraction should cease and cooling start

History

1880 Norman Lockyer proposes that stars are formed by gravitational contraction of meteoritic particles

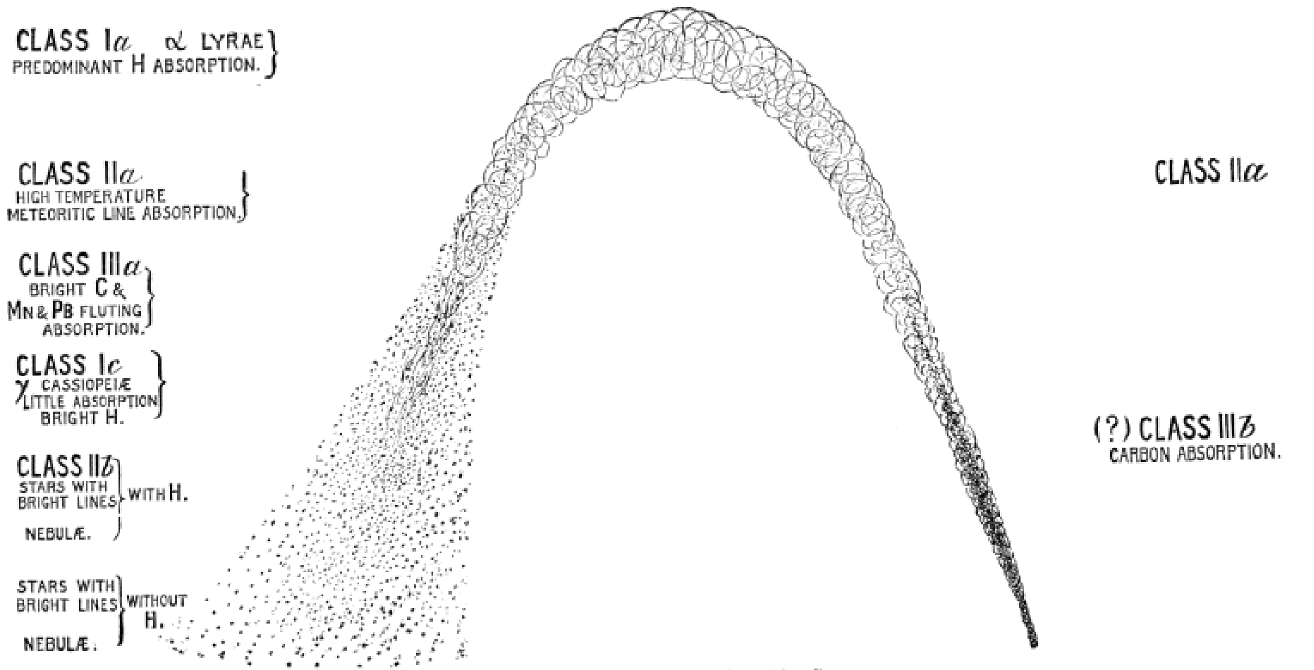

Fig. 67.—Temperature Curve (provisional).

N. Lockyer, The Meteoritic Hyphothesis, 1890, 375

→ Spectroscopic classes are different phases of contraction

→ Origin of the classification as early and late-type stars

History

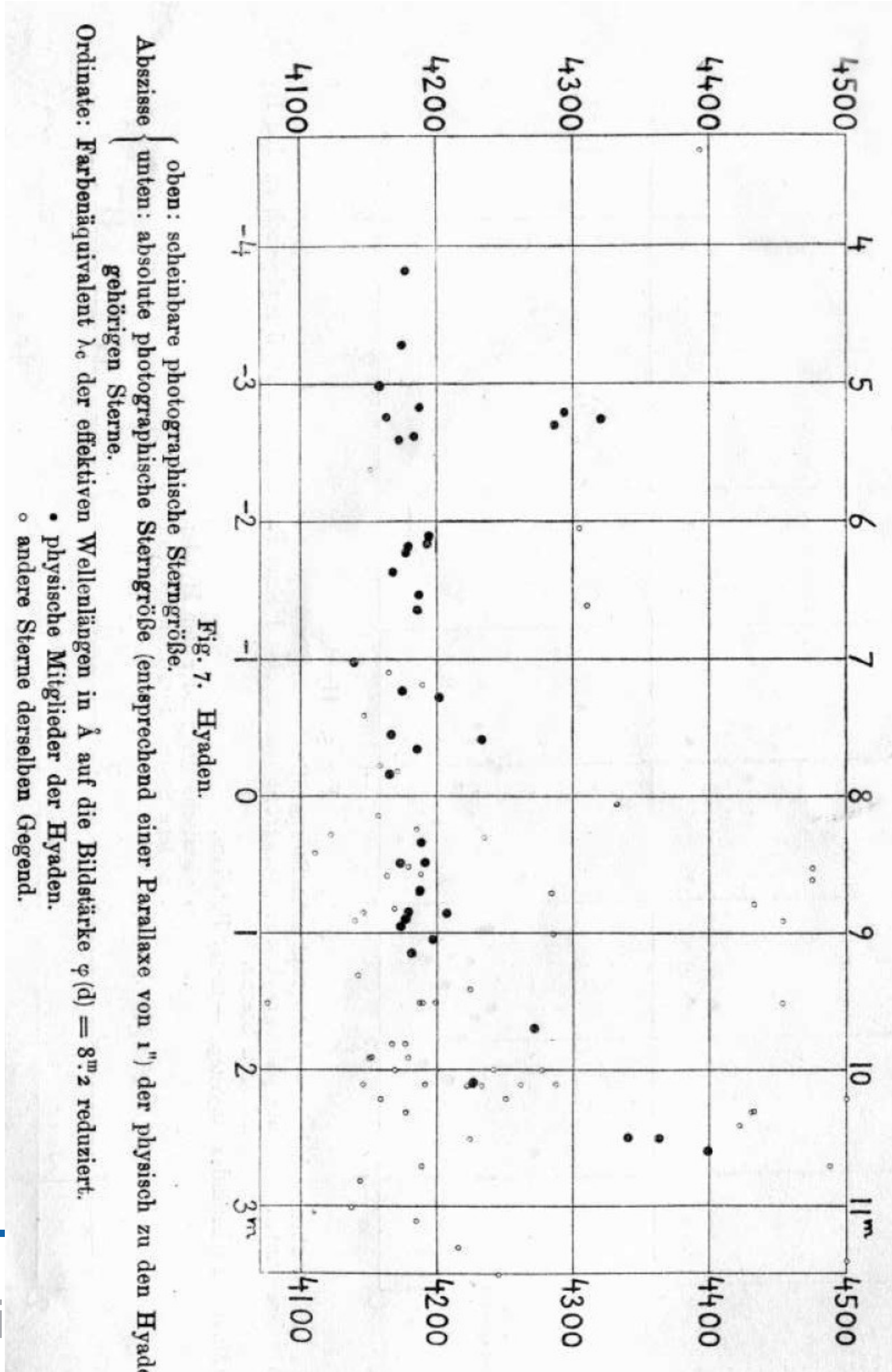

1911 Eijnar Hertzsprung

→ apparent magnitude against color for stars in the Pleiades and Hyades

→ no giants or supergiants in Pleiades and only a few in the Hyades

Gingerich 2013

History

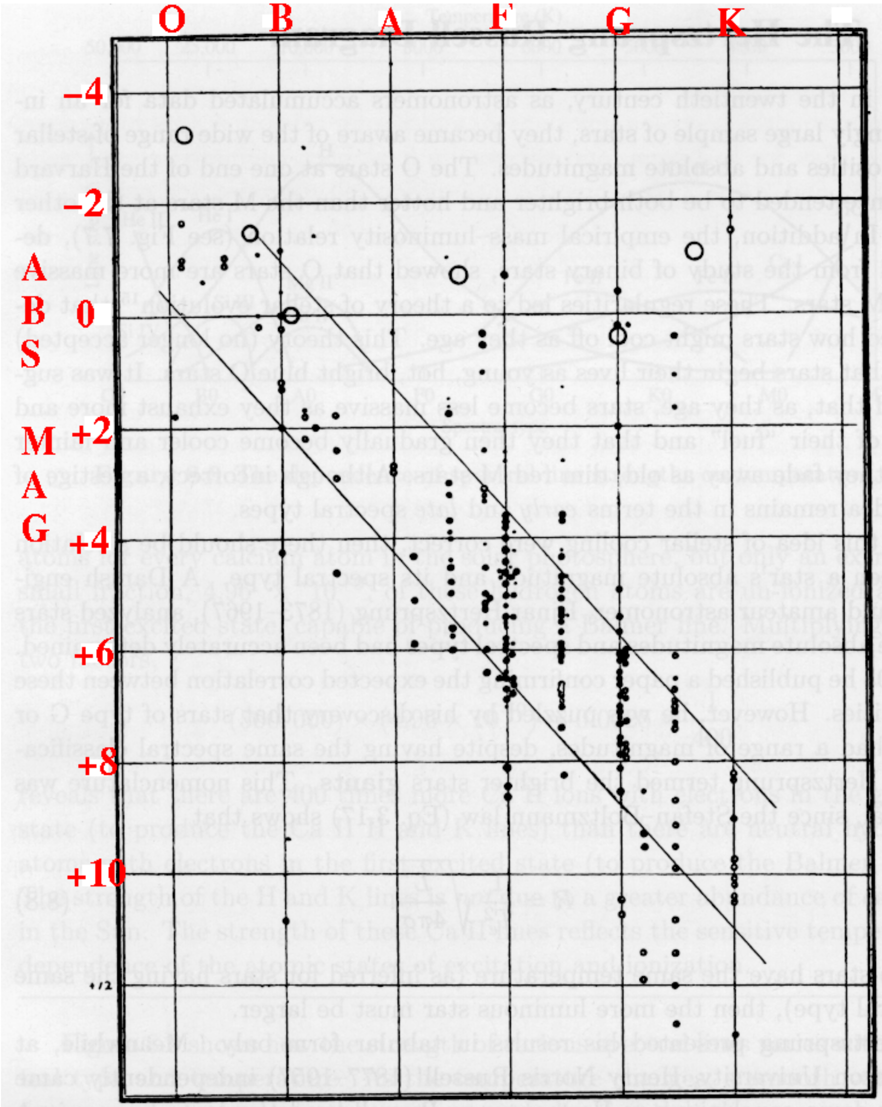

Figure 8.10 Henry Norris Russell's first diagram, with spectral types listed along the top and absolute magnitudes on the left-hand side. (Figure from Russell, *Nature*, *93*, 252, 1914.)

1913 Henry Norris Russell

→ Giant stars are contracting towards the main sequence

→ Main sequence stars stop contracting and cool down along the sequence

History

1907 Emden: Systematic work on polytropes, i.e., stellar models
where heat is transported solely by convection (book: Gaskugeln)

1926 F. J. M. Stratton: Spectroscopic similarities between early-type stars and planetary nebula, late-type stars and spiral nebula
$\rightarrow$ O, B stars and planetary nebula come from diffusive nebulosity
$\rightarrow$ M giants come from condensations in the arms of spiral nebula

1926 Eddington: The Internal Constitution of Stars
Perfect gas, uniform terrestrial (!) composition, constant opacity, constant energy generation, Theory of radiative heat transport (first suggested by Sampson in 1895 & K. Schwarzschild in 1906)
$\rightarrow$ Prediction of the mass-luminosity relation, opacity problem (debated)

1925 Cecilia Payne, PhD thesis: Stellar Atmospheres, A Contribution to the Observational Study of High Temperature in the Reversing Layers of Stars
$\rightarrow$ First application of Sahas ionization theory to spectral lines of stars
Strength and presence of lines depends more on temp. than on abundance
$\rightarrow$ Stars consist mainly of hydrogen (highly debated)

History

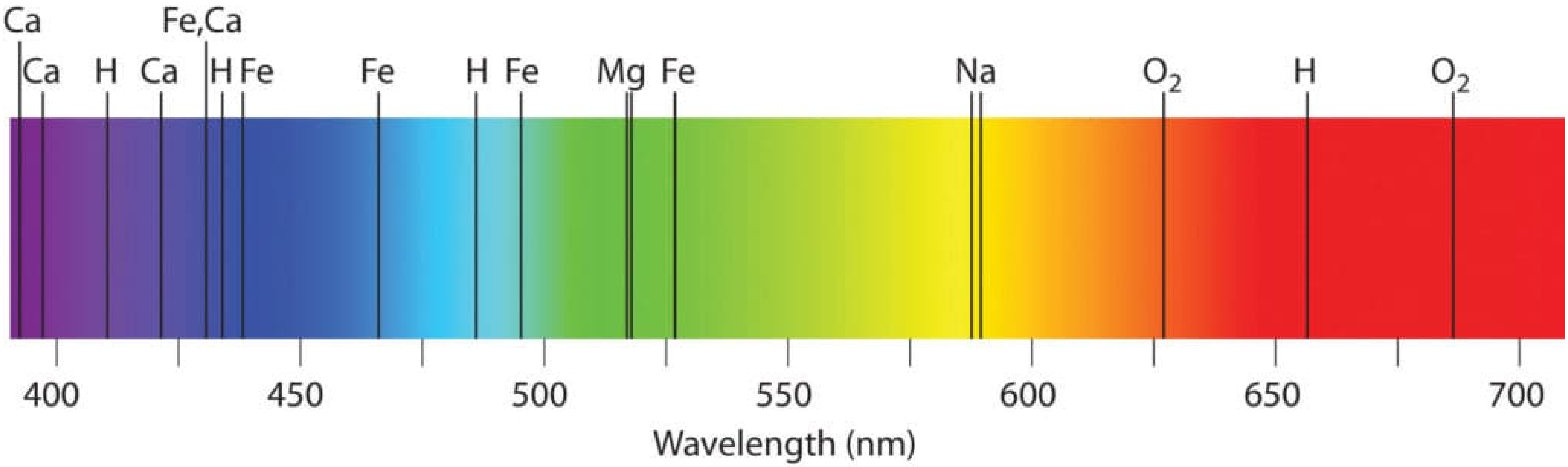

Metal lines are more abundant and stronger in the solar spectrum + Meteroids consist of rock and metals

Modern philosophy: Law of nature are universal

$\rightarrow$ Stars have terrestrial composition

History

January 14, 1925.

My dear Miss Payne:
Here, at last, are your notes on relative abundance which you were so good as to send me some time ago....
You have some very striking results which appear to me, in general, to be remarkably consistent. Several of the apparent discrepancies can be easily cleared up. [Here Russell discusses Mg, Mg+, and K in some detail.]
There remains one very much more serious discrepancy, namely, that for hydrogen, helium and oxygen. Here I am convinced that there is something seriously wrong with the present theory. It is clearly impossible that hydrogen should be a million times more abundant than the metals, and I have no doubt that the number of hydrogen atoms in the two quantum state is enormously greater than is indicated by the theory of Fowler and Milne. Compton and I sent a little note to 'Nature' *about metastable states, which may help to explain the difficulty....*

Very sincerely yours,
Henry Norris Russell

Gingerich 1995

Harvard College Observatory, Wikipedia

1932 Eddington and Bengt Strömgren resolve opacity problem with hydrogen-rich stellar models

1937 Strömgren: Determination of hydrogen content in stellar core

History

1904	Rutherford: radioactive energy to resolve age issue
1920s	Quantum mechanics becomes the standard in atomic physics
1928	Gamow: Theory of Coulomb barrier penetration (major breakthrough for considering nuclear reactions as energy source in stars)
1929	Atkinson and Houtermans apply Gamows theory of the tunnel effect to stellar interiors $\rightarrow$ Most effective interactions by light elements
1931	Theory of nucleosynthesis of heavy elements in stars $\rightarrow$ fusion of hydrogen to helium as energy source for the sun $\rightarrow$ Quadruple collision of hydrogen atoms unlikely $\rightarrow$ Successive absorption of protons
1938-39	Bethe and von Weizsäcker find the proper channels for the fusion of hydrogen to helium (p-p chain and CNO-cycle) $\rightarrow$ Nuclear fusion as energy source of stars confirmed
1940/50s	Nuclear reaction rates could finally be computed due to intensive laboratory work in nuclear physics

History

1916	Ernst Öpik derives the density of the recently discovered new luminosity class of white dwarfs to be 25000 times higher than the one of the Sun $\rightarrow$ "Impossible", Eddington: "Shut up. Don't talk nonsense."
1926	Fowler applies quantum mechanics and explains the high densities as degenerate matter
1930	Chandrasekhar derives a limiting mass for white dwarfs
1934	Baade and Zwicky: propose existence of neutron stars $\rightarrow$ Binding energy powers the newly identified class of supernova explosi
1952	Sandage and Schwarzschild show that the contraction of the core due to hydrogen exhaustion leads to an expansion of the envelope $\rightarrow$ Red giants are evolved stars $\rightarrow$ Explanation for connection between giants and dwarfs in cluster HRD
1951-54	Öpik, Salpeter and Hoyle show that carbon fusion by the triple-alpha process occurs in red giant cores

History

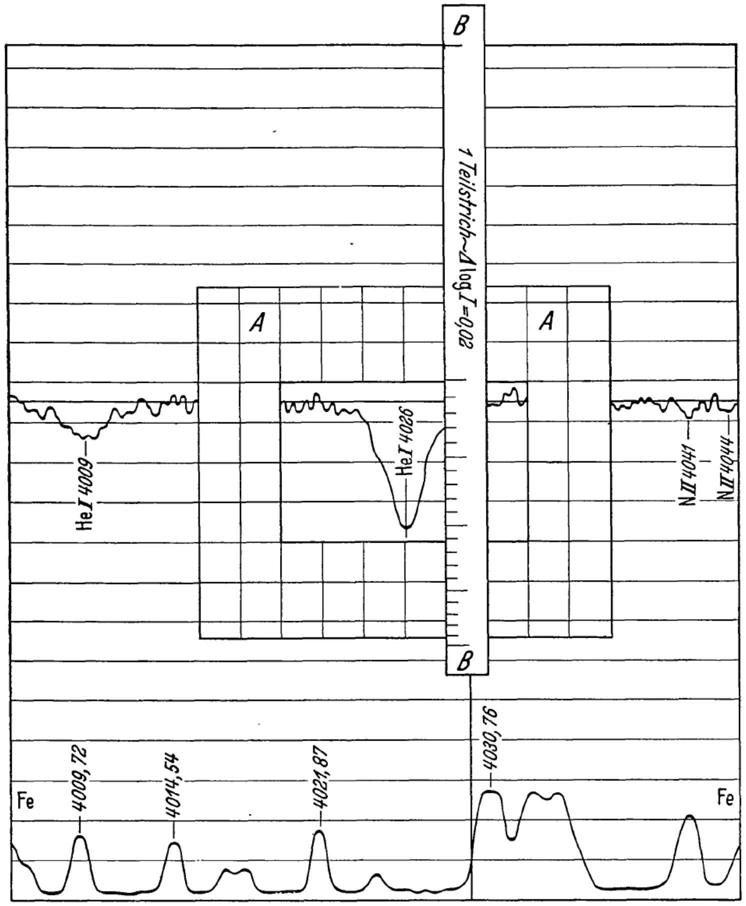

Unsöld 1942, ZA, 21, 10

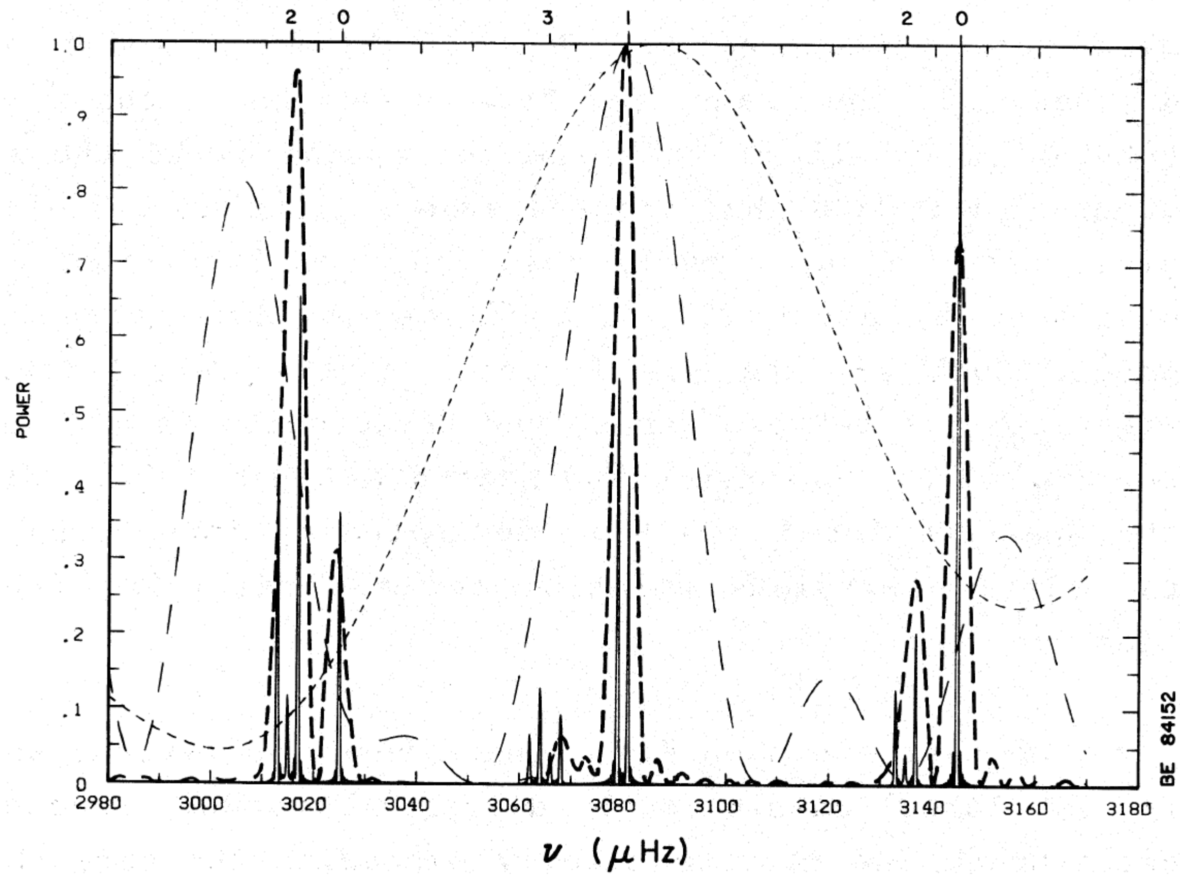

Christensen-Dalsgaard 1984, SRSPS Conf., 11

1939 Unsöld performs the first detailed spectroscopic analysis of a star other than the Sun → Quantitative spectral analysis

1980s Multi-mode pulsating stars are studied for the frist time → Helio- and asteroseismology

History

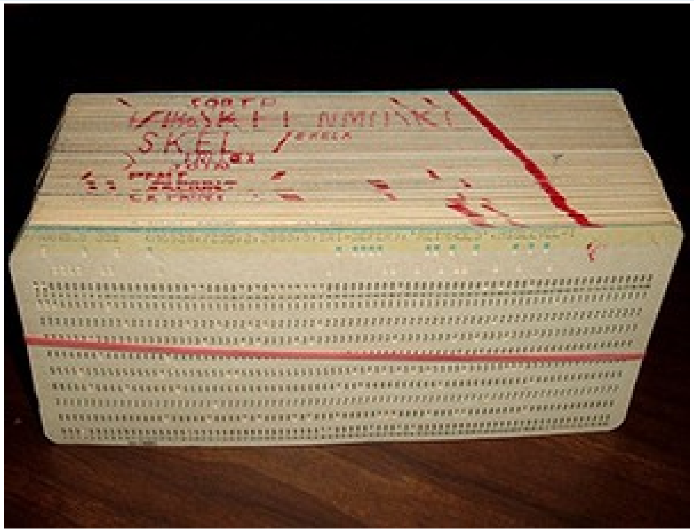

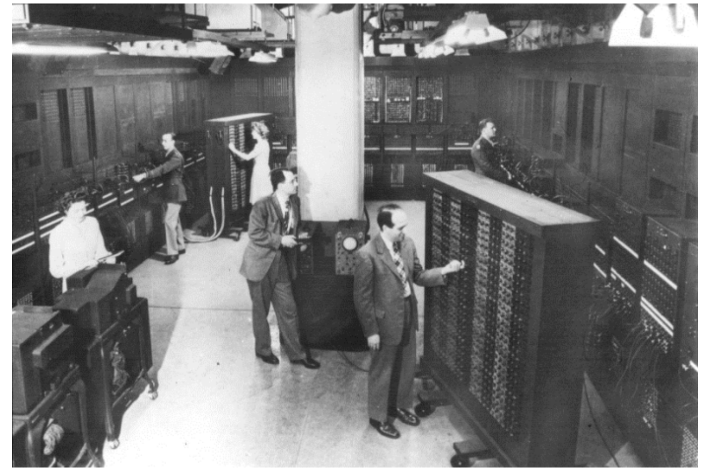

1950s	Stellar evolution modelling became a field of computational astrophysics
1958	Schwarzschild: Presentation of numerical models (based on hand integration techniques) that consistently account for energy production and energy transfer; breakthrough in model building
1967	Jocelyn Bell and Anthony Hewish discover the first pulsar
1972	Bolton, Luise Webster and Murdin discover the first stellar mass black hole in an X-ray binary
2014	LIGO detector discovers merging black holes from their gravitational wave signal
2017	LIGO and VIRGO detect neutron star merger, prove the connection to gamma ray bursts and the synthesis of heavy elements in this process

Observables of stars

Observables of stars

- Stars are observed as point sources (except our Sun)
- Electromagnetic radiation of very different wavelengths is emitted by stars
- The intensity I_0 of this radiation is transformed to the signal S measured by several wavelength dependent functions

$$S(\lambda) = I_0(\lambda)A(\lambda)O(\lambda)F(\lambda)Q(\lambda) \tag{4.1}$$

$A(\lambda)$ Extinction by the interstellar medium and the Earth atmosphere
$O(\lambda)$ Absorption by the telescope optics
$F(\lambda)$ Transmission function of the filter
$Q(\lambda)$ Quantum efficiency of the detector

Photometric filters

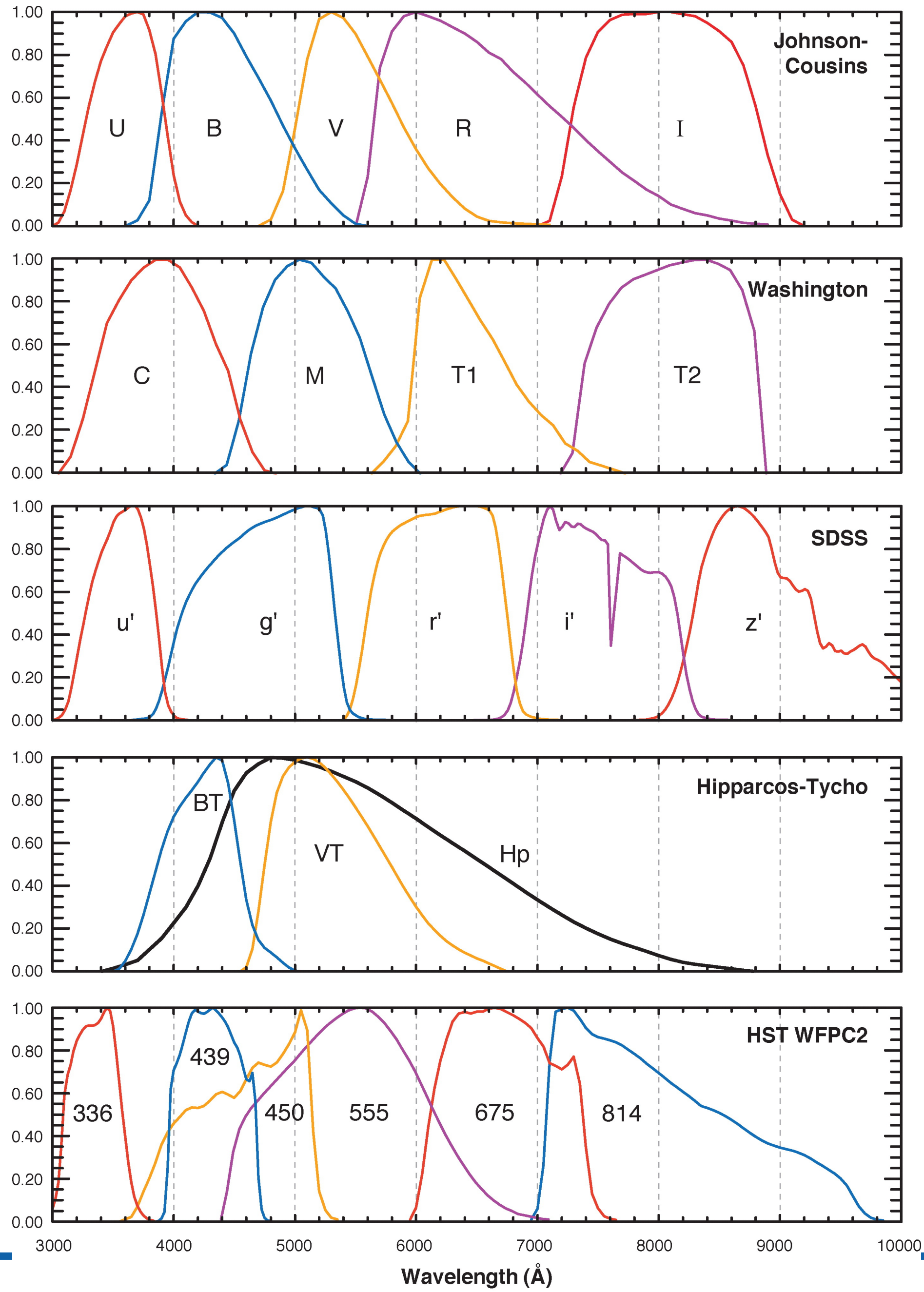

Bessell, MS. 2005
Annu. Rev. Astron. Astrophys. 43: 293–336

- measured brightness in a certain filter X is given as apparent magnitude

$$m_X = -2.5 \log_{10} \frac{F_X}{F_{X,0}} \qquad (4.2)$$

F_X flux density using filter X $F_{X,0}$ reference flux (zero-point) for this filter (Vega or AB-system)

- Magnitudes in different filters can be combined to determine colours

$$m_X - m_Y \rightleftarrows X - Y \qquad (4.3)$$

Photometric filters

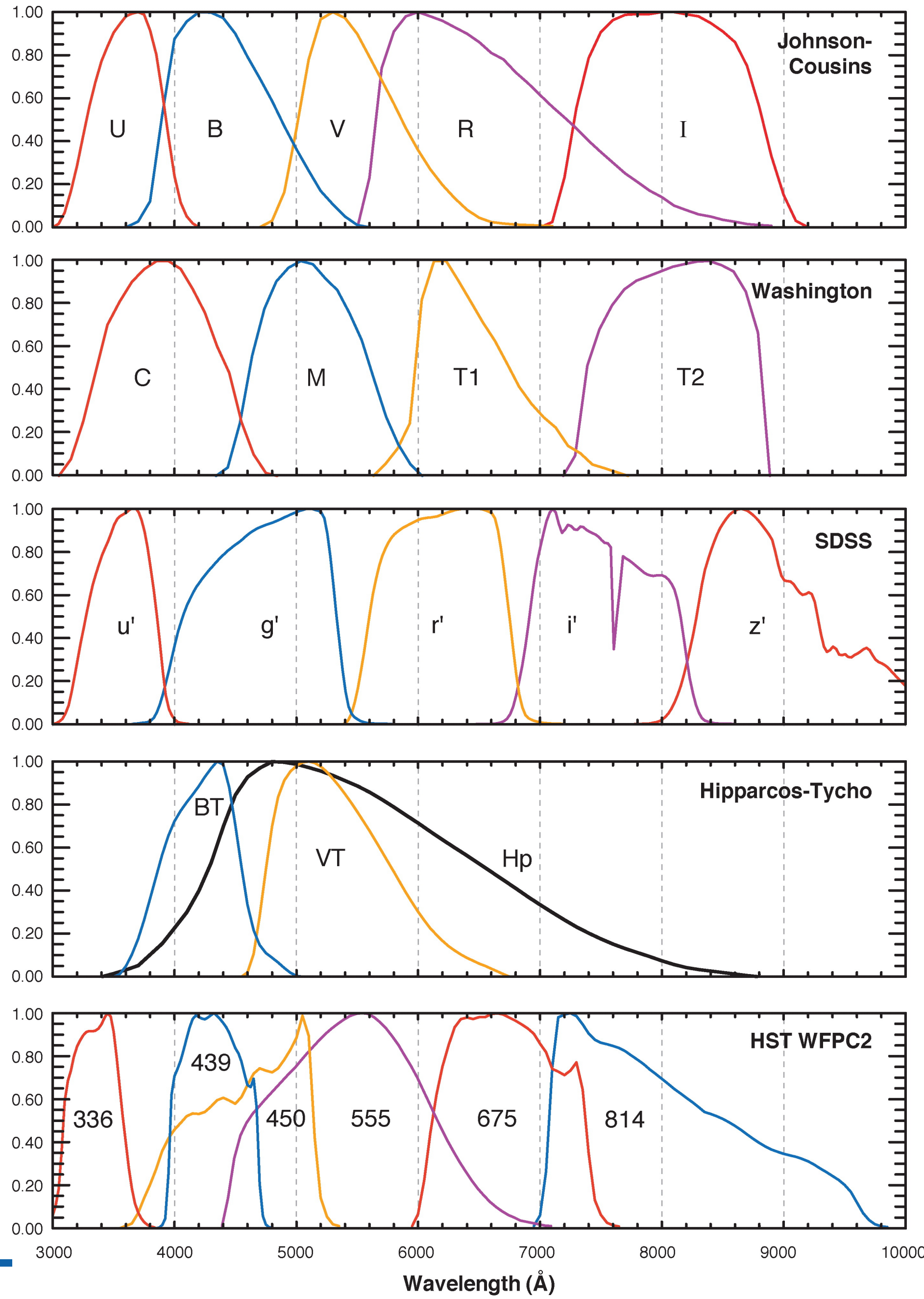

Bessell, MS. 2005
Annu. Rev. Astron. Astrophys. 43: 293–336

- system bases on the flux of Vega, $m_{\text{Vega}} \equiv 0$ **at all wavelengths**
- AB system: object with constant flux per unit frequency interval has zero color

$$m_{\text{AB}} = -2.5 \log(f(\lambda)) - 48.6 \quad (4.4)$$

$m_{\text{AB}} = V$ for a flat-spectrum source.

Abolute magnitude

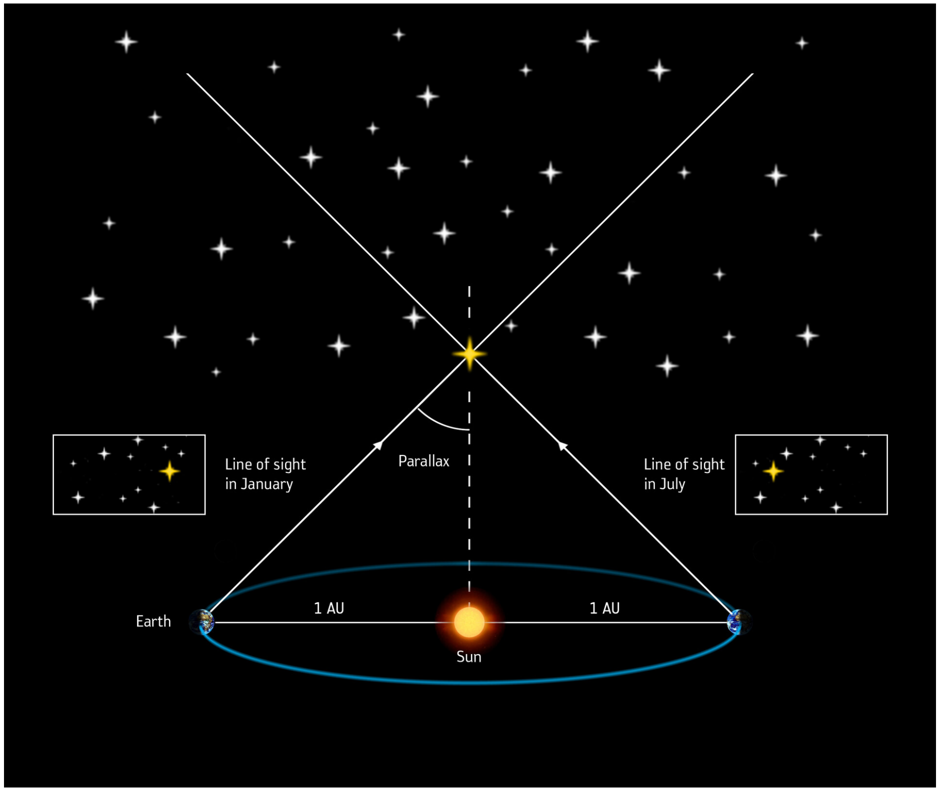

ESA

- Absolute magnitude M_X can be calculated from the apparent magnitude, if the distance d is known

$$m_X - M_X = 5 \log_{10} d - 5 \qquad (4.5)$$

distance modulus

- most direct distance measurement is using the parallax π

$$d = 1/\pi \qquad (4.6)$$

d in pc, π in arcsec

Bolometric magnitude and luminosity

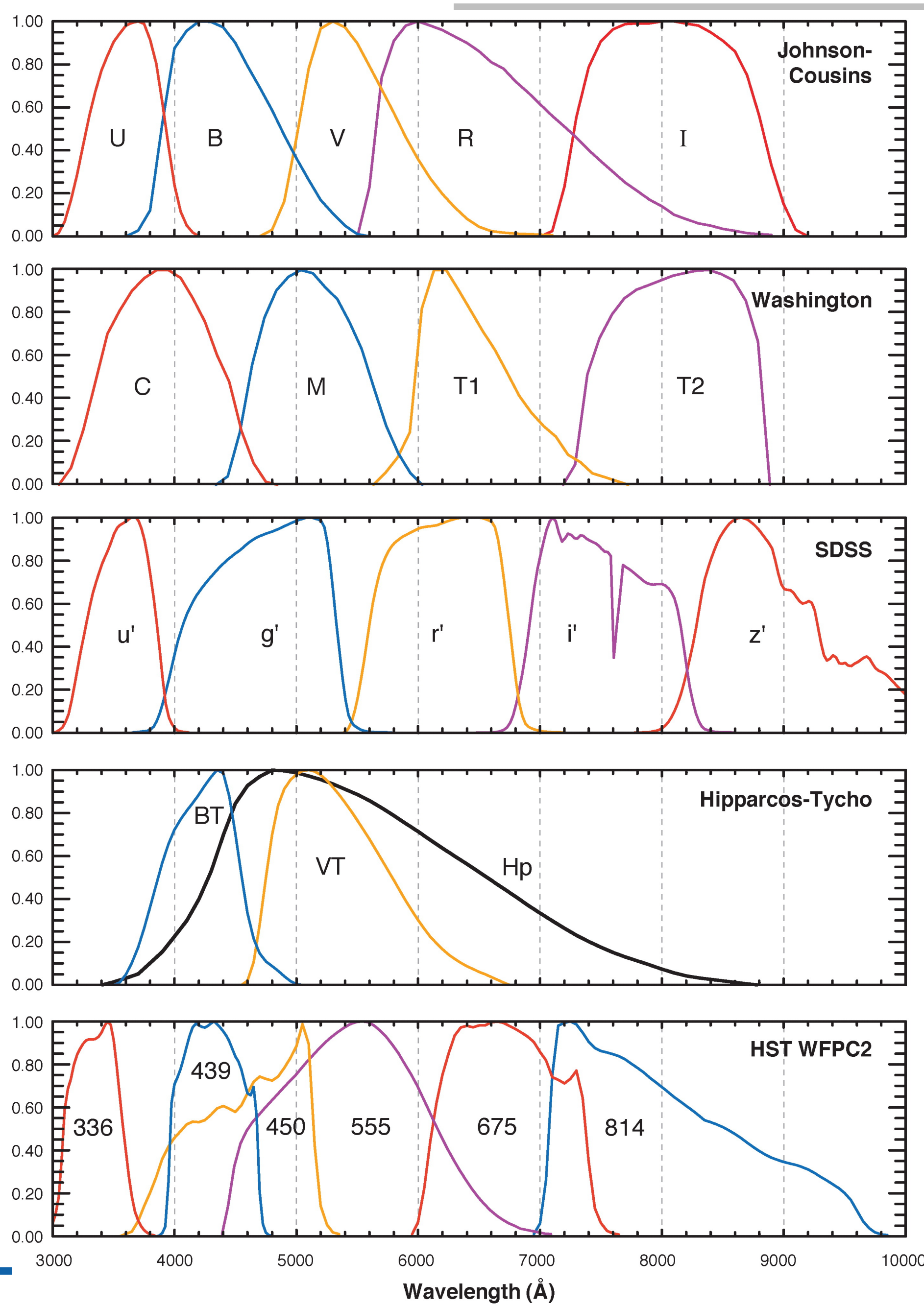

Bessell, MS. 2005
Annu. Rev. Astron. Astrophys. 43: 293–336

- bolometric magnitude M_{bol} is the integrated absolute magnitude over all wavelengths

$$M_{bol} = -2.5 \log_{10} \int_0^\infty I_\lambda \, d\lambda \qquad (4.7)$$

- to transform to bolometric magnitude a bolometric correction is necessary, which is calculated from stellar model fluxes for each stellar type

$$M_{bol} \equiv M_X - B.C. \qquad (4.8)$$

- luminosity of a star is related to the bolometric magnitude

$$\frac{L}{L_\odot} = 10^{(M_{bol} - M_{bol,\odot})/2.5} \qquad (4.9)$$

Interstellar Reddening

Extinction A_V

- absorption and scattering of electromagnetic radiation by dust and gas between an emitting astronomical object and the observer
- shorter wavelengths (blue) are more heavily reddened than longer (red) wavelengths
- measure colour index $B - V$

$$E(B-V) = (B-V) - (B-V)_0 \qquad (4.10)$$

$$A_V = 3.2E(B-V) \qquad (4.11)$$

- true distance

$$d = 10^{0.2(m-M+5-A_V)} \qquad (4.12)$$

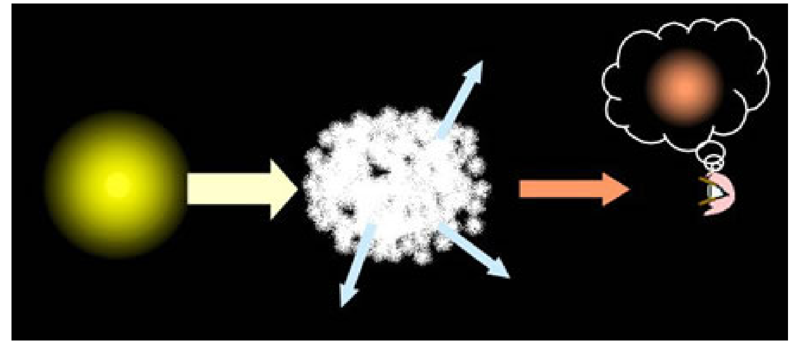

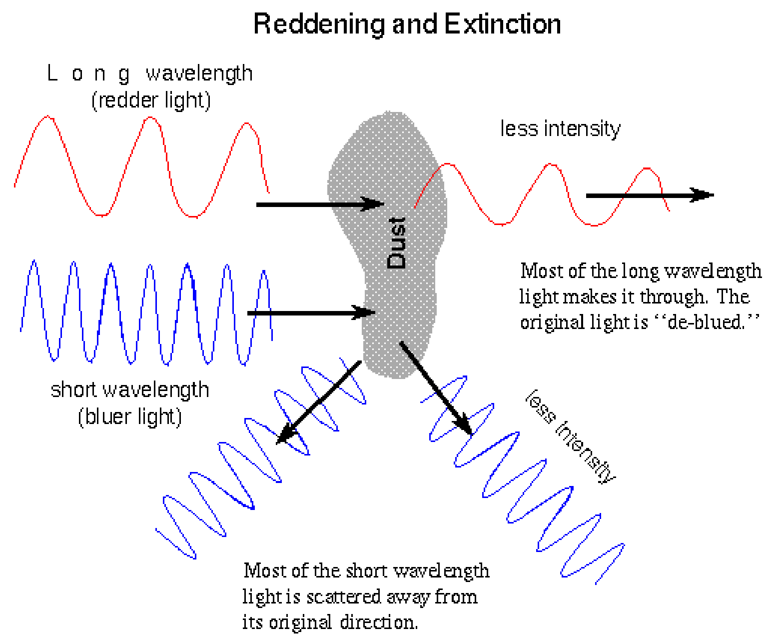

Atmospheric extinction

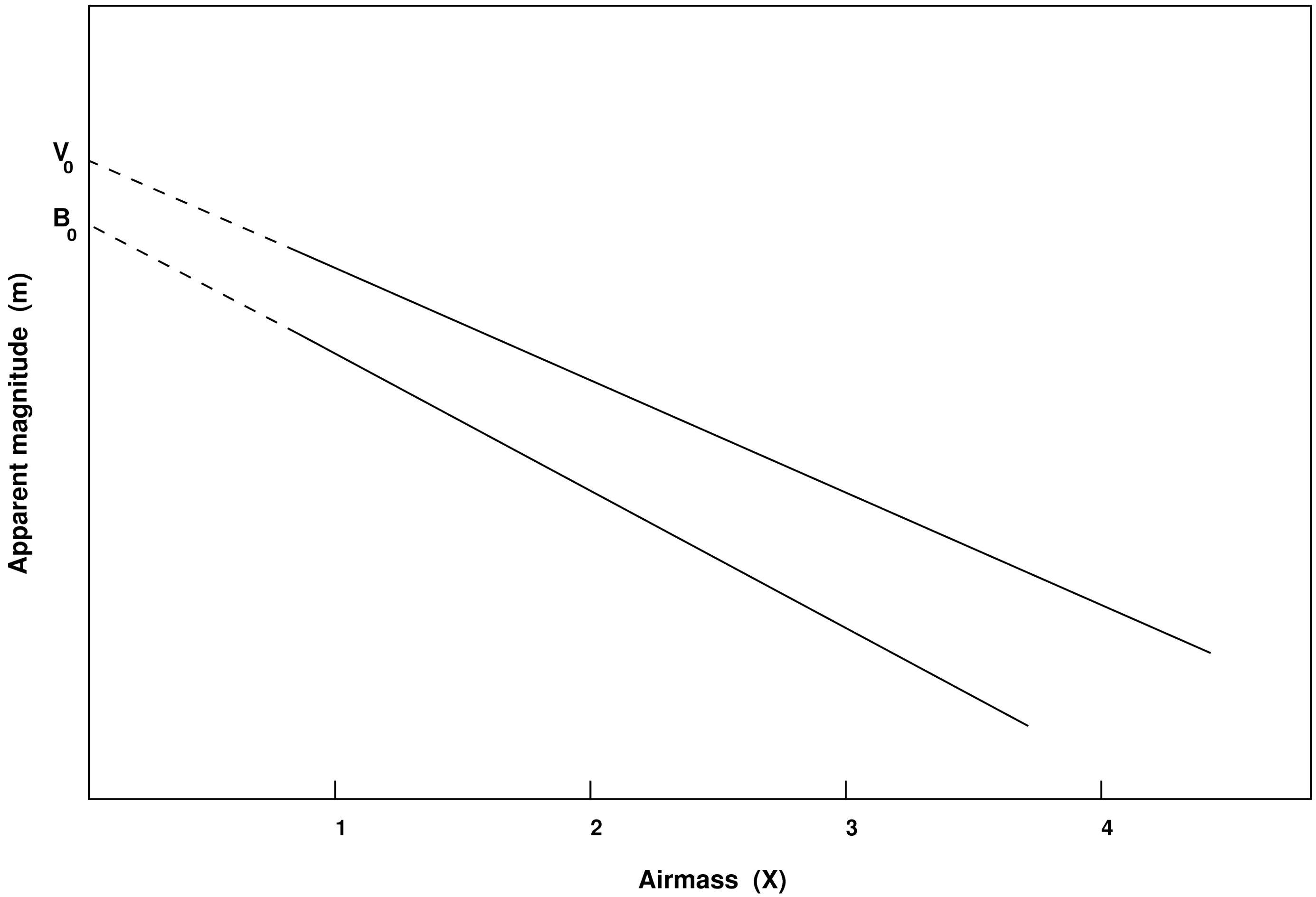

- $V = V_0 + \kappa(\lambda)X(z)$
  $\kappa(\lambda)$ is the extinction coefficient
  z is the zenith distance
  X is the air mass
  $X(z) \approx \cos^{-1} z$
- extinction greater for blue than for red

Standard stars to correct for atmospheric extinction and calibrate the sensitivity of the instrument

Atmospheric extinction

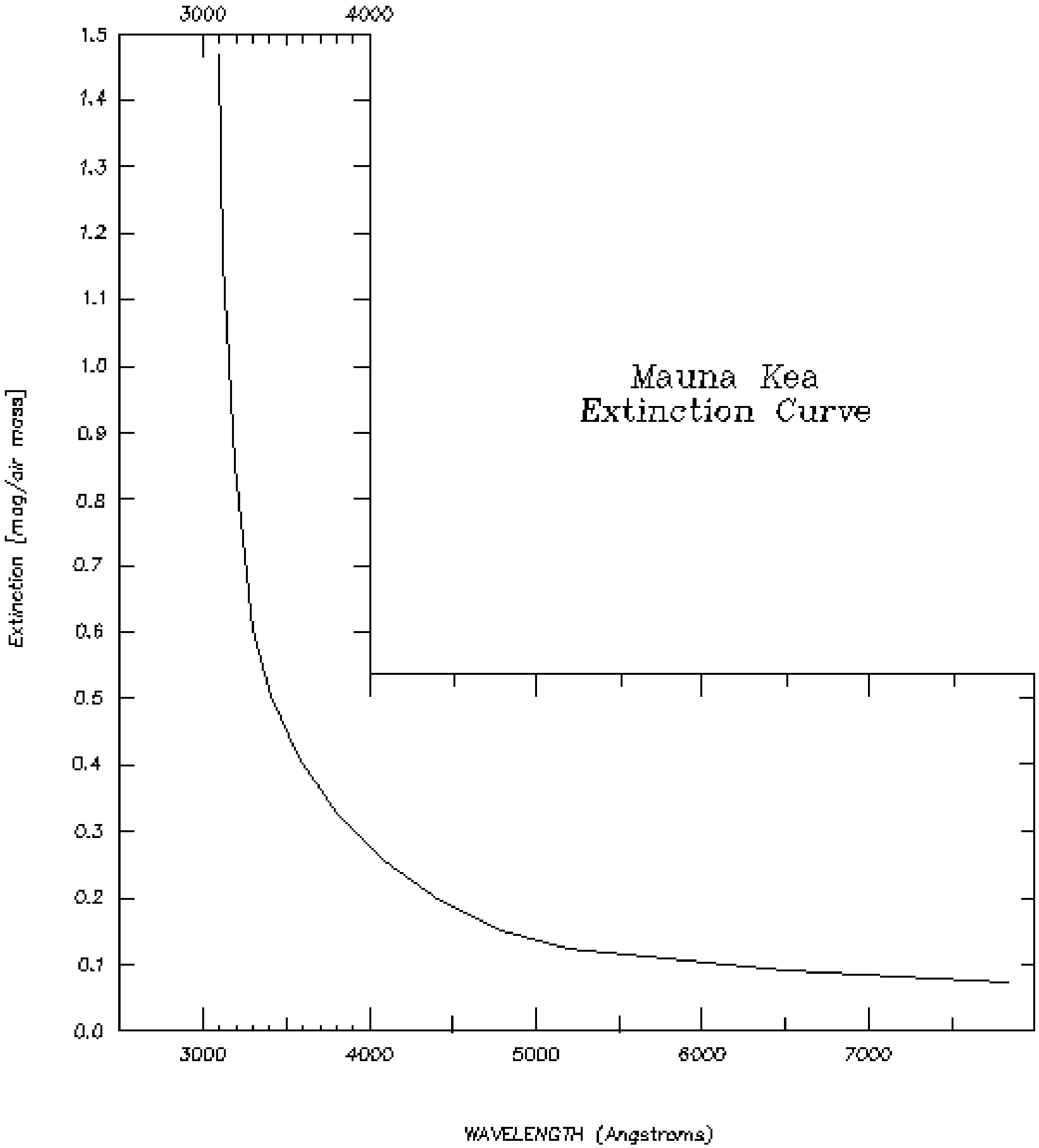

- $V = V_0 + \kappa(\lambda)X(z)$ $\kappa(\lambda)$ is the extinction coefficient
  z is the zenith distance
  X is the air mass
  $X(z) \approx \cos^{-1} z$
- extinction wavelength-dependent
- blue stars are getting weaker compared to red stars

Black body radiation

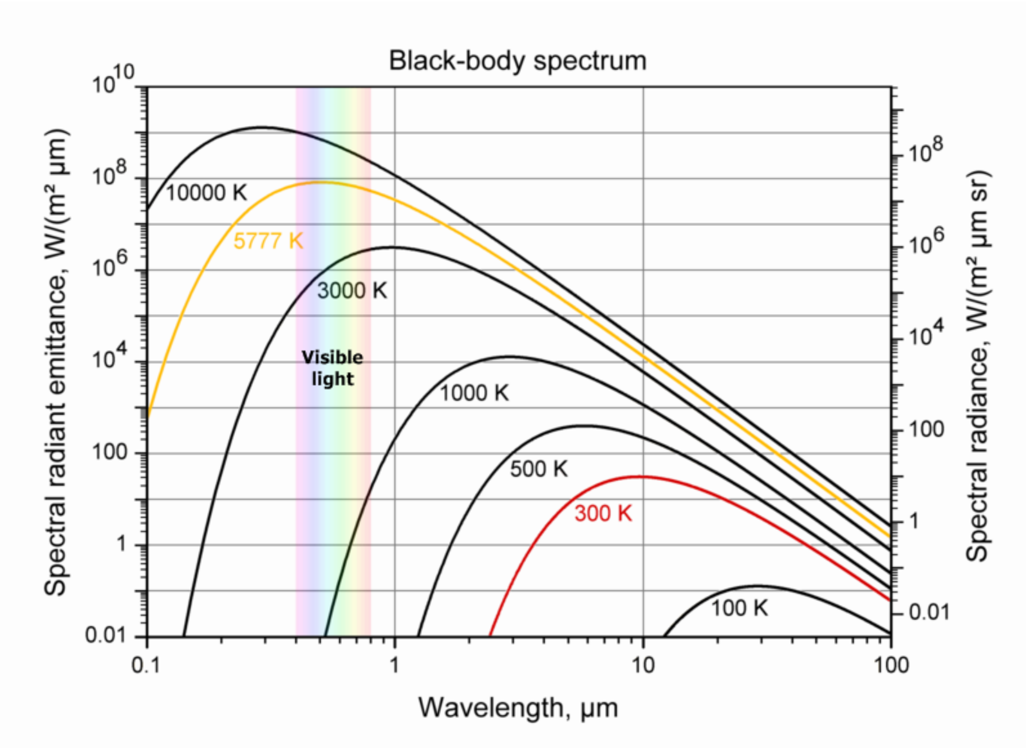

Definition

- in thermal equilibrium with its surroundings
- emits a continuous spectrum whose spectral shape is defined solely by its temperature $\rightarrow$ Planck function

Realisation in nature

- well recovered if photons are frequently absorbed and emitted, i.e., if the photons' mean free paths are short
- fulfilled in the stellar interior due to the high densities
- not fulfilled in stellar atmospheres where the densities are low
- useful first approximation

Derivation of the Planck function

closed box coupled to a heat bath

$\rightarrow$ photon gas inside is in thermal equilibrium

$\rightarrow$ energy density u of photons of frequency ν (h is the Planck constant, c speed of light, k Boltzmann constant)

$$u(\nu) = \frac{8\pi h\nu^3}{c^3}\frac{1}{\exp(h\nu/(kT)) - 1} \tag{4.13}$$

To derive Planck function $B(\nu)$ compute energy per unit area and unit time escaping through a tiny hole at, e.g., the bottom of the box:

$$B(\nu) = \frac{\text{escaping energy}}{\text{per unit area and unit time}} = \frac{\epsilon(\nu)}{\mathrm{d}At} \tag{4.14}$$

$\epsilon(\nu,\theta)\mathrm{d}\theta$ is the energy of photons with frequency ν escaping through the hole in unit time from all directions inclined at angle θ

$$\epsilon(\nu,\theta)\mathrm{d}\theta = u\,n(\theta)\,V(\theta) \stackrel{Fig}{=} u\frac{2\pi\sin\theta}{4\pi}\mathrm{d}A\,c\,\mathrm{d}t\cos\theta \tag{4.15}$$

$n(\theta)$ fraction of photons in prescribed cone, $V(\theta)$ volume occupied by those photons capable of passing through the hole in unit time

Derivation of the Planck function

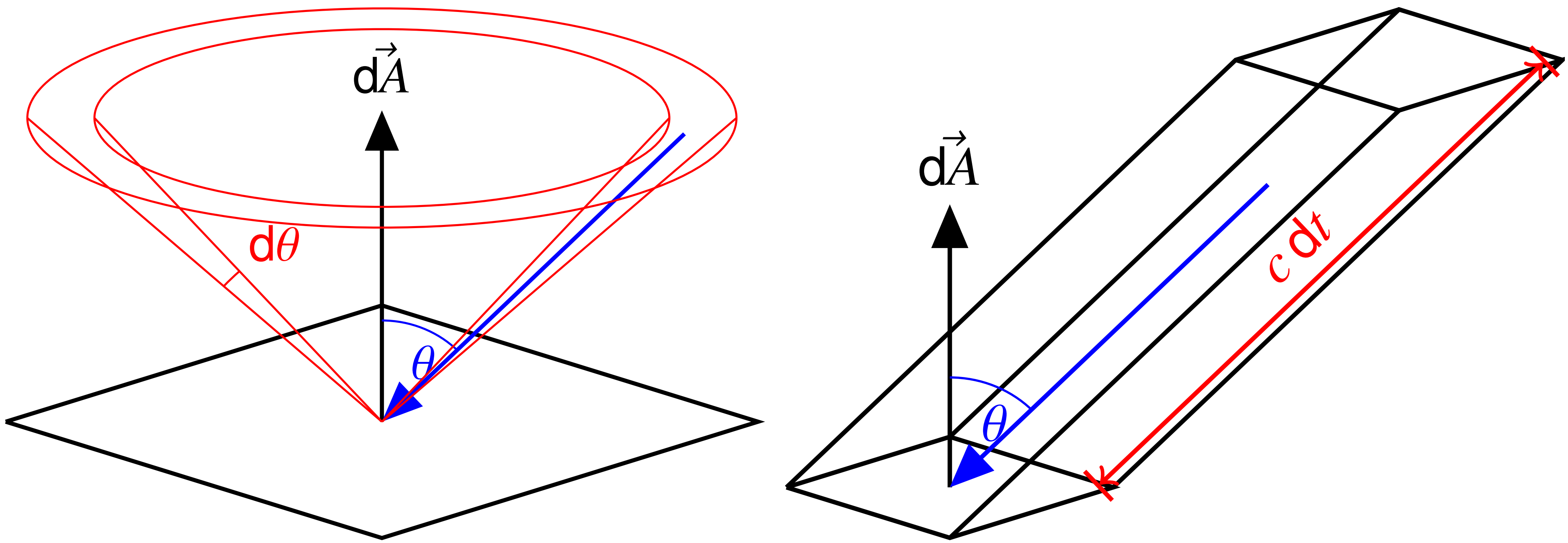

Integration over angle yields the Planck function $B(\nu)$:

$$B(\nu) = \int_0^{\pi/2} \epsilon(\nu, \theta) d\theta / (dA dt) = \frac{1}{4} c u(\nu) = \frac{2\pi h \nu^3}{c^2} \frac{1}{\exp(h\nu/(kT)) - 1} \tag{4.16}$$

Properties of the Planck function

- $B(\nu)$ is energy per unit area per unit time per unit frequency interval. Often Planck function per wavelength interval is useful. $\rightarrow B(\lambda)\mathrm{d}\lambda = B(\nu)\mathrm{d}\nu$:

$$B(\lambda) = B(\nu)\left|\frac{\mathrm{d}\nu}{\mathrm{d}\lambda}\right| \overset{\lambda\nu=c}{=} B\left(\frac{c}{\lambda}\right)\frac{c}{\lambda^2} = \frac{2\pi hc^2}{\lambda^5}\frac{1}{\exp(hc/(\lambda kT))-1} \tag{4.17}$$

- Integration over all wavelengths gives us the luminosity per area

$$\frac{L}{A} \overset{sphere}{=} \frac{L}{4\pi R^2} = \int_0^\infty B(\lambda)\mathrm{d}\lambda = S = \sigma T^4 \tag{4.18}$$

$\sigma = \frac{2\pi^5 k^4}{15c^2h^3} = 5.6705 \times 10^{-5}\mathrm{erg\,cm^{-2}\,s^{-1}K^{-4}}$ is the Stefan-Boltzmann constant

- Wien's displacement law states that the blackbody radiation curve for different temperatures peaks at a wavelength inversely proportional to the temperature

$$\frac{\mathrm{d}}{\mathrm{d}\lambda}B(\lambda_{\mathrm{max}}) \overset{!}{=} 0 \rightarrow \lambda_{\mathrm{max}}T = 2.898 \times 10^7\,\text{ÅK} \tag{4.19}$$

Planck function

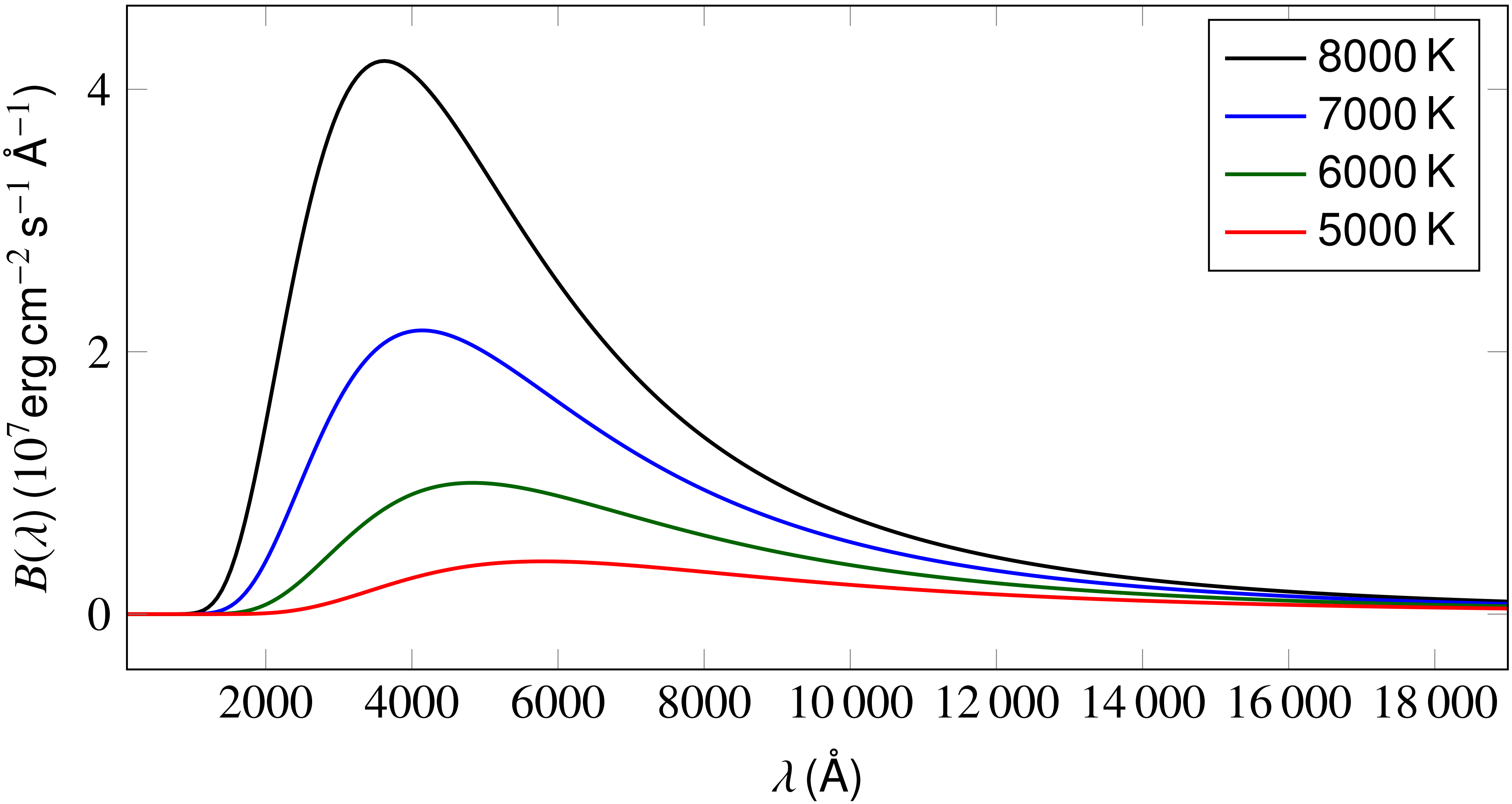

Wien approximation $\frac{h\nu}{kT} \gg 1 \rightarrow B_\nu(T) \simeq \frac{2h\nu^3}{c^2} \exp(-h\nu/(kT))$

Rayleigh-Jeans approximation $\frac{h\nu}{kT} \ll 1 \rightarrow B_\nu(T) \simeq \frac{2\nu^2 kT}{c^2}$

Planck function

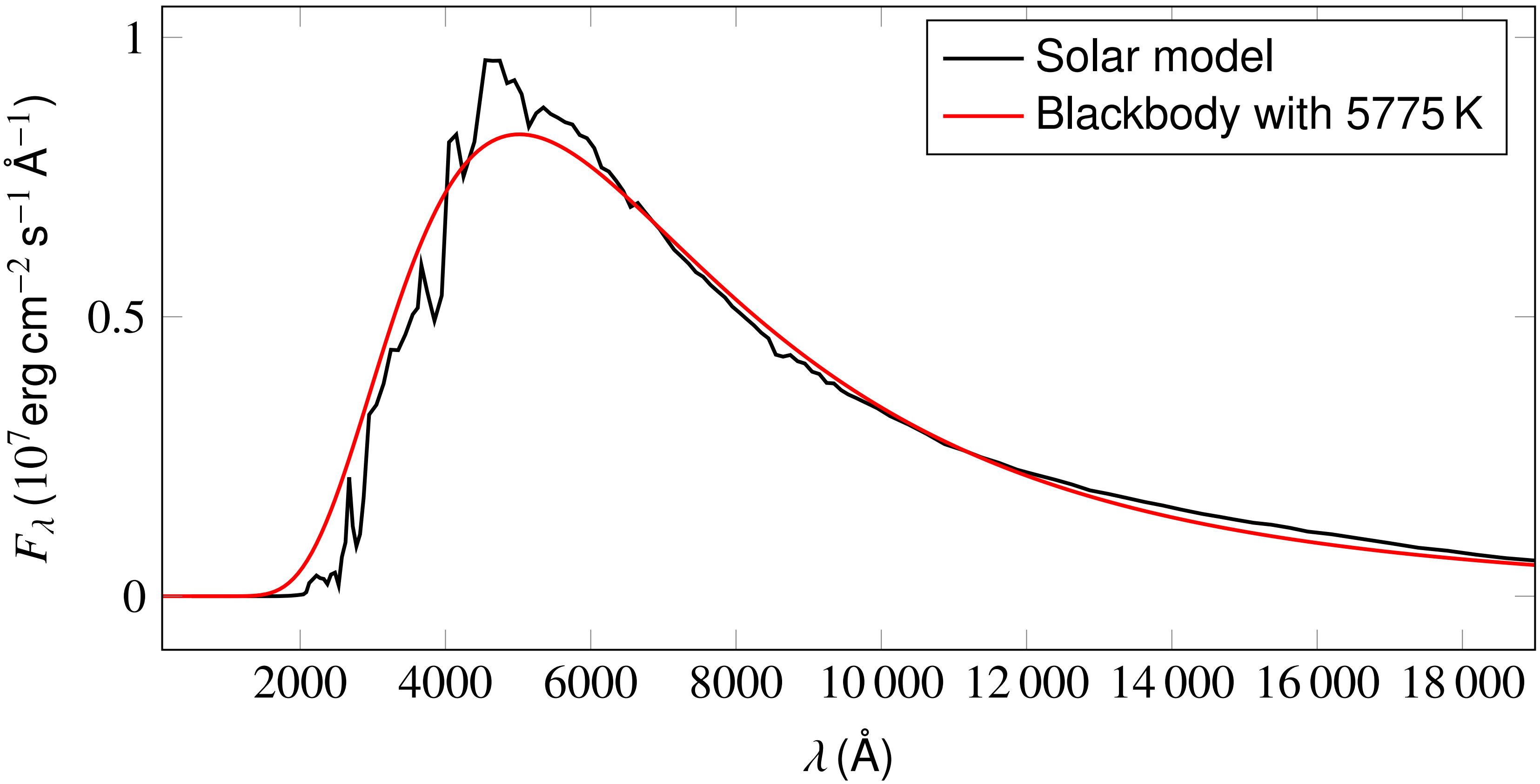

Definition of the effective temperature:

The effective temperature of a star is defined as the temperature of a blackbody having the same radiated power per unit area.

$$\int_0^\infty F(\lambda)\mathrm{d}\lambda \overset{!}{=} \sigma T_{\mathrm{eff}}^4 \tag{4.20}$$

Color-temperature relation

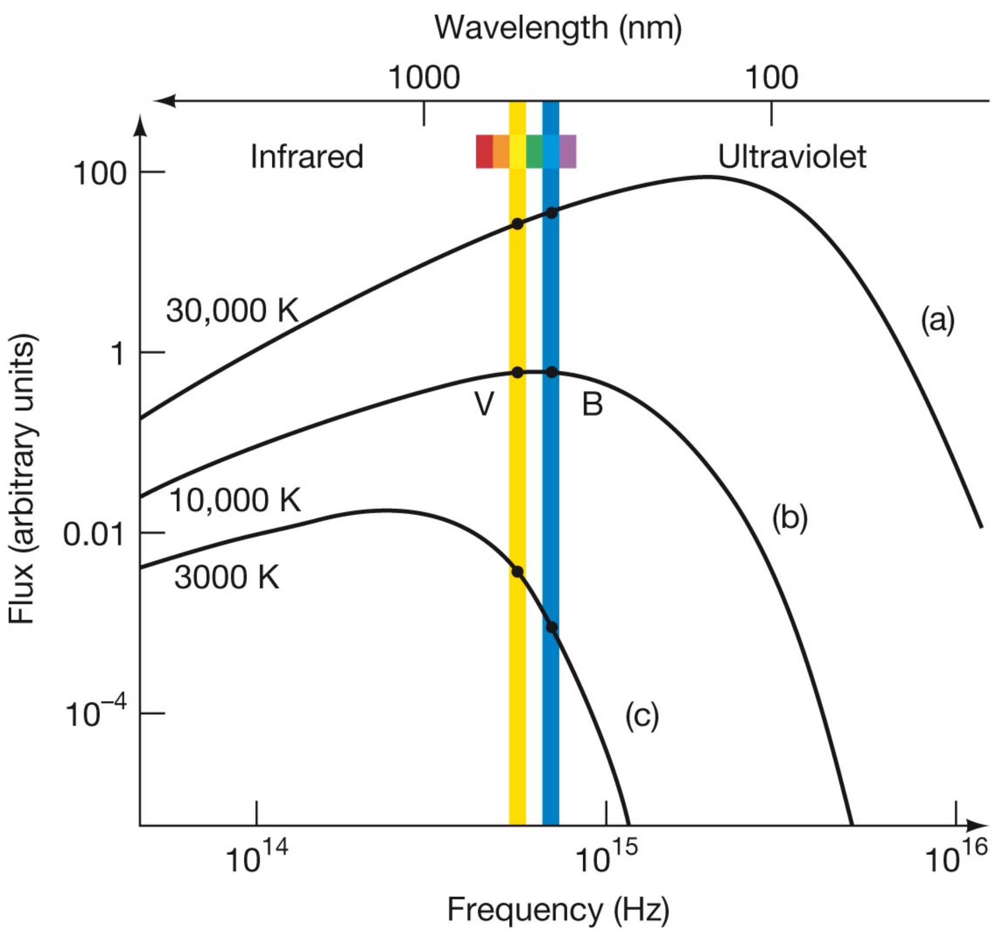

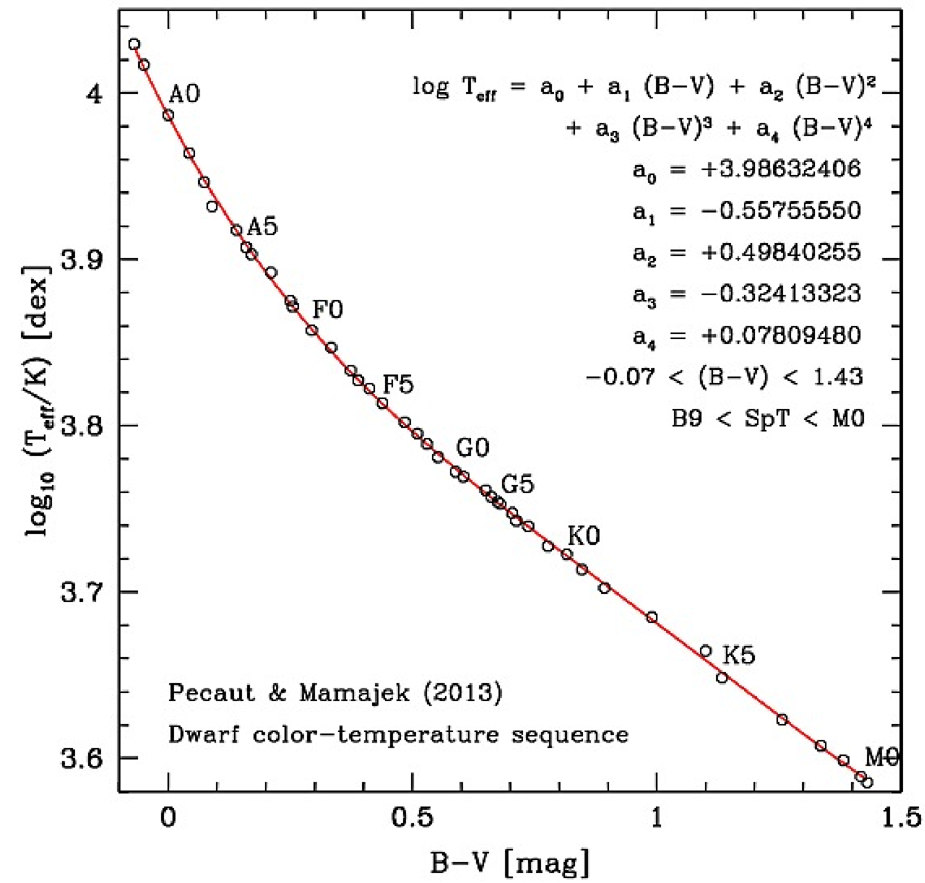

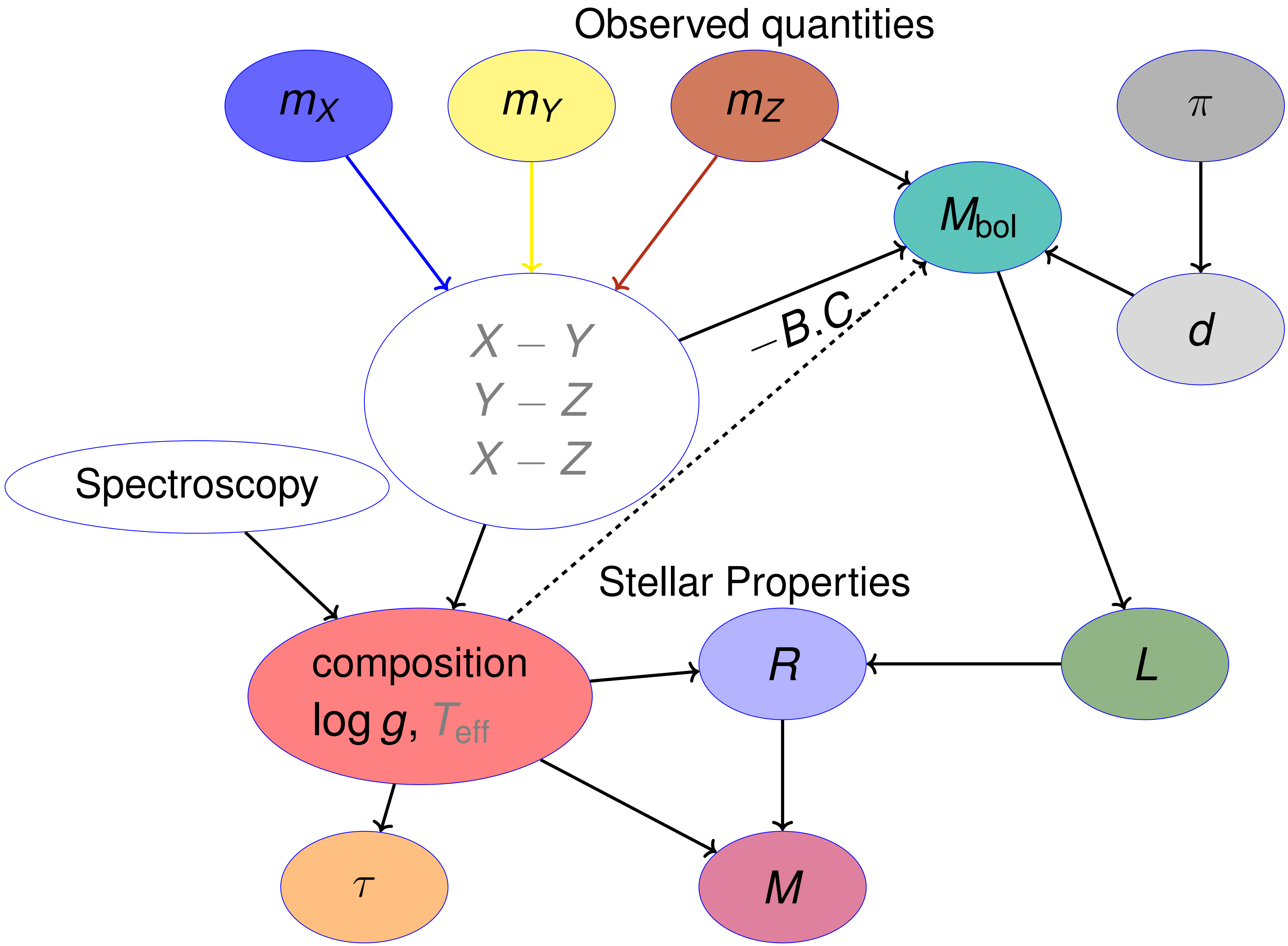

Observed quantities
m_X
m_Y
m_Z
π
M_{bol}
d
$X - Y$
$Y - Z$
$X - Z$
$-$B.C.
Spectroscopy
Stellar Properties
composition
$\log g$, T_{eff}
R
L
τ
M

Fundamental Parameters

Mass $M_\star$: Except for massive stars with strong stellar winds or stars in interacting multiple systems, the stellar mass is constant throughout a star's lifetime.
Possible range: 0.08 to several hundred $\mathrm{M}_\odot$

Radius $R_\star$: stellar radius is a probe for the evolutionary status.
Possible range: 0.5-1000 $\mathrm{R}_\odot$

Luminosity $L_\star$: total power radiated by the star: $L_\star = 4\pi R_\star^2 F = 4\pi R_\star^2 \sigma T_{\mathrm{eff}}^4$
Possible range: $10^{-2} - 10^7\,\mathrm{L}_\odot$

Age $\tau_\star$: age of the star. More massive stars have shorter lifetimes because
Typical range: millions to billions of years

Mass and radius linked via the surface gravity $g = GM_\star R_\star^{-2} \longrightarrow$ spectroscopy

Determination of fundamental parameters: Mass

Direct measurements of masses are only possible when stars occur in binary systems and when their orbital motion is known

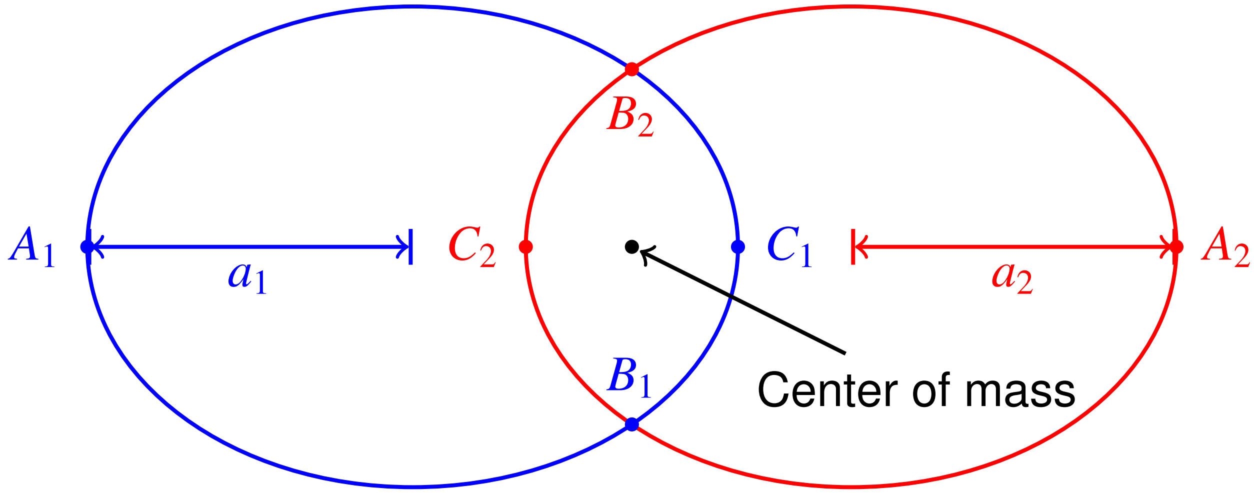

$M_{\star,1/2}$:	Mass of component 1 and 2
P :	Orbital period (measured)
d :	distance to the system (somehow known)
i :	Orbital inclination against the line of sight (somehow known).
$a_{1,2}$	Semimajor axis of the two stars' angular motion relative to center of mass (measured) – $a_{\mathrm{observ}} = a_{\mathrm{real}} \sin i$

- Keplers's third law with $a = a_1 + a_2$:

$$\frac{G(M_1 + M_2)}{4\pi^2} = \frac{a^3}{P^2} \tag{4.21}$$

- center-of-mass law

$$M_1 a_1 = M_2 a_2 \tag{4.22}$$

Determination of fundamental parameters: Mass

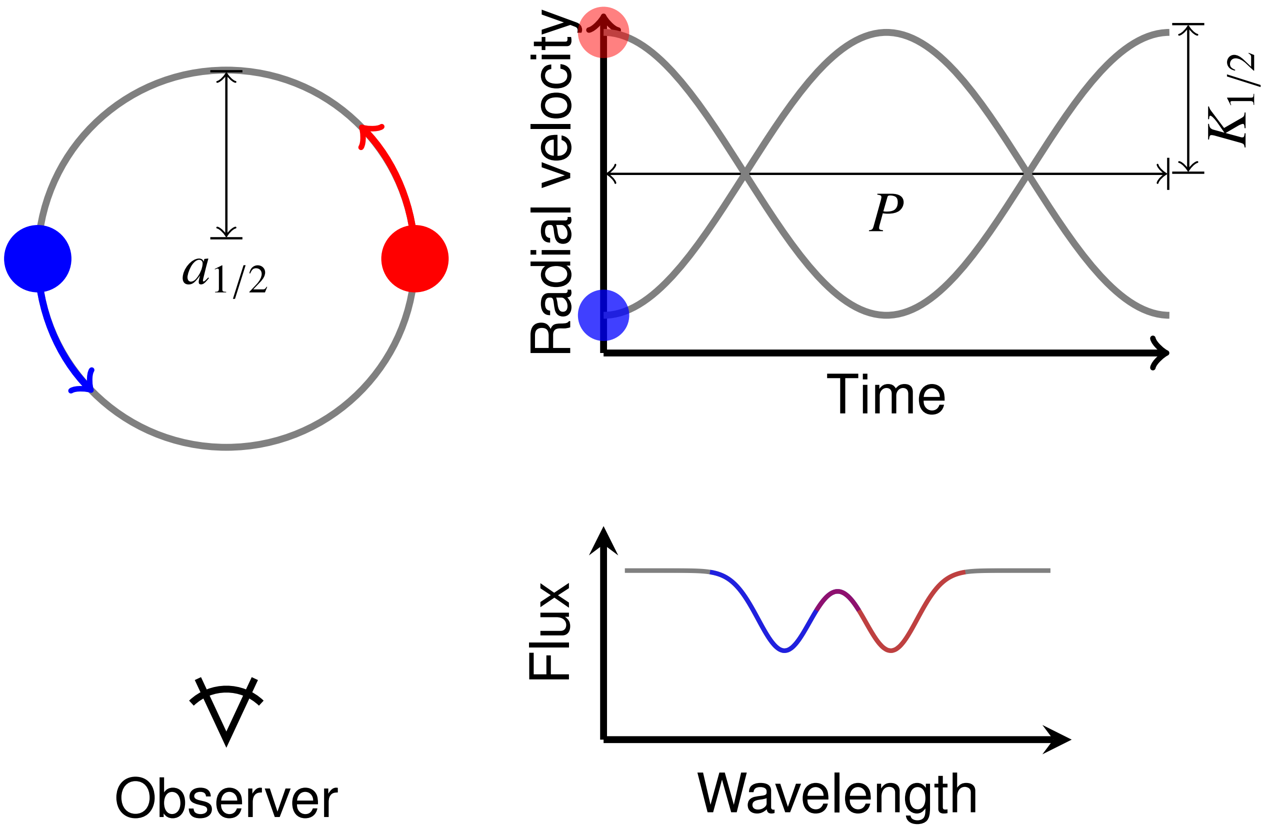

double-lined spectroscopic binary in circular orbit:

$$K_{1,2} = \frac{2\pi a_{1/2}}{P} \sin i \quad (4.23)$$

$K_{1/2}$ is the radial velocity amplitude

$\rightarrow$ three unknowns: i, M_1, M_2; two equations !

$\rightarrow$ inclination can be derived for eclipsing binaries ($i \sim 90^\circ$)

- momentum conservation:

$$M_1 K_1 = M_2 K_2 \qquad (4.24)$$

- Keplers's third law with $a = a_1 + a_2$:

$$(M_1 + M_2)\sin^3 i = \frac{P}{2\pi G}(K_1 + K_2)^3 \qquad (4.25)$$

Determination of fundamental parameters: Radius

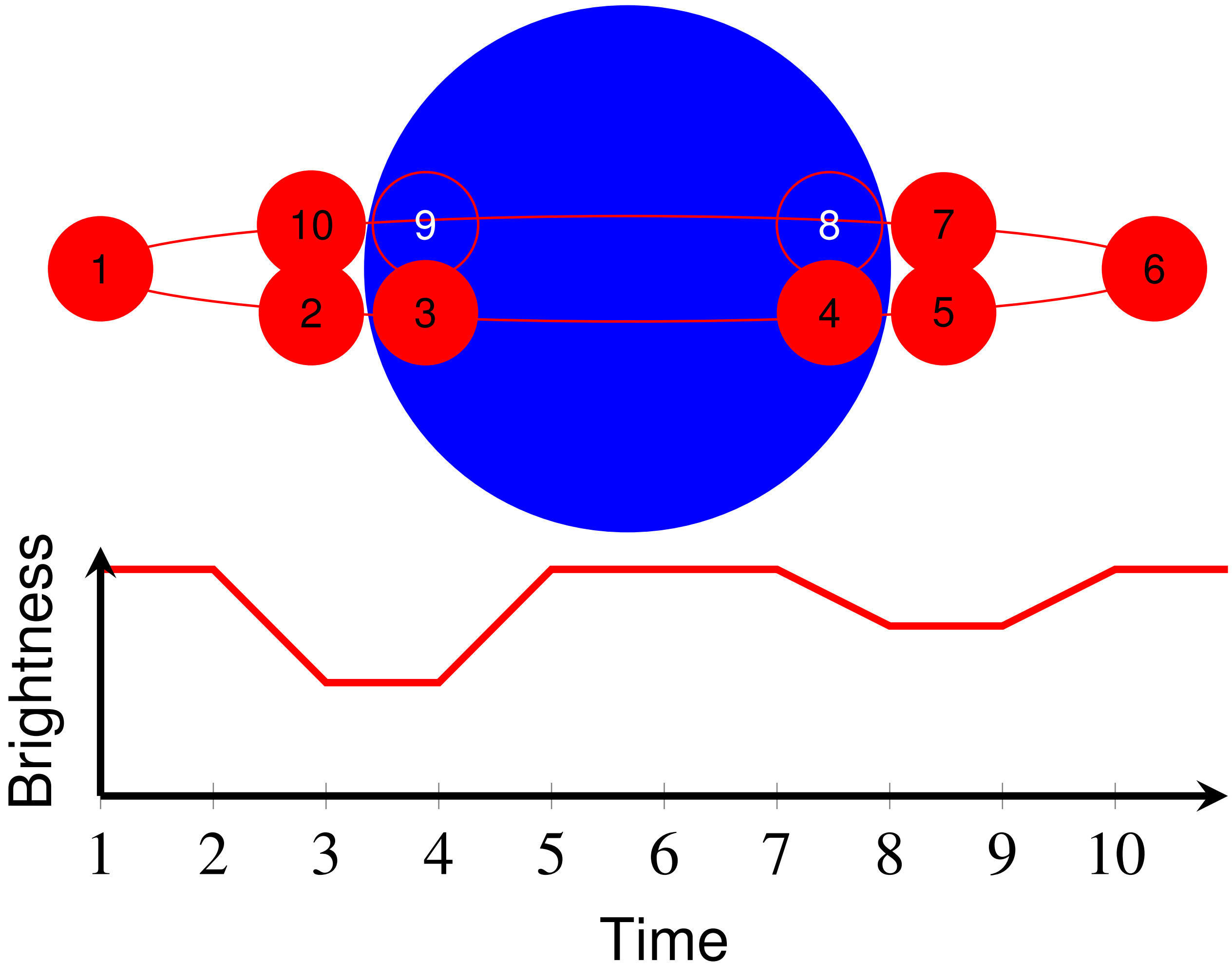

$$d_A + d_B = v(t_5 - t_2)$$

$$d_A - d_B = v(t_4 - t_3)$$

$d_{A,B}$ is the stars' diameter, v is the orbital velocity, t_i are the times of the eclipse

Determination of fundamental parameters: Radius and luminosity

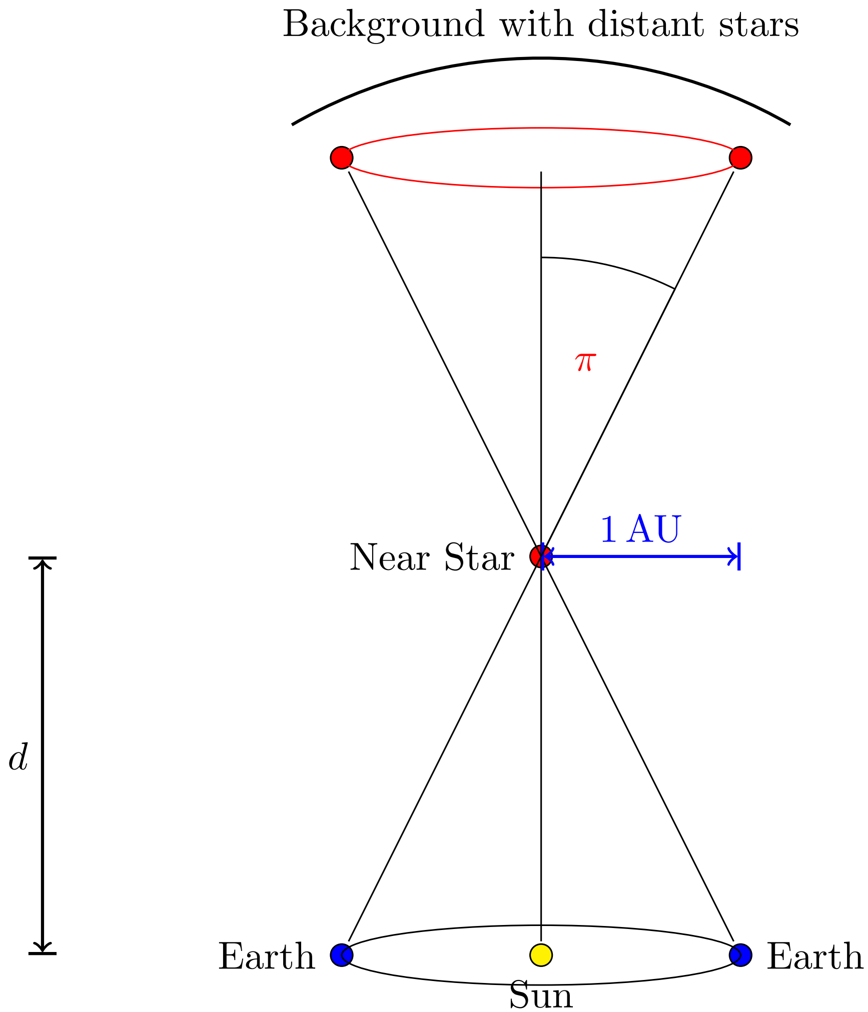

parallax π(arcsec) = $1/$d(pc)

$F = F(T_{\text{eff}})$ is the surface flux of the star, f is the flux arriving on Earth

$$4\pi d^2 f = 4\pi R^2 F \Rightarrow R = d\sqrt{f/F}$$

Luminosity L using Stefan-Boltzmann law

$$L = 4\pi R^2 \sigma T_{\text{eff}}^4$$

Determination of stellar parameters: Mass & age

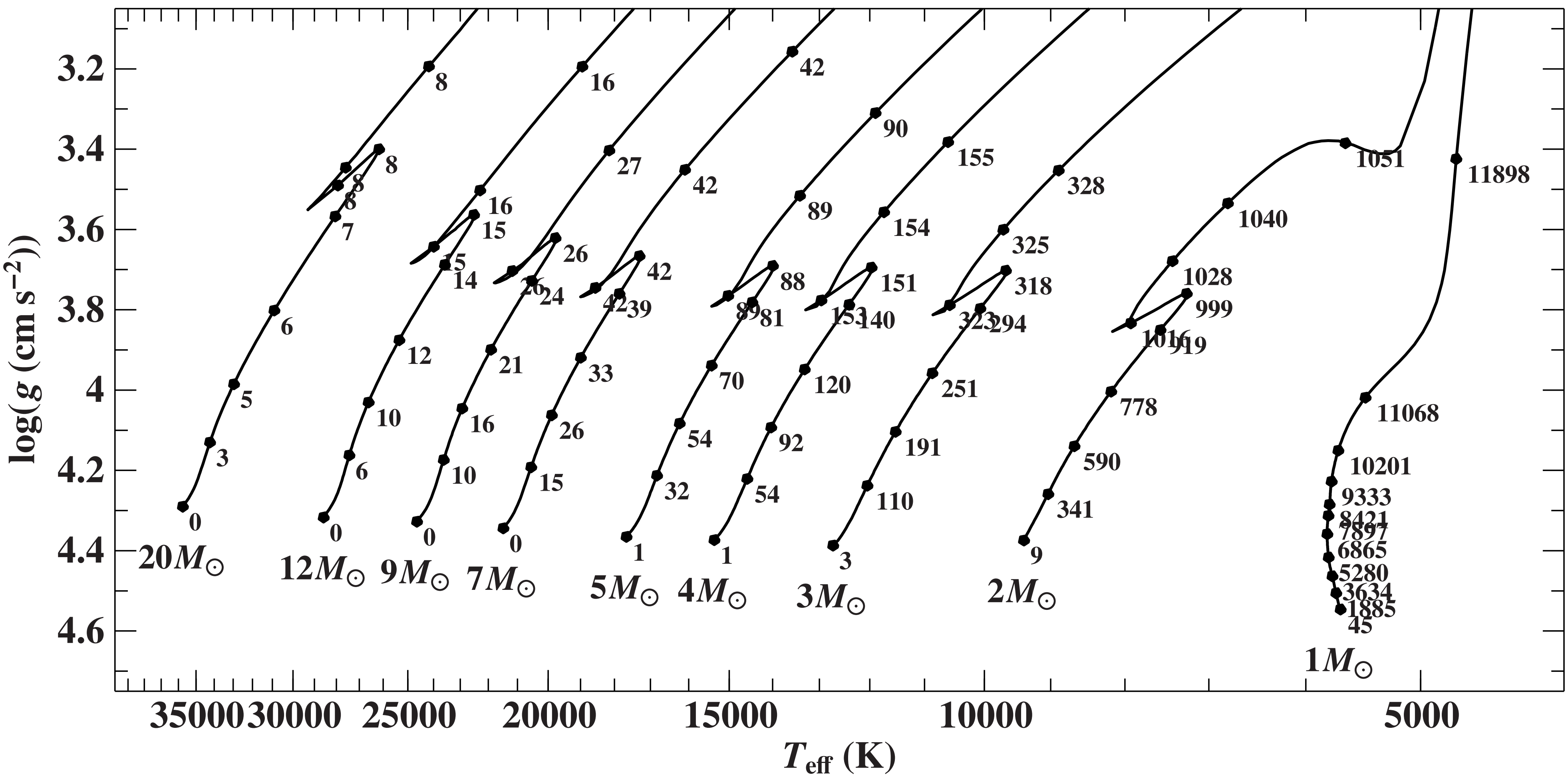

evolution tracks: circles give the age in Myr $\rightarrow$ (model dependent) mass and age from position in spectroscopic HRD

Hertzsprung-Russell diagram

Observational:

Colour-Magnitude diagram (CMD)

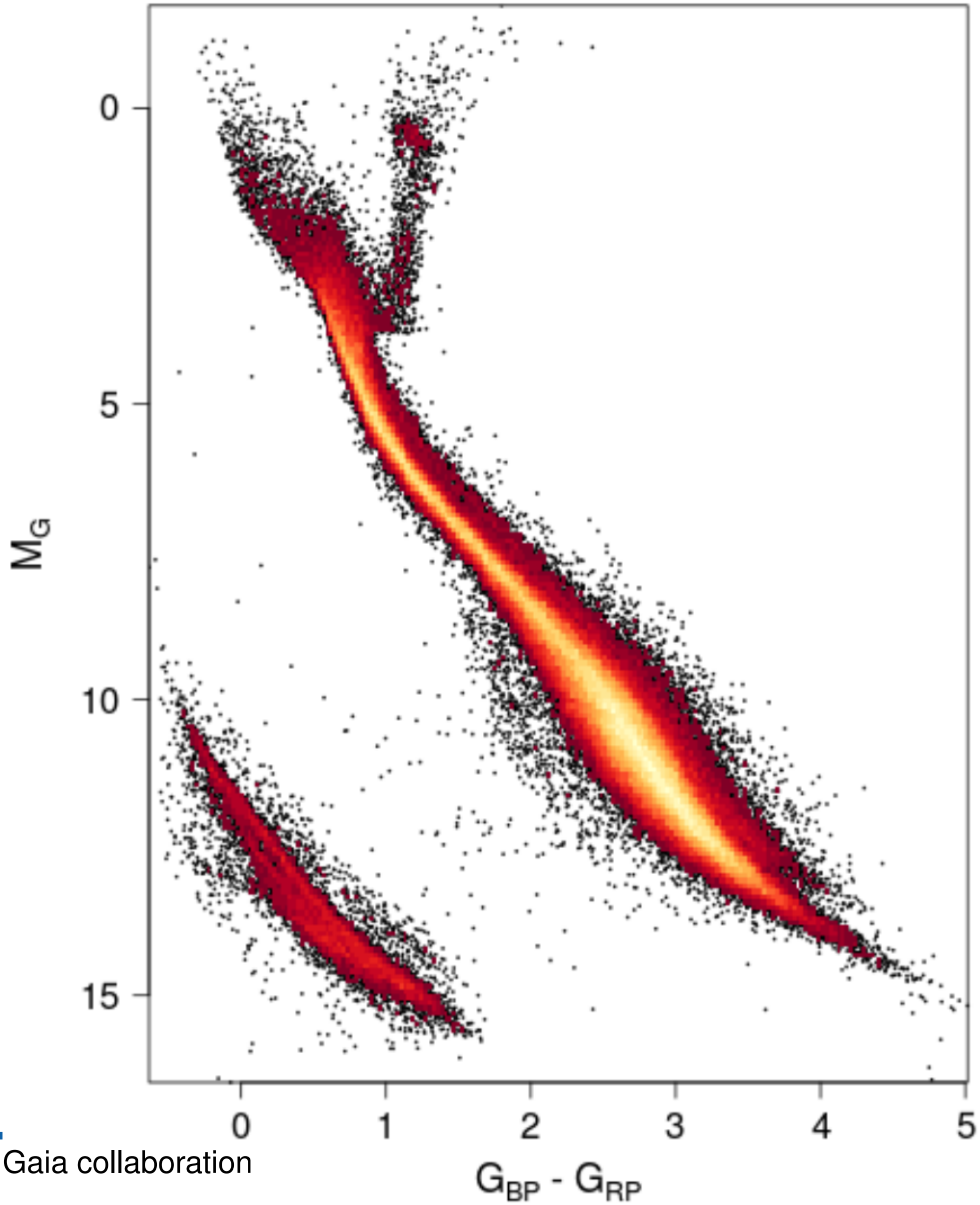

Gaia collaboration

Theoretical: Temperature-Luminosity

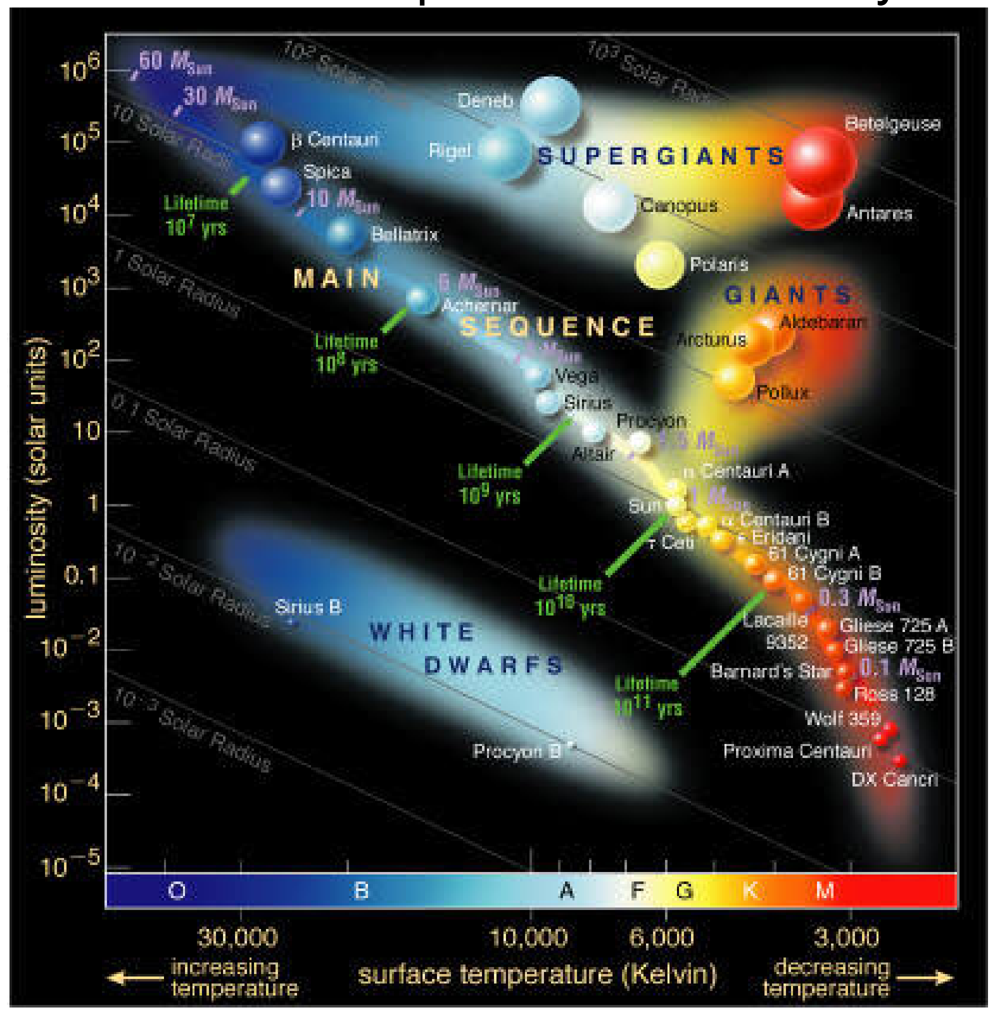

ESO

Hertzsprung-Russell diagram

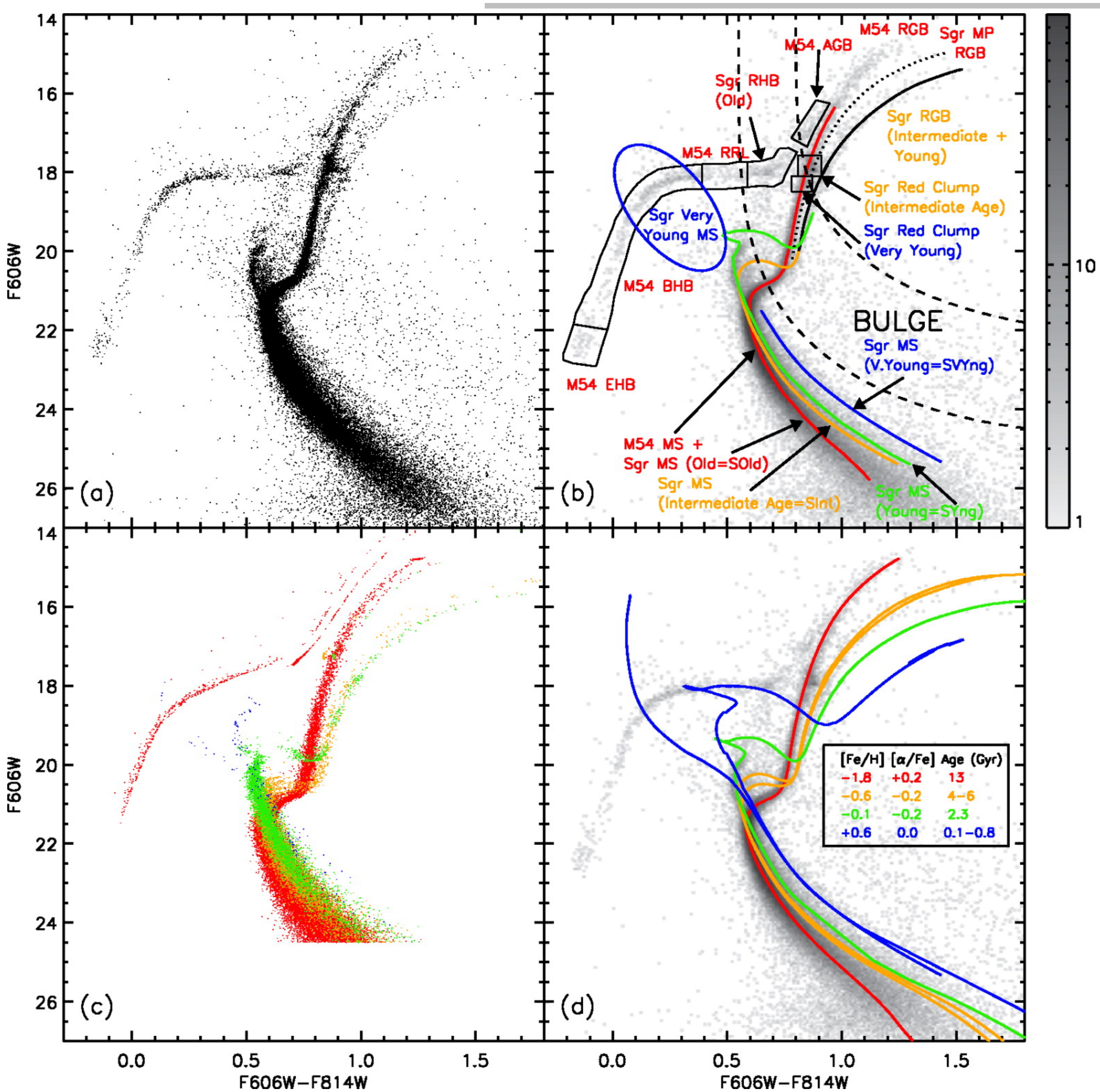

- Why are the stars distributed in that way?
- How can we learn about the temporal evolution of stars from such snapshots?

Siegel et al. 2007, ApJ, 667, L57

Stellar classification

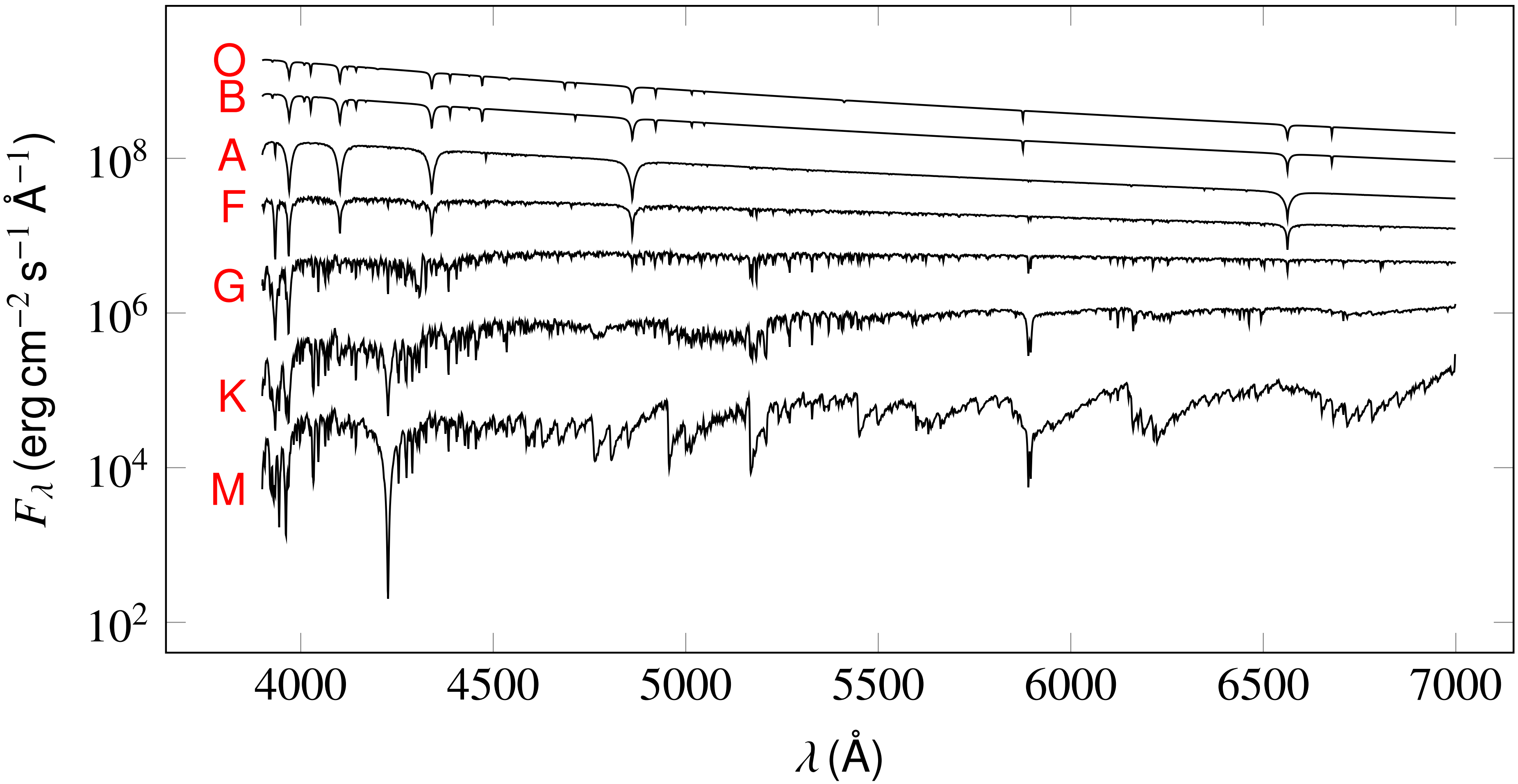

Angelo Secchi (1863): Stars have different spectra emitted from the visible stellar surface layers $\rightarrow$ Stellar atmosphere.

Annie Cannon introduced the Harvard classification scheme with seven spectral types (O, B, A, F, G, K, M) in 1901.

Stellar atmosphere

Energy from the stellar interior flows outward and leaves the star as radiation

- Hydrostatic equation
  $\rightarrow$ Pressure/temperature distribution in the surface layers
- Radiation transport equation
  $\rightarrow$ Emergence of radiative energy at the surface
  $\rightarrow$ Temperature distribution in the surface layers

$\Rightarrow$ Stellar atmosphere model

$\Rightarrow$ Model spectrum compared to observed spectrum

Main model parameters

- Effective temperature T_{eff}
- Surface gravity $g = \frac{GM}{R^2}$, usually used $\log g$
- Chemical composition: abundance of hydrogen X, helium Y and the other elements (metals) Z

Radiation theory

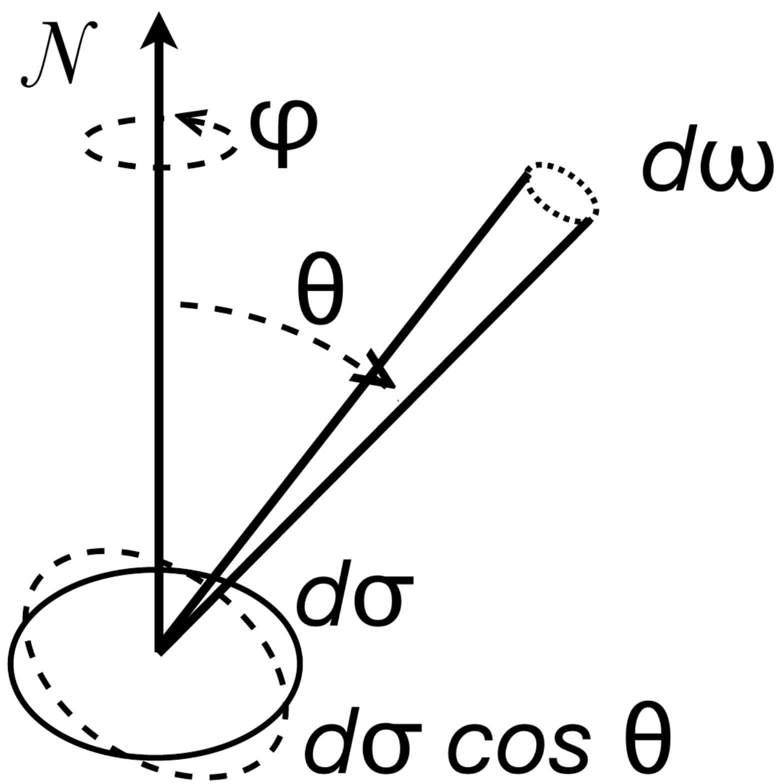

de Boer & Seggewiss 2008

Radiative intensity I_ν

$$I_\nu(\theta,\phi) = \frac{\mathrm{d}E_\nu}{\cos\theta\,\mathrm{d}t\,\mathrm{d}\nu\,\mathrm{d}\omega\,\mathrm{d}\sigma}$$

Energy $\mathrm{d}E_\nu$ within a frequency interval $\mathrm{d}\nu$ passing per unit time $\mathrm{d}t$ through a surface $\mathrm{d}\sigma$ and being directed into solid angle $\mathrm{d}\omega$

Integrated radiative intensity

$\rightarrow$ integrated over all frequencies

$$I(\theta,\phi) = \int_0^\infty I_\nu \mathrm{d}\nu$$

Mean intensity J $\rightarrow$ average of I_ν over all solid angles ω

$$J_\nu = \frac{1}{4\pi}\int_{\theta=0}^{\pi}\int_{\phi=0}^{2\pi} I_\nu(\theta,\phi)\cos\theta\sin\theta\,\mathrm{d}\phi\,\mathrm{d}\theta = \frac{1}{4\pi}\int I_\nu(\omega)\mathrm{d}\omega$$

Radiation theory

Radiative flux $\vec{F}_\nu$

$$\vec{F}_\nu = \int I_\nu \mathrm{d}\nu \cos\theta \mathrm{d}\omega$$

$\rightarrow$ net energy in the interval $\mathrm{d}\nu$ passing each second through a unit area in the direction of the vertical axis

$\rightarrow$ $F_\nu = F_\nu^+ + F_\nu^-$, F_ν^+ outward flux, F_ν^- inward flux
$\rightarrow$ Spherical star $J_\nu = \frac{1}{\pi} F_\nu$
$\rightarrow$ Isotropic radiation field $F_\nu = 0 \Rightarrow F_\nu^+ = -F_\nu^-$

Radiation density U_ν

$$U_\nu = \int \frac{\mathrm{d}E_\nu}{\mathrm{d}V} \mathrm{d}\omega = \frac{1}{c} \int I_\nu \mathrm{d}\omega$$

$\rightarrow$ Radiation energy $\mathrm{d}E_\nu$ passes in a time interval $\mathrm{d}t$ through a volume element $\mathrm{d}V = \mathrm{d}\sigma \mathrm{d}s$, where $\mathrm{d}s = c\mathrm{d}t$. Energy density found by integrating over all solid angles $\mathrm{d}\omega$
$\rightarrow$ Isotropic radiation $U_\nu = \frac{4\pi}{c} I_\nu$
$\rightarrow$ Total radiation density $U = \int U_\nu \mathrm{d}\nu = \frac{4\pi}{c} I$

Equation of radiative transport

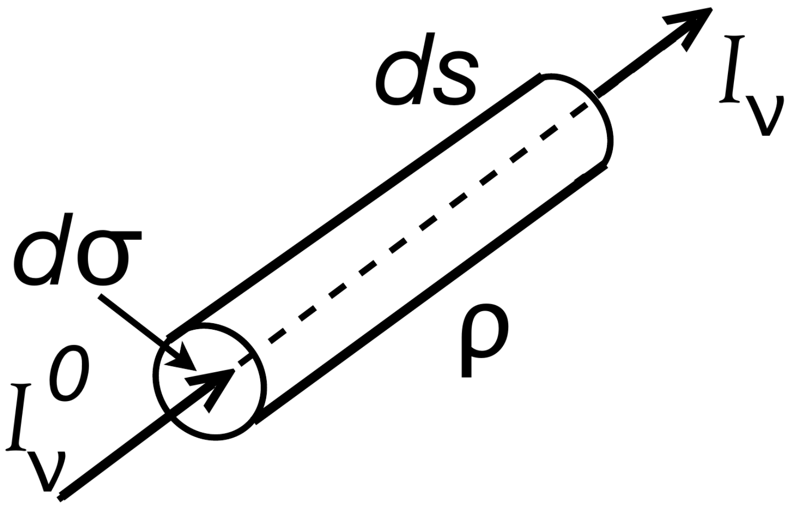

de Boer & Seggewiss 2008

- Optical depth τ_ν

$$\tau_\nu = \int_0^s \kappa_\nu \mathrm{d}s \qquad (4.26)$$

the mean free path of photons is $\Delta\tau_\nu = 1$

Intensity per volume element $\mathrm{d}V$ of length $\mathrm{d}s$ can change

- Emission $\rightarrow$ emission coefficient j_ν

$$j_\nu = \frac{\mathrm{d}E_\nu}{\mathrm{d}t\mathrm{d}V\mathrm{d}\nu\mathrm{d}\omega}$$

Energy emitted per volume element $\mathrm{d}V$ in a unit of time $\mathrm{d}t$ and frequency $\mathrm{d}\nu$ into a solid angle $\mathrm{d}\omega$

- Absorption $\rightarrow$ absorption coefficient κ_ν

$$\mathrm{d}I_\nu = -\kappa_\nu I_\nu \mathrm{d}s$$

Change in intensity due to absorption in the material over the path $\mathrm{d}s$

Equation of radiative transport

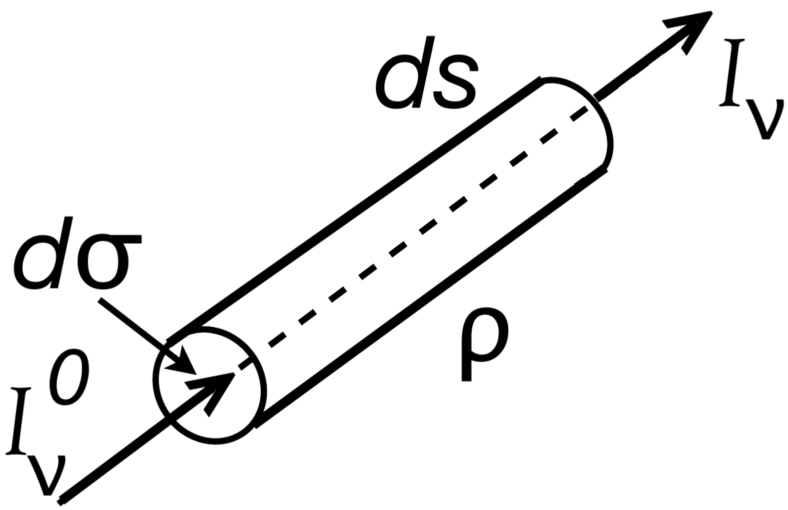

de Boer & Seggewiss 2008

Solving the differential equation

$$\mathrm{d}I_\nu = -\kappa_\nu I_\nu \mathrm{d}s = -I_\nu \mathrm{d}\tau_\nu$$

$$\Rightarrow I_\nu = I_\nu^0 e^{-\tau_\nu} = I_\nu^0 e^{-\int \kappa_\nu \mathrm{d}s}$$

$\rightarrow \tau = 1 \Rightarrow I_\nu = I_\nu^0 / e$

Large optical depth $\tau \gg 1$:

$\rightarrow$ Material opaque $I_\nu \ll I_\nu^0$

Small optical depth $\tau \ll 1$:

$\rightarrow$ Material transparent $I_\nu \simeq I_\nu^0$

Total change in intensity gives the radiative transport equation

$$\mathrm{d}I_\nu = -\kappa_\nu I_\nu \mathrm{d}s + j_\nu \mathrm{d}s \tag{4.27}$$

$$\frac{\mathrm{d}I_\nu}{\kappa_\nu \mathrm{d}s} = \frac{\mathrm{d}I_\nu}{\mathrm{d}\tau_\nu} = -I_\nu + \frac{j_\nu}{\kappa_\nu} = -I_\nu + S_\nu$$

Source function S_ν dependent on material: $S_\nu < 0$ more absorption than emission, $S_\nu > 0$ more emission than absorption

Equation of radiative transport

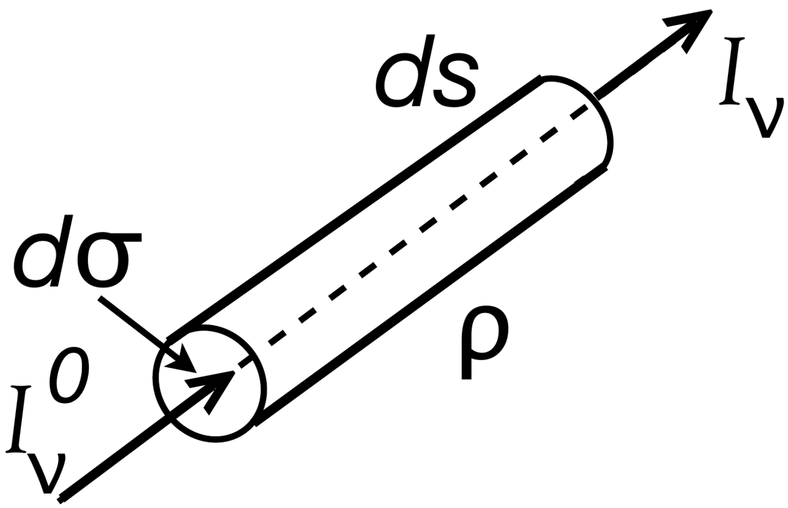

de Boer & Seggewiss 2008

- no background intensity $I_\nu^0 = 0$ and $\tau_\nu \to \infty$
  $\Rightarrow I_\nu \simeq B_\nu$
  Source function equals the Planck function

Solution for constant S_ν

$$I_\nu = I_\nu^0 e^{-\tau_\nu} + S_\nu(1 - e^{-\tau_\nu})$$

intensity entering the volume and intensity produced inside the box are diluted by the optical depth

- no background intensity $I_\nu^0 = 0$
  $\Rightarrow I_\nu = S_\nu(1 - e^{-\tau_\nu})$
- no background intensity $I_\nu^0 = 0$ and $\tau_\nu \ll 1$
  $\Rightarrow I_\nu = \tau_\nu S_\nu$
  All produced radiation can be seen by an observer
- no background intensity $I_\nu^0 = 0$ and $\tau_\nu \gg 1$
  $\Rightarrow I_\nu \simeq S_\nu$
  No photons can escape (they are immediately scattered or absorbed)

Equation of radiative transport

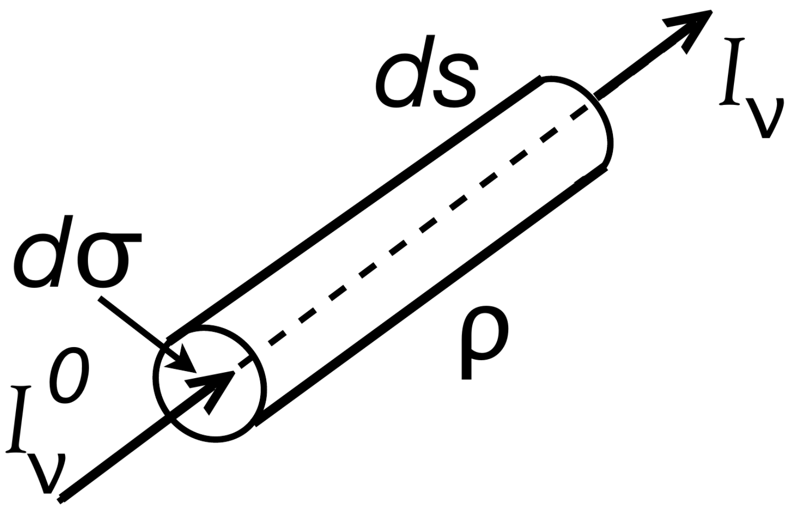

de Boer & Seggewiss 2008

- background intensity $I_\nu^0 \neq 0$
  $\Rightarrow I_\nu = S_\nu + (I_\nu^0 - S_\nu)e^{-\tau_\nu}$
  Applicable to stellar atmospheres
- background intensity $I_\nu^0 \neq 0$ and $\tau_\nu \ll 1$
  $\Rightarrow I_\nu = I_\nu^0 - \tau_\nu(I_\nu^0 - S_\nu)$
  $I_\nu^0 > S_\nu \rightarrow$ spectral absorption of an existing continuum
  $I_\nu^0 < S_\nu \rightarrow$ spectral emission superimposed on an existing continuum
- background intensity $I_\nu^0 \neq 0$ and $\tau_\nu \gg 1$
  $\Rightarrow I_\nu \simeq S_\nu$

General equation of radiative transport

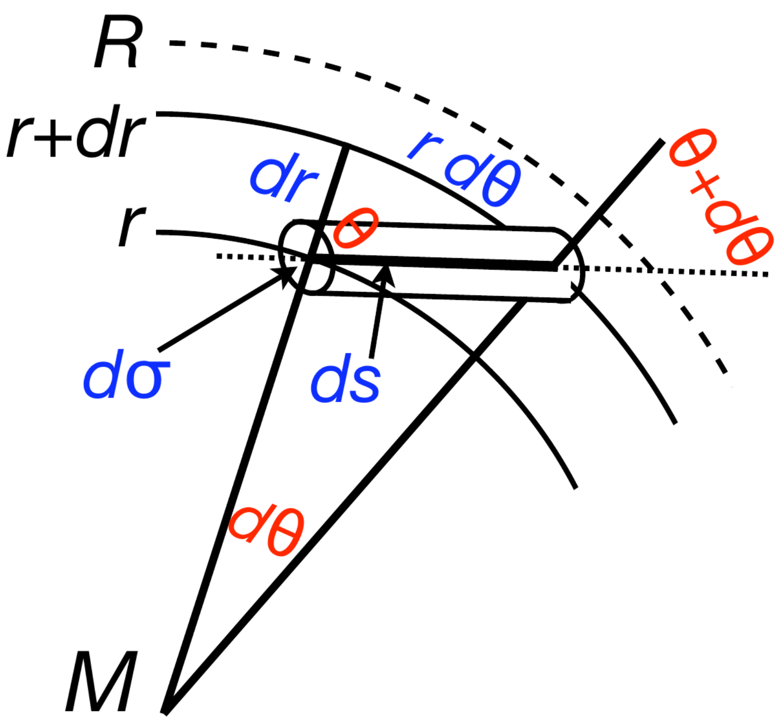

de Boer & Seggewiss 2008

In a stellar atmosphere, effects of geometry have to be considered

$$\mathrm{d}I_\nu(r,\theta) = -\kappa_\nu I_\nu(r,\theta)\mathrm{d}s + j_\nu \mathrm{d}s$$

$\mathrm{d}r = \mathrm{d}s\cos\theta$ and $r\mathrm{d}\theta = -\mathrm{d}s\sin\theta$:

General equation of radiative transport

$$\frac{\partial I_\nu}{\partial r}\cos\theta - \frac{\partial I_\nu}{\partial\theta}\frac{\sin\theta}{r} = -\kappa_\nu I_\nu + j_\nu \qquad (4.28)$$

Continuity equation

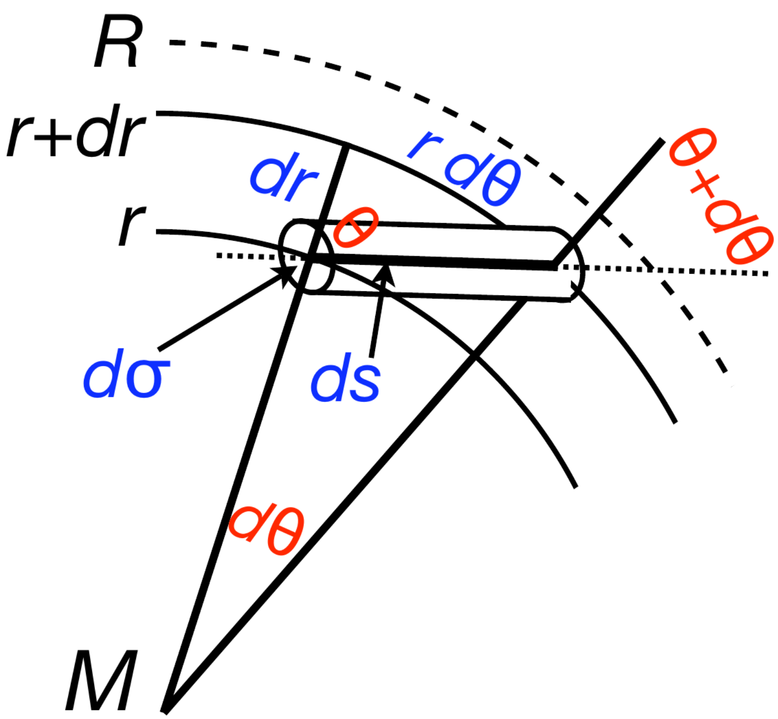

de Boer & Seggewiss 2008

radiative flux $\vec{F}_\nu$

$$\vec{F}_\nu = \int I_\nu(r,\theta)\mathrm{d}\nu\cos\theta\mathrm{d}\omega$$

$$\Rightarrow \frac{1}{4\pi}\frac{\mathrm{d}F_\nu}{\mathrm{d}r} = \kappa_\nu(I_\nu - S_\nu)$$

Energy transport only by radiation $\rightarrow \frac{\mathrm{d}F}{\mathrm{d}r} = 0$

Continuity equation

$$\frac{1}{4\pi}\int_0^\infty \kappa_\nu F_\nu \mathrm{d}\nu = \int_0^\infty \kappa_\nu S_\nu \mathrm{d}\nu \tag{4.29}$$

connection between the frequency dependent transport equations and the total radiative energy transport

Local Thermal Equilibrium

Thermodynamic equilibrium (TE)

- radiation is isotropic and in balance with the material
- all processes (absorption, emission) in balance
- no changes in time
- $I_\nu = S_\nu = B_\nu$ Black-body continuum $\rightarrow$ does not exist in the real universe

Local thermal equilibrium (LTE)

- locally, in small regions of the star TE (almost) fullfilled
- if the gas is not in LTE $\rightarrow$ non-LTE (NLTE)
- $S_\nu = B_\nu$ and $\frac{dI_\nu}{d\tau_\nu} = 0 \Rightarrow B_\nu = j\nu/\kappa_\nu$
- LTE can be assumed for some stellar atmospheres (high density, low temperature $\rightarrow$ radiation-matter interactions in balance)

Plane parallel atmosphere

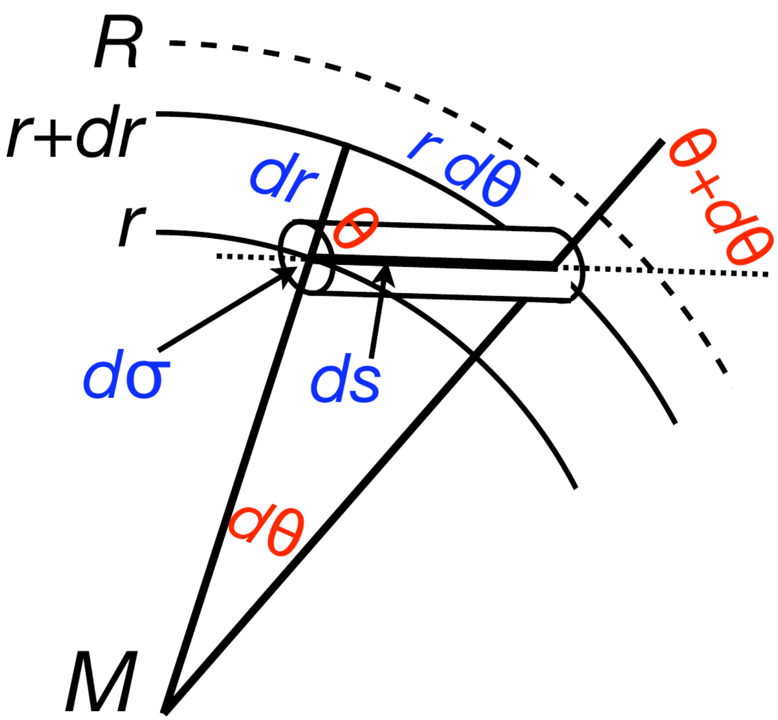

de Boer & Seggewiss 2008

Atmosphere with large radius

$\rightarrow$ Plane parallel atmosphere approximation

$$d\theta = 0 \text{ and } d\tau_\nu = -\kappa_\nu dr$$

$\rightarrow$ General energy transport equation

$$\frac{dI_\nu}{d\tau_\nu}\cos\theta = I_\nu - S_\nu$$

$\rightarrow$ total radiative flux F does not depend on the depth r (F = const = energy conservation)

$$F = \sigma T^4(r) = \sigma T_{\text{eff}}^4$$

Limb darkening

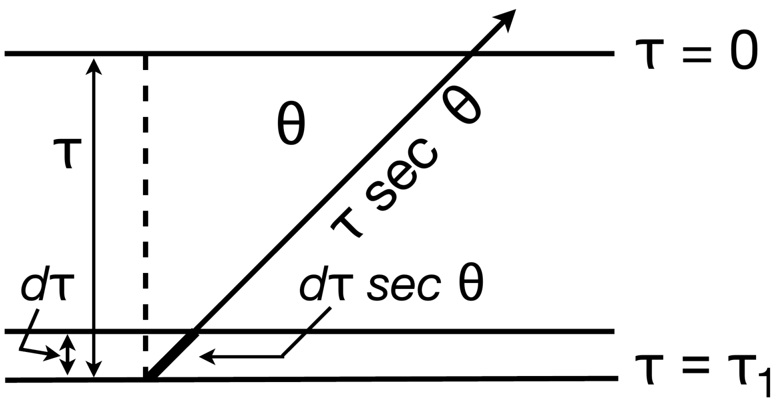

de Boer & Seggewiss 2008

approximation for the source function:

$$S_\nu(\tau_\nu) = a_\nu + b_\nu \tau_\nu$$

$$\rightarrow I_\nu(0,\theta) = a_\nu + b_\nu \cos\theta$$

Edge of stellar atmosphere

$\rightarrow$ Radiation field not isotropic

$\rightarrow$ Angular aspect θ relevant ($\sec\theta = 1/\cos\theta$)

$$Ie^{-\tau\sec\theta} = -\int_\tau Se^{-\tau'\sec\theta}\mathrm{d}\tau'\sec\theta$$

Outward component

$$I_\nu(0,\theta) = -\int_0^\infty S_\nu(\tau_\nu)e^{-\tau'\sec\theta}\mathrm{d}\tau'\sec\theta$$

$\rightarrow$ Edge of visible disk: $\theta = \frac{\pi}{2}, \sec\theta \rightarrow \infty$

$$I_\nu\left(0,\frac{\pi}{2}\right) = 0$$

$\rightarrow$ Center of visible disk: $\theta = 0, \sec\theta = 1$

$$I_\nu(0,0) = \int_0^\infty S_\nu(\tau_\nu)e^{-\tau_\nu}\mathrm{d}\tau_\nu$$

Gray atmosphere

Simplified expression for the absorption coefficient $\kappa_\nu \sim \bar{\kappa}$

$\rightarrow$ Rosseland opacity: flux-weighted mean opacity ($F = \int F_\nu \mathrm{d}\nu, \mathrm{d}\tau = \bar{\kappa}\mathrm{d}s$)

$$\frac{1}{\bar{\kappa}} = \frac{\int_0^\infty \frac{1}{\kappa_\nu}\frac{\mathrm{d}B_\nu}{\mathrm{d}T}\mathrm{d}\nu}{\frac{\mathrm{d}}{\mathrm{d}T}\int_0^\infty B_\nu \mathrm{d}\nu}$$

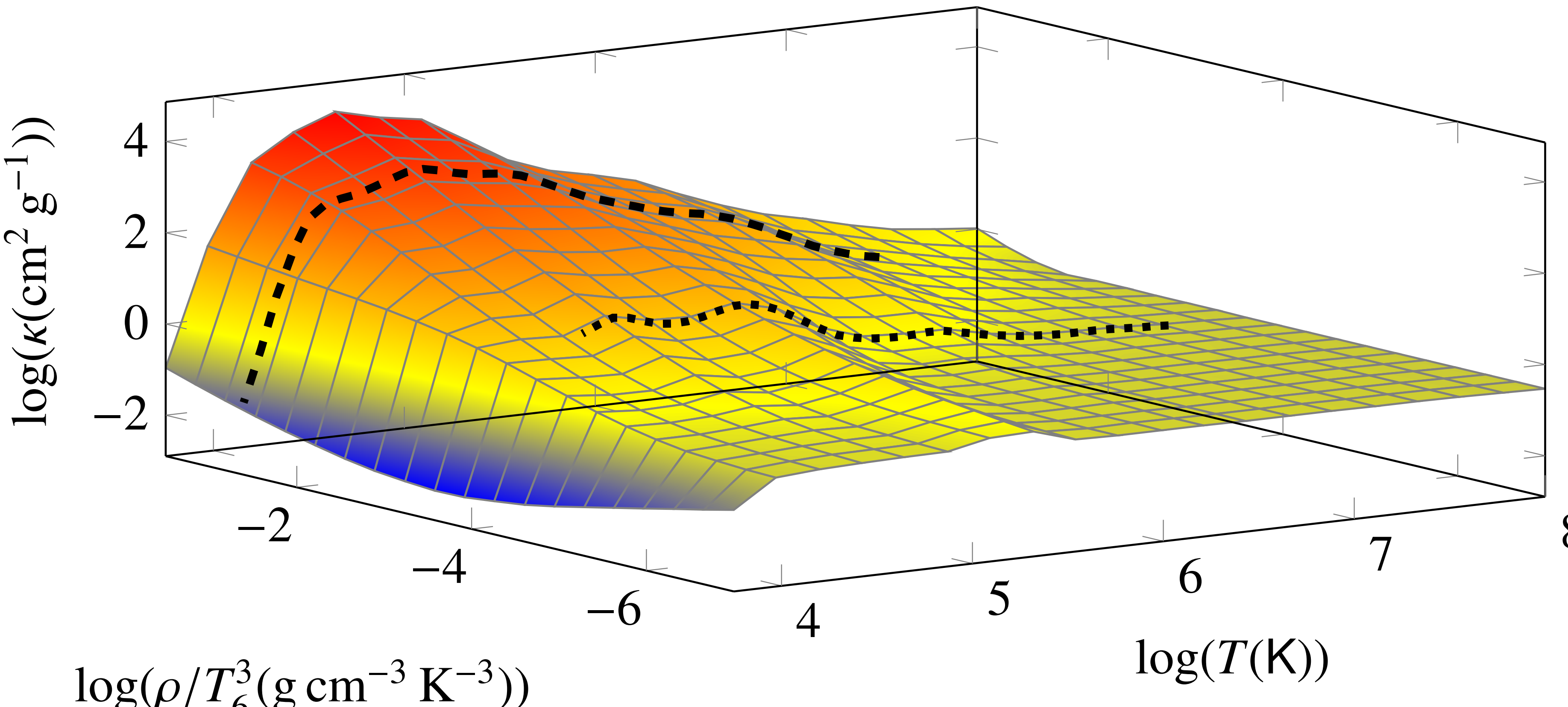

(http://cdsweb.u-strasbg.fr/topbase/OpacityTables.html)

Gray atmosphere

→ Simplified equation of radiation transport

$$\cos\theta \frac{\mathrm{d}I(\tau,\theta)}{\mathrm{d}\tau} = I(\tau,\theta) - S(\tau)$$

→ Simplified continuity equation

$$S(\tau) = \frac{1}{4\pi}F(\tau) \rightarrow S(\tau) = \frac{3}{4\pi}F\cdot(\tau + q(\tau))$$

$q(\tau) \simeq 0.7104 - 0.1331e^{-3.4488\tau}$ numerical function

→ Simple limb darkening law can be derived

$$\frac{I(0,\theta)}{I(0,0)} = \frac{2}{5}\left(1 + \frac{3}{2}\cos\theta\right)$$

Gray atmosphere

Temperature structure

- LTE ($S_\nu = B_\nu$) using Stefan-Boltzmann law

$$\pi S(\tau) = \sigma T^4(\tau)$$

- gray atmosphere

$$T^4(\tau) = \frac{3}{4} T_{\mathrm{eff}}^4 \cdot (\tau + q_\tau)$$

- at the surface ($\tau \to 0$) with $q_\tau = 2/3$

$$T_0 = \frac{1}{2^{1/4}} T_{\mathrm{eff}} \to T_{0,\odot} = 4860\,\mathrm{K}$$

Gray atmosphere

T vs. log(τ)

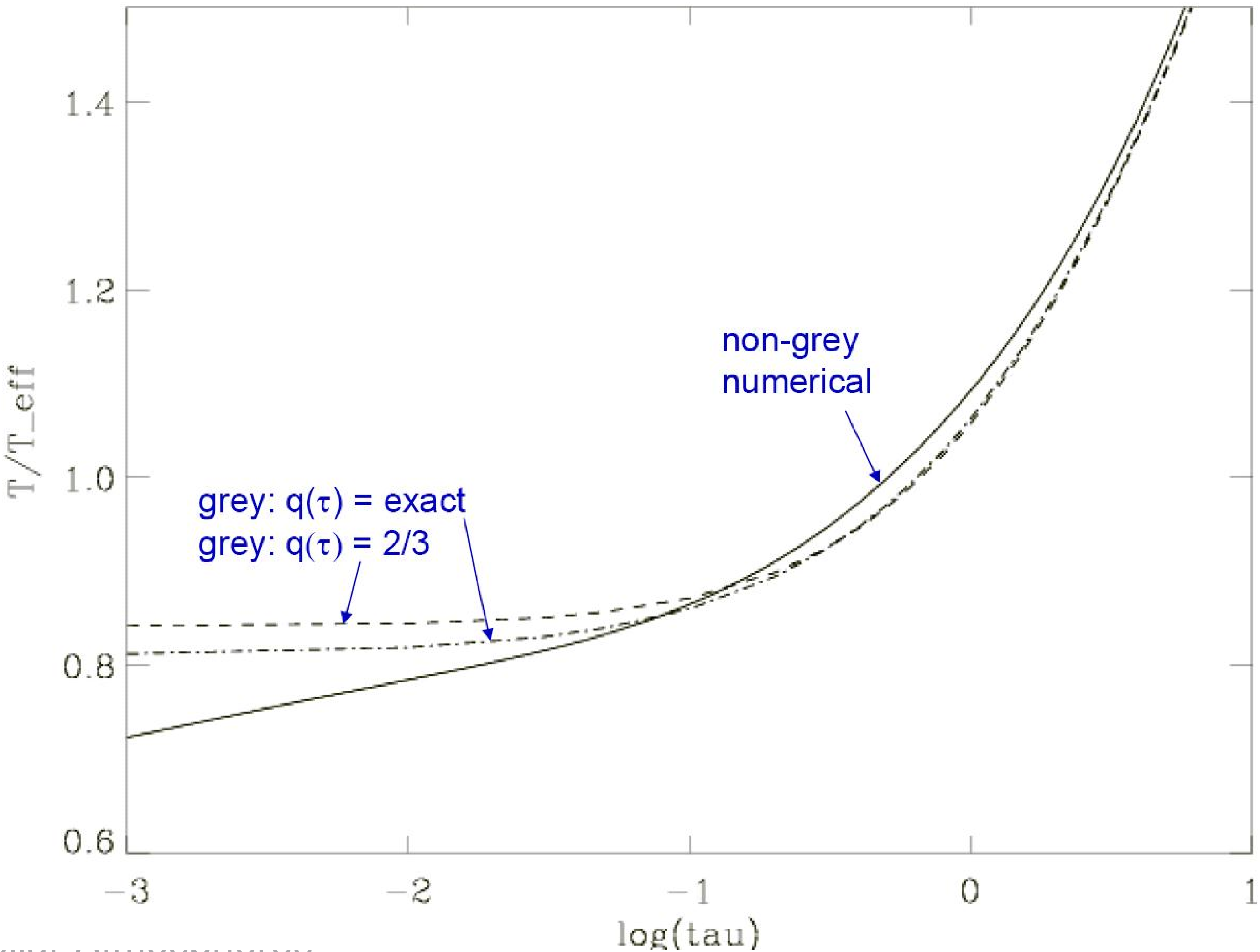

Gray atmosphere

pressure structure

- ideal gas $P_{\text{gas}} = nkT$, gas pressure $\mathrm{d}P_{\text{gas}} = -\rho g \mathrm{d}s$

$$\frac{\mathrm{d}P_{\text{gas}}}{\mathrm{d}\bar{\tau}} = \frac{g}{\bar{\kappa}_m}$$

  $\bar{\kappa}_m(T, P, XYZ)$ mass absorption coefficient $\rightarrow$ Numerical solution

- gray atmosphere and approximation $P_{\text{gas}} = (g/\bar{\kappa}_m)\bar{\tau}$

$\rightarrow$ Geometric structure

$$\frac{\mathrm{d}P_{\text{gas}}}{P_{\text{gas}}} = \mathrm{d}\ln P_{\text{gas}} = -\frac{\mathrm{d}r}{H_{\text{P}}}$$

with $H_{\text{P}} = \frac{kT}{\bar{\mu}g}$ the pressure scale height and $\bar{\mu}(T, P, XYZ)$ the mean molecular weight

Opacity

Opacity = ability of stellar material to absorb radiation

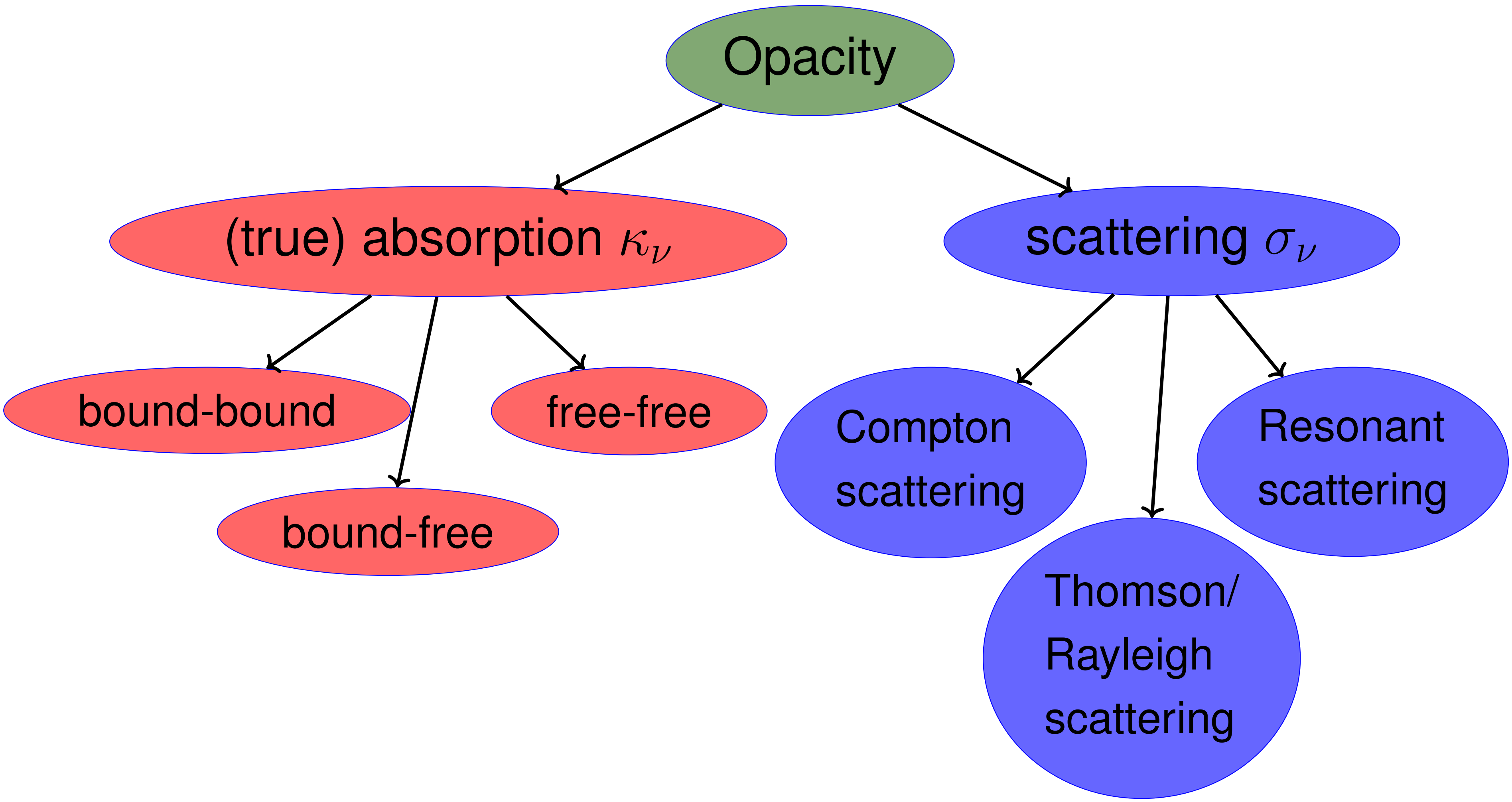

$$\kappa_{\nu,\mathrm{ges}} = \kappa_{\nu,bb} + \kappa_{\nu,bf} + \kappa_{\nu,ff} + \sigma_{\nu,C} + \sigma_{\nu,e} + \sigma_{\nu,R} \tag{4.30}$$

$\rightarrow$ True absorption is dominant in most stellar gases

Sources of opacity – bound-bound transitions

atom absorbs a photon and becomes excited

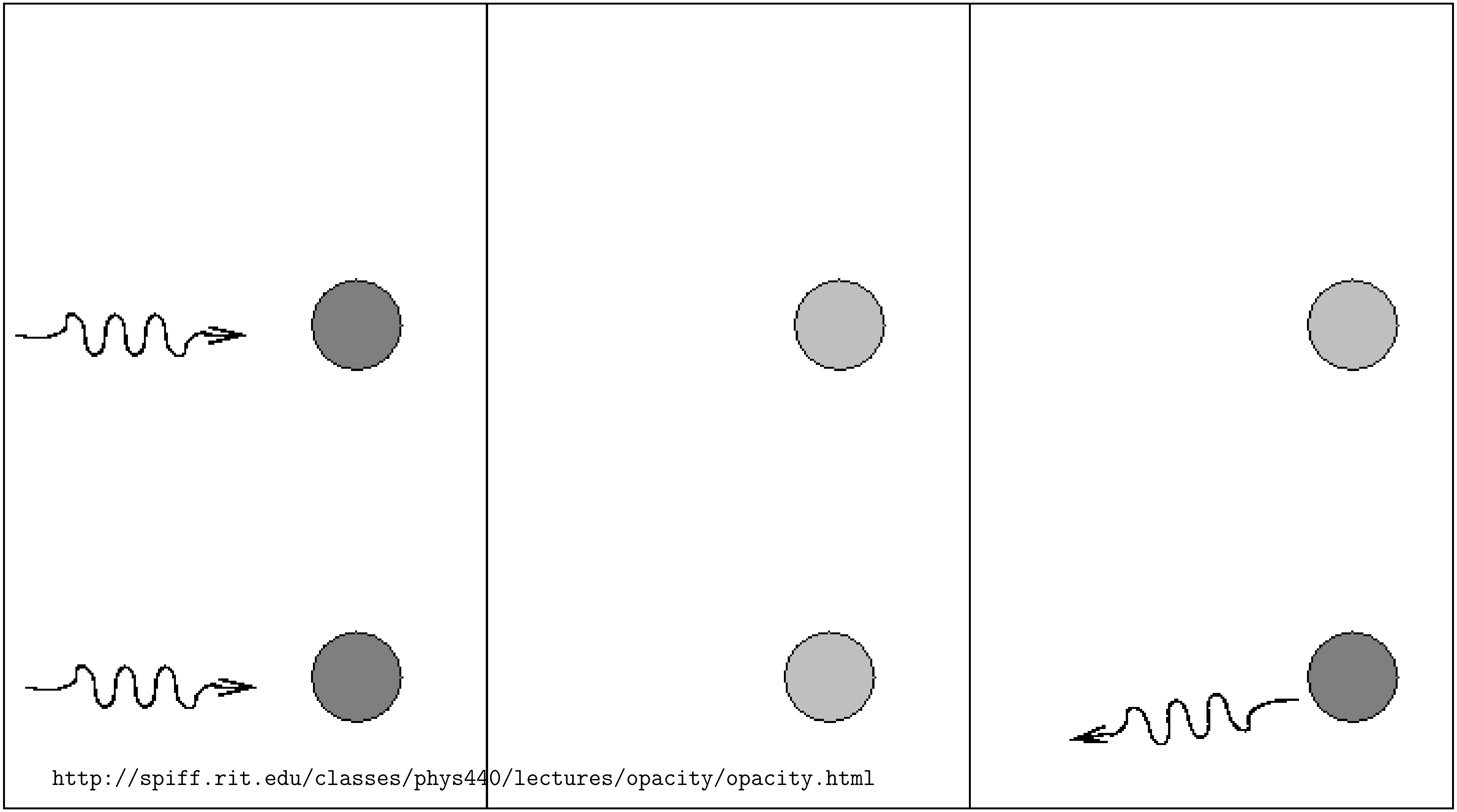

http://spiff.rit.edu/classes/phys440/lectures/opacity/opacity.html

Sources of opacity – bound-free transitions

ionizing absorption: if a photon has enough energy, its absorption can knock an electron free from an atom and send it off with the leftover energy in kinetic form

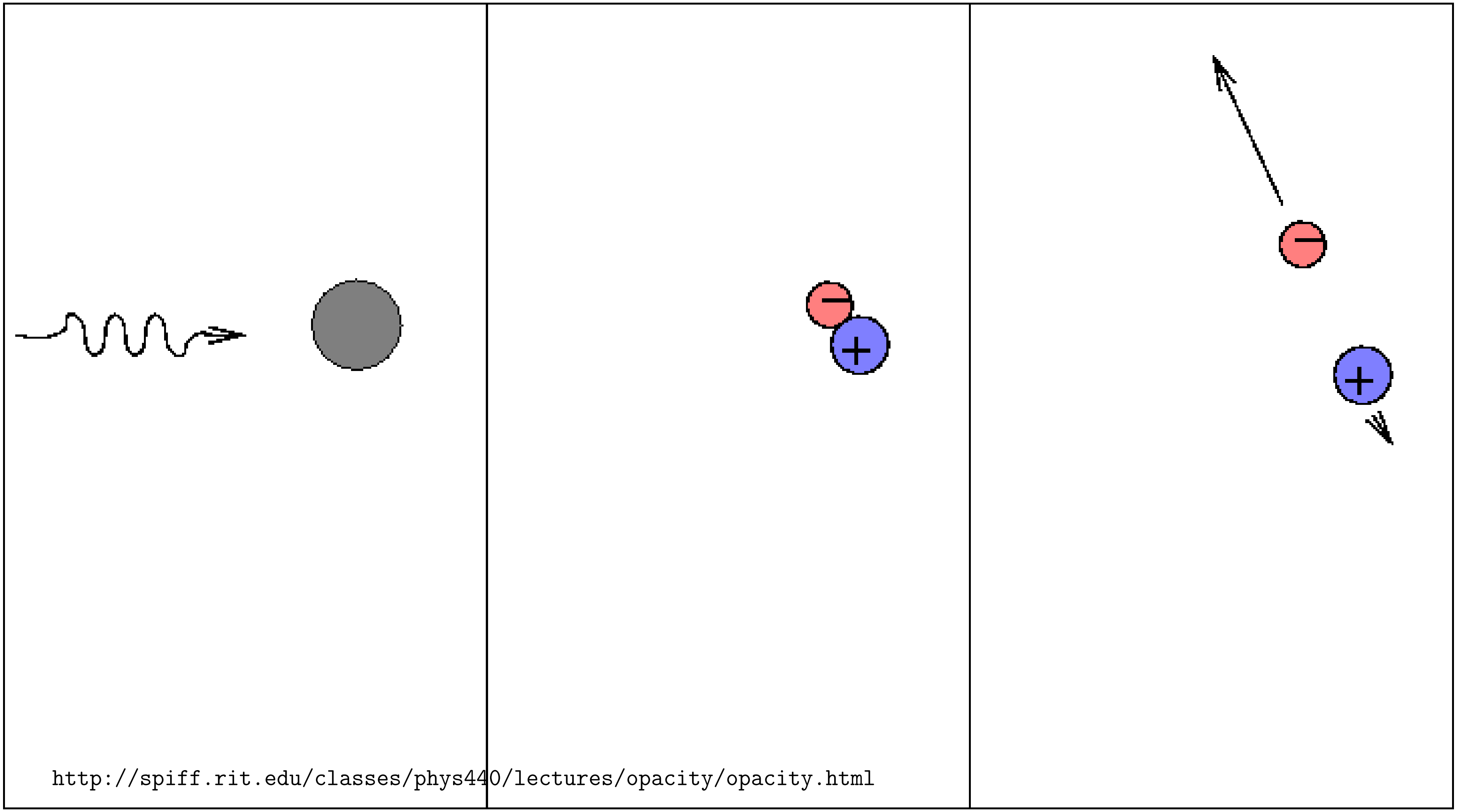

Sources of opacity – free-free transitions

When a free electron happens to be passing by a nucleus, it may absorb a photon (as opposed to scattering it). We call this a ”free-free” or bremsstrahlung process.

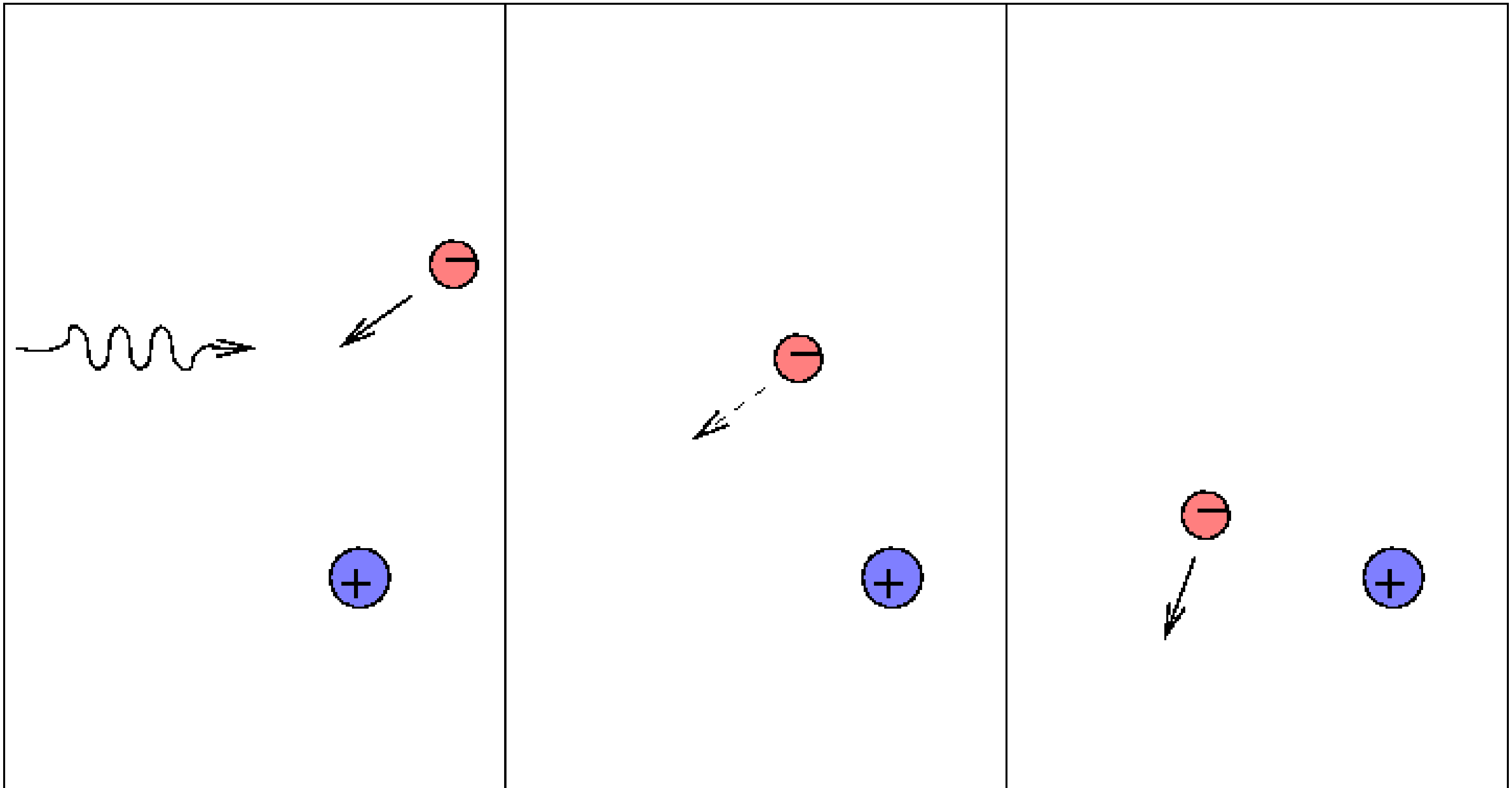

http://spiff.rit.edu/classes/phys440/lectures/opacity/opacity.html

Sources of opacity – (Thomson) scattering

A single, isolated electron cannot absorb a passing photon, but it can scatter it into some other direction. Scattering can also happen at atoms, ions and molecules.

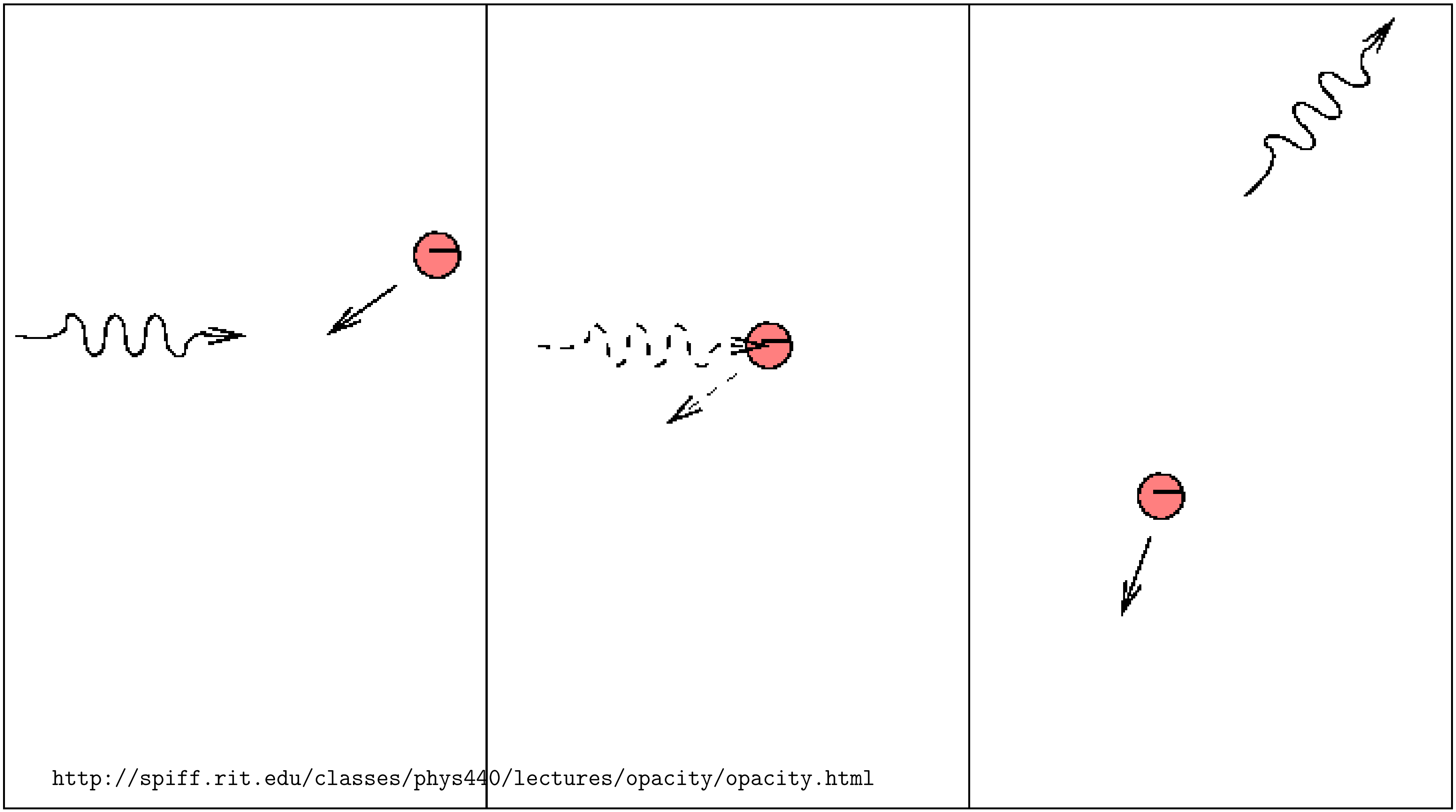

Absorption due to ionization

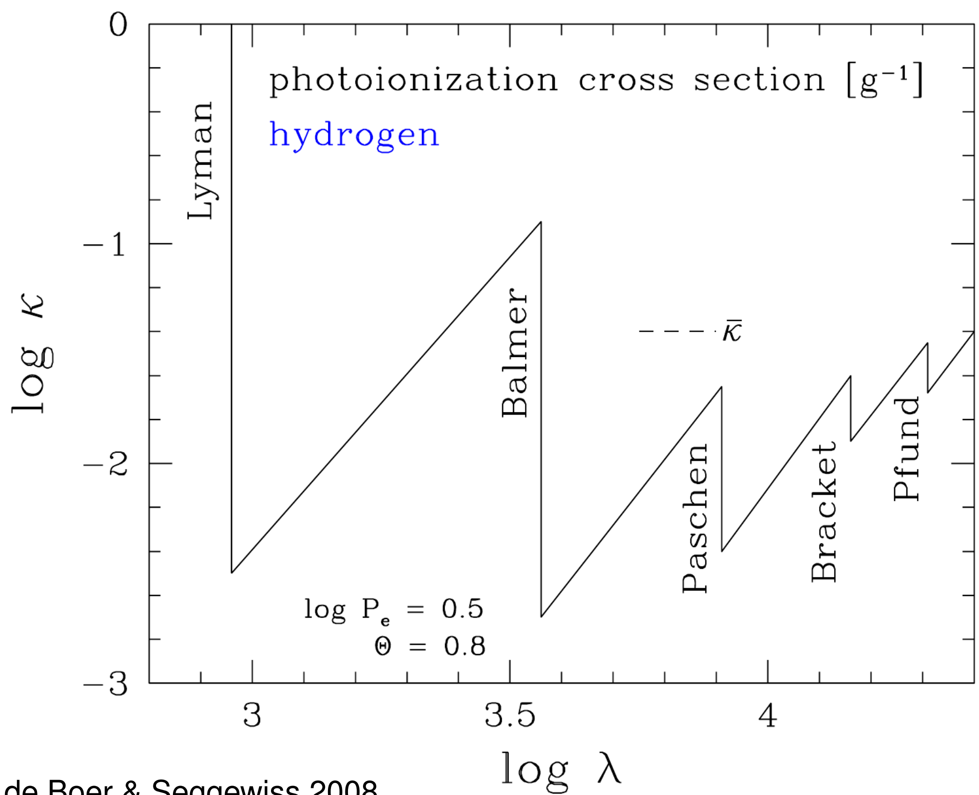

de Boer & Seggewiss 2008

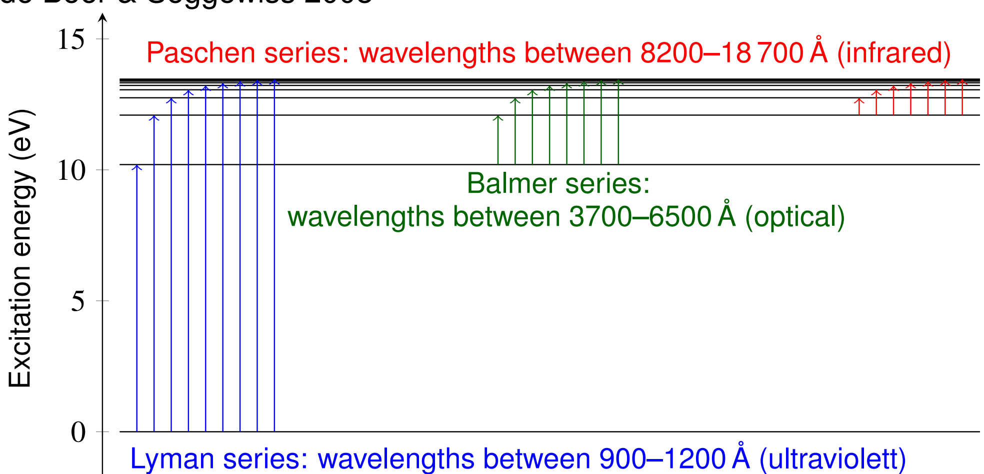

- Atoms are ionized by photons with
  $E_\gamma = h\nu > E_{\text{ion}}$
  $\rightarrow E_\gamma = E_{\text{ion}} + \frac{1}{2}m_e v_e^2 + \frac{1}{2}m_{\text{ion}} v_{\text{ion}}^2$

$\rightarrow$ E_{ion} depends on excitation state of atom

$\rightarrow$ bound-free (b-f) transition

- reverse process: recombination (f-b), photon produced
- ionization takes place for
  $\nu > \nu_{\text{ion}} = E_{\text{ion}}/h$
  $\rightarrow$ sharp depression of continuum: ionization edge

Absorption due to ionization

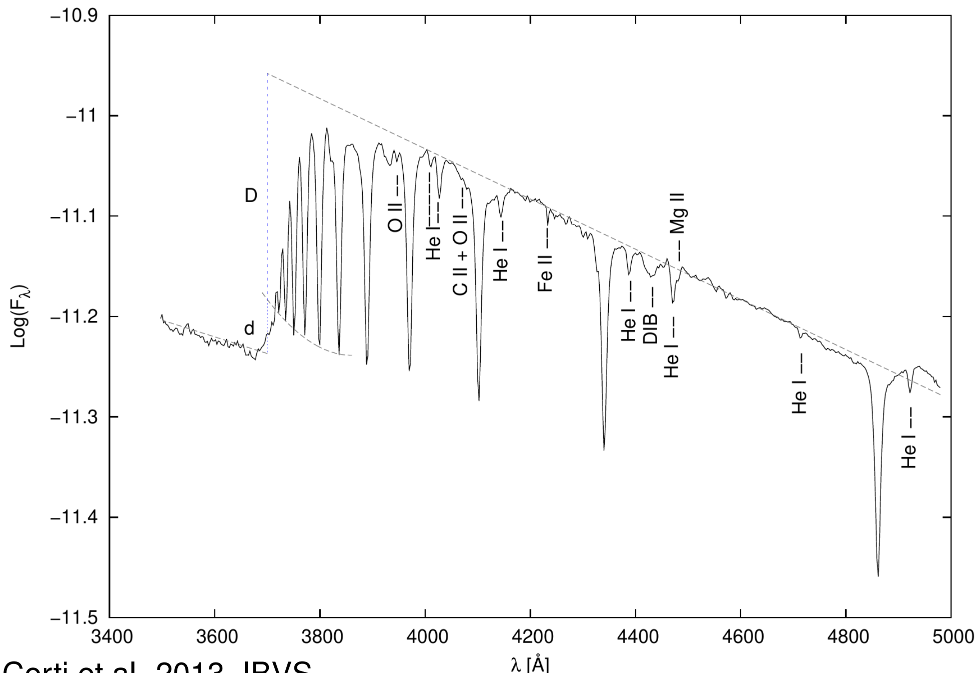

Corti et al. 2013, IBVS,

- ionization takes place for $\nu > \nu_\mathrm{ion} = E_\mathrm{ion}/h$
  $\longrightarrow$ sharp depression of continuum: ionization edge

$\longrightarrow$ Hydrogen-like atoms:

$$\nu_\mathrm{edge} = RZ^2 \frac{1}{n^2}$$

R Rydberg constant, Z nuclear charge

$\longrightarrow$ Helium: $\nu_\mathrm{edge} \simeq \frac{4}{n^2}$

$\longrightarrow$ Hydrogen: $\nu_\mathrm{edge} \simeq \frac{1}{n^2}$

$T \geq 20\,000\,\mathrm{K}$: hydrogen fully ionized, ionization edges disappear

$T \leq 6\,000\,\mathrm{K}$: hydrogen not ionized to level $n = 2$ Balmer and higher n absorption edges not present

Metals are less abundant in most stars and have lots of transitions and excitation stages $\longrightarrow$ ionization edges weaker

Absorption due to H^- dissociation

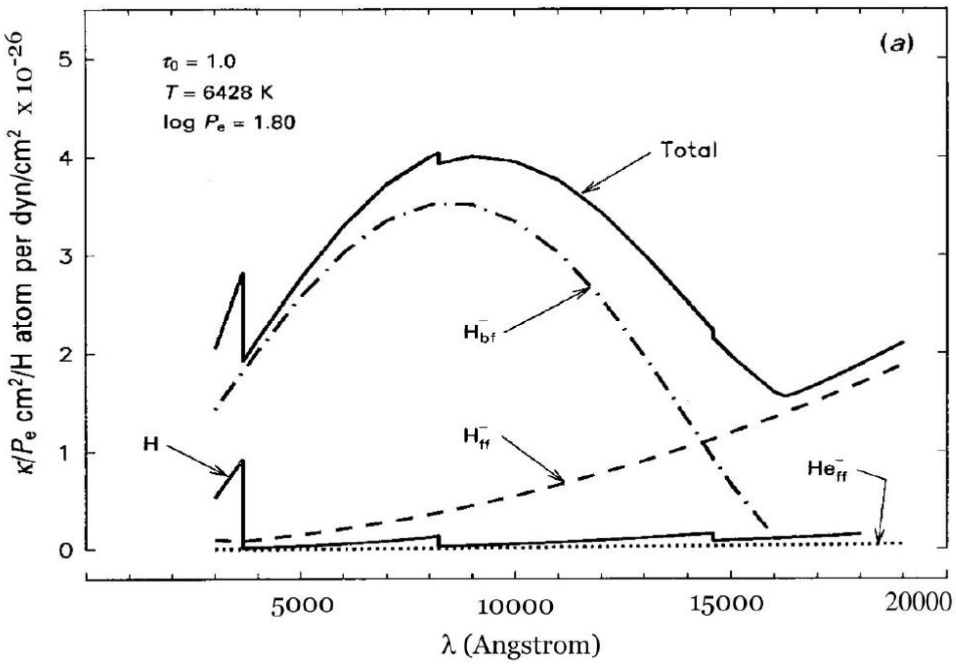

At temperature of 5000 to 6000 K most of the metals singly ionized

- Lots of electrons freed
- H^- anions created: $n(H^-) \simeq 3 \times 10^{-8} n(H)$
- binding energy 0.75 eV $\rightarrow$ easily dissociated

$\rightarrow$ Important source of absorption in the infrared range (around 16500 Å)

Absorption due to molecule dissociation

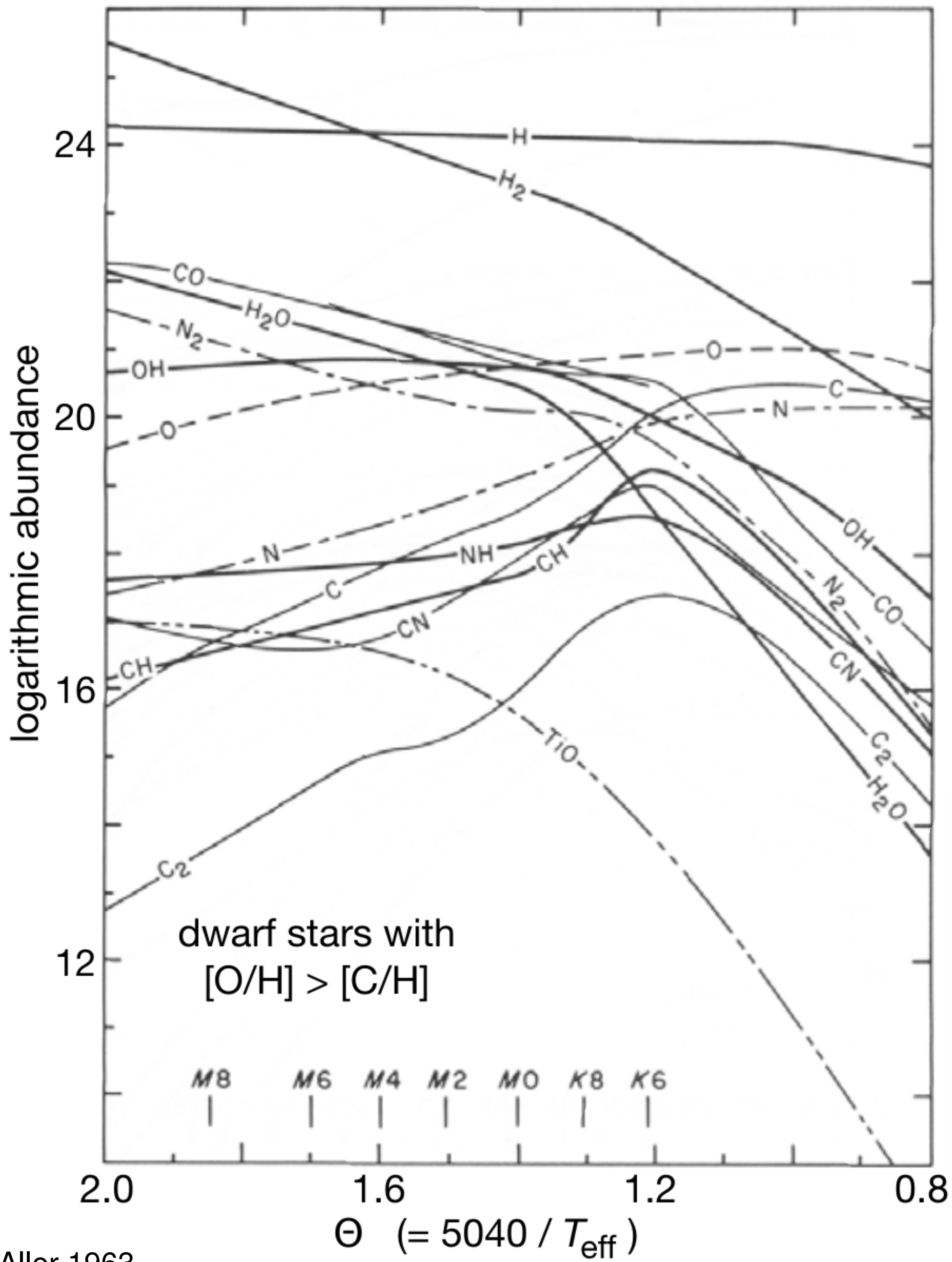

Aller 1963

At low temperatures $<$ 5000 K molecules (H_2, CO, TiO, ..) present in the stellar atmospheres

- molecules are dissociated by photons with $E_\gamma = h\nu > E_{\text{diss}}$
- molecule AB is dissociated into atoms A and B: $AB + h\nu_{\text{diss}} \rightarrow A + B$
- Energy is taken up to dissociate and kinetic energy as well as excitation energy: $E_\gamma = E_{\text{diss}} + E_{\text{kin}} + E_{\text{exc}}$
- Probability given by the dissociation constant

$$K_{AB} = \frac{P_A P_B}{P_{AB}} = kT \frac{n_A n_B}{n_{AB}}$$

assuming ideal gas $PV = nkT$

Absorption due to free-free transitions

At higher temperatures and higher electron densities, electrons passing by ions are accelerated in the Coulomb field and then radiate Coulomb-Bremsstrahlung

- Free-free (f-f) transition $\rightarrow$ free-free radiation
- energy can also be absorbed from the photon-field leading to acceleration (free-free absorption)
- Absorption coefficient (fully ionized gas (stellar interior), solar composition):

$$\kappa_{\nu,ff} = 1.32 \times 10^{-2} \frac{n_e^2}{T^{3/2}} \frac{1}{\nu^2} g$$

$g \simeq 1$ Gaunt correction factor

Opacity due to scattering

Resonant scattering on atoms and ions: absorption and instantaneous re-emission of the photon around the frequency of an transition ν_0 (absorption line)

$$\sigma_{\nu,\mathrm{R}} = \frac{8\pi e^4}{3m_e^2c^4}\left(\frac{\nu}{\nu_0}\right)^4 N$$

Photon scattered by electrons (**Thomson scattering**) or molecules (**Rayleigh scattering**)

$$\sigma_e = \frac{8\pi e^4}{3m_e^2c^4}n_e = 6.65 \times 10^{-25} n_e$$

$\rightarrow$ Thomson scattering important in hot atmospheres because of the higher electron density n_e

Compton scattering: Photons scattered by relativistic electrons gain energy $\rightarrow$ important in stellar interiors

Total opacity

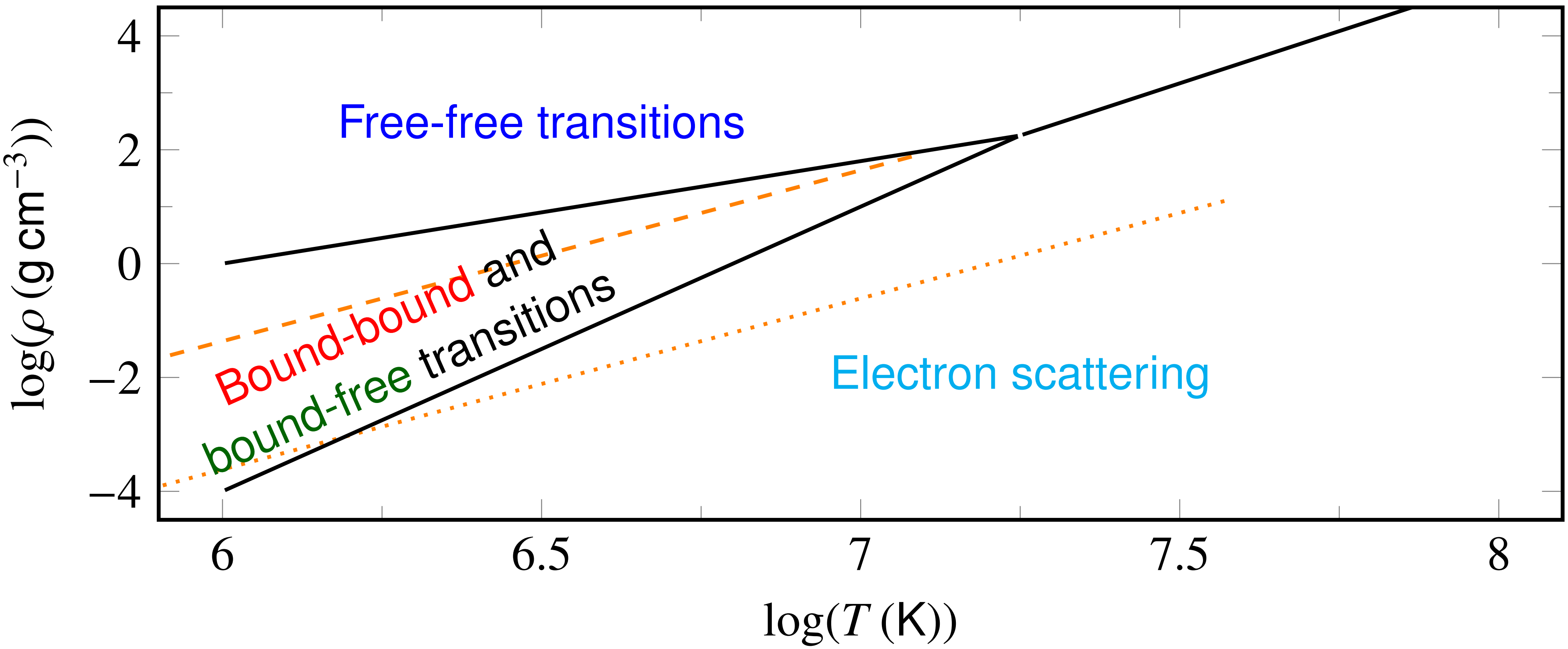

Total opacity

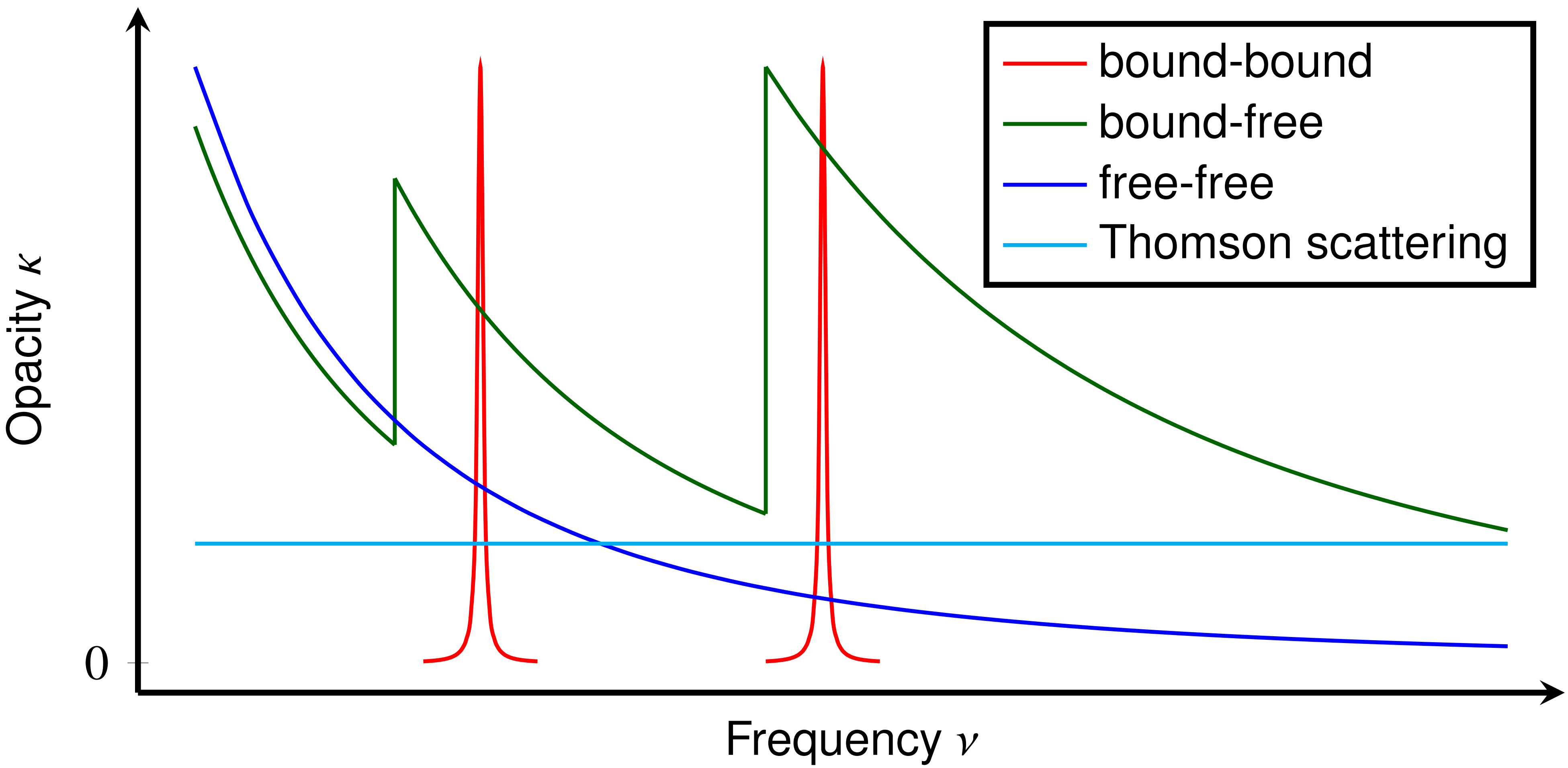

Total opacity

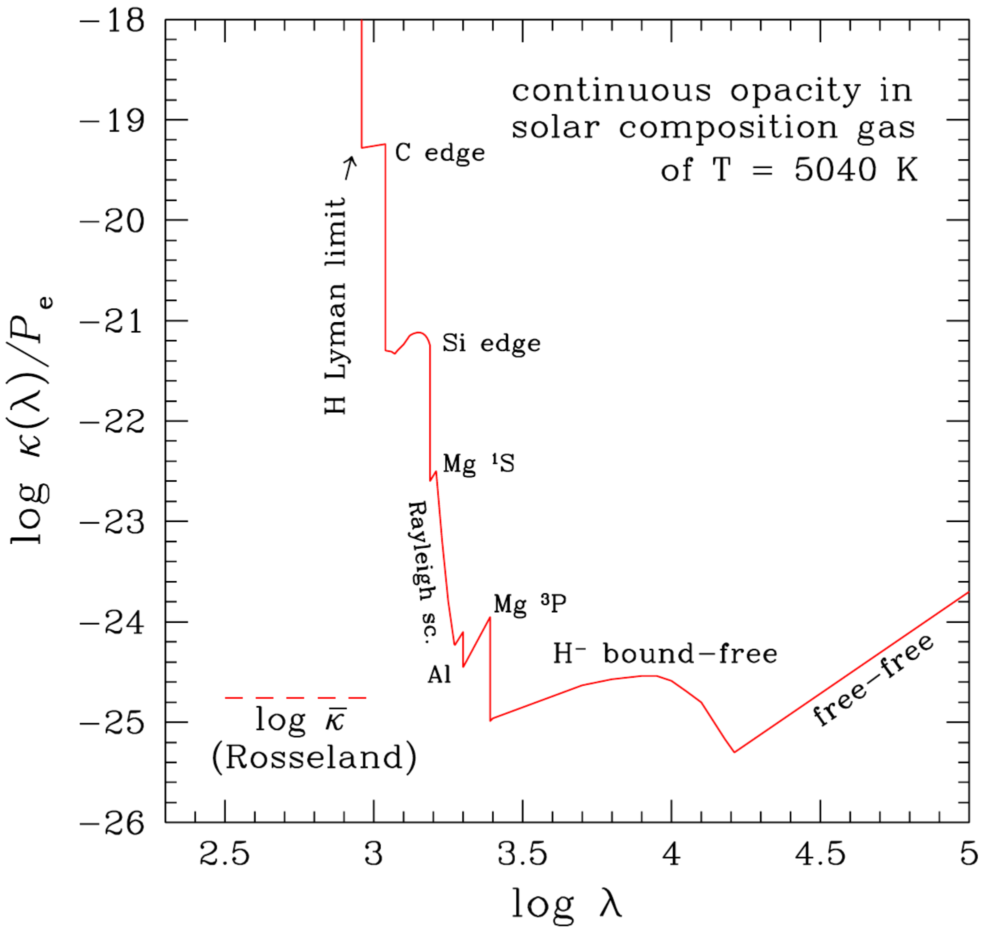

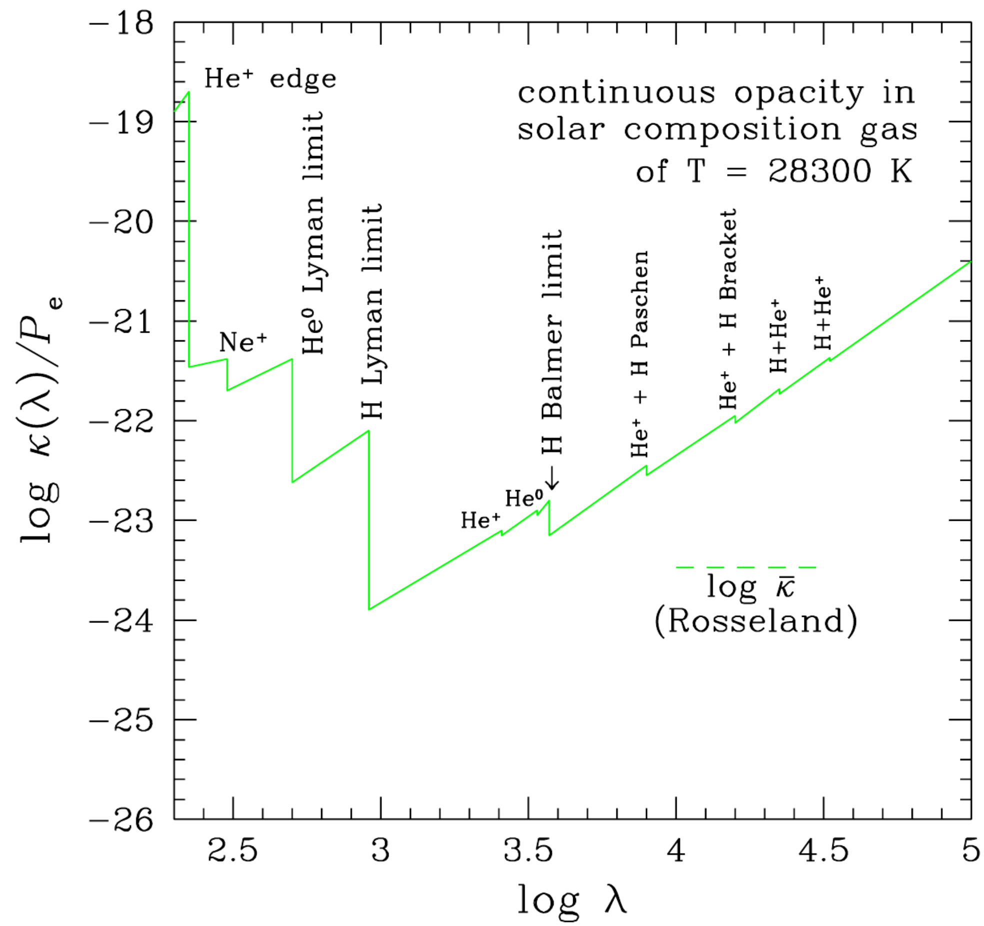

de Boer & Seggewiss 2008

Emission

Radiation continuum emitted by hot gas, can be described by Planck function inside the star as gas is in LTE

$$j_\nu = B_\nu(T)$$

Further sources:

- Free-free transitions or Coulomb-Bremsstrahlung
  $\rightarrow$ Electrons are accelerated and emit radiation
- Free-bound transitions or recombination radiation

Emission only significant, if the gas deviates from LTE

Spectral lines

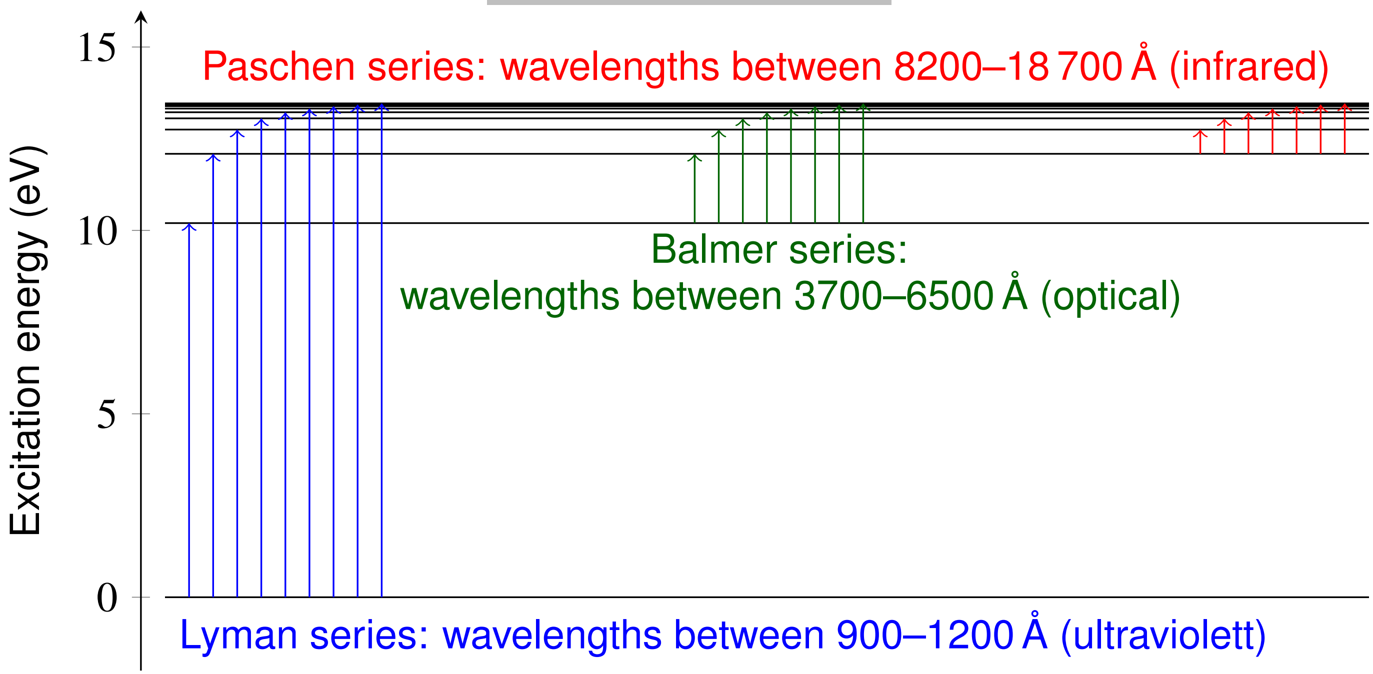

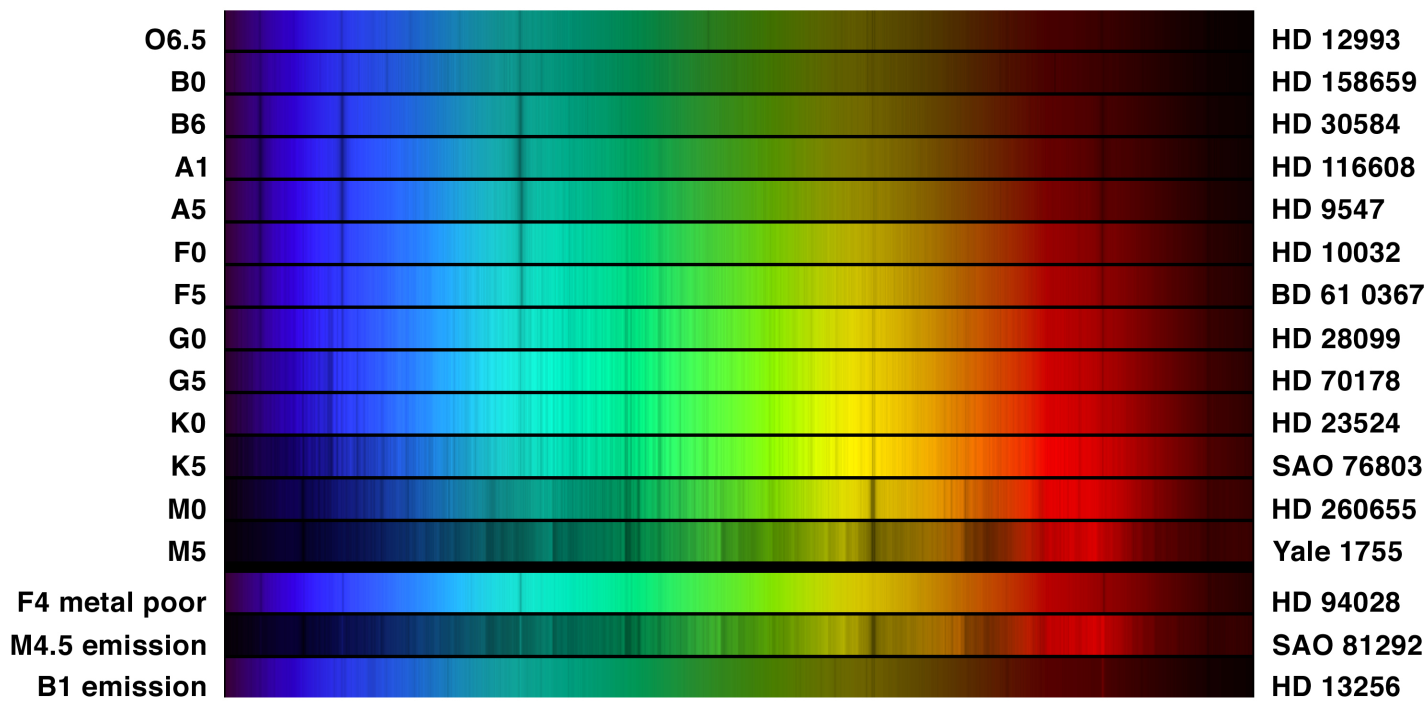

NOAO/AURA/NSF

Spectral lines

https://reddwarfs.wordpress.com/tag/spectra/

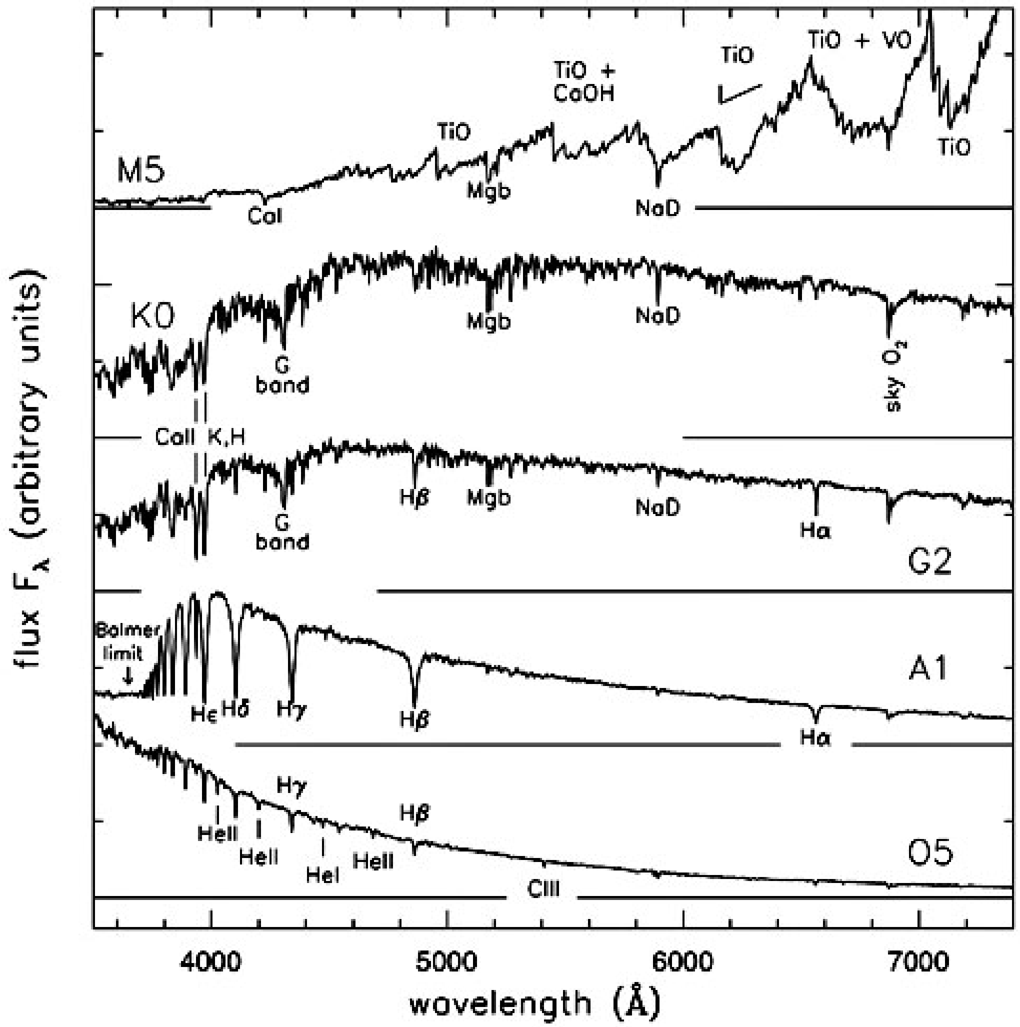

de Boer & Seggewiss 2008

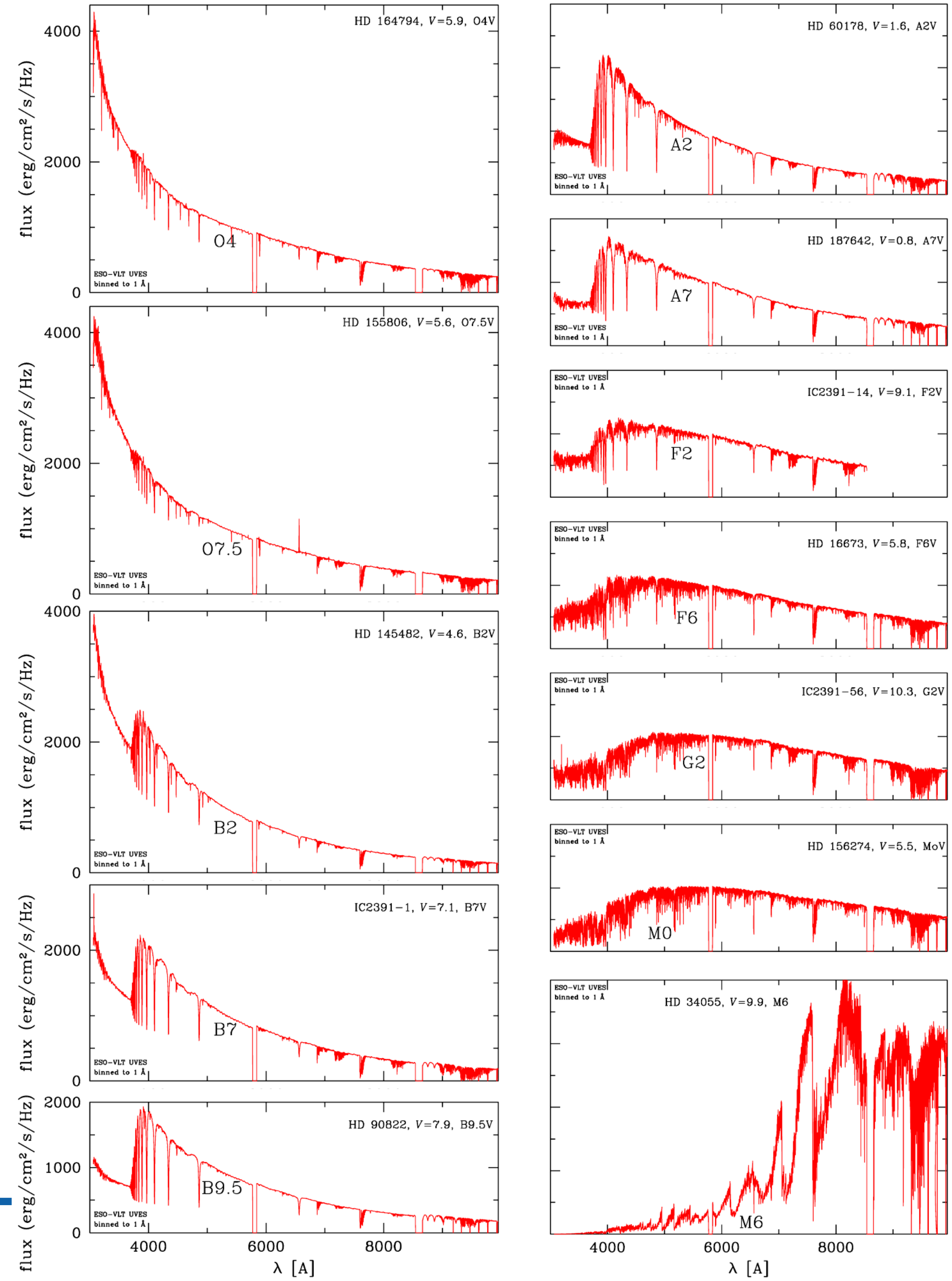

The shape of spectral lines is determined by quantum mechanics and the bulk properties of the gas

Line broadening mechanisms – Natural broadening

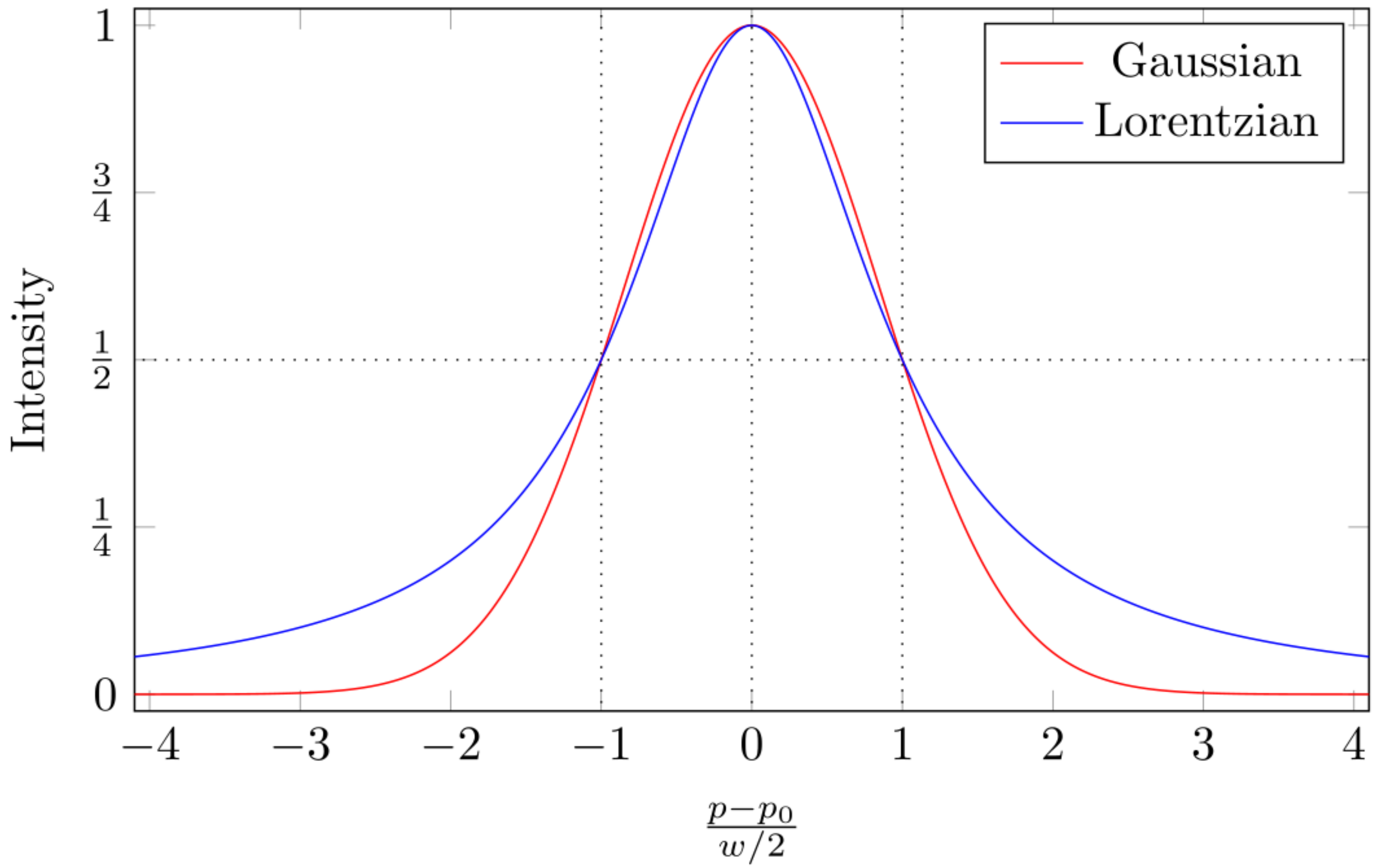

Wikipedia

Natural broadening: Lifetime of an excited state related to the uncertainty of the energy (uncertainty principle $\Delta E \Delta t = h \Delta \nu \Delta t \geq \frac{h}{4\pi}$)

$\rightarrow$ Lorentzian line profile with very small width $\Delta\lambda \approx 10^{-4}$ Å

Line broadening mechanisms – Pressure broadening

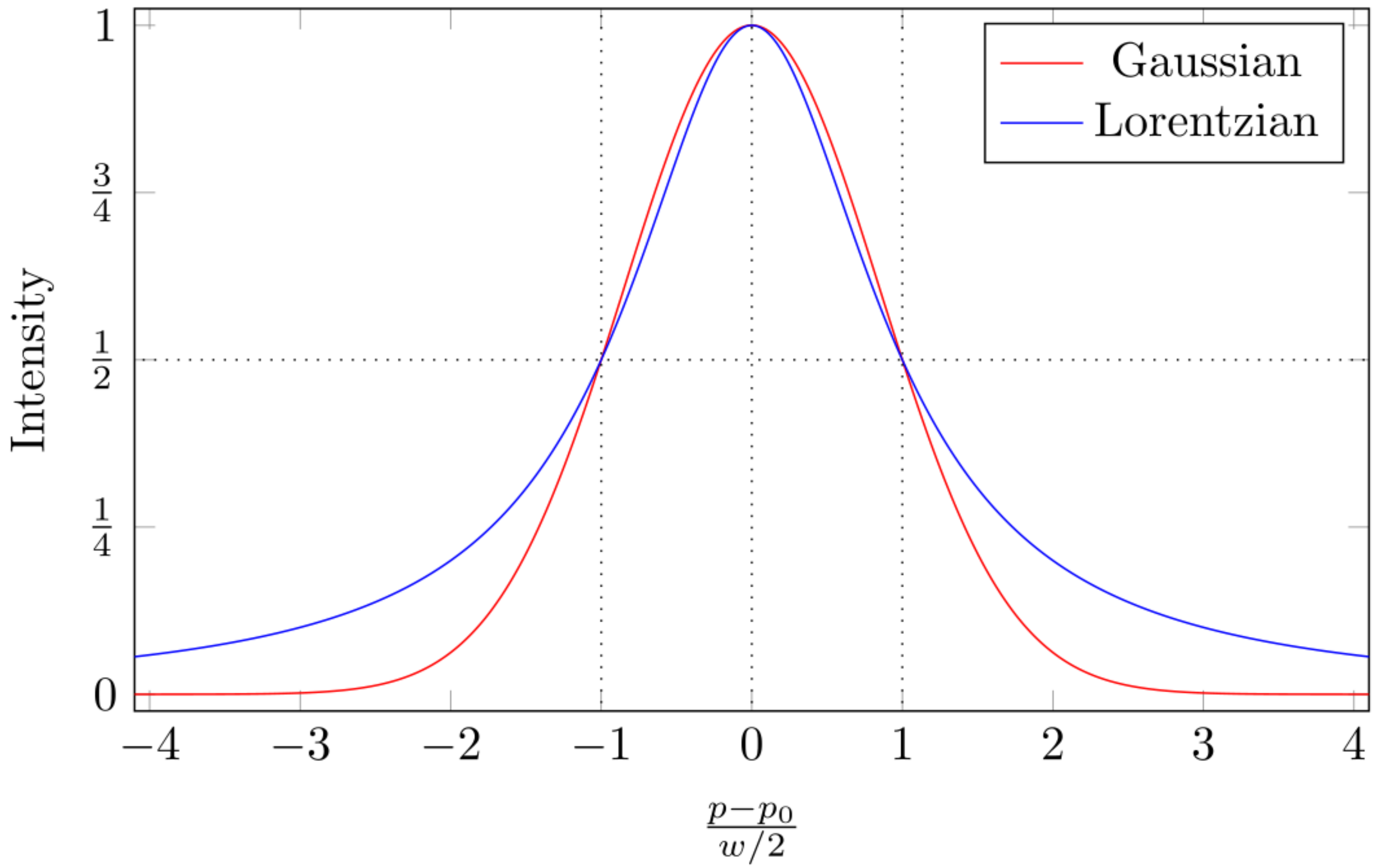

Wikipedia

Pressure broadening: Interaction of the emitting atom with the electric field of the surrounding plasma. Transition changed due to the Stark effect

$\rightarrow$ Lorentzian line profile width depends on pressure $\Delta\lambda \approx< 0.1 ... > 1000$ Å

Line broadening mechanisms – Pressure broadening

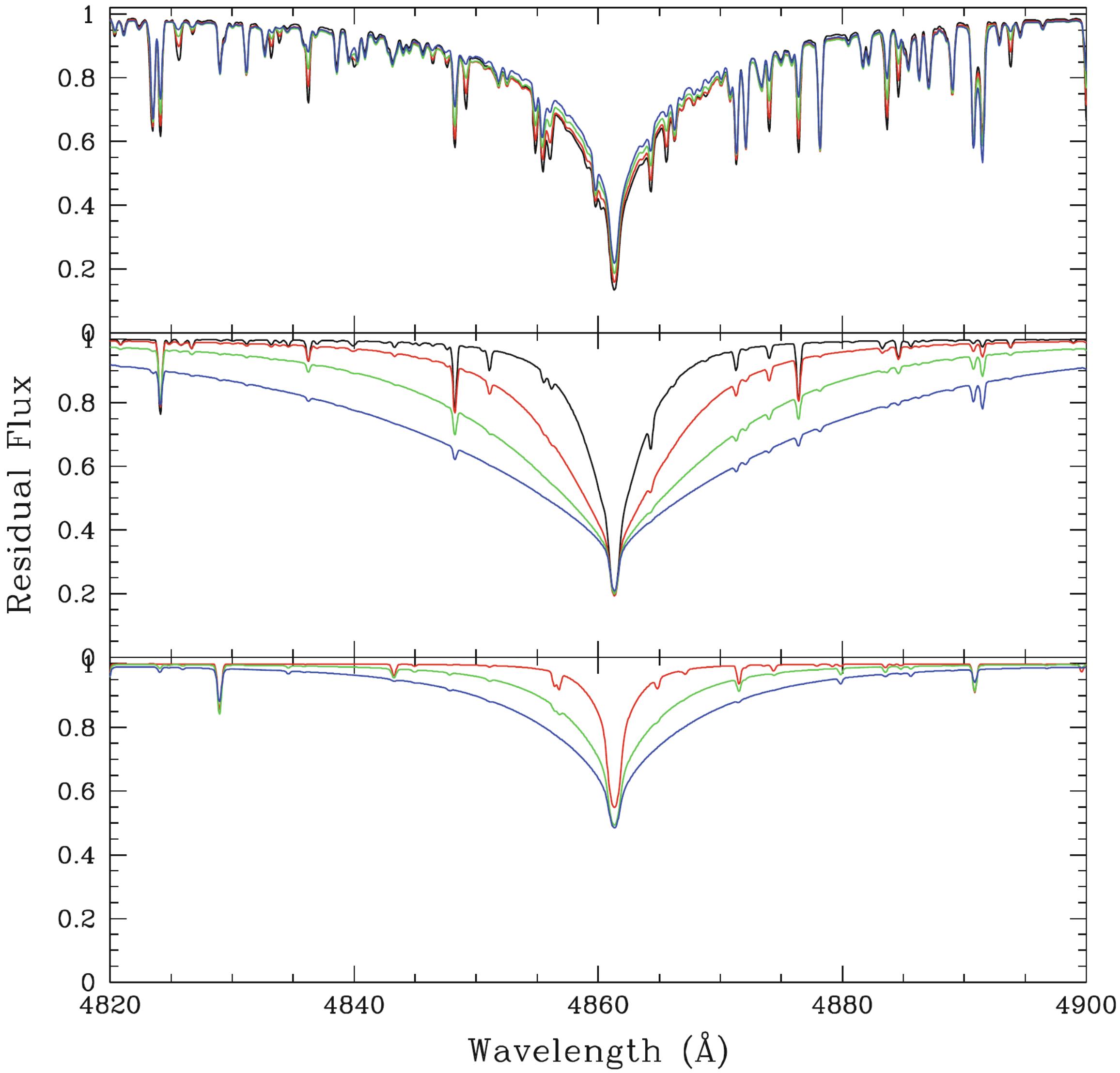

Niemczura, Smalley & Pych 2014

$H\beta$ for
$T_{\rm eff}$ = 7000, 10 000,
25 0000 K and
log g = 2.0 (black), 3.0 (red),
4.0 (green), 5.0 (blue)

Dependent on the surface gravity of the stars
$\rightarrow$ Distinction between dwarfs and giants possible

Line broadening mechanisms – thermal Doppler broadening

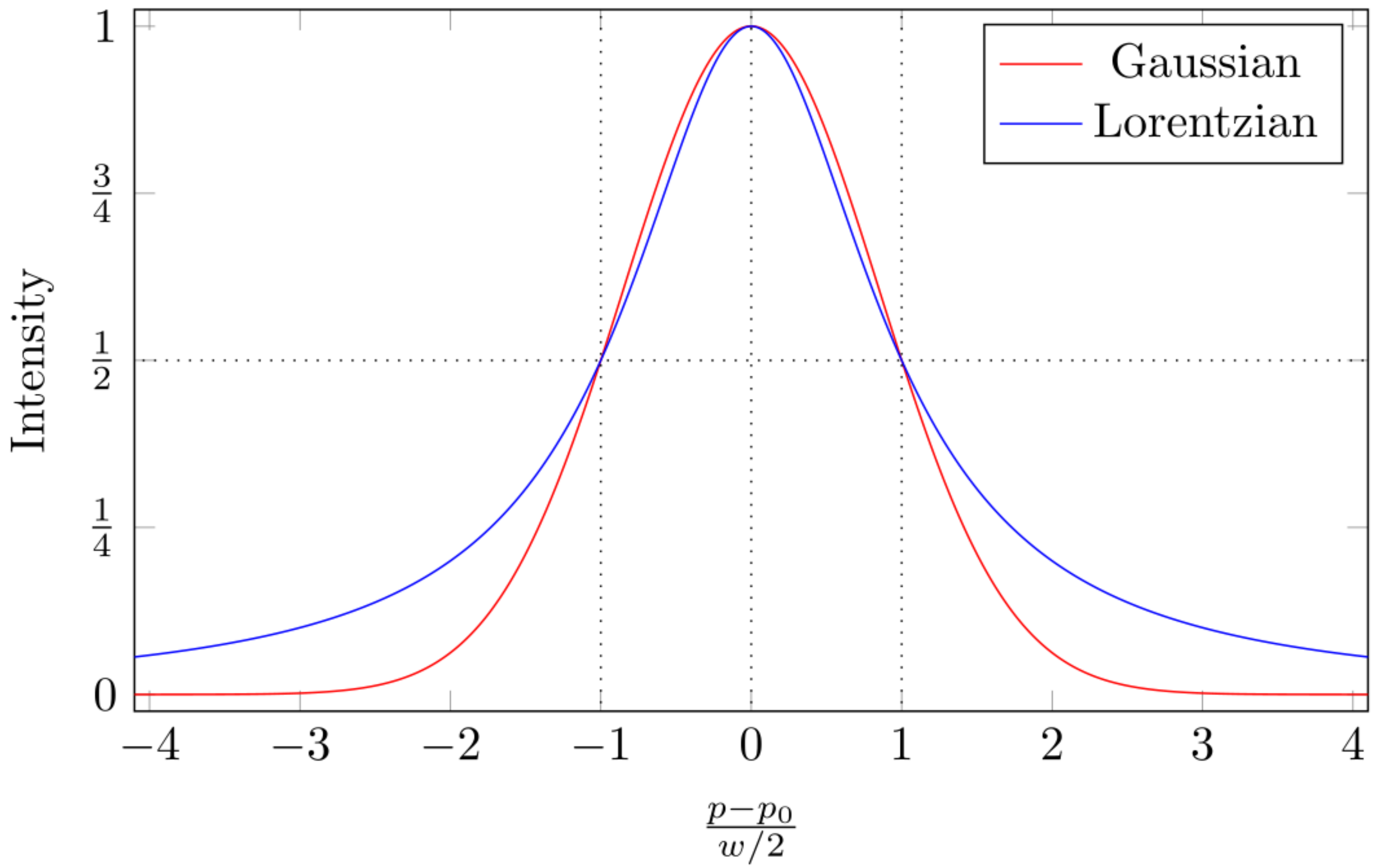

Wikipedia

Thermal Doppler broadening: Emitting atoms have a velocity distribution dependent on the plasma conditions

$\rightarrow$ Doppler effect causes Gaussian line broadening mostly dependent on temperature

Line profile

Voigt profile (α, w) : Convolution of Gaussian (thermal) function $\phi(\Delta\nu)$ and Lorentzian (pressure) function $\Psi(\nu)$

$$\phi(\Delta\nu) = \frac{1}{\Delta\nu_D\sqrt{\pi}} e^{-\left(\frac{\Delta\nu}{\Delta\nu_D}\right)^2}$$

$$\psi(\nu) = \frac{1}{\pi}\frac{\gamma/4\pi}{(\nu-\nu_0)^2 + (\gamma/4\pi)^2}$$

$$\int_{-\infty}^{+\infty} \psi(\nu\Delta\nu) \circledast \phi(\Delta\nu) \mathrm{d}(\Delta\nu)$$

$$= \frac{1}{\Delta\nu_D\sqrt{\pi}}\left[\frac{\gamma}{4\pi^2}\int_{-\infty}^{+\infty}\frac{e^{-\left(\frac{\Delta\nu}{\Delta\nu_D}\right)^2}}{(\nu-\nu_0-\Delta\nu)^2+(\gamma/4\pi)^2}\mathrm{d}(\Delta\nu)\right] = \frac{1}{\Delta\nu_D\sqrt{\pi}}H(\alpha, w)$$

$$\alpha = \frac{\gamma}{4\pi\Delta\nu_D} \qquad w = \frac{\nu-\nu_0}{\Delta\nu_D}$$

γ damping constant (pressure dependent), $\Delta\nu_D = \frac{\nu}{c}\sqrt{\frac{2kt}{\mu}}$ Doppler broadening

Line profile

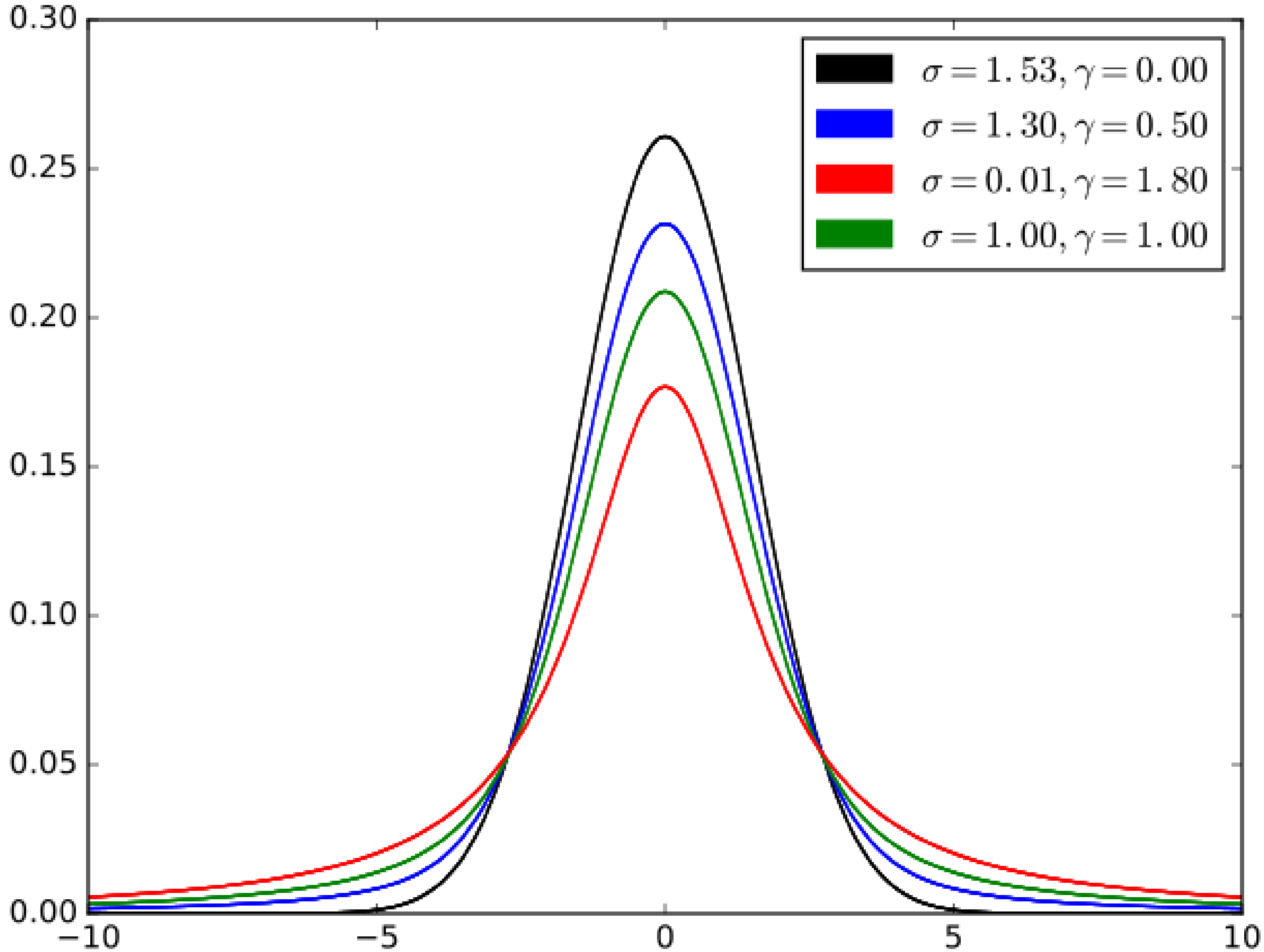

Wikipedia

Line shape and strength

shape due to frequency dependent absorption coefficient of the absorption line

$$\kappa_\nu^{\text{line}} = \frac{\pi e^2}{mc} n_l f_{lu} \frac{1}{\Delta\nu_D\sqrt{\pi}} H(\alpha, w)$$

n_l number density of atoms in the lower state l

f_{lu} probability for a transition from the lower state l to the upper state u with $\Delta E = E_u - E_l = h\nu \rightarrow$ oscillator strength

Continuum intensity I^{cont} is absorbed

$$I_\nu = I_\nu^{\text{cont}} e^{-\tau} \qquad \tau \sim H(\alpha, w)$$

Strength of spectral lines measured as **equivalent width**

$$W_\lambda = \int \frac{I^{\text{cont}} - I_\lambda}{I^{\text{cont}}} \mathrm{d}\lambda$$

$$\frac{W_\lambda}{\lambda} = \frac{W_\nu}{\nu} \rightarrow W_\nu = \int_{\text{line}} 1 - e^{-\tau_\nu} \mathrm{d}\nu$$

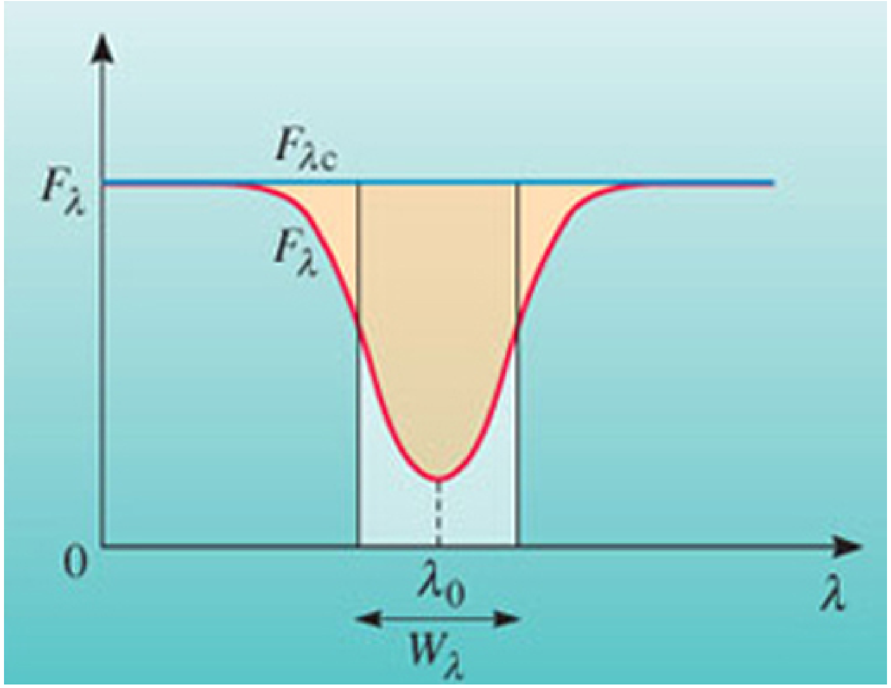

Open University

Line shape and strength

small optical depth in the line ($\tau \ll 1$ and/or $\alpha \ll 1$)

$\rightarrow 4\pi\Delta\nu_D \gg \gamma$:

Doppler- broadening is much more important than the effect of the damping

$\rightarrow$ absorption profile shows, only the central part, the Doppler core of the line

$$W_\nu = \int_{\text{line}} 1 - e^{-\tau_\nu}\mathrm{d}\nu = (\text{for small } \tau) = \int \tau_\nu \mathrm{d}\nu = \int_0^{+\infty}\int_{s_1}^{s_2} \kappa_\nu \mathrm{d}s\mathrm{d}\nu$$

$\rightarrow$ assuming material doing the absorption to be constant over the line of sight

$$W_\nu = \int \tau_\nu \mathrm{d}\nu = \int_0^{+\infty} \frac{\kappa_\nu}{n_l}\mathrm{d}\nu \cdot \int_{s_1}^{s_2} n_l \mathrm{d}s = \frac{\pi e^2}{mc} f_{lu} \cdot n_l L = \frac{\pi e^2}{mc} N_l f_{lu}$$

$\int n_l \mathrm{d}s = n_l L = N_l$ column density of the material, wavelength $\lambda = c/\nu$

$$\rightarrow \frac{W_\lambda}{\lambda} = \frac{\pi e^2}{mc^2} N_l f_{lu} \lambda$$

Line shape and strength

very large optical depth in the line ($\tau \gg 1$ and/or $\alpha \gg 1$)

$\rightarrow$ damping more important than Doppler broadening

$\rightarrow$ shape shows wide damping wings: $H(\alpha, w) \simeq \frac{\alpha}{\sqrt{\pi} w^2}$

$$\tau_\nu = \int_{s_1}^{s_2} \frac{\pi e^2}{mc} n_l f_{lu} \frac{1}{\Delta\nu_D \sqrt{\pi}} \frac{\alpha}{\sqrt{\pi} w^2} \mathrm{d}s$$

$\rightarrow$ Separating integration over line of sight and frequency

$$\frac{W_\lambda}{\lambda} = \frac{\pi^2 e^2}{mc^2} \sqrt{\frac{8}{3\lambda}} \sqrt{N_l f_{lu} \lambda} \tag{4.31}$$

Equivalent width proportional to square root of the amount of material and the line constant $f\lambda$

Intermediate τ **and/or** $\alpha \rightarrow$ Numerical integration: $\frac{W_\lambda}{\lambda} =\approx \log N_l f_{lu} \lambda$

$\rightarrow$ Equivalent width proportional to logarithm of the amount of material and the line constant $f\lambda$

Curve of growth

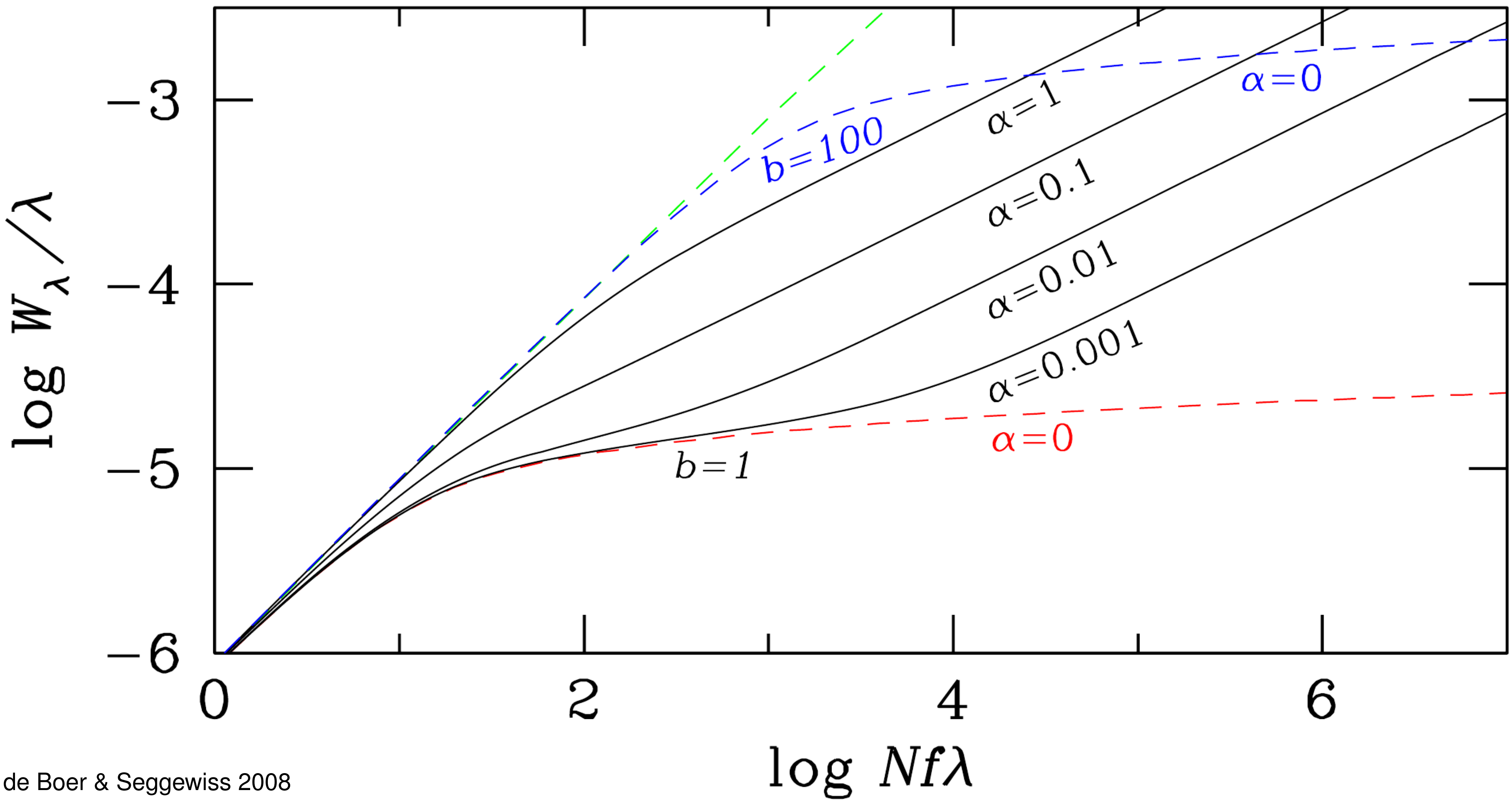

de Boer & Seggewiss 2008

$b = 2\sqrt{2}\Delta\nu_D(c/\nu_0)$ half width half maximum of Doppler broadening

Boltzmann equation

In (local) thermodynamic equilibrium all processes are in balance

$\rightarrow$ Population of energy levels determined by statistics

$\rightarrow$ Distribution of particles in the possible energetic states A and B given by **Boltzmann equation**

$$\frac{n_\mathrm{A}}{n_\mathrm{B}} = \frac{g_\mathrm{A}}{g_\mathrm{B}} e^{-\frac{\Delta E_\mathrm{AB}}{kT}} \tag{4.32}$$

$n_{\mathrm{A}/\mathrm{B}}$ number density, $g_{\mathrm{A}/\mathrm{B}}$ statistical weight, $\Delta E_\mathrm{AB} = E_\mathrm{A} - E_\mathrm{B}$

Ratio of particles in a given state to all particles of that kind

$$n_\mathrm{total} = \sum_i = \frac{n_1}{g_1} \cdot \left(g_1 + g_2 e^{-\frac{\Delta E_{12}}{kT}} + g_3 e^{-\frac{\Delta E_{13}}{kT}} + \ldots \right) \equiv \frac{n_1}{g_1} Q(T) e^{\frac{E_1}{kT}}$$

$Q(T) = \sum_i g_i e^{-E_i/kT}$ partition function

$$\Rightarrow \frac{n_j}{n} = \frac{g_j}{Q(T)} e^{-\frac{E_\mathrm{j}}{kT}}$$

population number of a given state j relative to total population

Saha equation

Distribution of particles in two different ionization stages a and b is given by

Saha equation

$$\frac{n_\mathrm{b}}{n_\mathrm{q}} n_e = 2\frac{Q_\mathrm{b}(T)}{Q_\mathrm{a}(T)} \cdot \left(\frac{2\pi mkT}{h^2}\right)^{\frac{3}{2}} e^{\frac{-\chi_\mathrm{ab}}{kT}} \tag{4.33}$$

χ_ab ionization energy, n_e electron number density

- equivalent width of a spectral lines depends on $N_l f_{lu} \lambda$
- fraction of the strength of two spectral lines with similar $f_{lu}\lambda$ in different excitation/ionization stages depends (mostly) on T

$\rightarrow$ Excitation/Ionization temperature can be determined

- Curve of growth (COG) analysis

4–73

Molecular bands

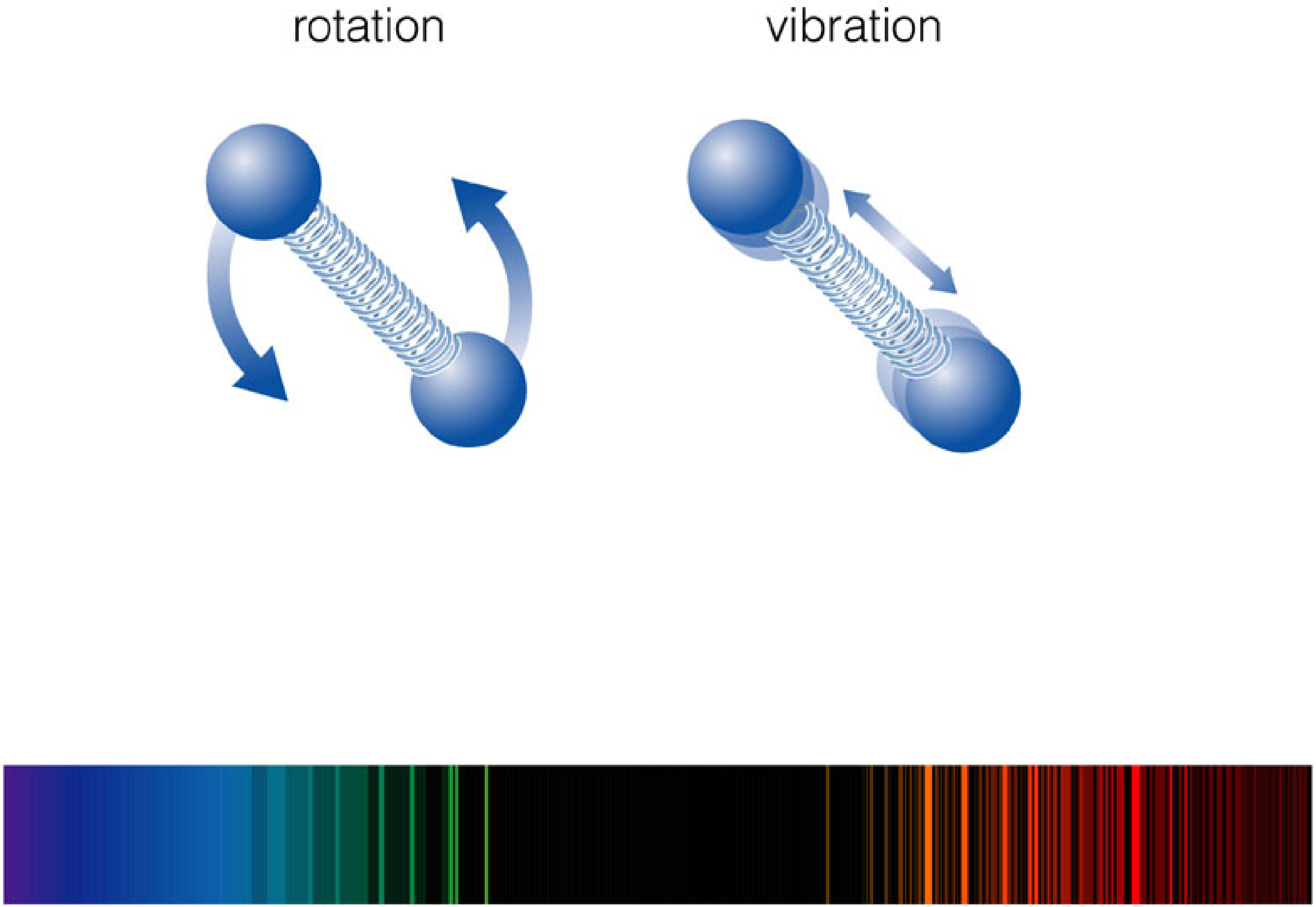

Molecular bands

- In cool stellar atmospheres atoms can form molecules, which contribute to the continuous (dissociation) and line opacity
- Molecules have additional energy levels due to vibration and rotation and form bands instead of single lines (e.g. G-band of CH molecule)
- In dense atmospheres, atoms can continuously form short-lived quasi-molecules, which quickly dissolve (e.g. H_2,H_2^+,He_2), but cause spectral features

Molecular bands

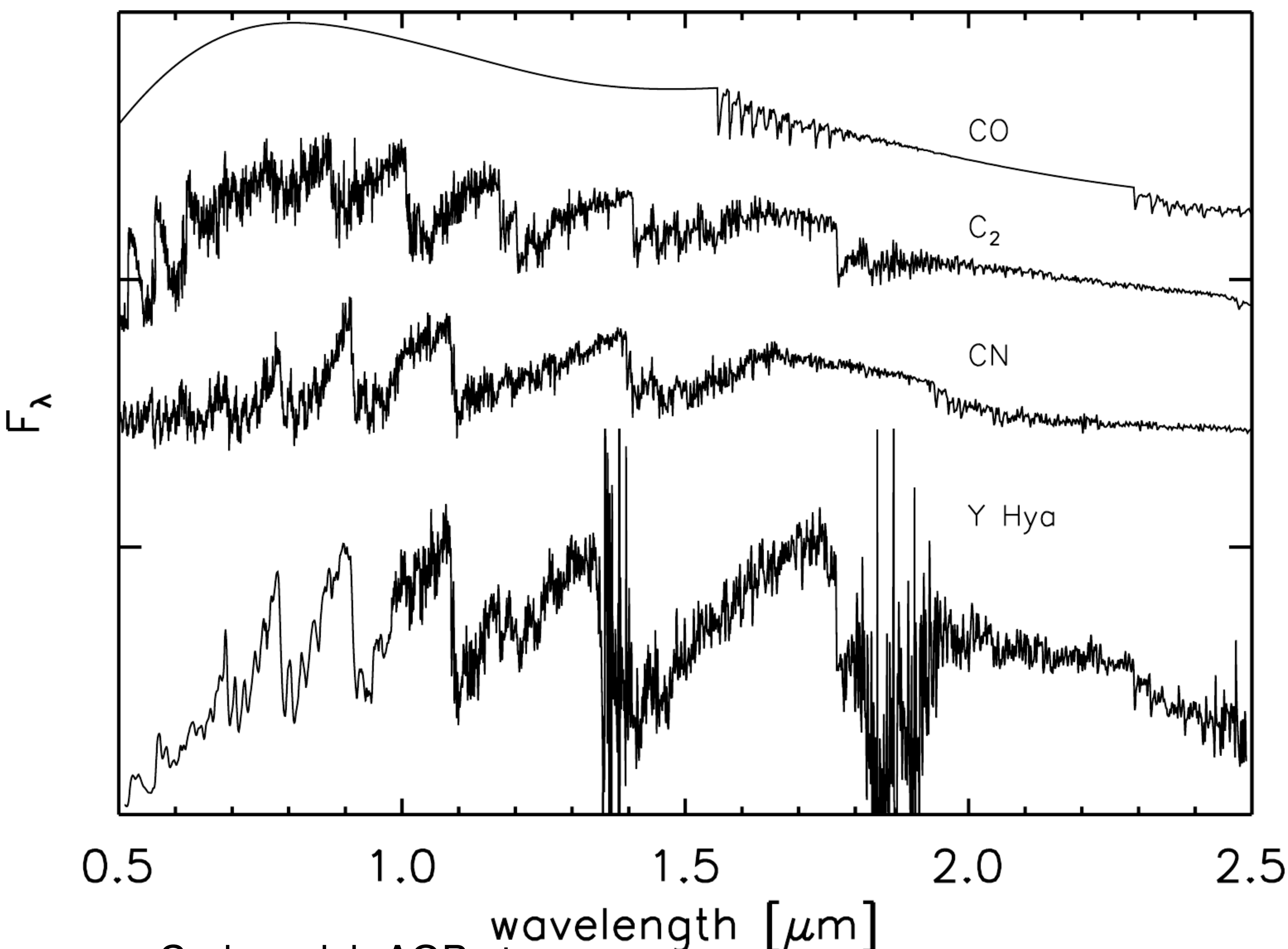

Loidl et al. 2001 Carbon-rich AGB star

Magnetic fields

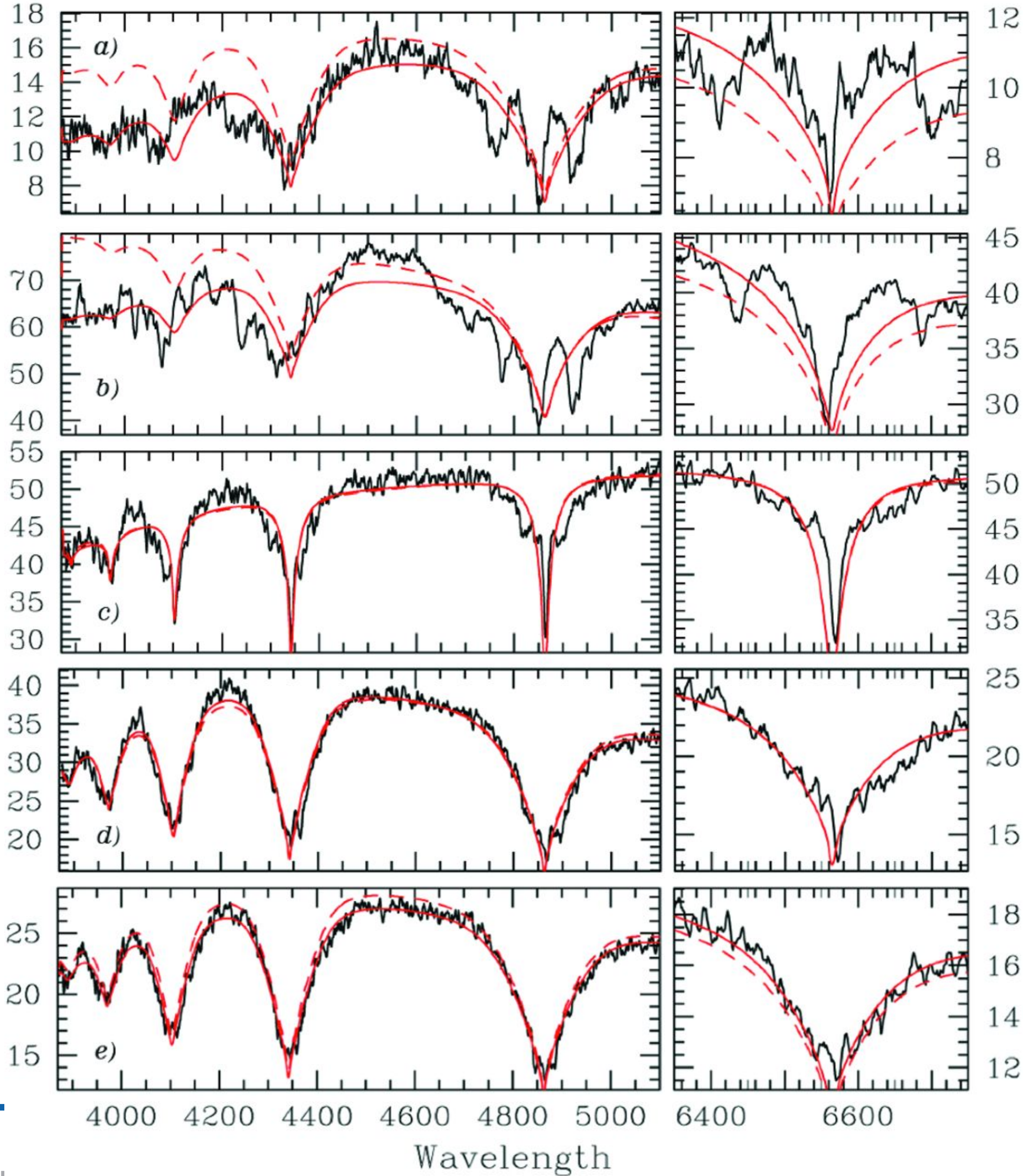

In stellar atmospheres with strong magnetic fields, spectral lines split based on interaction of the field and the electron spin (Zeeman effect)

$$\delta\lambda = g\frac{e\lambda^2}{4\pi mc^2}H \qquad (4.34)$$

H magnetic field strength

Magnetic white dwarfs with strong magnetic fields

Kepler et al. 2013, MNRAS, 429, 2934

Rotation

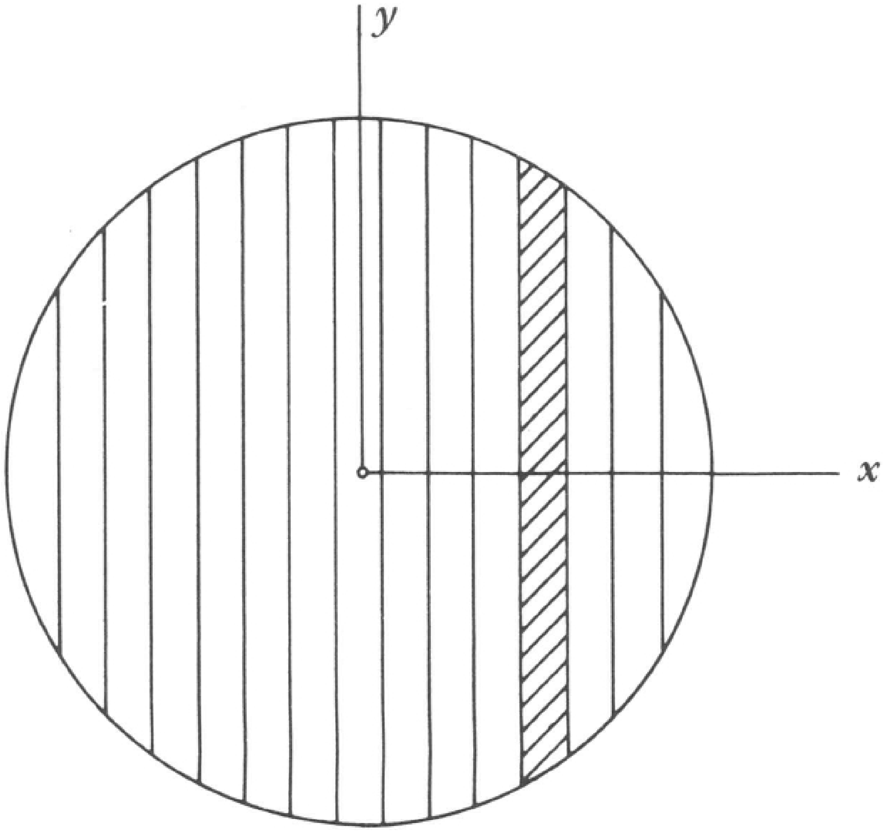

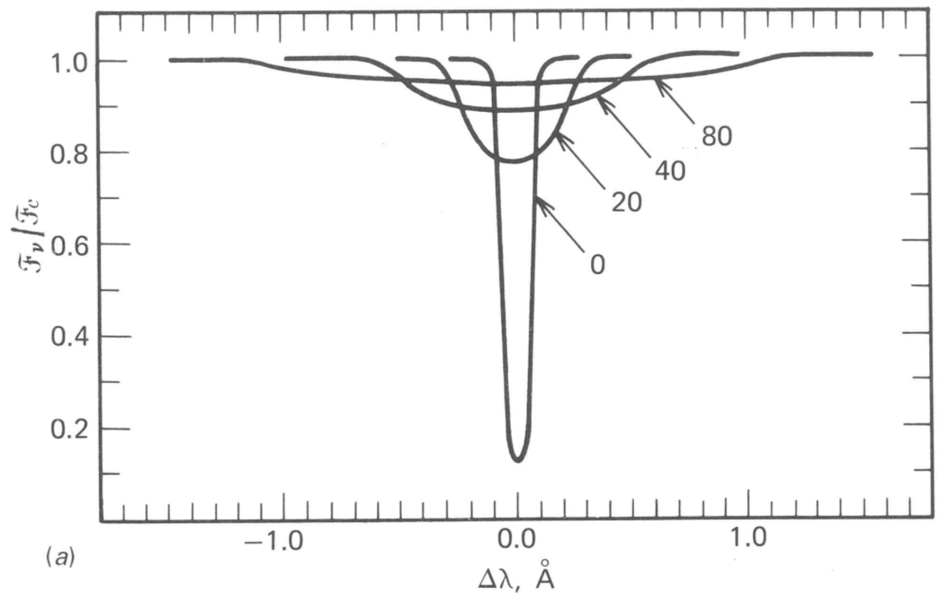

Gray 2008

Rotation

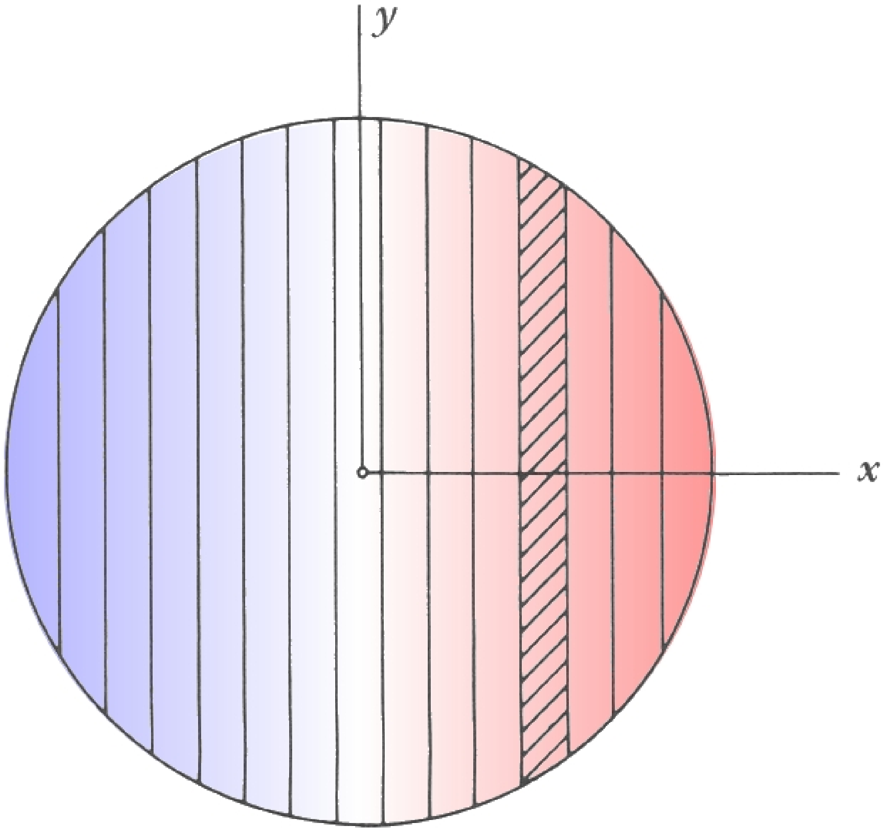

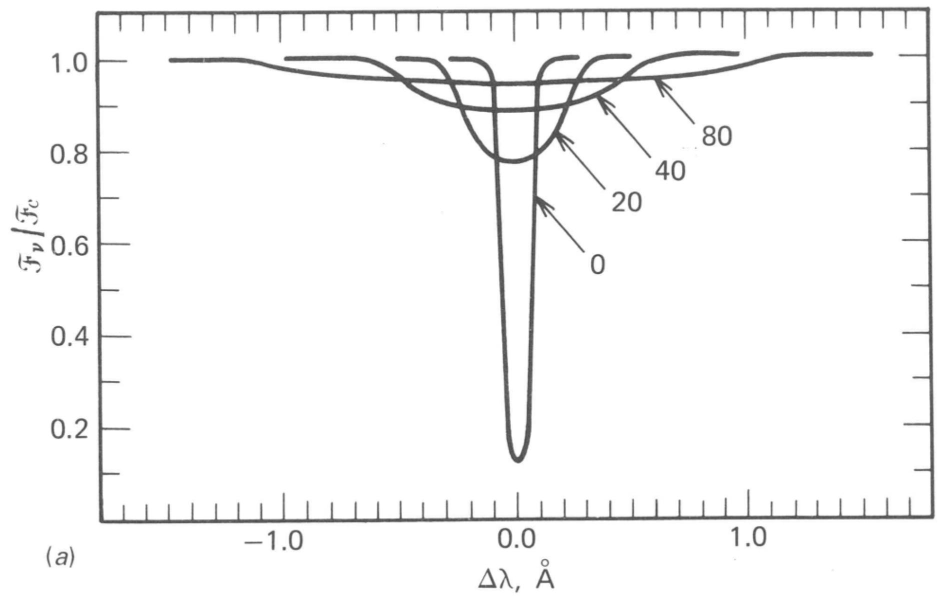

Gray 2008

Rotation

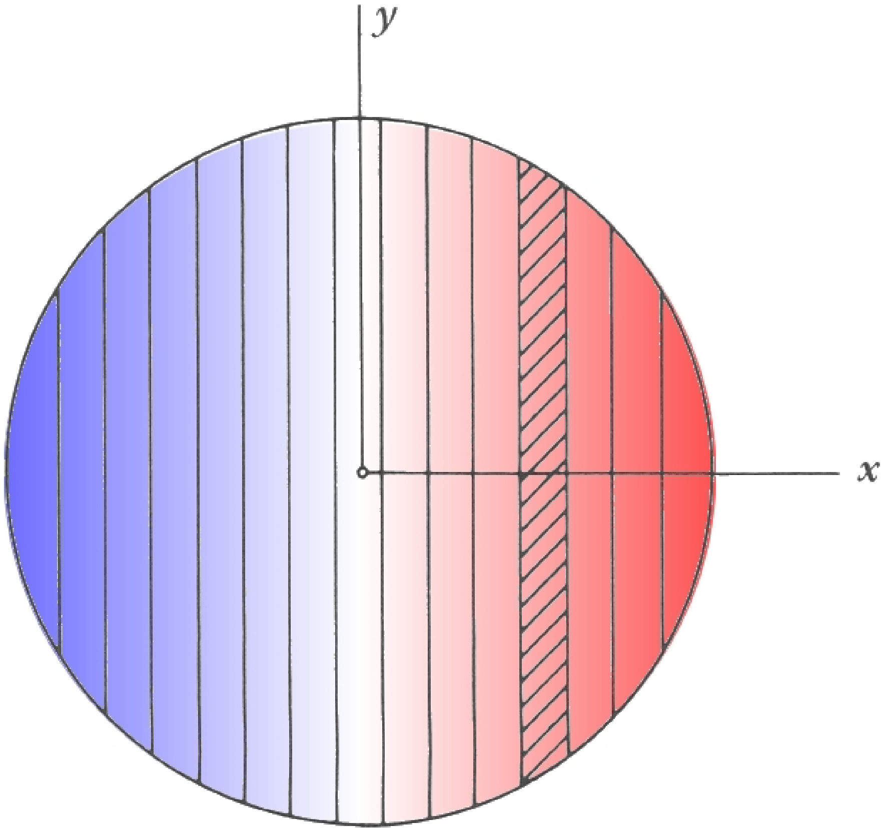

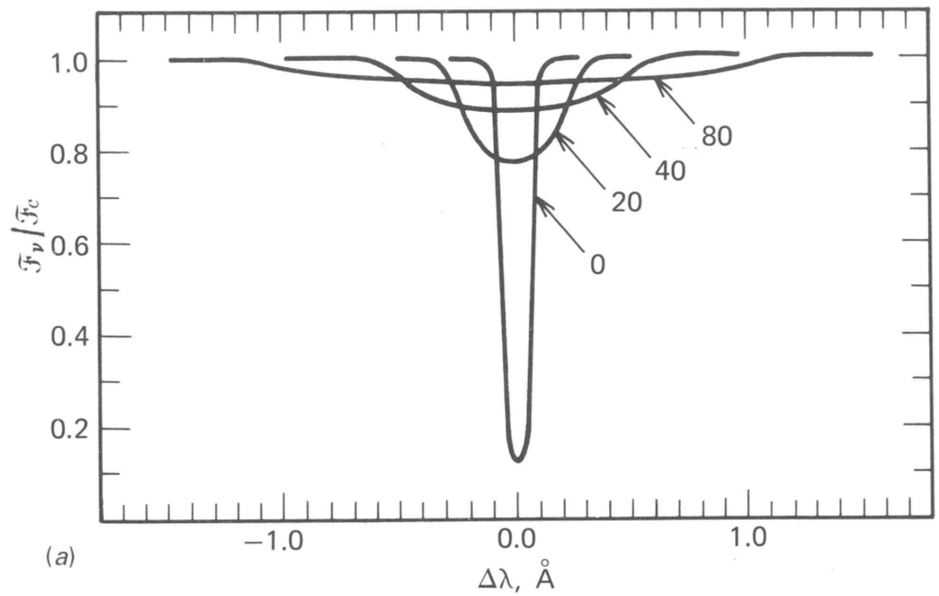

Gray 2008

Rotation

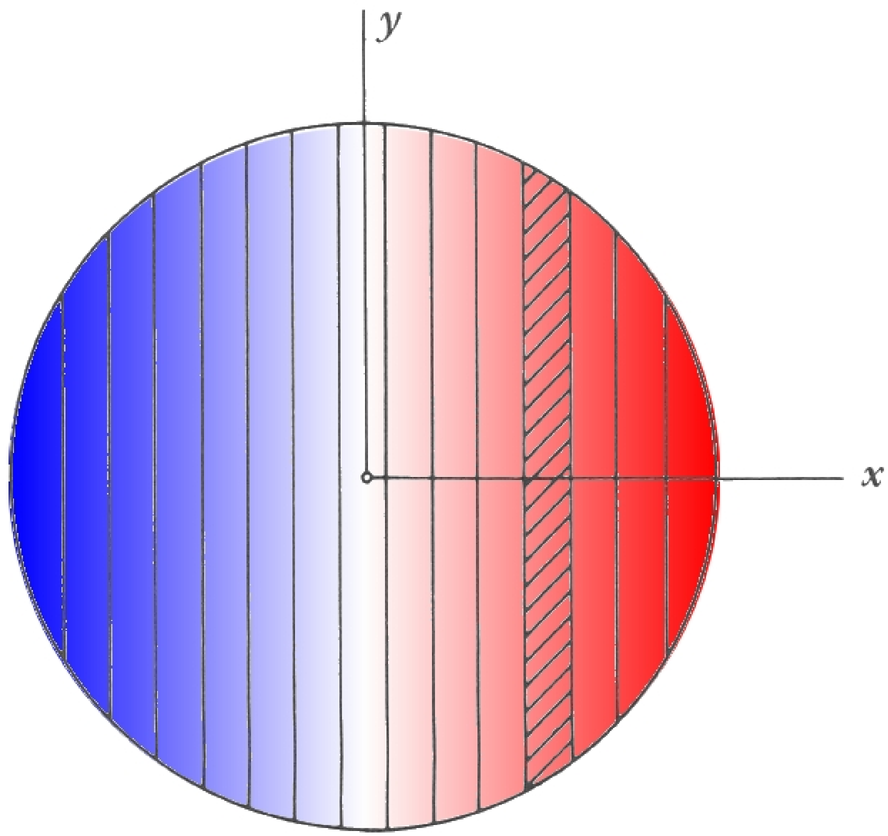

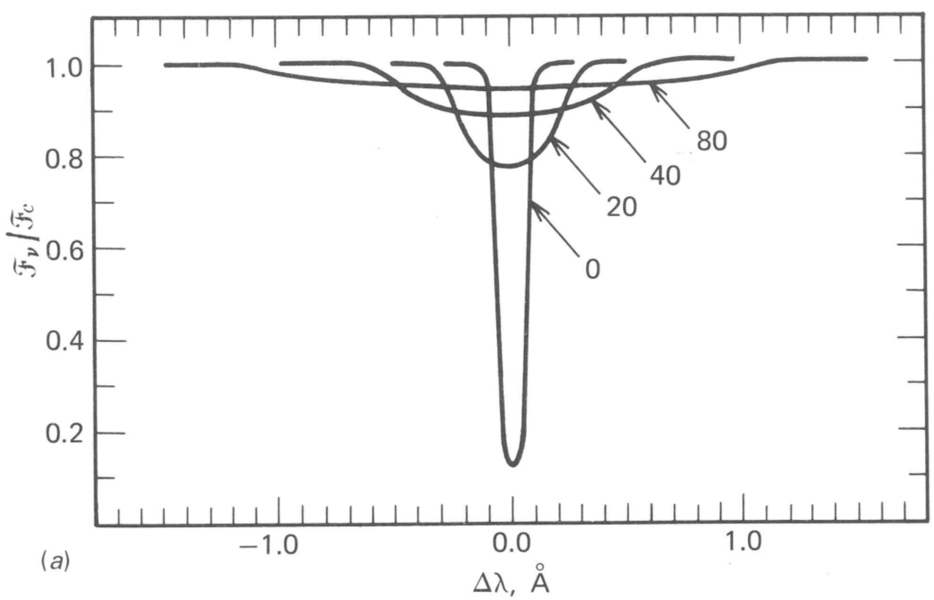

Gray 2008

Rotation

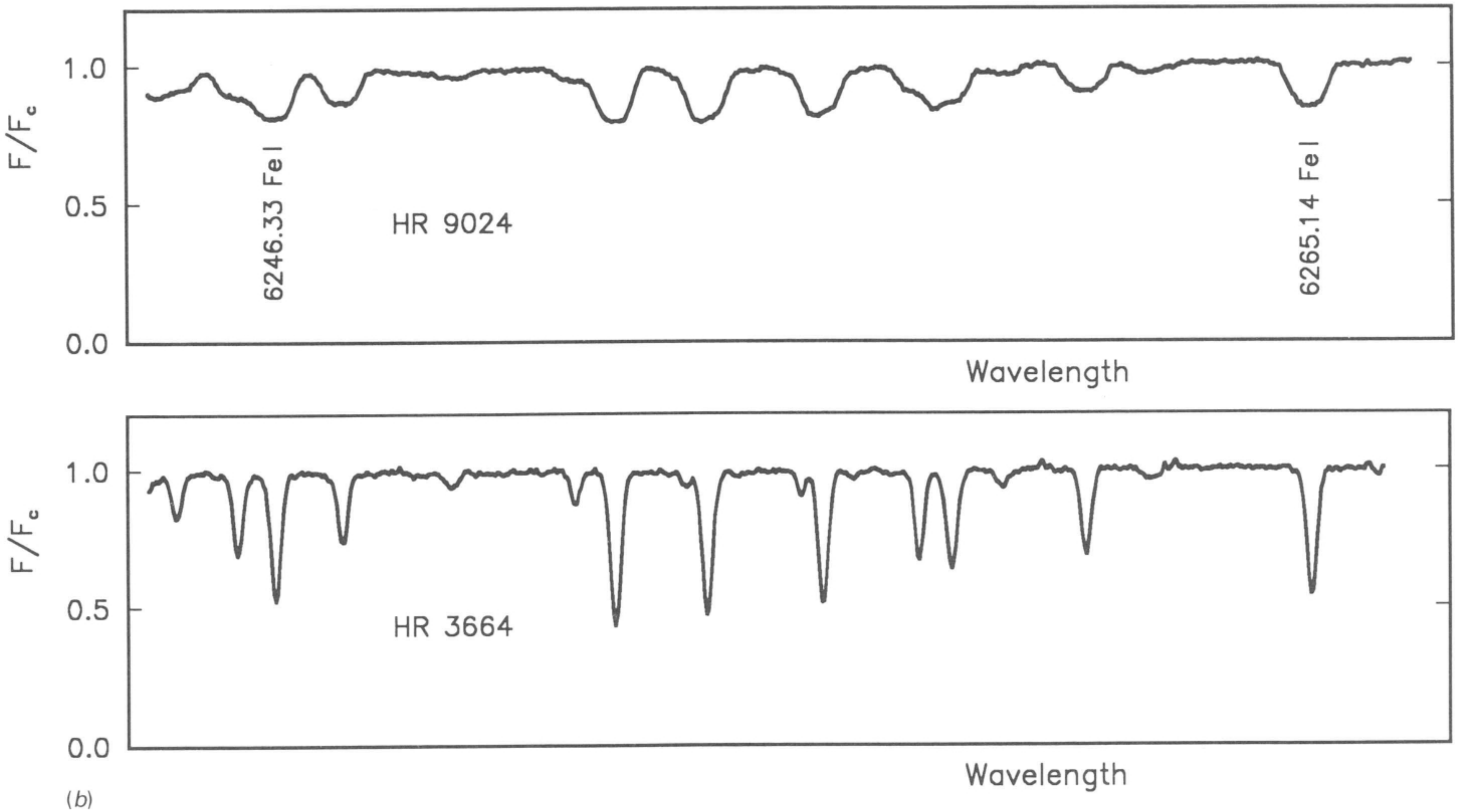

Gray 2008

Rotation

Stellar rotation leads to Doppler-shifts of the spectral lines across the stellar surface

$\rightarrow$ Integration over the entire visible surface leads to **rotational broadening** of the spectral lines

$$b = \frac{\lambda}{c} R\omega \sin i \rightarrow \frac{b}{\lambda} = \frac{v_{\mathrm{rot}}}{c} \sin i$$

b maximum FWHM broadening, ω angular rotational velocity, v_{rot} rotational velocity at equator, i inclination angle of the rotation axis

P Cygni profiles: signs of stellar wind

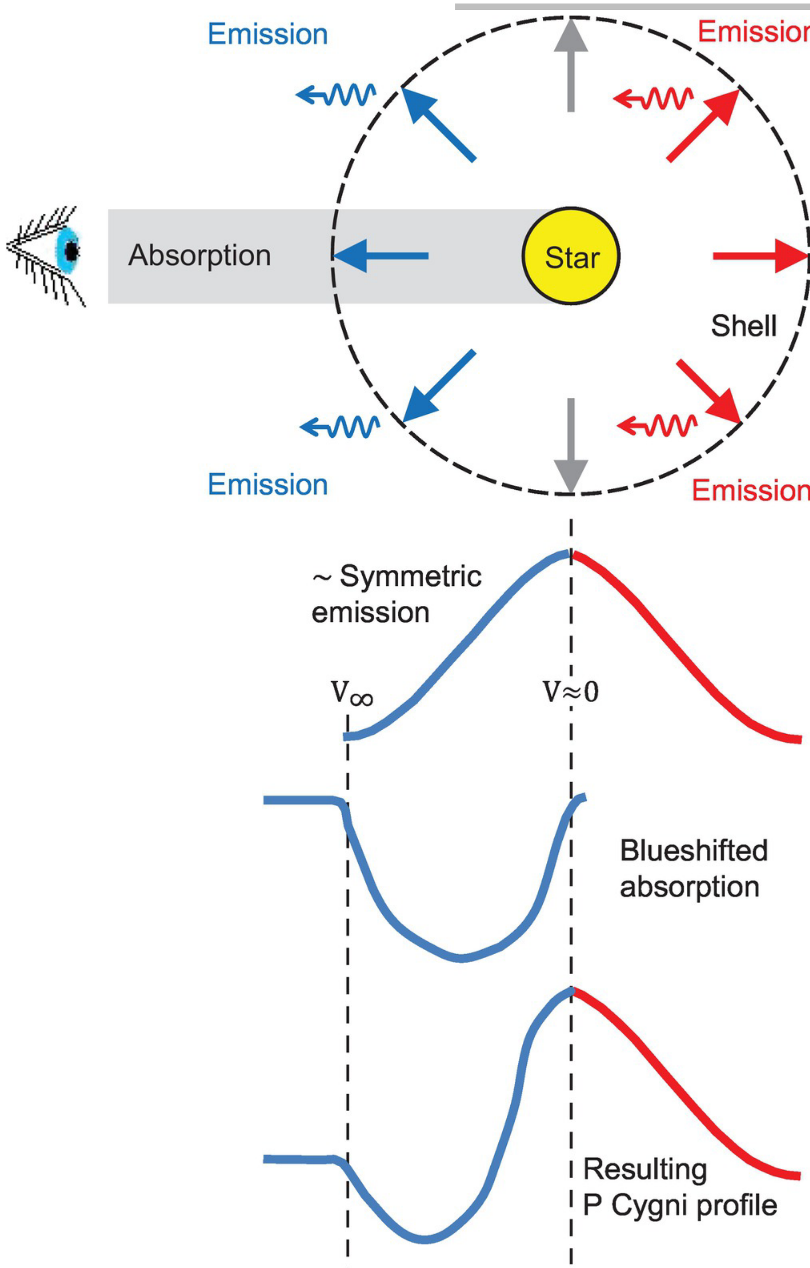

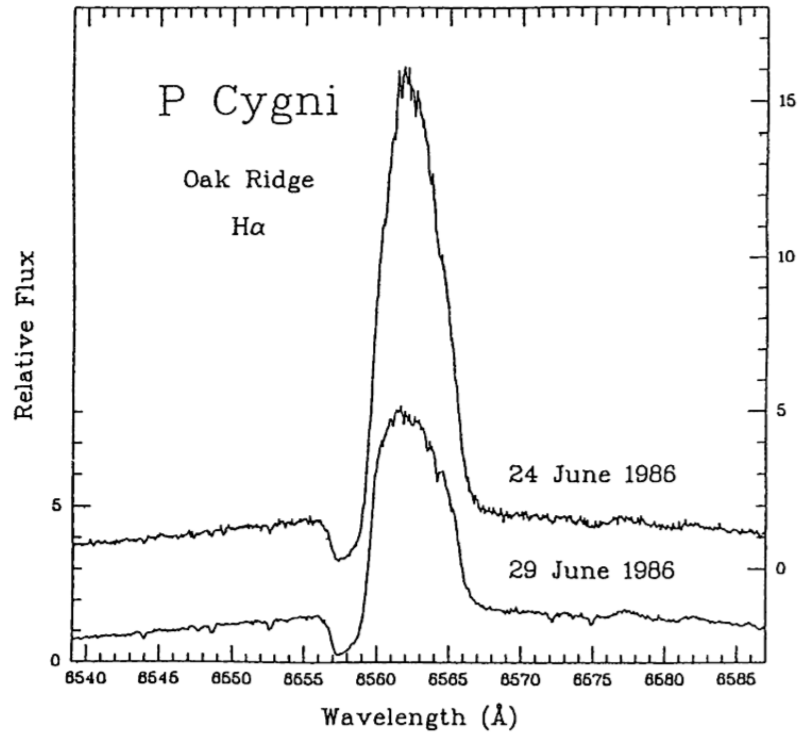

Figure 4. H-alpha profiles of P Cygni from Oak Ridge Observatory.

- Characteristic P Cygni profiles caused by optically thick stellar winds
- $\Delta\lambda/\lambda_0 = v_\infty/c$, terminal wind velocity v_∞
- Mass loss rate $\dot{M}$ determined with detailed models

Model atmosphere calculation

- **temperature and density** stratification of a model atmosphere is calculated by solving the basic equations of radiative transfer, hydrostatic equilibrium, radiative equilibrium, statistical equilibrium, charge and particle conservation iteratively
- Approximations have to be made dependent on the type of atmosphere (geometry, LTE/NLTE, static/wind, opacity sources)
- **spectrum synthesis code** take a previously computed atmospheric structure and solve, frequency-by-frequency, the radiative transfer equation, with a sufficiently high resolution in the frequency space to provide a reliable predicted spectrum to be compared with observations.
- Extended line lists containing of the order of $10^7 - 10^9$ of spectral line data are necessary

Model atmosphere calculation

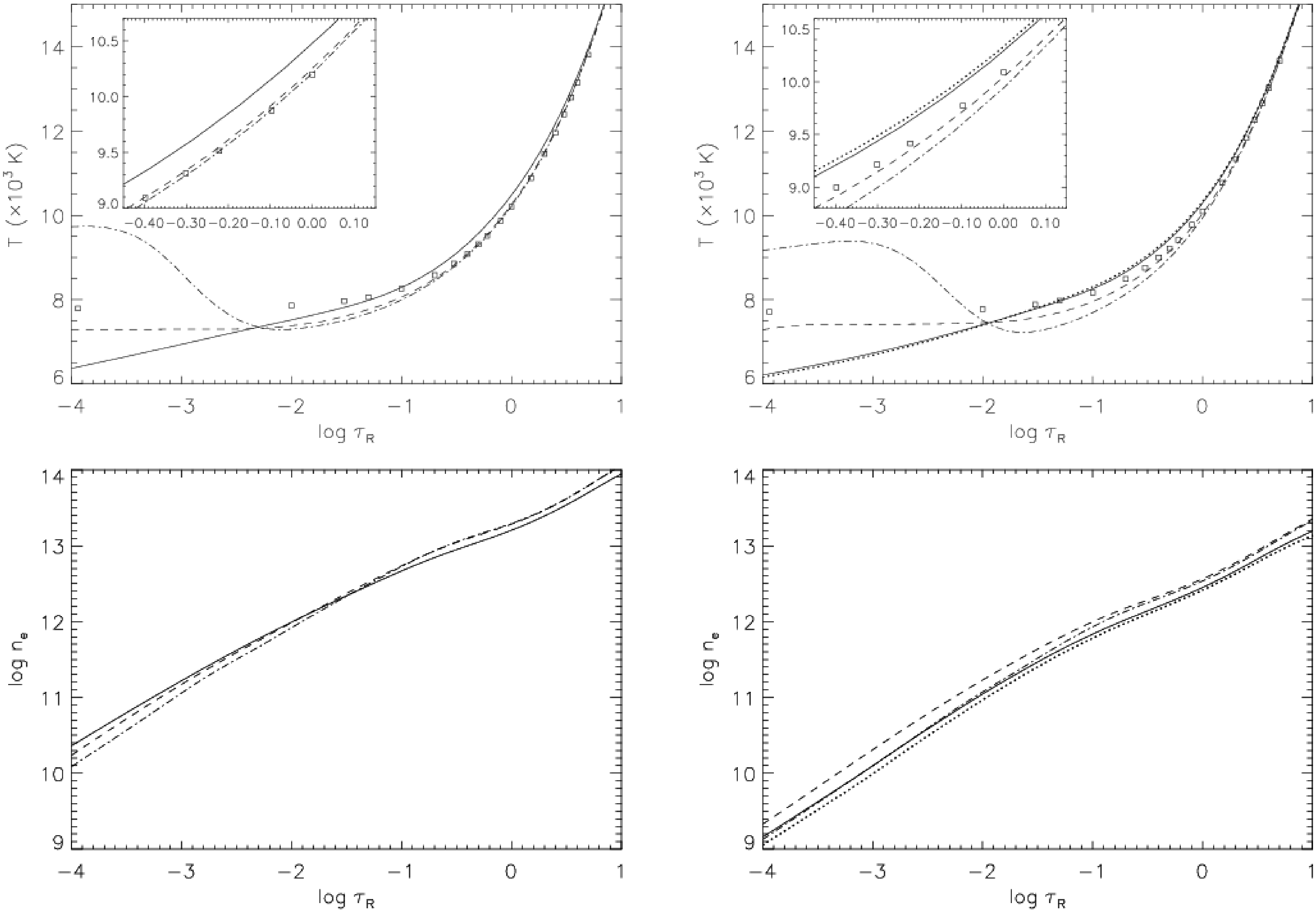

Przybilla et al. 2011, A&A, 445, 1099

Model atmosphere calculation

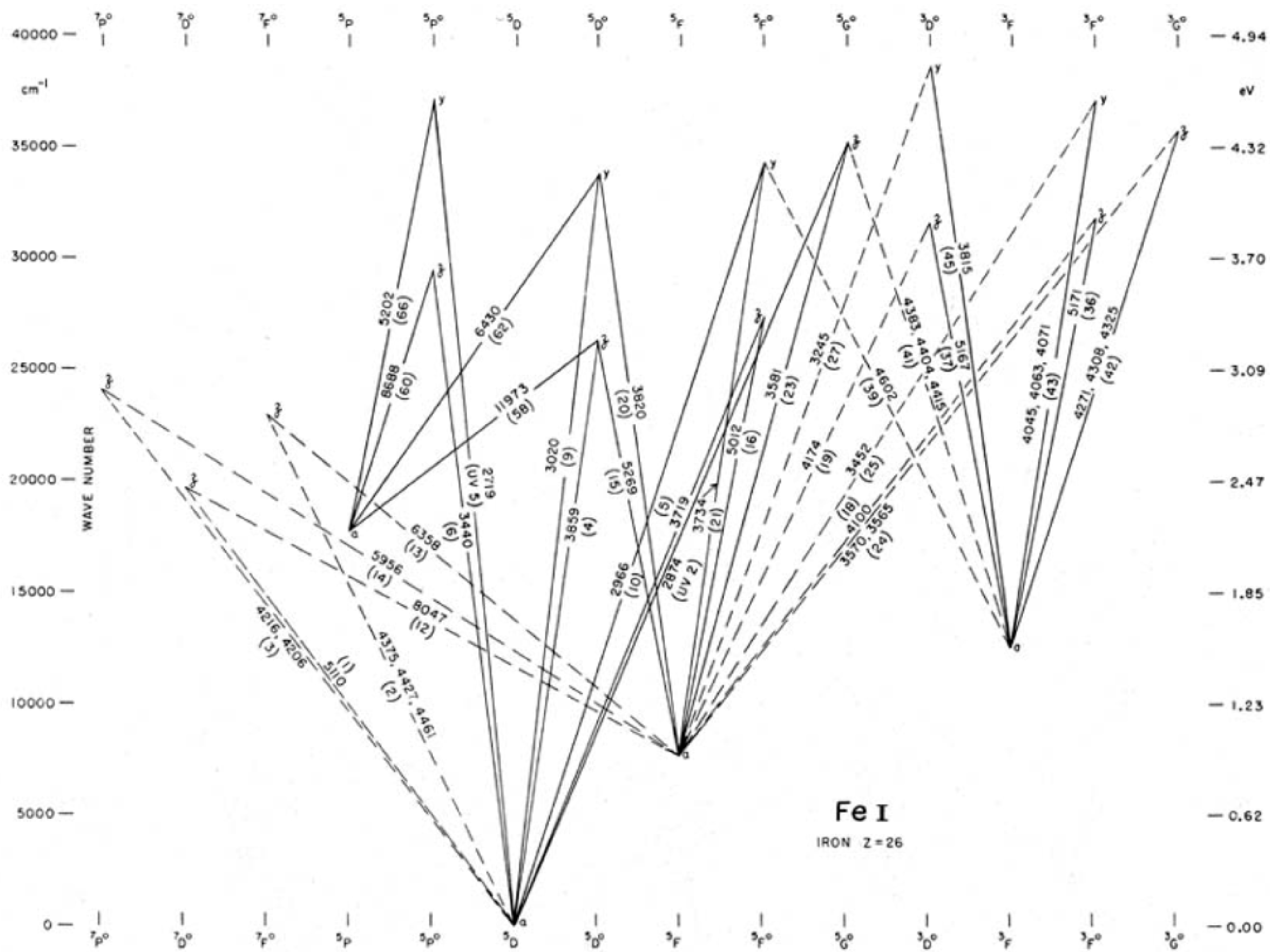

Moore & Merrill 1968

Model atmosphere calculation

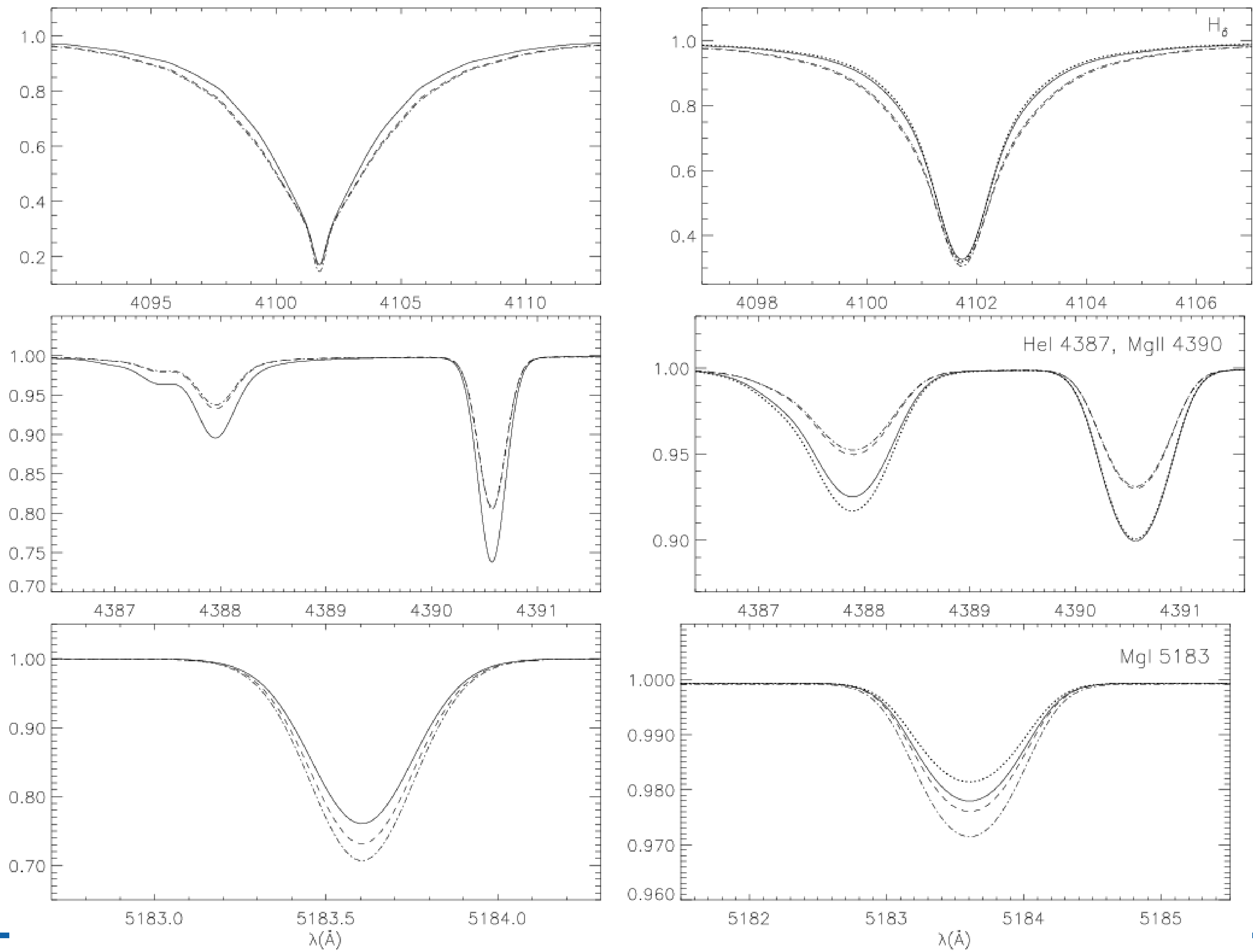

Przybilla et al. 2011, A&A, 445, 1099

Model atmosphere calculation

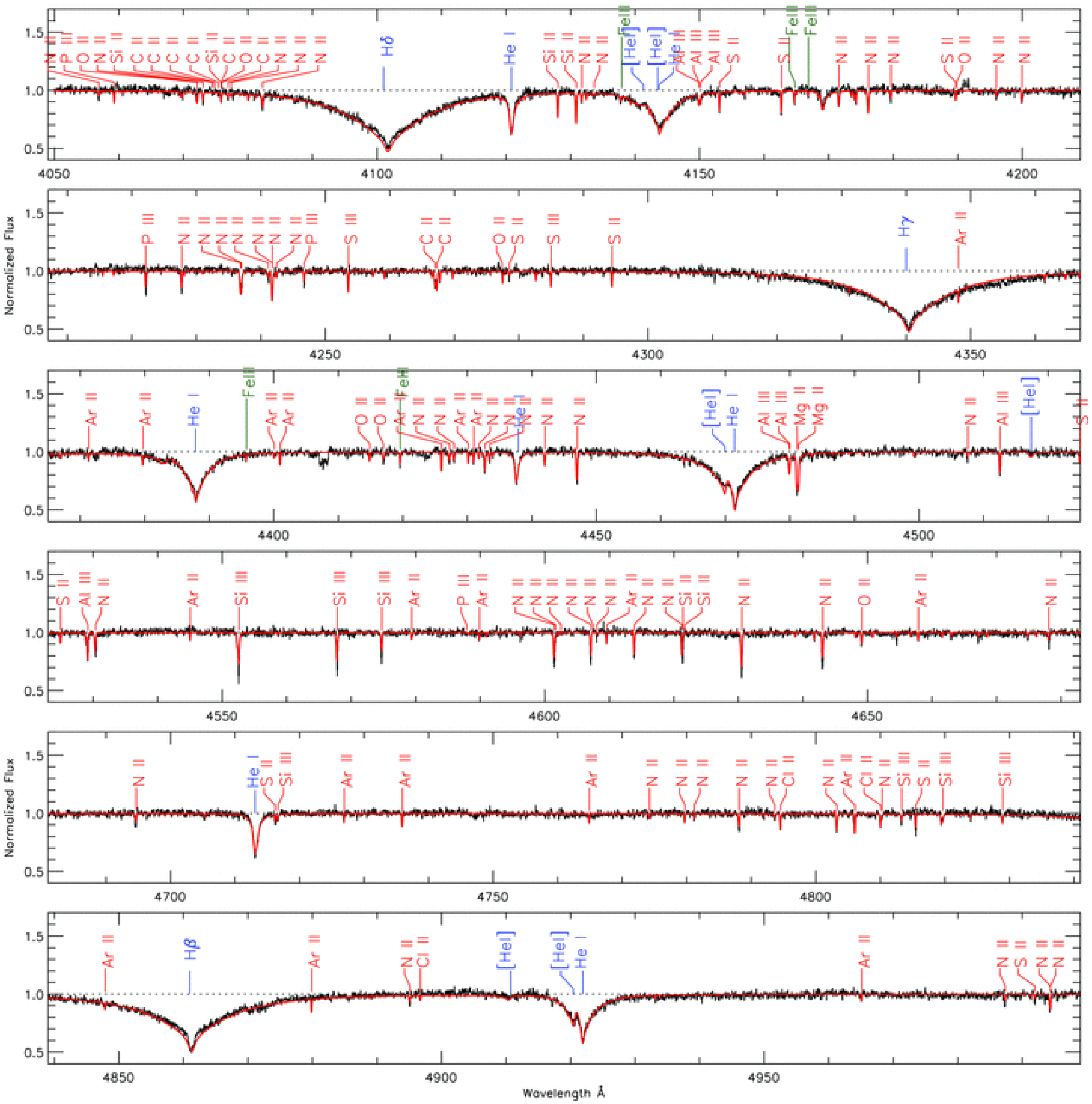

Models are fitted to observed spectra

Multidimensional model grids or individual models

Spectroscopic parameters (model dependent):

T_{eff}	Effective temperature
$\log g$	Surface gravity
$n(X)/n(H)$	Elemental abundances
[M/H]	Scaled metallicity (w.r.t Sun)
$V_{\mathrm{rot}} \sin i$	Projected rotational velocity
v_∞	Projected rotational velocity
$\dot{M}$	Mass loss rate
H	Magnetic field strength

Naslim et al. 2012, MNRAS, 423, 3031

Stellar classification

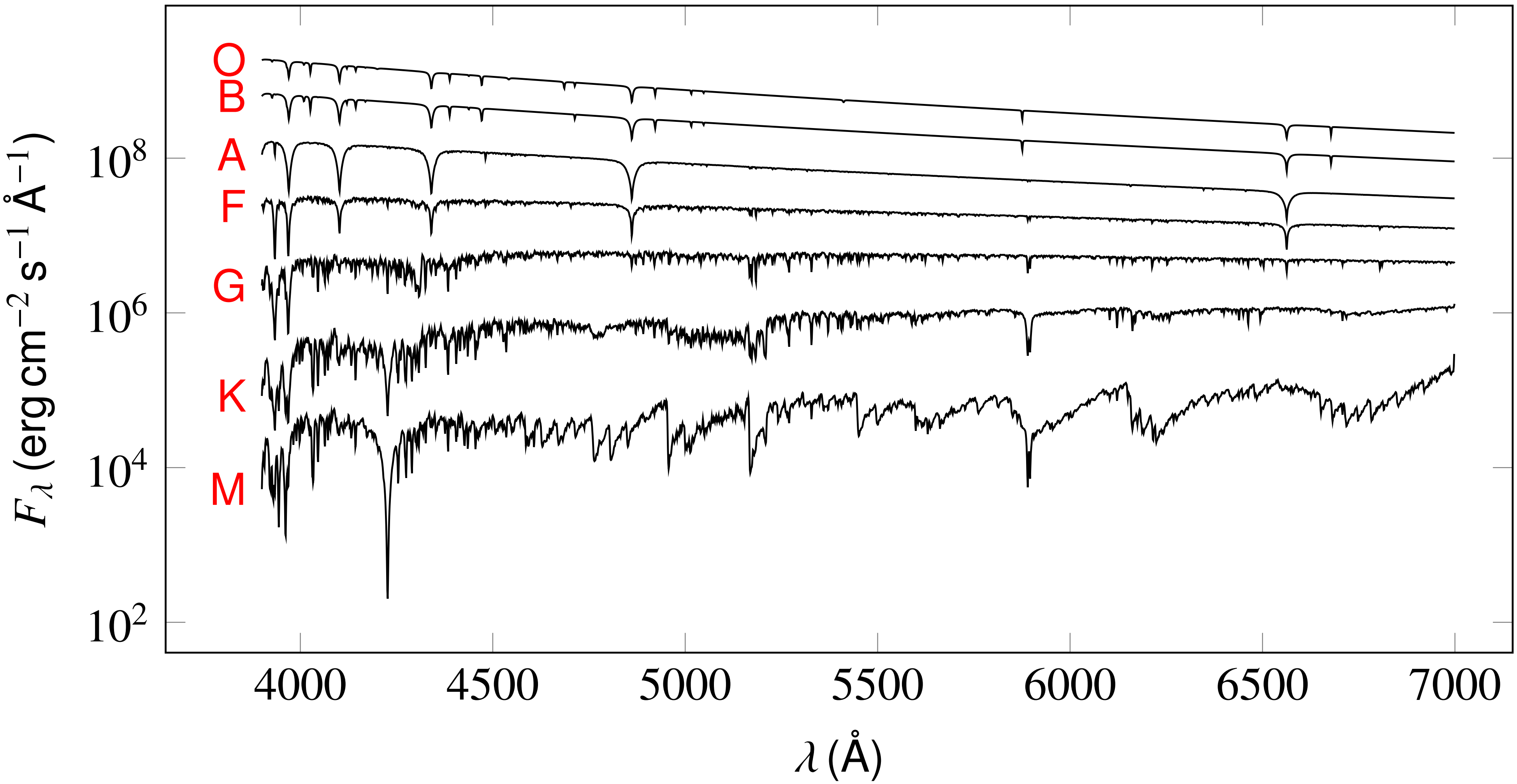

Annie Cannon introduced the Harvard classification scheme with seven spectral types (O, B, A, F, G, K, M) in 1901.

Harvard classification

The Harvard classification is based on the presence/absence and strength of absorption lines in low-resolution optical spectra:

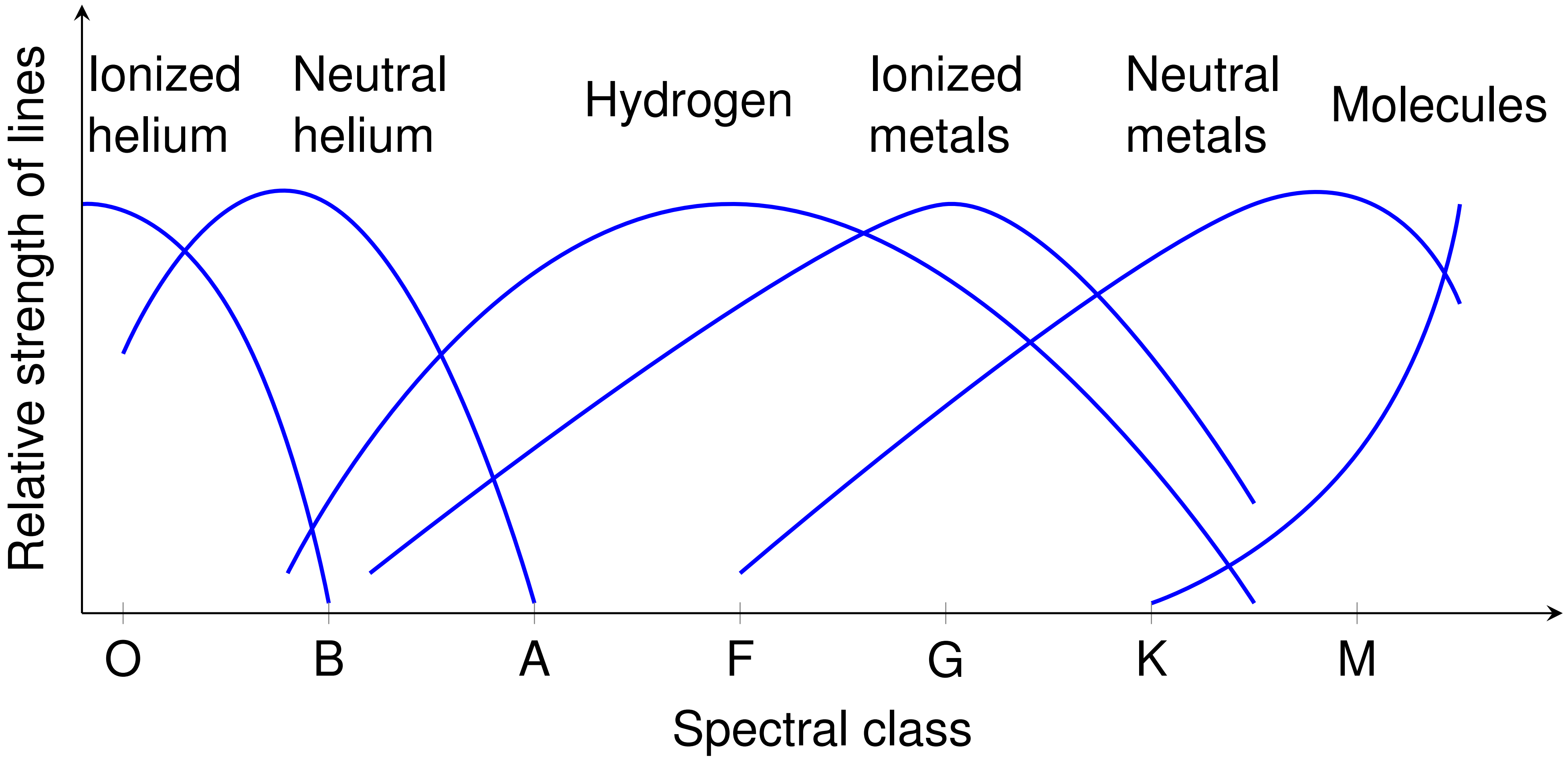

Harvard classification = temperature sequence

It turned out later that the spectral classes are actually a temperature sequence:

Class	Most prominent spectral features	Temperature
O	Ionized helium	45 000 – 25 000 K
B	Neutral helium lines	25 000 – 11 000 K
A	Hydrogen lines	11 000 – 7500 K
F	Ionized metals	7500 – 6000 K
G	Ionized and neutral metals	6000 – 5000 K
K	Neutral metals and molecules	5000 – 3500 K
M	Molecular bands	3500 – 2200 K

The ordering of the letters is due to historic reasons. Also for historic reasons, the hotter stars are sometimes called “early-type stars” while the cooler ones are called “late-type stars”. This has nothing to do with age.

Link between spectral class and temperature

- Spectral classes based on absorption lines in optical spectra
- atom in ionization stage r and absorption line from transition from lower state $\epsilon_{\mathrm{r,l}}$ to upper state $\epsilon_{\mathrm{r,u}}$
  $\rightarrow$ strength S of line scales with number of absorbers $n_{\mathrm{r,l}}$: $S \propto n_{\mathrm{r,l}}$
- likelihood to find an atom in state given by Boltzmann distribution $\epsilon_{\mathrm{r,l}}$:
  $n_{\mathrm{r,l}} \propto n_r \exp(-\epsilon_{\mathrm{r,l}}/(kT))$
- degree of ionization given by the Saha equation:
  $\frac{n_e n_{r+1}}{n_r} \propto \frac{(2\pi m_e kT)^{3/2}}{h^3} \exp(-\frac{(\epsilon_{r+1}-\epsilon_r)}{kT}) \rightarrow n_r = n_r(T)$

$$S \propto n_r(T) \exp(-\epsilon_l/(kT)) \tag{4.35}$$

$\rightarrow$ interplay between excitation and ionization effect

Link between spectral class and temperature – Hydrogen as example

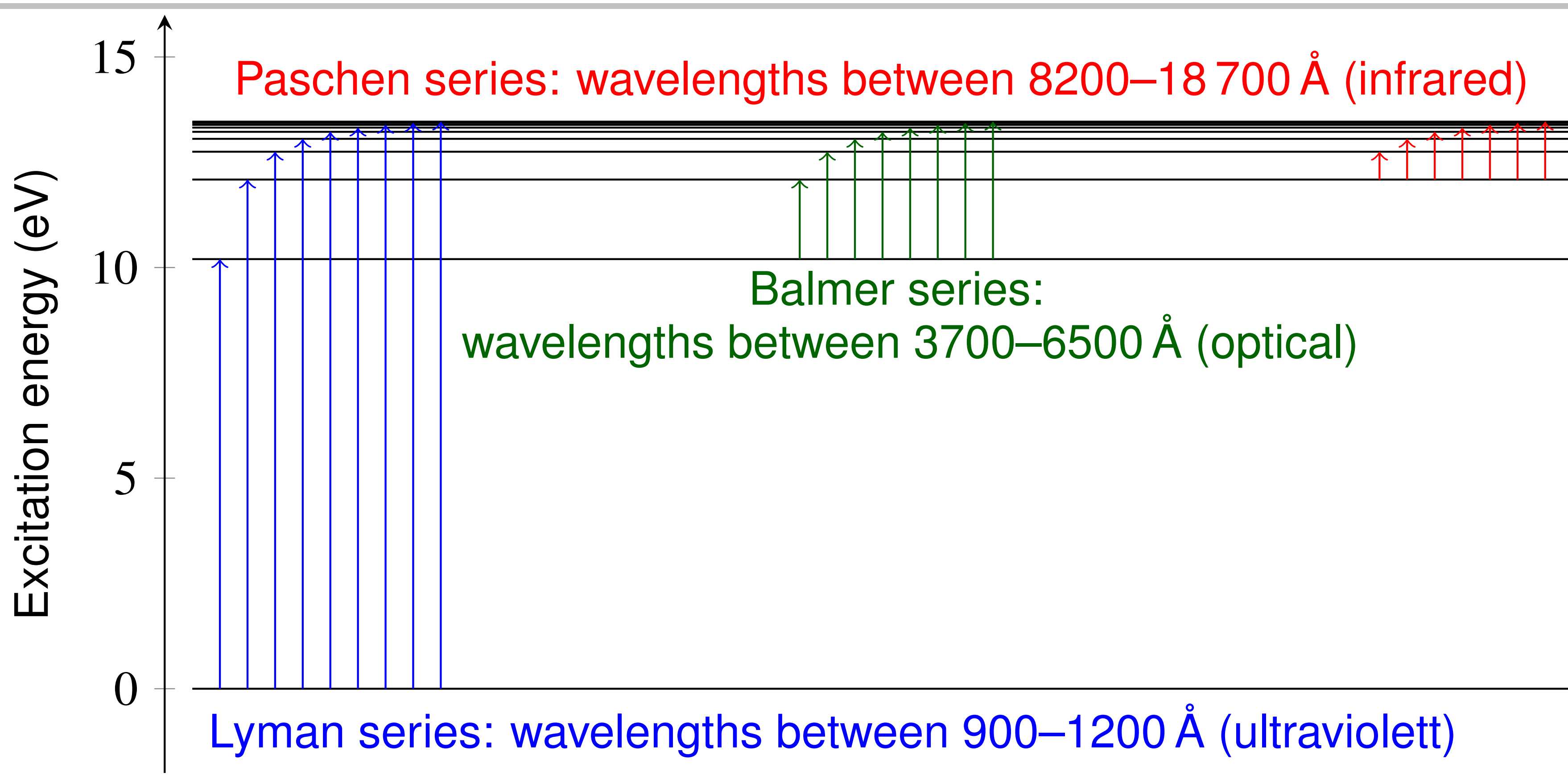

- Optical transitions only if first excited state is populated
- low temperatures, most atoms are in the ground state (Lyman series, UV)
- with increasing temperature first excited state gets populated (Balmer series, optical)
- for high temperatures hydrogen atoms get ionized, less atoms in first excited state

Luminosity classes

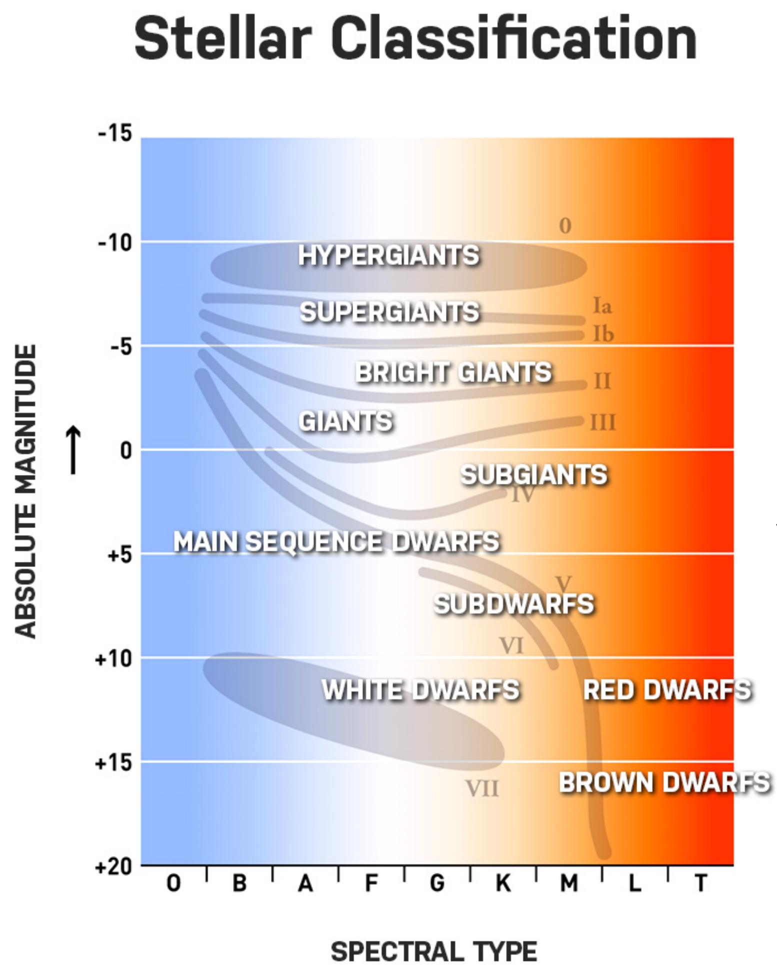

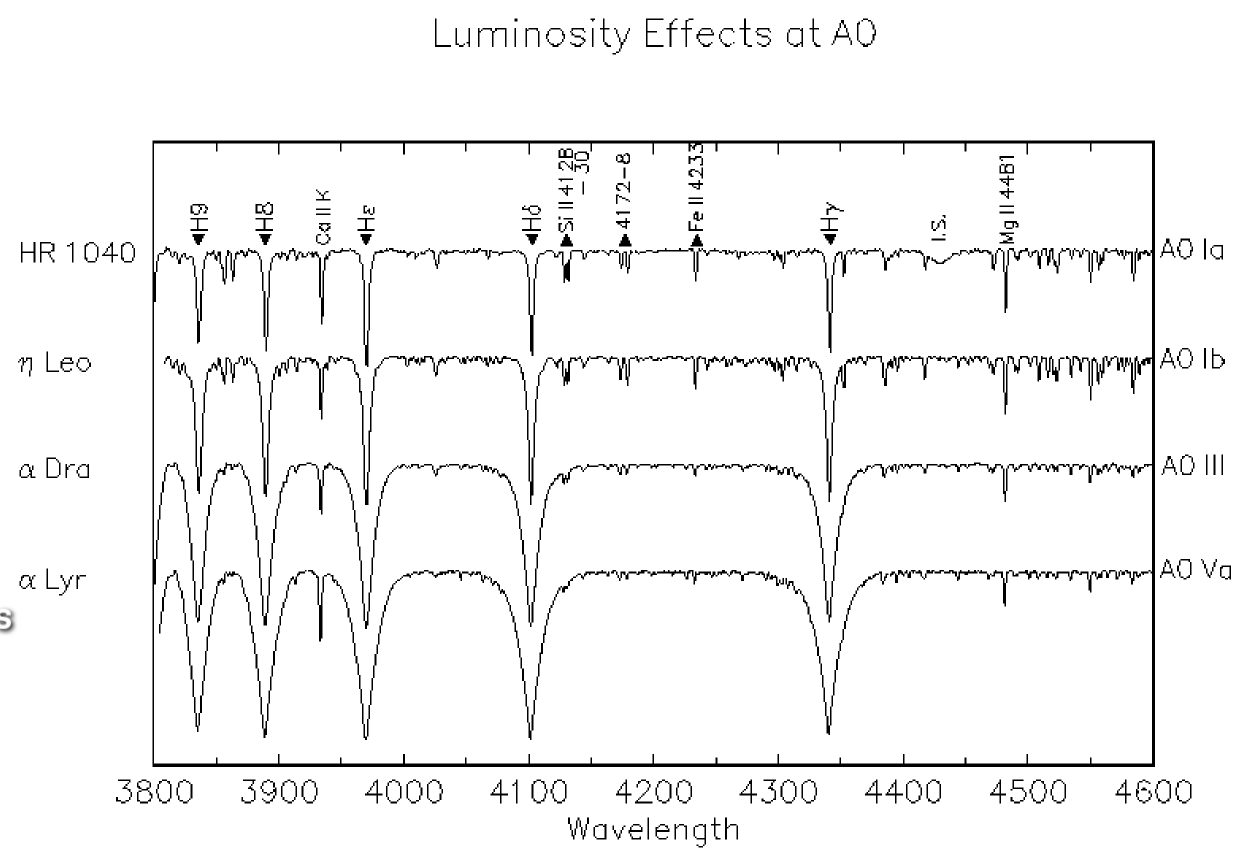

Wikipedia

http://ned.ipac.caltech.edu/level5/Gray/frames.html

Stellar structure equations

Mathematical preliminaries

Gradient of scalar field

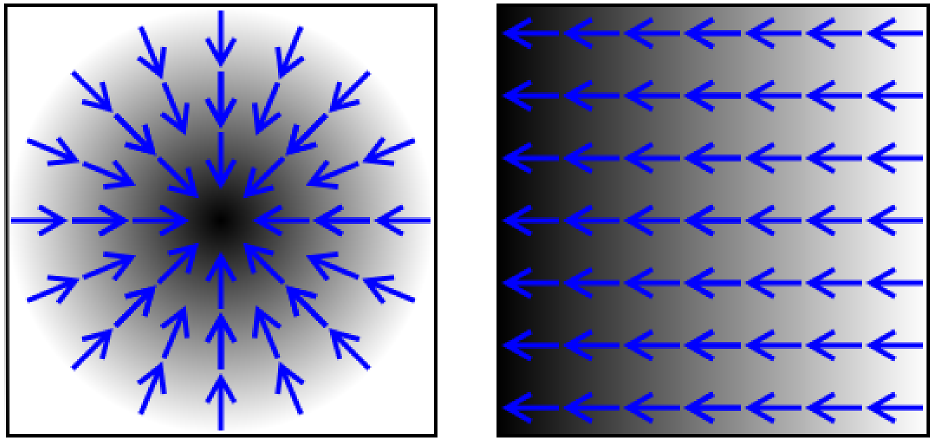

Scalar field: scalar value to every point in a space (e.g. temperature, gravitational potential)

Divergence of a vector field

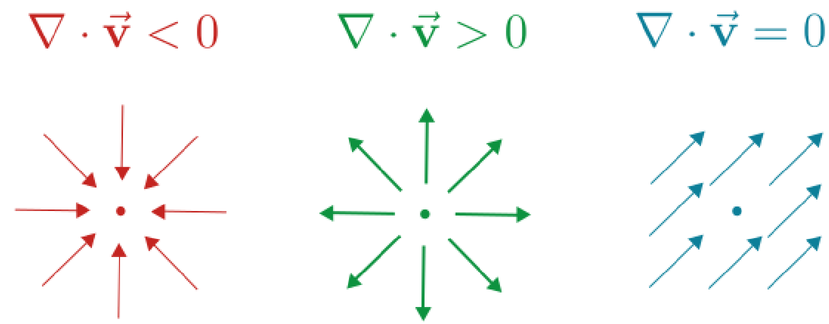

vector field: vector to each point in a subset of space (e.g. velocity field in a fluid)

Mathematical preliminaries

Spherical polar coordinates: scalar field V and vector field $\mathbf{F}$

$$\mathbf{F} = F_r\mathbf{a}_r + F_\theta\mathbf{a}_\theta + F_\phi\mathbf{a}_\phi \tag{5.1}$$

gradient of V

$$\nabla V = \frac{\partial V}{\partial r}\mathbf{a}_r + \frac{1}{r}\frac{\partial V}{\partial \theta}\mathbf{a}_\theta + \frac{1}{r\sin\theta}\frac{\partial V}{\partial \phi}\mathbf{a}_\phi \tag{5.2}$$

divergence of $\mathbf{F}$

$$\operatorname{div}\mathbf{F} = \frac{1}{r^2}\frac{\partial}{\partial r}(r^2F_r) + \frac{1}{r\sin\theta}\frac{\partial}{\partial\theta}(\sin\theta F_\theta) + \frac{1}{r\sin\theta}\frac{\partial F_\phi}{\partial\phi} \tag{5.3}$$

Laplacian of V: $\nabla^2 V = \operatorname{div}(\nabla V)$

$$\nabla^2 V = \frac{1}{r^2}\frac{\partial}{\partial r}\left(r^2\frac{\partial V}{\partial r}\right) + \frac{1}{r^2\sin\theta}\frac{\partial}{\partial\theta}\left(\sin\theta\frac{\partial V}{\partial\phi}\right) + \frac{1}{r^2\sin^2\theta}\frac{\partial^2 V}{\partial\phi^2} \tag{5.4}$$

horizontal component of vector $\mathbf{F}$

$$\mathbf{F}_\mathrm{h} = F_\theta\mathbf{a}_\theta + F_\phi\mathbf{a}_\phi \tag{5.5}$$

Coordinates and symmetries

Stars are clumps of gas, which are stabilized by the equilibrium of self-gravity and pressure

$\rightarrow$ Spherically symmetric configuration

$\rightarrow$ 3D problem reduces to 1D problem

$\rightarrow$ To characterize the full star and its evolution, one needs a temporal coordinate t and a spatial coordinate

Coordinates and symmetries

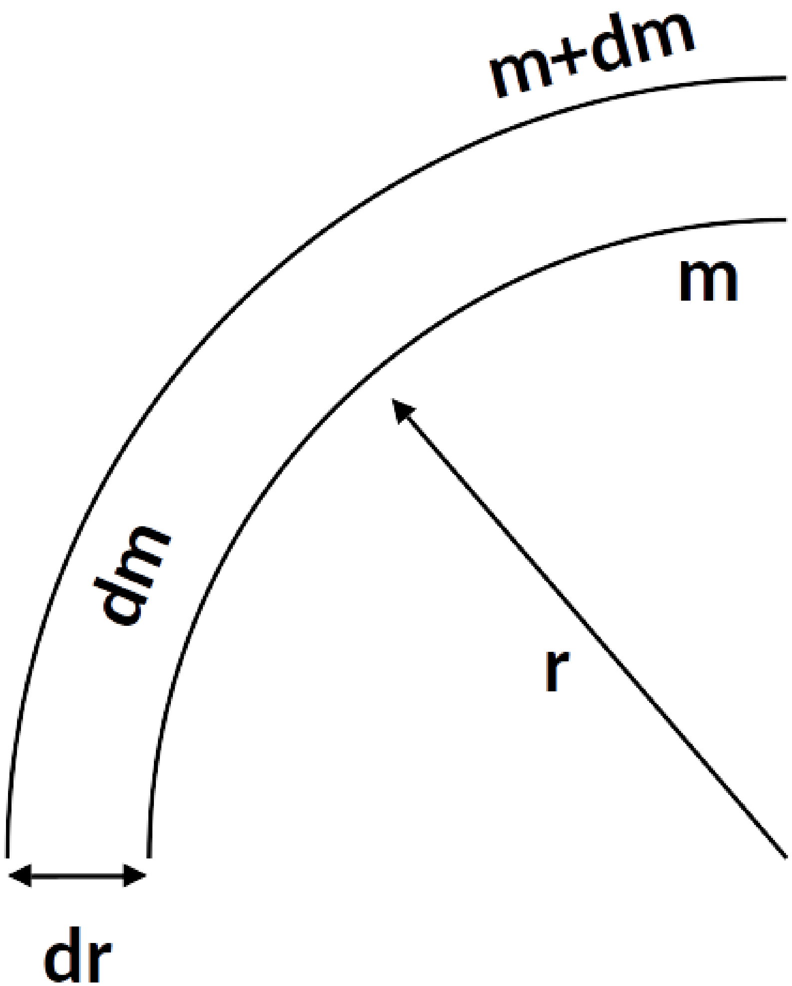

Eulerian description

- Spatial coordinate is distance r from the stellar center $\Rightarrow 0 \leq r \leq R$
- $m(r, t)$ mass of sphere of radius r at the time t

$$\Rightarrow \mathrm{d}m = 4\pi r^2 \rho \mathrm{d}r - 4\pi r^2 \rho v \mathrm{d}t$$

$\rho(r, t)$ density, v radial velocity

Conservation of mass

Coordinates and symmetries

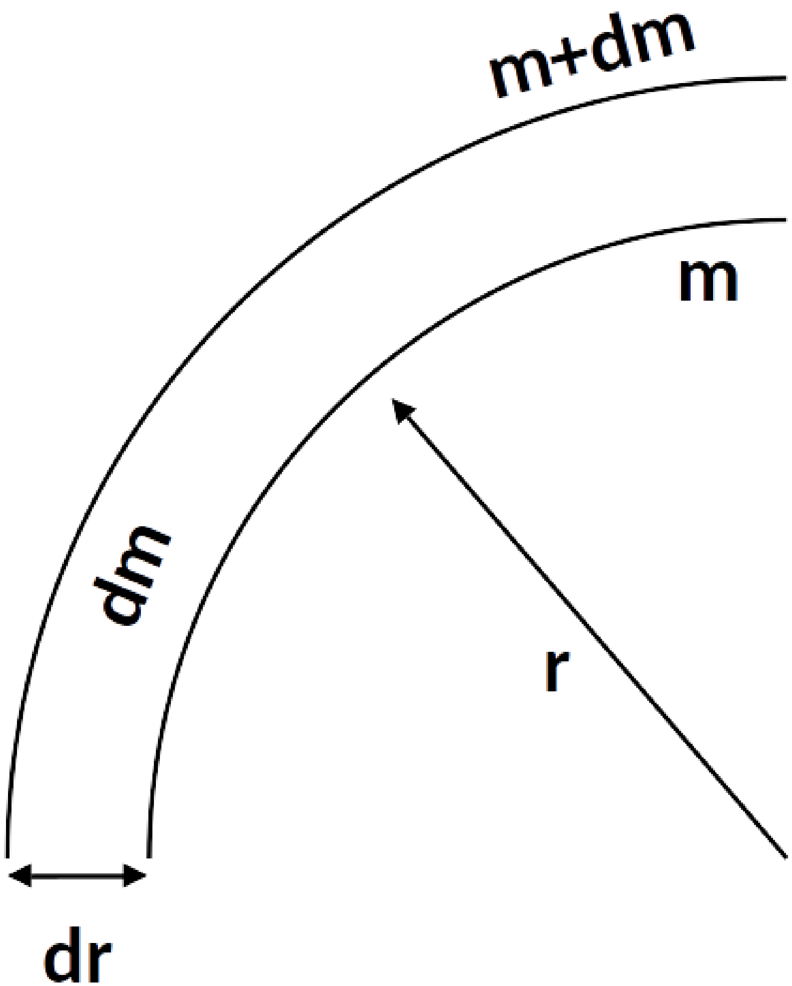

- Mass in sphere $r + \mathrm{d}r$ at constant t

$$\frac{\partial m}{\partial r} = 4\pi r^2 \rho \tag{5.6}$$

- Mass flow out of sphere $r + \mathrm{d}r$ due to radial velocity v within $\mathrm{d}t$

$$\frac{\partial m}{\partial t} = -4\pi r^2 \rho v \tag{5.7}$$

Conservation of mass (basic equation)

Coordinates and symmetries

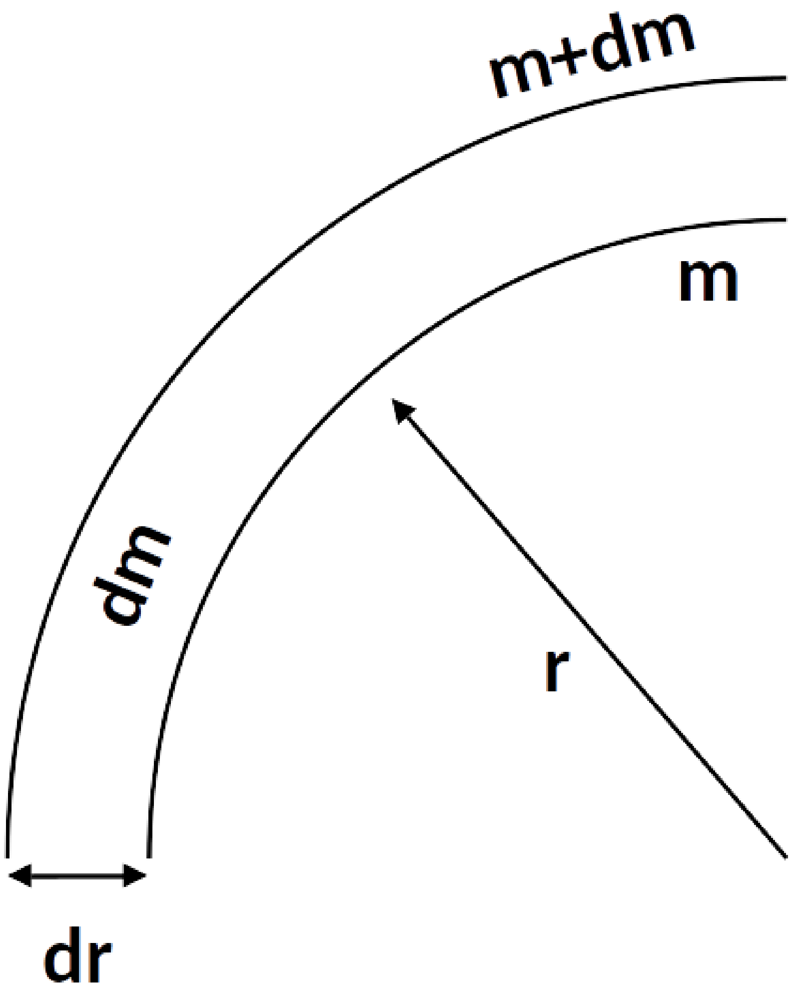

$$\frac{\partial}{\partial t}\left(\frac{\partial m}{\partial r}\right) = \frac{\partial}{\partial t}4\pi r^2\rho$$

$$\frac{\partial}{\partial r}\left(\frac{\partial m}{\partial t}\right) = \frac{\partial}{\partial r}[-4\pi r^2\rho v]$$

Symmetry

$$\frac{\partial}{\partial t}\left(\frac{\partial m}{\partial r}\right) = \frac{\partial}{\partial r}\left(\frac{\partial m}{\partial t}\right)$$

$$\Rightarrow 4\pi\frac{\partial}{\partial t}r^2\rho = -4\pi\frac{\partial}{\partial r}r^2\rho v$$

r independent of t

$$\Rightarrow \frac{\partial\rho}{\partial t} = -\frac{1}{r^2}\frac{\partial(\rho r^2 v)}{\partial r} = -\nabla\cdot(\rho v) \quad (5.8)$$

Continuity equation of hydrodynamics

Coordinates and symmetries

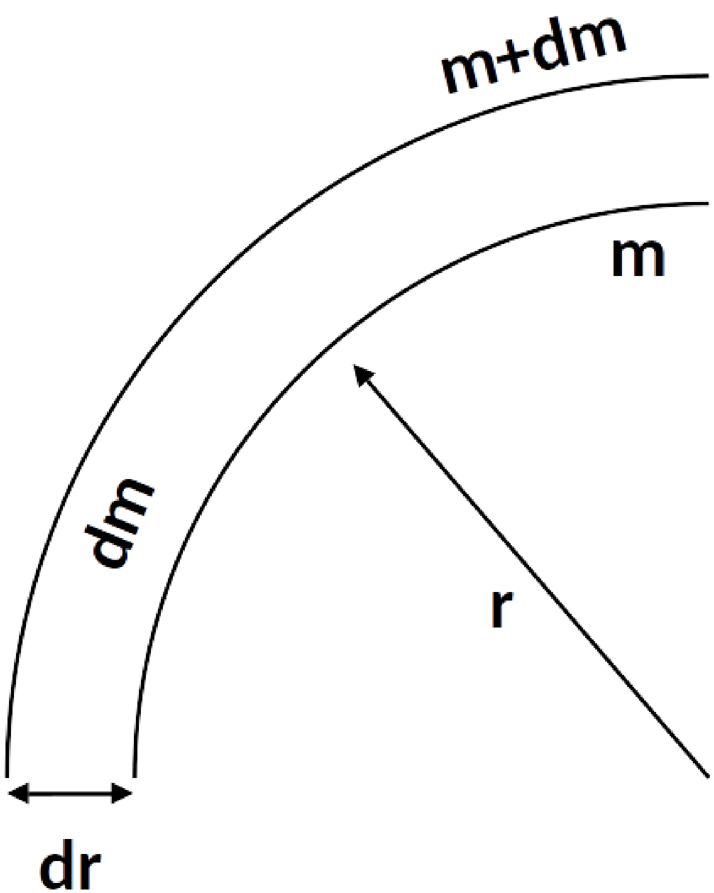

Advantageous as the mass of a star varies much less than the radius during stellar evolution
$\frac{M_{\max}}{M_{\min}} \sim 2-10$, $\frac{R_{\max}}{R_{\min}} \sim 10^3-10^8$

Lagrangian description

- Spatial coordinate is mass m contained in a concentric sphere
  $\Rightarrow m(r,t),\ 0 \le r \le R$
- $m(0,t) = 0$ mass at the center,
  $m(R,t) = M$ total mass

Coordinate transformation from (r,t) to (m,t)

$$\frac{\partial}{\partial m} = \frac{\partial}{\partial r} \cdot \frac{\partial r}{\partial m}$$

$$\left(\frac{\partial}{\partial t}\right)_m = \frac{\partial}{\partial r} \cdot \left(\frac{\partial r}{\partial t}\right)_m + \left(\frac{\partial}{\partial t}\right)_r$$

transformation between operators

$$\frac{\partial r}{\partial m} = \frac{1}{4\pi r^2 \rho} \Rightarrow \frac{\partial}{\partial m} = \frac{1}{4\pi r^2 \rho}\frac{\partial}{\partial r}$$

Gravitational field

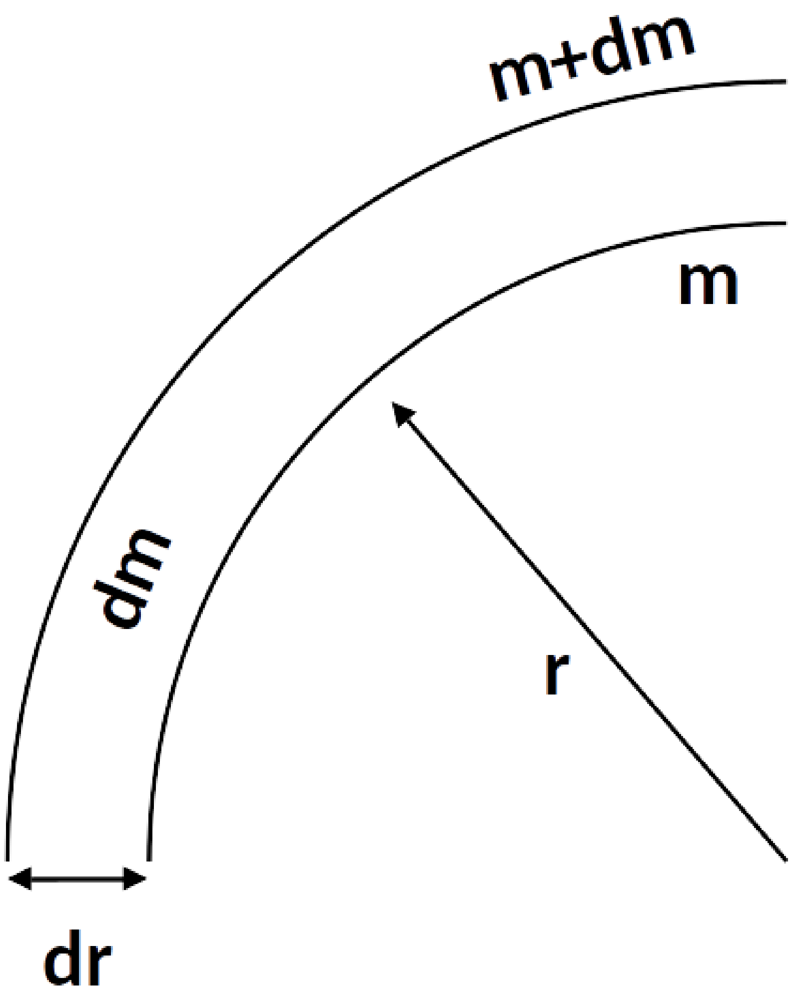

Inside a spherically symmetric body, the absolute value of gravitational acceleration g at r does not depend on the mass elements outside r

The gravitational potential Φ is a solution of the Poisson equation

$$\nabla^2\Phi = \frac{1}{r^2}\frac{\partial}{\partial r}\left(r^2\frac{\partial\phi}{\partial r}\right) = 4\pi G\rho$$

$$\Rightarrow g = \frac{\partial\Phi}{\partial r} = \frac{Gm}{r^2}$$

with G the gravitational constant

$$\Rightarrow \Phi(r) = \int_0^r \frac{Gm}{r^2}\mathrm{d}r + \text{constant}$$

$\Phi \to 0$ for $r \to \infty$

Hydrostatic equilibrium

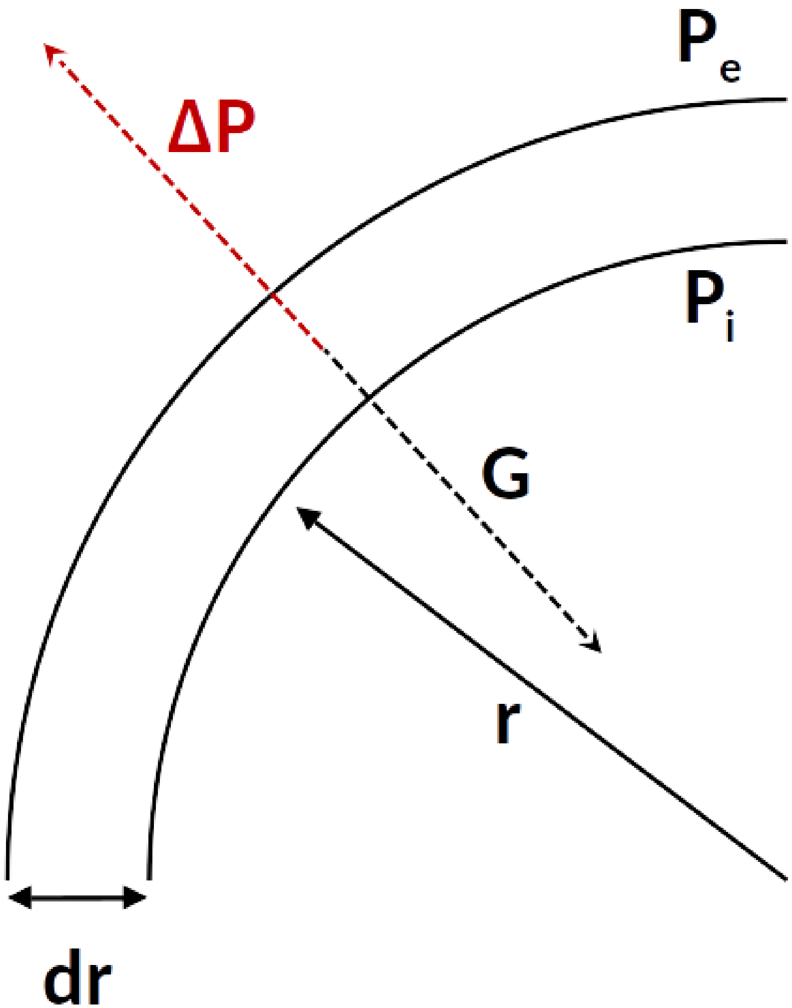

Gravitational force acting on shell at r with thickness dr inward

$$f_G = \frac{F_G}{dA} = -g\frac{dm}{dA} = -g\rho dr$$

Balanced by buoyancy force due to pressure difference outward

$$F_B = P_e dA - P_i dA = -dA\frac{\partial P}{\partial r}dr$$

In equilibrium, the sum of the two forces has to be zero ($F_G + F_B \overset{!}{=} 0$)

$$\rightarrow \frac{\partial P}{\partial r} = -g\rho \Leftrightarrow \frac{\partial P}{\partial m} = -\frac{g}{4\pi r^2} \qquad (5.9)$$

Equation of hydrostatic equilibrium (basic equation)

Equation of motion

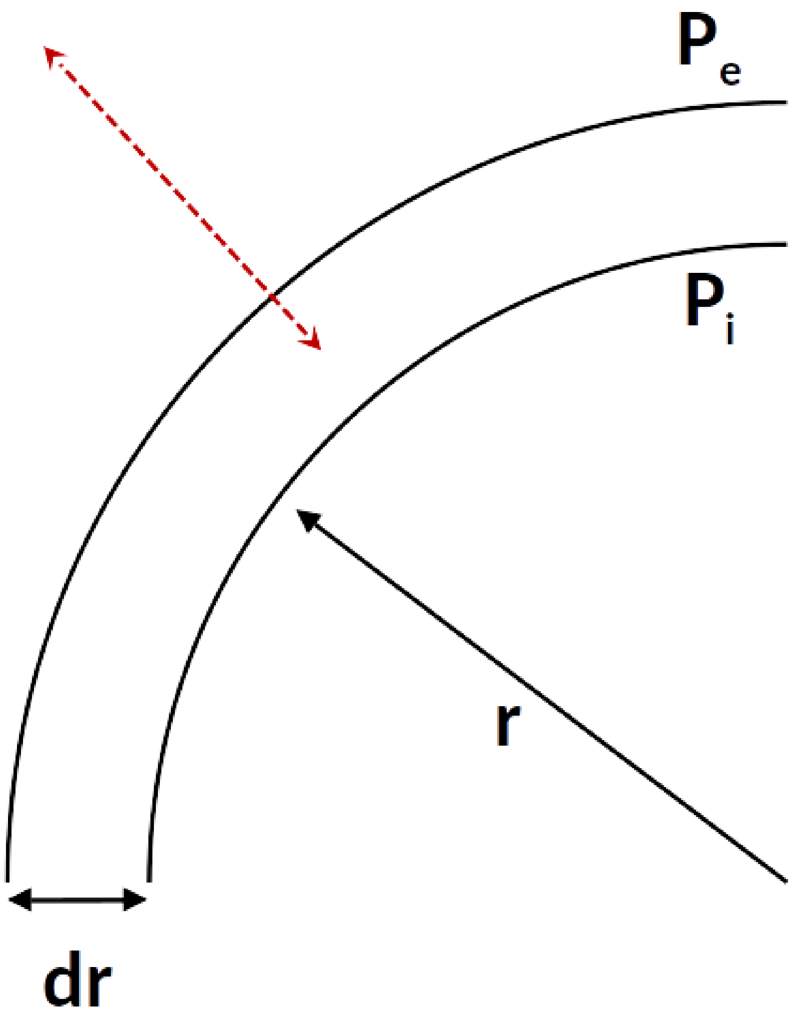

Star undergoes accelerated radial motion

$$0 \neq -\frac{\partial P}{\partial m} - \frac{g}{4\pi r^2}$$

Mass shell will be accelerated

$$\frac{\mathrm{d}m}{4\pi r^2}\frac{\partial^2 r}{\partial t^2} = f_\mathrm{G} + f_\mathrm{B} = -\frac{\partial P}{\partial m}\mathrm{d}m - g\frac{\mathrm{d}m}{4\pi r^2}$$

$$\frac{1}{4\pi r^2}\frac{\partial^2 r}{\partial t^2} = -\frac{\partial P}{\partial m} - \frac{g}{4\pi r^2} \qquad (5.10)$$

Equation of motion

Free-fall timescale

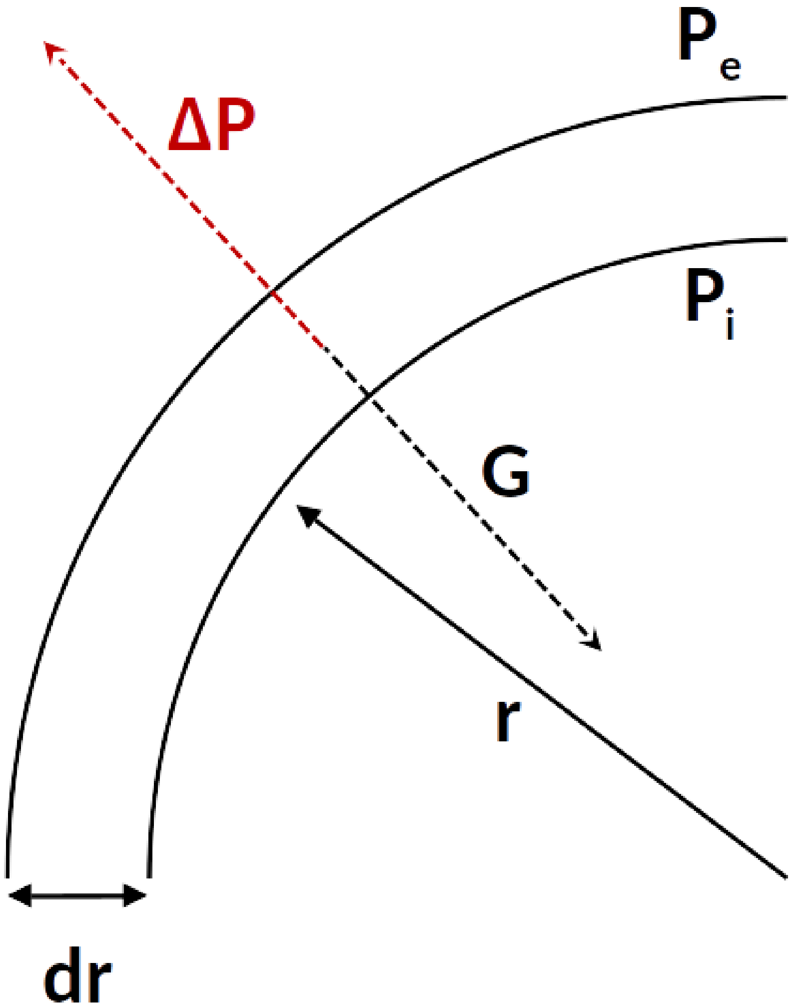

Reaction of the star to vanishing pressure

$$\frac{1}{4\pi r^2}\frac{\partial^2 r}{\partial t^2} = -\frac{g}{4\pi r^2}$$

Exercise sheet III

Calculation of free-fall timescale τ_{ff}

Explosive timescale

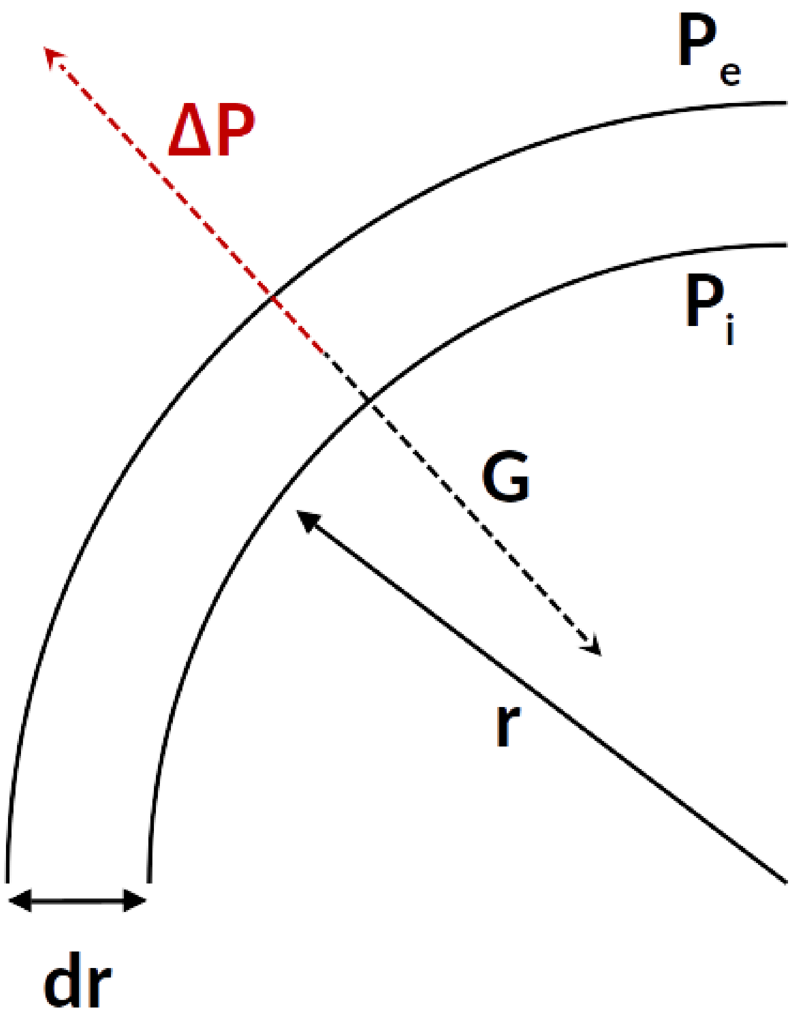

Reaction of the star to vanishing gravity

$$\frac{1}{4\pi r^2}\frac{\partial^2 r}{\partial t^2} = -\frac{\partial P}{\partial m}$$

Lagrangian/Eulerian transformation

$$4\pi r^2 \frac{\partial P}{\partial m} = \frac{\partial P}{\partial r}\frac{1}{\rho} = \frac{\bar{P}}{R\bar{\rho}}$$

$$\Rightarrow \frac{\partial^2 r}{\partial t^2} = -\frac{\bar{P}}{R\bar{\rho}}$$

Defining the characteristic **explosion timescale** τ_{expl}

$$\left|\frac{\partial^2 r}{\partial t^2}\right| = \frac{R}{\tau_{\mathrm{expl}}^2} = \frac{\bar{P}}{R\bar{\rho}}$$

$$\Rightarrow \tau_{\mathrm{expl}} \approx R\left(\frac{\bar{\rho}}{\bar{P}}\right)^{1/2}$$

τ_{expl} of the order of the time a sound wave needs to travel from center to surface

Hydrostatic time-scale

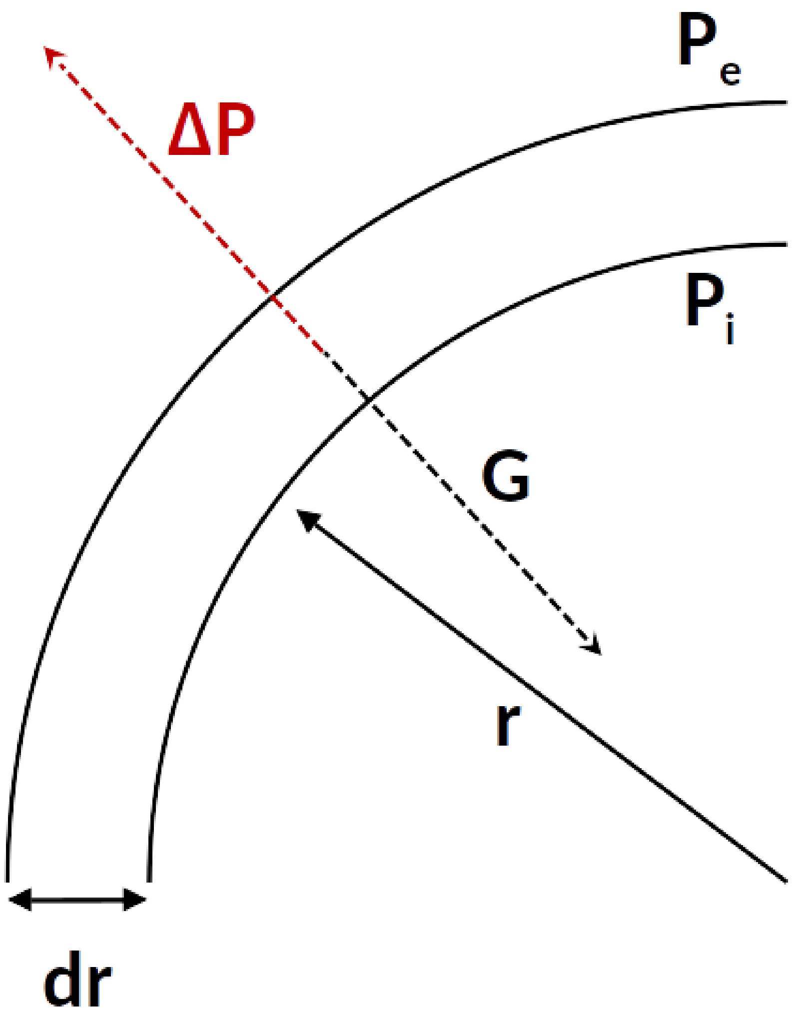

In near hydrostatic equilibrium

$$\tau_{\rm expl} \approx \tau_{\rm ff} = \tau_{\rm hydr}$$

$\tau_{\rm hydr}$ **hydrostatic time-scale** typical time in which a (dynamically stable) star reacts on a slight perturbation of hydrostatic equilibrium

$$\tau_{\rm hydr} \approx \left(\frac{R^3}{GM}\right)^{1/2} \approx \frac{1}{2}(G\bar{\rho})^{-1/2}$$

Much shorter than stellar evolution times $10^8 - 10^{10}$ yr

see Exercise sheet III

Virial theorem

Integrating the basic equation of hydrostatic equilibrium $\frac{\partial P}{\partial m} = -\frac{g}{4\pi r^2}$ over dm from center to surface and multiplying by the Volume $V = 4/3\pi r^3$

$$\Rightarrow \int_0^M \frac{Gm}{r}\mathrm{d}m = 3\int_0^P \frac{P}{\rho}\mathrm{d}m \tag{5.11}$$

Derivation Exercise sheet III

E_G **gravitational energy**: Potential energy of all mass elements dm of the star due to the gravitational field

$$E_\mathrm{G} := -\int_0^M \frac{Gm}{r}\mathrm{d}m$$

Energy needed to expand all mass shells to infinity

Virial theorem

What is the meaning of $3\int_0^P \frac{P}{\rho}\mathrm{d}m$?

Assuming an ideal gas with equation of state

$$P = nkT = \frac{R}{\mu}\rho T$$

with $\rho = n\mu m_\mathrm{u}$, n number of particles per volume, μ mean molecular weight, m_u atomic mass unit, k Boltzmann constant, $R = \frac{k}{m_\mathrm{u}}$ universal gas constant

$$\rightarrow \frac{P}{\rho} = \frac{R}{\mu}T = (c_\mathrm{P} - c_\mathrm{V})T = (\gamma - 1)c_\mathrm{V})T$$

with $c_{\mathrm{V,P}}$ specific heat capacities for constant V or P, $\frac{R}{\mu} = c_\mathrm{P} - c_\mathrm{V}$, $\gamma = \frac{c_\mathrm{P}}{c_\mathrm{V}}$ **for monoatomic gas:** $\gamma=\frac{5}{3}$

$$\Rightarrow \frac{P}{\rho} = \frac{2}{3}u$$

with $u = c_\mathrm{V}T$ internal energy per unit mass

Virial theorem

Virial theorem for monoatomic gas

$$\int_0^M \frac{Gm}{r}\mathrm{d}m = 2\int_0^M u\mathrm{d}m$$

$$E_\mathrm{G} = -2E_\mathrm{i} \tag{5.12}$$

E_i **internal energy** $:= \int_0^M u\mathrm{d}m$

E_G **gravitational energy** $:= -\int_0^M \frac{Gm}{r}\mathrm{d}m$

General virial theorem

$$\zeta E_\mathrm{i} + E_\mathrm{G} = 0 \tag{5.13}$$

where $\zeta u = 3\frac{P}{\rho}$

Ideal gas $\zeta = 3(\gamma - 1)$, monoatomic $\zeta = 2$

Virial theorem

W **Total energy**

$$W = E_\mathrm{i} + E_\mathrm{G}$$

for gravitationally bound systems $W < 0$

$$W = (1 - \zeta)E_\mathrm{i} = \frac{\zeta - 1}{\zeta}E_\mathrm{G}$$

All energy forms are coupled!

Energy loss via radiation with luminosity L

$$\frac{\mathrm{d}W}{\mathrm{d}t} + L = 0$$

$$\Rightarrow L = (\zeta - 1)\frac{\mathrm{d}E_\mathrm{i}}{\mathrm{d}t} = -\frac{\zeta - 1}{\zeta}\frac{\mathrm{d}E_\mathrm{G}}{\mathrm{d}t}$$

Contraction $\frac{\mathrm{d}E_\mathrm{G}}{\mathrm{d}t} < 0$ and ideal monoatmoic gas $L = -\frac{1}{2}\frac{\mathrm{d}E_\mathrm{G}}{\mathrm{d}t} = \frac{\mathrm{d}E_\mathrm{i}}{\mathrm{d}t}$

$\rightarrow$ Half of the energy radiated away, half heats the star

$\rightarrow$ Stars in hydrostatic equilibrium have a negative heat capacity, become hotter upon losing energy

Kelvin-Helmholtz/ thermal timescale

Evolutionary time for a contracting and cooling star

$$\tau_{\mathrm{KH}} := \frac{|E_{\mathrm{G}}|}{L} \approx \frac{E_{\mathrm{i}}}{L}$$

Rough estimate for $|E_{\mathrm{G}}| \approx \frac{G\bar{m}^2}{\bar{r}} \approx \frac{GM^2}{2R}$

$$\tau_{\mathrm{KH}} \approx \frac{GM^2}{2RL}$$

For the Sun $\tau_{\mathrm{KH}} \approx 1.6 \times 10^7$ yr

Thermodynamic relations

First law of thermodynamics

$$\mathrm{d}q = \mathrm{d}u + P\mathrm{d}V \tag{5.14}$$

q heat per unit mass, u internal energy per unit mass, $V = 1/\rho$ specific volume per unit mass

General equations of state $\rho = \rho(P, T, (X_i))$, $u = u(\rho, T, (X_i))$
$\to \mathrm{d}\rho/\rho = \alpha \mathrm{d}P/P - \delta \mathrm{d}T/T$

Derivatives with respect to P, T, other quantity stays constant

$$\alpha = \left(\frac{\partial \ln \rho}{\partial \ln P}\right)_T = -\frac{P}{V}\left(\frac{\partial V}{\partial P}\right)_T$$

$$\delta = \left(\frac{\partial \ln \rho}{\partial \ln T}\right)_P = -\frac{T}{V}\left(\frac{\partial V}{\partial T}\right)_P$$

c_P, c_V **specific heats**

$$c_P = \left(\frac{\mathrm{d}q}{\mathrm{d}T}\right)_P = \left(\frac{\partial u}{\partial T}\right)_P + P\left(\frac{\partial V}{\partial T}\right)_P \tag{5.15}$$

$$c_V = \left(\frac{\mathrm{d}q}{\mathrm{d}T}\right)_V = \left(\frac{\partial u}{\partial T}\right)_V$$

Thermodynamic relations

Total derivative

$$\mathrm{d}u = \left(\frac{\partial u}{\partial V}\right)_T \mathrm{d}V + \left(\frac{\partial u}{\partial T}\right)_V \mathrm{d}T$$

$\rightarrow$ change of the **specific entropy** $\mathrm{d}s = \mathrm{d}q/T$

$$\mathrm{d}s = \frac{\mathrm{d}q}{T} = \frac{1}{T}\left[\left(\frac{\partial u}{\partial V}\right)_T + P\right]\mathrm{d}V + \frac{1}{T}\left(\frac{\partial u}{\partial T}\right)_V \mathrm{d}T$$

Symmetry of total derivative: $\partial^2 s/\partial T\partial V = \partial^2 s/\partial V\partial T$

$$\frac{\partial}{\partial T}\left[\frac{1}{T}\left(\frac{\partial u}{\partial V}\right)_T + \frac{P}{T}\right] = \frac{1}{T}\frac{\partial^2 u}{\partial T\partial V} \Rightarrow \left(\frac{\partial u}{\partial V}\right)_T = T\left(\frac{\partial P}{\partial T}\right)_V - P$$

analogue you can derive $\left(\frac{\partial u}{\partial T}\right)_P$ and use it for calculating the specific heats:

$$c_P - c_V = \left(\frac{\partial u}{\partial T}\right)_P + P\left(\frac{\partial V}{\partial T}\right)_P - \left(\frac{\partial u}{\partial T}\right)_V = \left(\frac{\partial V}{\partial T}\right)_P\left(\frac{\partial P}{\partial T}\right)_V T$$

using the definitions for α and δ

$$\left(\frac{\partial P}{\partial T}\right)_V = -\frac{\left(\frac{\partial V}{\partial T}\right)_P}{\left(\frac{\partial V}{\partial P}\right)_T} = \frac{P\delta}{T\alpha} \Rightarrow c_P - c_V = T\left(\frac{\partial V}{\partial T}\right)_P\frac{P\delta}{T\alpha} = \frac{P\delta^2}{\rho T\alpha} = \frac{R}{\mu} \text{ (perfect gas)}$$

Thermodynamic relations

rewrite the first law of thermodynamics in Terms of T and P

$$dq = du + PdV = \left(\frac{\partial u}{\partial T}\right)_V dT + \left[\left(\frac{\partial u}{\partial V}\right)_T + P\right] dV = \left(\frac{\partial u}{\partial T}\right)_V dT + T\left(\frac{\partial P}{\partial T}\right)_V dV$$

using the previous relations and use $\rho = 1/V$ instead of V (Kippenhahn & Weigert 2012 for more details)

$$dq = c_P dT - \frac{\delta}{\rho} dP \tag{5.16}$$

next we define the adiabatic temperature gradient $\nabla_{\rm ad}$:

$$\nabla_{\rm ad} := \left(\frac{\partial \ln T}{\partial \ln P}\right)_s$$

valid for constant entropy $\rightarrow ds = dq/T = 0$

$$0 = dq = c_P dT - \frac{\delta}{\rho} dP \Rightarrow \left(\frac{dT}{dP}\right)_s = \frac{\delta}{\rho c_P}$$

$$\nabla_{\rm ad} \equiv \left(\frac{P}{T}\frac{dT}{dP}\right)_s = \frac{P\delta}{T\rho c_P} \tag{5.17}$$

Mean molecular weight and perfect gas

Equation of state for perfect gas consisting of n particles per unit volume with molecular weight μ having a density of $\rho = n\mu m_\mathrm{u}$ ($R = \frac{k}{m_\mathrm{u}}$)

$$P = nkT = \frac{R}{\mu}\rho T$$

Gas in stellar interiors is usually fully ionized $\rightarrow$ Mixture of nuclei and free electron gas, can be treated like a one-component gas, if all gases are perfect

Mixture of i kinds of fully ionized nuclei with weight fractions X_i, molecular weight μ_i, charge number Z_i, number of nuclei per volume n_i, and partial density ρ_i (Mass of the electrons is neglected here)

$$X_i = \rho_i/\rho \qquad n_i = \frac{\rho_i}{\mu_i m_\mathrm{u}} = \frac{\rho}{m_\mathrm{u}}\frac{X_i}{\mu_i}$$

Total pressure P is sum of the partial pressures due to the nuclei P_i and the electrons P_e

$$P = P_e + \sum_i P_i = \left(n_e + \sum_i n_i\right) kT$$

Mean molecular weight and perfect gas

Contribution of one completely ionized atom to the total number of particles is one nucleus and Z_i electrons

$$\Rightarrow n = n_e + \sum_i n_i = \sum_i (1 + Z_i) n_i = \sum_i (1 + Z_i) \frac{\rho}{m_\mathrm{u}} \frac{X_i}{\mu_i}$$

$\rightarrow$ Equation of state

$$P = nkT = \sum_i \frac{k}{m_\mathrm{u}} \frac{X_i(1 + Z_i)}{\mu_i} \rho T = \frac{R}{\mu} \rho T \tag{5.18}$$

Mean molecular weight μ:

$$\mu = \left(\sum_i \frac{X_i(1 + Z_i)}{\mu_i} \right)^{-1} \tag{5.19}$$

Thermodynamic quantities for perfect, monoatomic gas

Internal energy is kinetic energy of translational motion of the particles only

$$u = \frac{3}{2}kT\frac{n}{\rho}$$

$$c_P = \frac{5}{2}\frac{R}{\mu} \qquad c_V = \frac{3}{2}\frac{R}{\mu}$$

$$\nabla_{\mathrm{ad}} = \frac{R}{\mu c_P} = \frac{2}{5} \qquad \alpha = \delta = 1$$

adiabatic changes

$$\gamma_{\mathrm{ad}} := \left(\frac{\partial \ln P}{\partial \ln \rho}\right)_s = \frac{c_P}{c_V} = \frac{1}{\alpha - \delta\nabla_{\mathrm{ad}}} = \frac{5}{3} \tag{5.20}$$

Conservation of energy

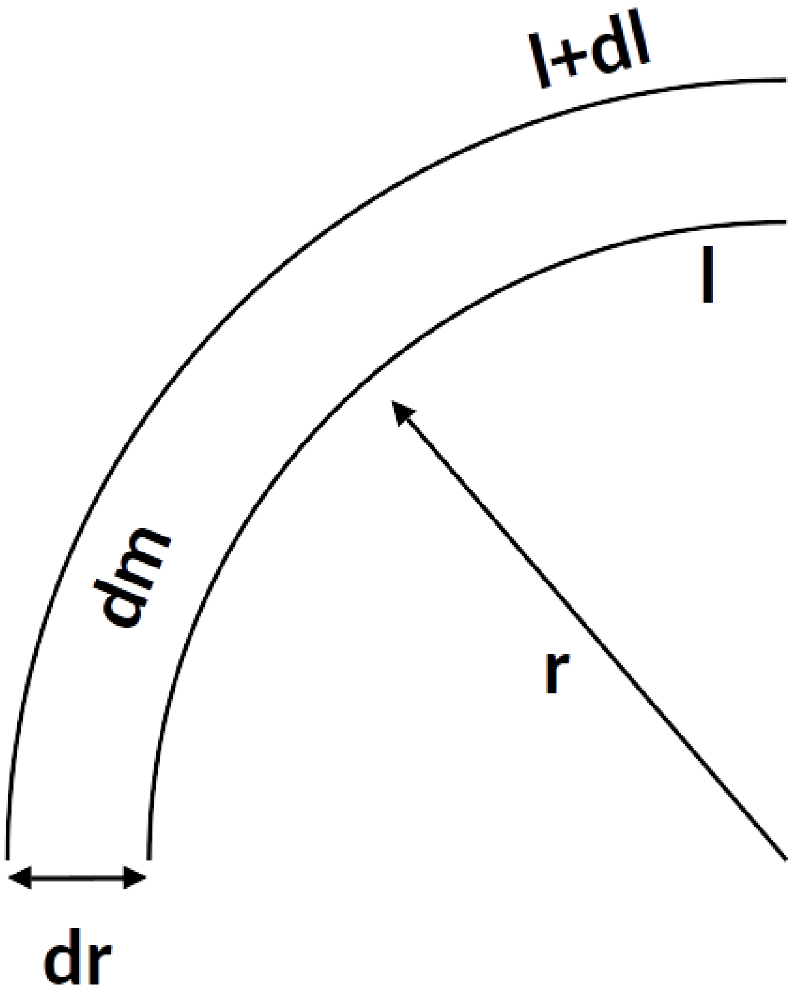

Net energy $l(r)$ per second passing outward through a sphere with radius r

$l(0) = 0$ at center, $l(R) = L$ at surface

$\rightarrow$ in between dependent of distribution of sources and sinks of energy

Stationary case $\mathrm{d}l$ due to release of nuclear energy only, ϵ nuclear energy per unit mass and second

$$\mathrm{d}l = 4\pi r^2 \rho\epsilon \mathrm{d}r = \epsilon \mathrm{d}m \Rightarrow \frac{\partial l}{\partial m} = \epsilon$$

Non-Stationary case $\mathrm{d}l$ can change its internal energy and exchange mechanical work

$$\mathrm{d}q = \left(\epsilon - \frac{\partial l}{\partial m}\right) \mathrm{d}t$$

$\mathrm{d}q$ heat per unit mass added to shell in $\mathrm{d}t$

Conservation of energy

$$\mathrm{d}u + P\mathrm{d}V \overset{5.14}{=} \mathrm{d}q = \left(\epsilon - \frac{\partial l}{\partial m}\right)\mathrm{d}t \overset{5.16}{=} c_P\mathrm{d}T - \frac{\delta}{\rho}\mathrm{d}P$$

$$\Rightarrow \frac{\partial l}{\partial m} = \epsilon - \frac{\partial u}{\partial t} - P\frac{\partial V}{\partial t} \overset{V=1/\rho}{=} \epsilon - \frac{\partial u}{\partial t} - \frac{P}{\rho^2}\frac{\partial \rho}{\partial t}$$

$$\Rightarrow \frac{\partial l}{\partial m} = \epsilon - c_P\frac{\partial T}{\partial t} + \frac{\delta}{\rho}\frac{\partial P}{\partial t} \qquad (5.21)$$

Conservation of energy (basic equation)

terms containing the time derivatives combined in a source function

$$\epsilon_\mathrm{g} := -T\frac{\partial s}{\partial t} \overset{\mathrm{d}s=\mathrm{d}q/T}{=} -c_P\frac{\partial T}{\partial t} + \frac{\delta}{\rho}\frac{\partial P}{\partial t} \overset{5.17}{=} -c_P T\left(\frac{1}{T}\frac{\partial T}{\partial t} - \frac{\nabla_\mathrm{ad}}{P}\frac{\partial P}{\partial t}\right)$$

$$\frac{\partial l}{\partial m} = \epsilon + \epsilon_\mathrm{g}$$

Conservation of energy

Neutrino losses have to be considered. Formed by nuclear energy reactions or other reactions, but do not interact with stellar material and act as energy sink.

Complete energy equation:

$$\frac{\partial l}{\partial m} = \epsilon - \epsilon_\nu + \epsilon_{\rm g} \tag{5.22}$$

The energy per second carried away from the star by neutrinos is often called the **neutrino luminosity**:

$$L_\nu := \int_0^M \epsilon_\nu \mathrm{d}m$$

Nuclear timescale

Star balances its energy loss L essentially by release of nuclear energy. If L is constant this can go on for a **nuclear timescale** τ_n:

$$\tau_\mathrm{n} := \frac{E_\mathrm{n}}{L} \tag{5.23}$$

E_n total nuclear energy

Example Sun completely consisting of hydrogen:

$E_\mathrm{n} = QM_\odot = 6.3 \times 10^{18}\mathrm{erg\,g}^{-1} M_\odot = 1.25 \times 10^{52}\mathrm{erg},\ L = 4 \times 10^{33}\mathrm{erg/s}$

$\Rightarrow \tau_\mathrm{n} = 10^{11}\ \mathrm{yr}$

For stars with stable nuclear burning of hydrogen or helium

$$\tau_\mathrm{n} \gg \tau_\mathrm{KH} \gg \tau_\mathrm{hydr}$$

In this case, the equation of energy conservation simplifies to

$$\frac{\partial l}{\partial m} \approx \epsilon$$

Transport of energy

- energy the star radiates away replenished from reservoirs situated in the very hot central region $\rightarrow$ effective transfer of energy through the stellar material
- possible due to a non-vanishing temperature gradient in the star
- Depending on the local physical situation, transfer can occur mainly via radiation, conduction, and convection
- ”particles” (photons, atoms, electrons, ”blobs” of matter) are exchanged between hotter and cooler parts
- their mean free path together with the temperature gradient of the surroundings will play a decisive role

Energy transport by radiation

Mean free path $l_{\rm ph}$ of a photon in the stellar interior

$$l_{\rm ph} = \frac{1}{\kappa\rho} \tag{5.24}$$

κ average absorption coefficient

For sun: $\kappa \approx 1\,\mathrm{cm^2g^{-1}}$, $\rho_\odot \approx 3\mathrm{M}_\odot/4\pi\mathrm{R}_\odot^3 \Rightarrow \mathrm{l_{ph}} \approx 2\,\mathrm{cm}$

Stellar interiors are extremely opaque

Mean free path of photons is much smaller than stellar radius

$\rightarrow$ Energy transport can be simplified as diffusion process

typical **Temperature gradient**

$$\frac{\Delta T}{\Delta r} \approx \frac{T_{\rm center} - T_{\rm surface}}{R_\odot} \approx \frac{10^7\,\mathrm{K} - 10^4\,\mathrm{K}}{R_\odot} \approx 1.4 \times 10^{-4}\,\mathrm{K\,cm^{-1}} \tag{5.25}$$

differences of temperature very small $\rightarrow$ in stellar interiors very close to thermal equilibrium, radiation very close to black body

energy density of radiations $u \sim T^4$

$\rightarrow$ relative anisotropy $4\Delta T/T \sim 10^{-10}$: carrier of the stars' huge luminosity

Energy transport by radiation

diffusive flux j of particles (per unit area and time) between different particle densities n

$$\mathbf{j} = -D\nabla n \tag{5.26}$$

Coefficient of diffusion $D = \frac{1}{3} v l_\mathrm{p}$ with v mean velocity and l_p mean free path of the particles

transition from particles to radiation

$$\begin{aligned} n &\rightarrow U = aT^4 \\ \mathbf{j} &\rightarrow \mathbf{F} \\ l_\mathrm{p} &\rightarrow l_\mathrm{ph} \\ v &\rightarrow c \end{aligned}$$

Energy density of radiation U (a radiation density constant), $\mathbf{F}$ radiative flux

Spherical symmetry

$$F_r = |\mathbf{F}| = F$$

$$\nabla U \rightarrow \frac{\partial U}{\partial r}$$

Energy transport by radiation

$$\Rightarrow \frac{\partial U}{\partial r} = 4aT^3 \frac{\partial T}{\partial r}$$

with 5.24 and 5.26 follows for the flux:

$$F = -\frac{4ac}{3}\frac{T^3}{\kappa\rho}\frac{\partial T}{\partial r} \tag{5.27}$$

using the local luminosity $l = 4\pi r^2 F$ we can solve for the temperature gradient

$$\frac{\partial T}{\partial r} = -\frac{3}{16\pi ac}\frac{\kappa\rho l}{r^2 T^3} \Leftrightarrow \frac{\partial T}{\partial m} = -\frac{3}{64\pi^2 ac}\frac{\kappa l}{r^4 T^3} \tag{5.28}$$

Basic equation for **radiative transport** of energy

Only valid in the stellar interior!

κ needs to be a mean over all frequencies (e.g. Rosseland mean)

$$\frac{\partial T}{\partial P} = \frac{\partial T/\partial m}{\partial P/\partial m} \overset{\frac{\partial P}{\partial m} = -\frac{Gm}{4\pi r^4}}{=} \frac{3}{16\pi acG}\frac{\kappa l}{mT^3}$$

$$\nabla_{\mathrm{rad}} = \left(\frac{\mathrm{d}\ln T}{\mathrm{d}\ln P}\right)_{\mathrm{rad}} = \frac{3}{16\pi acG}\frac{\kappa l P}{mT^4} \tag{5.29}$$

Gradient describing the temperature variation with depth

Energy transport by conduction

Heat conduction: Energy transfer via collisions of particles (electrons, nuclei or atoms, molecules) in random thermal motion

$\rightarrow$ mean free paths and velocities several orders of magnitude less than for photons

$\rightarrow$ in ”ordinary” stellar matter negligible

$\rightarrow$ Important for degenerate matter(high densities), e.g. interiors of white dwarfs: increases velocities and mean free path of electrons

$\rightarrow$ Diffusion approximation can be used as well

$$F_{\text{cond}} = -\frac{4ac}{3}\frac{T^3}{\kappa_{\text{cond}}\rho}\frac{\partial T}{\partial r} \tag{5.30}$$

$$\Rightarrow \mathbf{F} = \mathbf{F}_{\text{rad}} + \mathbf{F}_{\text{cd}}$$

Stability against convection

Heat and mass transfer occurs via streams of stellar gas

$\rightarrow$ Hot gas bubbles rise, while cooler material sinks down

$\rightarrow$ Whether or not convection is driven in certain regions of the star depends on the stability of the material against small perturbations and give rise to macroscopic local (non- spherical) motions that are also statistically distributed over the sphere

Stability against convection

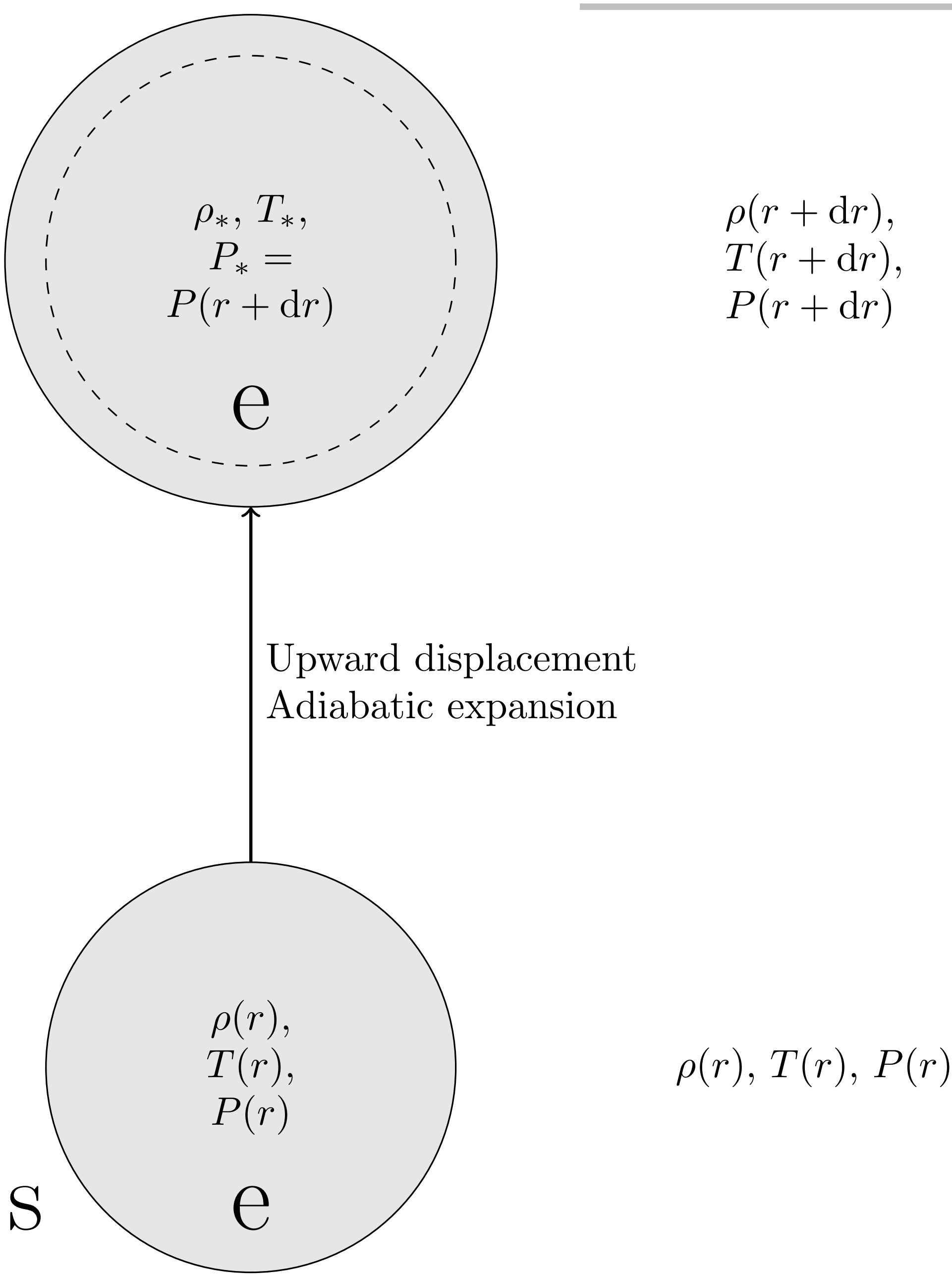

Dynamic instability

$\rightarrow$ No heat exchange of moving elements: adiabatic

$\rightarrow$ pressure equilibrium with surrounding

Change of property of mass element e with respect to surrounding s for any quantity A:

$$DA = A_\mathrm{e} - A_\mathrm{s}$$

Stability against convection

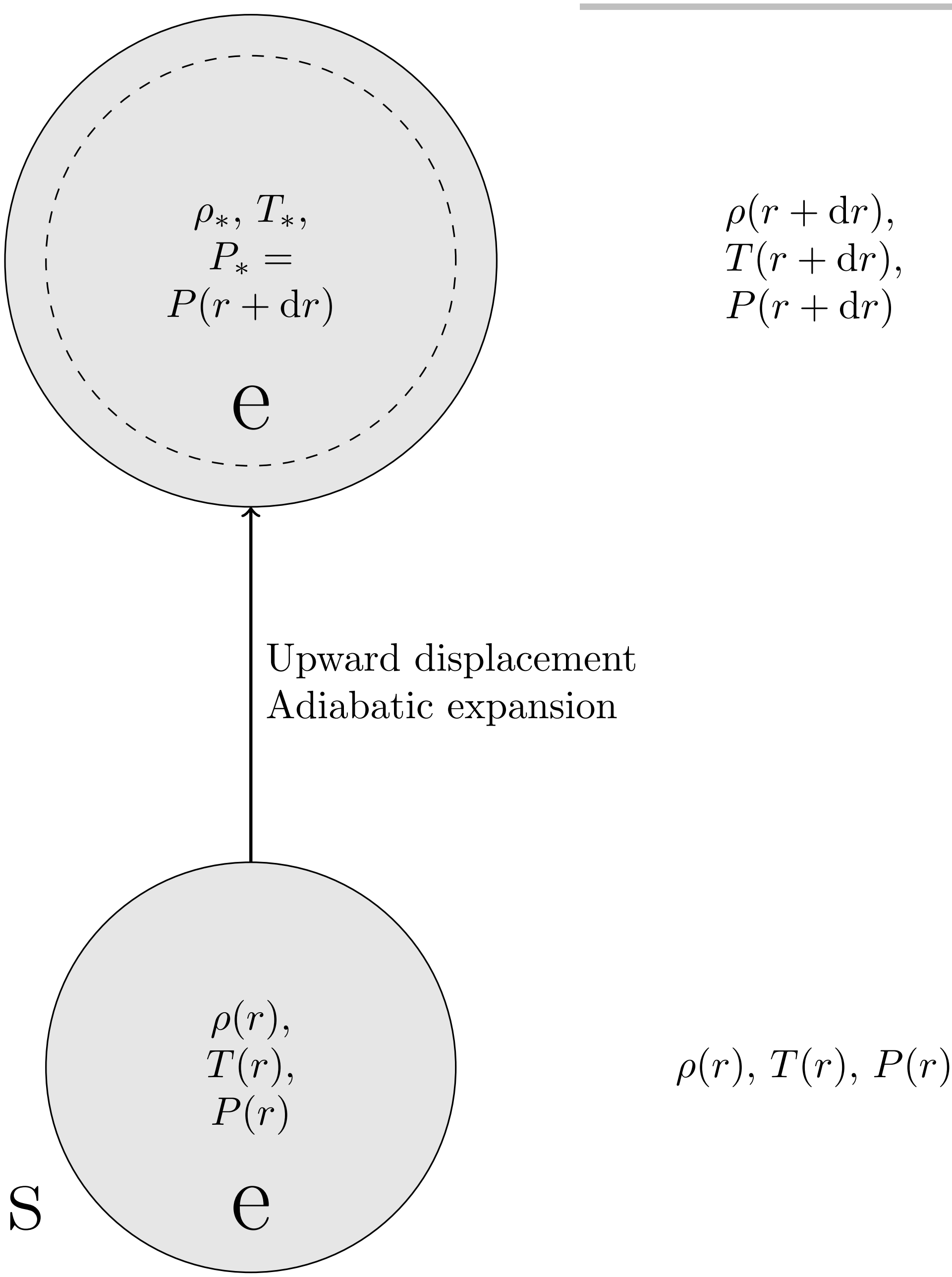

slightly hotter element

$$DT > 0$$

No increase in pressure, because elements will expand immediately

$$DP = 0$$

perfect gas with $\rho \sim P/T$:

$$D\rho < 0$$

$\Rightarrow$ Element is lighter than surrounding material

$\Rightarrow$ Buoyancy force will lift it upward

Stability against convection

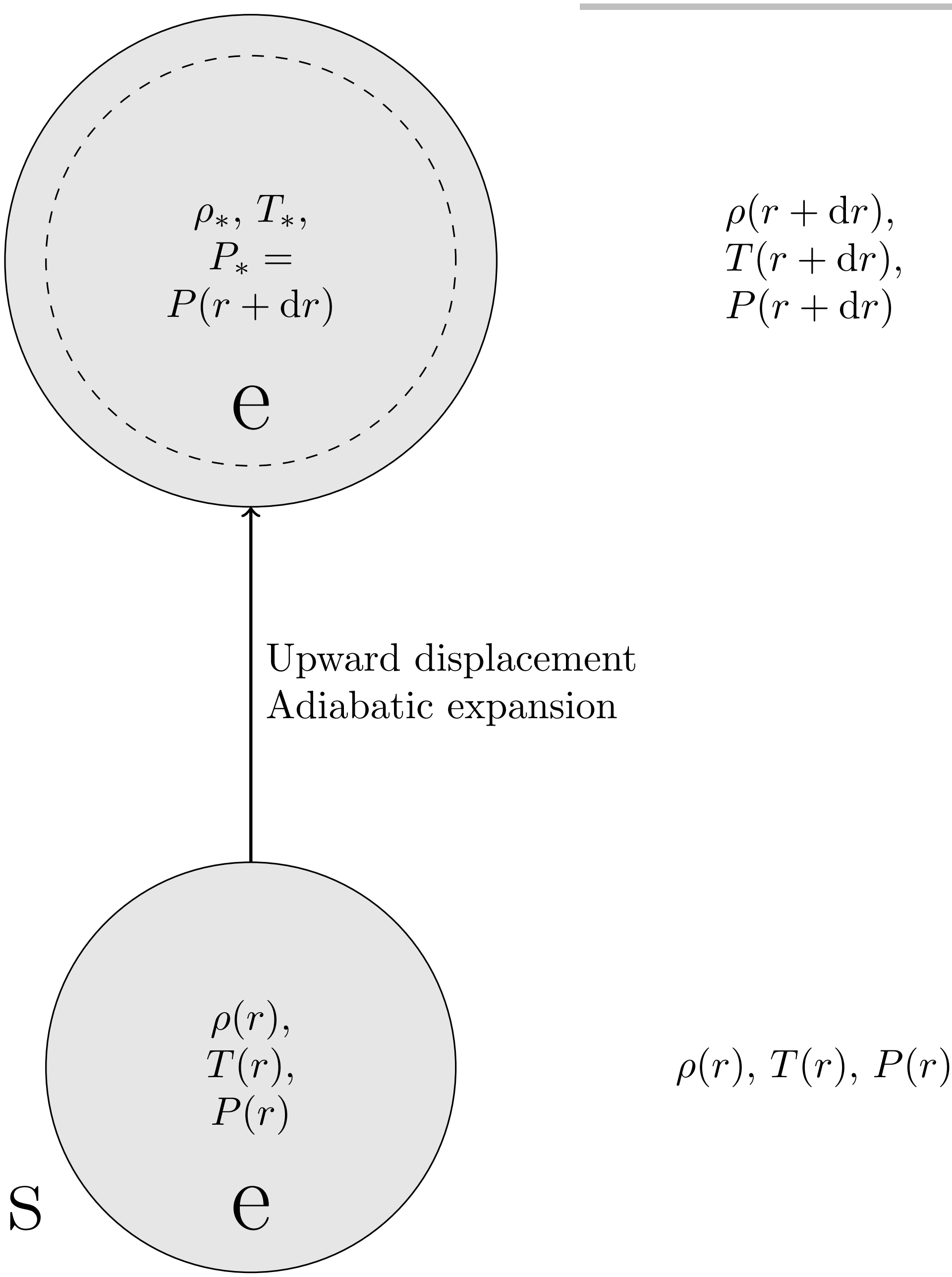

Density difference at new position

$$D\rho = \left[\left(\frac{\mathrm{d}\rho}{\mathrm{d}r}\right)_\mathrm{e} - \left(\frac{\mathrm{d}\rho}{\mathrm{d}r}\right)_\mathrm{s}\right]\mathrm{d}r$$

For $D\rho < 0$:

Boyancy force $K_r = -gD\rho > 0$ is directed upward

$\rightarrow$ perturbation is increased

Unstable!

For $D\rho > 0$:

Boyancy force $K_r = -gD\rho > 0$ is directed downward

$\rightarrow$ perturbation is removed

Stable!

Stability against convection

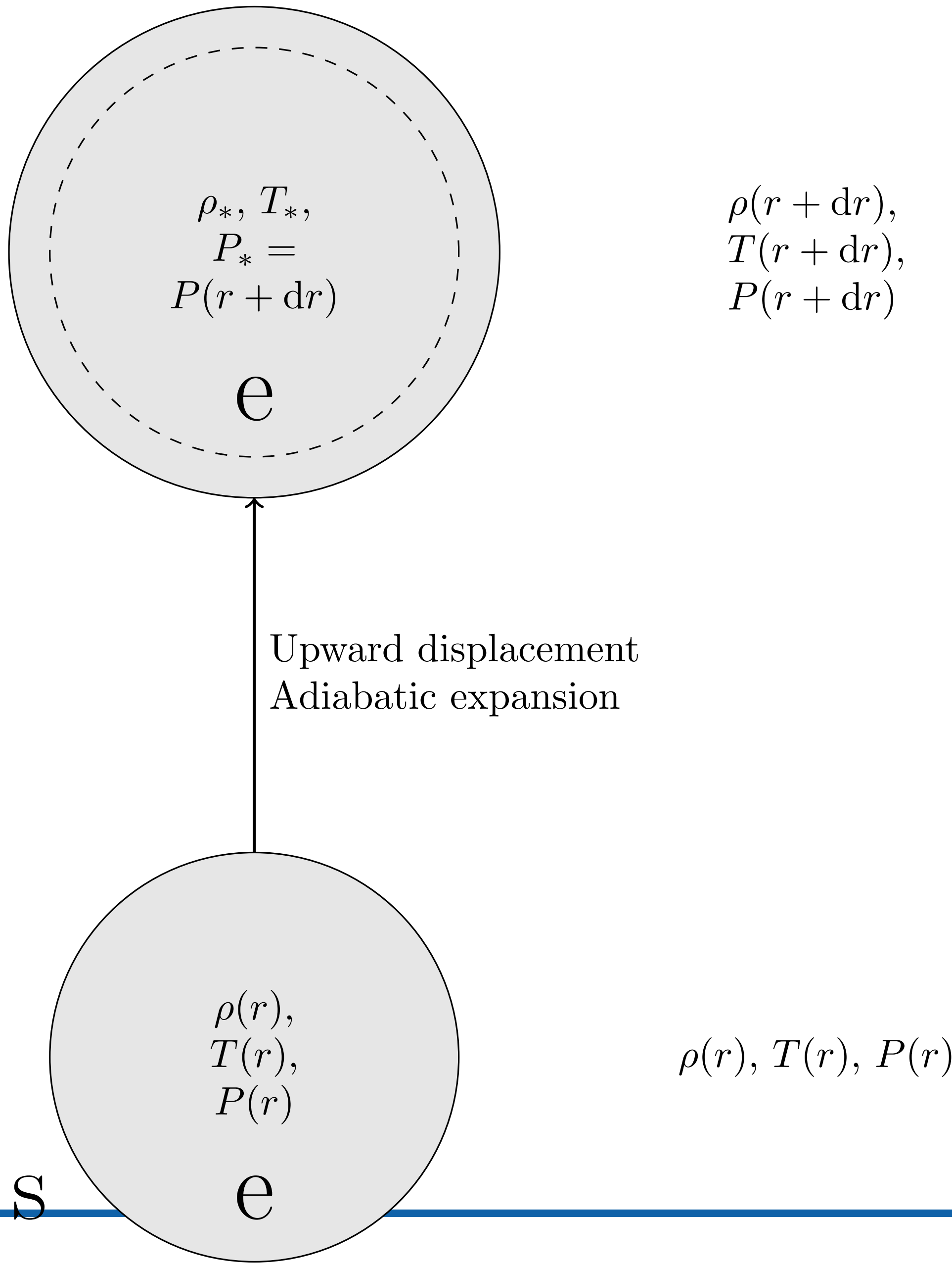

Stability criterion

$$\left(\frac{\mathrm{d}\rho}{\mathrm{d}r}\right)_{\mathrm{e}} - \left(\frac{\mathrm{d}\rho}{\mathrm{d}r}\right)_{\mathrm{s}} > 0$$

Density gradient not part of basic equations

$\rightarrow$ Transformation to temperature gradients:

Equation of state $\rho(P, T, \mu)$ in differential form

$$\frac{\mathrm{d}\rho}{\rho} = \alpha\frac{\mathrm{d}P}{P} - \delta\frac{\mathrm{d}T}{T} + \varphi\frac{\mathrm{d}\mu}{\mu}$$

Perfect gas $\alpha = \delta = \varphi = 1$

$$\alpha = \left(\frac{\partial \ln \rho}{\partial \ln P}\right)_{T,\mu} \quad \delta = \left(\frac{\partial \ln \rho}{\partial \ln T}\right)_{P,\mu} \tag{5.31}$$

$$\varphi = \left(\frac{\partial \ln \rho}{\partial \ln \mu}\right)_{P,T}$$

Stability against convection

$$\frac{\mathrm{d}\rho}{\rho} = \alpha\frac{\mathrm{d}P}{P} - \delta\frac{\mathrm{d}T}{T} + \varphi\frac{\mathrm{d}\mu}{\mu}$$

$$\rightarrow \frac{\mathrm{d}\rho}{\mathrm{d}r} = \rho\left(\frac{\alpha}{P}\frac{\mathrm{d}P}{\mathrm{d}r} - \frac{\delta}{T}\frac{\mathrm{d}T}{\mathrm{d}r} + \frac{\varphi}{\mu}\frac{\mathrm{d}\mu}{\mathrm{d}r}\right)$$

$$\left(\frac{\mathrm{d}\rho}{\mathrm{d}r}\right)_{\mathrm{e}} - \left(\frac{\mathrm{d}\rho}{\mathrm{d}r}\right)_{\mathrm{s}} > 0$$

$$\rightarrow \left(\frac{\alpha}{P}\frac{\mathrm{d}P}{\mathrm{d}r}\right)_{\mathrm{e}} - \left(\frac{\delta}{T}\frac{\mathrm{d}T}{\mathrm{d}r}\right)_{\mathrm{e}} + \left(\frac{\varphi}{\mu}\frac{\mathrm{d}\mu}{\mathrm{d}r}\right)_{\mathrm{e}} - \left(\frac{\alpha}{P}\frac{\mathrm{d}P}{\mathrm{d}r}\right)_{\mathrm{s}} + \left(\frac{\delta}{T}\frac{\mathrm{d}T}{\mathrm{d}r}\right)_{\mathrm{s}} - \left(\frac{\varphi}{\mu}\frac{\mathrm{d}\mu}{\mathrm{d}r}\right)_{\mathrm{s}} > 0$$

- $\mathrm{d}\mu$ change in chemical composition: $\mathrm{d}\mu_{\mathrm{e}} = 0$ for moving element
- $DP = 0 \rightarrow \left(\frac{\alpha}{P}\frac{\mathrm{d}P}{\mathrm{d}r}\right)_{\mathrm{e}} = \left(\frac{\alpha}{P}\frac{\mathrm{d}P}{\mathrm{d}r}\right)_{\mathrm{s}}$

Introducing the **scale height of pressure** H_P

$$H_P = \frac{\mathrm{d}r}{\mathrm{d}\ln P} = -P\frac{\mathrm{d}r}{\mathrm{d}P} \tag{5.32}$$

with hydrostatic equilibrium $\frac{\partial P}{\partial r} = -g\rho \Rightarrow H_P = \frac{P}{\rho g}$

Stability against convection

$$\left[-\left(\frac{\delta}{T}\frac{dT}{dr}\right)_e + \left(\frac{\delta}{T}\frac{dT}{dr}\right)_s - \left(\frac{\varphi}{\mu}\frac{d\mu}{dr}\right)_s\right] \overbrace{\frac{dr}{d\ln P}}^{H_P} > 0$$

$$\Rightarrow \left[-\left(\frac{\delta}{T}\frac{dT}{d\ln P}\right)_e + \left(\frac{\delta}{T}\frac{dT}{d\ln P}\right)_s - \left(\frac{\varphi}{\mu}\frac{d\mu}{d\ln P}\right)_s\right] > 0$$

$$\Rightarrow -\left(\delta\frac{d\ln T}{d\ln P}\right)_e + \left(\delta\frac{d\ln T}{d\ln P}\right)_s - \left(\varphi\frac{d\ln\mu}{d\ln P}\right)_s > 0$$

Condition for stability

$$\Rightarrow \left(\frac{d\ln T}{d\ln P}\right)_s < \left(\frac{d\ln T}{d\ln P}\right)_e + \frac{\varphi}{\delta}\left(\frac{d\ln\mu}{d\ln P}\right)_s \tag{5.33}$$

$$\nabla := \left(\frac{d\ln T}{d\ln P}\right)_s \qquad \nabla_e := \left(\frac{d\ln T}{d\ln P}\right)_e \qquad \nabla_\mu := \left(\frac{d\ln\mu}{d\ln P}\right)_s$$

∇, ∇_μ variation of T and μ in the surrounding material with depth (P taken as measure of depth)

∇_e variation of T in the moving element, position is measured by P

Stability against convection

$$\nabla < \nabla_\mathrm{e} + \frac{\varphi}{\delta}\nabla_\mu \tag{5.34}$$

Stability of radiative layer $\nabla = \nabla_\mathrm{rad}$ with adiabatic change of elements: $\nabla_\mathrm{e} = \nabla_\mathrm{ad}$

$$\nabla_\mathrm{rad} < \nabla_\mathrm{ad} + \frac{\varphi}{\delta}\nabla_\mu \tag{5.35}$$

Ledoux criterion for dynamical stability ($\Delta_\mu > 0$ is stabilizing)

region with homogeneous chemical composition: $\nabla_\mu = 0$

$$\nabla_\mathrm{rad} < \nabla_\mathrm{ad} \tag{5.36}$$

Schwarzschild criterion for dynamical stability

Dynamically stable layers with different chemical compositions can become unstable under nonadiabatic conditions ($DT \neq 0$, $D\mu \neq 0$, $\nabla_\mu = 0$)
$\rightarrow$ Specific weight is temperature dependent

Secular or thermal instability

Stability against convection

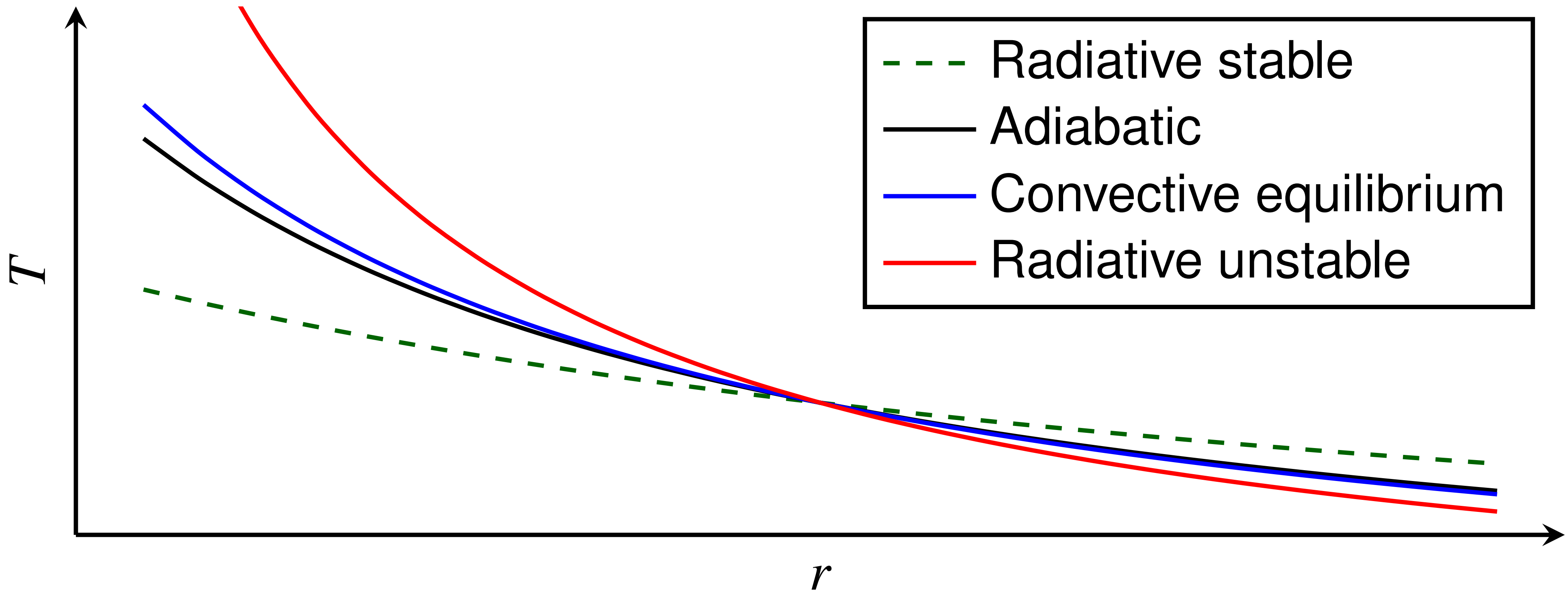

$$\frac{\partial T}{\partial r} \approx \nabla_{\mathrm{ad}} \frac{T}{P} \frac{\partial P}{\partial r} \text{ (convection)}$$

$$\frac{\partial T}{\partial r} = -\frac{3}{16\pi ac} \frac{\kappa \rho l}{r^2 T^3} \text{ (Radiation)}$$

Energy transport by convection

Theoretical treatment of convective motions and transport of energy is extremely difficult

- Hydrodynamic equations cannot be solved easily
- Conditions in stellar interiors are unfavorable: turbulent motion transports enormous fluxes of energy in a very compressible gas (differences in properties over many orders of magnitude)
- Full 3D numerical simulations are demanding in terms of computer power

$\rightarrow$ Mixing-length theory provides a simple model, which is still used today

Energy transport by convection

Herwig 2018, Youtube

Energy transport by convection

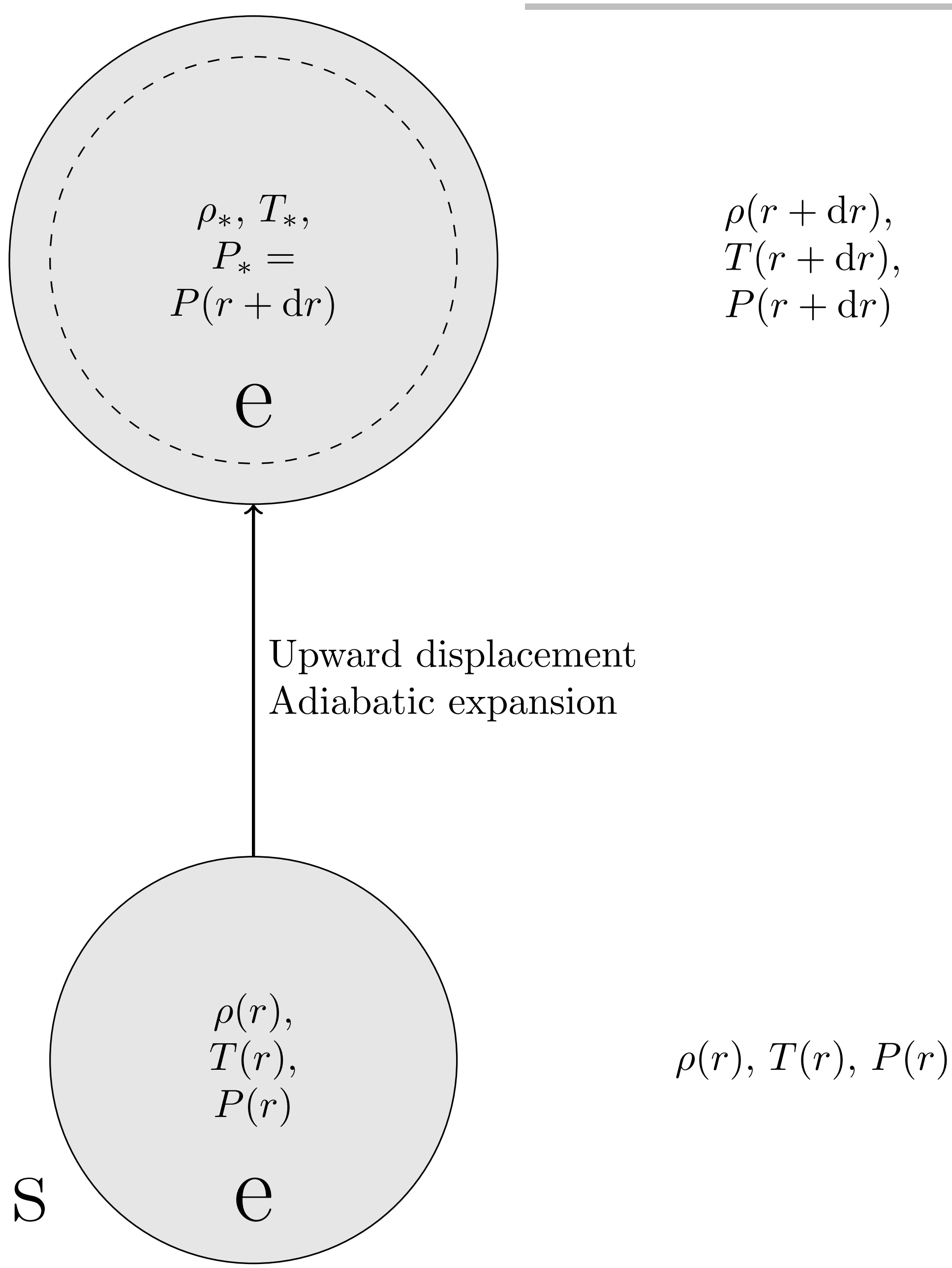

Mixing length theory:

- Convective element with $DT > 0$ and $DP = 0$
- Local convective flux

$$F_{\text{con}} = \rho v c_P DT$$

- Average convective flux: vDT must be replaced by mean value over the full concentric sphere and all elements
- All elements started as small perturbations $DT_0 = 0$ and $v_0 = 0$
- Due to differences in temperature gradients and buoyancy force DT and v increase

Energy transport by convection

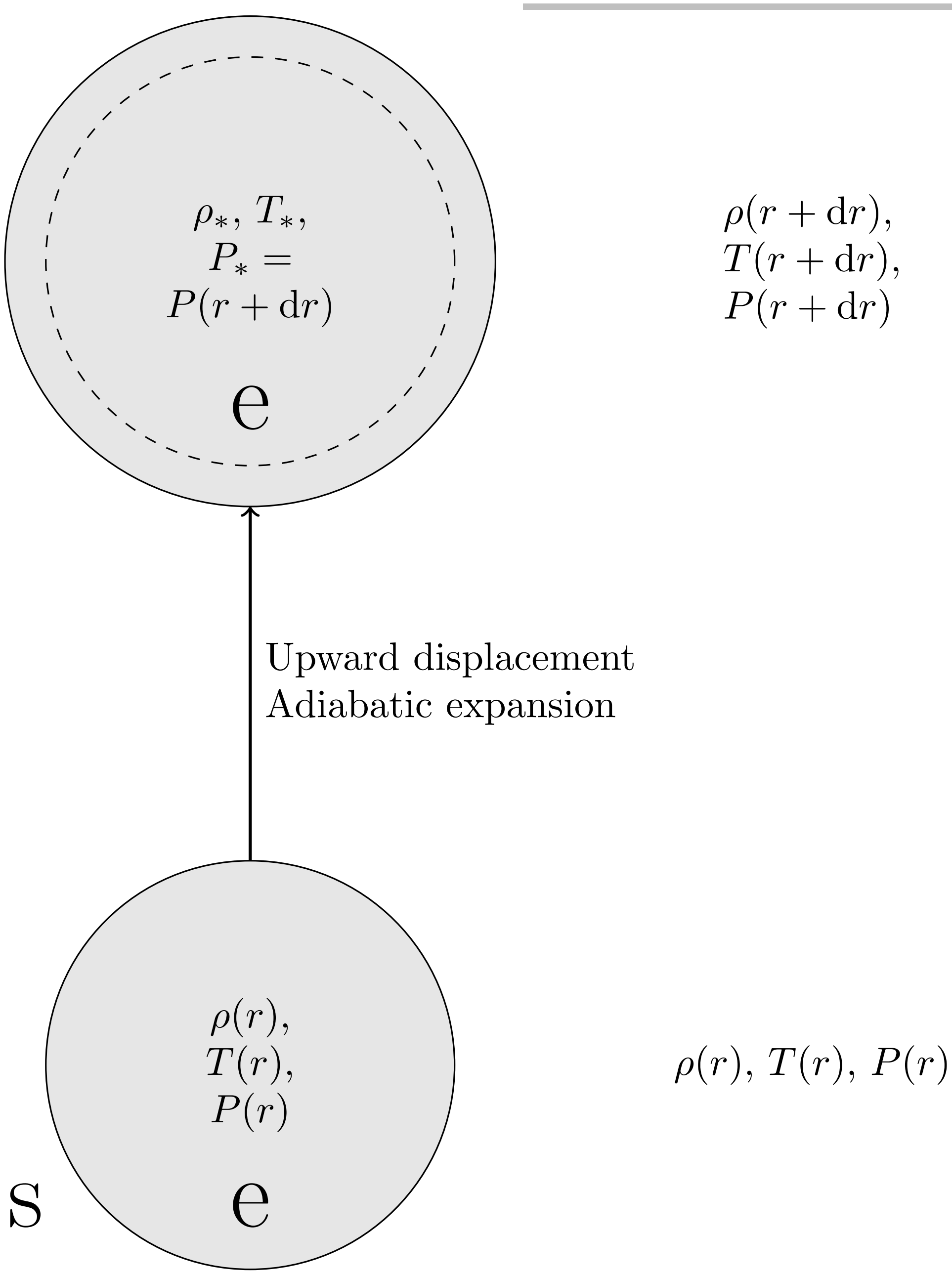

- After a distance l_m the elements dissolves and mixes with the surroundings (l_m mixing length)
- Assuming that the average element moved $l_\mathrm{m}/2$ in the sphere

$$\frac{DT}{T} = \frac{1}{T}\frac{\partial(DT)}{\partial r}\frac{l_\mathrm{m}}{2} = (\nabla - \nabla_\mathrm{e})\frac{l_\mathrm{m}}{2}\frac{1}{H_P}$$

- Density difference ($DP = D\mu = 0$)

$$\frac{D\rho}{\rho} = -\frac{\delta DT}{T}$$

- Buyoncy force

$$k_r = -g\frac{D\rho}{\rho}$$

Energy transport by convection

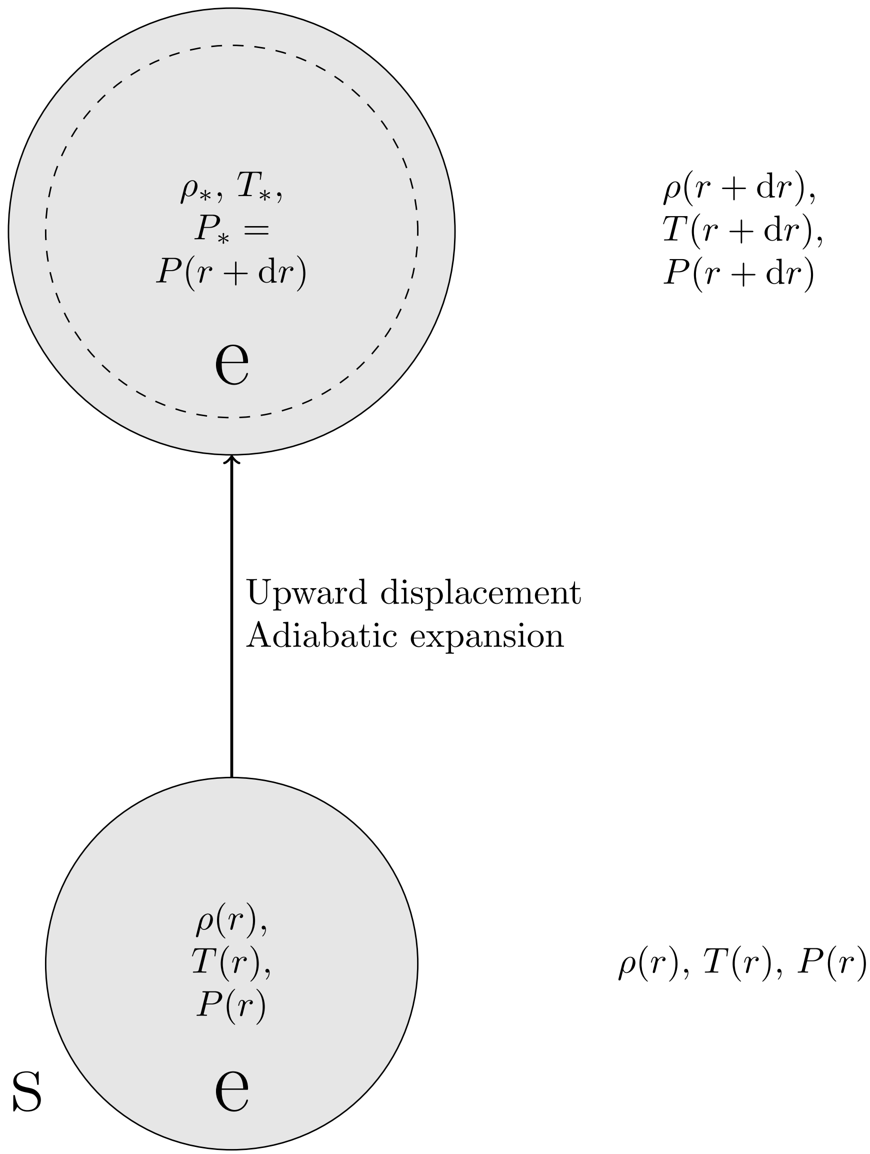

- Half of the buoyancy force may have acted on the element over its motion $\rightarrow$work done is

$$\frac{1}{2}k_r\frac{l_\mathrm{m}}{2} = g\delta(\nabla - \nabla_\mathrm{e})\frac{l_\mathrm{m}^2}{8H_P}$$

- Half of the work goes into kinetic energy

$$v^2 = g\delta(\nabla - \nabla_\mathrm{e})\frac{l_\mathrm{m}^2}{8H_P}$$

- **convective flux**

$$F_\mathrm{con} = \rho c_P T\sqrt{g\delta}\frac{l_\mathrm{m}^2}{4\sqrt{2}}H_P^{-3/2}(\nabla - \nabla_\mathrm{e})^{3/2}$$

- l_m or mixing-length parameter $\alpha_\mathrm{MLT} = \frac{l_\mathrm{m}}{H_P}$ are free parameters estimated by plausible assumptions and comparison with observations

Chemical composition

The chemical composition of stellar matter is very important, since it directly influences basic properties

- absorption by radiation
- generation of energy by nuclear reactions

$\rightarrow$ reactions also alter the composition: record of the nuclear history

- composition is extremely simple compared to that of terrestrial bodies: no chemical compounds, atoms mostly ionized because of high temperature and pressure $\rightarrow$ sufficient to count different types of nuclei

Chemical composition

- X_i fraction of a unit mass which consists of nuclei of type i

$$\sum_i X_i \stackrel{!}{=} 1$$

- chemical composition of a star at time t: $X_i = X_i(m, t)$, $0 < m < M$
- particle number n_i in a volume of nuclei with mass m_i is related to mass abundance

$$X_i = \frac{m_i n_i}{\rho}$$

- only few X_i to consider: most elements too rare, not important or constant
- sufficient to specify mass fraction of hydrogen, helium, "rest" (metals)

$$X \equiv X_{\mathrm{H}} \qquad Y \equiv X_{\mathrm{He}} \qquad Z \equiv 1 - X - Y$$

- relative distribution of the elements Z necessary (especially C,N and O)
- most stars in their envelopes, contain an overwhelming amount of hydrogen and helium:

$$X = 0.65...0.75 \qquad Y = 0.30...0.25 \qquad Z = 0.05...0.0001$$

Chemical composition

In radiative regions, no exchange of matter between different mass shells, if we can neglect diffusion

$\rightarrow$ frequency of a certain reaction is described by the reaction rate r_{lm}: number of reactions per unit volume and time that transform nuclei from type l into m

$$\frac{\partial X_i}{\partial t} = \frac{m_i}{\rho}\left[\sum_j r_{ji} - \sum_k r_{ik}\right], \qquad i = 1 \ldots I$$

r_{ji} reaction rates for creation and change of n_i per second

r_{ki} reaction rates for destruction and change of n_i per second

reaction $p \rightarrow q$ may release energy e_{pq}: energy generation rate ϵ per unit mass

$$\epsilon = \sum_{p,q} \epsilon_{p,q} = \frac{1}{\rho}\sum_{p,q} r_{pq} e_{pq}$$

energy generated when one mass unit of type p nuclei is transformed to type q:

$$q_{pq} = \frac{e_{pq}}{m_p}$$

Chemical composition

$$\Rightarrow \frac{\partial X_i}{\partial t} = \frac{m_i}{\rho}\left[\sum_j \frac{\epsilon_{ji}}{q_{ji}} - \sum_k \frac{\epsilon_{ik}}{q_{ik}}\right]$$

I different nuclei simultaneously subject to nuclear transformations form a set of I differential equations, called a ”nuclear reactions network”

For hydrogen burning:

$$\frac{\partial X}{\partial t} = -\frac{\epsilon_{\mathrm{H}}}{q_{\mathrm{H}}} \Leftrightarrow \frac{\partial Y}{\partial t} = -\frac{\partial X}{\partial t} \tag{5.37}$$

Reaction rates and energies are calculated or measured

Chemical composition

Diffusion:

microscopic effects can also change the chemical composition in a star

- concentration diffusion tends to smooth out the differences
- heavier atoms can migrate towards the regions of higher temperature due to temperature diffusion
- Heavier nuclei diffuse towards higher pressure due to pressure diffusion (gravitational settling, sedimentation)

$$j_\mathrm{D} = c v_\mathrm{D} = -D \nabla c \Rightarrow v_\mathrm{D} = -\frac{1}{c} D(\nabla c + k_T \nabla \ln T + k_P \nabla \ln P)$$

  v_D diffusion velocity
- In the the outer regions, where atoms are formed, radiative levitation can lead to enrichment of heavy elements

Chemical composition

mixing due to turbulent **convective motion** very rapid compared to change of the chemical composition by nuclear reactions

$\rightarrow$ composition in a convective region remains homogeneous

$$\frac{\partial X_i}{\partial m} = 0$$

- Boundaries of convective layers can be different and change with time

$\rightarrow$ composition can still change if the boundaries move into a region of inhomogeneous composition, e.g. "ashes" of earlier nuclear burnings may be brought to the surface, fresh fuel may be carried into a zone of nuclear burning, or discontinuities can be produced that drastically influence the later evolution.

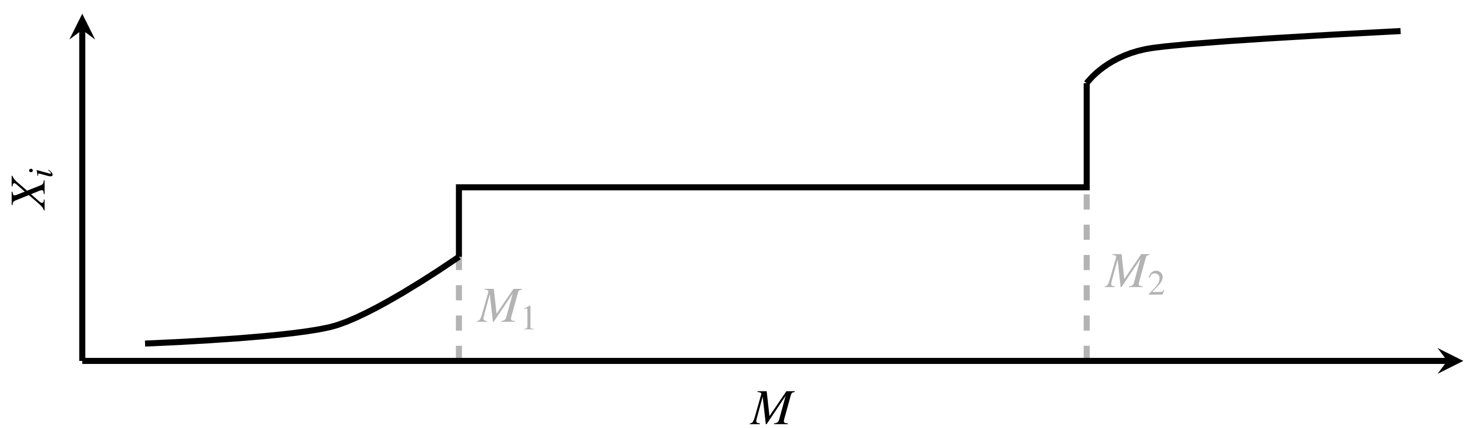

Mass loss

Due to interaction of photons emitted from the photosphere with atoms (radiation driven wind), molecules, or dust grains (dust-driven wind) in the atmosphere stellar winds are formed and lead to mass loss

- mass loss of the sun: $10^{-14}\,\mathrm{M}_\odot/\mathrm{yr}$
- AGB stars: $10^{-4}\,\mathrm{M}_\odot/\mathrm{yr}$
- Evidence for mass loss and estimates of its size from direct detection of circumstellar matter and from spectral signatures, such as Doppler shifts and spectral line shapes
- wind velocities: few km/s up to a few thousand km/s
- Complicated radiation-hydrodynamics problem

$\rightarrow$ Only empirical formulations, e.g. Reimers law

$$\dot{M}_\mathrm{R} = -4^{-13}\eta\frac{L}{gR}\cdot\frac{\mathrm{g}_\odot\mathrm{R}_\odot}{\mathrm{L}_\odot}$$

parameter η varies between 0.2...1, lower for metal-poor stars

Full set of stellar structure equations

Mass conservation: $$\frac{\partial m}{\partial r} = 4\pi r^2\rho \qquad \frac{\partial r}{\partial m} = \frac{1}{4\pi r^2\rho} \tag{5.38}$$

Hydrostatic equilibrium: $$\frac{\partial P}{\partial r} = -\frac{Gm\rho}{r^2} \qquad \frac{\partial P}{\partial m} = -\frac{Gm}{4\pi r^4} \tag{5.39}$$

Energy production: $$\frac{\partial l}{\partial m} = \epsilon_\mathrm{n} - \epsilon_\nu - c_P\frac{\partial T}{\partial \rho} + \frac{\delta}{\rho}\frac{\partial P}{\partial t} \tag{5.40}$$

Energy transport: $$\frac{\partial T}{\partial r} = -\rho\frac{GmT}{r^2P}\nabla_{\mathrm{conv/rad}} \qquad \frac{\partial T}{\partial m} = -\frac{GmT}{4\pi r^4 P}\nabla_{\mathrm{conv/rad}} \tag{5.41}$$

temperature gradient: $$\nabla = \left(\frac{\mathrm{d}\ln T}{\mathrm{d}\ln P}\right)$$

$$\nabla_{\mathrm{rad}} = \frac{3}{16\pi acG}\frac{\kappa l P}{mT^4} \qquad \nabla_{\mathrm{conv}} \approx \nabla_{\mathrm{ad}} = (\nabla)_S$$

$$\frac{\partial X_i}{\partial t} = \frac{m_i}{\rho}\left(\sum_j r_{ji} - \sum_k r_{ik}\right), \; i = 1, \ldots, I \tag{5.42}$$

change in chemical composition

Full set of stellar structure equations

Equations 5.38 to 5.42 contain functions which describe properties of the stellar material such as ρ, ϵ_n, ϵ_ν, κ, c_P, ∇_ad, δ and reaction rates r_{ij}

If we assume them to be known functions of P, T and the chemical composition by functions $X_i(m, t)$, we have the equations of state:

$$\rho = \rho(P, T, X_i) \tag{5.43}$$

and equations for the other thermodynamic properties of the stellar matter

$$c_P = c_P(P, T, X_i) \tag{5.44}$$

$$\delta = \delta(P, T, X_i) = \left(\frac{\partial \ln \rho}{\partial \ln T}\right)_{P,\mu} \tag{5.45}$$

$$\nabla_\mathrm{ad} = \nabla_\mathrm{ad}(P, T, X_i) \tag{5.46}$$

as well as the Rosseland mean of the opacity (including conduction)

$$\kappa = \kappa(P, T, X_i) \tag{5.47}$$

Full set of stellar structure equations

and nuclear reaction rates and the energy production and energy loss via neutrinos:

$$r_{jk} = r_{jk}(P, T, X_i) \tag{5.48}$$

$$\epsilon_{\mathrm{n}} = \epsilon_{\mathrm{n}}(P, T, X_i) \tag{5.49}$$

$$\epsilon_{\nu} = \epsilon_{\nu}(P, T, X_i) \tag{5.50}$$

X_i stand for **all** types of nuclei ($i = 1, ..., I$)

I different types of nuclei being affected by reactions form a set of $4 + I$ differential equations for the $4 + I$ variables $r, P, T, l, X_1, ..., X_I$.

Independent variables m and t. If total mass of the star M is constant and time of start of evolution $t = t_0$: solutions in the interval $0 \leq m \leq M, t \geq t_0$

set of non-linear, partial differential equations $\rightarrow$ Boundary conditions necessary

For full problem: specification of $r(m, t_0)$, $\dot{r}(m, t_0)$, $s(m, t_0)$ and $X_i(m, t_0)$

Stellar model: solution $r(m), P(m), ..., X_i(m)$ for given time t in interval $[0, M]$

Boundary conditions

Central conditions

- $m = 0$: $r = 0$ $l = 0$
- $m \to 0$
  - $\mathrm{d}(r^3) = \frac{3}{4\pi\rho_c}\mathrm{d}m \to r = \left(\frac{3}{4\pi\rho_c}\right)^{1/3} m^{1/3}$
  - $l = (\epsilon_n - \epsilon_\nu + \epsilon_g)_c m$
  - $\frac{\mathrm{d}P}{\mathrm{d}m} = -\frac{G}{4\pi}\left(\frac{4\pi\rho_c}{3}\right)^{4/3} m^{-1/3} \to P - P_c = -\frac{3G}{8\pi}\left(\frac{4\pi}{3}\rho_c\right)^{4/3} m^{2/3}$
  - radiative case: $\frac{\mathrm{d}T}{\mathrm{d}m} = -\frac{3}{64\pi^2 ac}\frac{\kappa l}{r^4 T^3}$
    $\to T^4 - T_c^4 = -\frac{1}{2ac}\left(\frac{3}{4\pi}\right)^{2/3} \kappa_c(\epsilon_n - \epsilon_\nu + \epsilon_g)_c \rho_c^{4/3} m^{2/3}$
  - convective case: $\ln T - \ln T_c = -\left(\frac{\pi}{6}\right) G \frac{\nabla_{\mathrm{ad,c}}\rho_c^{4/3}}{P_c} m^{2/3}$

Numerical approaches needed to solve the system of equations: e.g. Shooting method, Henyey method

Boundary conditions

Surface conditions

- naive "zero conditions" – $m \to M : P \to 0, T \to 0$
- more real: extended transition to the finite values of P, T of the diffuse interstellar medium
- find "surface" that defines total stellar radius $r = R$: photosphere, from where the bulk of the radiation is emitted into space: $\tau := \int_R^\infty \kappa\rho \mathrm{d}r = \bar{\kappa} \int_R^\infty \rho \mathrm{d}r = 2/3$
- $P_{r=R} \int_R^\infty g\rho \mathrm{d}r = g_0 \int_R^\infty \rho \mathrm{d}r \overset{\tau=2/3}{=} \frac{GM}{R^2}\frac{2}{3}\frac{1}{\bar{\kappa}}$
- temperature of the photosphere equal to effective temperature $T_{r=R} = T_{\mathrm{eff}}$ $\to L = 4\pi R^2 \sigma T_{\mathrm{eff}}^4, \sigma = ac/4$
- temperature dependency of κ: Eddington approximation – grey atmosphere $T^4(\tau) = \frac{3}{4}(L/4\pi R^2\sigma)\left(\tau + \frac{2}{3}\right) \Rightarrow T = T_{\mathrm{eff}}$ for $\tau = 2/3$
- $\mathrm{d}r/\mathrm{d}\tau = -1/(\kappa\rho) \qquad \mathrm{d}P/\mathrm{d}r = -g\rho \qquad \to \frac{\mathrm{d}P}{\mathrm{d}\tau} = \frac{Gm}{r^2\kappa}$
- generally: interior solution should fit smoothly to solution of the stellar-atmosphere problem

Properties of stellar matter

Properties of stellar matter

- basic variables: m, r, P, T, l
- differential equations also contain density, nuclear energy generation, or opacity $\rightarrow$ describe properties of stellar matter for given P, T and chemical composition, do not depend on m, r, l at given point in the star, could be determined in a laboratory

$\rightarrow$ position in the star not necessary to describe them

$\rightarrow$ dependence of density ρ on P, T: **equation of state**

- simple if we have a perfect gas
- **but!** radiation and ionization also influence the pressure and the internal energy $\rightarrow$ have to be included

Perfect gas with radiation

Radiation pressure

- pressure in a star not only given by that if the gas but photons in the stellar interior contribute significantly
- radiation is practically that of a black body

$$P_{\mathrm{rad}} = \frac{1}{3}U = \frac{a}{3}T^4 \Rightarrow P = P_{\mathrm{gas}} + P_{\mathrm{rad}} = \frac{R}{\mu}\rho T + \frac{a}{3}T^4$$

- importance of the radiation pressure

$$\beta := \frac{P_{\mathrm{gas}}}{P}, \qquad 1 - \beta = \frac{P_{\mathrm{rad}}}{P}$$

$\rightarrow \beta = 1 \Rightarrow P_{\mathrm{rad}} = 0$, $\beta = 0 \Rightarrow P_{\mathrm{gas}} = 0$

Perfect gas with radiation

Thermodynamic Quantities

$$\stackrel{5.31}{\Rightarrow} \alpha = \frac{1}{\beta} \qquad \delta = \frac{4-3\beta}{\beta} \qquad \varphi = 1$$

internal energy per unit mass

$$u = \frac{3}{2}\frac{R}{\mu}T + \frac{aT^4}{\rho} = \frac{RT}{\mu}\left[\frac{3}{2} + \frac{3(1-\beta)}{\beta}\right]$$

specific heat

$$c_P \stackrel{5.15}{=} \frac{R}{\mu}\left[\frac{3}{2} + \frac{3(4+\beta)(1-\beta)}{\beta^2} + \frac{4-3\beta}{\beta^2}\right]$$

adiabatic gradient

$$\nabla_{\mathrm{ad}} \stackrel{5.17}{=} \left(1 + \frac{(1-\beta)(4+\beta)}{\beta^2}\right) \Big/ \left(\frac{5}{2} + \frac{4(1-\beta)(4+\beta)}{\beta^2}\right)$$

perfect gas without radiation see 5.20 $\Rightarrow \quad \gamma_{\mathrm{ad}} \rightarrow \frac{5}{3}, \quad \nabla_{\mathrm{ad}} \rightarrow \frac{2}{5}$

gas dominated by pressure $\Rightarrow \quad \gamma_{\mathrm{ad}} \rightarrow \frac{4}{3}, \quad \nabla_{\mathrm{ad}} \rightarrow \frac{1}{4}$

Perfect gas with radiation

Adiabatic coefficients (Chandrasekkar)

$$\Gamma_1 := \left(\frac{d\ln P}{d\ln\rho}\right)_{ad} = \gamma_{ad} \qquad (6.1)$$

$$\frac{\Gamma_2}{\Gamma_2 - 1} := \left(\frac{d\ln P}{d\ln T}\right)_{ad} = \frac{1}{\nabla_{ad}} \qquad (6.2)$$

$$\Gamma_3 := \left(\frac{d\ln T}{d\ln\rho}\right)_{ad} + 1 \qquad (6.3)$$

$$\Rightarrow \frac{\Gamma_1}{\Gamma_3 - 1} = \frac{\Gamma_2}{\Gamma_2 - 1}$$

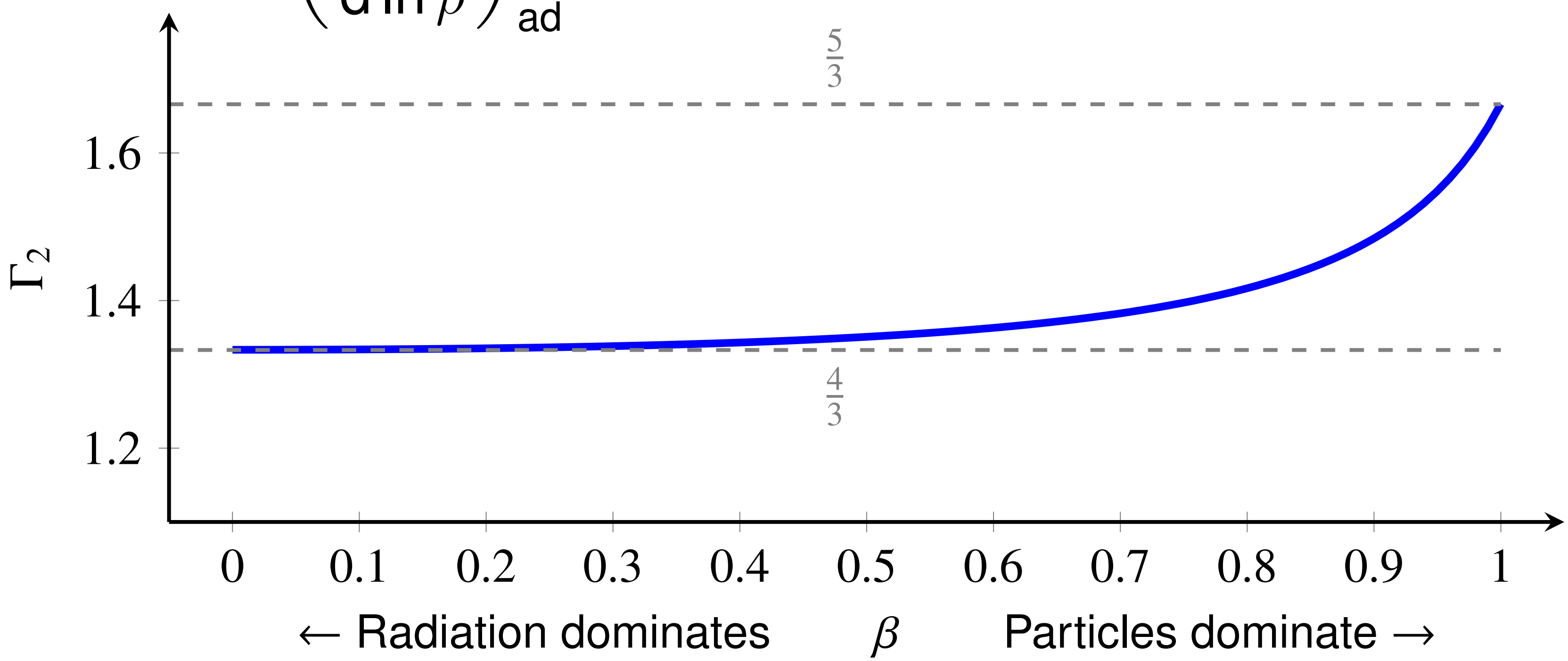

cores of massive stars: ionized, ideal gas plus photon field

Perfect gas with radiation

Adiabatic coefficients (Chandrasekkar)

$$\Gamma_1 := \left(\frac{d\ln P}{d\ln \rho}\right)_{ad} = \gamma_{ad} \qquad (6.4)$$

$$\frac{\Gamma_2}{\Gamma_2 - 1} := \left(\frac{d\ln P}{d\ln T}\right)_{ad} = \frac{1}{\nabla_{ad}} \qquad (6.5)$$

$$\Rightarrow \frac{\Gamma_1}{\Gamma_3 - 1} = \frac{\Gamma_2}{\Gamma_2 - 1}$$

$$\Gamma_3 := \left(\frac{d\ln T}{d\ln \rho}\right)_{ad} + 1 \qquad (6.6)$$

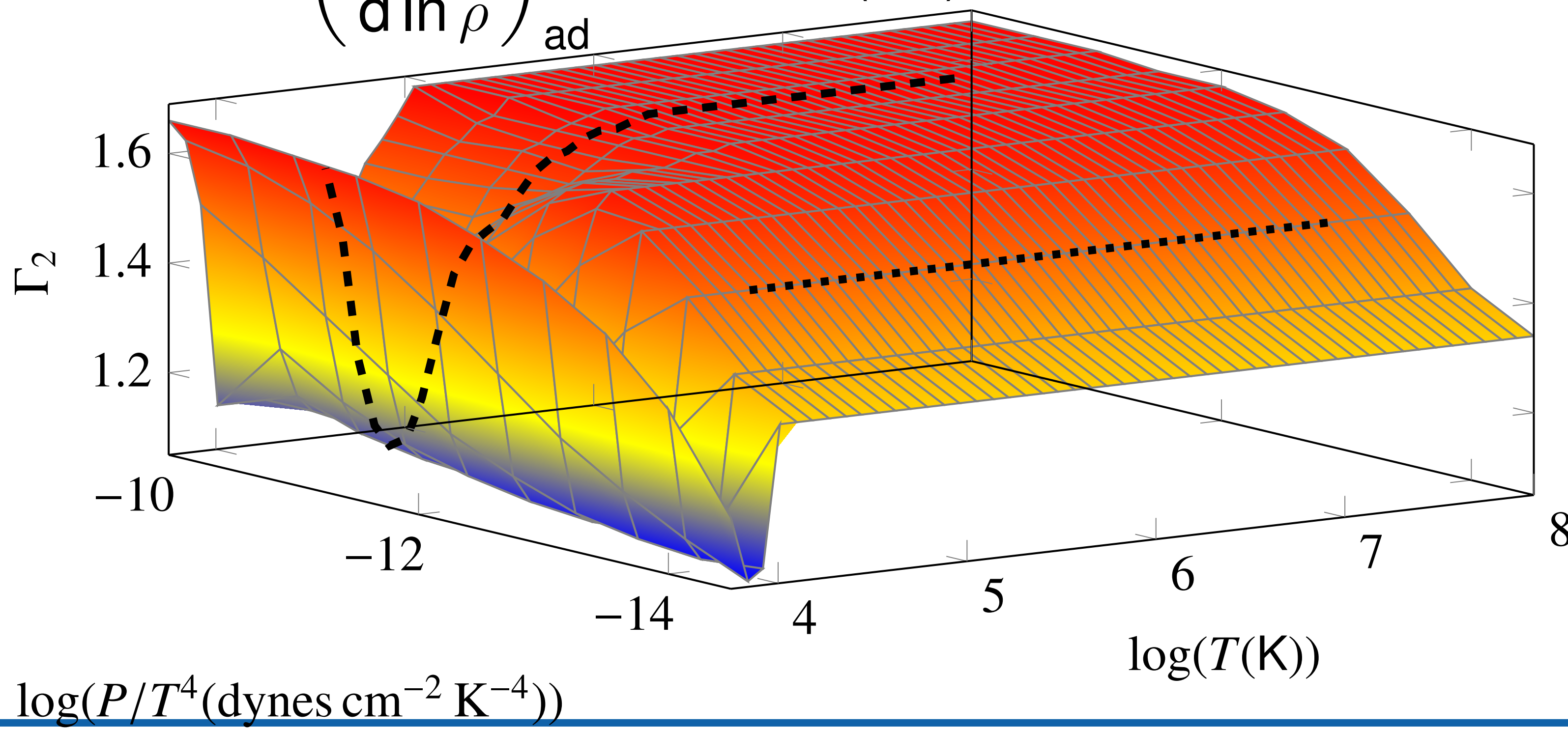

Ionization

- complete ionization of all atoms good approximation in the very deep interior, where T and P sufficiently large
- in outer regions and stellar atmospheres atoms can only be partially ionized
- mean molecular weight and thermodynamic properties such as c_p, Γ_2 depend on degree of ionization
- Ionization fraction given by Saha equation

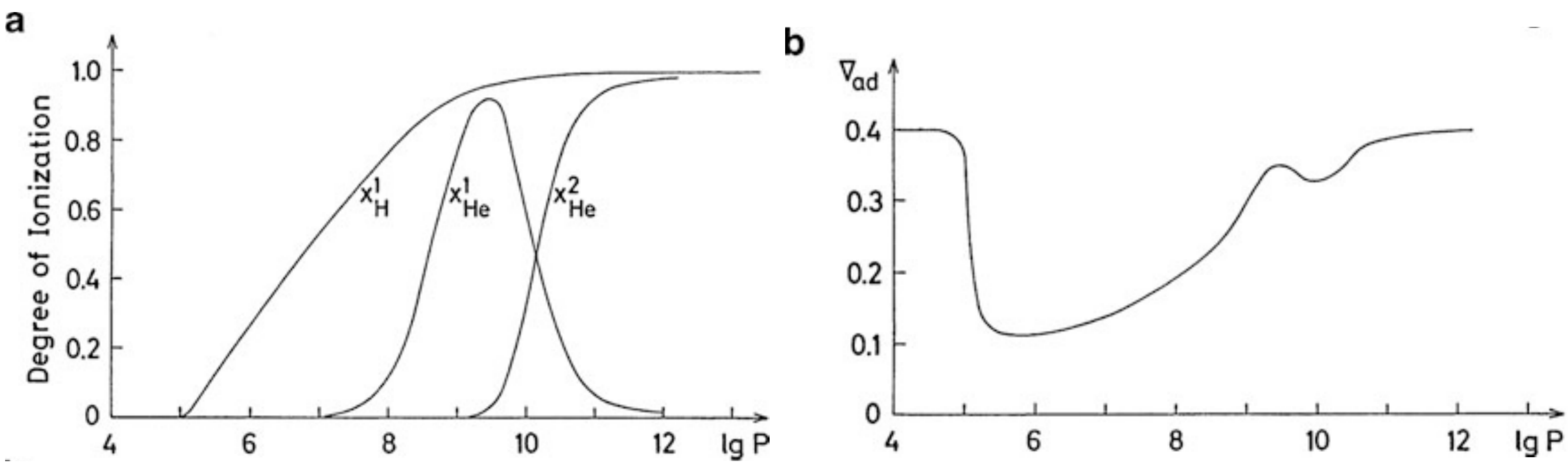

Kippenhahn, Weigert & Weiss 2012

Ionization

Adiabatic coefficients (Chandrasekkar)

$$\Gamma_1 := \left(\frac{\mathrm{d}\ln P}{\mathrm{d}\ln\rho}\right)_{\mathrm{ad}} = \gamma_{\mathrm{ad}} \qquad (6.7)$$

$$\frac{\Gamma_2}{\Gamma_2 - 1} := \left(\frac{\mathrm{d}\ln P}{\mathrm{d}\ln T}\right)_{\mathrm{ad}} = \frac{1}{\nabla_{\mathrm{ad}}} \qquad (6.8)$$

$$\Rightarrow \frac{\Gamma_1}{\Gamma_3 - 1} = \frac{\Gamma_2}{\Gamma_2 - 1}$$

$$\Gamma_3 := \left(\frac{\mathrm{d}\ln T}{\mathrm{d}\ln\rho}\right)_{\mathrm{ad}} + 1 \qquad (6.9)$$

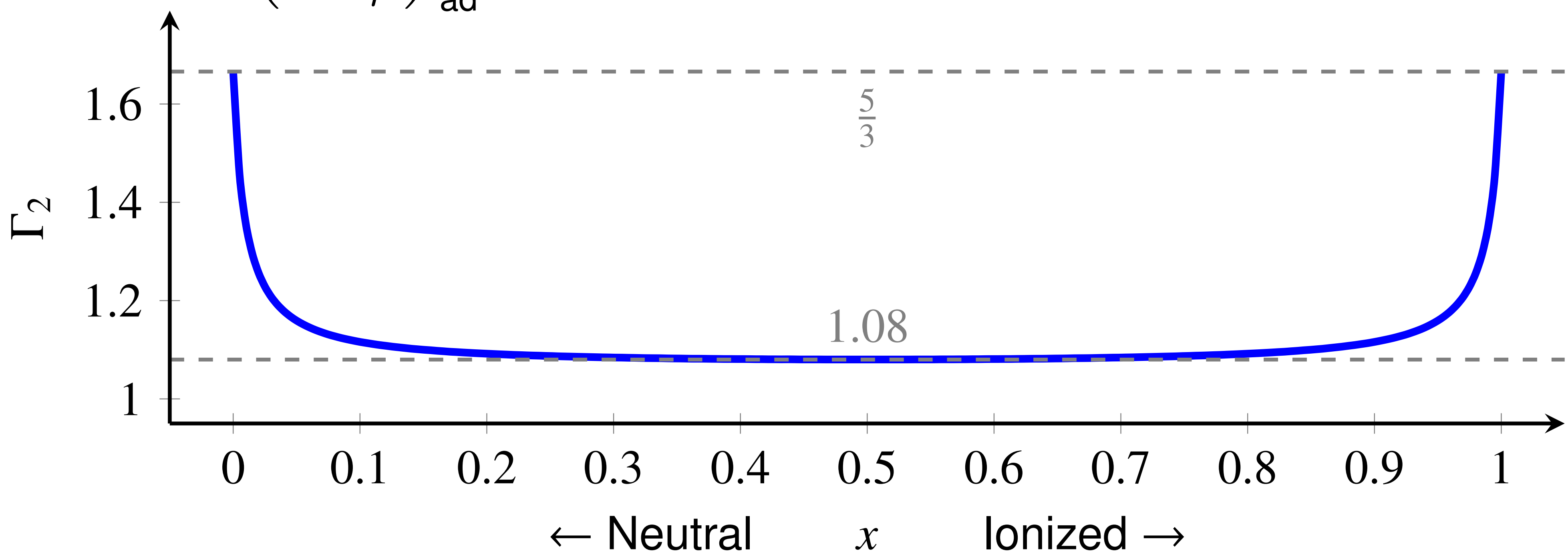

stellar envelopes of low-mass stars: Γ_2 dominated by ionization effects on H

Pressure ionization

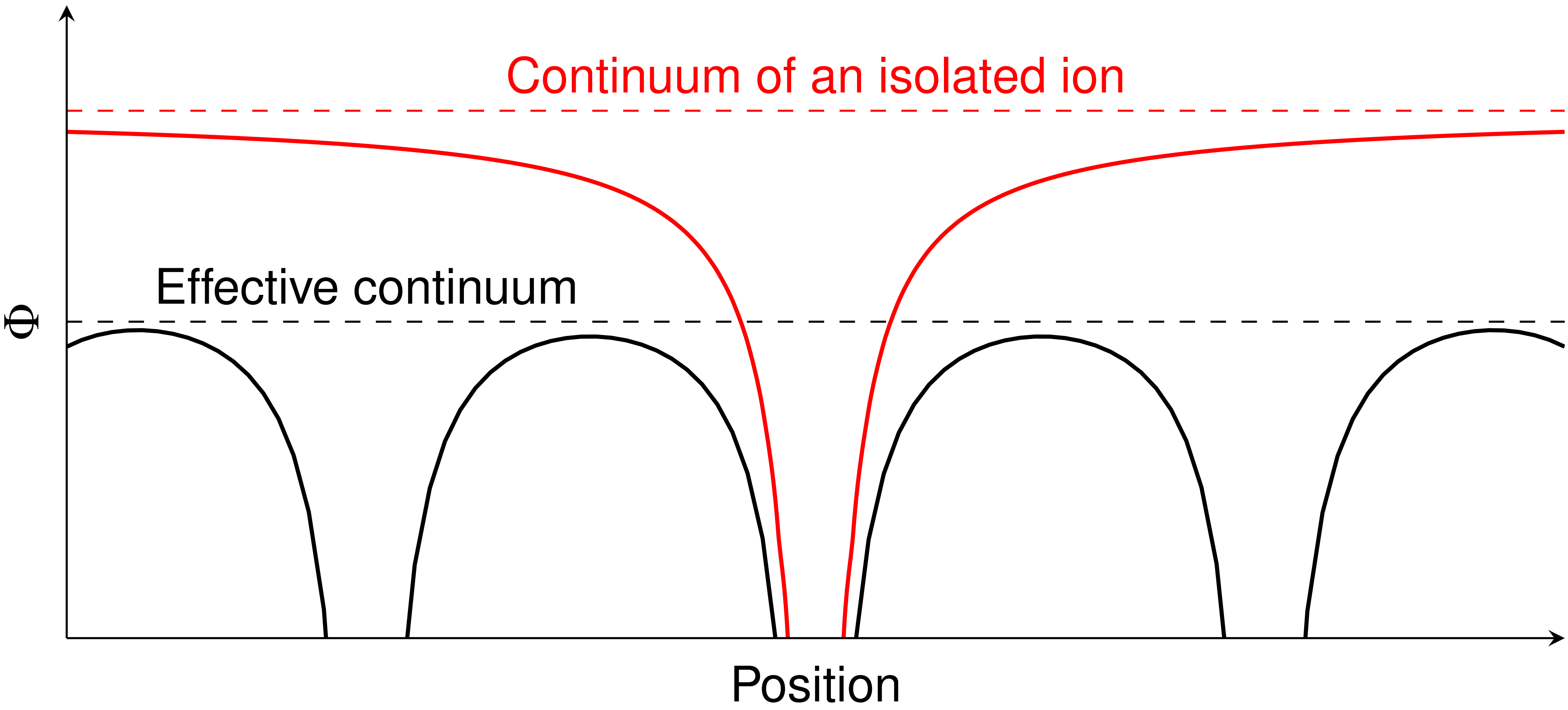

Limitation of Saha formula for high pressure, when pressure ionization sets in $\rightarrow$ Saha equation will underestimate the degree of ionization once this effect becomes important enough

Degenerate electron gas

- gas with sufficiently high density in volume $\mathrm{d}V$: fully pressure ionized
- free electrons of number density n_e
- velocity distribution given by Boltzmann statistics $\rightarrow E_\mathrm{kin,mean} = 3/2kT$
- in momentum space p_x, p_y, p_z each electron in a given volume $\mathrm{d}V$ represented by a point, points forming a spherical symmetric "cloud" around the origin
- p is the absolute value of the momentum ($p^2 = p_x^2 + p_y^2 + p_z^2$)
- number of electrons in spherical shell $[p, p+\mathrm{d}p]$ given by Boltzmann distribution function

$$f(p)\mathrm{d}p\mathrm{d}V = n_\mathrm{e}\frac{4\pi p^2}{(2\pi m_\mathrm{e}kT)^{3/2}}\exp\left(-\frac{p^2}{2m_\mathrm{e}kT}\right)\mathrm{d}p\mathrm{d}V$$

- for constant electron density: $p_\mathrm{max} = (2m_\mathrm{e}kT)^{1/2}$

$\rightarrow$ smaller T, maximum of distribution p_max at smaller p, maximum of $f(p)$ higher ($n_\mathrm{e} \sim \int\limits_0^\infty f(p)\mathrm{d}p$)

Degenerate electron gas

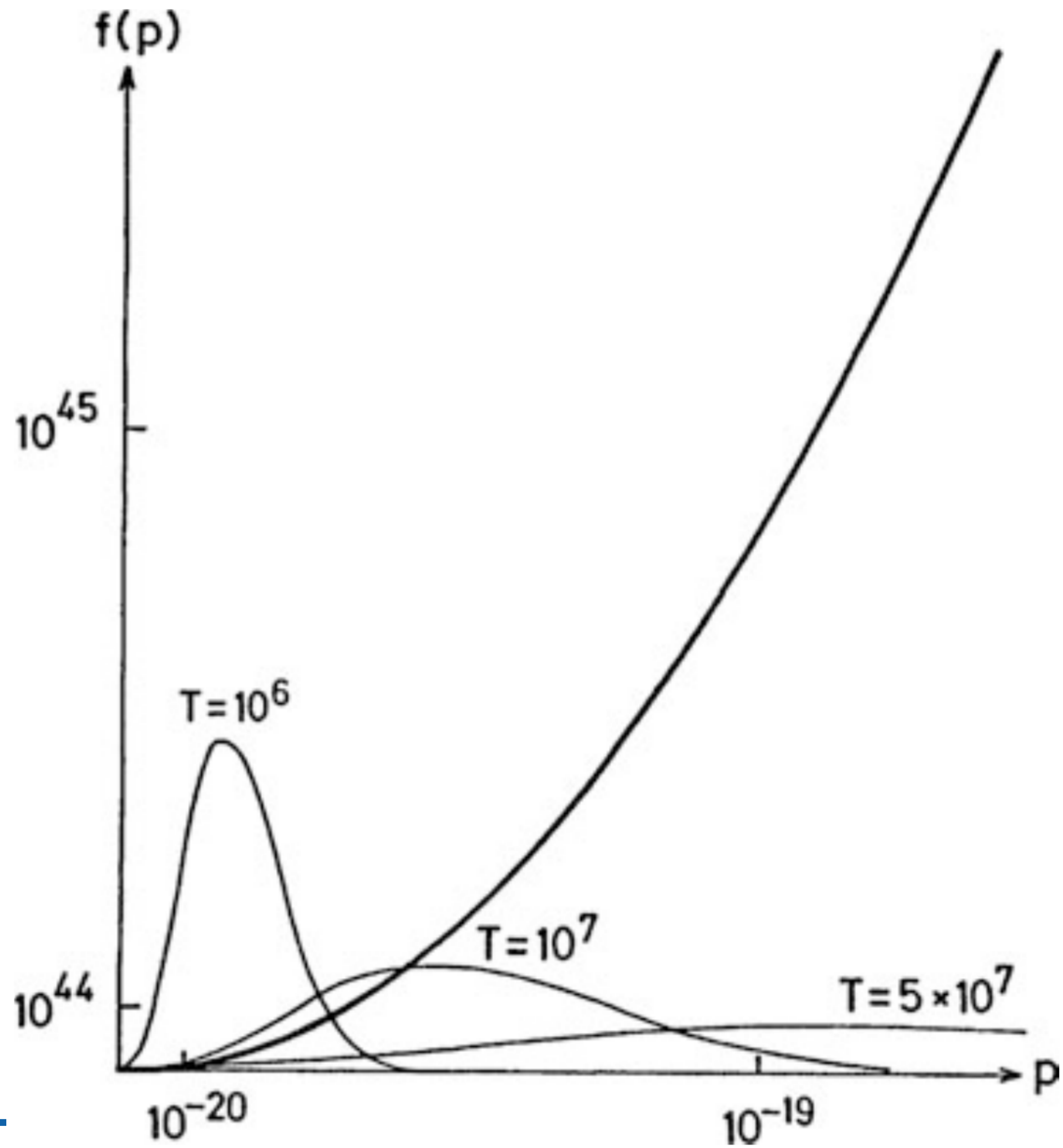

Kippenhahn, Weigert & Weiss 2012

Degenerate electron gas

Pauli principle

- electrons are fermions

$\rightarrow$ Pauli's exclusion principle: each quantum cell of the six-dimensional phase space $(x; y; z; p_x; p_y; p_z)$ cannot contain more than two electrons

- $x; y; z$ are the space coordinates of the electrons with $\mathrm{d}V = \mathrm{d}x\mathrm{d}y\mathrm{d}z$
- volume of quantum cell is $\mathrm{d}p_x\mathrm{d}p_y\mathrm{d}p_z\mathrm{d}V = h^3$ (h is Planck's constant)

$\rightarrow$ in shell $[p, p + \mathrm{d}p]$ are $4\pi p^2\mathrm{d}p\mathrm{d}V/h^3$ quantum cells with two electrons per cell

- quantum mechanics demands:

$$f(p)\mathrm{d}p\mathrm{d}V \leq 8\pi p^2\mathrm{d}p\mathrm{d}V/h^3$$

- Boltzmann distribution is in contradiction with quantum mechanics for too low temperatures or too high densities
- electrons become **degenerate**

Degenerate electron gas

Completely degenerate electron gas:

- all electrons have the lowest energy without violating Pauli's principle
- all phase cells up to p_F are filled, all other phase cells above p_F empty

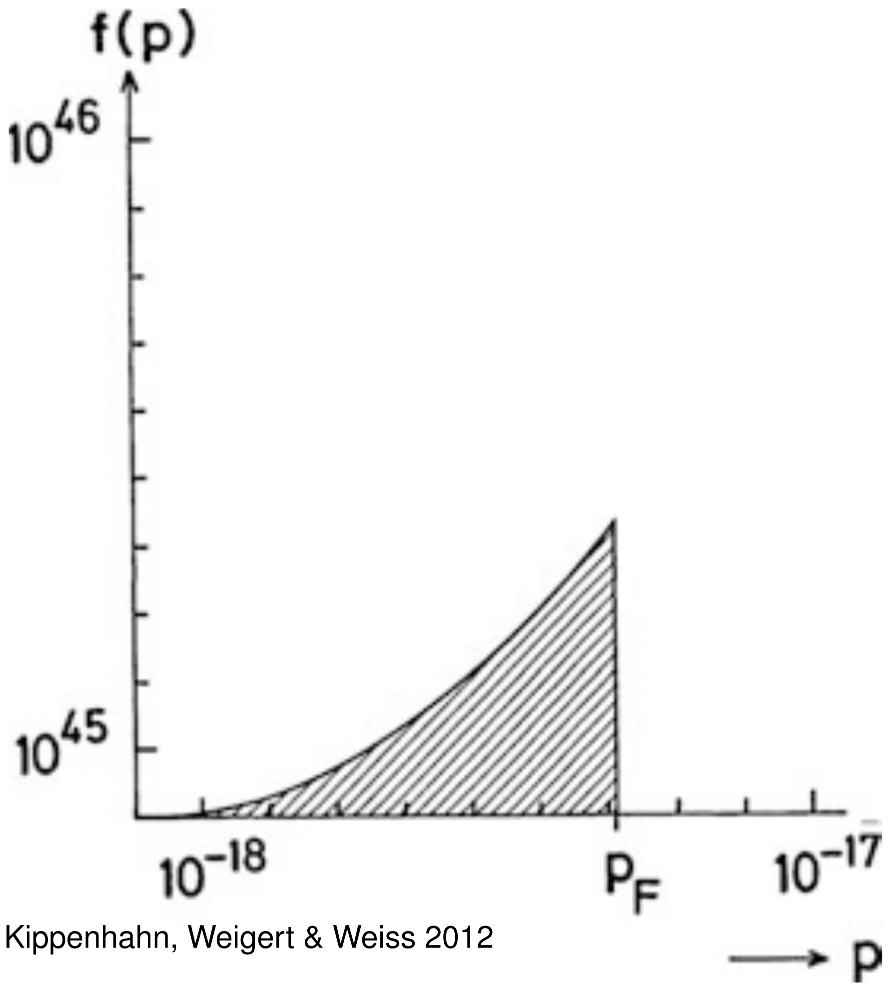

Kippenhahn, Weigert & Weiss 2012

$$f(p) = \frac{8\pi p^2}{h^3} \quad \textbf{for } p \leq p_F$$
$$f(p) = 0 \quad \textbf{for } p > p_F$$

Total number of electrons in dV

$$n_e dV = dV \int_0^{p_F} \frac{8\pi p^2 dp}{h^3} = \frac{8\pi}{3h^3} p_F^3 dV \tag{6.10}$$

Fermi momentum $p_F \sim n_e^{1/3}$

$\rightarrow E_F = p_F^2/2m_e \sim n_e^{2/3}$ Fermi energy

Degenerate electron gas

Completely degenerate electron gas:

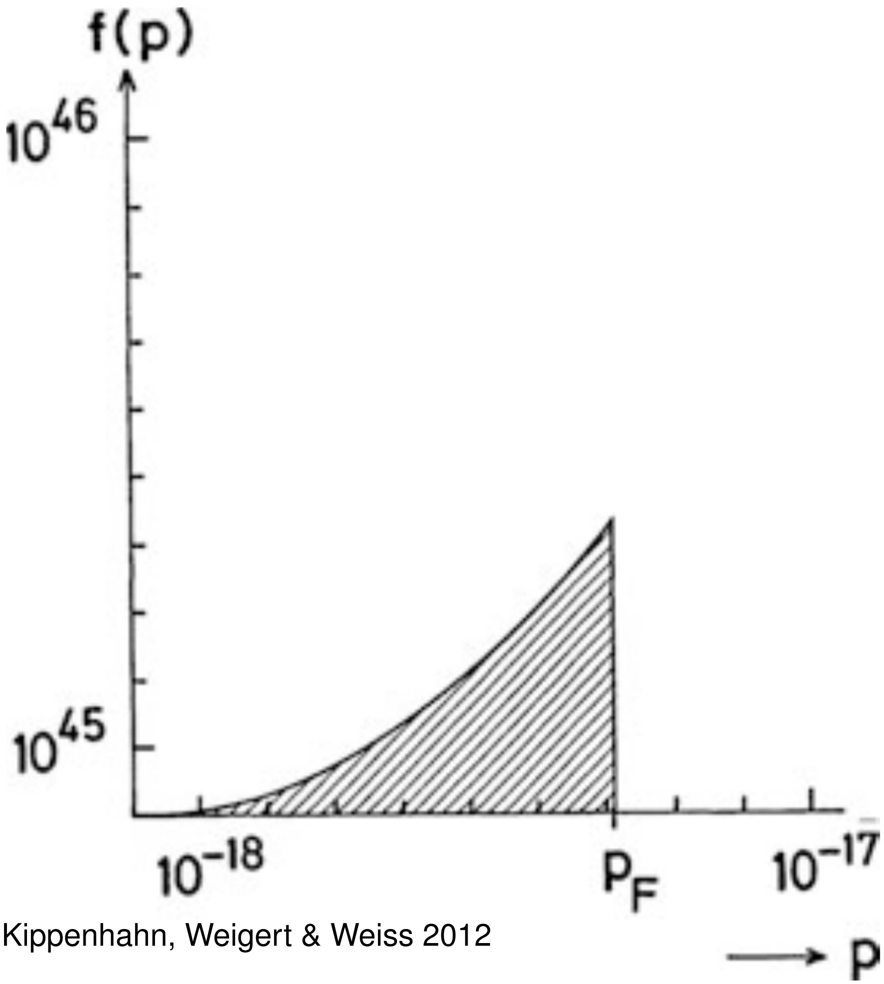

Kippenhahn, Weigert & Weiss 2012

- temperature of electron gas is zero
- but, electrons have energies up to finite Energies E_F
- for sufficiently large electron densities: p_F so high that fastest electrons have $v \sim c$

$$p = \frac{m_e v}{\sqrt{1 - v^2/c^2}}$$

$$E_{tot} = \frac{m_e c^2}{\sqrt{1 - v^2/c^2}} = m_e c^2 \sqrt{1 + \frac{p^2}{m_e^2 c^2}} \tag{6.11}$$

$$\Rightarrow \frac{1}{c}\frac{\partial E_{tot}}{\partial p} = \frac{p/(m_e c)}{[1 + p^2/(m_e^2 c^2)]^{1/2}} = \frac{v}{c}$$

Kinetic energy $E = E_{tot} - m_e c^2$

Degenerate electron gas

Completely degenerate electron gas:

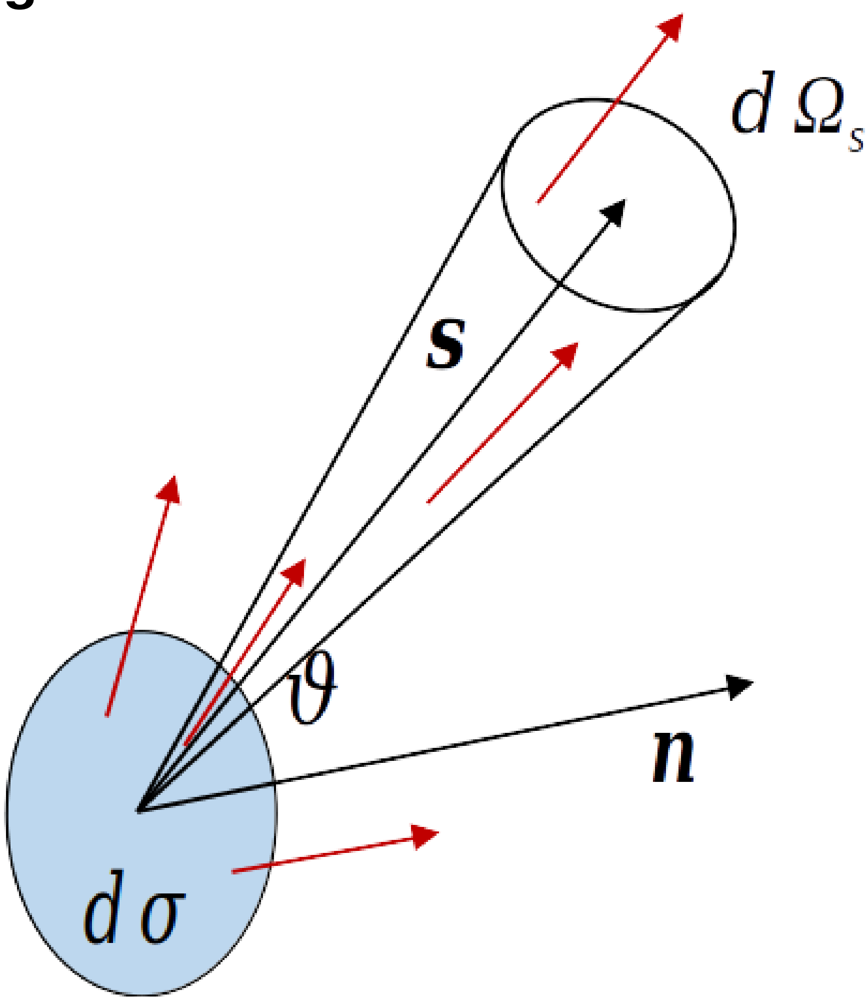

Derive equation of state

→ pressure needed: flux of momentum through a unit surface per second

→ Number of electrons with momentum between $[p, p + \mathrm{d}p]$ per second going through $\mathrm{d}\sigma$ into solid angle $\mathrm{d}\Omega_\mathrm{S}$ around direction **s**

→ $f(p)\mathrm{d}p\mathrm{d}\Omega_\mathrm{S}/(4\pi)$ electrons per unit volume at the location of the surface element with right momentum $[p, p + \mathrm{d}p]$

→ $f(p)\mathrm{d}p\mathrm{d}\Omega_\mathrm{S} v(p) \cos\vartheta \mathrm{d}\sigma/(4\pi)$ electrons per second move through the surface element $\mathrm{d}\sigma$ into the solid-angle element $\mathrm{d}\Omega_\mathrm{S}$

→ momentum in direction **n** : $p \cos\vartheta$

Completely degenerate electron gas

Electron pressure by integration over all directions **s** and all values of p

$$P_\mathrm{e} = \int\limits_{2\pi} \int\limits_0^\infty f(p) v(p) p \cos^2\vartheta \, \mathrm{d}p \, \mathrm{d}\Omega_\mathrm{S} / (4\pi) = \frac{4\pi}{3} \frac{8\pi}{h^3} \int\limits_0^{p_\mathrm{F}} p^2 p v(p) \mathrm{d}p / (4\pi)$$

$$P_\mathrm{e} = \frac{8\pi}{3h^3} \int\limits_0^{p_\mathrm{F}} p^3 v(p) \mathrm{d}p = \frac{8\pi c}{3h^3} \int\limits_0^{p_\mathrm{F}} p^3 \frac{p/(m_\mathrm{e} c)}{[1 + p^2/(m_\mathrm{e}^2 c^2)]^{1/2}} \mathrm{d}p$$

with $\xi = \frac{p}{m_\mathrm{e} c}$ and $x = \frac{p_\mathrm{F}}{m_\mathrm{e} c}$

$$P_\mathrm{e} = \frac{8\pi m_\mathrm{e}^4 c^5}{3h^3} \int\limits_0^x \frac{\xi^4 \mathrm{d}\xi}{(1 + \xi^2)^{1/2}} = \frac{\pi c^5 m_\mathrm{e}^4}{3h^3} f(x)$$

$$f(x) = x(2x^2 - 3)(1 + x^2)^{1/2} + 3 \ln[x + (1 + x^2)^{1/2}]$$

$$\stackrel{6.10}{\Rightarrow} n_\mathrm{e} = \frac{\rho}{\mu_\mathrm{e} m_\mathrm{u}} = \frac{8\pi m_\mathrm{e}^3 c^3}{3h^3} x^3$$

Completely degenerate electron gas

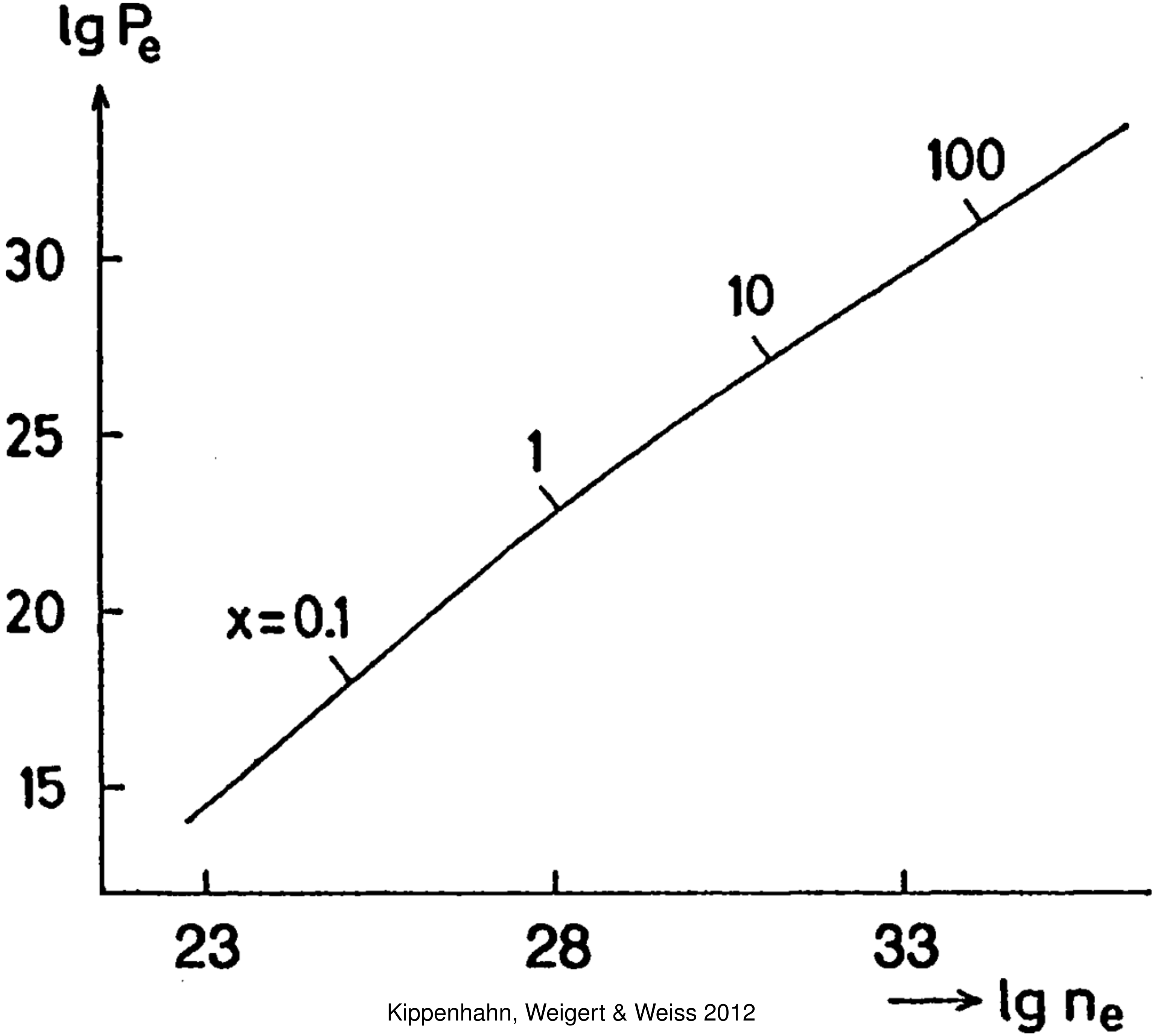

Kippenhahn, Weigert & Weiss 2012

Completely degenerate electron gas

Internal energy:

$$U_\mathrm{e} = \int_0^{p_\mathrm{F}} f(p) E(p) \mathrm{d}p = \frac{8\pi}{h^3} \int_0^{p_\mathrm{F}} E(p) p^2 \mathrm{d}p \stackrel{6.11}{=} \frac{\pi m_\mathrm{e}^4 c^5}{3h^3} g(x)$$

$g(x) = 8x^3[(x^2+1)^{1/2} - 1] - f(x)$

numerical values of $f(x)$, $g(x)$ can be found in Chandrasekhar 1939, Table 23.

x: **importance of relativistic effects** for electrons with the highest momentum

$$x = \frac{p_\mathrm{F}}{m_\mathrm{e} c} = \frac{v_\mathrm{F}/c}{(1 - v_\mathrm{F}^2/c^2)^{1/2}} \qquad \textbf{or} \qquad \frac{v_\mathrm{F}^2}{c^2} = \frac{x^2}{1+x^2}$$

For $x \ll 1 \Rightarrow v_\mathrm{F}/c \ll 1$: Non-relativistic case

For $x \gg 1 \Rightarrow v_\mathrm{F}/c \approx 1$: Relativistic case

Completely degenerate electron gas

Non-relativistic case

$$x \to 0 : f(x) \to \frac{8}{5}x^5, \qquad g(x) \to \frac{12}{5}x^5$$

$$\Rightarrow P_\mathrm{e} = \frac{8\pi m_\mathrm{e}^4 c^5}{15h^3}x^5$$

equation of state for a completely degenerate non-relativistic electron gas:

$$P_\mathrm{e} = \frac{1}{20}\left(\frac{3}{\pi}\right)^{2/3}\frac{h^2}{m_\mathrm{e}}n_\mathrm{e}^{5/3} = \frac{1}{20}\left(\frac{3}{\pi}\right)^{2/3}\frac{h^2}{m_\mathrm{e}m_\mathrm{u}^{5/3}}\left(\frac{\rho}{\mu_\mathrm{e}}\right)^{5/3}$$

degeneracy pressure:

$$P_\mathrm{e} = 1.0036 \times 10^{13}\left(\frac{\rho}{\mu_\mathrm{e}}\right)^{5/3} \text{(cgs)}$$

$$P_\mathrm{e} = \frac{2}{3}U_\mathrm{e}$$

Completely degenerate electron gas

Extreme relativistic case

see exercise sheet III

equation of state for a completely degenerate extreme relativistic electron gas:

$$P_\mathrm{e} = 1.2435 \times 10^{15} \left(\frac{\rho}{\mu_\mathrm{e}}\right)^{4/3} \text{(cgs)}$$

$$P_\mathrm{e} = \frac{1}{3} U_\mathrm{e}$$

Partial Degeneracy of the Electron Gas

For finite temperatures, degeneracy not complete

$\rightarrow$ transition to Boltzmann distribution

Fermi-Dirac statistics

$$f(p)\mathrm{d}p\mathrm{d}V = \frac{8\pi p^2\mathrm{d}p\mathrm{d}V}{h^3}\frac{1}{1+e^{E/kT-\psi}}$$

$$n_\mathrm{e} = \frac{8\pi}{h^3}\int_0^\infty \frac{p^2\mathrm{d}p}{1+e^{E/kT-\psi}}$$

$$P_\mathrm{e} = \frac{8\pi}{3h^3}\int_0^\infty p^3 v(p)\frac{\mathrm{d}p}{1+e^{E/kT-\psi}}$$

$$U_\mathrm{e} = \frac{8\pi}{h^3}\int_0^\infty \frac{Ep^2\mathrm{d}p}{1+e^{E/kT-\psi}}$$

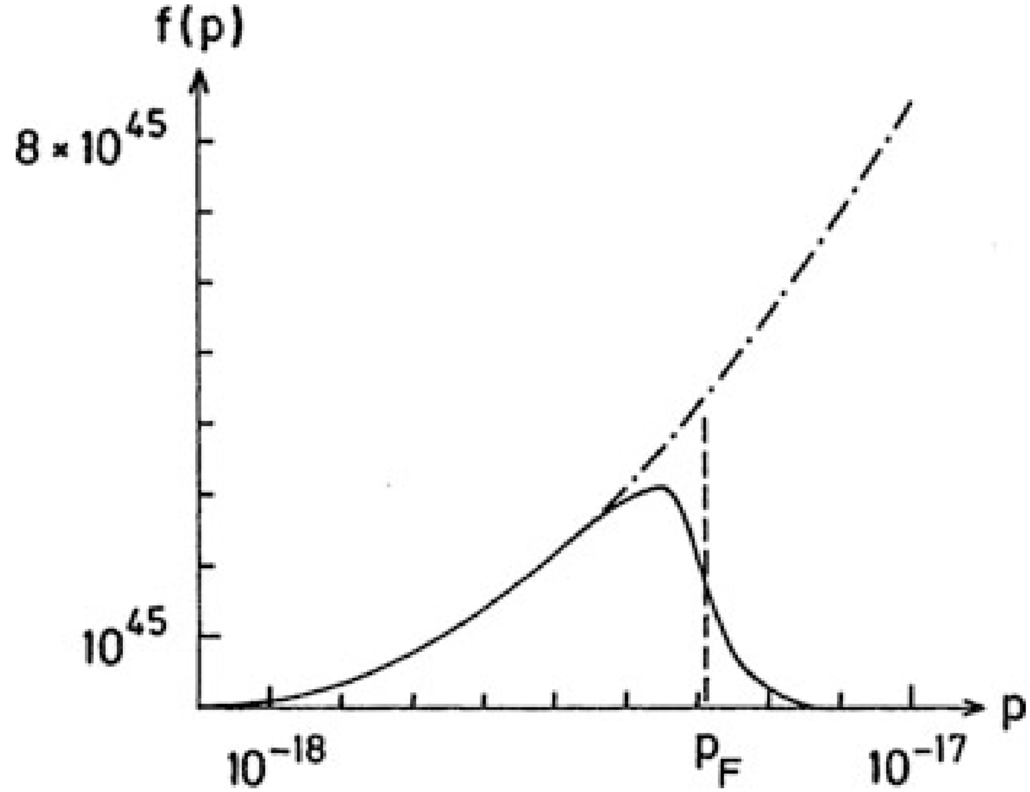

Kippenhahn, Weigert & Weiss 2012

degeneracy parameter $\psi = \psi\left(\frac{n_\mathrm{e}}{T^{3/2}}\right)$

$\rightarrow$ equation of state in the case of partial degeneracy cannot be derived analytically, analytical approximations are possible for the non-relativistic and extreme relativistic case

For details see: Kippenhahn, Weigert & Weiss 2012, p. 145-150

Partial Degeneracy of the Electron Gas

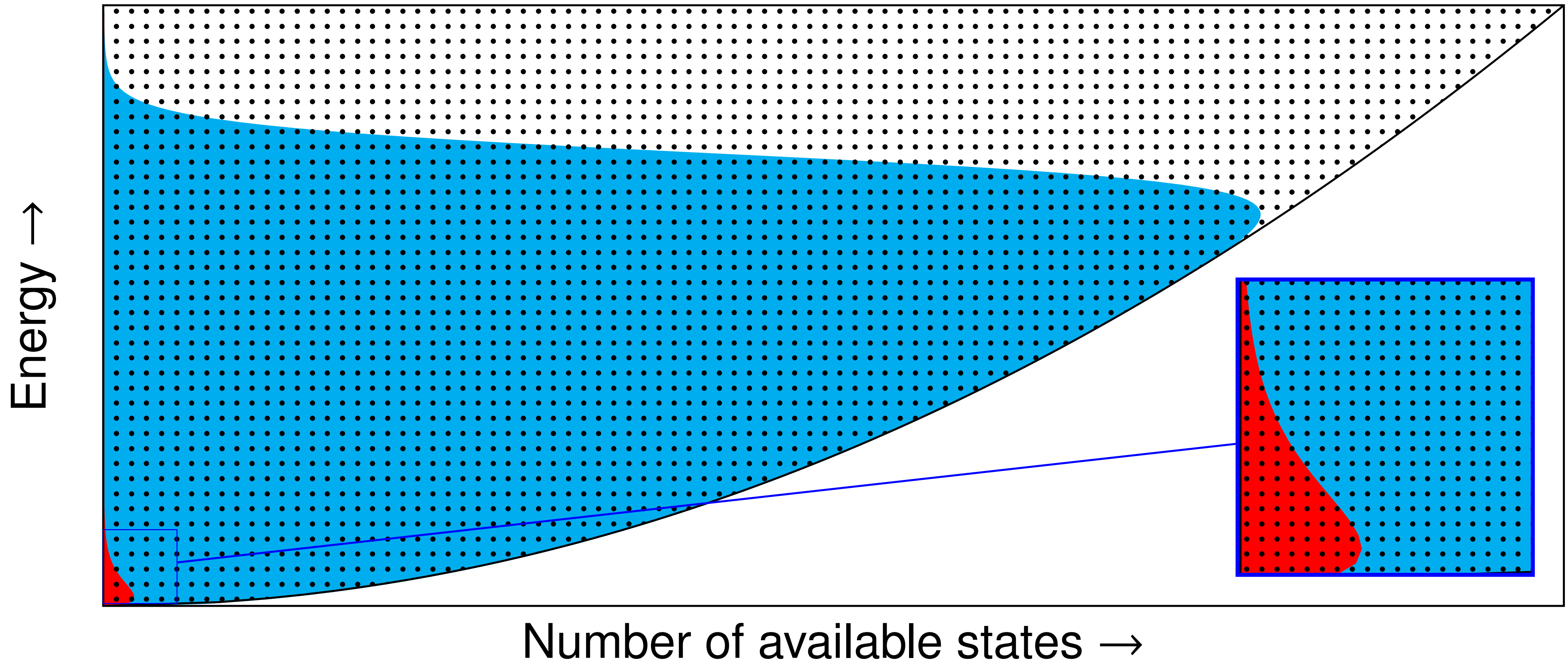

- low-density gas (red) behaves like ideal gas: Maxwell-Boltzmann distribution
- high-density gas (cyan) highly degenerate, i.e., all low energetic states are occupied and electrons are forced into high-lying states causing degeneracy pressure
- in complete degeneracy, all states up to the Fermi energy are filled

Equation of state of stellar matter

In real stellar matter all components, which are ions, electrons and radiation are mixed

$$P = P_{\mathrm{ion}} + P_{\mathrm{e}} + P_{\mathrm{rad}} = \frac{R}{\mu_0}\rho T + \frac{8\pi}{3h^3}\int_0^\infty p^3 v(p)\frac{\mathrm{d}p}{1+e^{E/kT-\psi}} + \frac{a}{3}T^4$$

$$\rho = \frac{4\pi}{h^3}(2m_{\mathrm{e}})^{3/2} m_{\mathrm{u}}\mu_{\mathrm{e}}\int_0^\infty \frac{E^{1/2}\mathrm{d}E}{1+e^{E/kT-\psi}},\ v(p) = \frac{\partial E}{\partial p},\ E = m_{\mathrm{e}}c^2\left(\sqrt{1+\frac{p^2}{m_{\mathrm{e}}^2c^2}}-1\right)$$

- Local equation of state depends on the conditions in the plasma
- Both electron and ion gas can become degenerate at low temperatures and/or high densities
  $\rightarrow$ Critical density for ions $(m_{\mathrm{ion}}/m_{\mathrm{e}})^{3/2} \sim 10^5$ times higher
  $\rightarrow$ Electron gas can be degenerate and ion gas ideal at the same time
- For high densities and low temperatures, the ions start to interact with each other via Coulomb interactions
  $\rightarrow$ Perfect gas approximation breaks down

Equation of state of stellar matter

In real stellar matter all components, which are ions, electrons and radiation are mixed

$$P = P_{\text{ion}} + P_{\text{e}} + P_{\text{rad}} = \frac{R}{\mu_0}\rho T + \frac{8\pi}{3h^3}\int_0^\infty p^3 v(p)\frac{\mathrm{d}p}{1 + e^{E/kT-\psi}} + \frac{a}{3}T^4$$

$$\rho = \frac{4\pi}{h^3}(2m_{\text{e}})^{3/2} m_{\text{u}}\mu_{\text{e}} \int\limits_0^\infty \frac{E^{1/2}\mathrm{d}E}{1 + e^{E/kT-\psi}},\ v(p) = \frac{\partial E}{\partial p},\ E = m_{\text{e}}c^2\left(\sqrt{1 + \frac{p^2}{m_{\text{e}}^2c^2}} - 1\right)$$

- ions start to form a lattice to minimize total energy as soon as the thermal energy $\frac{3}{2}kT$ becomes similar to the Coulomb energy per ion of charge: $-Ze$
- This **crystallization** is not important in normal stars, but becomes important at the late stages of stellar evolution
- Other **real gas effects** (e.g. van der Waals forces: attractive forces of electrically neutral, but polarized particles important at low temperatures; electron shielding: clouds of electrons gather around ions from distance the ion electron cloud appears electrically neutral, low densities) have to be taken into account in modern equations of state for stellar models

Equation of state of stellar matter

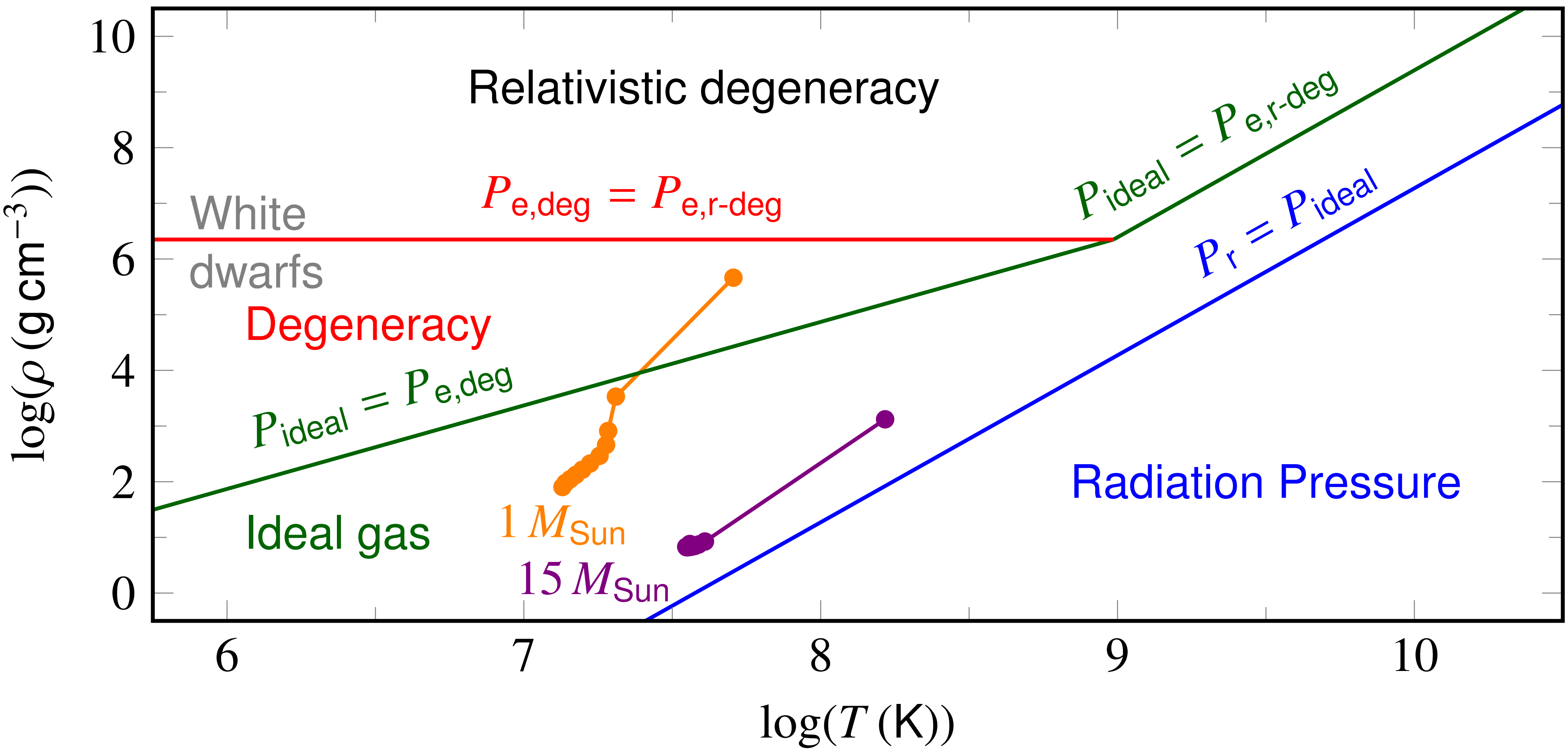

Equation of state of stellar matter

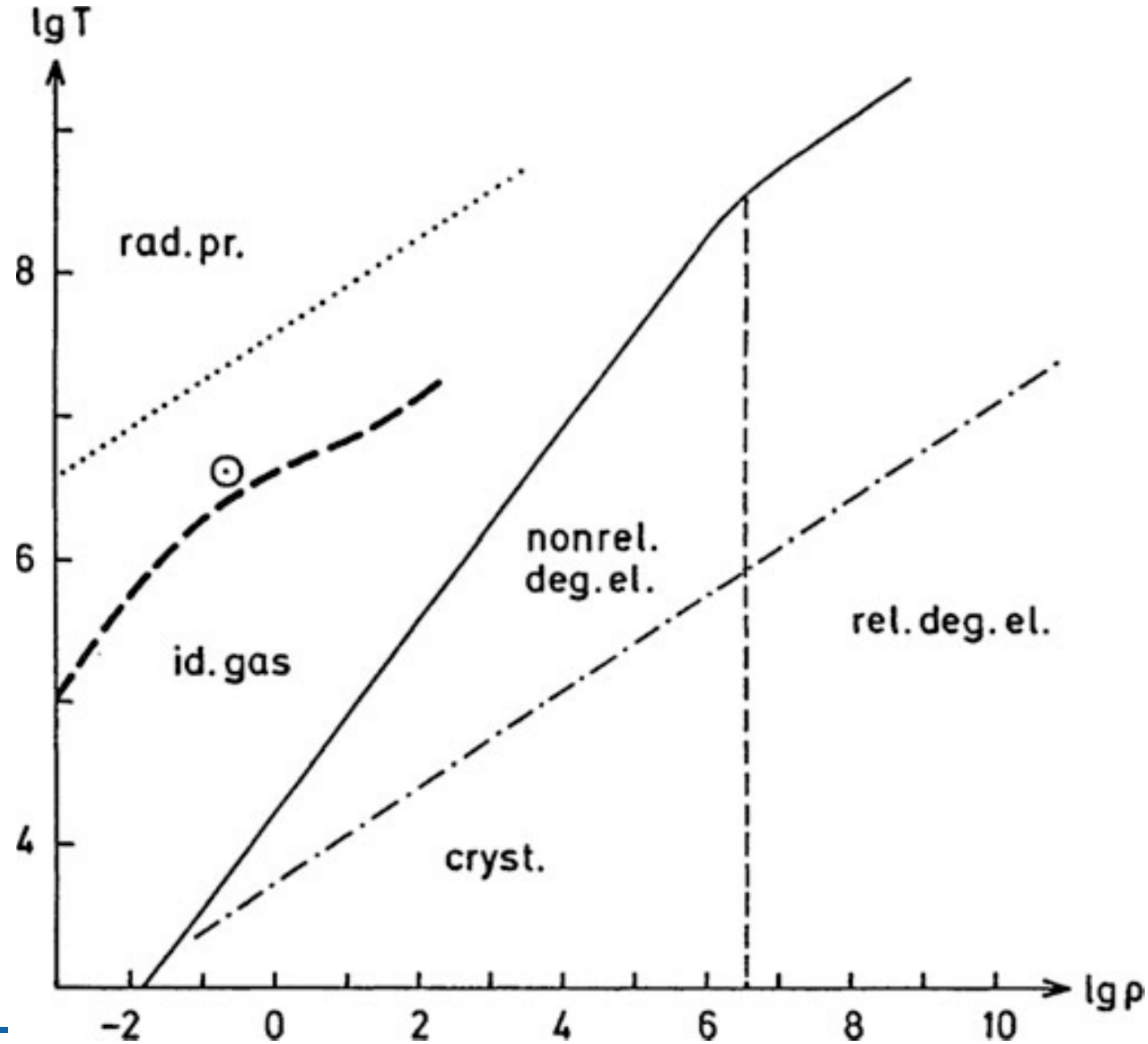

Kippenhahn, Weigert & Weiss 2012

Opacity

- The material function $\kappa(\rho, T)$ for stellar-structure calculations is nowadays computed numerically for different chemical mixtures
- main opacity mechanisms have already been introduced in the stellar atmosphere part of this course:
  - Electron scattering
  - Absorption due to free-free, bound-free and bound-bound transitions
  - Absorption due to H^- dissociation
  - Absorption due to dissociation of molecules
  - Conduction (for white dwarfs only)
- Groups spezialised on different aspects published extensive tables for different chemical mixtures, temperatures and densities
  - Atomic absorption (OPAL, Opacity Project)
  - Molecular and dust absorption below 10^4 K (Alexander & Ferguson 1994)
  - Electron conduction (Itoh et al.)
- The tables must be combined to cover the whole stellar structure
- To find $\kappa(\rho, T, X_i)$ for a given point in a star, the value has to be interpolated from the grid points

Nuclear energy production

- Stars produce energy through **thermonuclear fusion**
  $\rightarrow$ Thermal motions induce fusions of lighter elements to form a heavier one
- Before the reaction, the nuclei j have a total mass $\sum_j M_j$, which is different from the mass of the reaction product M_y

$$\Delta M = \sum_j M_j - M_y$$

  ΔM is called **mass defect**
  $\rightarrow$ this mass is released as energy $E = \Delta M c^2$ (Einstein's formula)
- **Binding energy** E_B of a nucleus with mass M_nuc and atomic mass number A: Z protons of mass m_p and $(A - Z)$ neutrons of mass m_n

$$E_\mathrm{B} = [(A - Z)m_\mathrm{n} + Zm_\mathrm{p} - M_\mathrm{nuc}]c^2$$

- Average **binding energy per nucleon** f

$$f = \frac{E_\mathrm{B}}{A}$$

Nuclear energy production

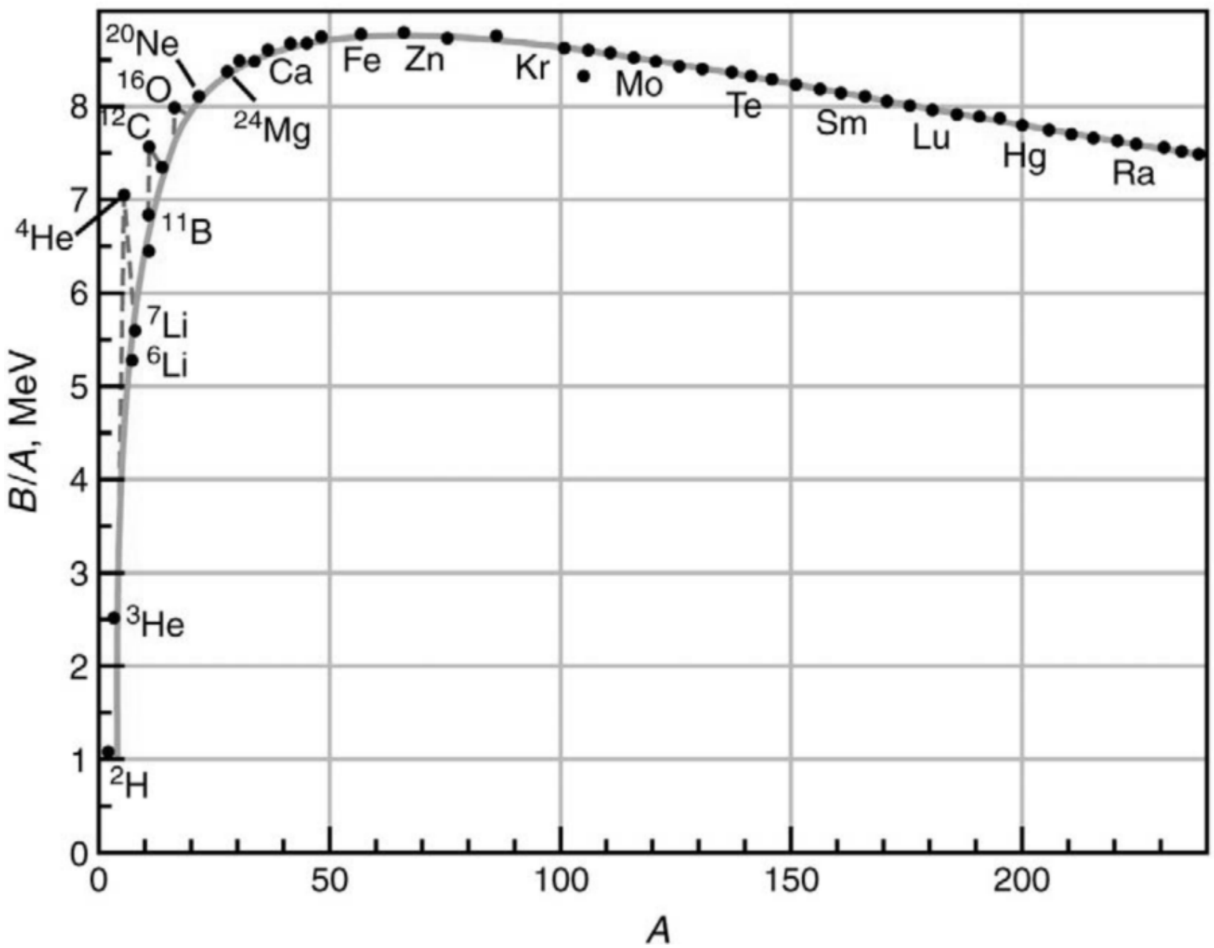

Abdullah 2014, Fundamentals in nuclear physics

Increase for $A < 56$

surface effect: particles at the surface of the nucleus experience less attraction by nuclear forces than those in the interior

$\rightarrow$ volume rises faster than surface area

$f(^{56}\text{Fe}) = 8.5\,\text{MeV}$

$\rightarrow$ increasing repulsion by the Coulomb forces for $A > 56$

Energy generation: **Fusion** of light nuclei $A < 56$ and **Fission** of heavy nuclei $A > 56$

Nuclear energy production

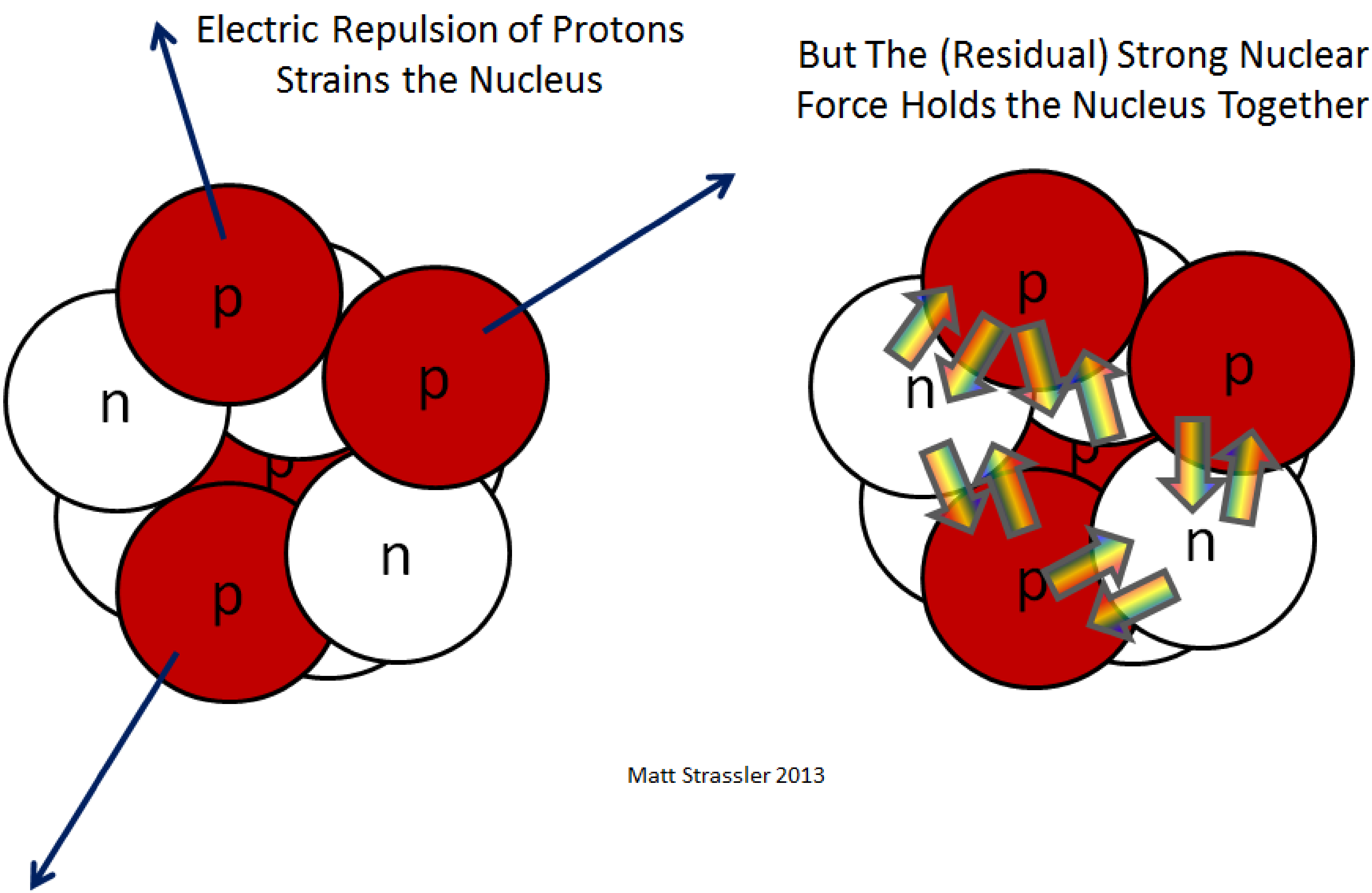

Nuclear energy production

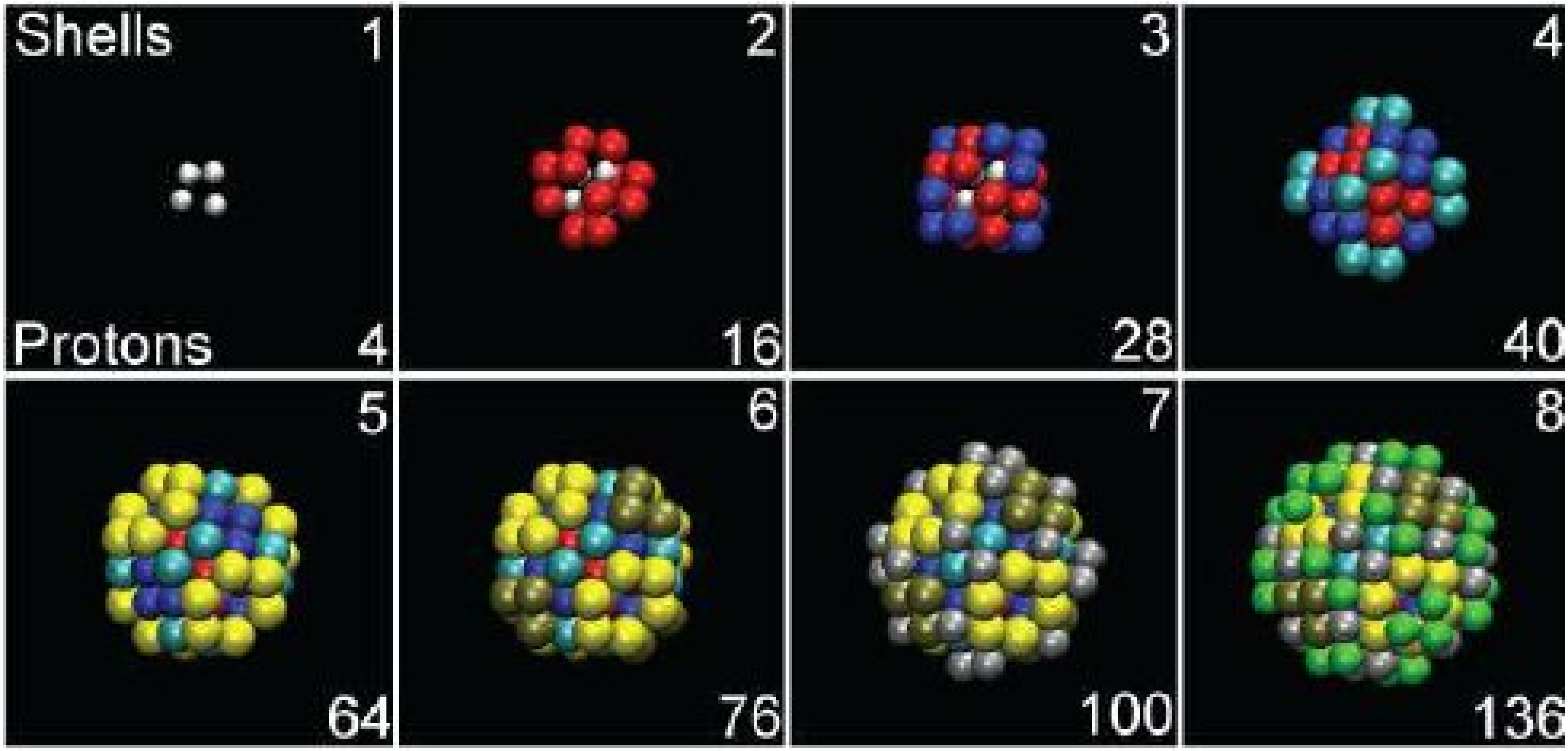

Hofer 2013, Journal of Physics Conference Series 504, 1

Coulomb barrier

For fusion two particles with charges Z_1 and Z_2 must be close enough to overcome the repulsive Coulomb forces

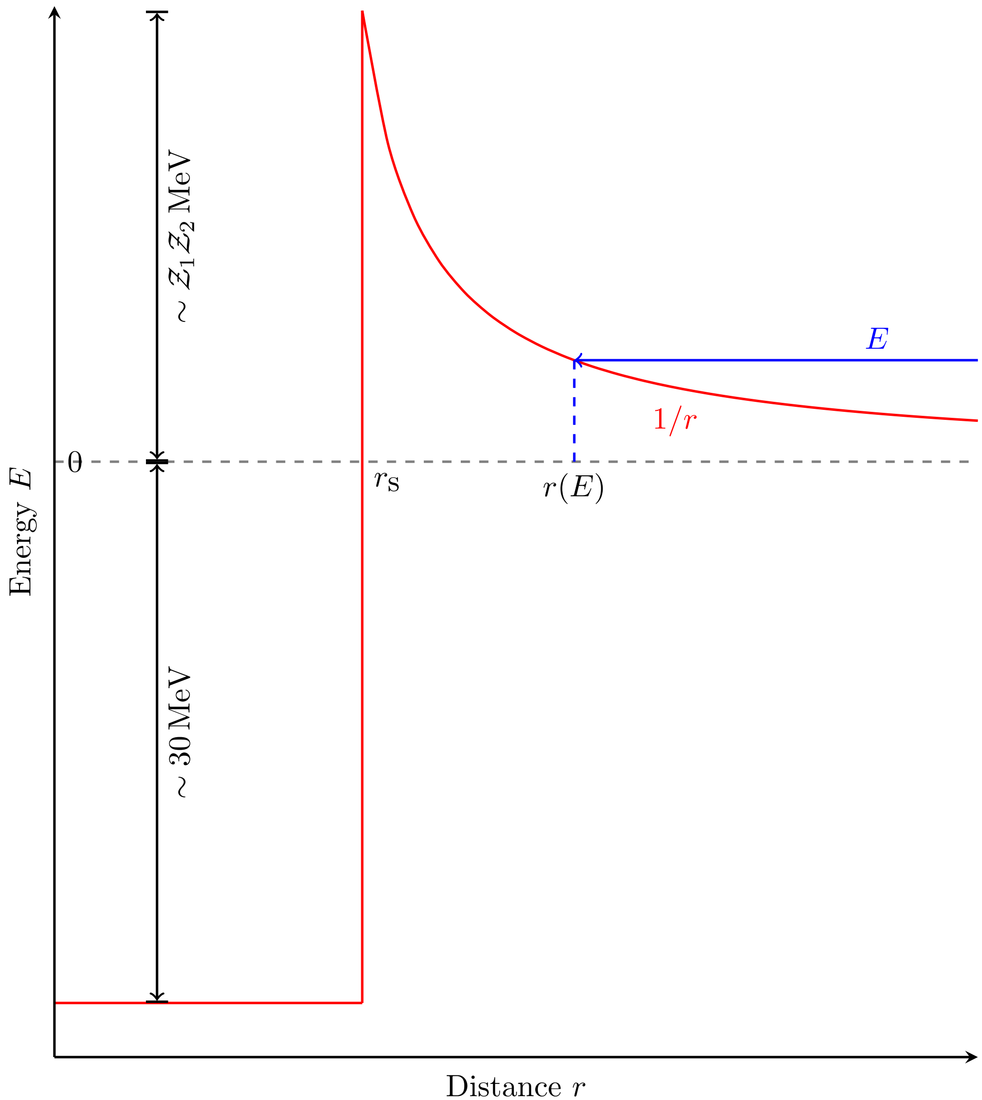

$$E_{\mathrm{Coul}} = \frac{Z_1 Z_2 e^2}{r} \tag{6.12}$$

Distances smaller than $r_S \approx A^{1/3} 1.44 \times 10^{-13}\,\mathrm{cm}$: attractive nuclear forces dominate

$\rightarrow$ Sharp drop in potential energy

Coulomb barrier with height of $E_{\mathrm{Coul}}(r_S) \approx Z_1 Z_2$ MeV

Coulomb barrier

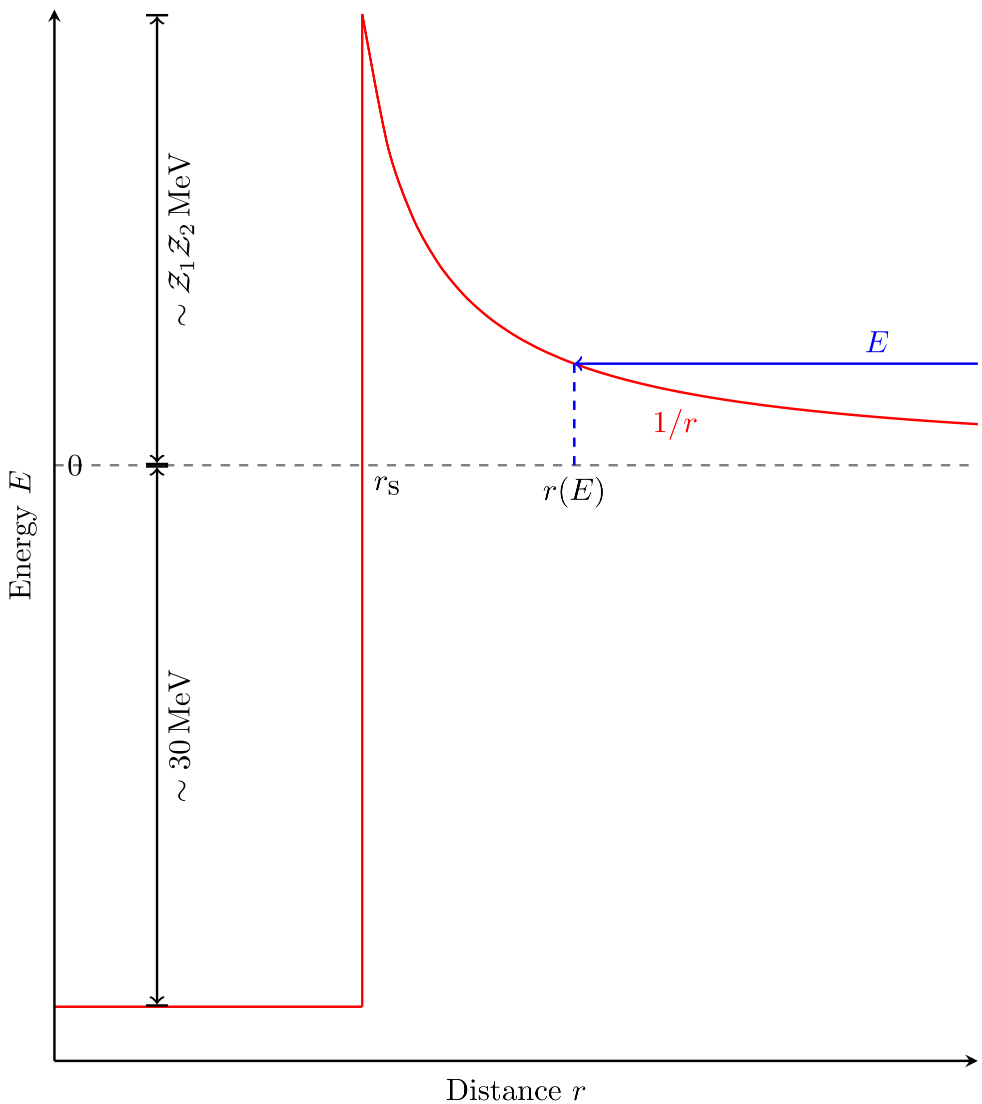

Classical case

Kinetic energy of particle (given by Maxwell-Boltzmann statistics) must be higher than Coulomb barrier

e.g. center of the sun $T \approx 10^7$ K
$\Rightarrow E_{\text{kin}}/E_{\text{Coul}} \approx 10^{-3}$
(no fusion possible)

Quantum mechanics

Small probability P_0 **to tunnel** the Coulomb barrier

$$P_0 = p_0 E^{-1/2} e^{-2\pi\eta}$$

$$\eta = \left(\frac{m}{2}\right)^{1/2} \frac{Z_1 Z_2 e^2}{\hbar E^{-1/2}}$$

m reduced mass, p_0 parameter depends on properties of colliding nuclei

Coulomb barrier

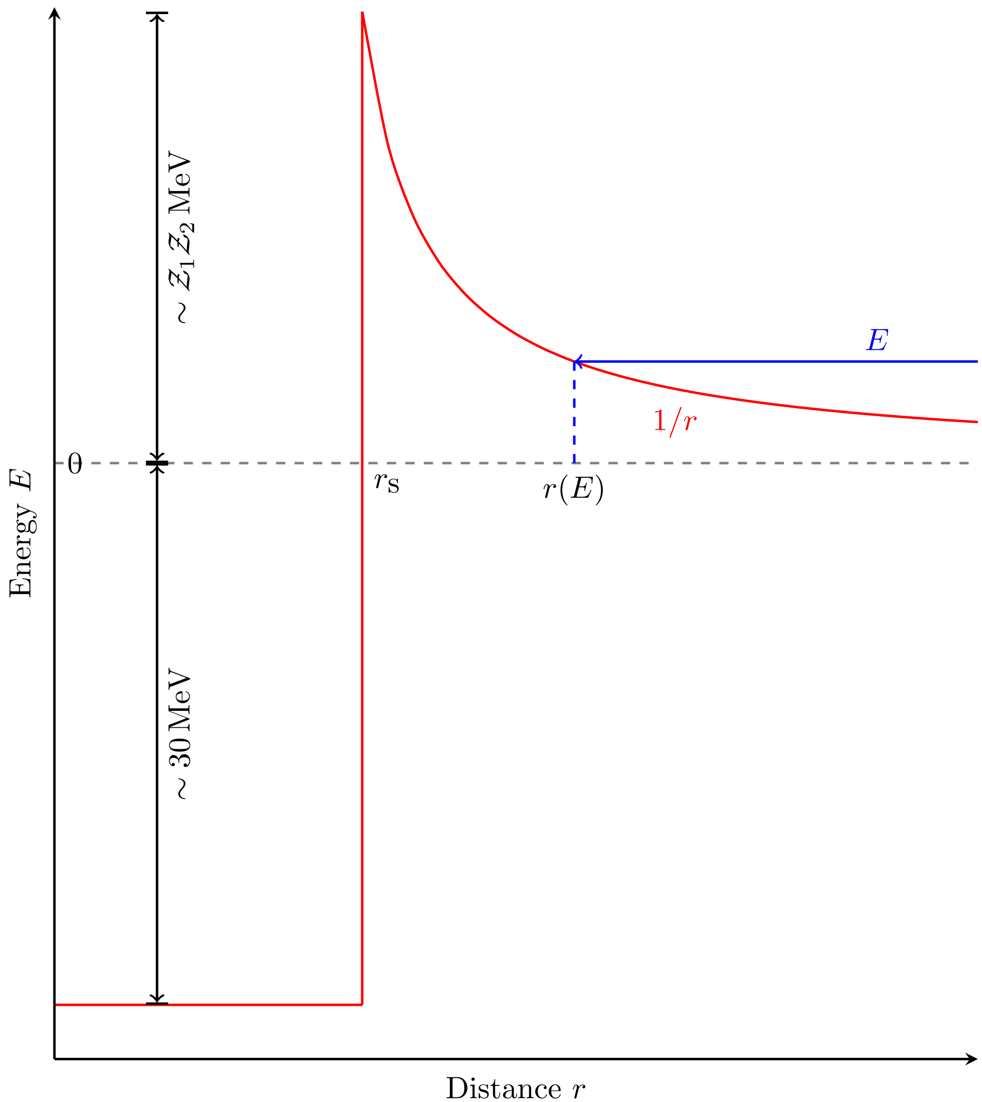

Example: Hydrogen fusion in center of the Sun $T \approx 10^7$ K, $Z_1 Z_2 = 1$

$$\Rightarrow P_0 \approx 10^{-20}$$

Probability increases with E and decreases with $Z_1 Z_2$

$\rightarrow$ Lightest elements fuse first

$\rightarrow$ Heavy element require much higher energies

Coulomb barrier

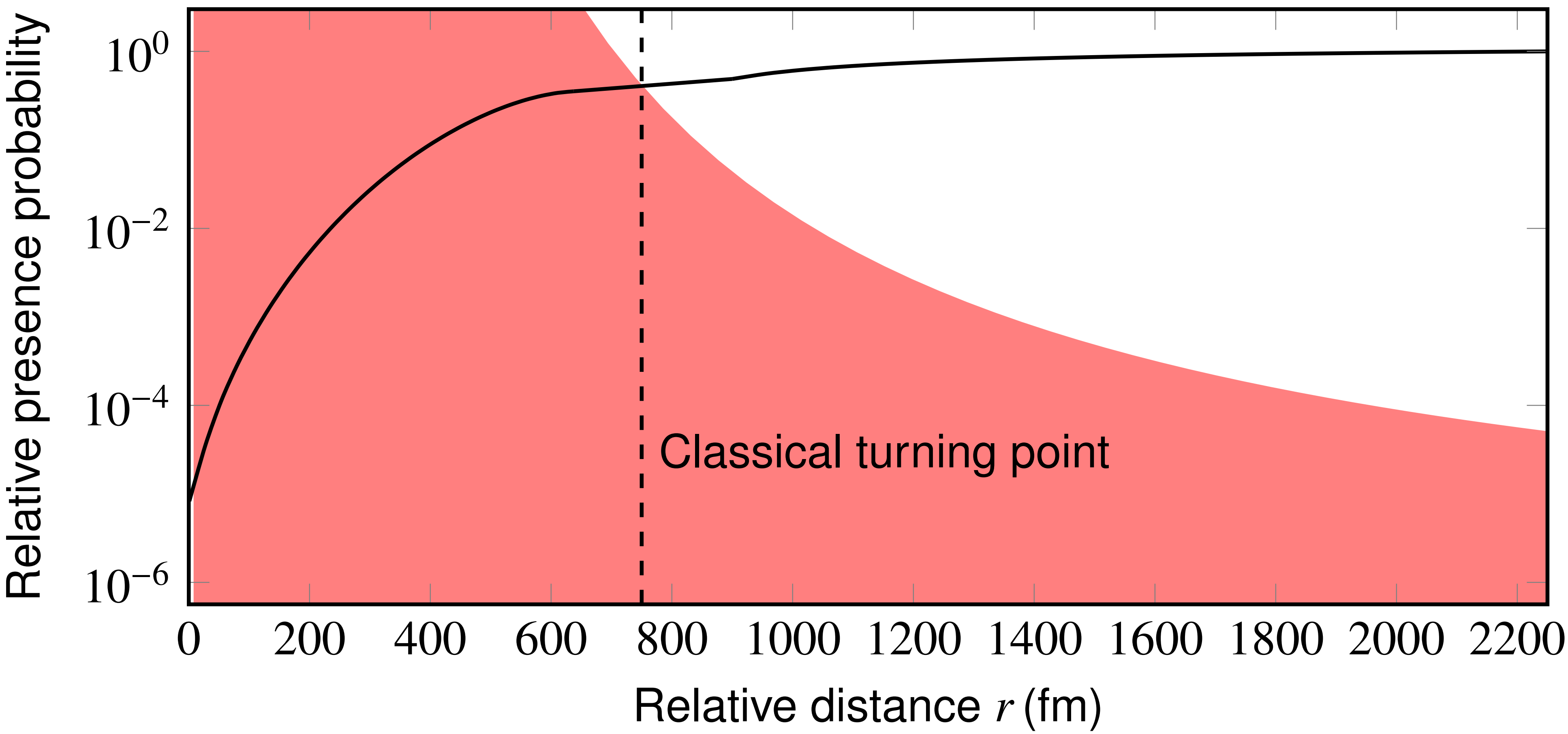

Small probability P_0 **to tunnel** the Coulomb barrier

$$P_0 = p_0 E^{-1/2} e^{-2\pi\eta}$$

Gamow factor $\hat{T} \equiv e^{-2\pi\eta}$

Thermonuclear reaction rate

thermonuclear reaction rates have to be computed to get the fusion rates

reaction of the nucleus X with the particle a by which the nucleus Y and the particle b are formed:

$$\mathrm{a} + \mathrm{X} \longrightarrow \mathrm{Y} + \mathrm{b} \qquad \Leftrightarrow \qquad X(a,b)Y$$

velocity-dependent cross section σ of the reaction

$$\sigma(v) = \frac{\text{number of reactions per nucleus } X \text{ per unit time}}{\text{number of incident particles } a \text{ per unit area per unit time}}$$

name cross section:
comes from assuming that each nucleus X has a cross-sectional area and that a reaction occurs each time an a particle strikes that area (symmetric in type of particle)

$\rightarrow$ not physically correct picture, but helpful for understanding

Thermonuclear reaction rate

thermonuclear reaction rate r per unit volume with the relative velocity (between a and X) v in range $[v, v + \mathrm{d}v]$ given by the velocity distribution $P(v)$:

$$r = \sigma(v) v n_a n_X \Rightarrow r_{aX} = \frac{1}{1+\delta_{aX}} n_a n_X \int_0^\infty v\sigma(v) P(v) \mathrm{d}v = \frac{1}{1+\delta_{aX}} n_a n_X \langle \sigma v \rangle$$

Replacing particle number n_i by mass fractions $X_i \rho = n_i m_i$ and introducing the energy released per reaction Q

$\rightarrow$ **Energy generation** per unit mass

$$\epsilon_{aX} = \frac{1}{1+\delta_{aX}} \frac{Q}{m_a m_X} \rho X_a X_X \langle \sigma v \rangle$$

$\rightarrow$ **nuclear lifetime** $\tau_a(X)$

$$\left(\frac{\partial n_X}{\partial t}\right)_a = -\frac{n_X}{\tau_a(X)}, \qquad \tau_a(X) = \frac{1}{1+\delta_{aX}} \frac{n_X}{r_{aX}} \rightarrow \frac{1}{\tau(X)} = \sum_i \frac{1}{\tau_i(X)}$$

Nuclear cross section

nuclear cross section

- inversely proportional to the number of incident particles per unit time and react more often with each other when they spend more time close to each other $\sigma(v) \sim v^{-2} \overset{E=\frac{1}{2}mv^2}{\sim} E^{-1}$
- Nuclear reactions only when the particles can penetrate the Coulomb barrier
- nuclear structure of the involved particles will play a role $\rightarrow$ S-factor

$$\sigma(E) \equiv \frac{S(E)}{E} e^{-2\pi\eta} \Rightarrow \langle \sigma v \rangle = \int_0^\infty \sigma(E) v \overbrace{\frac{2}{\sqrt{\pi}} \frac{E^{1/2}}{(kT)^{3/2}} e^{-E/kT}}^{f(E)} \mathrm{d}E$$

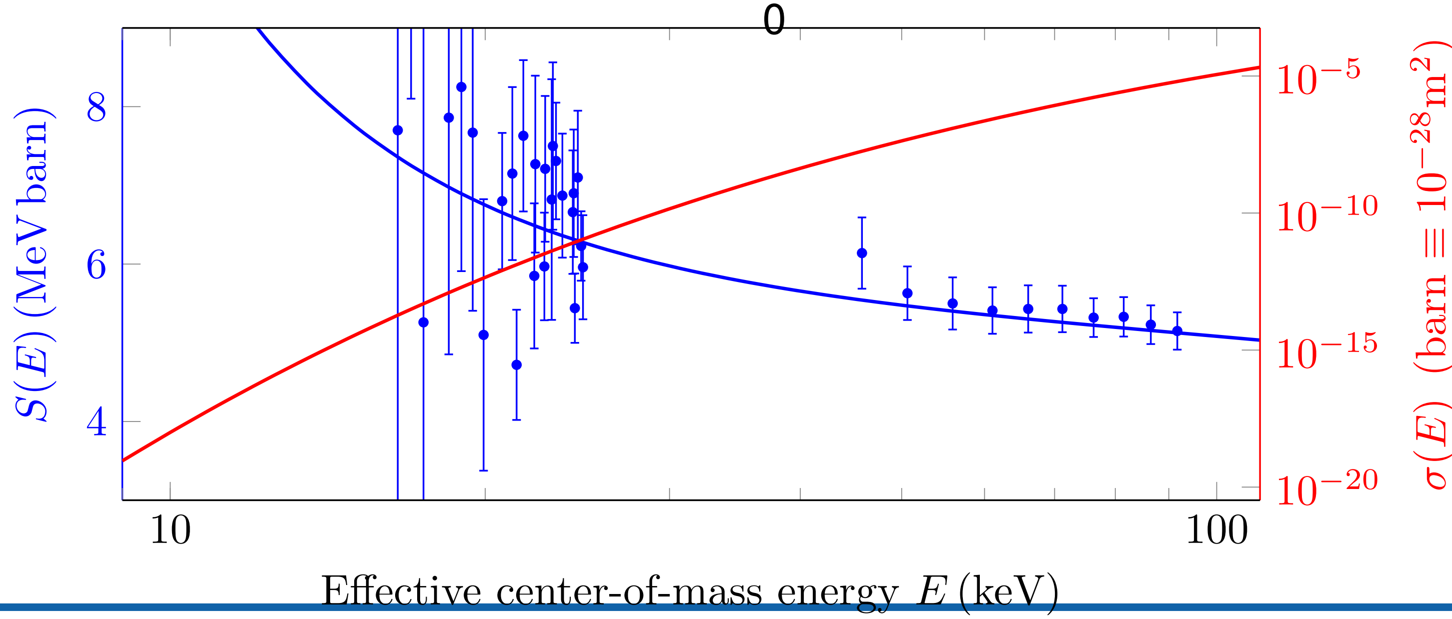

$^3He + {}^3He \longrightarrow {}^4He + 2\,p$ measured by LUNA (Junker et al. 1997, Bonetti et al. 1999)

Gamow peak

The product (black) of rapidly falling Maxwell-Boltzmann exponential (blue) and increasing Gamow penetration factor (red) has a sharp peak, the **Gamow peak**, at energy $E_0 = \left(\frac{2\pi\eta}{\sqrt{E}}\frac{kT}{2}\right)^{2/3} = \left(\frac{\sqrt{2m}\pi Z_1 Z_2 e^2}{\hbar}\frac{kT}{2}\right)^{2/3} \approx 5 - 100 \times kT$

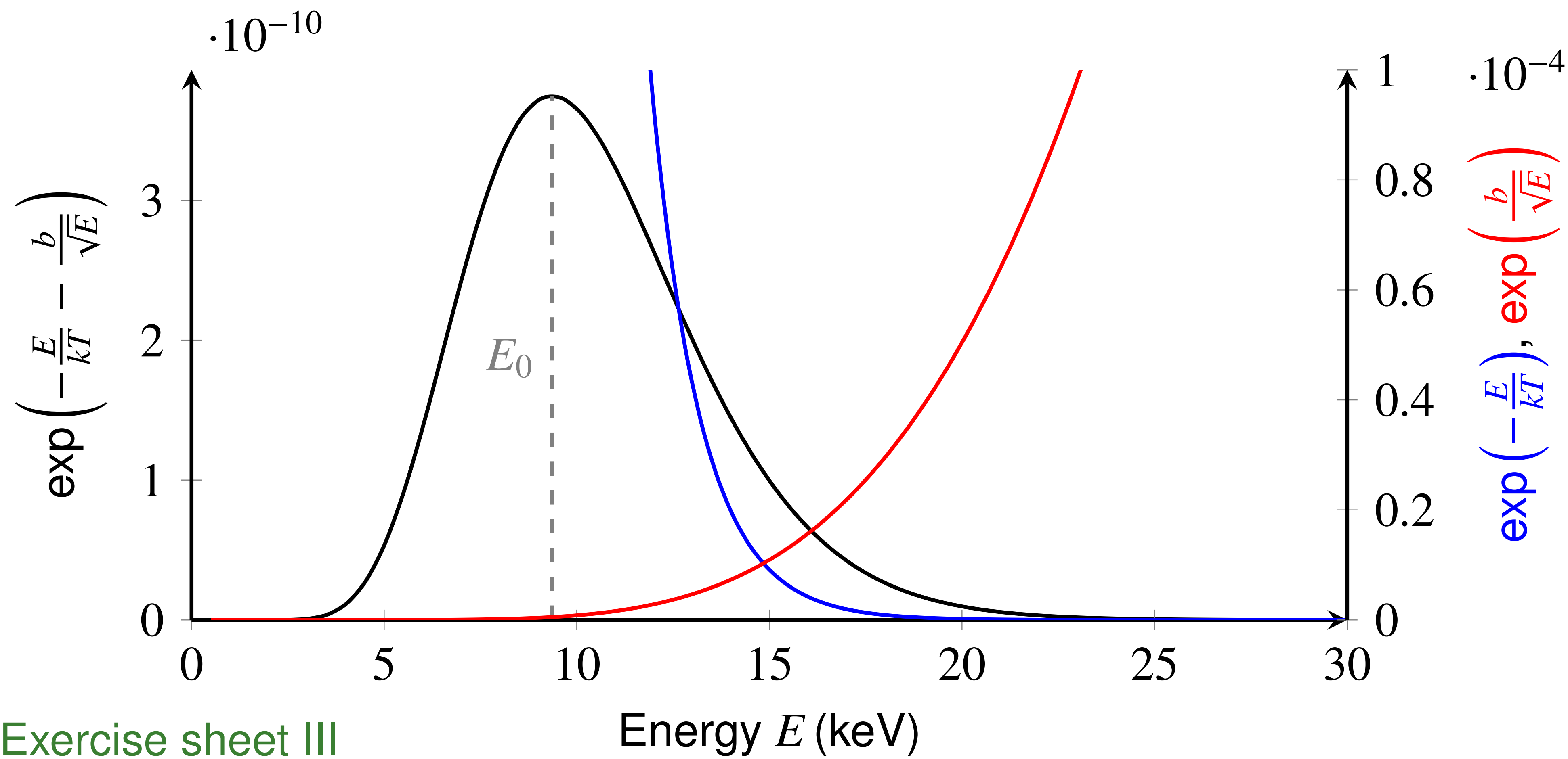

Exercise sheet III

Gamow peak

Maximum and area of Gamow peak extremely dependent on temperature

$$\langle \sigma v \rangle \sim \int_0^\infty e^{-E/kT - 2\pi\eta} \mathrm{d}E \approx \langle \sigma v \rangle_0 \left(\frac{T}{T_0} \right)^\nu , \qquad \nu \approx \frac{E_0}{kT}, \nu \approx 5 - 20$$

Each reaction has a well defined energy range separate from other reactions

→ **Separate burning stages** dependent mostly on temperature

→ The heavier the nuclei, the higher the temperature dependence

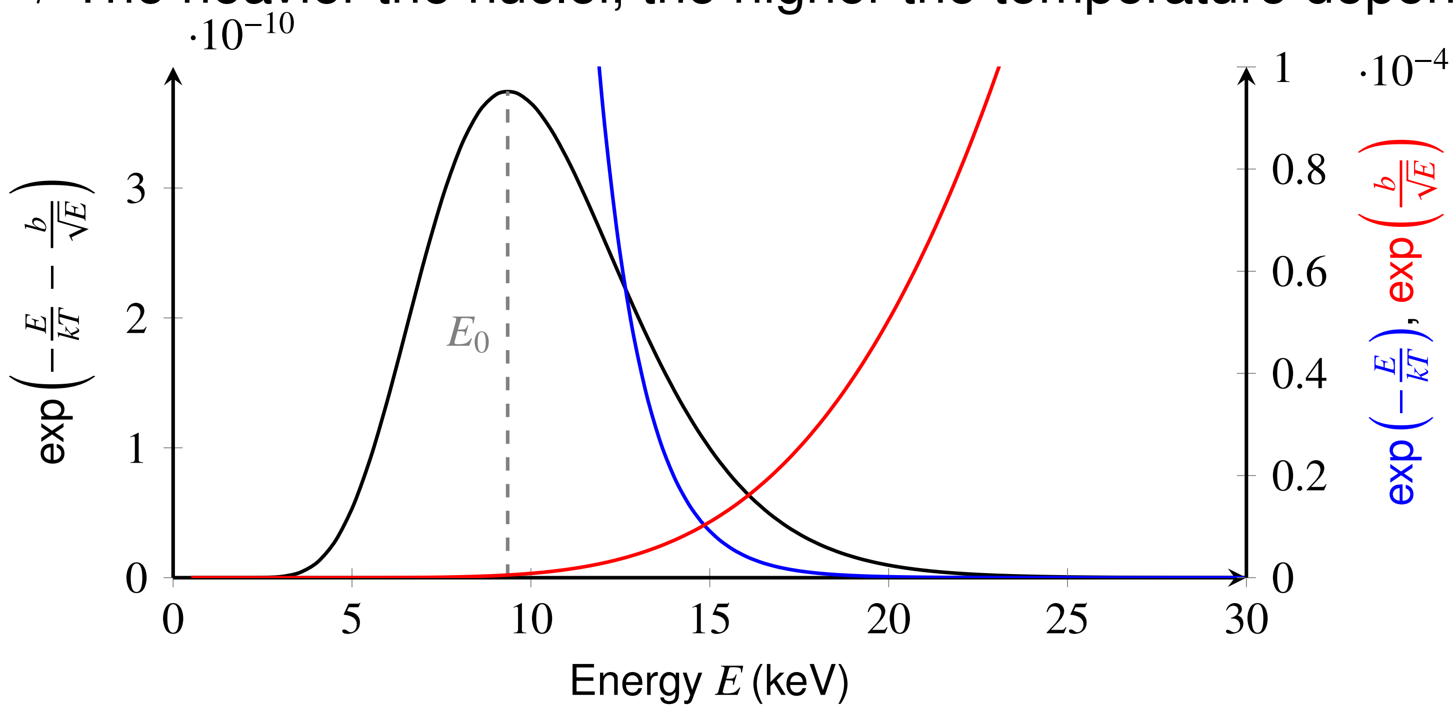

Nuclear reactions

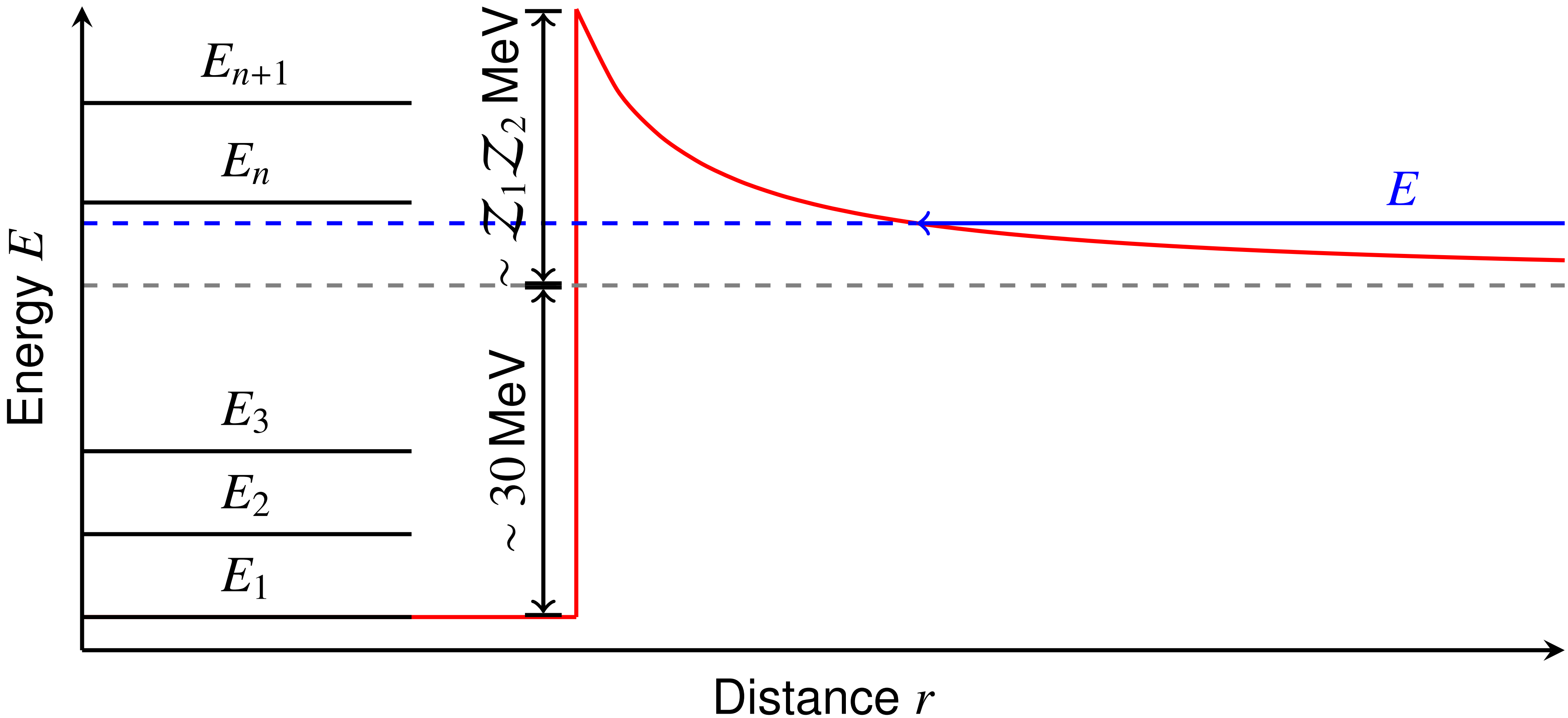

- Right after a particle is absorbed by the nucleus, a new compound nucleus is formed for a short time

$\rightarrow$ Similar to the energy levels of atoms, this nucleus has certain energy levels

$\rightarrow$ if energy of absorbed particle matches one of those energy levels: resonance

Nuclear reactions

Resonant reactions

- if configuration of the compound nucleus is similar to a stable excited state of the newly formed nucleus, the reaction is said to be resonant.
- respective cross sections vary strongly with energy (since the energy uncertainty of a stable state is small) and are relatively large

Non-resonant reactions

- If configuration of the compound nucleus is far from any stable excited state of the newly formed nucleus, the reaction is said to be non-resonant.
- compound nucleus is, by definition, not stable and decays or de-excites instantaneously
- cross sections are roughly constant with energy (since the energy uncertainty of an unstable state is huge) and are relatively small

Nuclear reactions

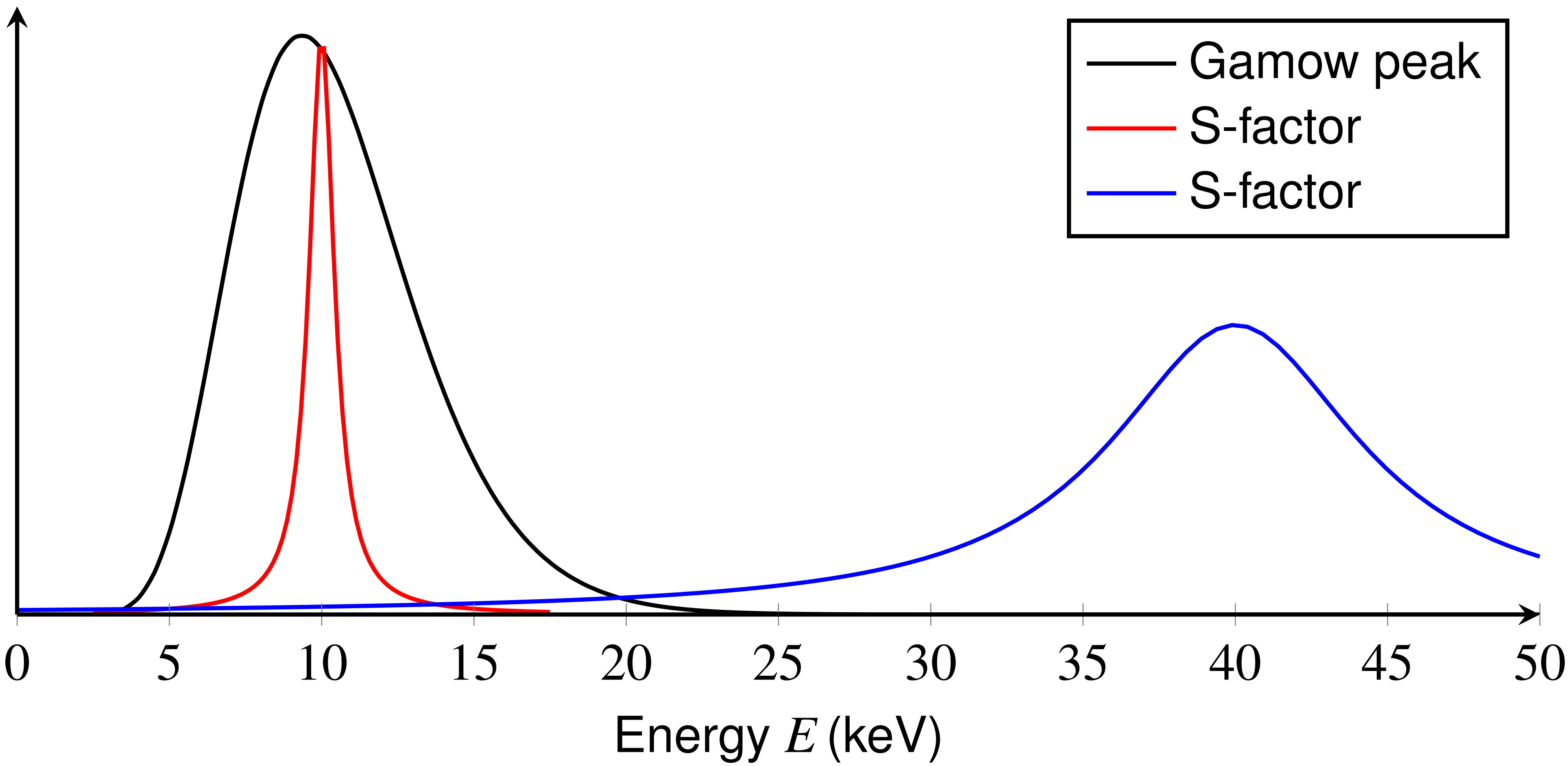

Nuclear reactions

Energy dependence of reaction cross section $\sigma(E)$ has another factor of typical resonance form around the resonance energy E_{res} in resonance case

$$\xi(E) \sim \frac{1}{(E - E_{\text{res}})^2 + (\Gamma/2)^2}$$

$\Gamma = \hbar/\tau$ energy width of the level, τ lifetime on this level

Introducing the de Broglie wavelength of the particle with relative momentum p and reduced mass $m = m_1 m_2/(m_1 m_2)$

$$\lambda = \frac{\hbar}{p} = \frac{\hbar}{(2mE)^{1/2}}$$

$$\sigma(E) \sim \pi\lambda^2 P_0(E)\xi(E) = \xi(E)\frac{\pi p_0 \hbar^2 E^{-1/2}}{2m}\frac{e^{-2\pi\eta}}{E} \equiv \frac{S(E)}{E}e^{-2\pi\eta}$$

”Astrophysical factor” $S(E)$ contains all intrinsic nuclear properties of the reaction, $\xi(E) \to 1$ away from resonances

$\to$ Can in principle be calculated, but is more reliable when measured

$\to$ Problem: energies in stellar interiors very small ≈ 10 keV: $\sigma(E)$ very small

Nuclear reactions

^{2}H(p, γ)^{3}He

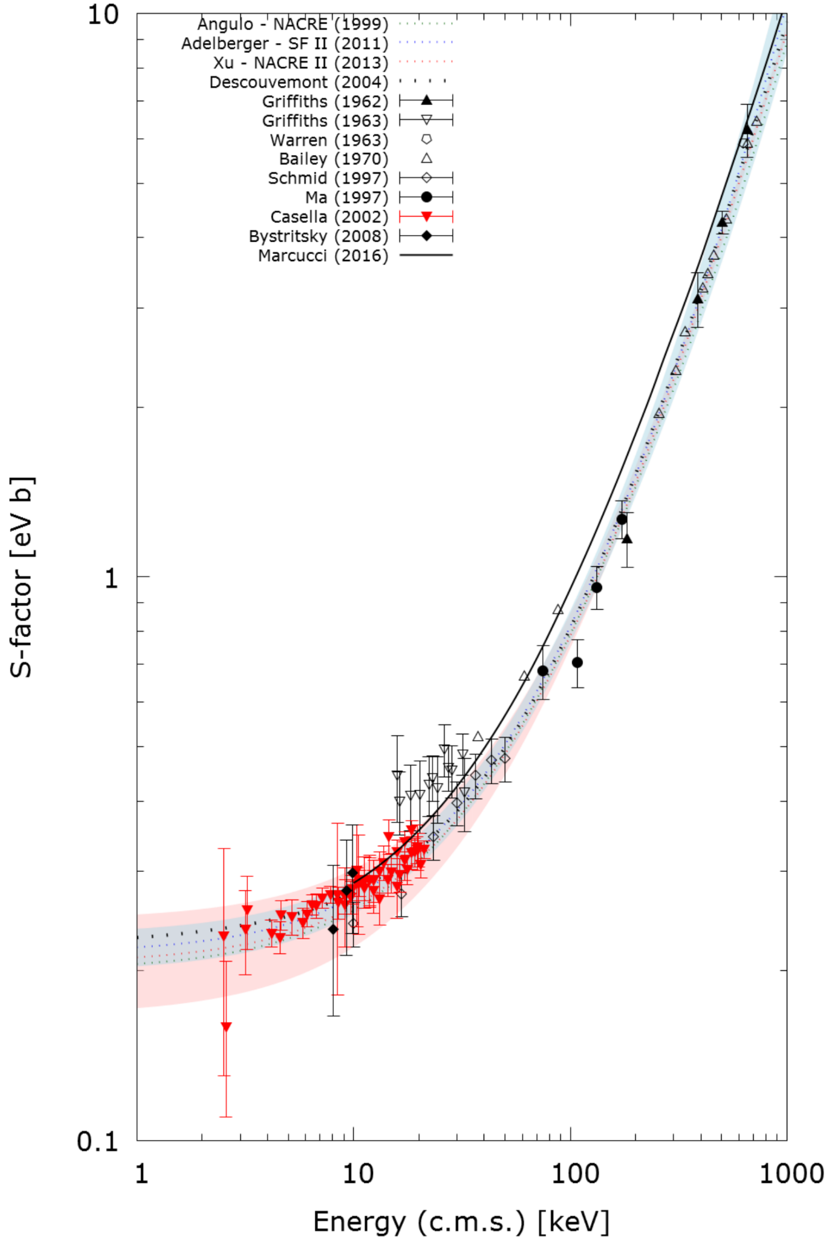

Cavanna et al. 2018

Laboratory measurements with particle accelerators(LUNA experiment at Gran Sasso (1999-2014)):

^{3}He(^{3}He, 2 p)^{4}He, ^{17}O(p, γ)^{18}F, ^{2}H(α, γ)^{6}Li, ^{2}H(p, γ)^{3}He

$S(E)$ must be extrapolated to lower energies in most cases

$\rightarrow$ Easily possible in the non-resonant case, because $S(E)$ varies slowly with energy

$\rightarrow$ Not possible, if hidden resonances are present

Nuclear reactions

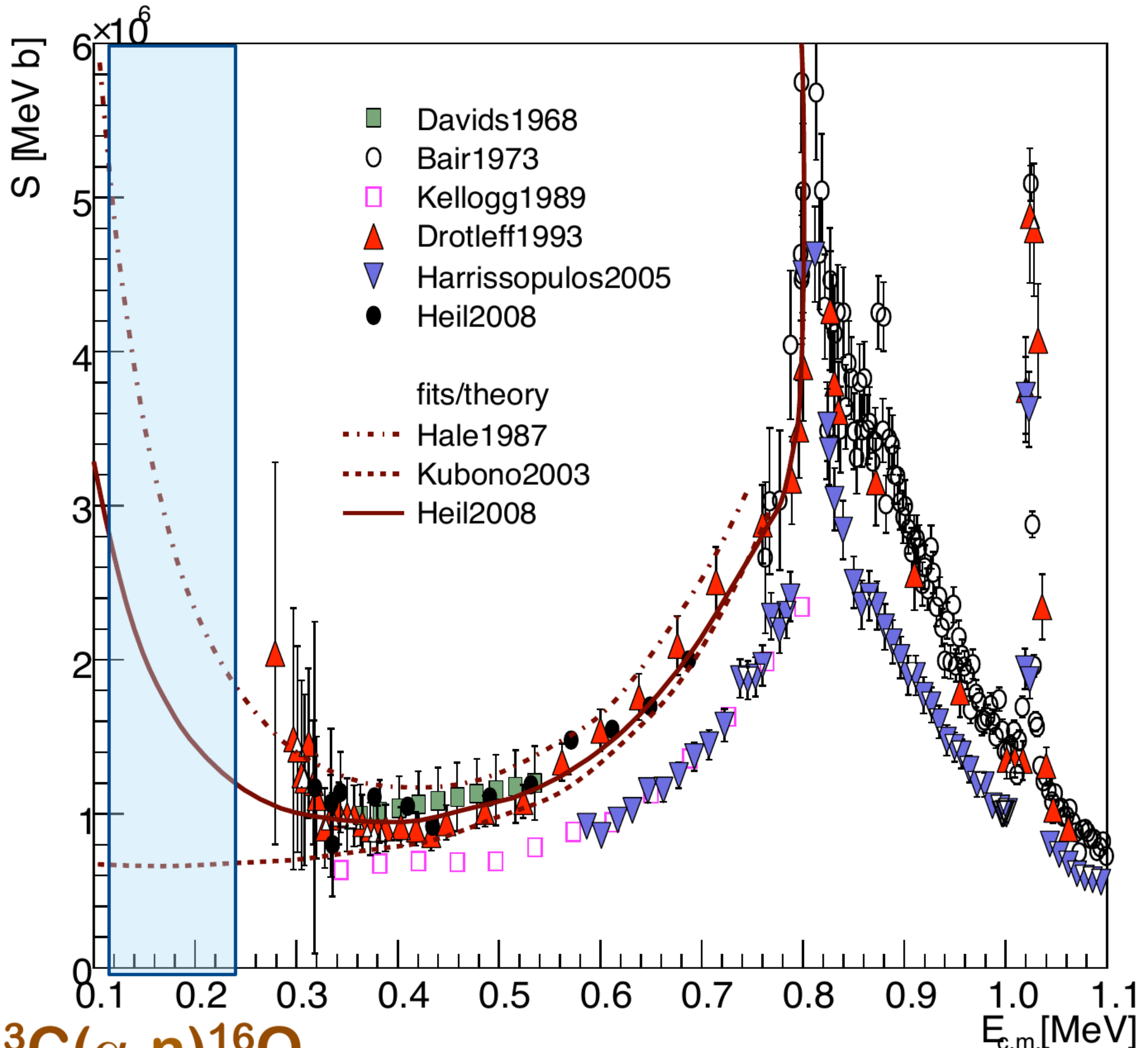

$^{13}C(\alpha,n)^{16}O$

Sandra Zavatarelli 2017

Laboratory measurements with particle accelerators(LUNA experiment at Gran Sasso (1999-2014)):

$^3He(^3He, 2p)^4He$, $^{17}O(p,\gamma)^{18}F$, $^2H(\alpha,\gamma)^6Li$, $^2H(p,\gamma)^3He$

$S(E)$ must be extrapolated to lower energies in most cases

$\rightarrow$ Easily possible in the non-resonant case, because $S(E)$ varies slowly with energy

$\rightarrow$ Not possible, if hidden resonances are present

Hydrogen burning

Hydrogen is the lightest and most abundant element

$\rightarrow$ Fusion reactions are happening at the lowest energies

fusion of hydrogen to helium liberates 26.64 MeV of total energy due to the mass defect Δm

$\rightarrow$ not all of this energy converted to thermal energy

$\rightarrow$ some fraction (2 to 30%) carried by neutrinos, which are created by the conversion of two protons into two neutrons via the β^{+} decay

$\rightarrow$ low cross sections with matter, almost all neutrinos escape from the star without interaction and their energy is lost (2×0.262 MeV)

$\rightarrow$ detection of solar neutrinos was the verification of nuclear energy generation in stars

$4\,\mathrm{H} \longrightarrow {}^{4}\mathrm{He}$: requires fusion of 4 protons at the same time

$\rightarrow$ reaction extremely unlikely

$\rightarrow$ Chain of reactions necessary

$\rightarrow$ Two different reaction processes: **p-p chains** and **CNO cycle**

p-p chains

backbone of the p-p chain – proton-proton reaction:

$$^{1}\mathrm{H} + {}^{1}\mathrm{H} \longrightarrow {}^{2}\mathrm{D} + \mathrm{e}^{+} + \nu_e$$

$\rightarrow$ liberated energy via the mass defect Δm is 0.420 MeV, annihilation of the positron and an electron brings the total energy release to 1.442 MeV

$\rightarrow$ close encounter between two protons **and** a simultaneous decay of a proton into a neutron

$\rightarrow$ cross section extremely small, never possible to measure it in the laboratory ($\tau_p(p) \approx 10^{10}$ yr)

$\rightarrow$ theoretical understanding good enough: $S(E_0) \approx 3.78^{-22}$ keV barns

cross-section of deuterium-deuterium reaction very small $\rightarrow$ deuterium reacts with protons:

$$^{2}\mathrm{D} + {}^{1}\mathrm{H} \longrightarrow {}^{3}\mathrm{He} + \gamma$$

$\rightarrow$ $\tau_{\mathrm{p}(^2\mathrm{D})} \approx 2.8$ s for conditions in center of the Sun

$\rightarrow$ created deuterium atom will almost immediately be converted to ^{3}He, deuterium-deuterium reaction can be neglected

p-p chains

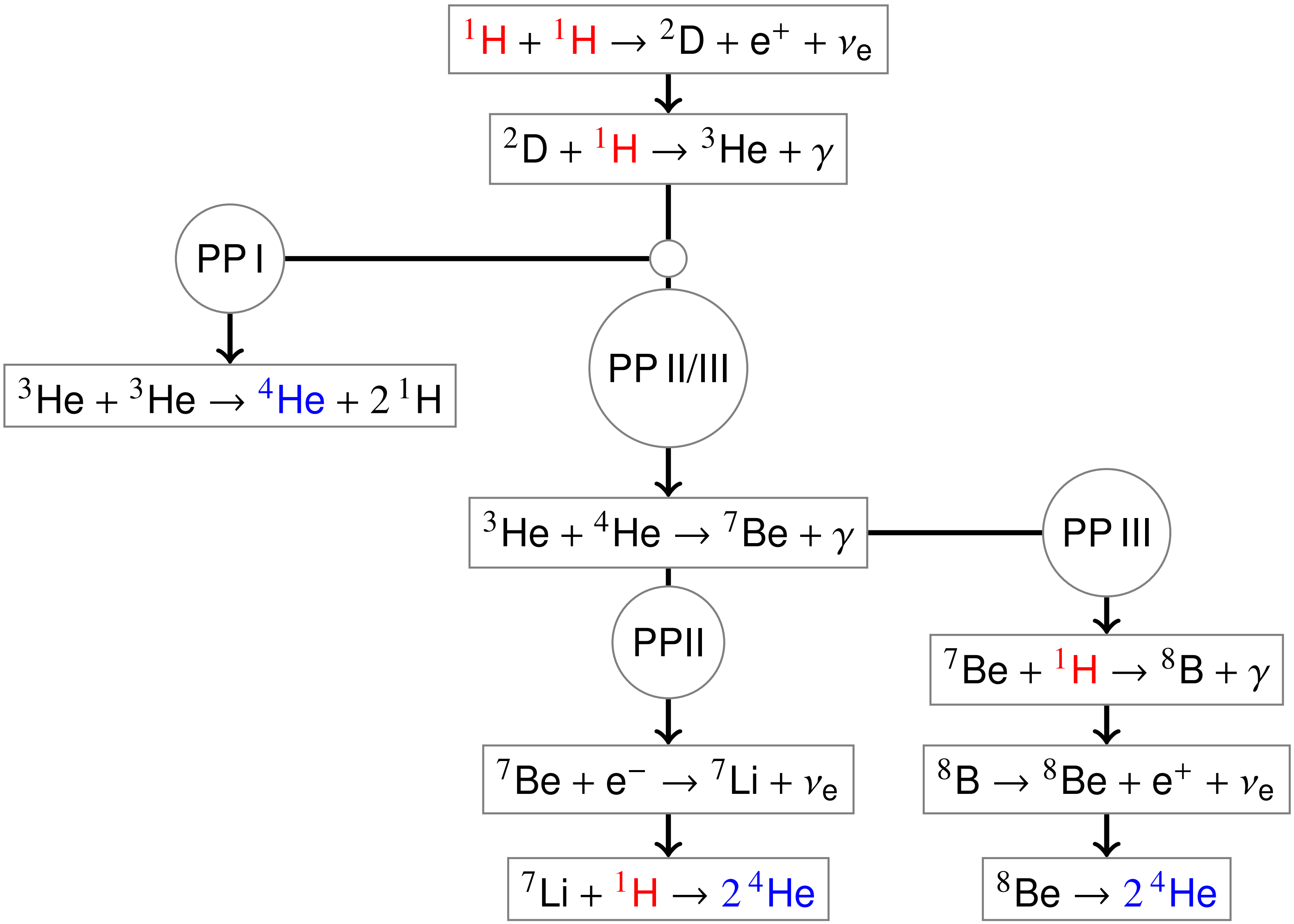

Reaction rate determined by the slowest reaction: p-p reaction (10^{10} yr)

p-p chains

Chemical composition similar to center of the Sun ($X = 0.35$, $Y = 0.6465$)

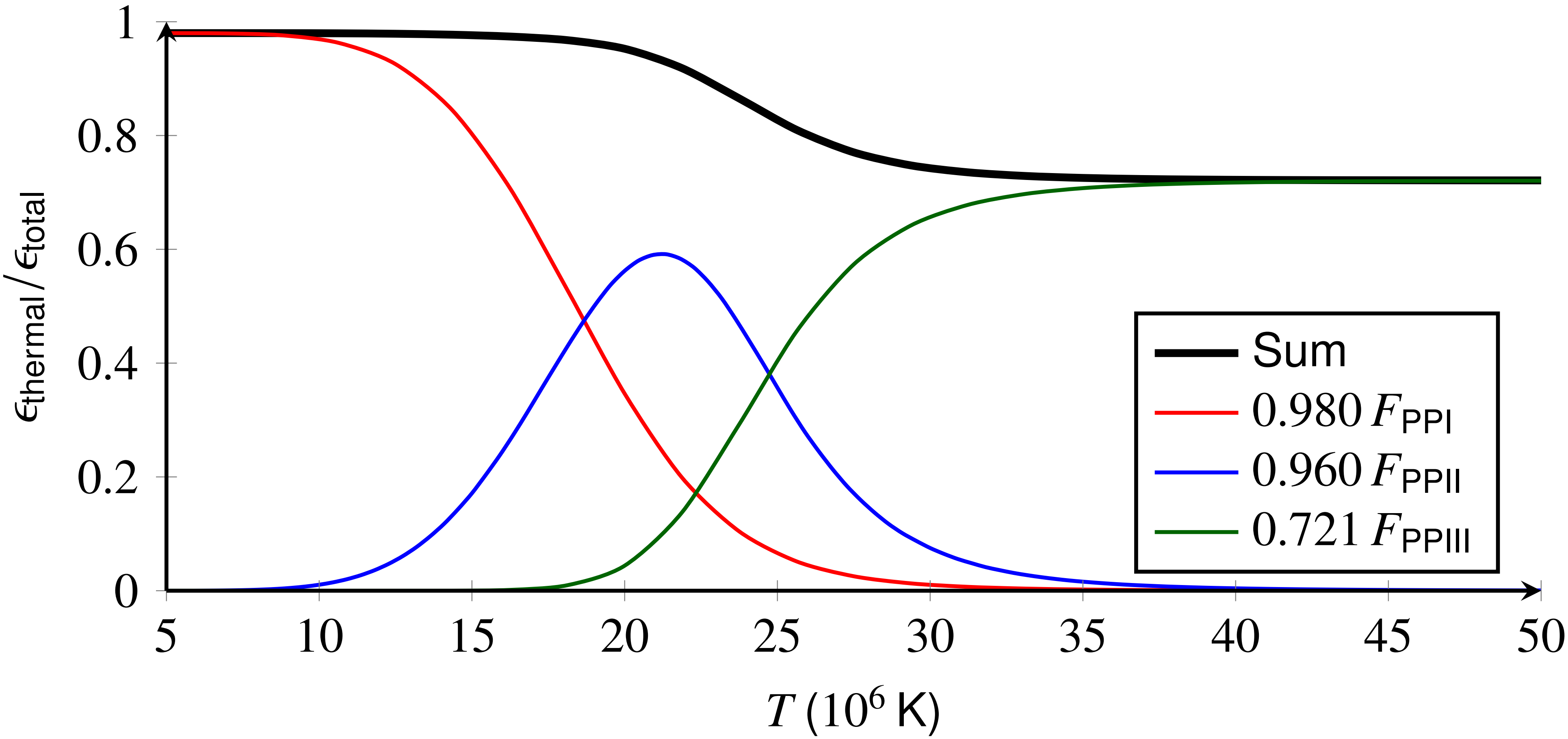

- relative contribution of the chains depends on the temperature, density and abundances
- Energy released: $Q \approx 25$ MeV; reaction rate $\langle \sigma v \rangle \sim \rho T^{4.6}$

CNO bi-cycle

C,N and O are present with relatively small abundances in all stars

$\rightarrow$ These nuclei can induce another chain of reactions to transform hydrogen to helium acting as catalysts only

$$^{12}\mathrm{C} + {}^{1}\mathrm{H} \rightarrow {}^{13}\mathrm{N} + \gamma$$

$$^{13}\mathrm{N} \rightarrow {}^{13}\mathrm{C} + \mathrm{e}^{+} + \nu_{\mathrm{e}}$$

$$^{13}\mathrm{C} + {}^{1}\mathrm{H} \rightarrow {}^{14}\mathrm{N} + \gamma$$

$$^{14}\mathrm{N} + {}^{1}\mathrm{H} \rightarrow {}^{15}\mathrm{O} + \gamma$$

$$^{15}\mathrm{O} \rightarrow {}^{15}\mathrm{N} + \mathrm{e}^{+} + \nu_{\mathrm{e}}$$

99.96%

$$^{15}\mathrm{N} + {}^{1}\mathrm{H} \rightarrow {}^{12}\mathrm{C} + {}^{4}\mathrm{He}$$

0.04%

$$^{15}\mathrm{N} + {}^{1}\mathrm{H} \rightarrow {}^{16}\mathrm{O} + \gamma$$

$$^{16}\mathrm{O} + {}^{1}\mathrm{H} \rightarrow {}^{17}\mathrm{F} + \gamma$$

$$^{17}\mathrm{F} \rightarrow {}^{17}\mathrm{O} + \mathrm{e}^{+} + \nu_{\mathrm{e}}$$

$$^{17}\mathrm{O} + {}^{1}\mathrm{H} \rightarrow {}^{14}\mathrm{N} + {}^{4}\mathrm{He}$$

CNO bi-cycle

In massive stars also the CNO3 and CNO4 cycle becomes significant

$$^{18}\mathrm{F} \rightarrow {}^{18}\mathrm{O} + \mathrm{e}^{+} + \nu_\mathrm{e}$$

$$^{17}\mathrm{O} + {}^{1}\mathrm{H} \rightarrow {}^{18}\mathrm{F} + \gamma$$

$$^{18}\mathrm{O} + {}^{1}\mathrm{H} \rightarrow {}^{15}\mathrm{N} + {}^{4}\mathrm{He}$$

$$^{17}\mathrm{F} \rightarrow {}^{17}\mathrm{O} + \mathrm{e}^{+} + \nu_\mathrm{e}$$

$$^{15}\mathrm{N} + {}^{1}\mathrm{H} \rightarrow {}^{16}\mathrm{O} + \gamma$$

$$^{17}\mathrm{O} + {}^{1}\mathrm{H} \rightarrow {}^{18}\mathrm{F} + \gamma$$

$$^{16}\mathrm{O} + {}^{1}\mathrm{H} \rightarrow {}^{17}\mathrm{F} + \gamma$$

$$^{18}\mathrm{F} \rightarrow {}^{18}\mathrm{O} + \mathrm{e}^{+} + \nu_\mathrm{e}$$

$$^{19}\mathrm{F} + {}^{1}\mathrm{H} \rightarrow {}^{16}\mathrm{O} + {}^{4}\mathrm{He}$$

$$^{18}\mathrm{O} + {}^{1}\mathrm{H} \rightarrow {}^{19}\mathrm{F} + \gamma$$

CNO bi-cycle

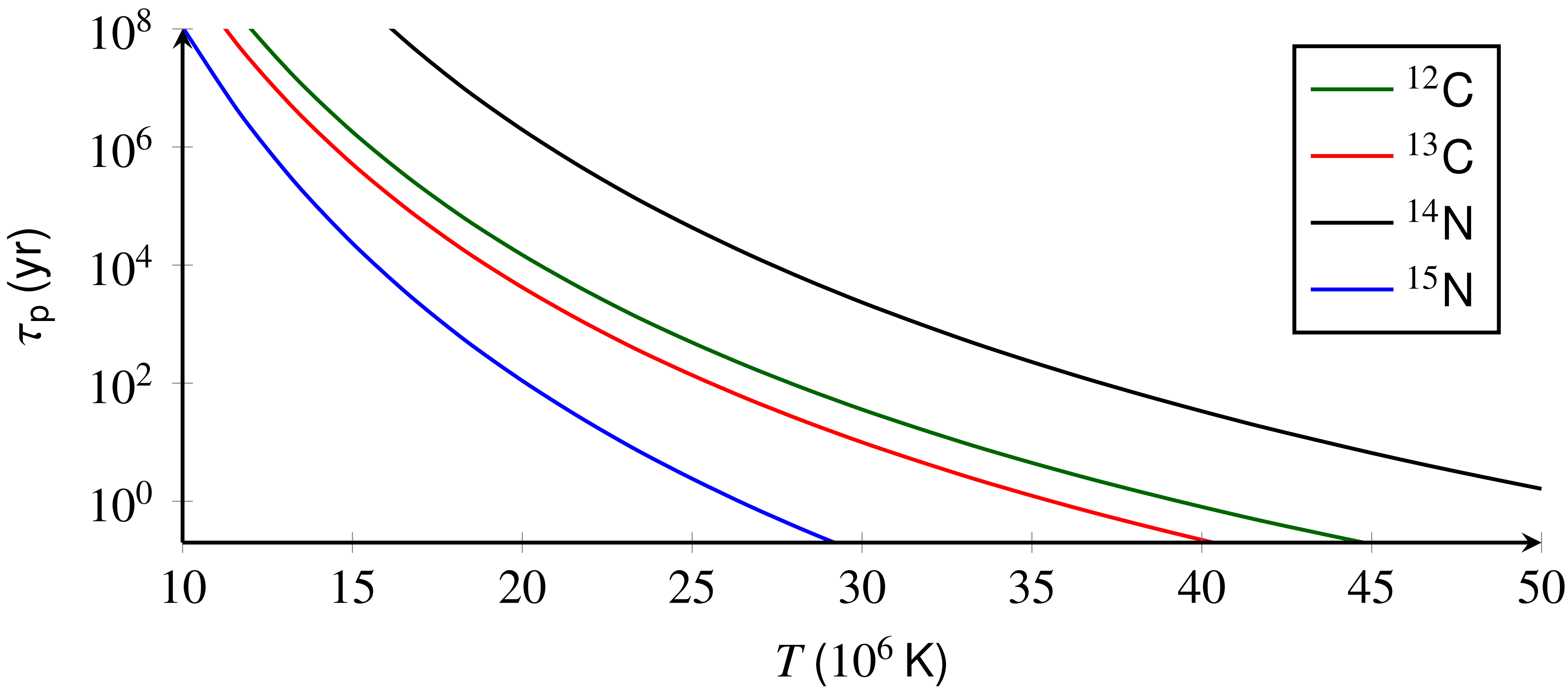

- Slowest reaction: ^{14}N + H $\longrightarrow$ ^{15}O + γ: pace of the CN cycle, and its energy generation rate, is given by the decay of ^{14}N against protons
- non-resonant reaction, contribution of ON cycle negligible
- Energy released: $Q = [4m_\mathrm{p} - M_{^4\mathrm{He}}]c^2 - E_{\nu_\mathrm{e}} \approx 26$ MeV
- reaction rate $\langle \sigma v \rangle \sim \rho T^{16.7}$

CNO bi-cycle

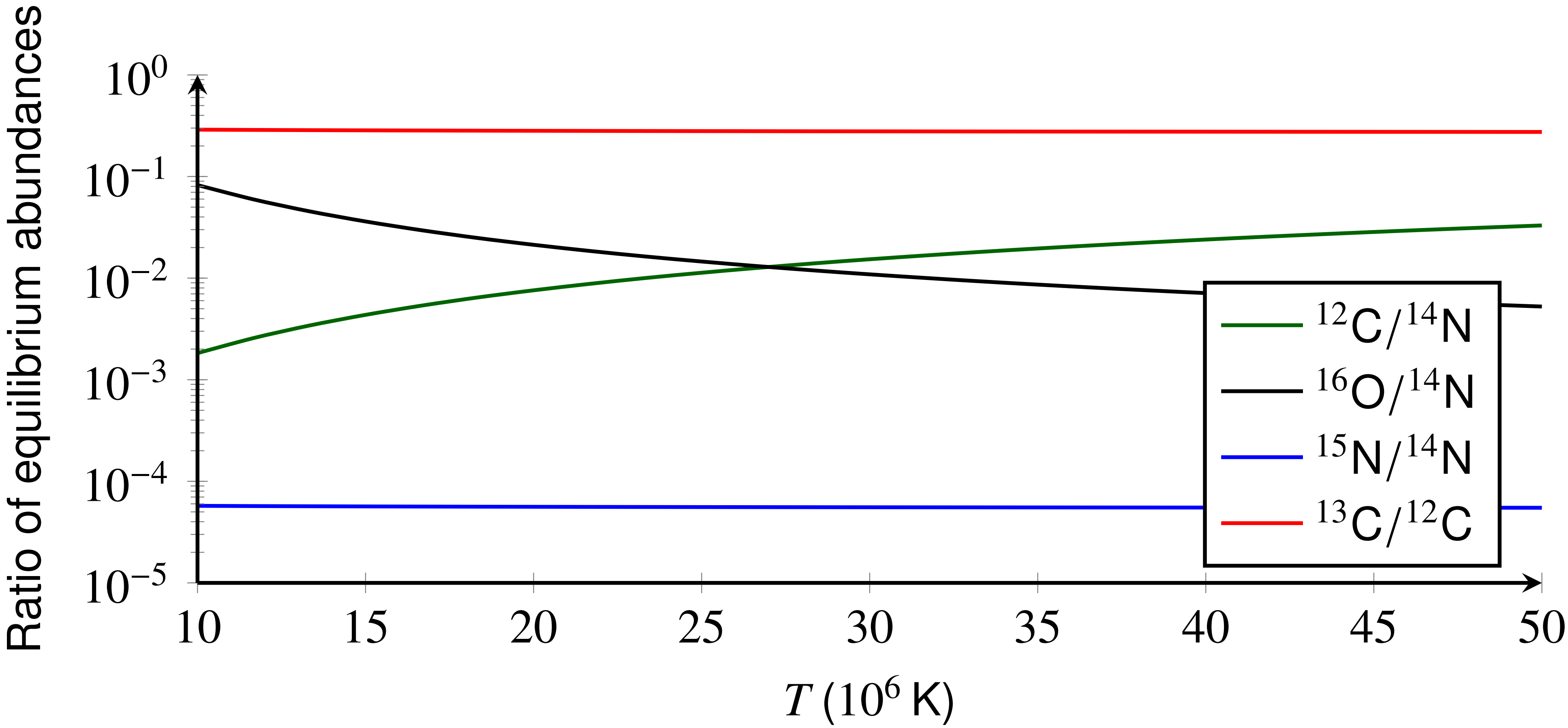

- Slowest reaction: ^{14}N + H $\longrightarrow$ ^{15}O + γ
  $\rightarrow$ overabundance of *N* w.r.t. *C* and *O* indication for CNO cycle as most of ^{12}C, ^{13}C and ^{15}N will be converted to ^{14}N
- isotopic ratio $^{13}\text{C}/^{12}\text{C} \approx 0.3$ important observational signature of CNO cycle

CNO bi-cycle

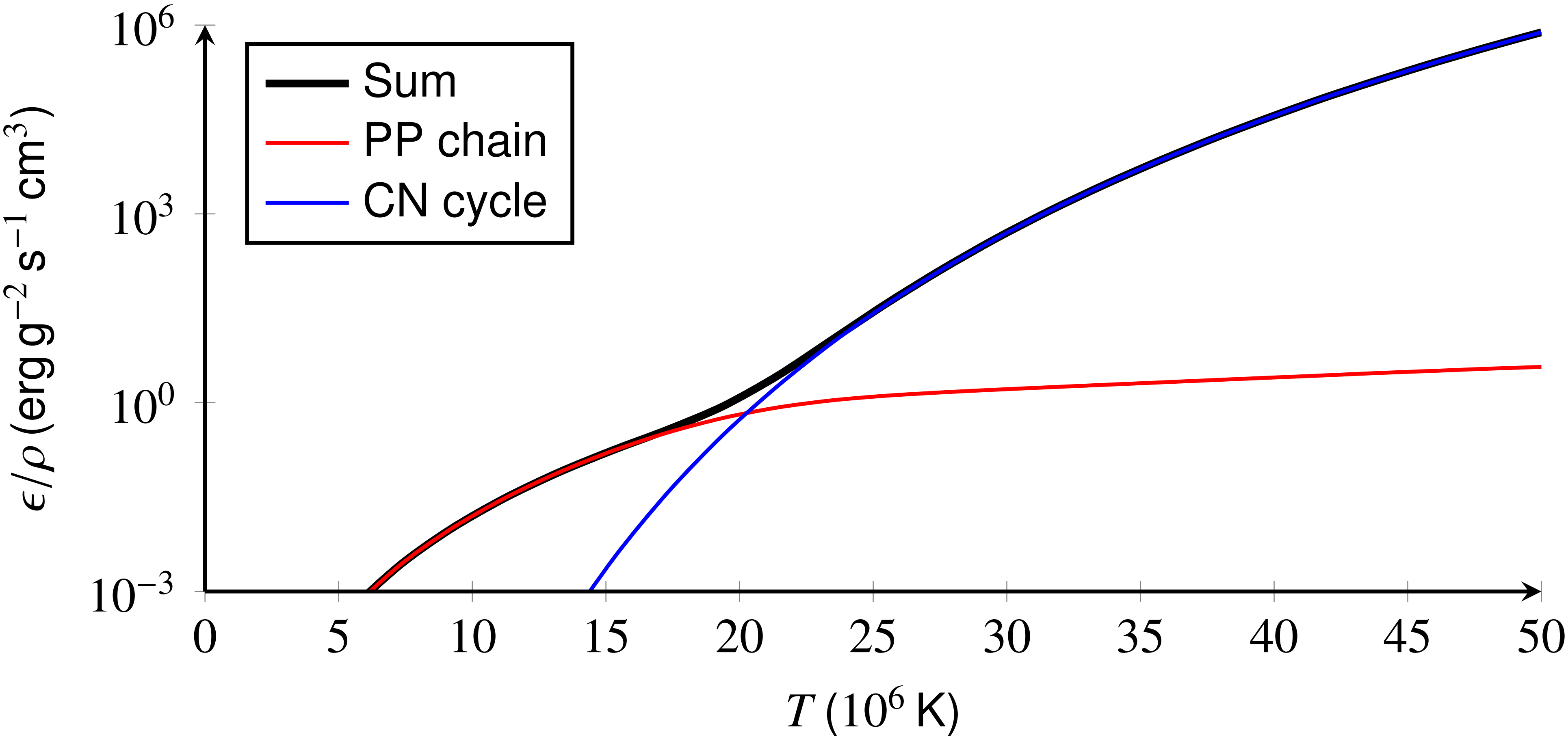

- Energy generation in massive stars sharply peaked at the stellar center where temperatures are largest
- very steep temperature gradients to get rid of the huge amounts of energy

$\rightarrow$ convective core

CNO bi-cycle

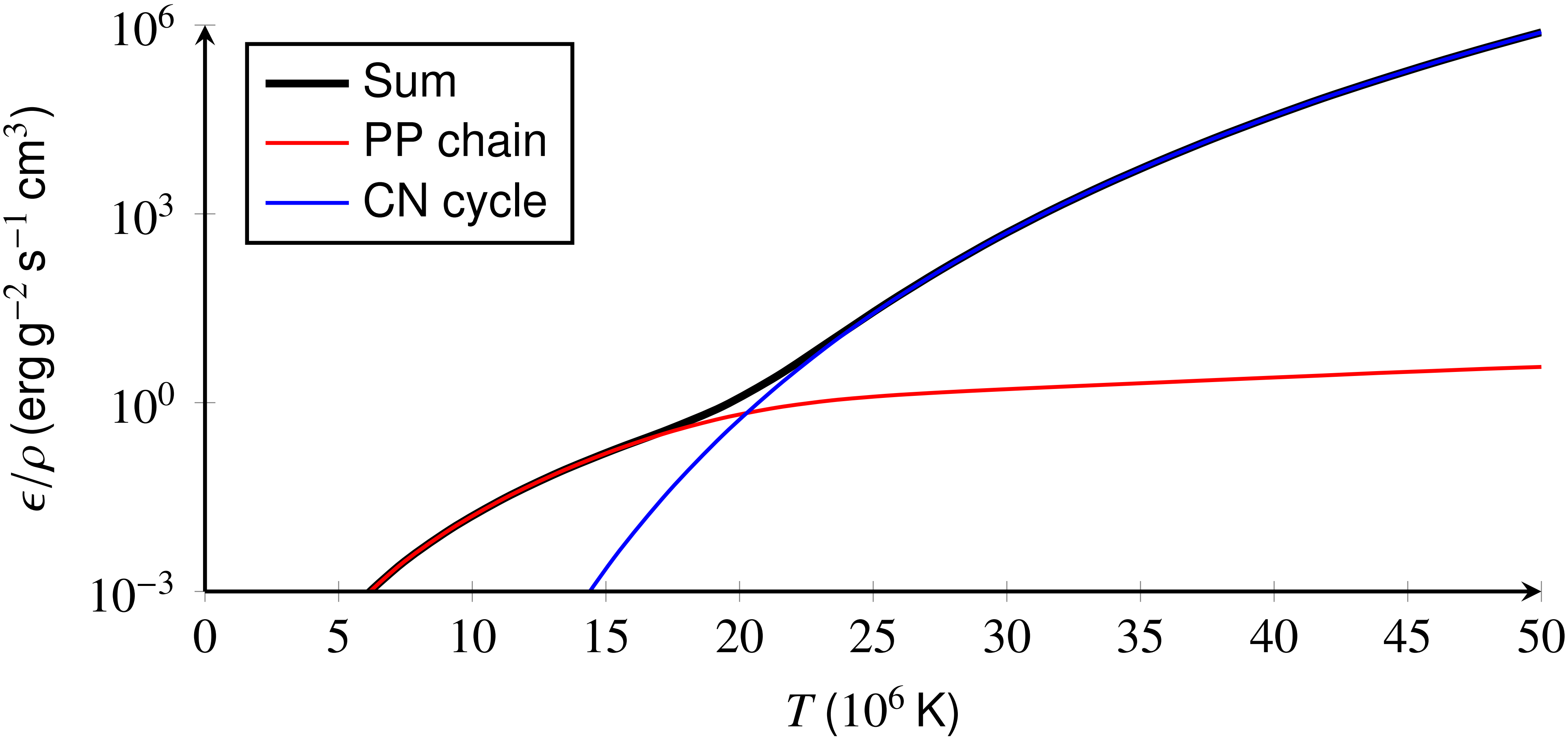

$$\langle\sigma v\rangle_{\mathrm{pp}} \sim \rho T^{4.6} \text{ at } 10\times10^6\,\mathrm{K} \quad\Leftrightarrow\quad \langle\sigma v\rangle_{\mathrm{CNO}} \sim \rho T^{16.7} \text{ at } 25\times10^6\,\mathrm{K}$$

- CNO cycle dominates for stars of mass $\gtrsim 1.5\,\mathrm{M}_\odot$

Helium burning

Helium burning often written as a triple alpha reaction: $3\,{}^4\mathrm{He} \longrightarrow {}^{12}\mathrm{C} + \gamma$

- two succesive reactions: creation of unstable isotope ^{8}Be by

$$^4\mathrm{He} + {}^4\mathrm{He} \longrightarrow {}^8\mathrm{Be}$$

  and an instantaneous catch of a third alpha particle via a resonant reaction

$$^8\mathrm{Be} + {}^4\mathrm{He} \longrightarrow {}^{12}\mathrm{C} + \gamma$$

- lifetime of ^{8}Be: $\tau_{^8\mathrm{Be}} = 2.6 \times 10^{-16}$ s, still longer than mean collision time with an alpha particle at $T \sim 10^8$ K
- Helium burning becomes important only for high helium mass fractions Y and for very high temperatures ($T \gtrsim 10^8$ K)
- at later stages of stellar evolution when the temperature of the helium core increases via gravitational contraction
- if helium burning is ignited in a stellar core supported by electron degeneracy, i.e., the pressure is independent of temperature, an explosive event, the so-called **helium flash**, is expected to occur.

Helium burning

As soon as enough carbon has accumulated another alpha-capture reaction is possible

$$^{12}\mathrm{C} + {}^{4}\mathrm{He} \longrightarrow {}^{16}\mathrm{O}$$

- probabilities for other alpha-captures is very unlikely due to the Coulomb barrier
- products of He-burning by the **triple-alpha process** are C and O
- Energy released by the net reactions

$$Q = [3m_\alpha - M_{^{12}\mathrm{C}}]c^2 = 7.275\,\mathrm{MeV}$$

$$Q = [4m_\alpha - M_{^{16}\mathrm{O}}]c^2 = 7.162\,\mathrm{MeV}$$

- very strong temperature dependence $\langle \sigma v \rangle \sim \epsilon_{3\alpha} \sim T^{40}$ near $T \approx 10^8$ K

Advanced burning stages

In all massive stars ($M \gtrsim 8\,\mathrm{M}_\odot$), helium burning in the core is succeeded by carbon and (for ($M \gtrsim 12\,\mathrm{M}_\odot$)) oxygen burning

- Fusion of carbon is possible for temperatures higher than 5×10^8 K

$$
\begin{aligned}
{}^{12}\mathrm{C} + {}^{12}\mathrm{C} &\longrightarrow {}^{24}\mathrm{Mg} + \gamma \\
&\longrightarrow {}^{23}\mathrm{Mg} + \mathrm{n} \\
&\longrightarrow {}^{23}\mathrm{Na} + \mathrm{p} \\
&\longrightarrow {}^{20}\mathrm{Ne} + \alpha \\
&\longrightarrow {}^{16}\mathrm{O} + 2\,\alpha
\end{aligned}
$$

- Fusion of oxygen is possible for temperatures higher than 10^9 K

$$
\begin{aligned}
{}^{16}\mathrm{O} + {}^{16}\mathrm{O} &\longrightarrow {}^{32}\mathrm{S} + \gamma \\
&\longrightarrow {}^{31}\mathrm{S} + \mathrm{n} \\
&\longrightarrow {}^{31}\mathrm{P} + \mathrm{p} \\
&\longrightarrow {}^{28}\mathrm{Si} + \alpha \\
&\longrightarrow {}^{24}\mathrm{Mg} + 2\,\alpha
\end{aligned}
$$

Advanced burning stages

Core carbon burning

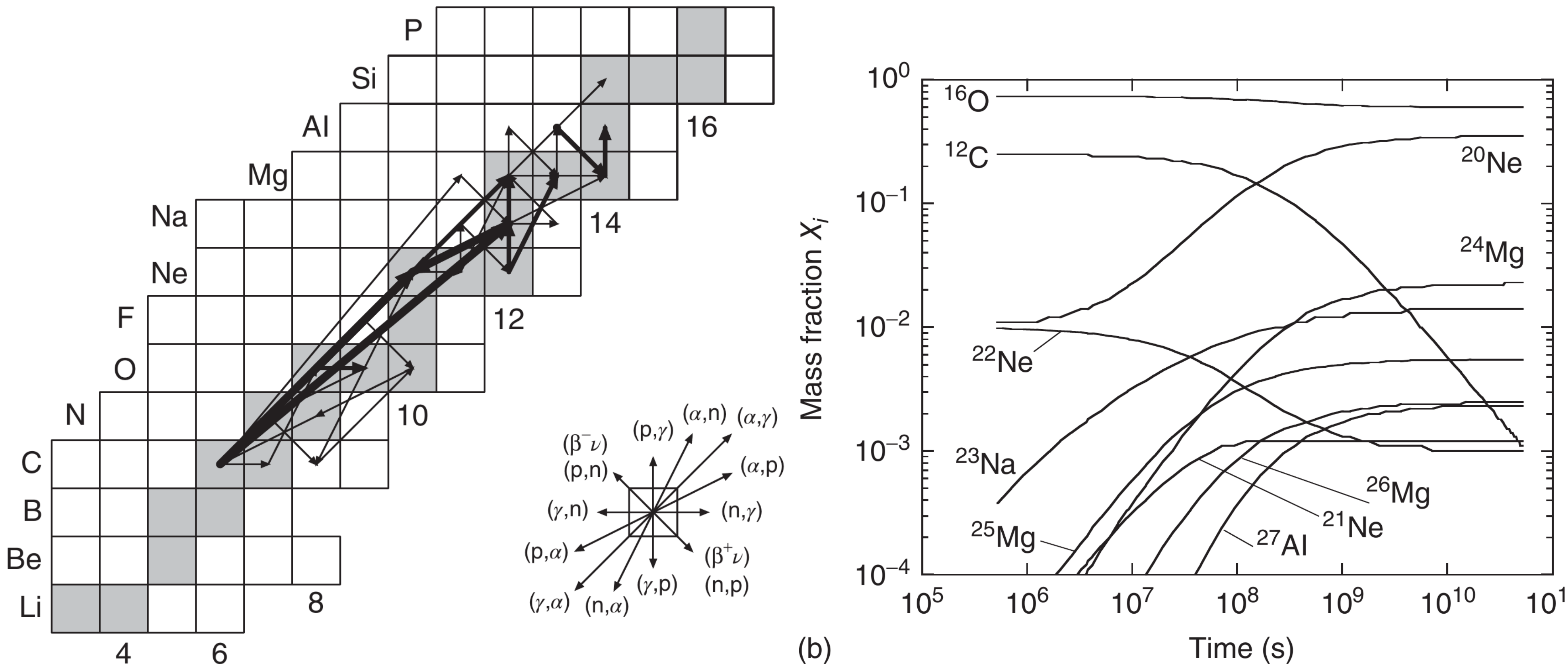

(b)

Iliadis 2015

Advanced burning stages

- Energy released by the net reactions between 13 MeV and 16 MeV
- The particles produced in those reactions lead to the formation of many different isotopes by secondary reactions $\rightarrow$ **Major reaction** product is ^{28}Si
- for temperatures $T > 10^9$ K photodisintegration of nuclei that are not too strongly bound get important, e.g. neon disintegration dominating over inverse reaction for $T > 1.5 \times 10^9$ K

$$
\begin{aligned}
{}^{20}\mathrm{Ne} + \gamma &\rightleftharpoons {}^{16}\mathrm{O} + \alpha, & Q &= -4.73\,\mathrm{MeV} \\
2\,{}^{20}\mathrm{Ne} + \gamma &\rightleftharpoons {}^{16}\mathrm{O} + {}^{24}\mathrm{Mg} + \gamma, & Q &= +4.583\,\mathrm{MeV} \\
{}^{24}\mathrm{Mg} + \alpha &\longrightarrow {}^{28}\mathrm{Si} + \gamma, & Q &= 0.984\,\mathrm{MeV}
\end{aligned}
$$

- near end of oxygen burning: photodisintegration of ^{28}Si and eject n, p and α particles followed by a large number of reactions
- created nuclei (Al, Mg, Ne) also subject to photodisintegration leading to the existence of an appreciable amount of free n, p and α particles
- react with the remaining ^{28}Si building up gradually heavier nuclei, until ^{56}Fe is reached

Advanced burning stages

- forward and reverse reactions achieve equilibrium, with increasing temperature and progressing time several pairs of nuclides link together to form quasi-equilibrium clusters ($24 \le A \le 40$, $A > 45 \to A > 24$)
  $\to$ photodisintegration rearrangement
- ^{56}Fe so strongly bound, it may survive this melting pot as the only (or dominant) species
- ultimately net-conversion of two ^{28}Si into ^{56}Fe: Silicon burning

$$\begin{aligned} {}^{28}\mathrm{Si} + {}^{28}\mathrm{Si} &\longrightarrow {}^{56}\mathrm{Ni} + \gamma \\ {}^{56}\mathrm{Ni} &\longrightarrow {}^{56}\mathrm{Co} + \mathrm{e}^{+} + \nu_{\mathrm{e}} \\ {}^{56}\mathrm{Ni} &\longrightarrow {}^{56}\mathrm{Fe} + 2\,\mathrm{e}^{+} + 2\,\nu_{\mathrm{e}} \end{aligned}$$

- at the end of silicon burning, the temperature in the stellar core increases steadily $\to$ nonequilibrated reactions in the $A < 24$ region come into equilibrium as well: **Nuclear Statistical Equilibrium**
- for $T > 5 \times 10^9$ K photodisintegration breaks up even the ^{56}Fe into α particles: supernova explosions

Nuclear Statistical Equilibrium

At high temperatures compositium can be aproximated by Nuclear Statistical Equilibrium

- Composition is given by a minimum of the Free Energy: $F = U - TS$ conservation of number of nucleons and charge neutrality

$$\mathrm{A(Z,N)} \rightleftharpoons \mathrm{Zp} + \mathrm{Nn} + \gamma$$

- It is assumed that all nuclear reactions operate in a time scale much shorter than any other timescale in the system
- favors free nucleons at high temperatures and iron group nuclei at low temperatures
- nuclei follow Boltzmann statistics, results in a Saha equation

$$^{20}\mathrm{Ne} + \gamma \rightleftharpoons {}^{16}\mathrm{O} + \alpha$$

$$\frac{n_\mathrm{O} n_\alpha}{n_\mathrm{Ne}} = \frac{1}{h^3}\left(\frac{2\pi m_\mathrm{O} m_\alpha kT}{m_\mathrm{Ne}}\right)^{3/2} \frac{G_\mathrm{O} G_\alpha}{G_\mathrm{Ne}} e^{-Q/kT}$$

Nuclear Statistical Equilibrium

At high temperatures compositium can be aproximated by Nuclear Statistical Equilibrium

- Composition is given by a minimum of the Free Energy: $F = U - TS$ conservation of number of nucleons and charge neutrality

$$\mathrm{A(Z,N)} \rightleftharpoons \mathrm{Zp} + \mathrm{Nn} + \gamma$$

- It is assumed that all nuclear reactions operate in a time scale much shorter than any other timescale in the system
- favors free nucleons at high temperatures and iron group nuclei at low temperatures
- nuclei follow Boltzmann statistics, results in a Saha equation

$$Y(Z,A) = \frac{G_{Z,A}(T)A^{3/2}}{2^A}\left(\frac{\rho}{m_\mathrm{u}}\right)^{A-1} Y_\mathrm{p}^Z Y_\mathrm{n}^{A-Z}\left(\frac{2\pi\hbar^2}{m_\mathrm{u}kT}\right)^{3(A-1)/2} e^{B(Z,A)/kT}$$

$G_{Z,A} = \sum_i (2J_i+1)e^{-E_i(Z,A)/kT}$ partition function

Composition depends on two parameters: Y_p, Y_n

Nucleosynthesis

solar abundances

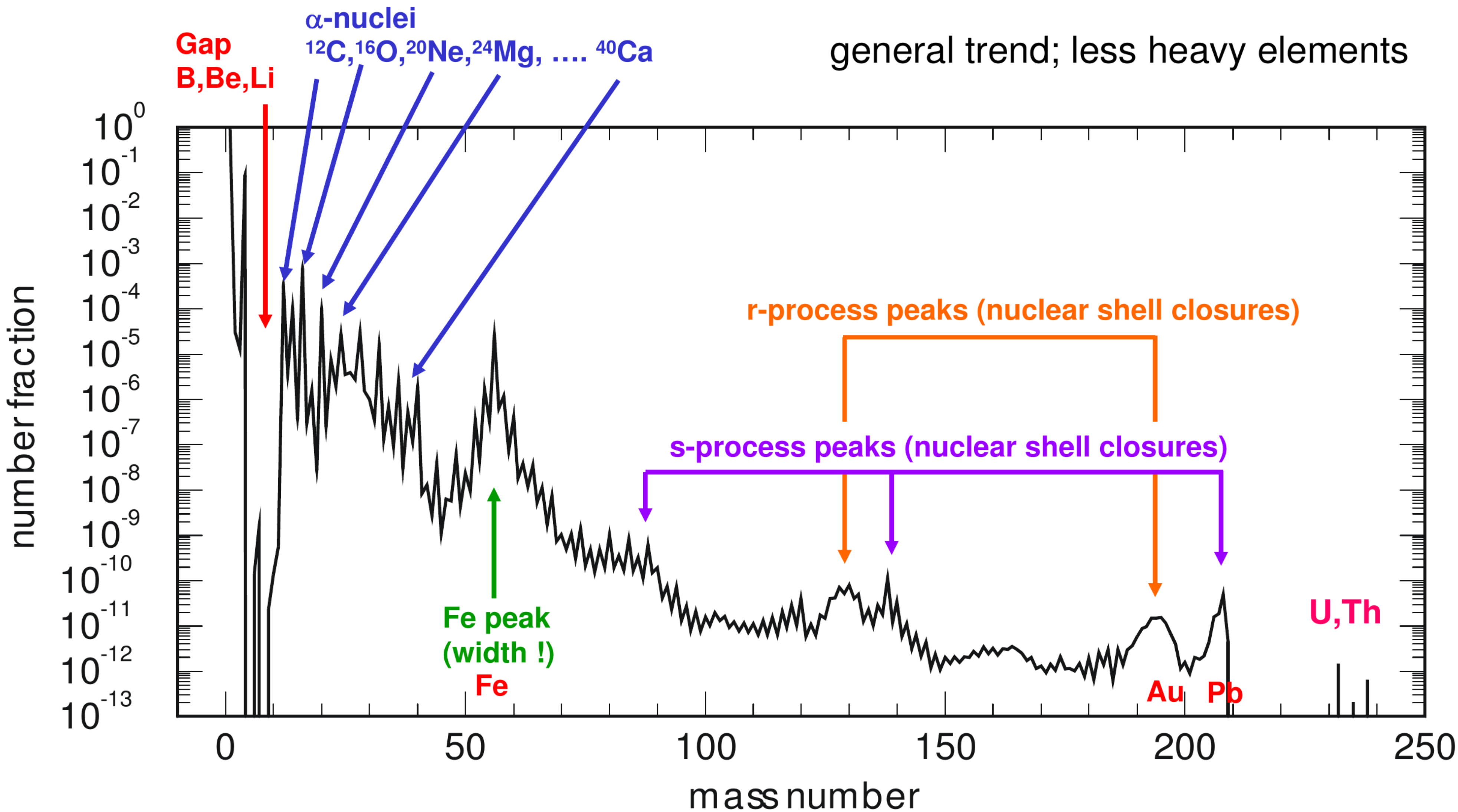

Pinedo 2017

Nucleosynthesis

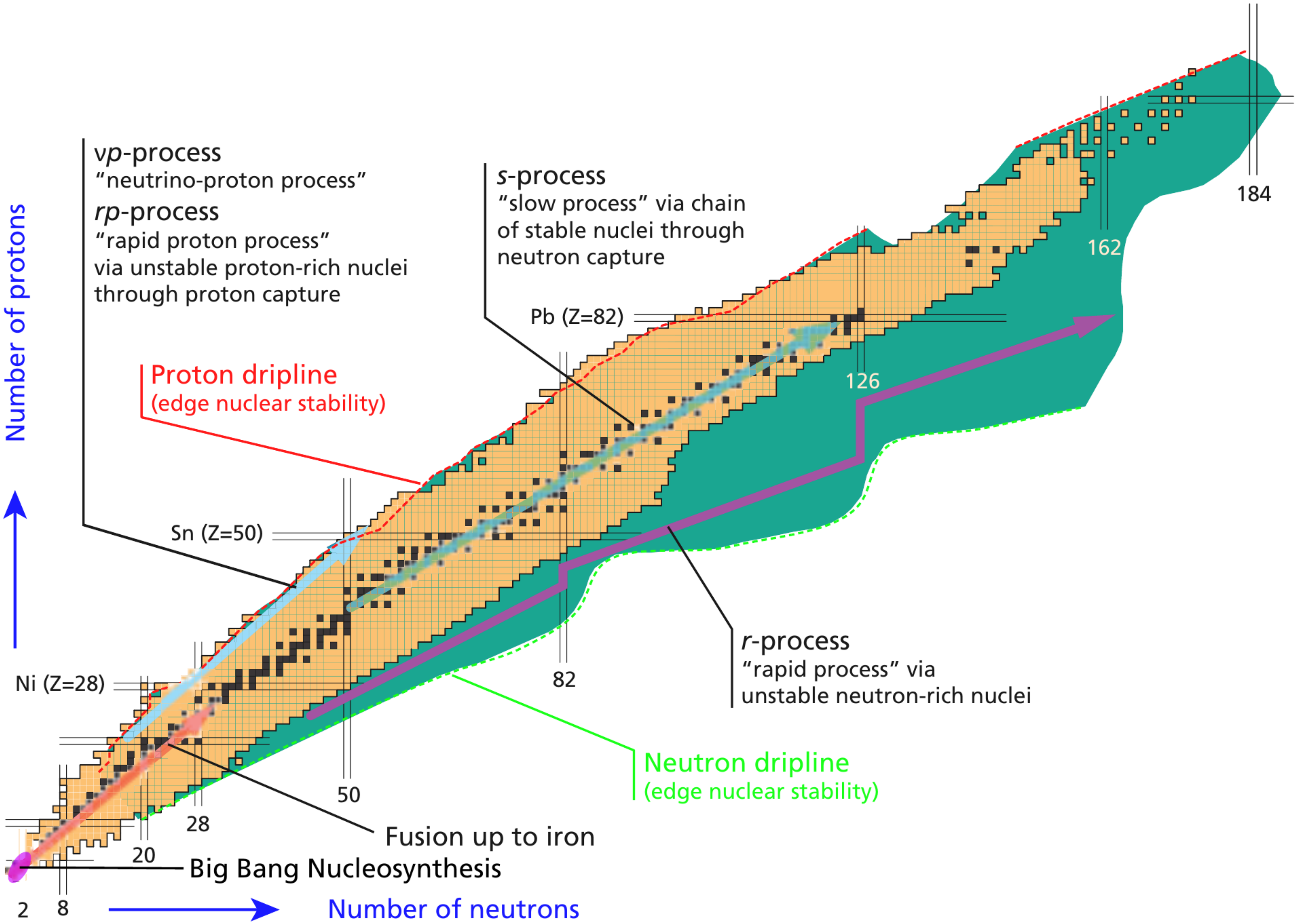

Pinedo 2017

Neutron-Capture Nucleosynthesis

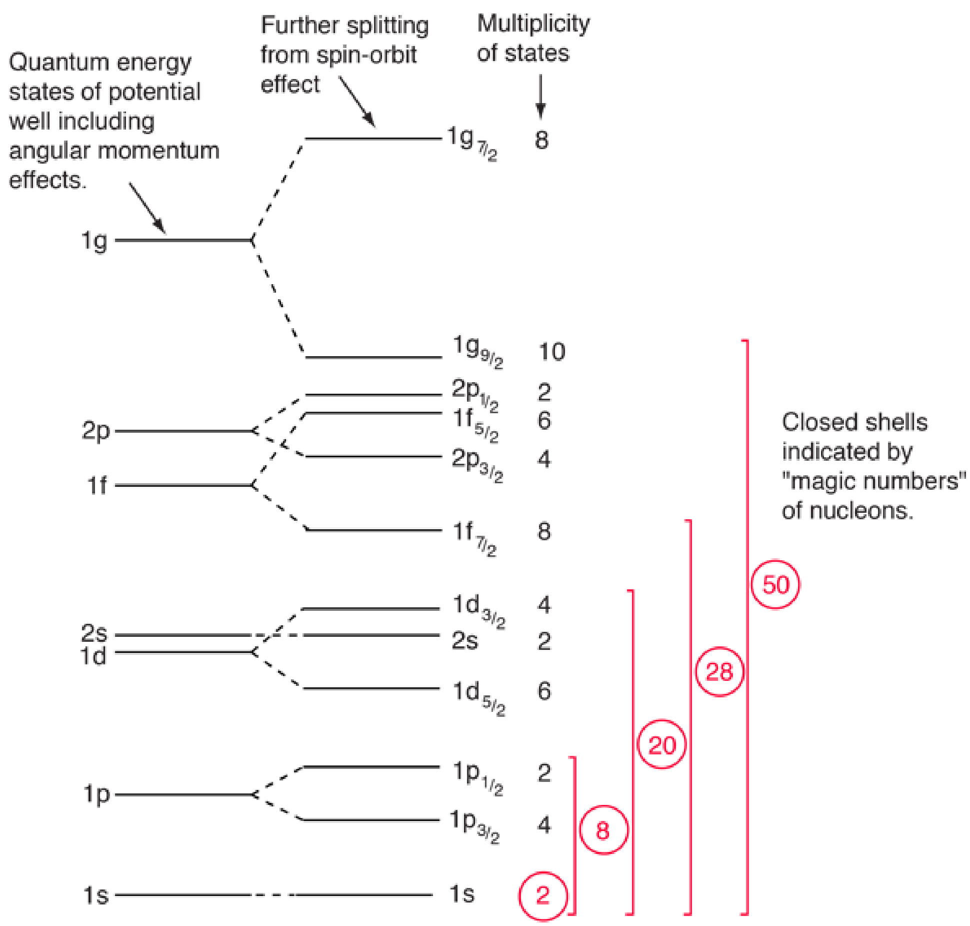

http://hyperphysics.phy-astr.gsu.edu/hbase/Nuclear/shell.html

- nuclear burning able to produce only elements up to iron: creation of elements heavier than the ”iron peak” is endothermic, electrostatic repulsion increasing with nuclear charge
- peaks in abundances reflect stability of isotopes against further addition of neutrons and protons: due to the structure of the nuclei – shell model of nuclear physics
- isotopes with even and equal numbers of neutrons and protons very stable $\rightarrow$ more abundant
- during hydrostatic burning phases, elements beyond the iron peak produced only if other reactions with lighter nuclei provide enough energy and, by the capture of neutrons (electrically neutral), heavier isotopes: unstable

Neutron-Capture Nucleosynthesis

general sequence of reactions is

$$(Z, A) + n \longrightarrow (Z, A+1) + \gamma$$
$$(Z, A+1) \longrightarrow (Z+1, A+1) + e^- + \nu_e$$

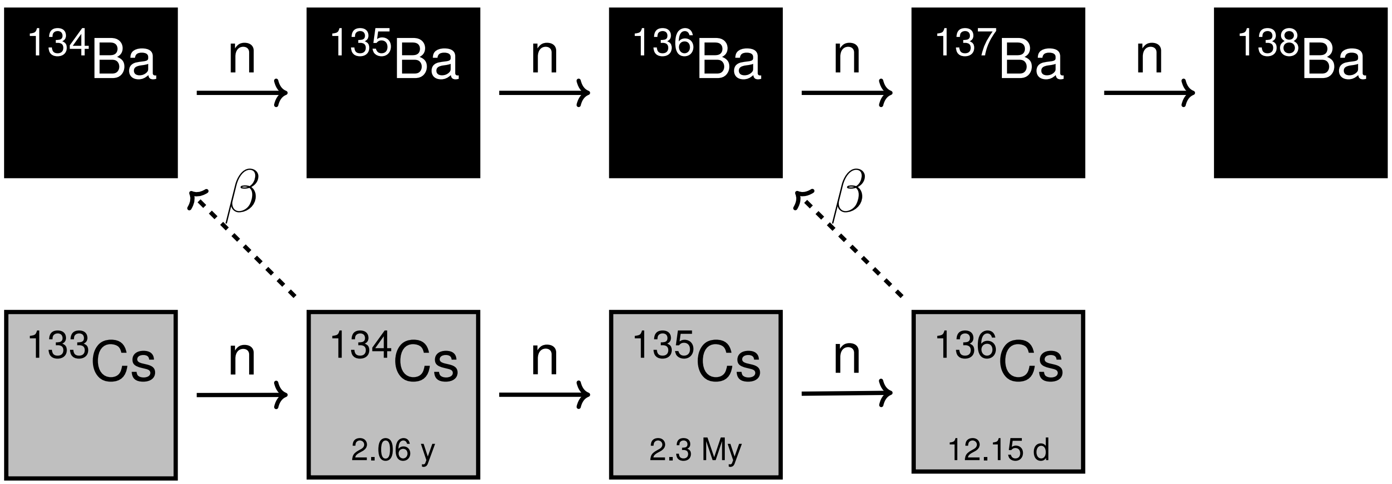

- neutron-capture time is long compared to the β-decay time: slow neutron-capture process or simply the **s-process** – close to the line of β-stability in the nuclear chart
- neutron-capture time is very short compared to the β-decay time: rapid neutron-capture process or **r-process** – Subsequent neutron captures and β-decays will lead to the creation of heavy elements

Neutron-Capture Nucleosynthesis

s-process

- taking place in stars of intermediate mass ($M \approx$ 2...5$M_\odot$) in an advanced phase of evolution: shell burning on the asymptotic giant branch: $\rightarrow$ $^{13}C(\alpha, n)^{16}O$, $^{22}Ne(\alpha, n)^{25}Mg$
- short-lived isotopes of heavy elements (e.g. ^{99}Tc,$\tau_{1/2} = 211,000$ y) found in the atmospheres, could only have been created in the stars themselves
- unimportant for the energy budget and the structure of stars, mainly due to the extremely low abundances

r-process

- astrophysical site for the r-process is not clearly identified, but is probably to be found in supernova explosions and/or neutrino-driven winds after neutron star mergers
- very high neutron fluxes $\rightarrow$ neutron capture until nuclear shell closure, stable against more neutron capture: $\beta -$ *decay*

proton capture: responsible for proton-rich nuclei (p-process, rp- process, νp-process): supernovae, neutrino driven winds

Simple stellar models

Polytropic Gaseous spheres

Accurate stellar models need to be calculated numerically

$\rightarrow$ simple analytic models can be useful to understand general rules and dependencies

$\rightarrow$ earliest such models are called **polytropes**

Temperature does not appear in the mechanical equations of stellar structure.

Assuming hydrostatic equilibrium

$$\frac{\mathrm{d}P}{\mathrm{d}r} = -\frac{Gm}{r^2}\rho \stackrel{\frac{\mathrm{d}\Phi}{\mathrm{d}r}=\frac{Gm}{r^2}}{\Longrightarrow} \frac{\mathrm{d}P}{\mathrm{d}r} = -\frac{\mathrm{d}\Phi}{\mathrm{d}r}\rho$$

together with Poisson's equation

$$\nabla^2\Phi = \frac{1}{r^2}\frac{\mathrm{d}}{\mathrm{d}r}\left(r^2\frac{\mathrm{d}\phi}{\mathrm{d}r}\right) = 4\pi G\rho$$

Temperature enters via equation of state $\rho = \rho(P, T)$, simplest case: $\rho = \rho(P)$

$\rightarrow$ two equations can be solved for P and Φ without the other equations

Polytropic Gaseous spheres

Assuming such a simple relation between P and ρ of the form

$$P = K\rho^{\gamma} = K\rho^{1+\frac{1}{n}}, \qquad n = \frac{1}{\gamma - 1} \tag{7.1}$$

polytropic relation: K polytropic constant, γ polytropic exponent, n polytropic index

$$\Rightarrow \frac{d\Phi}{dr} = -K\rho^{\gamma-2}\frac{d\rho}{dr}$$

If $\gamma \neq 1$ and $\Phi = 0$ at the surface ($\rho = 0$), integration gives

$$\rho = \left(\frac{-\Phi}{(n+1)K}\right)^{n}$$

With the Poisson equation, we obtain an ordinary differential equation for Φ

$$\frac{d^2\Phi}{dr^2} + \frac{2}{r}\frac{d\Phi}{dr} = 4\pi G\left(\frac{-\Phi}{(n+1)K}\right)^{n} \tag{7.2}$$

Lane-Emden equation

define dimensionless variables z, w and Φ_c, ρ_c at the center

$$z = Ar,\;\; A^2 = \frac{4\pi G}{(n+1)^n K^n}(-\phi_c)^{n-1} = \frac{4\pi G}{(n+1)K}(\rho_c)^{\frac{n-1}{n}},\;\; w = \frac{\Phi}{\Phi_c} = \left(\frac{\rho}{\rho_c}\right)^{1/n}$$

Lane-Emden equation

$$\frac{1}{z^2}\frac{d}{dz}\left(z^2\frac{dw}{dz}\right) + w^n = 0 \tag{7.3}$$

interested in solutions that are finite at the centre, $z = Ar = 0 \rightarrow dw/dz \equiv w' = 0$

$$\rho(r) = \rho_c w^n, \qquad \rho_c = \left[\frac{-\Phi_c}{(n+1)K}\right]^n$$

$$\Rightarrow P(r) = P_c w^{n+1}, \qquad P_c = K\rho_c^\gamma$$

Lane-Emden equation

regular singularity at $z = 0$, expand into a power series:

$$w(z) = 1 + a_1 z + a_2 z^2 + a_3 z^3 + \ldots, \qquad \stackrel{\text{Lane-Emden}}{\Longrightarrow} w(z) = 1 - \frac{1}{6}z^2 + \frac{n}{120}z^4 + \ldots$$

with $a_1 = w'(0), 2a_2 = w''(0), \ldots$ Analytical solutions only for three values of

- $n = 0 : w(z) = 1 - \frac{1}{6}z^2$
- $n = 1 : w(z) = \frac{\sin z}{z}$
- $n = 5 : w(z) = \frac{1}{(1+z^2/3)^{1/2}}$

Surface of the polytrope of index n defined by value $z = z_n$, for which $\rho = p = 0$ and $w = 0$

$$\Rightarrow z_0 = \sqrt{6}, \qquad z_1 = \pi, \qquad z_5 = \infty$$

$\rightarrow$ Only polytropes with $n < 5$ have finite radii

$\rightarrow$ In general, values of z_n and related functions have to be calculated numerically

$\rightarrow$ published in tabular form

Lane-Emden equation

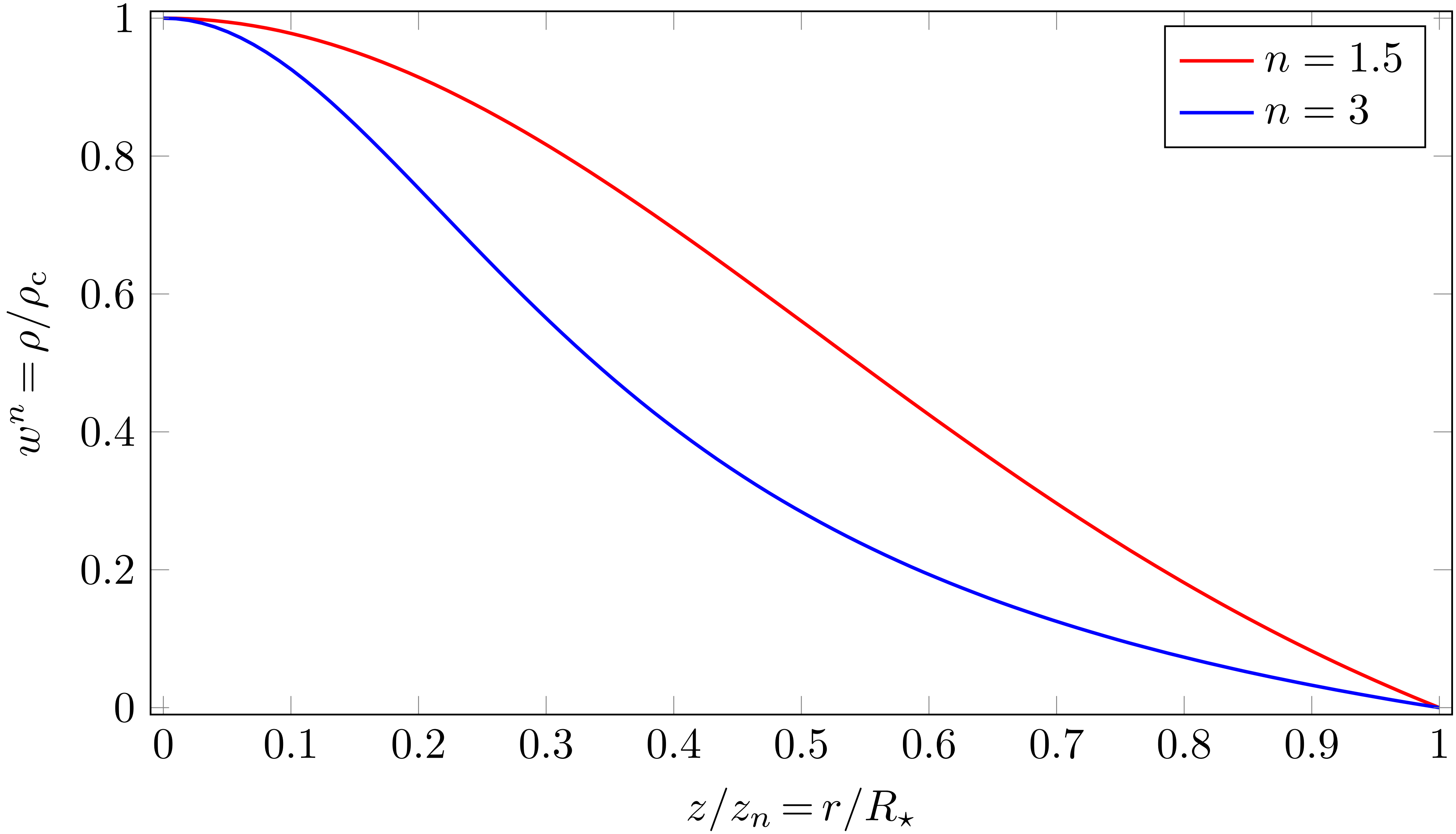

Lane-Emden equation

n	$R_n \equiv z_n$	$M_n \equiv \left(-z^2 \frac{\mathrm{d}w(z)}{\mathrm{d}z}\right)\Big\vert_{z=z_n}$	$D_n \equiv -\left(\frac{3}{z}\frac{\mathrm{d}w(z)}{\mathrm{d}z}\right)^{-1}\Big\vert_{z=z_n}$	$B_n \equiv \frac{R_n^{\frac{n-3}{n}}(3D_n)^{\frac{3-n}{3n}}}{(n+1)M_n^{\frac{n-1}{n}}}$
0	2.44949	4.89898	1.00000	undefined
0.5	2.75270	3.78865	1.83514	0.27432
1	3.14159	3.14159	3.28987	0.23310
1.5	3.65375	2.71407	5.99066	0.20558
2	4.35287	2.41113	11.40216	0.18538
2.5	5.35528	2.18721	23.40630	0.16957
3	6.89685	2.01824	54.18229	0.15654
3.25	8.01894	1.94983	88.15187	0.15076
3.5	9.53581	1.89060	152.88022	0.14534
5	∞	1.73205	∞	∞

$$D_n \equiv \left(\frac{\rho_c}{\bar{\rho}}\right)_{z=z_n}$$

Application to stars

polytropic models for a given index $n < 5$ and for given values of $M_\star$ and $R_\star$

$$m(r) = \int_0^r 4\pi\rho r^2 \mathrm{d}r = 4\pi\rho_\mathrm{c} \int_0^r w^n r^2 \mathrm{d}r \overset{z=Ar}{=} 4\pi\rho_\mathrm{c} \frac{r^3}{z^3} \int_0^z w^n z^2 \mathrm{d}z$$

Using the Lane-Emden equation

$$-\frac{\mathrm{d}}{\mathrm{d}z}\left(z^2 \frac{\mathrm{d}w}{\mathrm{d}z}\right) = w^n z^2 \Rightarrow m(r) = 4\pi\rho_\mathrm{c} r^3 \left(-\frac{1}{z}\frac{\mathrm{d}w}{\mathrm{d}z}\right)$$

At the surface $z = z_n$

$$M_\star = 4\pi\rho_\mathrm{c} R_\star^3 \left(-\frac{1}{z}\frac{\mathrm{d}w}{\mathrm{d}z}\right)_{z=z_n} = -4\pi A^{-3}\rho_\mathrm{c}\left(z^2 \frac{\mathrm{d}w}{\mathrm{d}z}\right)_{z=z_n} \tag{7.4}$$

introducing the mean density $\bar{\rho} = 3M_\star/(4\pi R_\star^3)$

$$\frac{\bar{\rho}}{\rho_\mathrm{c}} = \left(-\frac{3}{z}\frac{\mathrm{d}w}{\mathrm{d}z}\right)$$

higher $n \rightarrow$ smaller $\frac{\bar{\rho}}{\rho_\mathrm{c}} \Rightarrow$ higher density concentration in the center

Polytropic model

1. Measuring or assuming values for $M_\star$ and $R_\star$
2. Pick the appropriate polytropic index n
   $\rightarrow$ Numerical solution of Lane-Emden equation (R_n, M_n, D_n, B_n)
3. Calculating $\bar{\rho} = \frac{3M_\star}{4\pi R_\star^3}$ and $\rho_\mathrm{c} = -z_n/(3\mathrm{d}w/\mathrm{d}z)_{z=z_n}\bar{\rho}$
4. turning the dimensionless z scale to r scale with $A = z_n/R_\star$
5. density distributon: $\rho(r) = \rho_\mathrm{c} w^n(z)$
6. From $A^2 = \frac{4\pi G}{(n+1)K}\rho_\mathrm{c}^{\frac{n-1}{n}}$ follows $K = \frac{4\pi G}{(n+1)A^2}\rho_\mathrm{c}^{\frac{n-1}{n}}$
7. Pressure distribution: $P(r) = K\rho_\mathrm{c}^{(n+1)/n} w^{n+1}$
   $\rightarrow P_\mathrm{c} = (4\pi)^{\frac{1}{3}} \frac{R_n^{\frac{n-3}{n}}(3D_n)^{\frac{3-n}{3n}}}{(n+1)M_n^{\frac{n-1}{n}}} GM_\star^{\frac{2}{3}}\rho_\mathrm{c}^{\frac{4}{3}} \equiv (4\pi)^{\frac{1}{3}} B_n G M_\star^{\frac{2}{3}}\rho_\mathrm{c}^{\frac{4}{3}} = K\rho_\mathrm{c}^{\gamma}$.
   polytropic constants R_n, M_n, D_n, and B_n see table
8. Mass distribution: $m(r) = 4\pi\rho_\mathrm{c} r^3 \left(-\frac{1}{z}\frac{\mathrm{d}w}{\mathrm{d}z}\right)$

Polytropic model – Sun

Example: Sun

1. $M_\odot = 1.989 \times 10^3 3$ g, $R_\odot = 6.96 \times 10^{10}$ cm
2. Polytropic index $n = 3 \rightarrow z_3 = 6.897$
3. $\bar{\rho} = 1.41\,\mathrm{g\,cm^{-1}}$, $\rho_\mathrm{c} = 76.39\,\mathrm{g\,cm^{-1}}$
4. $A = 9.91 \times 10^{-11}$
5. $\rho(r) = \rho_\mathrm{c} w^3(z)$
6. $K = 3.85 \times 10^{14}$

$\rightarrow$ central pressure $P_\mathrm{c} = 1.24 \times 10^{17}\,\mathrm{dyn\,cm^{-2}}$

Assuming an ideal gas with $X = 0.7$ and $Y = 0.3 \Rightarrow \mu = 0.62$

$\rightarrow$ central temperature $T_\mathrm{c} = 1.2 \times 10^7$ K

$\rightarrow$ detailed calculations $T_\mathrm{c} = 1.5 \times 10^7$ K

$\rightarrow$ **Polytropic model does work quite well**

Polytropic model – Sun

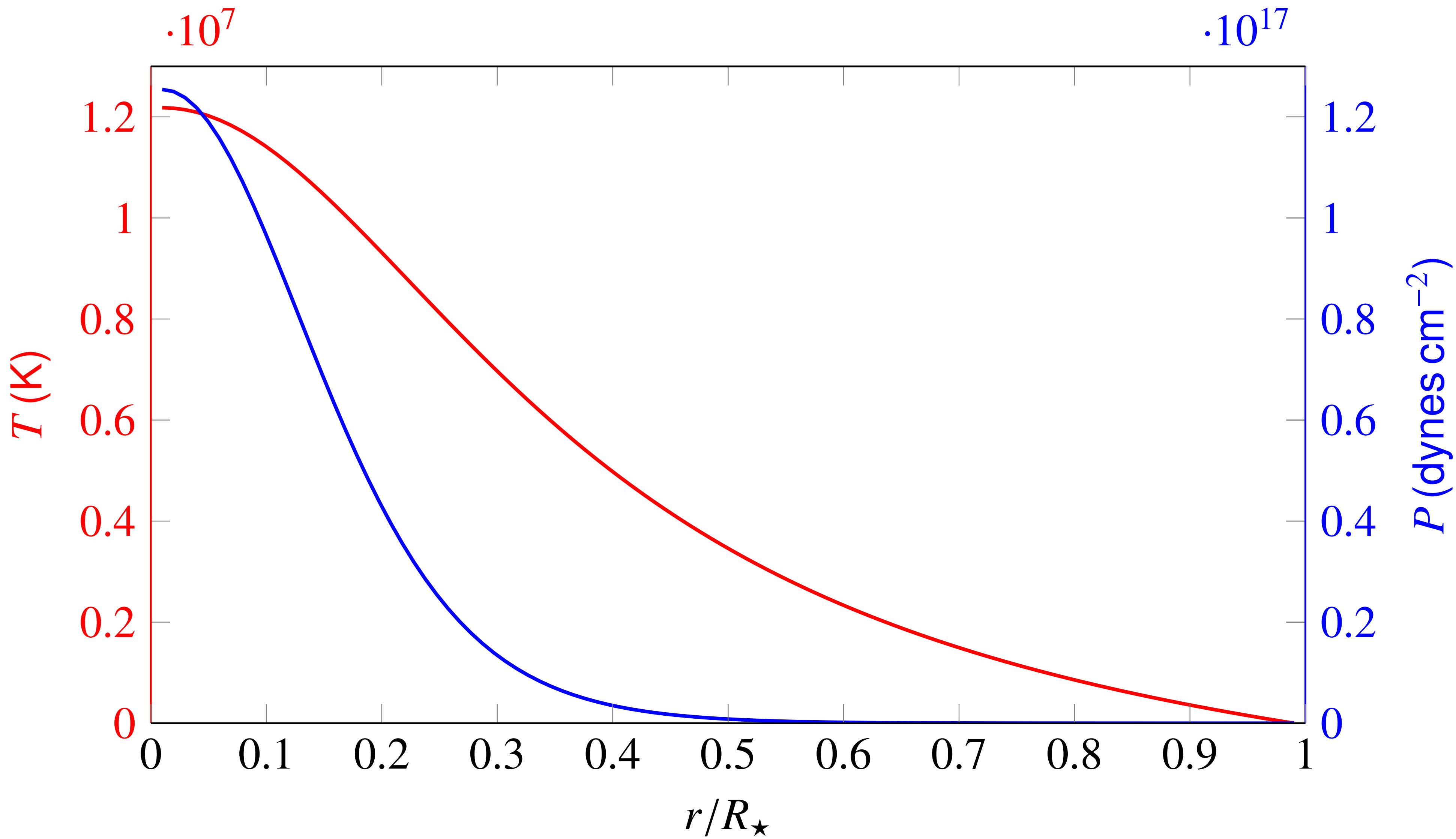

Polytropic model: $n = 3$ – Standard model

$\Rightarrow$ Eddingtons ”standard model”

Ideal gas with radiation pressure, $\beta = P_{\text{gas}}/P$

$$P = \frac{R}{\mu}\rho T + \frac{a}{3}T^4 = \frac{R}{\mu\beta}\rho T$$

Assuming β to be constant throughout the star ($0 > \beta > 1$)

$$\Rightarrow 1 - \beta = \frac{P_{\text{rad}}}{P} = \frac{aT^4}{3P} \Rightarrow T^4 \sim P$$

Equation of state becomes a polytropic relation with $n = 3$

$$P = \left(\frac{3R^4}{a\mu^4}\right)^{1/3}\left(\frac{1-\beta}{\beta^4}\right)^{1/3}\rho^{4/3} = K\rho^{1+\frac{1}{n}} \tag{7.5}$$

$\rightarrow$ K free parameter, which depends on choice of β: two free parameters: ρ_{c}, β

$\rightarrow$ can be replaced by $M_\star, R_\star \Rightarrow P_{\text{c}} = P_{\text{c}}(M_\star, R_\star),\ T_{\text{c}} = T_{\text{c}}(M_\star, R_\star)$

$$P_{\text{c}} = 1.24\times 10^{17}\left(\frac{M_\star}{M_\odot}\right)^2\left(\frac{R_\odot}{R_\star}\right)^4 \text{dyn}\,\text{cm}^{-2}, \qquad \text{T}_{\text{c}} = 19.5\times 10^6\mu\beta\frac{\text{M}_\star}{\text{M}_\odot}\frac{\text{R}_\odot}{\text{R}_\star}\,\text{K}$$

Polytropic model: $n = 3$ – Standard model

with 7.5, 7.4 and the definition of A we get the Eddington quartic equation:

$$1-\beta = \frac{a}{3R^4}\frac{(\pi G)^3(3D_3/4\pi)^2}{z_3^6}M^2\mu^4\beta^4 = 0.003\left(\frac{M_\star}{M_\odot}\right)^2\mu^4\beta^4, \ \rightarrow \beta = \beta(\mu, M_\star)$$

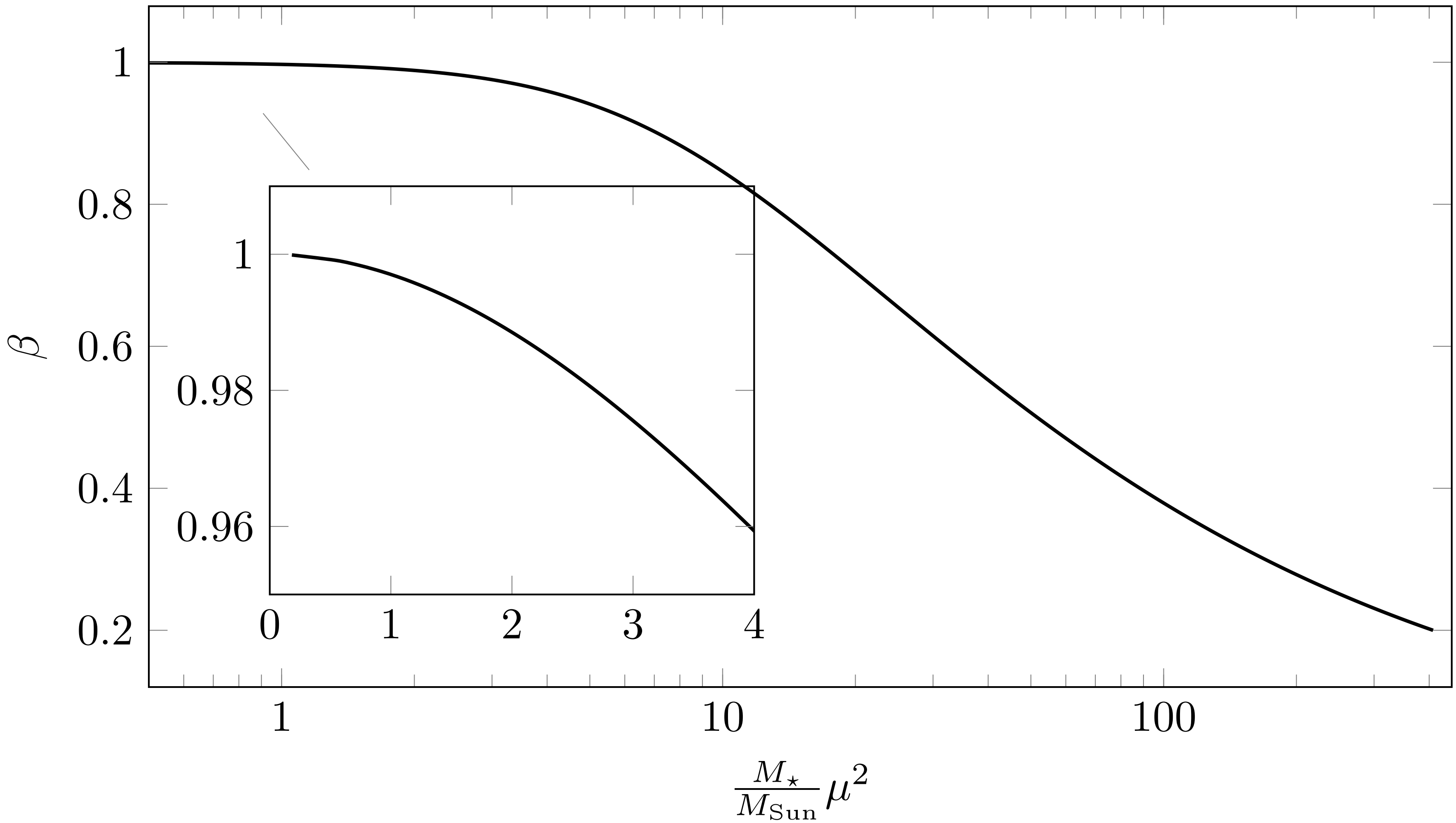

Polytropic model for radiative and fully convective stars

from the radiative temperature gradient we can derive the radiation pressure gradient $\frac{dP_r}{dr} = \frac{4}{3}aT^3\frac{dT}{dr} = -\frac{\kappa\rho L}{4\pi c r^2}$, and obtain for $n = 3$:

$$\frac{dP_r}{dP} \overset{\frac{dP}{dr}=-\frac{GM\rho}{r^2}}{=} \frac{\kappa L}{4\pi cGM} = 1-\beta(r) = 0.003\left(\frac{M_\star}{M_\odot}\right)^2\mu^4\beta^4$$

$$\frac{L_\star}{L_\odot} = \frac{4\pi cGM_\odot}{\kappa L_\odot}0.003\mu^4\beta^4(\mu, M_\star)\left(\frac{M_\star}{M_\odot}\right)^3 \text{ (mass-luminosity relation)} \qquad (7.6)$$

For fully convective stars the temperature gradient is given by the adiabatic temperature gradient

$$\frac{dT}{dr} = \frac{\Gamma_2-1}{\Gamma_2}\frac{T}{P}\frac{dP}{dr} \Leftrightarrow \frac{dT}{T} = \frac{\Gamma_2-1}{\Gamma_2}\frac{dP}{P}\,.$$

If we assume the adiabatic coefficient Γ_2 to be constant and the radiation pressure negligible, the equation of state is that of an ideal gas

$$T \sim P/\rho \Rightarrow P \sim \rho^{\Gamma_2}, \qquad \Rightarrow n = 1/(\Gamma_2-1) \Rightarrow TP^{\frac{1-\Gamma_2}{\Gamma_2}} = \text{const} \qquad (7.7)$$

$\rightarrow$ pre-main-sequence stars following the Hayashi line

Polytropic model with K = const

Now we assume K to be fixed and construct a model with index n for a given central density $\rho_c \Rightarrow \rho = \rho_c w^n$, $A^{-2} = \left(\frac{r}{z}\right)^2 = \frac{1}{4\pi G}(n+1)K\rho_c^{\frac{1-n}{n}}$
Using $R_\star = \frac{z_n}{A}$ we get a mass-radius relation, for a given K and n:

$$R_\star \sim \rho_c^{\frac{1-n}{2n}},\ M_\star \sim \rho_c R_\star^3$$

$$\Rightarrow M_\star = C_1 \rho_c^{\frac{3-n}{2n}};\ C_1 = 4\pi \left(-\frac{1}{z}\frac{dw}{dz}\right)_{z=z_n} z_n^3 \left(\frac{n+1}{4\pi G}\right)^{3/2} K^{3/2}$$

$$\Rightarrow R_\star \sim M_\star^{\frac{1-n}{3-n}} \tag{7.8}$$

Polytropic model for a degenerate electron gas

Non-relativistic, degenerate electron gas

$$P_e = \frac{1}{20}\left(\frac{3}{\pi}\right)^{2/3}\frac{h^2}{m_e m_u^{5/3}}\left(\frac{\rho}{\mu_e}\right)^{5/3}$$

Considering the chemical composition μ_e to be fixed:

$$P_e = \frac{1}{20}\left(\frac{3}{\pi}\right)^{2/3}\frac{h^2}{m_e(\mu_e m_u)^{5/3}}\rho^{5/3}$$

$\rightarrow$ Equation of state is polytropic: $P = K\rho^{1+\frac{1}{n}}$

with polytropic index $n = \frac{3}{2}$ and polytropic constant $K = \frac{1}{20}\left(\frac{3}{\pi}\right)^{2/3}\frac{h^2}{m_e(\mu_e m_u)^{5/3}}$

with the mass-radius relation 7.8, do we get a mass-radius relation for this case

$$R_\star \sim M_\star^{-1/3} \tag{7.9}$$

$\rightarrow$ The higher the mass, the smaller the radius

Polytropic model for a degenerate electron gas

for high densities, the degenerate electron gas becomes **relativistic**:

$$P_e = \left(\frac{3}{\pi}\right)^{1/3} \frac{hc}{8(\mu_e m_u)^{4/3}} \rho^{4/3}$$

Equation of state is (again) polytropic: $P = K\rho^{1+\frac{1}{n}}$
with polytropic index $n = 3$ and polytropic constant $K = \left(\frac{3}{\pi}\right)^{1/3} \frac{hc}{8(\mu_e m_u)^{4/3}}$

$$\Rightarrow M_\star = 4\pi \left(-\frac{1}{z}\frac{dw}{dz}\right)_{z=z_3} z_3^3 \left(\frac{K}{\pi G}\right)^{3/2} \underbrace{\rho_c^0}_{1} = M_{Ch}$$

Mass does not vary with central density!

$\rightarrow$ only one possible mass for relativistic degenerate polytropes:

$$\textbf{Chandrasekhar mass}: \qquad M_{Ch} = \frac{5.836}{\mu_e^2} M_\odot \qquad (7.10)$$

For white dwarfs $\mu_e = 2 \Rightarrow M_{Ch} = 1.46\,\mathrm{M}_\odot$
$\rightarrow$ **Highest possible (and observed) mass for WDs**

Polytropic model for a degenerate electron gas

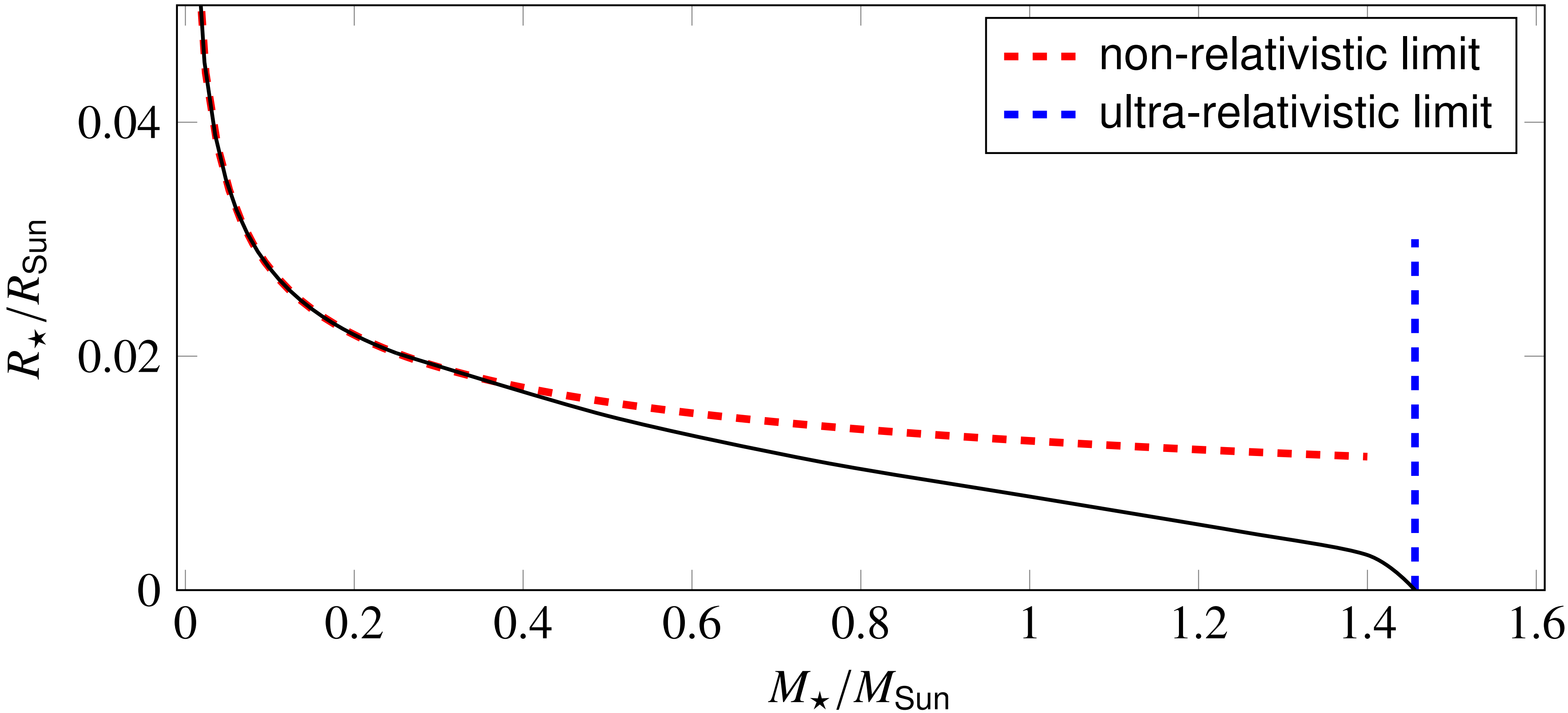

mass-radius relation for white dwarfs with $\mu_e = 2$, transition between non-relativistic limit and ultra-relativistic limit can be derived by using an equation of state accounting for relativistic effects (for $M_{\mathrm{WD}} \gtrsim 0.5\,\mathrm{M}_\odot$), which is then no longer a polytropic equation of state.

Homology Relations

For stars with similar density structure, there are simple relations between their parameters

$$x = \frac{m}{M} = \frac{m'}{M'} \text{ then } \frac{r(x)}{r'(x)} = \frac{R}{R'}$$

$\rightarrow$ This follows from the stellar structure equations

$\rightarrow$ Such stars are called **homologous**

Homology relations can be formulated for the fundamental parameters and material functions, e.g.

$$\frac{\rho}{\rho'} = \frac{M/M'}{(R/R')^3}, \qquad \frac{P}{P'} = \frac{(M/M')^2}{(R/R')^4} = \left(\frac{\rho}{\rho'}\right)^{4/3}\left(\frac{M}{M'}\right)^{2/3}$$

Homology Relations

Assuming an ideal gas $P \sim (1/\mu)\rho T$

$$\frac{T}{T'} = \frac{\mu}{\mu'}\frac{M}{M'}\left(\frac{R}{R'}\right)^{-1}$$

$\rightarrow$ If a star is compressed, R becomes smaller and T higher

$\rightarrow$ Higher T leads to more fusion, higher internal energy and expansion

$\rightarrow$ Star behave like a thermostat

Assuming an ideal gas and radiative energy transport

$$\frac{L}{L'} = \left(\frac{\kappa}{\kappa'}\right)^{-1}\left(\frac{M}{M'}\right)^{3}\left(\frac{\mu}{\mu'}\right)^{4}, \qquad \frac{L}{L'} = \frac{\epsilon}{\epsilon'}\frac{M}{M'}$$

$\rightarrow$ Luminosity is a strong function of mass $L \sim M^3$

$\rightarrow$ Stars with smaller metal content (smaller opacity κ) have higher L

$\rightarrow$ Stars with higher μ have higher L

Stellar populations

Stellar populations

First stars (Population III)

- formed with the primordial composition of the Universe (H, He, Li ,Be, B)
  $\rightarrow$ Metal-free composition (not observed yet)
  $\rightarrow$ No CNO-cycle possible
- Star forming gas clouds cool much slower, because the transitions of metals make cooling more efficient
  $\rightarrow$ instability for collapse to stars might happen at **higher masses** $M \approx 100 - 1000\,\mathrm{M}_{\odot}$
  The mass distribution of the first stars is currently debated
- after 10^6 yr first supernovae (core collapse, pair production) enrich the interstellar medium
  $\rightarrow$ Nucleosynthesis dominated by α-elements from C/O burning (C, O, Ne, Mg, Si, S, Ar, Ca)
  $\rightarrow$ Due to the short evolutionary times, no s-process elements are formed
  $\rightarrow$ Due to the extreme properties of the first stars, r-process elements might have been formed

Stellar populations

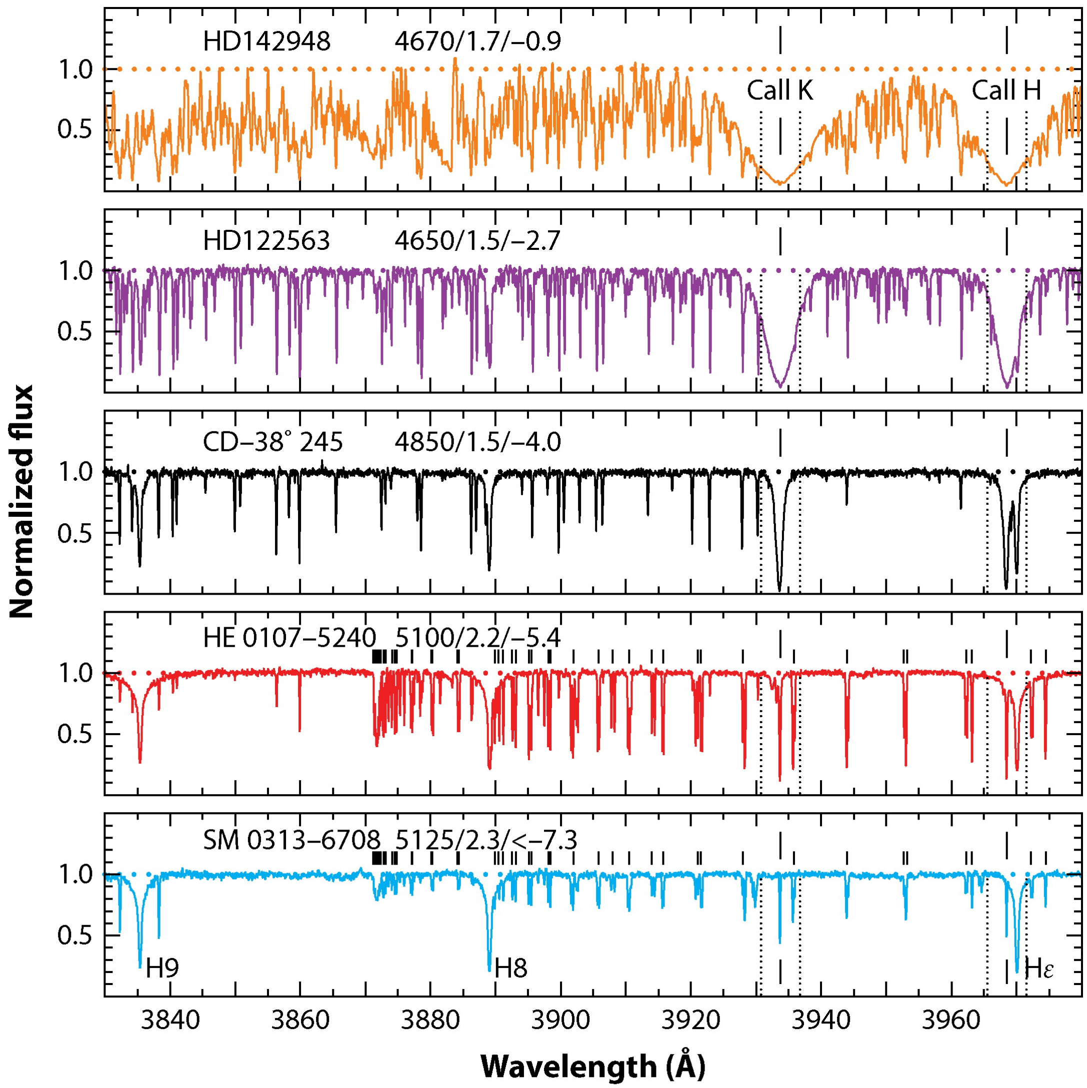

Frebel A, Norris JE. 2015.
Annu. Rev. Astron. Astrophys. 53:631–88

Extremely metal-poor (EMP), low-mass stars (MS, red giants) with $[\mathrm{Fe}/\mathrm{H}] < -7.0 \ldots -3.0$ have been observed

- Due to their long lifetimes, they allow us to study the enrichment by the first generations of stars
- Stellar archaeology
- Near-field cosmology

Stellar populations

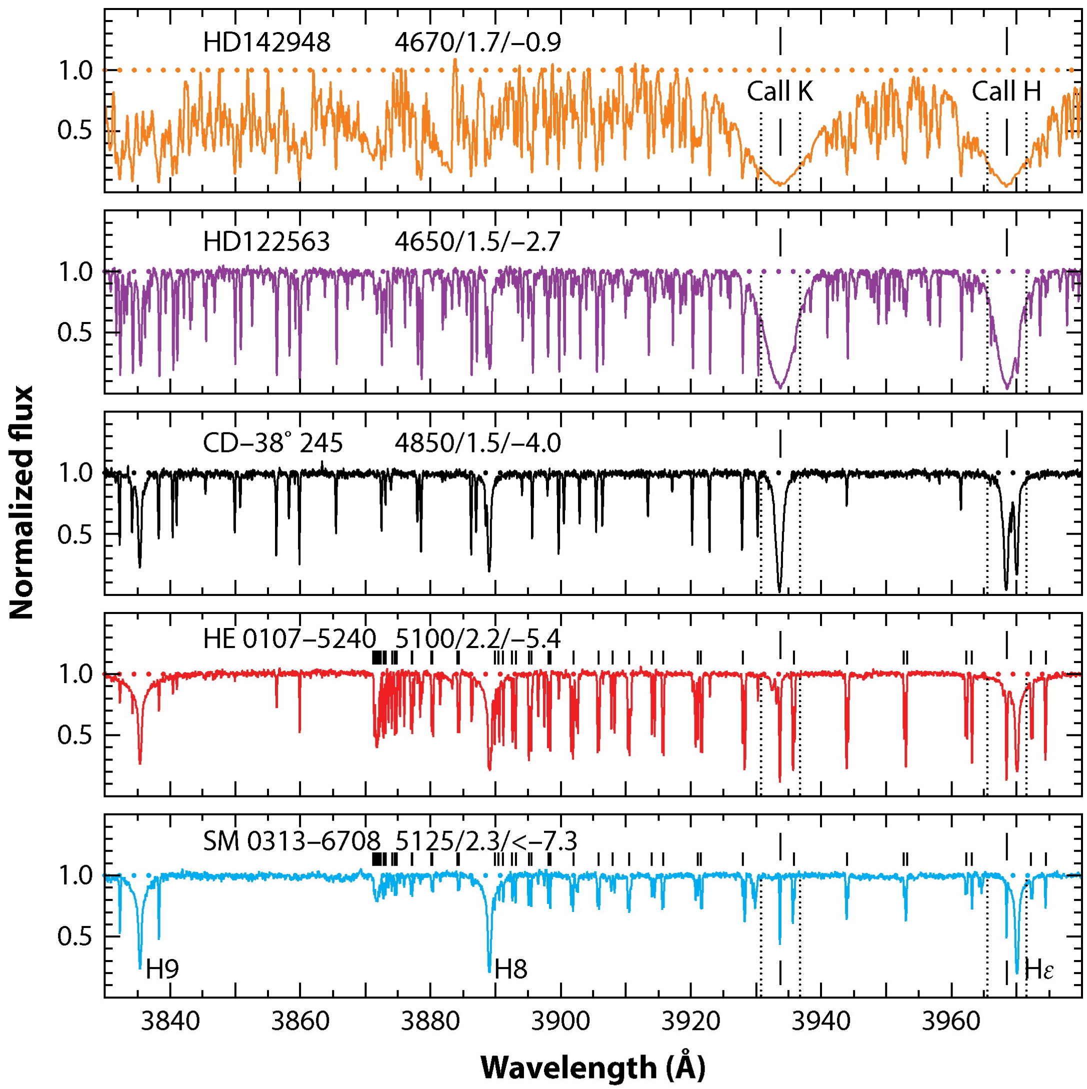

Frebel A, Norris JE. 2015. Annu. Rev. Astron. Astrophys. 53:631–88

Extremely metal-poor (EMP), low-mass stars (MS, red giants) with $[Fe/H] < -7.0 \ldots -3.0$ have been observed

- Lithium abundances and isotope ratio in conflict with predictions for primordial nucleosynthesis
- Carbon enrichment $[C/Fe] > 1.0$ detected in a large fraction of stars $\rightarrow$ CEMP stars
- Enrichment with r- and s-process elements $\rightarrow$ (C)EMP-r/s stars

Enrichment by Pop III stars?

Nucleosynthesis predictions by early supernovae highly uncertain

Stellar populations

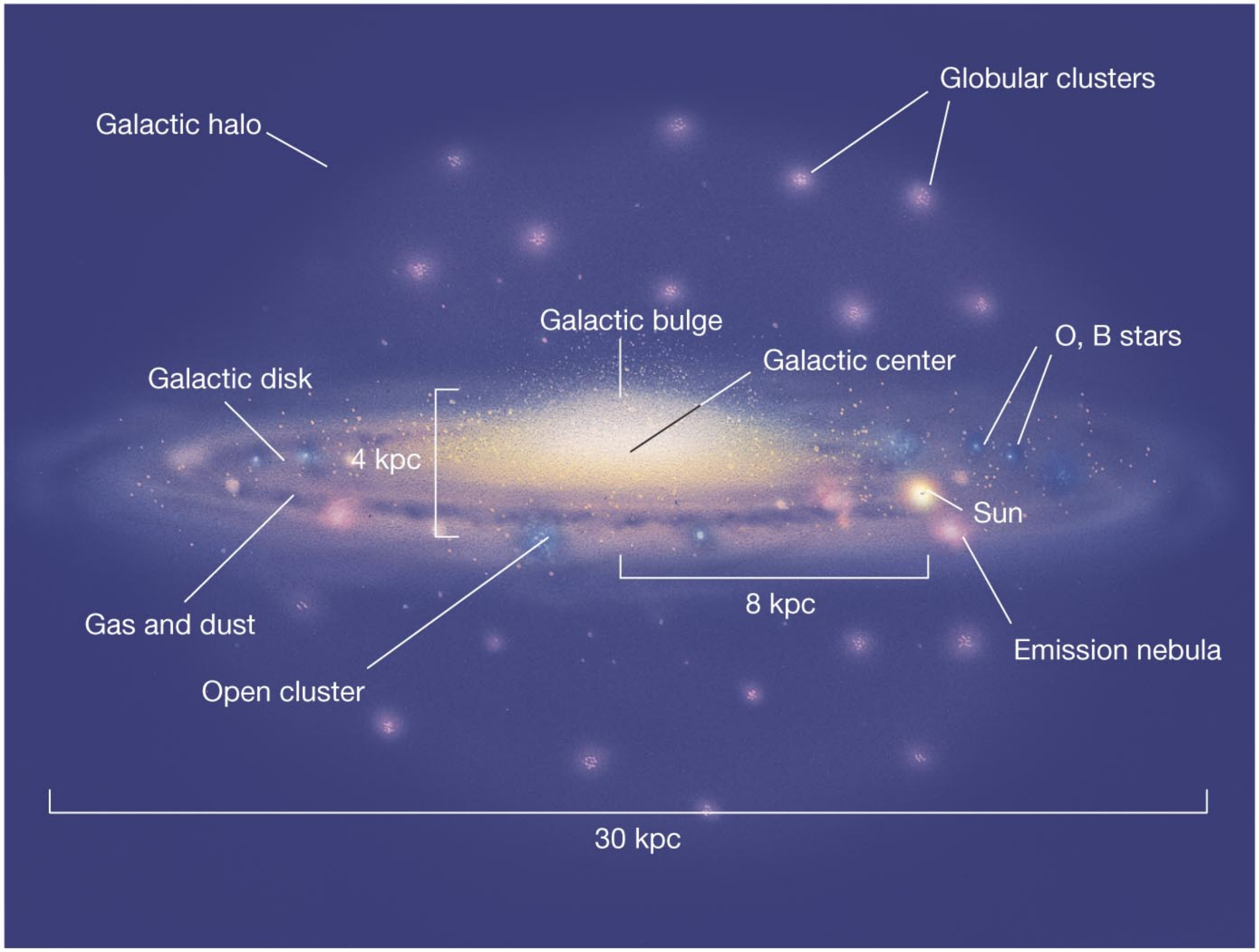

Subsequent generations of stars enriched the ISM

- Stellar populations become more metal-rich
- Massive stars most important for enrichment (winds, SN II), but short-lived (α-elements)
- AGB-stars (s-process elements)
- SN Ia (iron)

Stellar populations

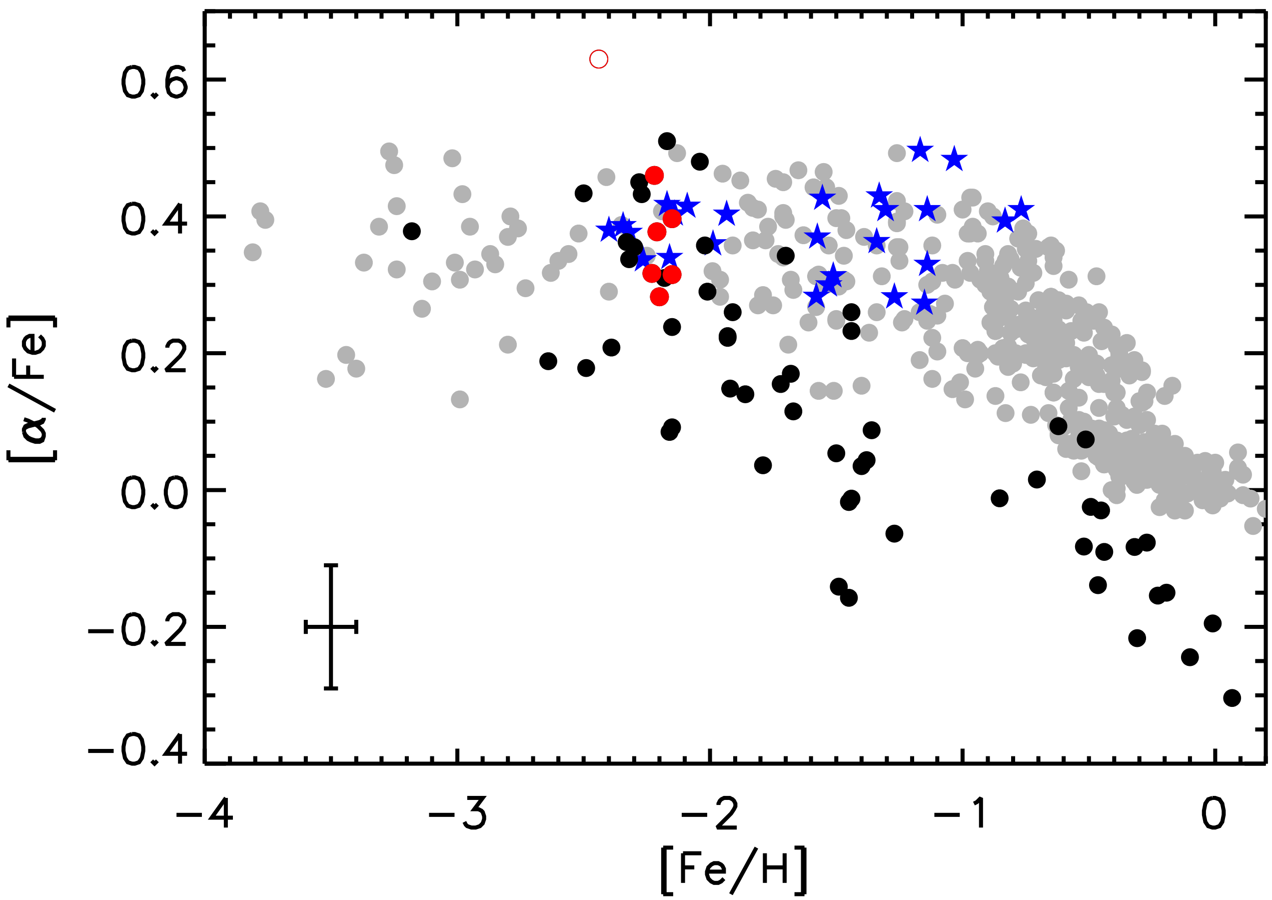

San Roman 2015, A&A, 579, 6

SN Ia require low-mass stars to evolve to WDs first
$\rightarrow$ starting to contribute later than core collapse SN from massive stars
$\rightarrow$ The relative abundance of $\alpha-$elements w.r.t iron [α/Fe decreases with time

Stellar populations

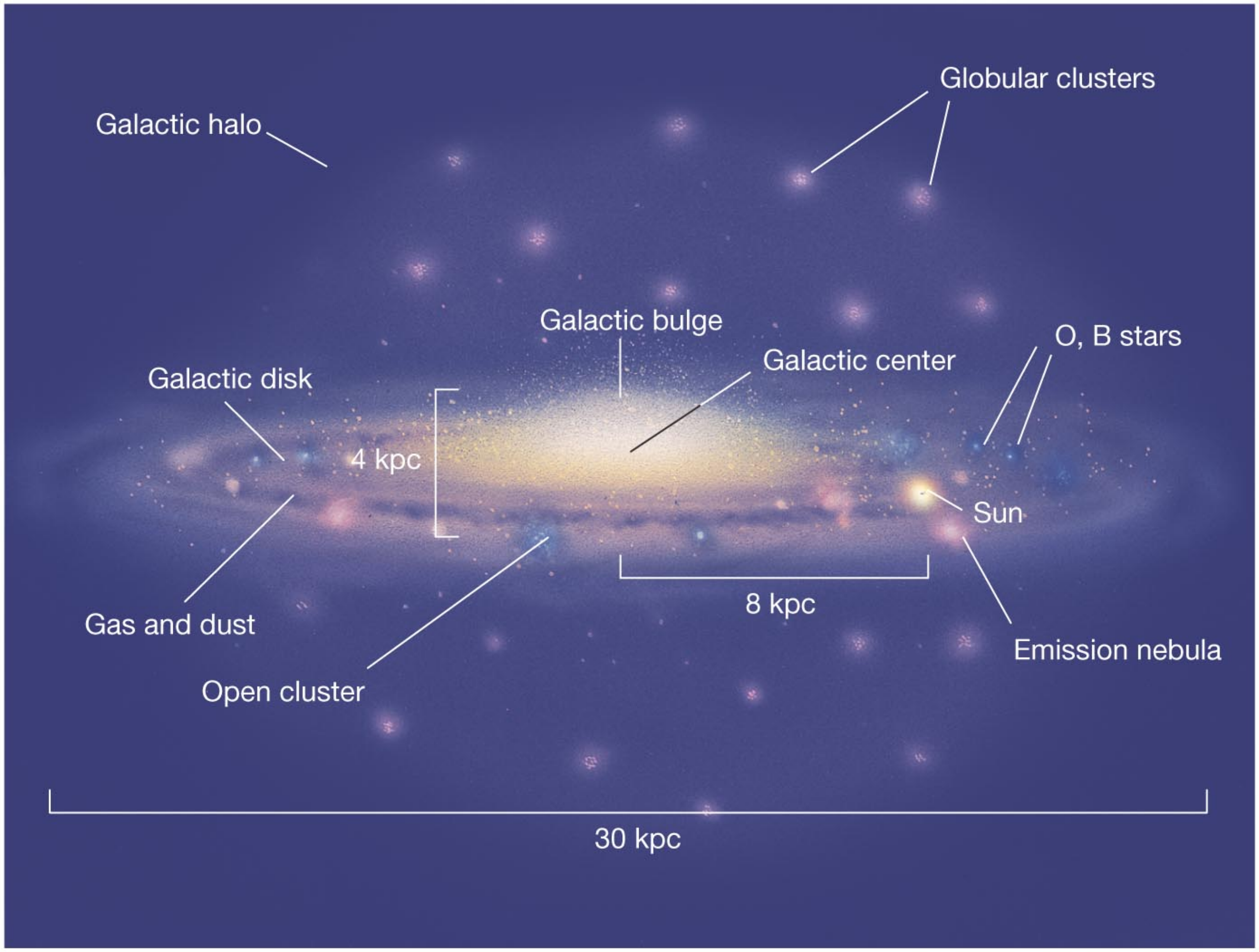

Population II

Oldest Galactic population

- Associated with **Galactic halo**
- $[\mathrm{Fe}/\mathrm{H}] < -2.2 \ldots -1.6$
- Stars $< 0.8\,\mathrm{M}_\odot$ still on main sequence
- Age < 13 Gyr

Stellar populations

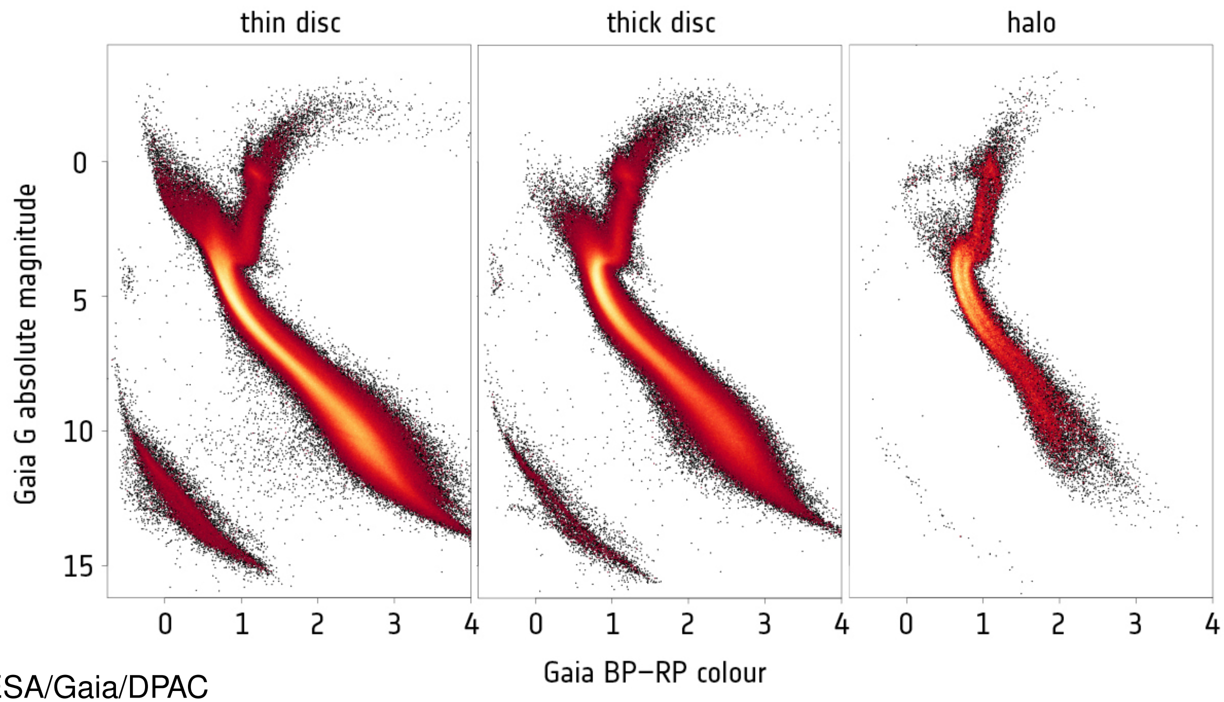

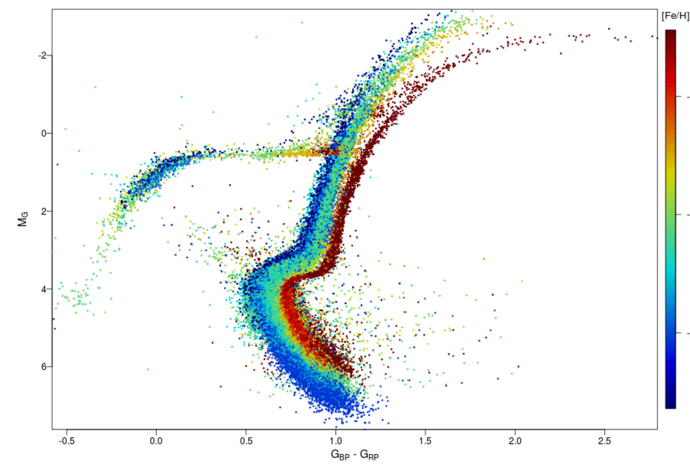

ESA/Gaia/DPAC

Lower metallicity shifts the MS

Pop II stars below the ZAMS of sub-solar metallicity are called subdwarfs (sdA/F/G/K/M)

Gaia revealed split in Pop II!

Stellar populations

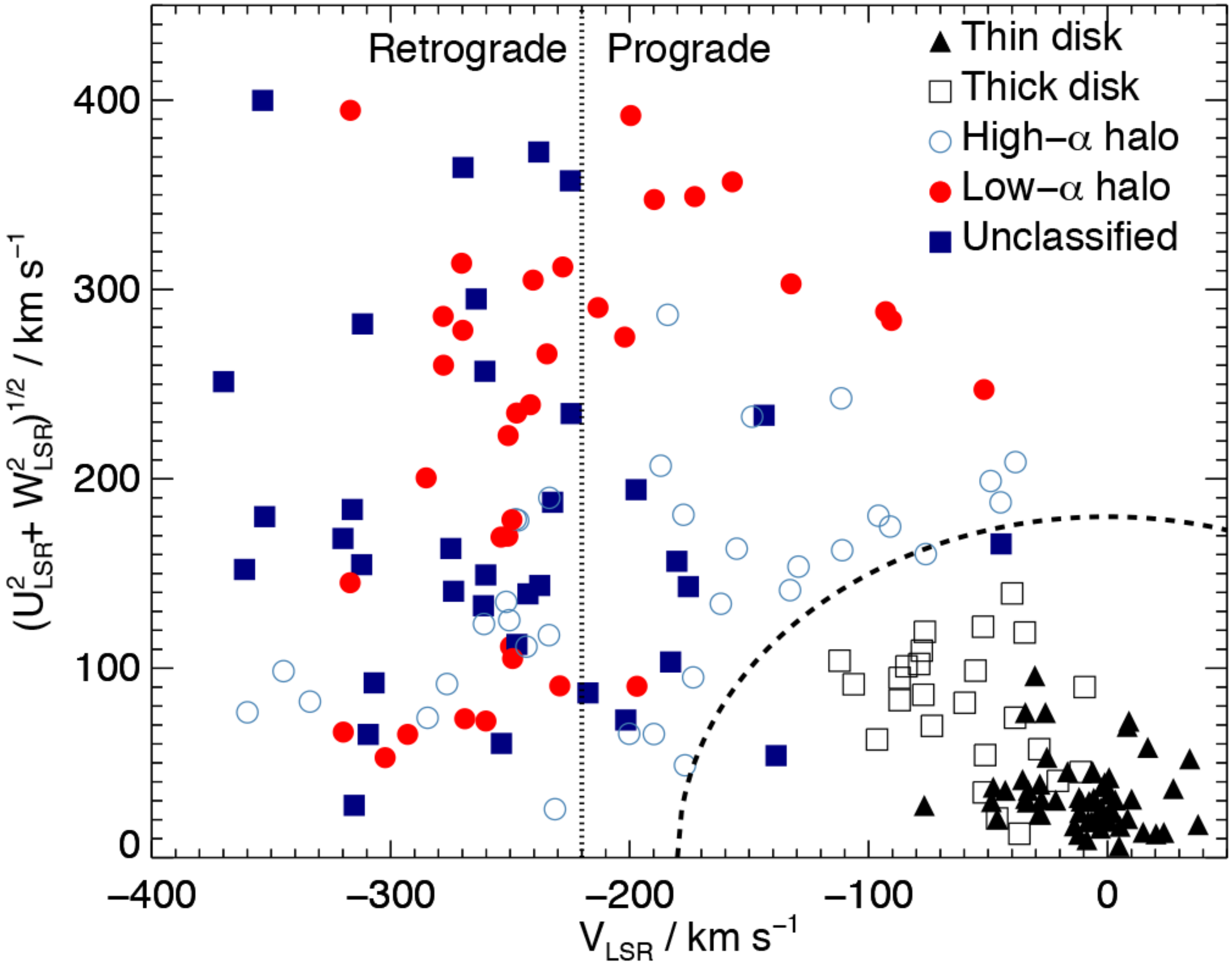

Amarsi et al. 2019, A&A, 630, 104

Galactic space velocity (km/s): U Velocity (km/s) toward the Galactic center; V in the direction of Galactic rotation; W toward the North Galactic Pole

Kinematic selection

Stellar populations

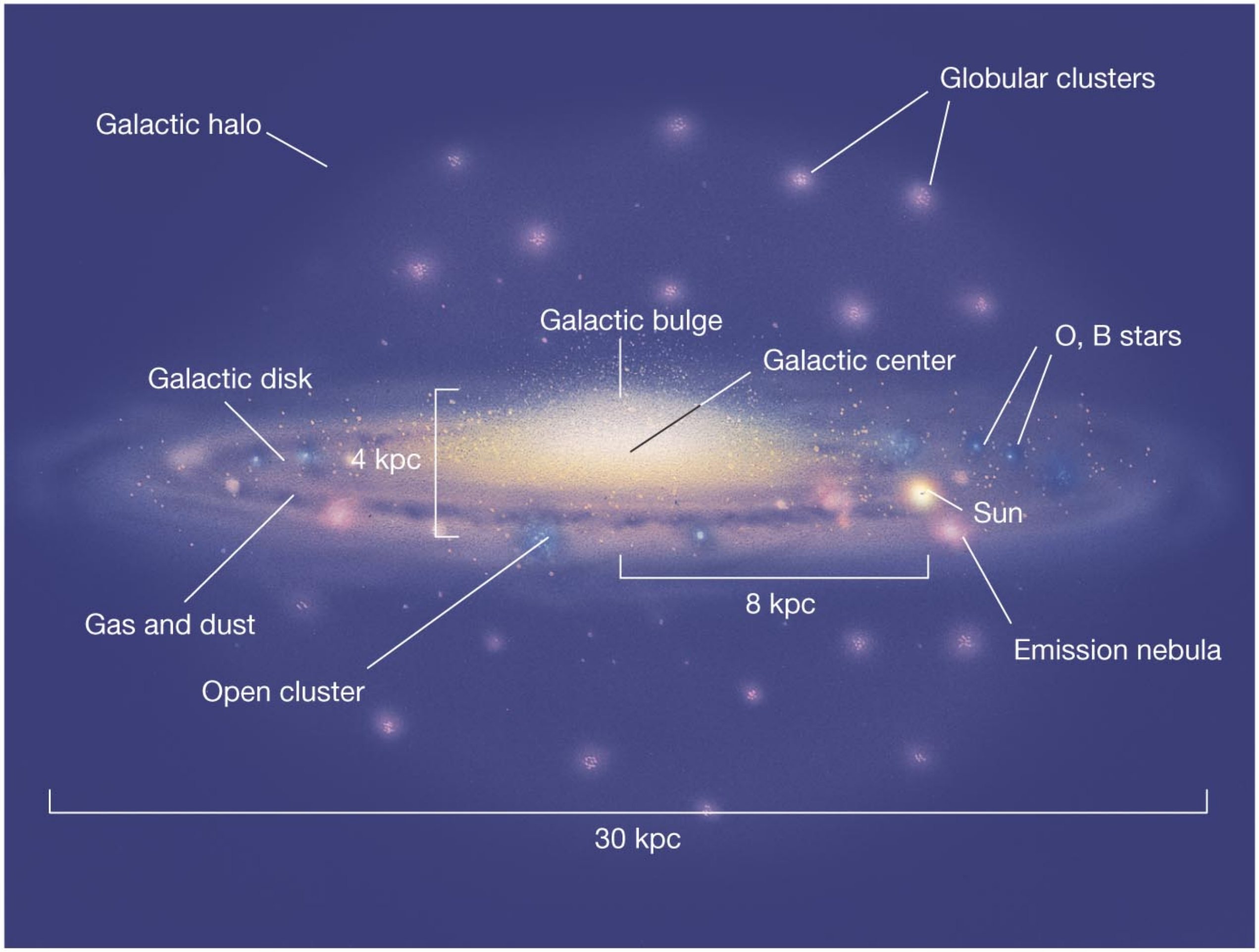

Globular clusters represent old sub-populations with up to $\sim 10^6$ stars

- Part of the Galactic halo
- $[\mathrm{Fe}/\mathrm{H}] < -2.3 \ldots -1.6$
- Cluster stars have formed at the same time
- MS-turnoff depends on age
- Problem: Multiple populations

Stellar populations

NASA/ESA

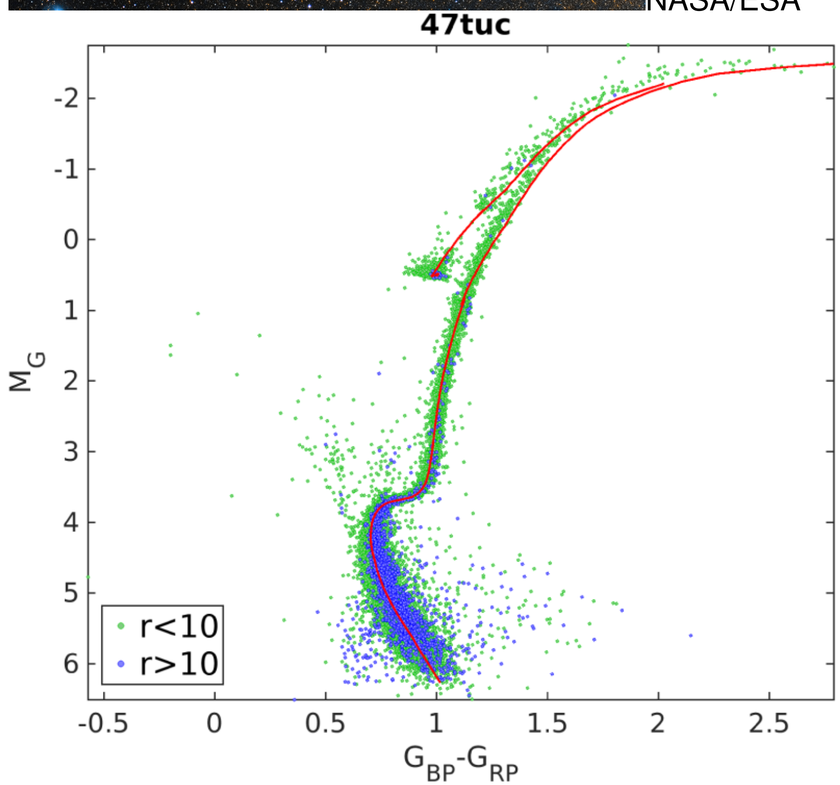

ESA/Gaia/DPAC

Globular clusters represent old sub-populations with up to $\sim 10^6$ stars

- Part of the Galactic halo
- $[\mathrm{Fe}/\mathrm{H}] < -2.3 \ldots -1.6$
- Cluster stars have formed at the same time
- MS-turnoff depends on age
- Problem: Multiple populations

Stellar populations

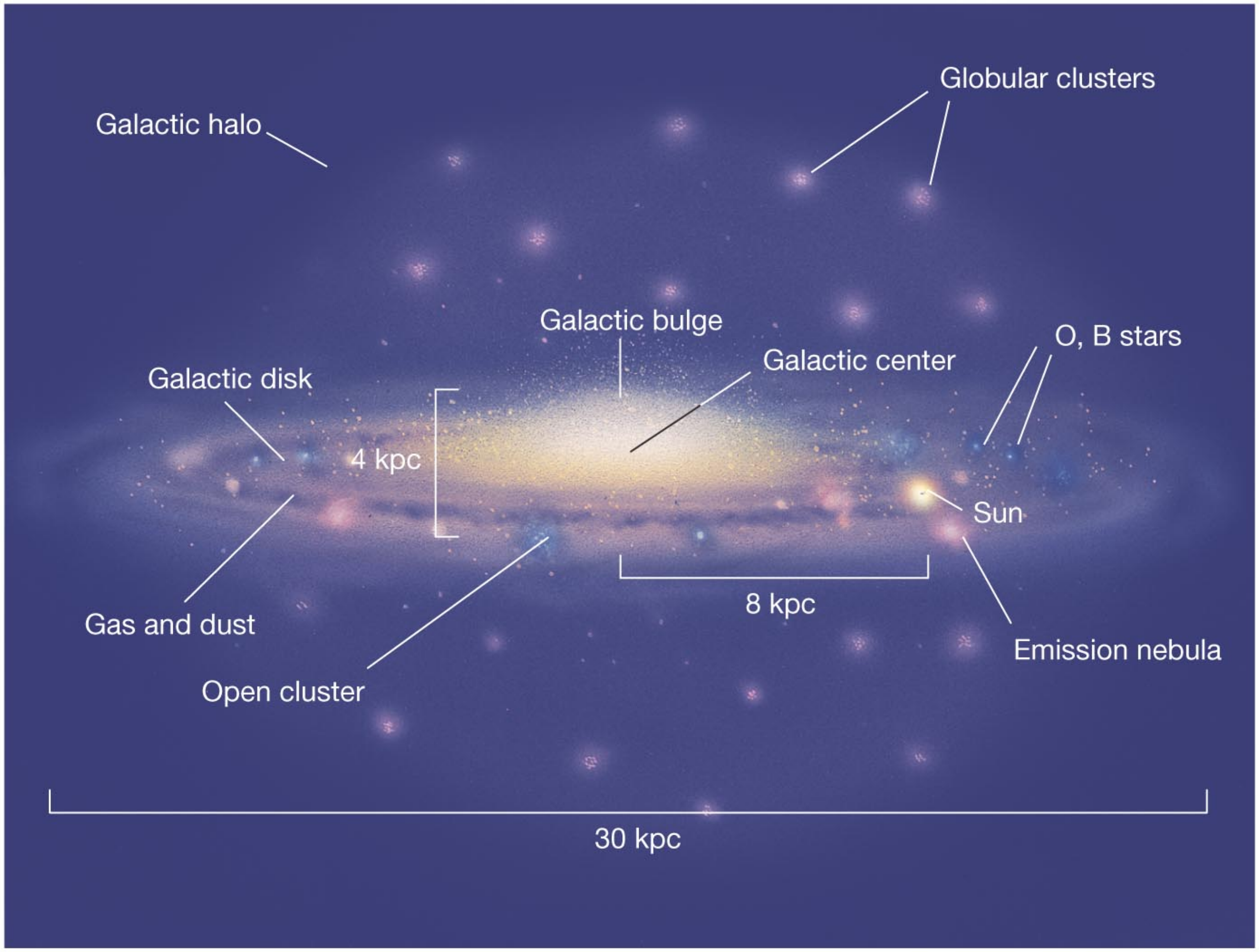

Population I

Youngest Galactic population

- Associated with Galactic disk/bulge
- $[\mathrm{Fe}/\mathrm{H}] < -0.2 \ldots -0.6$
- Star formation ongoing in the disk

Stellar populations

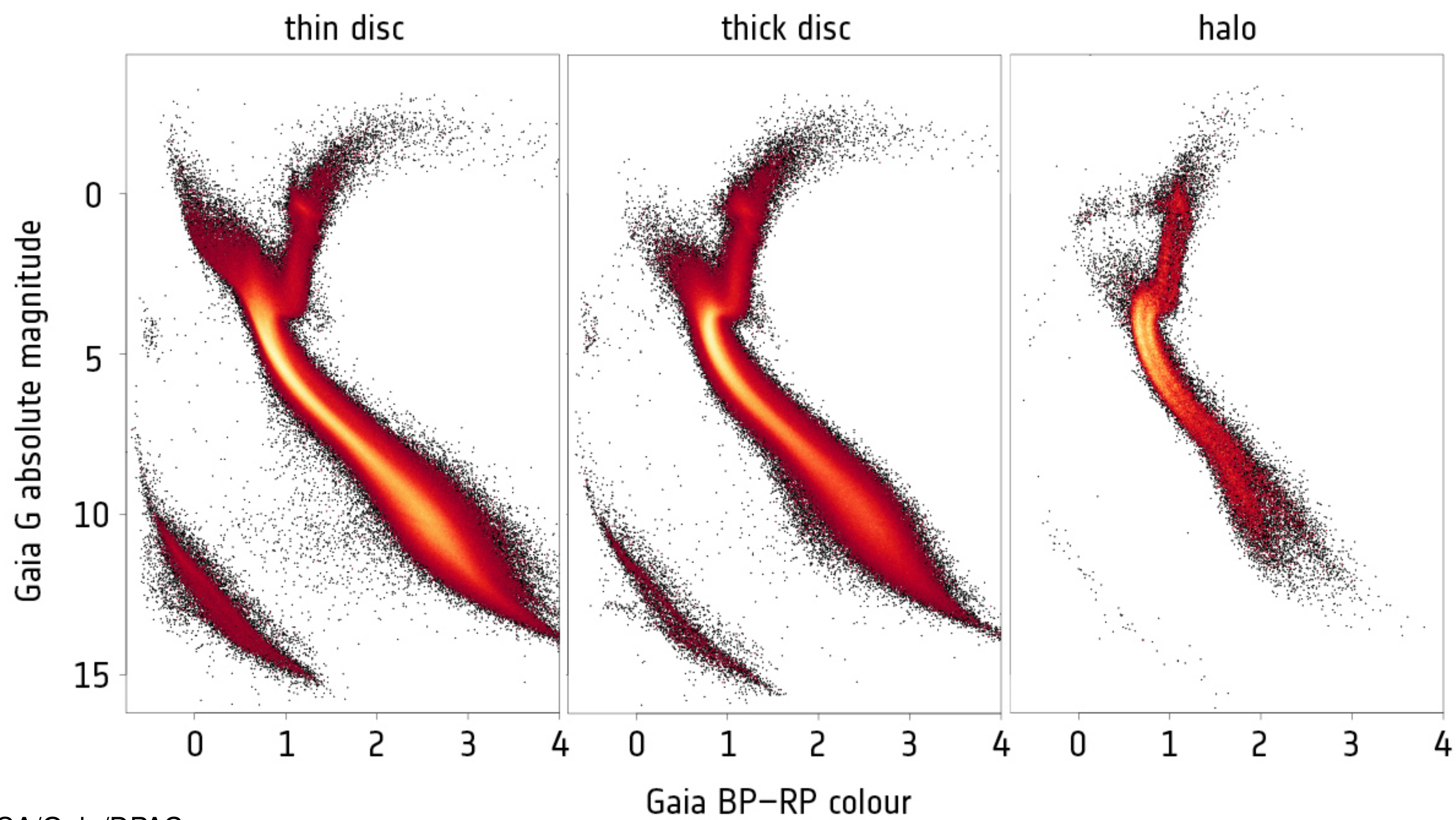

ESA/Gaia/DPAC

MS extended towards young and massive stars

WDs and low-mass MS stars present

$\rightarrow$ Selection effect: Sun belongs to the disk

Stellar populations

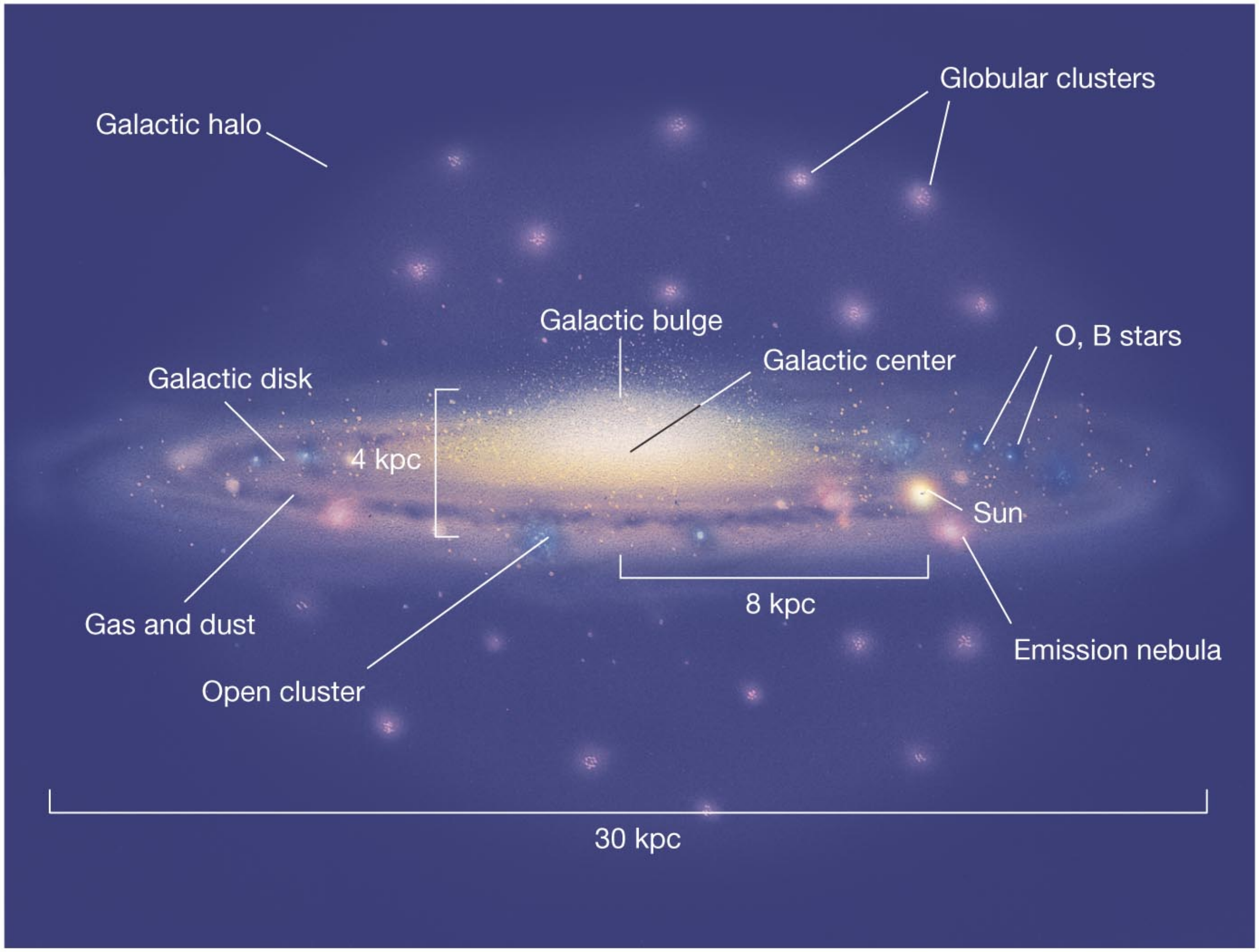

Open clusters represent sub-populations with up to $\sim 10^3$ stars

- Part of the Galactic disk
- Cluster stars have formed at the same time
- MS-turnoff depends on age

Stellar populations

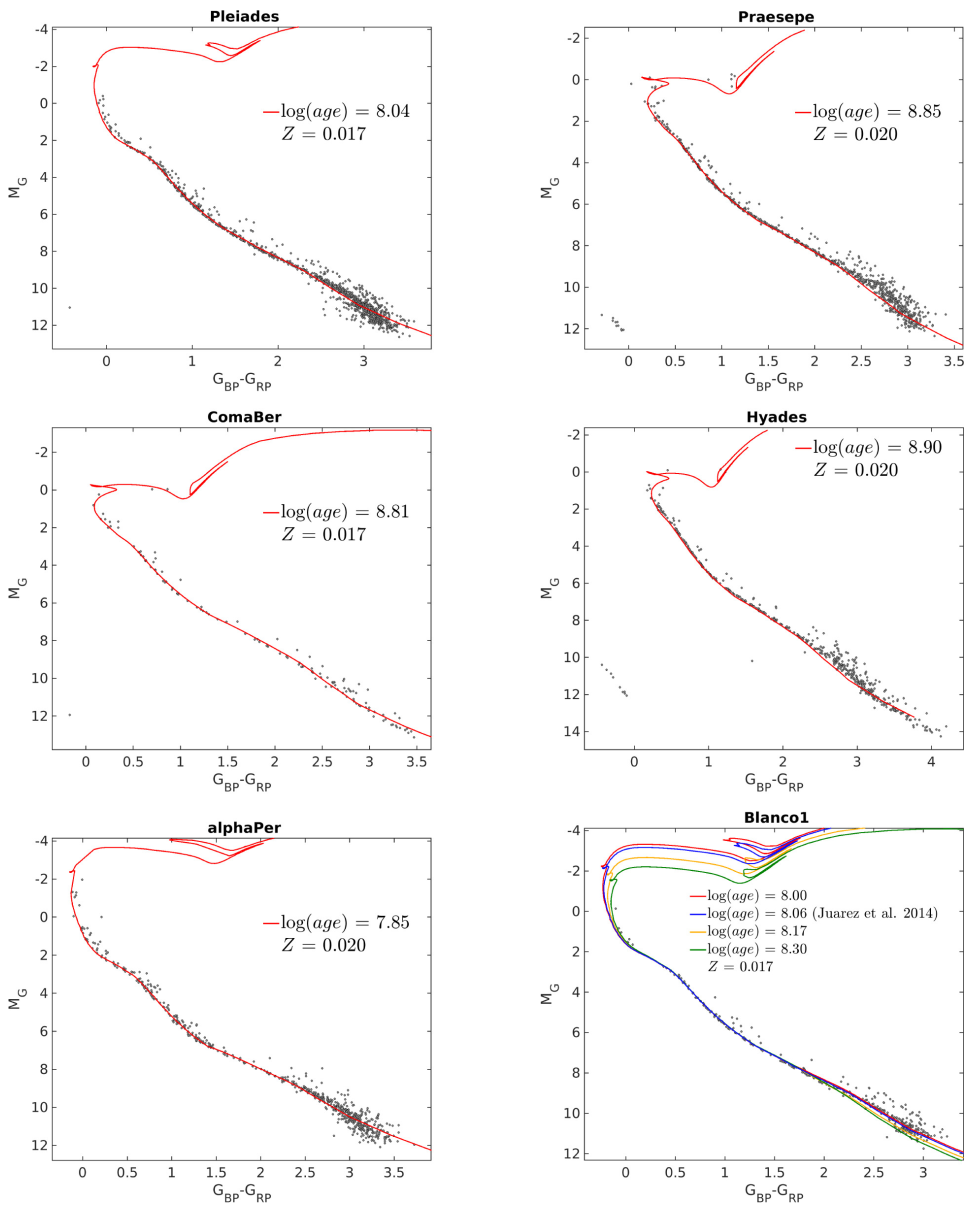

ESA/Gaia/DPAC

Open clusters represent sub-populations with up to $\sim 10^3$ stars

- Part of the Galactic disk
- Cluster stars have formed at the same time
- MS-turnoff depends on age

NA

ESA, AURA/Caltech, Palomar Observatory

Stellar populations

Age determination of clusters by isochrones

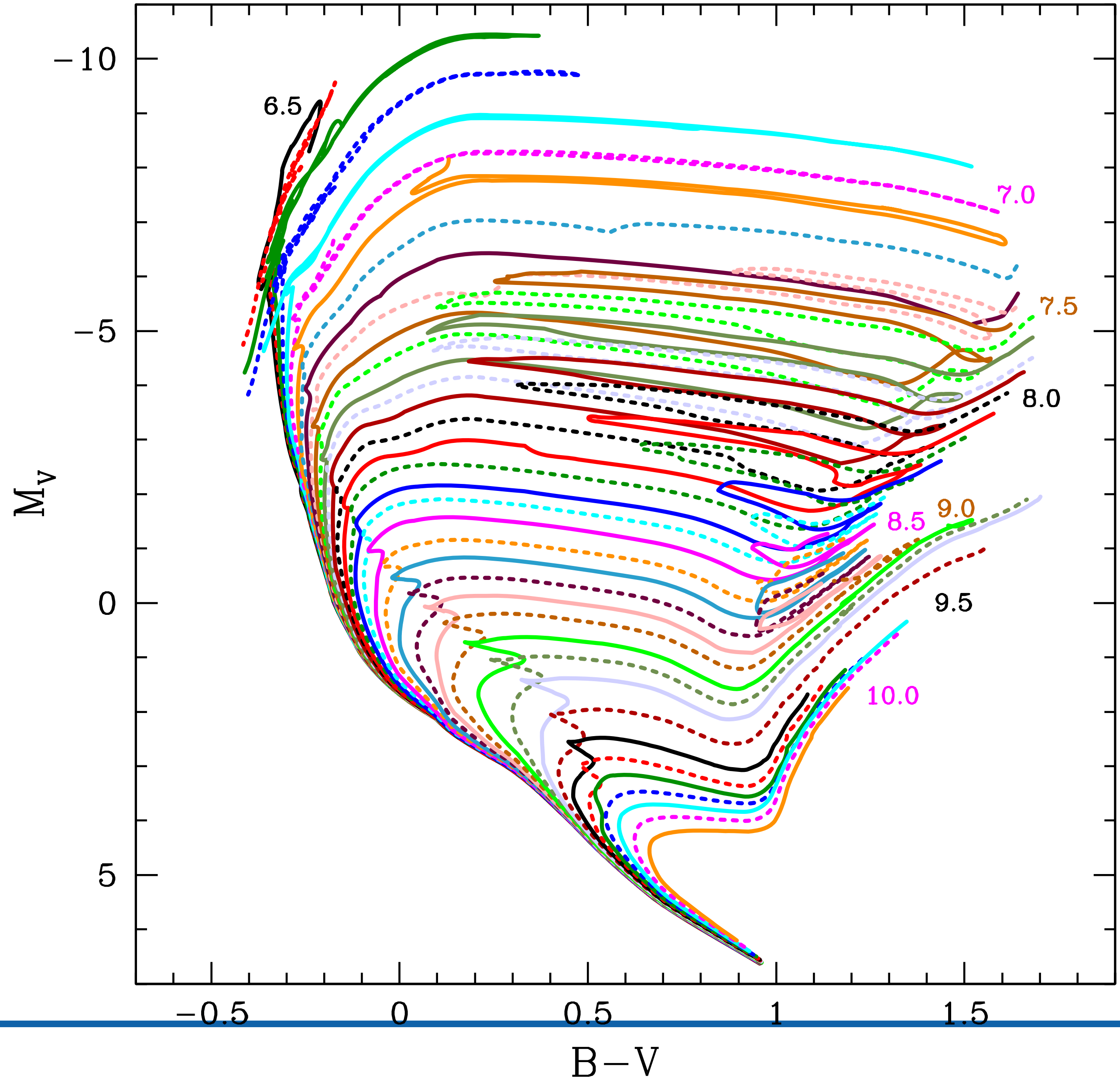

Ekström et al. 2012, A&A, 37, A146

Stellar evolution

Cosmic cycle of matter

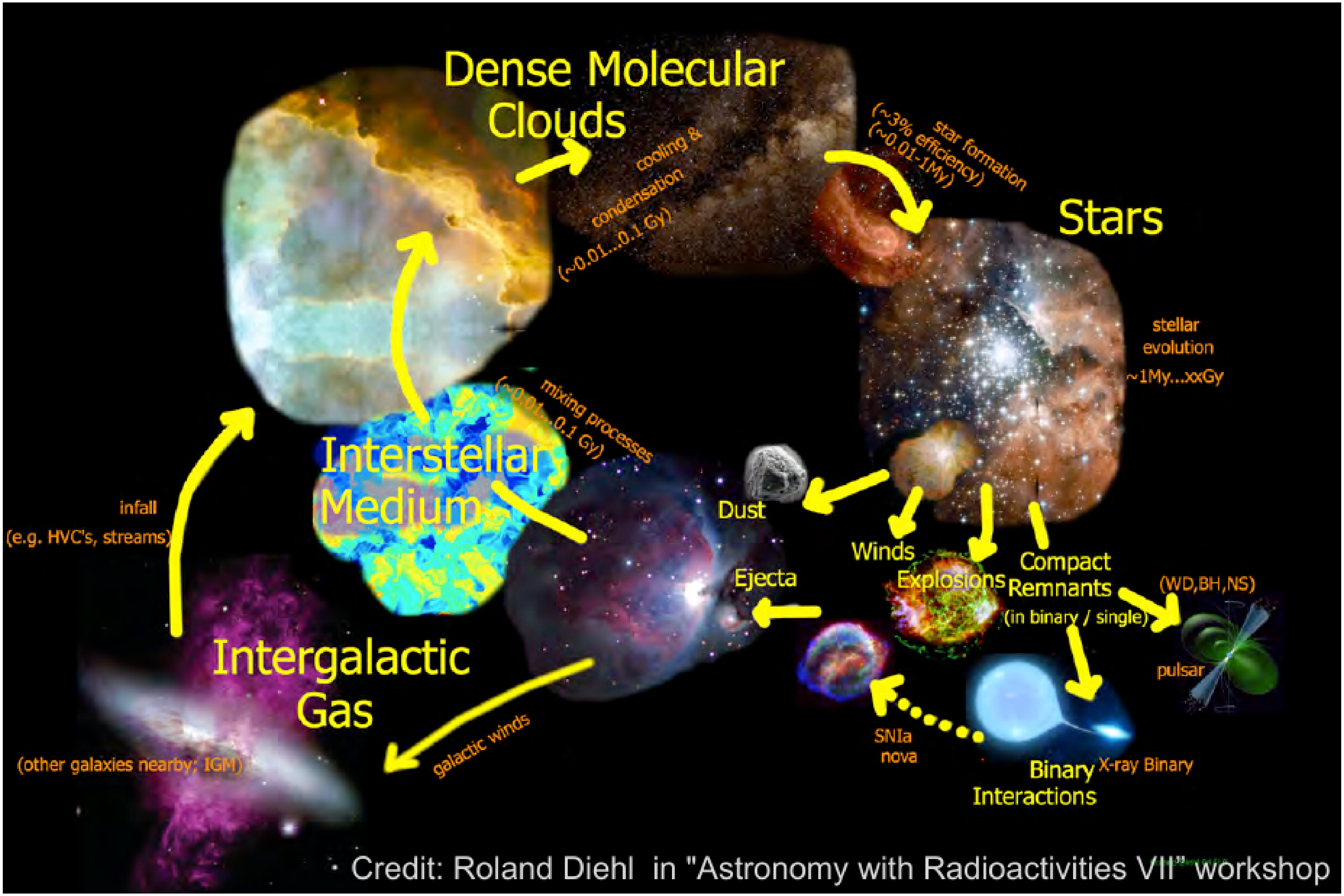

Molecular clouds

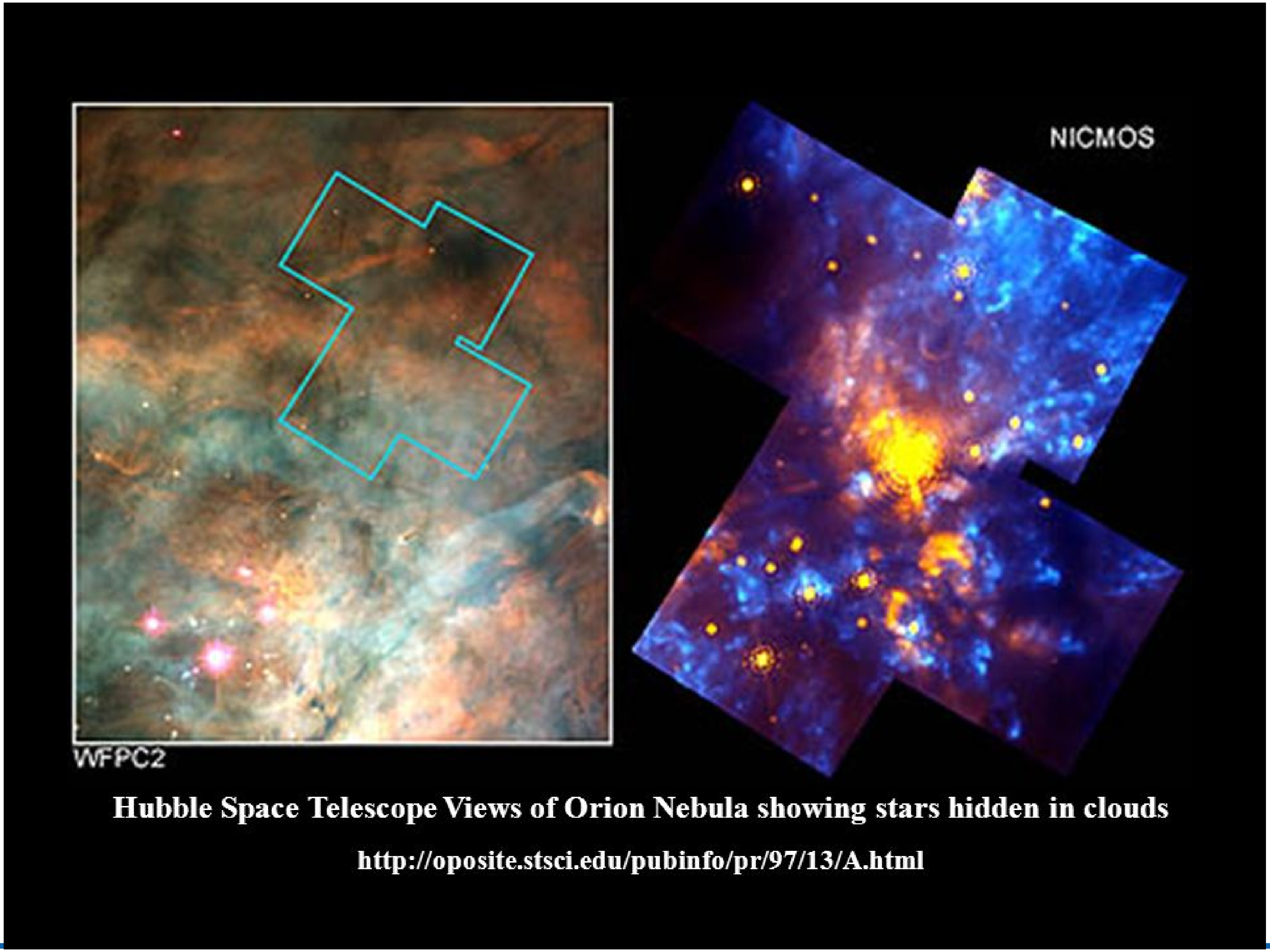

Cloud collapse

In equilibrium:

$$-E_g = 2E_k$$

$$\frac{3}{5}\frac{GM^2}{R} = \frac{3}{2}kT\frac{M}{m}$$

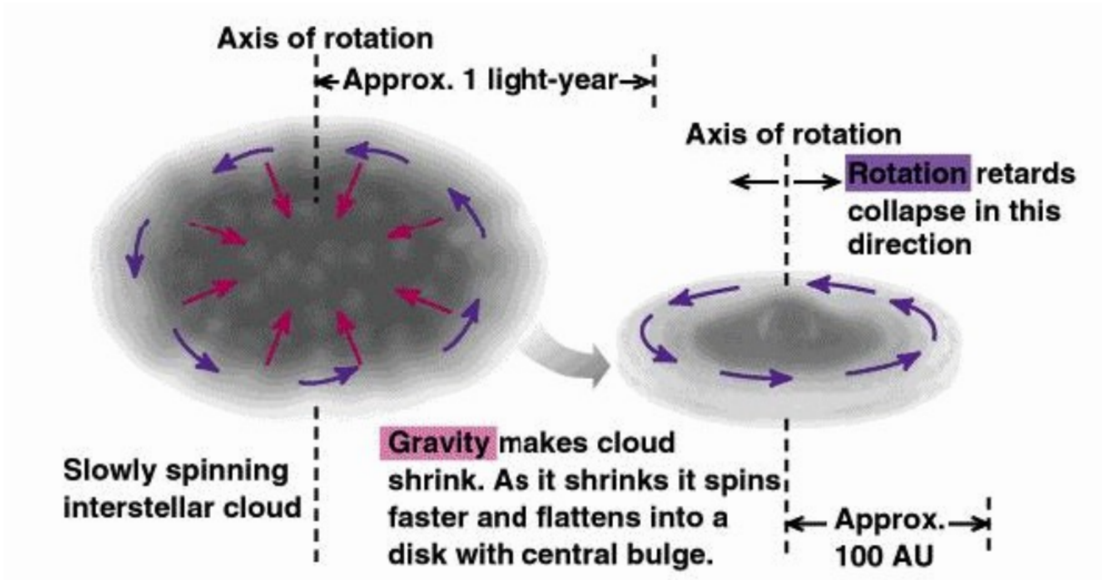

During collapse:

$$-\frac{1}{2}E_g > E_k$$

$$M > M_J = 9 \cdot 10^4 M_{\odot} \left(\frac{T^3_{(K)}}{n_{(m^{-3})}}\right)^{\frac{1}{2}}$$

For a MC with:

T=10K
n=100 cm^{-3} } $M_J \sim 10^2 M_S$

- new stars can be formed in an environment of dense interstellar (molecular hydrogen H_2) clouds. Under certain circumstances (e.g. by shock waves from supernovae) these clouds can become gravitationally unstable to contraction.
- not strictly necessary to have such massive clouds. There are inhomogeneities that will cause the cloud to fragment leading to the formation of more than one star.

Cloud collapse

In equilibrium:

$$-E_g = 2E_k$$

$$\frac{3}{5}\frac{GM^2}{R} = \frac{3}{2}kT\frac{M}{m}$$

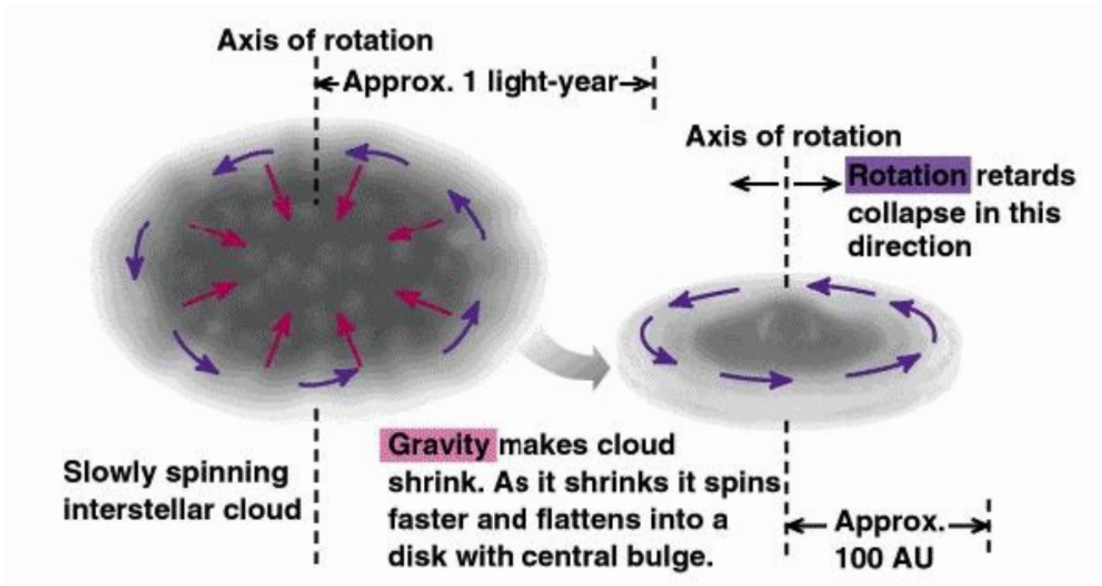

During collapse:

$$-\frac{1}{2}E_g > E_k$$

$$M > M_J = 9\cdot 10^4 M_\odot \left(\frac{T^3_{(K)}}{n_{(m^{-3})}}\right)^{\frac{1}{2}}$$

For a MC with:

T=10K
n=100 cm^{-3} } M_J~$10^2 M_S$

Jeans mass

- Gravitational pressure has to overcome gas pressure ($\theta = 3/5$ for homogenous sphere)

$$|P_{\text{gas}}| < |P_{\text{grav}}| \to \frac{R}{\mu}\rho T < \theta\frac{GM^2}{4\pi R^4}$$

$$\Rightarrow M_{Jeans} = \frac{27}{16}\left(\frac{3}{\pi}\right)^{1/2}\left(\frac{R}{\theta G}\right)^{3/2}\sqrt{\frac{T^3}{\mu^3\bar{\rho}}}$$

$$\Rightarrow M_{Jeans} = 1.1 M_\odot \left(\frac{T}{10\,\mathrm{K}}\right)^{3/2}\left(\frac{\rho}{10^{-19}\,\mathrm{g\,cm^{-3}}}\right)^{-1/2}\left(\frac{\mu}{2.3}\right)^{-3/2)}$$

Cloud collapse

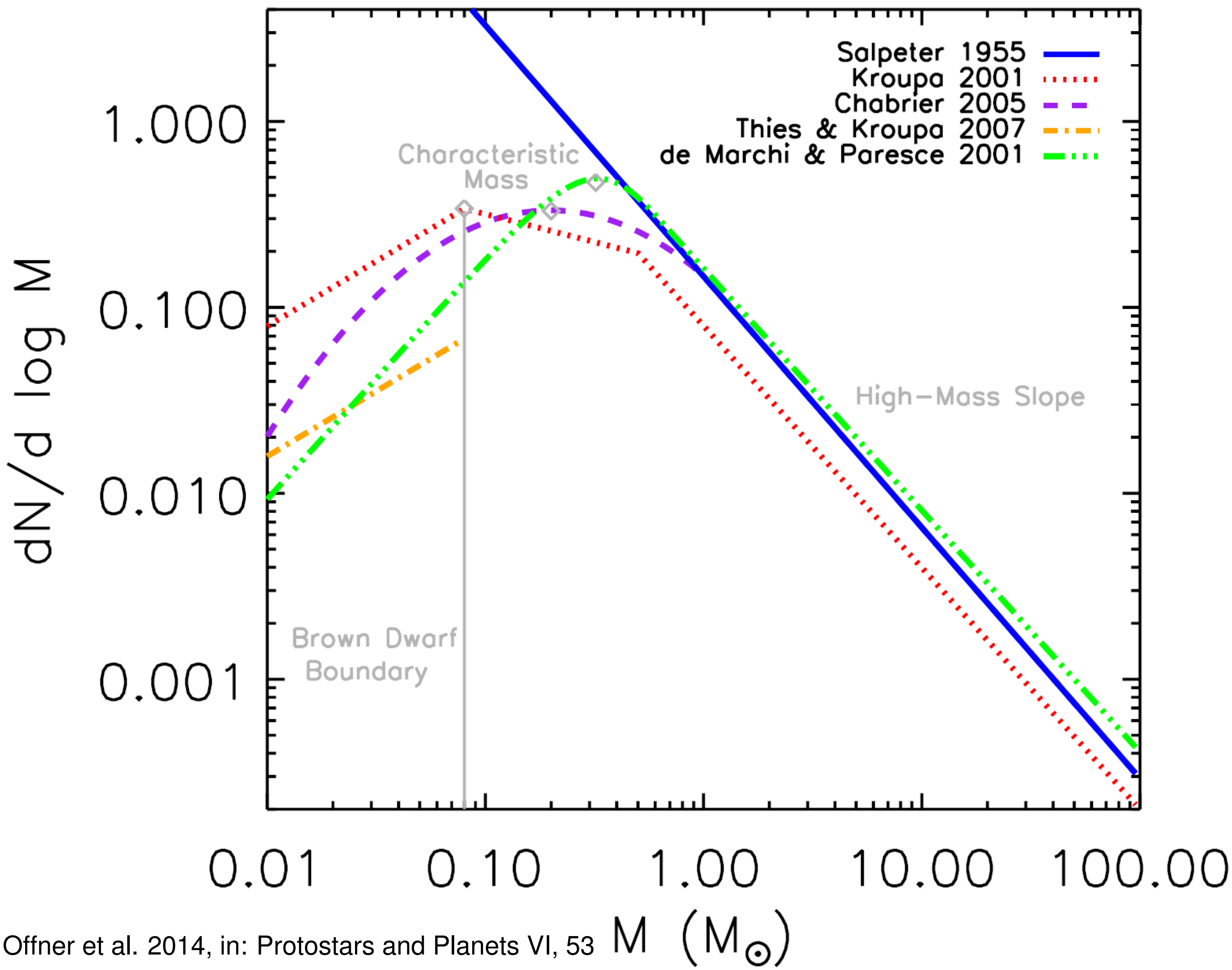

Offner et al. 2014, in: Protostars and Planets VI, 53

Low-mass stars are more frequent $\rightarrow$ peak at $M = 0.2\,M_\odot$

Cloud collapse

Molecular clouds highly turbulent $\rightarrow M_{\text{Jeans}} \sim \sqrt{\frac{T^3}{\mu^3\rho}}\mathcal{M}^{-1}$, $\mathcal{M} = \frac{v_{\text{shock}}}{v_{\text{sound}}}$
with Mach number $\mathcal{M}$

Star formation

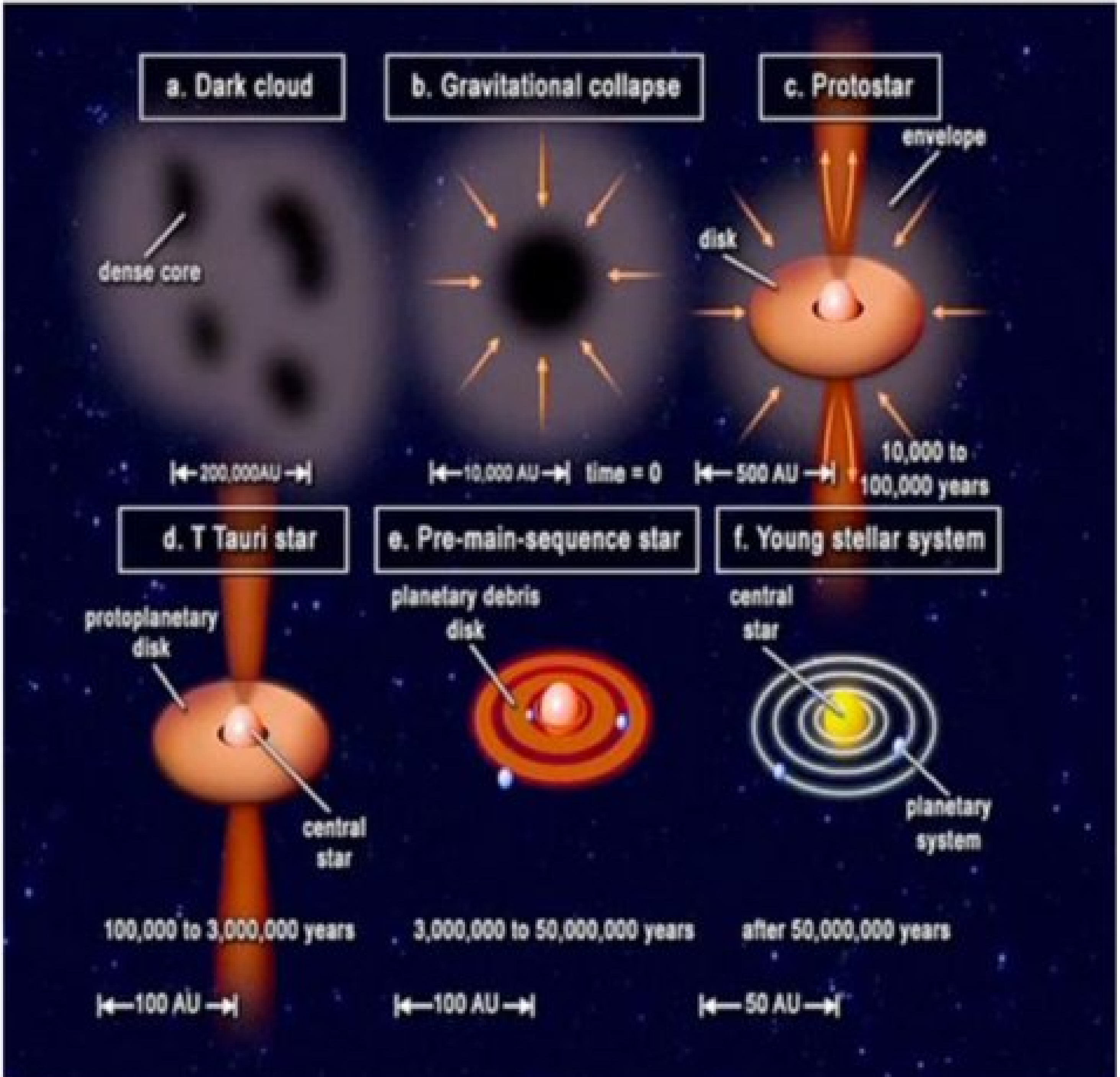

Young stellar objects (YSOs)

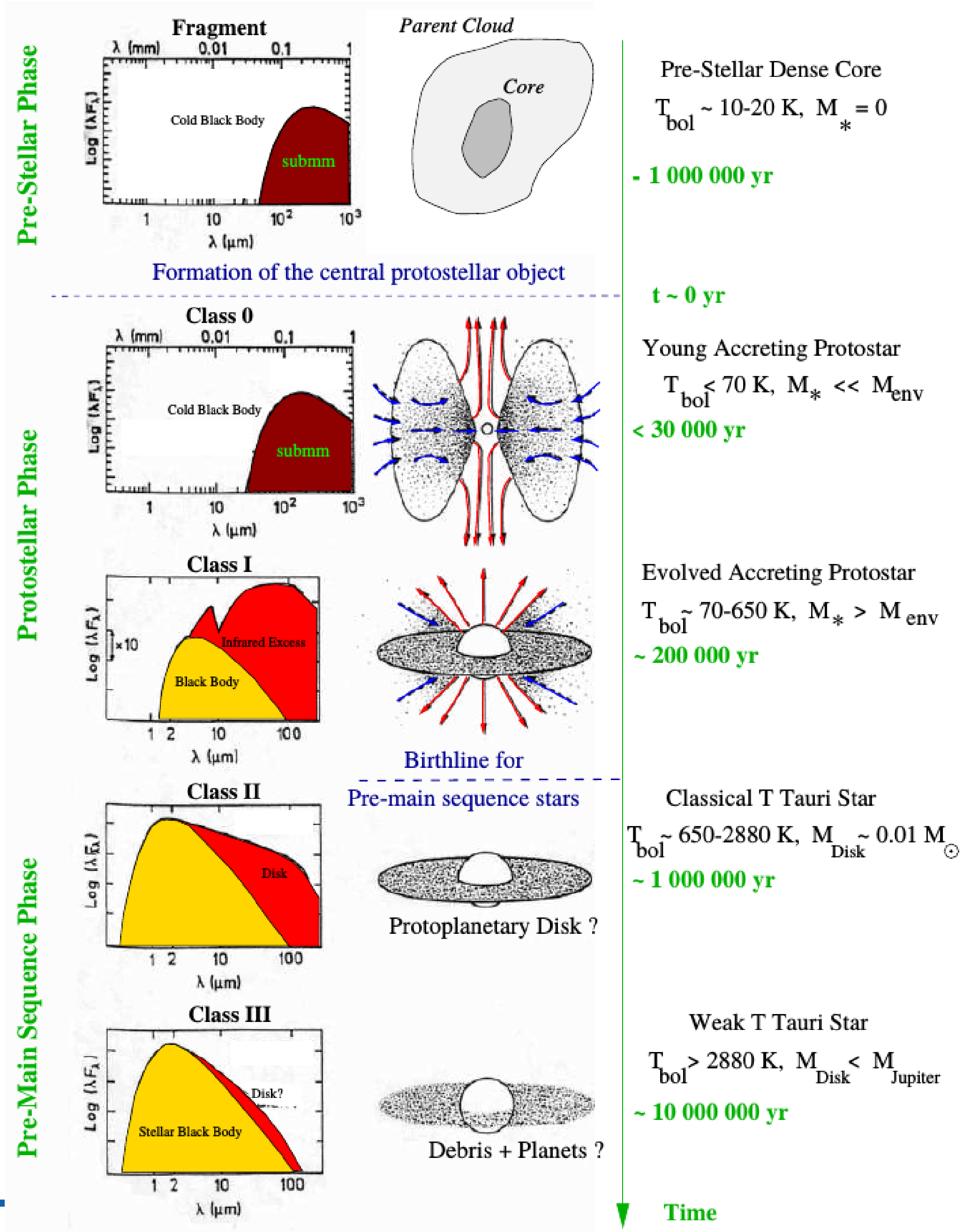

André 2002

- isothermal phase: $T \sim 10$ K, density low enough that gravitational energy can be radiated away, temperature remains low and it keeps contracting, visible through far infrared emission
- adiabatic phase: density increases until cloud becomes opaque, temperature rises until contraction stops because pressure built up (hydrostatic equilibrium), protostar forms, cloud is detectable from radiation from dust in IR

Young stellar objects (YSOs)

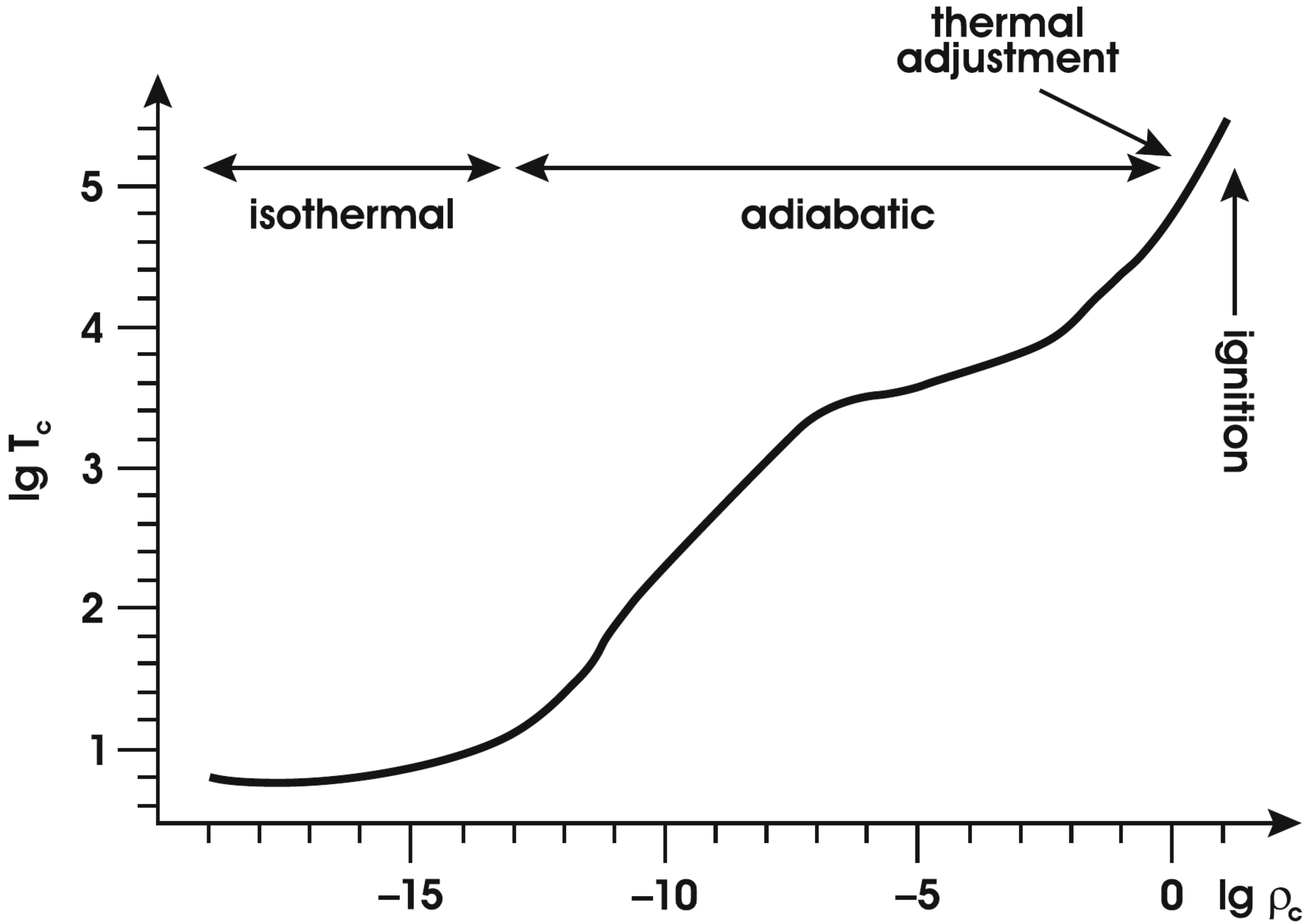

Evolution of cloud collapse and early pre-main sequence in the HRD

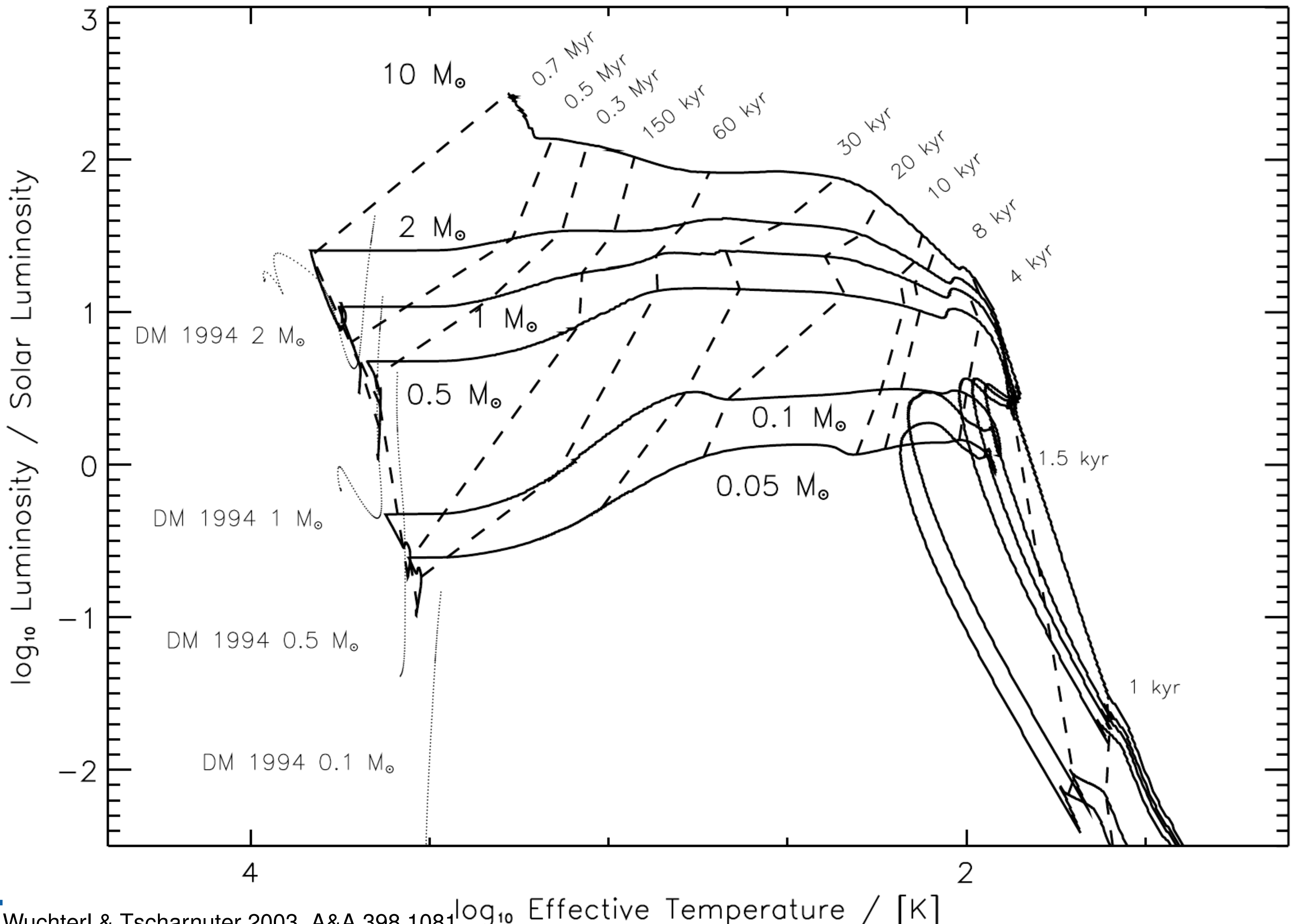

Wuchterl & Tscharnuter 2003, A&A 398,1081

Evolution of cloud collapse and early pre-main sequence in the HRD

- collapsing cloud remains an infrared object as long as the envelope is opaque to visible radiation $\rightarrow$ evolutionary track starts extremely far to the right
- thinning out of the envelope has several effects:
  - becomes more transparent
  - photosphere moves downwards until it has reached the surface of the hydrostatic core
  - with decreasing R: T_{eff} must increase in order to radiate away the energy
  - luminosity is produced by accretion $\rightarrow$ with decreasing $\dot{M}$: L decreases until it is finally provided by contraction of the core
- for low-mass stars accretion onto the protostar stops well before central temperatures for hydrogen ignition is reached
- For massive stars, accretion continues while central hydrogen burning has already set in $\rightarrow$ already consumed part of its hydrogen fuel when it becomes visible

Hayashi lines

The Hayashi line (HL) is defined as the locus in the HRD of fully convective stars of given parameters (mass M and chemical composition)

$\rightarrow$ located far to the right in the HRD, typically at $T_{\text{eff}} \approx 3000...5000$ K, very steep, in large parts almost vertical

$\rightarrow$ borderline between an "allowed" region (on its left) and a forbidden" region (on its right), for all stars in hydrostatic equilibrium and being fully convective

$\rightarrow$ cooler T_{eff} than Hayashi line not stable because temperature gradients would have to be steeper than the adiabatic one

interior part of convective star has an adiabatic stratification $\mathrm{d}\ln T/\mathrm{d}\ln P = \nabla_{\text{ad}}$

$\rightarrow$ if we assume a fully ionized ideal gas: $\nabla_{\text{ad}} = \text{ const } = 0.4$

$\rightarrow$ simple $P - T$ relation: $P = CT^{1+n} = CT^{5/2}$

$\rightarrow$ star is polytropic with an index $n = 1/\nabla_{\text{ad}} - 1 = 3/2$, $C = K^{-n}(R/\mu)^{1+n}$

$$K \sim \rho_c^{1/3} A^{-2} \sim \rho_c^{1/3} R^2 \sim M^{1/3} R \Rightarrow C = C'(n,\mu) R^{-3/2} M^{-1/2}$$

$$\Rightarrow \lg T = 0.4 \lg P + 0.4 \left(\frac{3}{2} \lg R + \frac{1}{2} \lg M - \lg C' \right)$$

Hayashi lines

with the hydrostatic equation and the Stephan-Boltzmann law we get the Hayashi lines in the HRD

$$\lg T_{\text{eff}} = A \lg L + B \lg M + C \lg \mu + \text{constant} \tag{9.1}$$

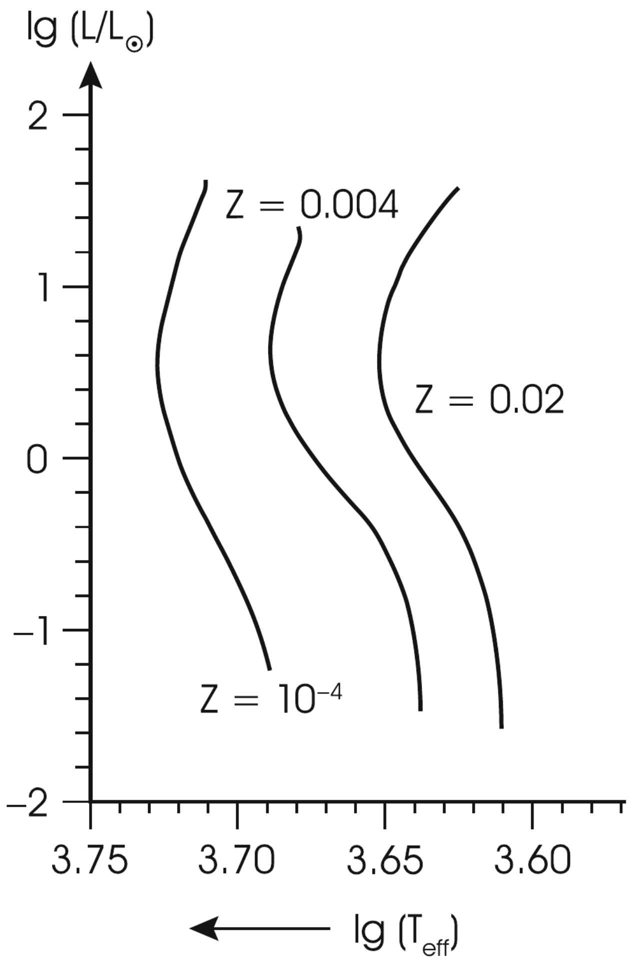

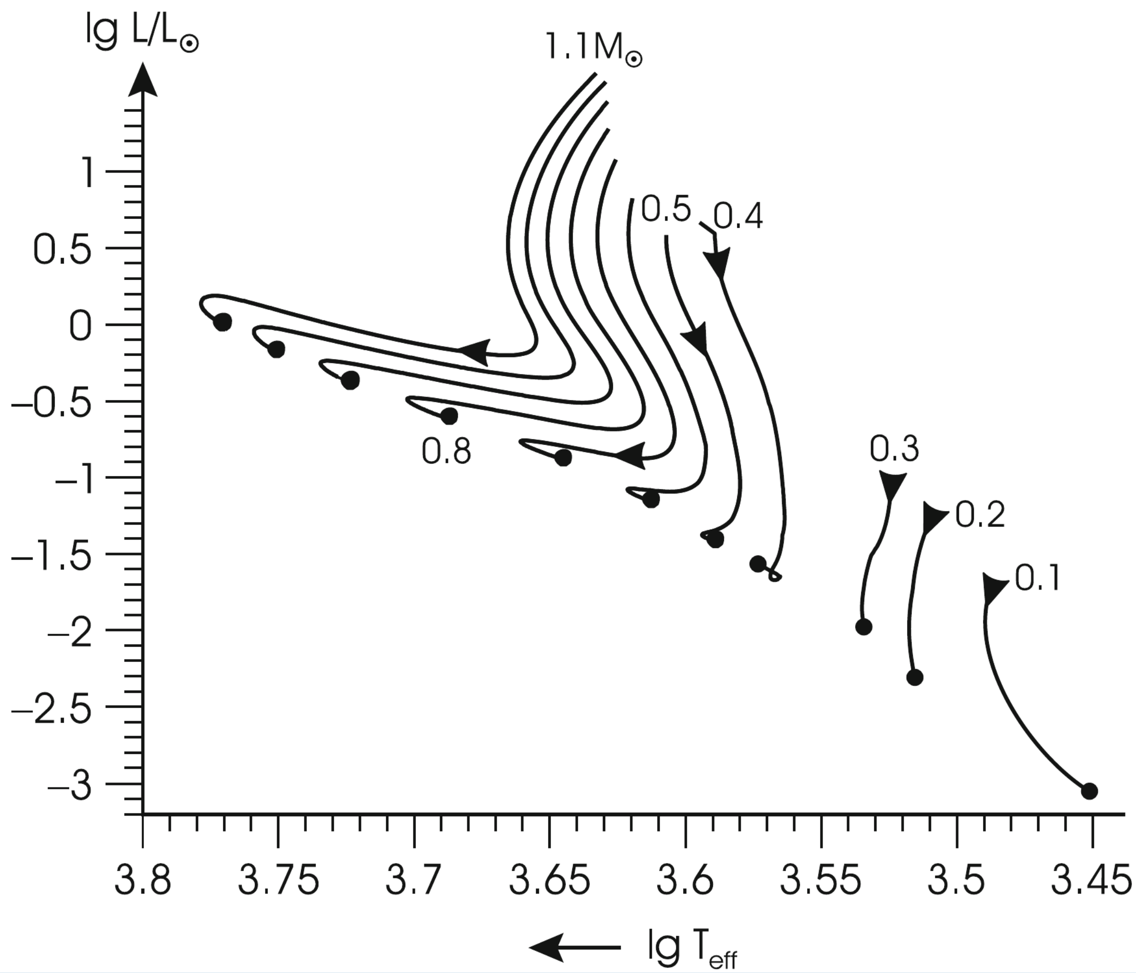

Kippenhahn, Weigert & Weiss 2012

Further evolution of pre-main sequence in the HRD

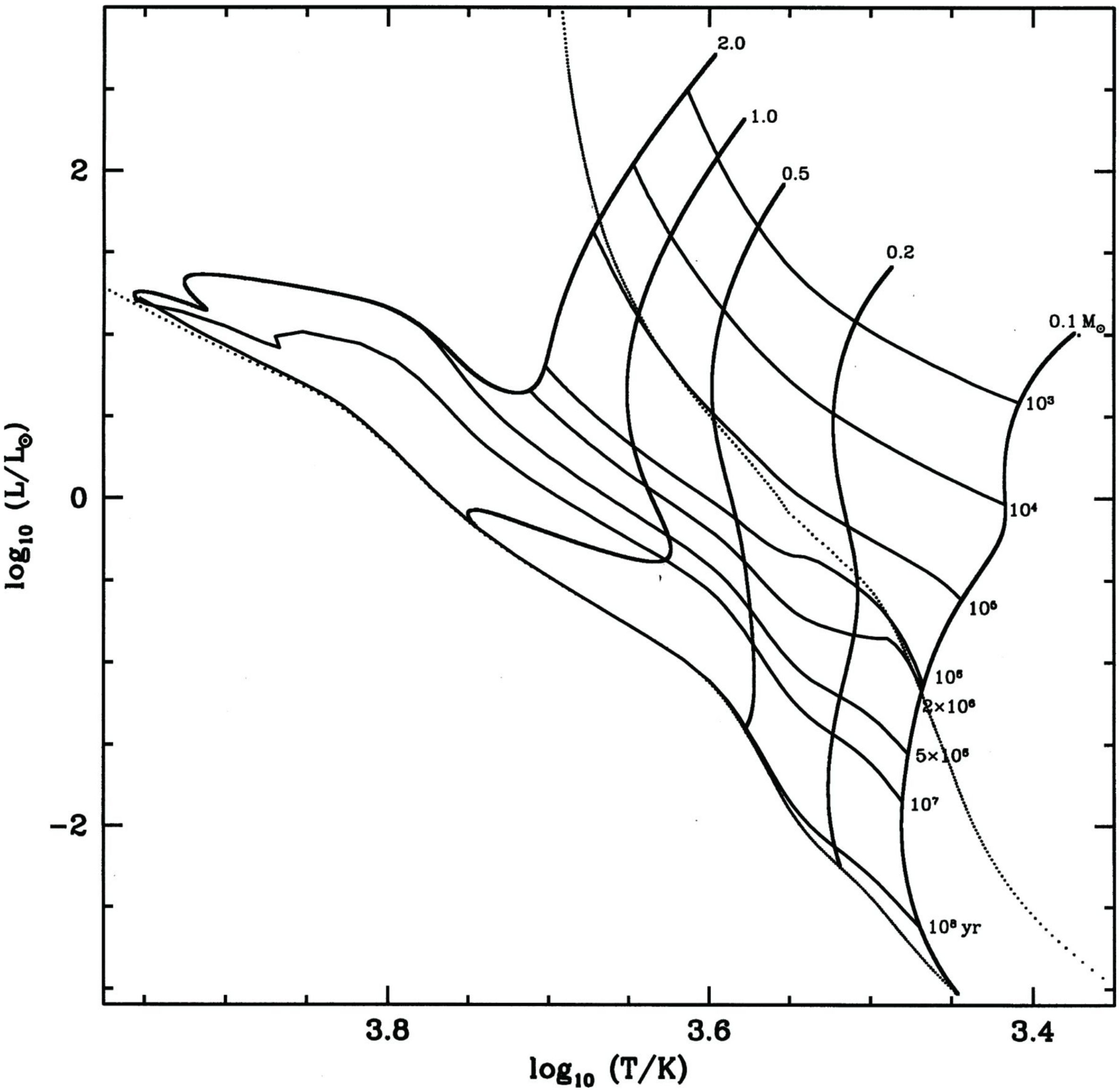

Tout et a. 1999, MNRAS, 310, 360

PMS tracks with constant masses

- later phases a short episode of nuclear burning sets in

$$\mathrm{D} + \mathrm{H} \longrightarrow {}^{3}_{2}\mathrm{He} + \gamma$$

- Low-mass PMS $\leq \quad 0.5\,\mathrm{M}_\odot$ evolve along the Hayashi tracks
- High-mass PMS $> \quad 0.5\,\mathrm{M}_\odot$ leave or never follow the Hayashi tracks because a radiative zone develops

Further evolution of pre-main sequence in the HRD

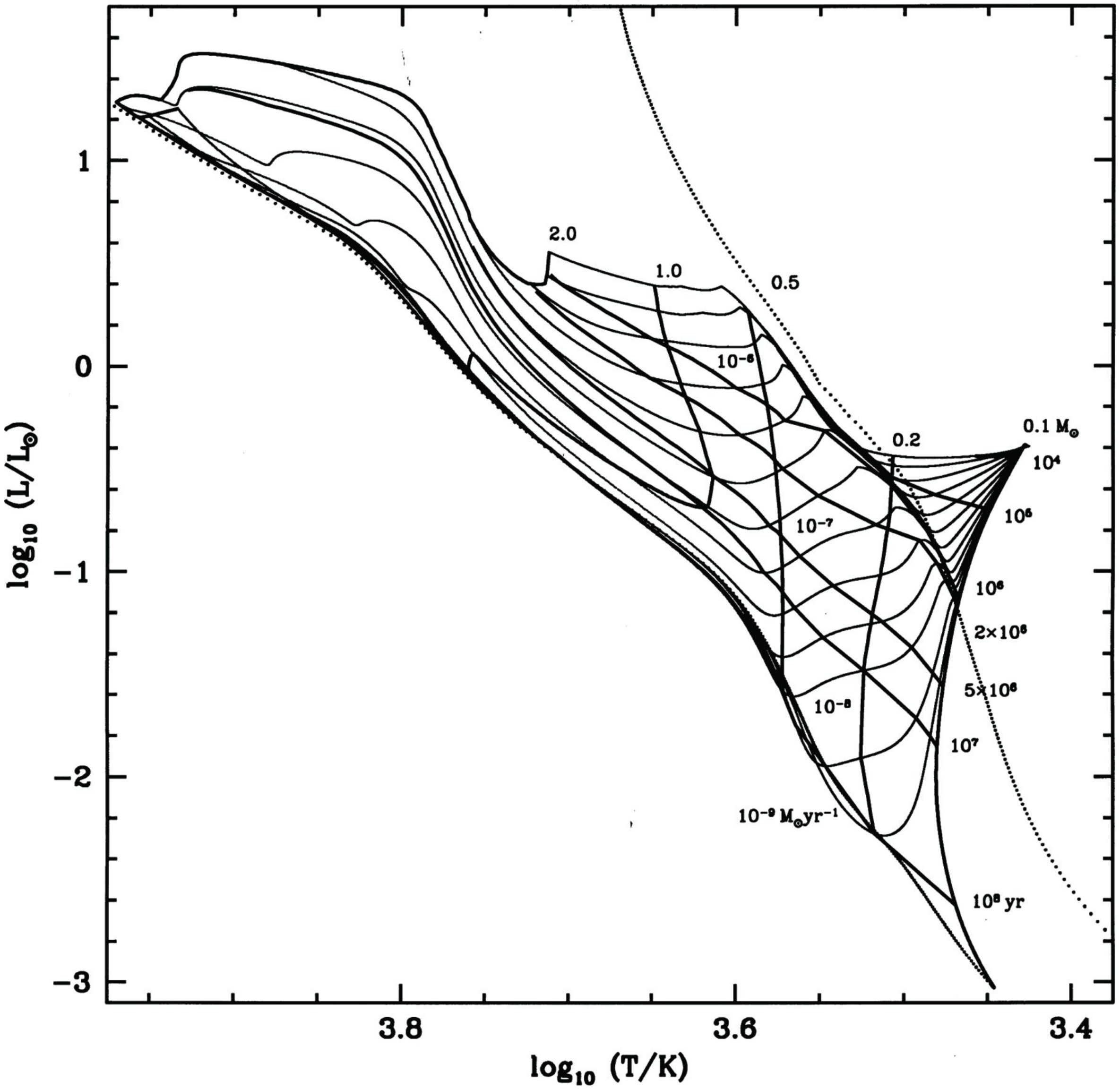

Tout et a. 1999, MNRAS, 310, 360

PMS tracks for constant accretion and an initial mass of $0.1\,M_\odot$

$\rightarrow$ Much more complicated

Further evolution of pre-main sequence in the HRD

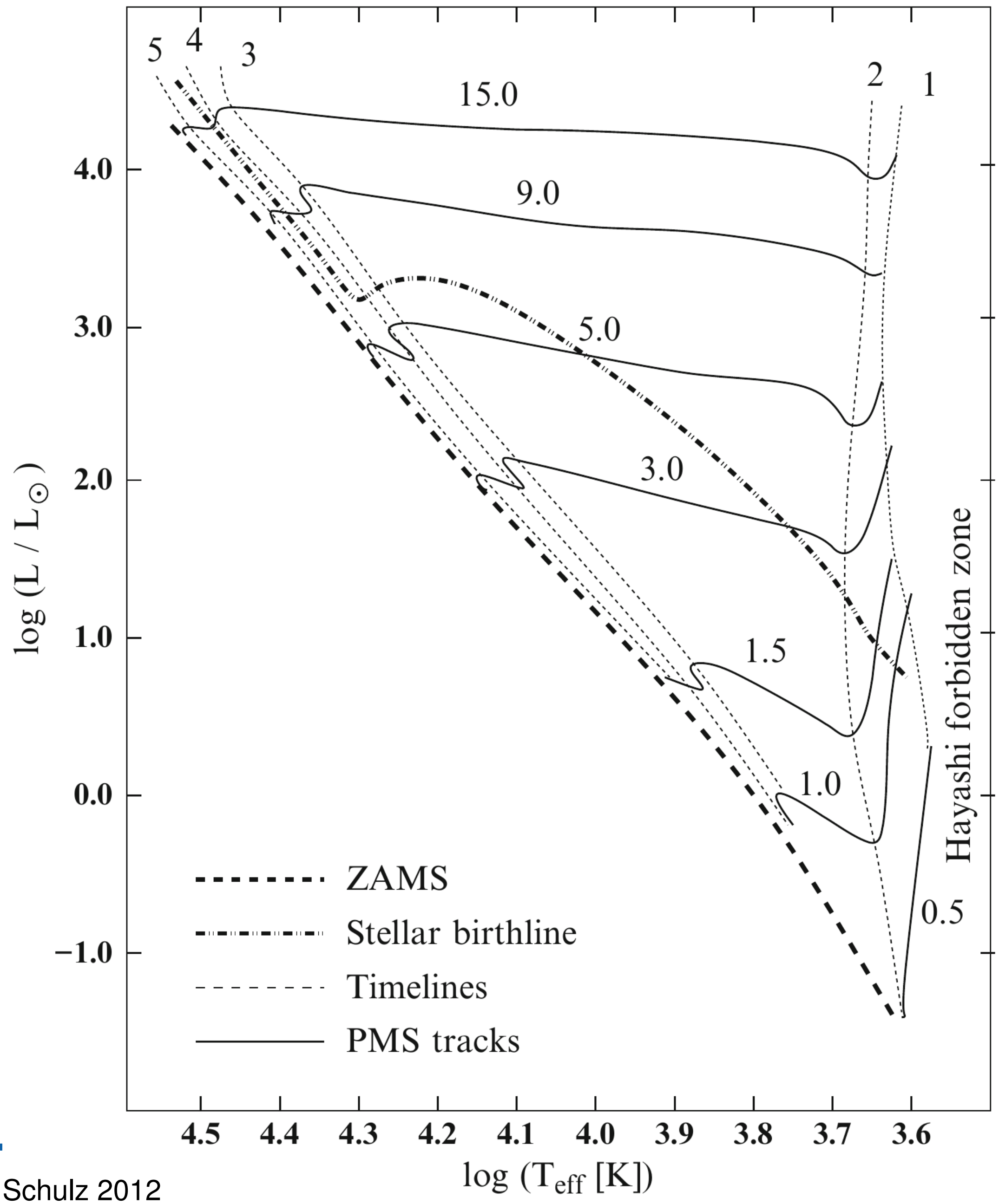

Schulz 2012

When the opacity drops the internal temperature rises and the convective zone recedes from the center, evolutionary path of the star in the HR-diagram to move away from the Hayashi track toward higher effective temperatures

→ radiative track of the HR-diagram (timelines 2-5)

Protostars

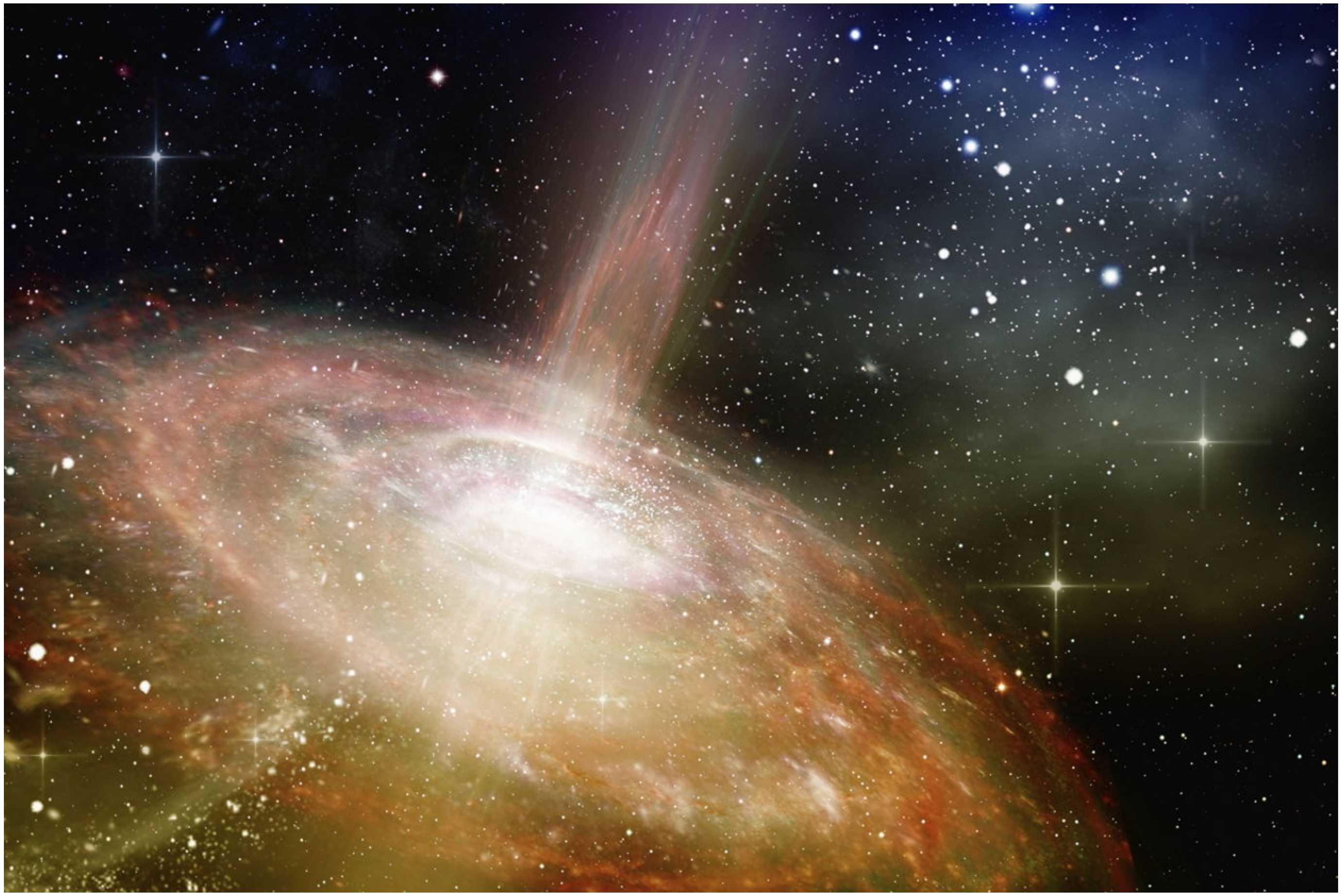

T_{central} of pre-main-sequence (PMS) stars too low to ignite hydrogen burning
$\rightarrow$ Energy source is gravitational energy of infalling material $L_{\text{proto}} = \frac{GM\dot{M}}{R}$
$\rightarrow$ evolution on Kelvin-Helmholtz timescale $\tau_{KH} = \frac{GM^2}{2RL_{\text{proto}}} \sim 10^7\,\text{yr}$
$\rightarrow$ presence of infalling envelope of gas and dust is the defining characteristic

Lithium abundance in solar type stars

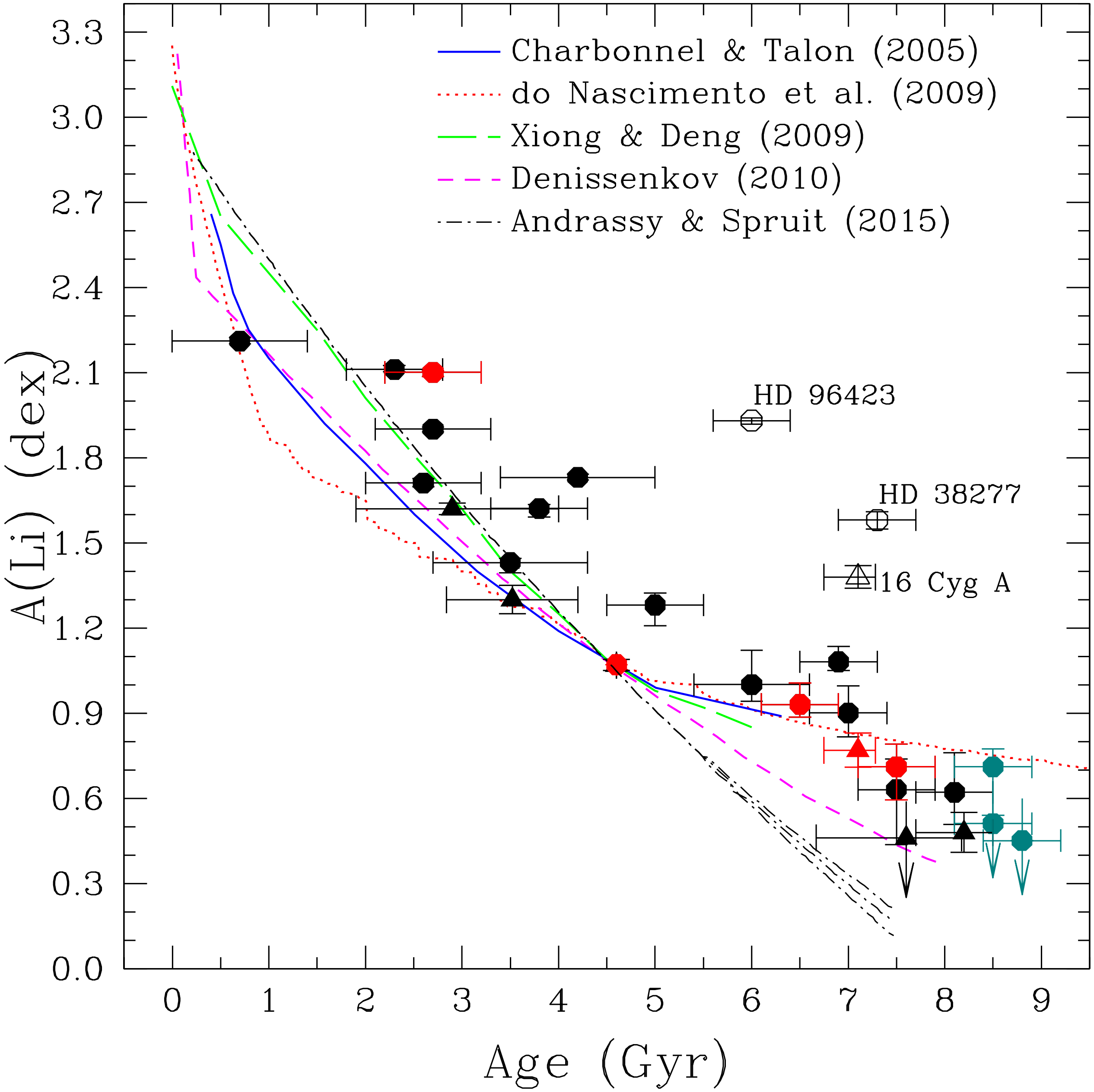

Identification as young star via the presence of lithium in their spectra

$\rightarrow$ Lithium is consumed in stars with $T > 2 \times 10^6$ K

$^7\text{Li} + \text{H} \longrightarrow {}^4\text{He} + {}^4\text{He}$

Carlos et al. 2015

Structure of a protostellar system

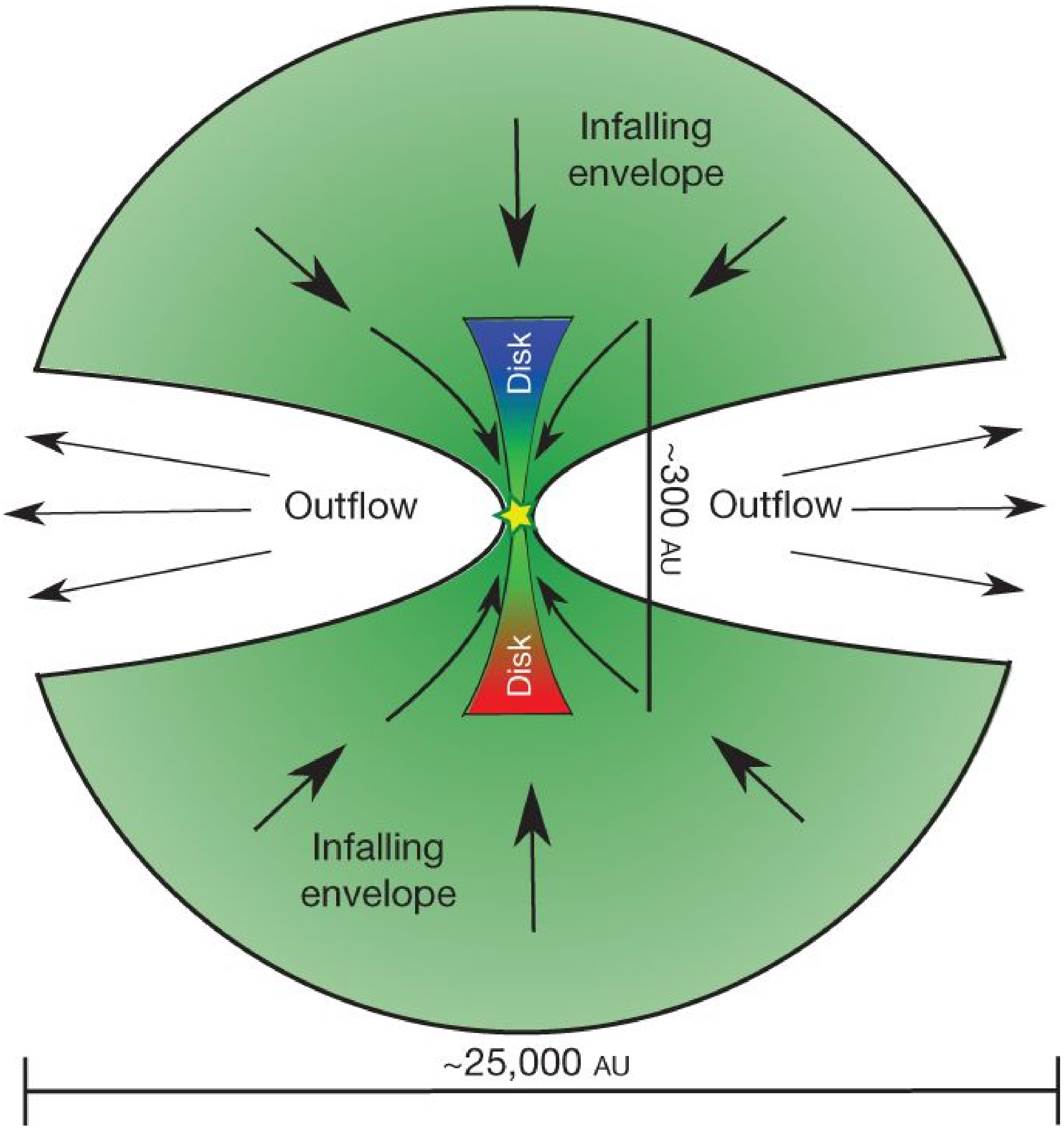

Tobin et al. 2012

- infalling envelope surrounding the protostar and disk
- infalling material has some net rotation $\rightarrow$ falls onto a disk
- Keplerian rotation of the disk around the protostar
- Mass is transported from the envelope to the disk and then it is accreted through the disk and onto the protostar
- protostar and disk both work together and drive a bipolar outflow
- $>$ 50% are variable

Protostellar luminosity problem

Total protostellar luminosity

Photospheric luminosity

Protostellar mass

Protostellar mass accretion rate

$$L_p = L_{\rm phot} + \underbrace{f_{\rm acc}\frac{Gm\dot{m}}{r}}_{\text{Accretion luminosity}}$$

Protostellar radius

Radiative efficiency of accretion shock

$\sim$ 10 times less luminous than expected

How do stars accrete their mass?

Protostellar luminosity problem

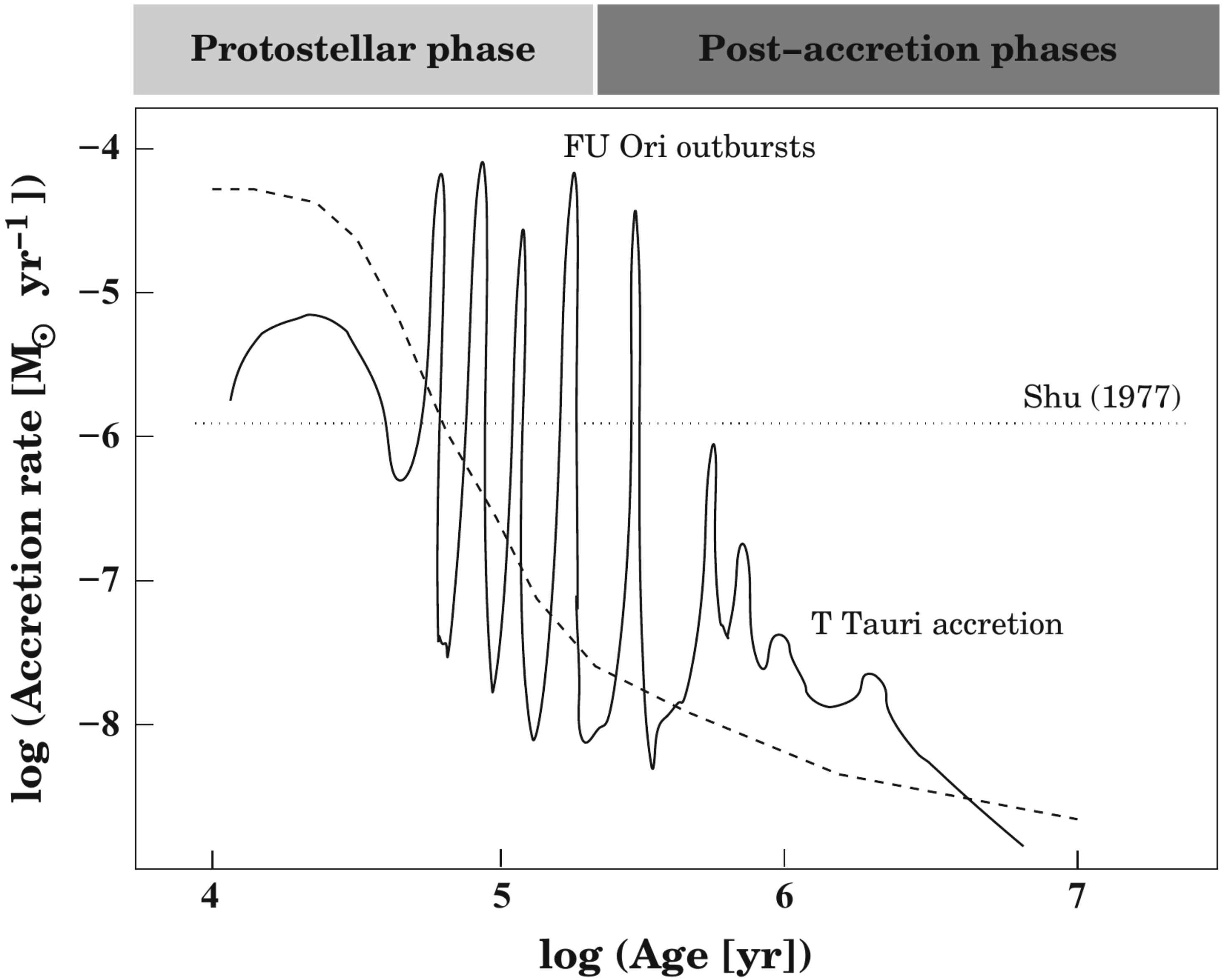

episodic acretion

Schulz 2012

Magnetospheric Accretion in T Tauri stars

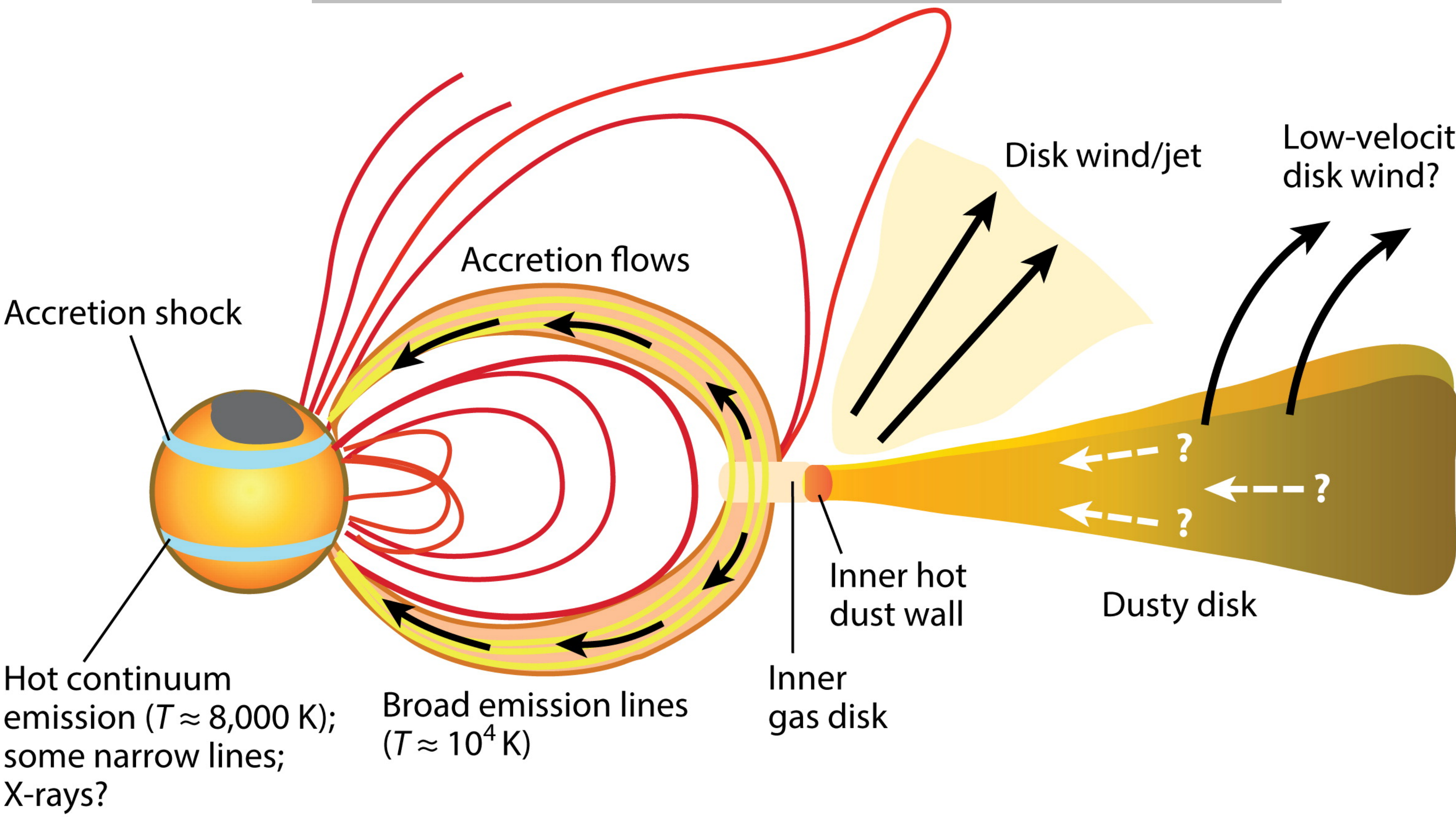

Hartmann L, et al. 2016.
Annu. Rev. Astron. Astrophys. 54:135–80

UV and X-ray excess in T Tauri stars

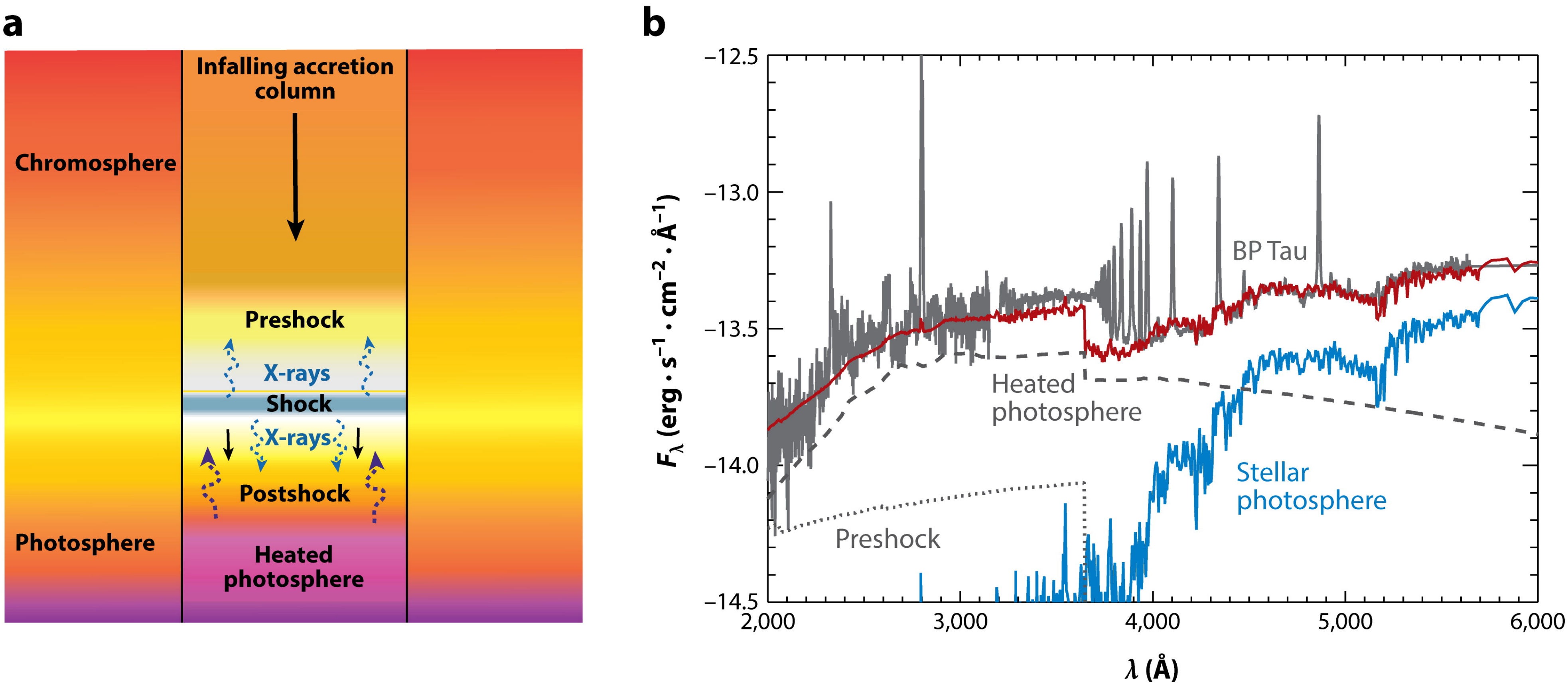

Hartmann L, et al. 2016.
Annu. Rev. Astron. Astrophys. 54:135–80

Variable stars of spectral types Me to Fe are called T Tauri stars

Variability of pre-main sequence stars

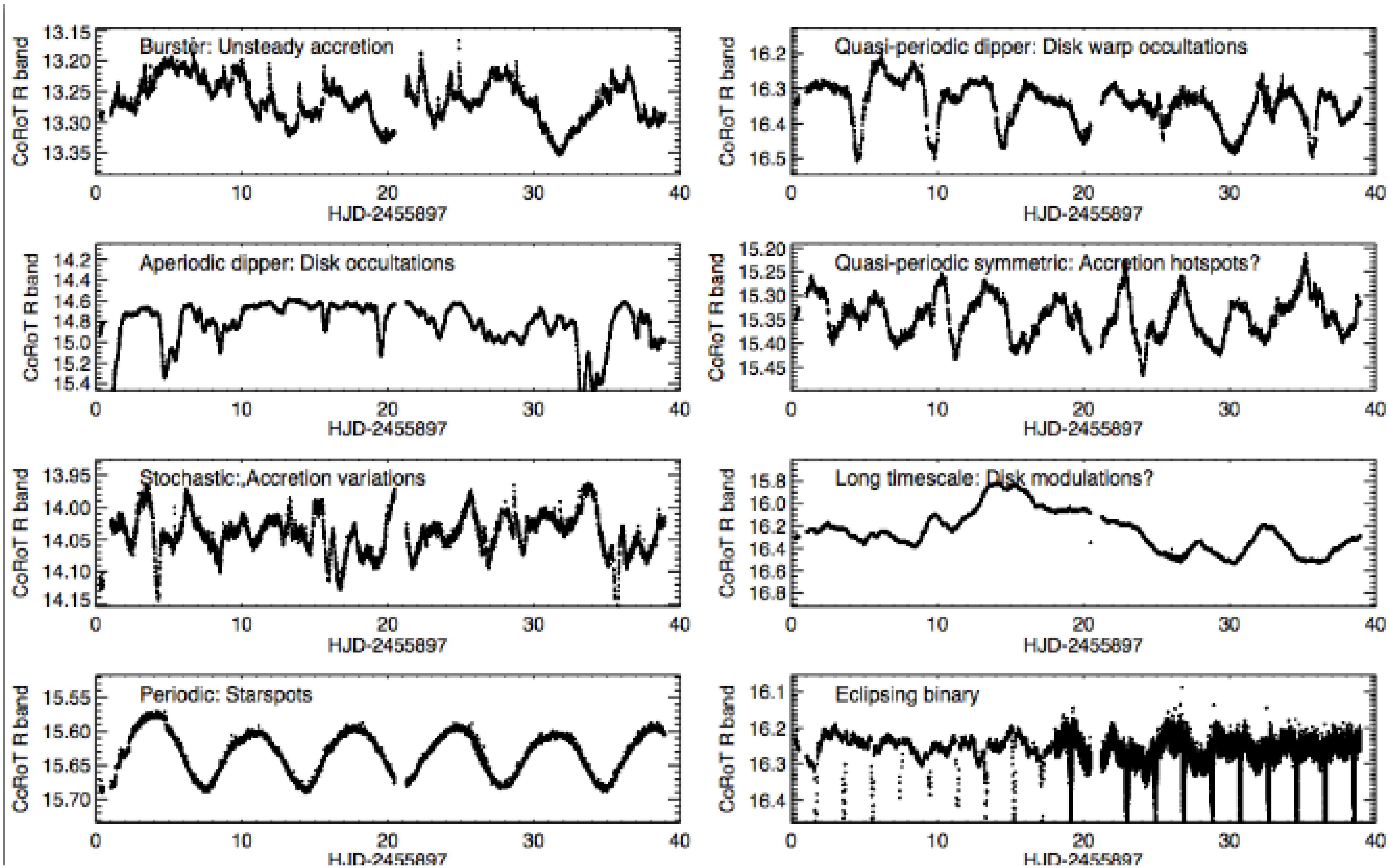

Cody et al. 2014, AJ, 147, 4

T Tauris stars in the HRD

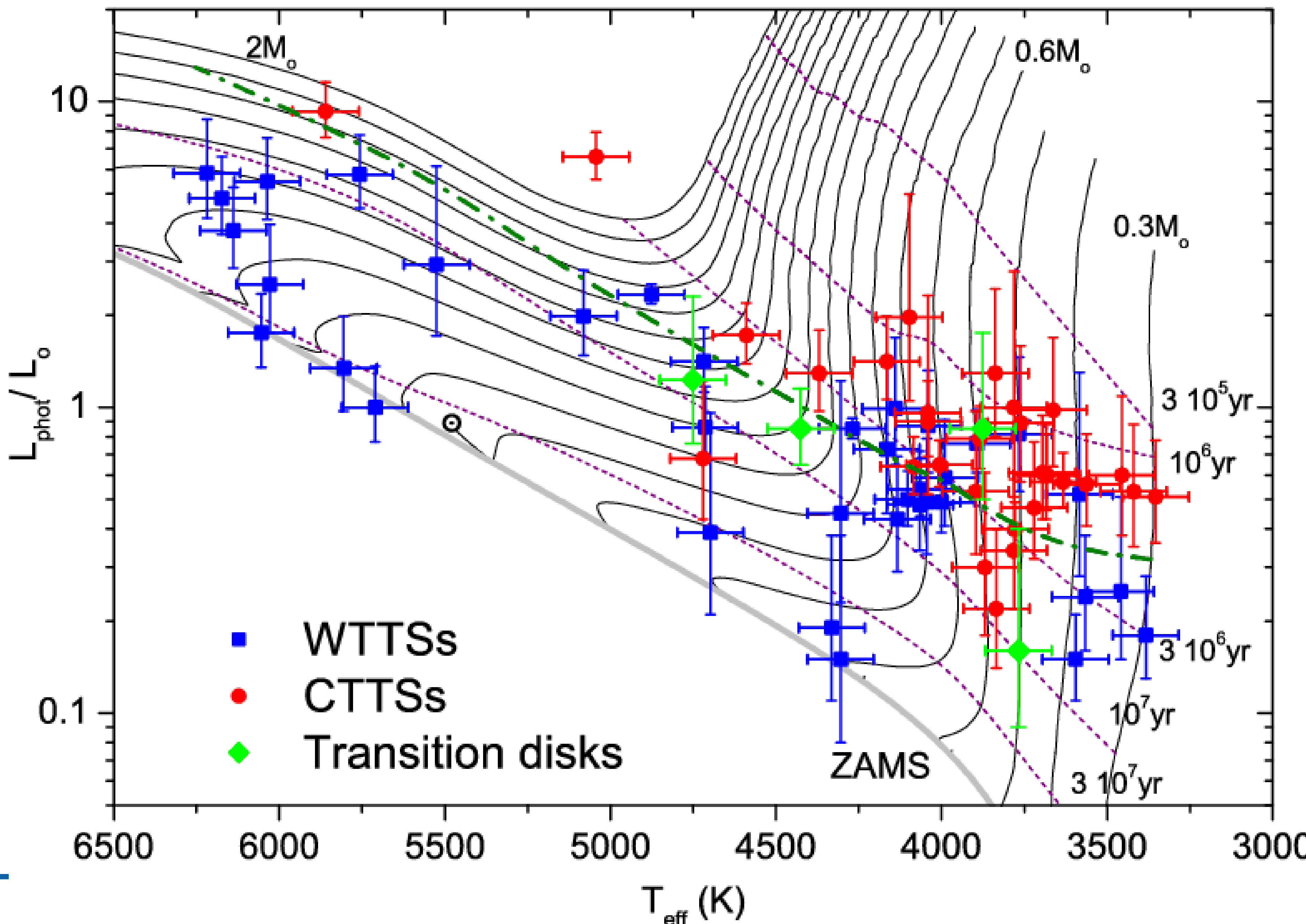

Bertout et al. 2007, A&A, 473, L21

Protoplanetary discs

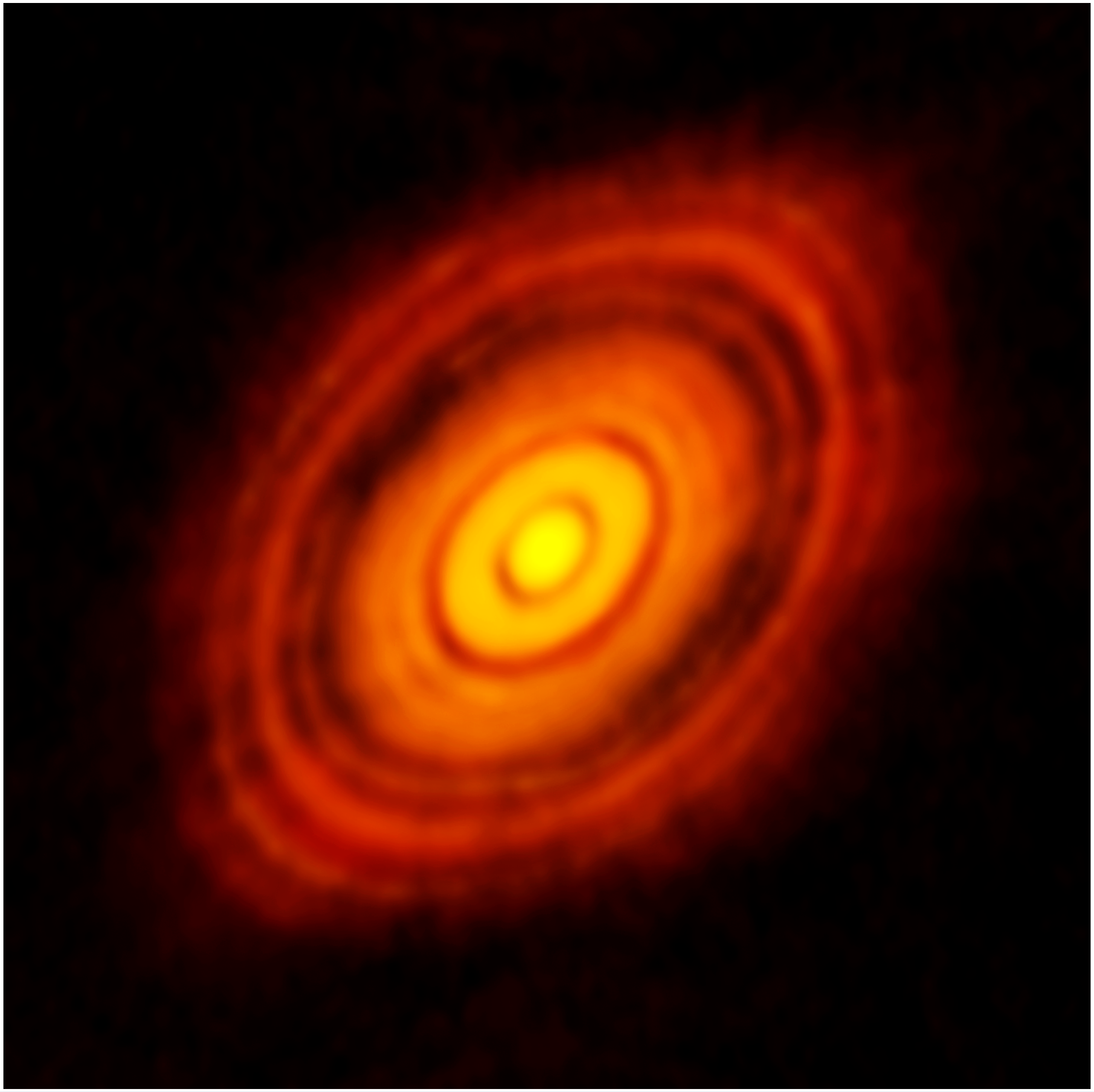

HL Tau, ALMA

Protoplanetary discs

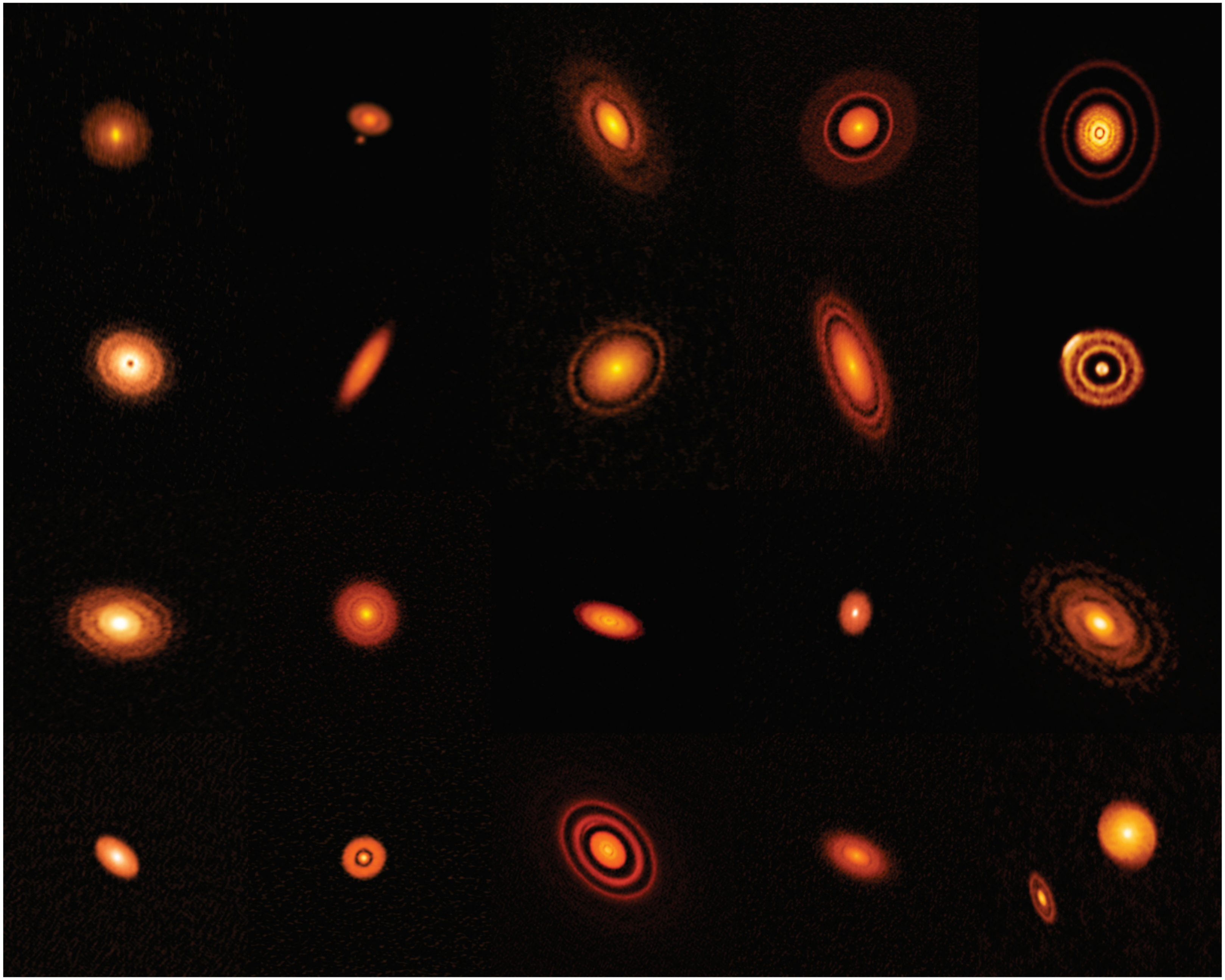

ALMA / ESO / NAOJ / NRAO / S. Andrews et al / AUI / NSF / S. Dagnello

Herbig Ae/Be stars

- Pre-MS stars of intermediate mass, higher-mass ($2\,M_\odot < M < 10\,M_\odot$) analogs of TTS
- within mass range of HAeBes change in accretion mechanism from magnetically to an unknown mechanism for high mass stars (radiative, non-magnetic)
- Herbig Ae and T-Tauri stars behave more similarly than Herbig Be stars, and Herbig Ae and Herbig Be stars have different observational properties

Massive young stellar objects (MYSOs)

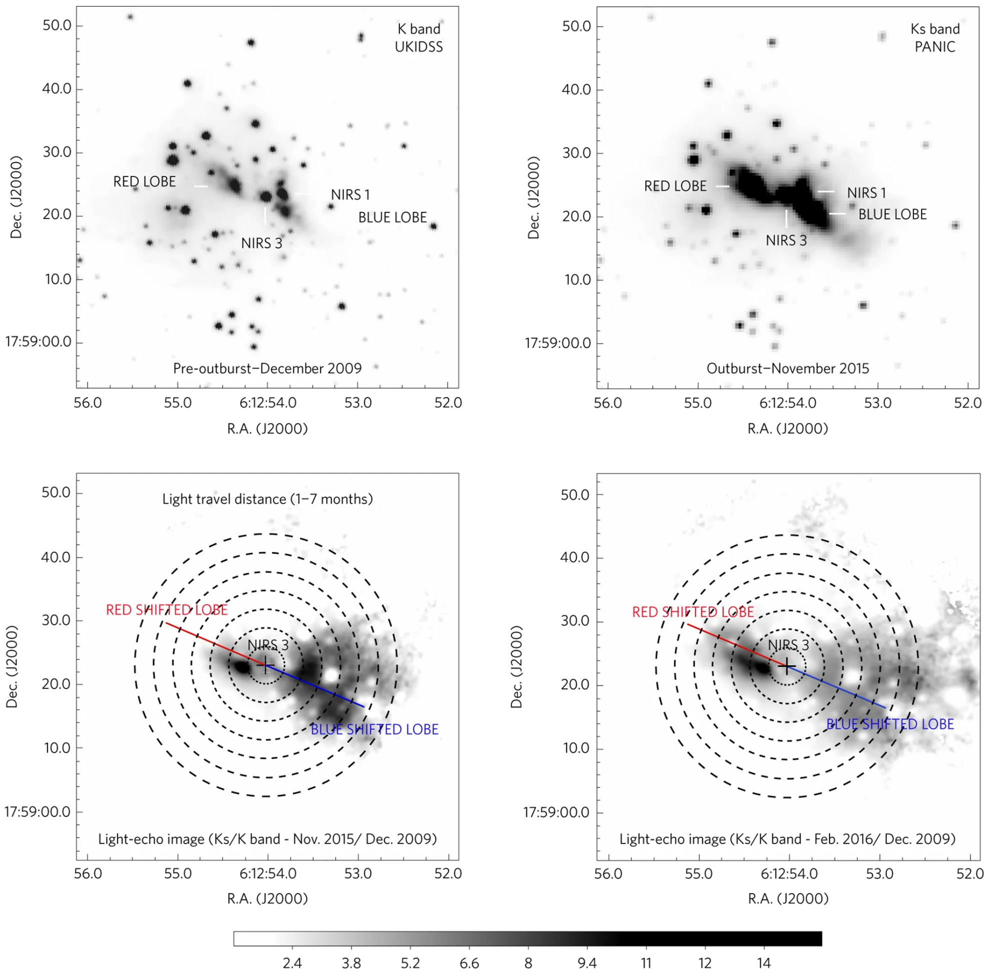

Caratti o Garatti et al 2017

- massive young stellar objects (MYSO) spend their brief youth while deeply embedded in extremely dense molecular cores
- optically visible massive stars should have already arrived on the zero-age-main-sequence with very little episodic accretion activity
- massive stars can form from clumpy discs of material – in much the same way as less massive stars
- accretion bursts might reduce the radiation pressure of the central source and allow the star to form

Zero-Age Main Sequence (ZAMS)

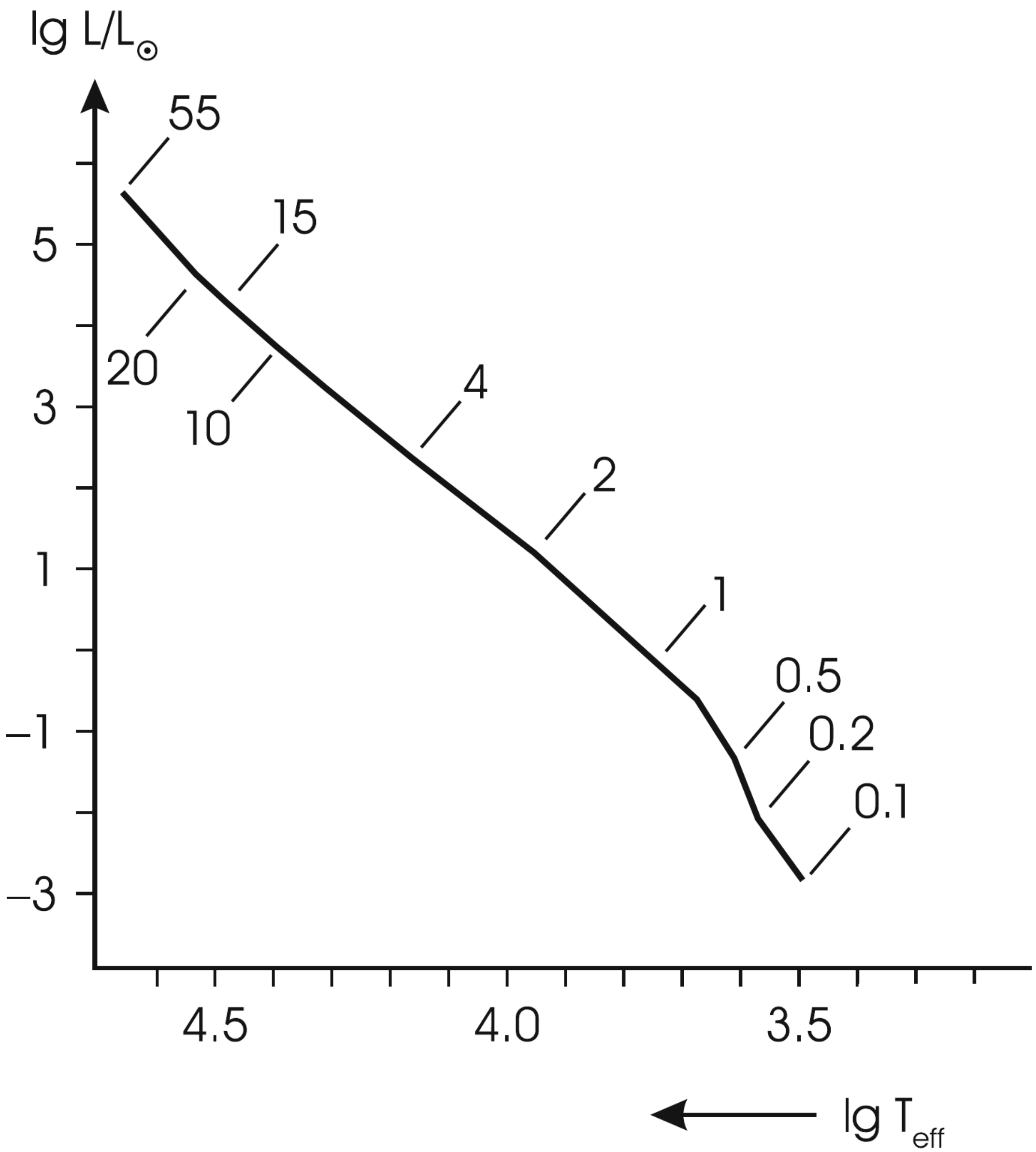

Kippenhahn, Weigert & Weiss 2012

As soon as the conditions in the core are fulfilled, **stable burning of hydrogen starts**

Since $\tau_{\rm nuc} \gg \tau_{KH}$ this phase can be described by **homogeneous models** in thermal equilibrium

For solar-like stars the chemical composition is

$$X = 0.70, \quad Y = 0.28 \; Z = 0.02$$

The sequence of such models is called

Zero Age Main Sequence

Zero-Age Main Sequence (ZAMS)

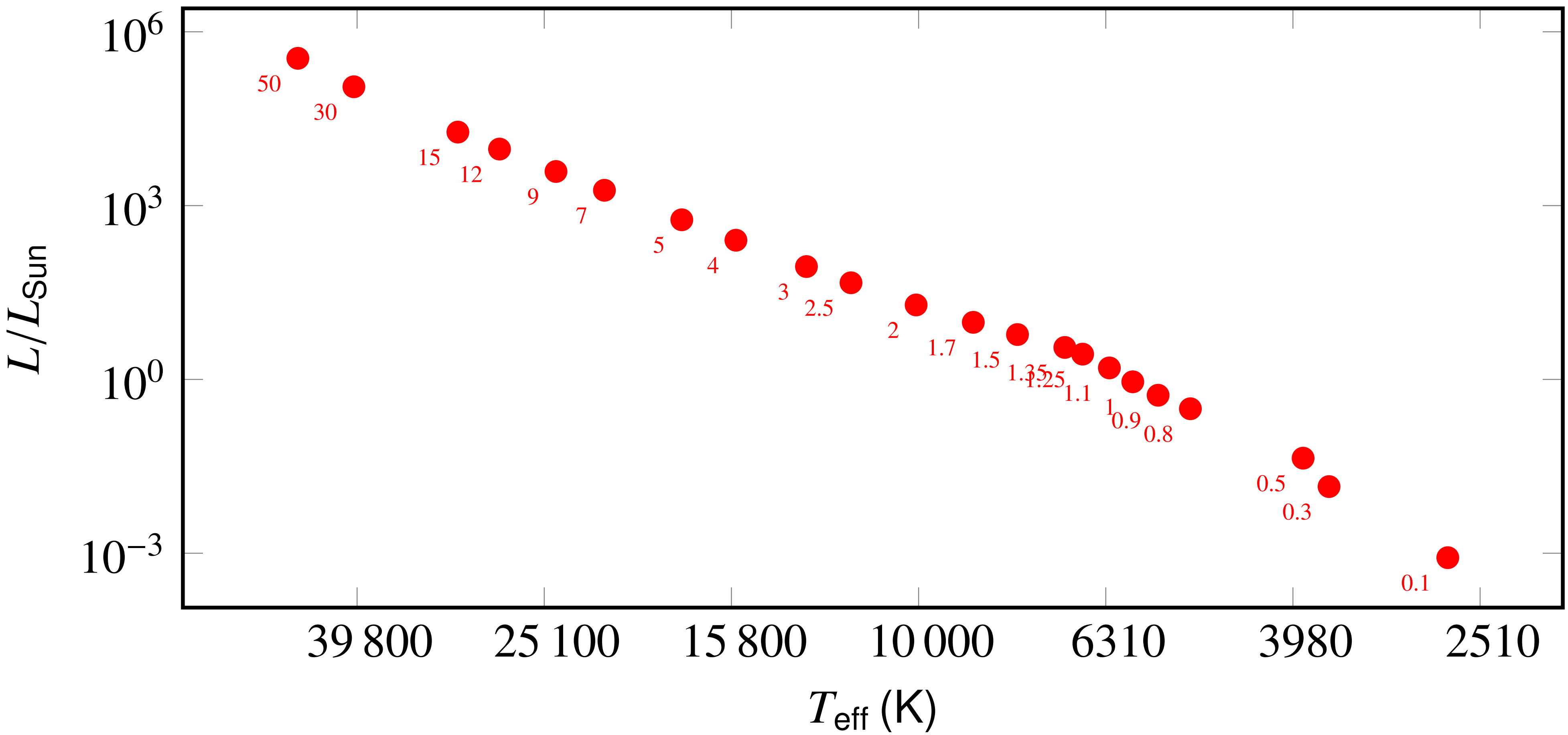

prediction of the ZAMS by a sophisticated stellar structure and evolution code (EZ: `http://www.astro.wisc.edu/~townsend/static.php?ref=ez-web`)

Zero-Age Main Sequence (ZAMS)

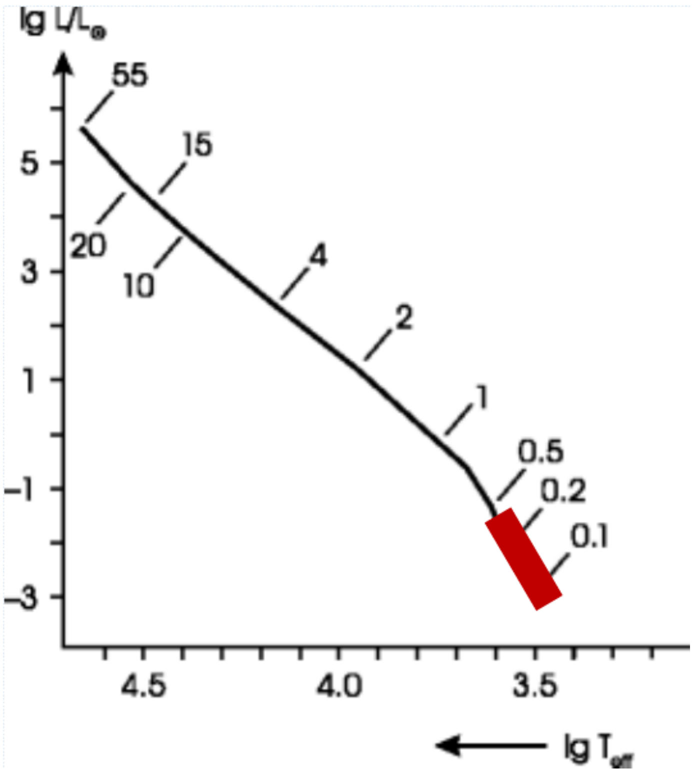

Kippenhahn, Weigert & Weiss 2012

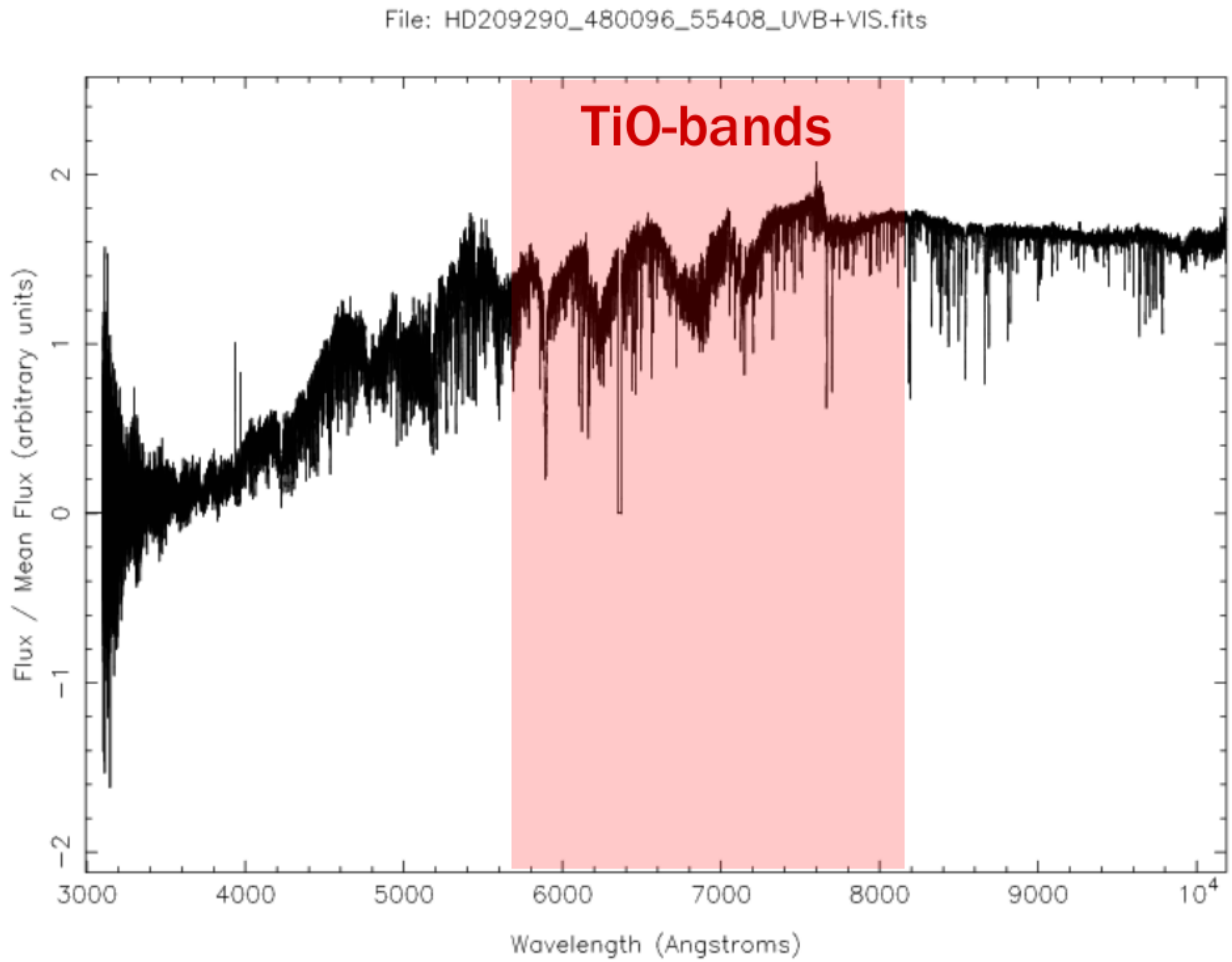

X-Shooter spectral library, `http://xsl.u-strasbg.fr/`

Spectral-type M

$T_{\mathrm{eff}} = 2400 - 3700\,\mathrm{K}$

Zero-Age Main Sequence (ZAMS)

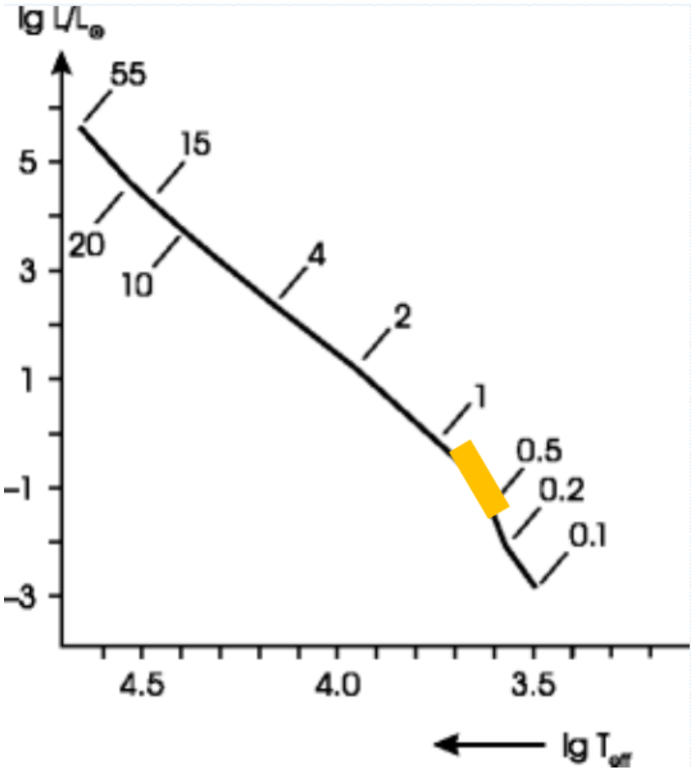

Kippenhahn, Weigert & Weiss 2012

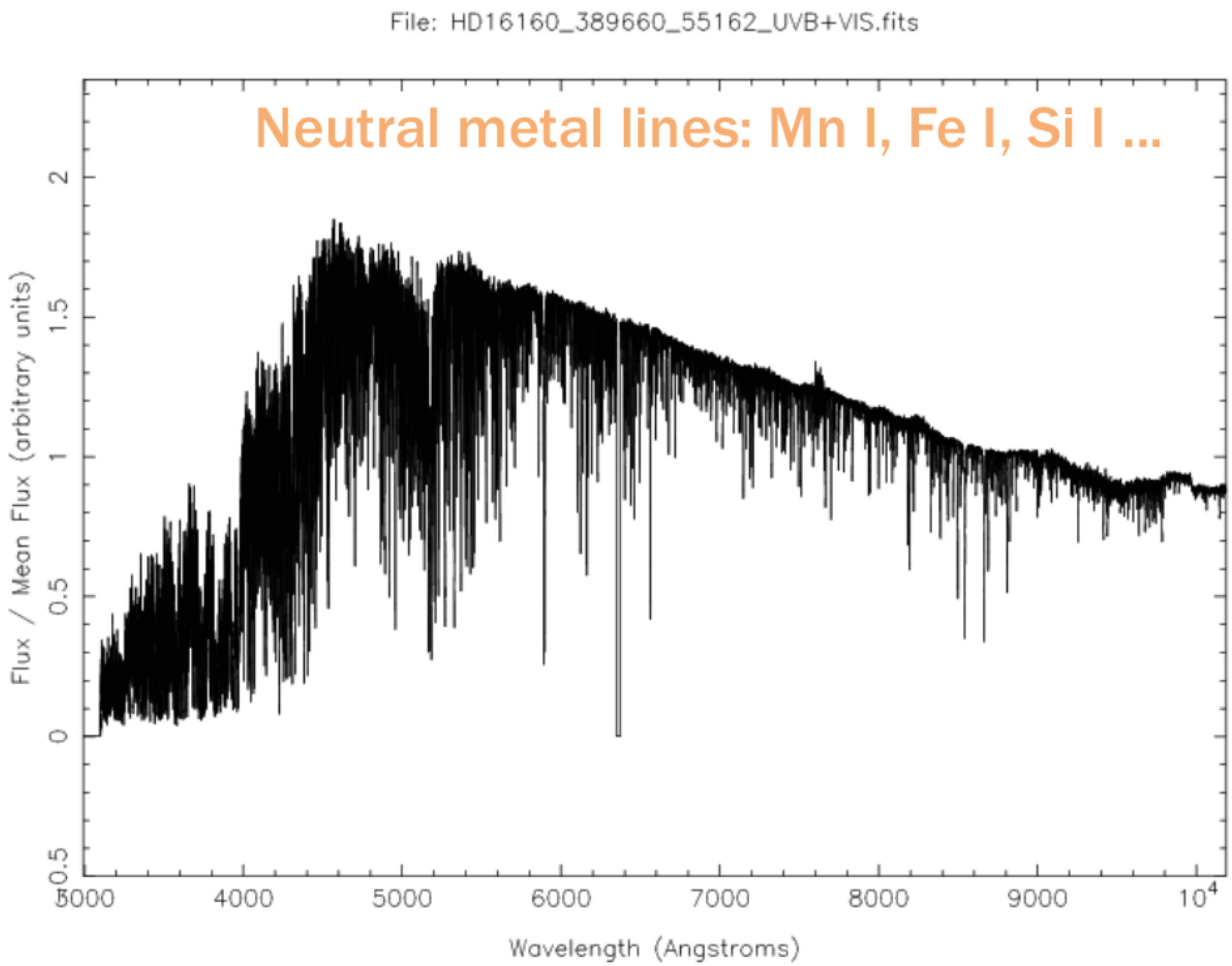

X-Shooter spectral library, `http://xsl.u-strasbg.fr/`

Spectral-type K

$T_{\rm eff} = 3700 - 5200\,\mathrm{K}$

Zero-Age Main Sequence (ZAMS)

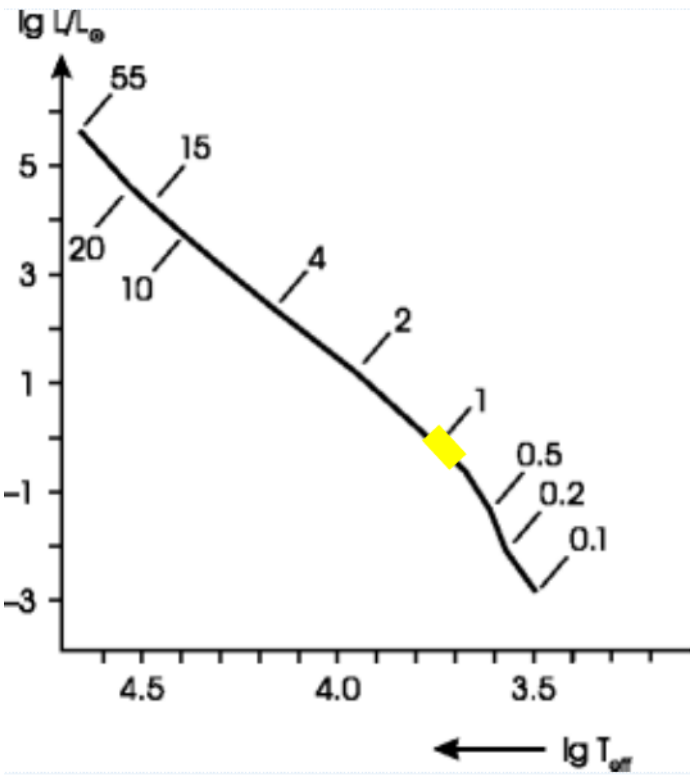

Kippenhahn, Weigert & Weiss 2012

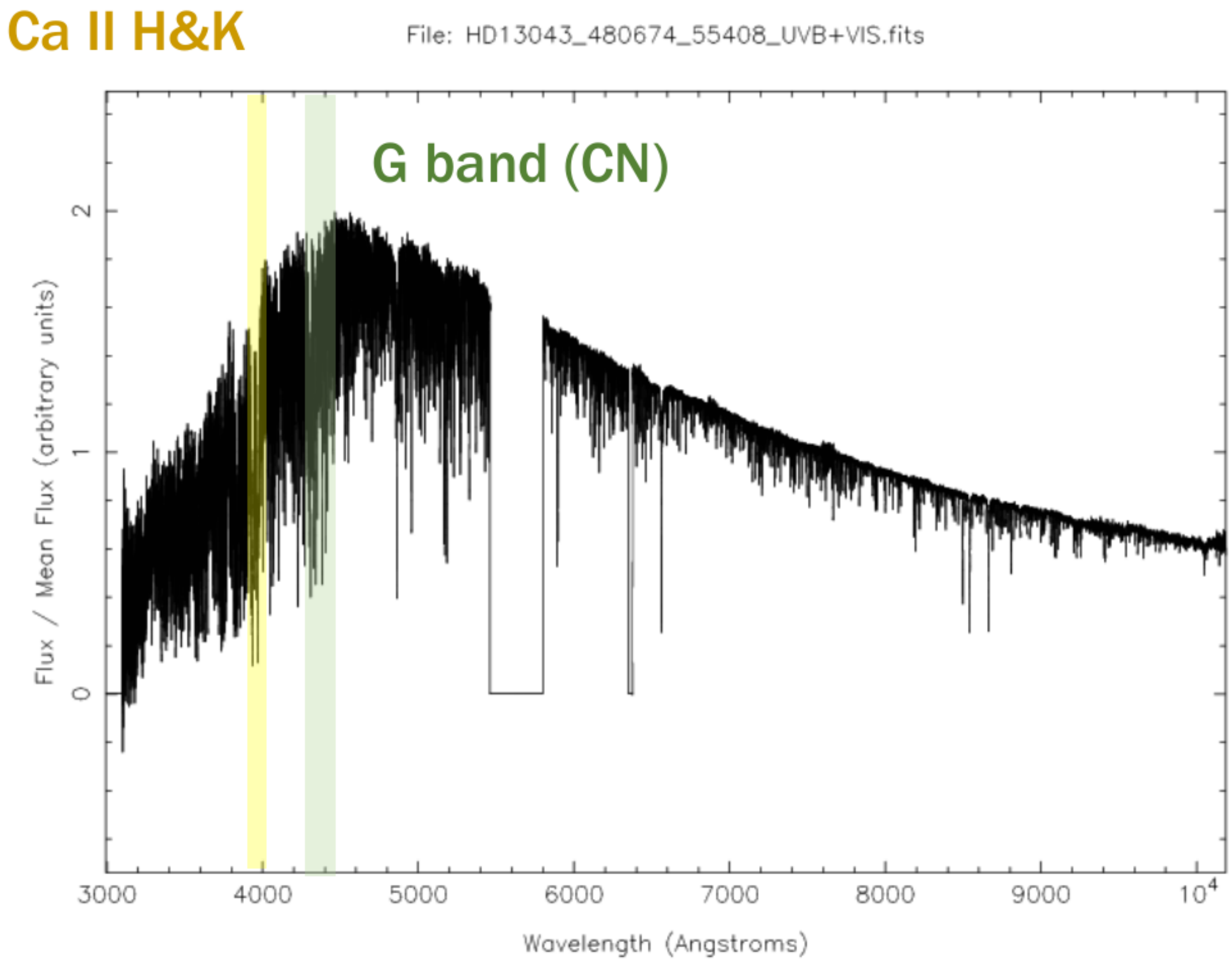

X-Shooter spectral library, `http://xsl.u-strasbg.fr/`

Spectral-type G

$T_{\mathrm{eff}} = 5200 - 6000\,\mathrm{K}$

Zero-Age Main Sequence (ZAMS)

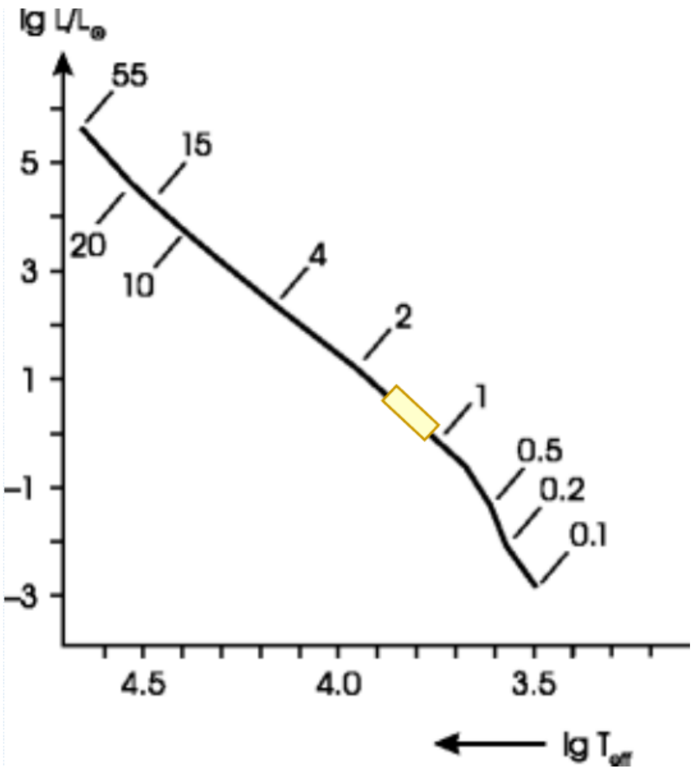

Kippenhahn, Weigert & Weiss 2012

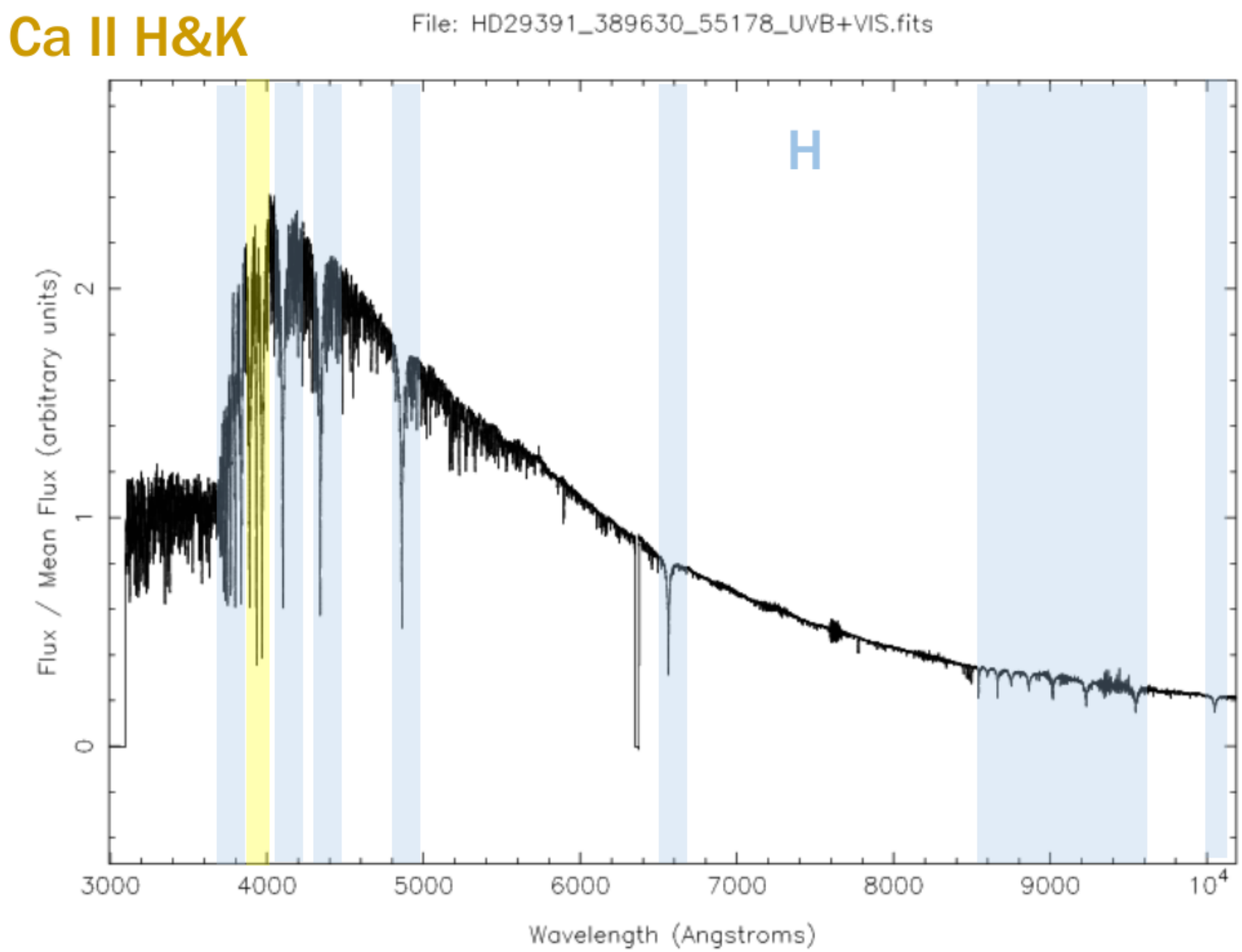

X-Shooter spectral library, `http://xsl.u-strasbg.fr/`

Spectral-type F

$T_{\mathrm{eff}} = 6000 - 7500\,\mathrm{K}$

Zero-Age Main Sequence (ZAMS)

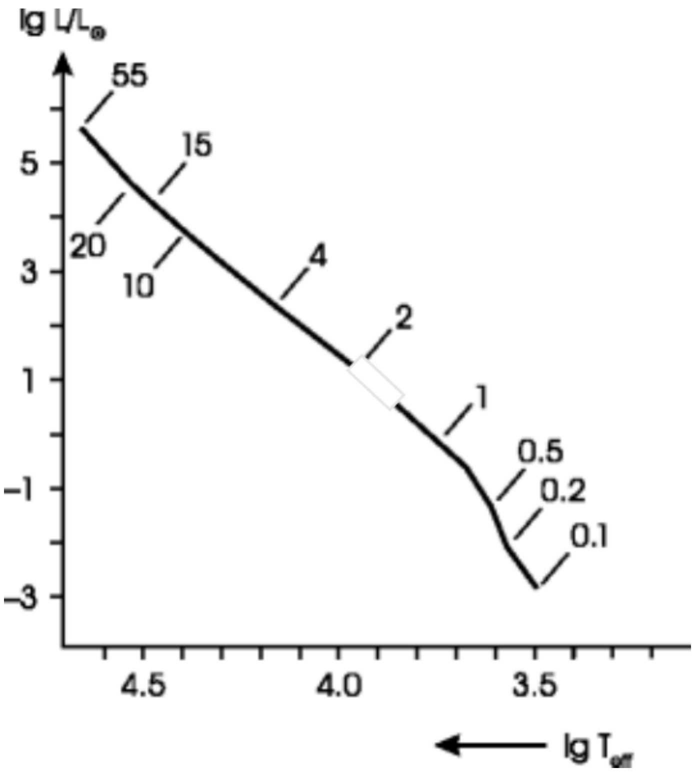

Kippenhahn, Weigert & Weiss 2012

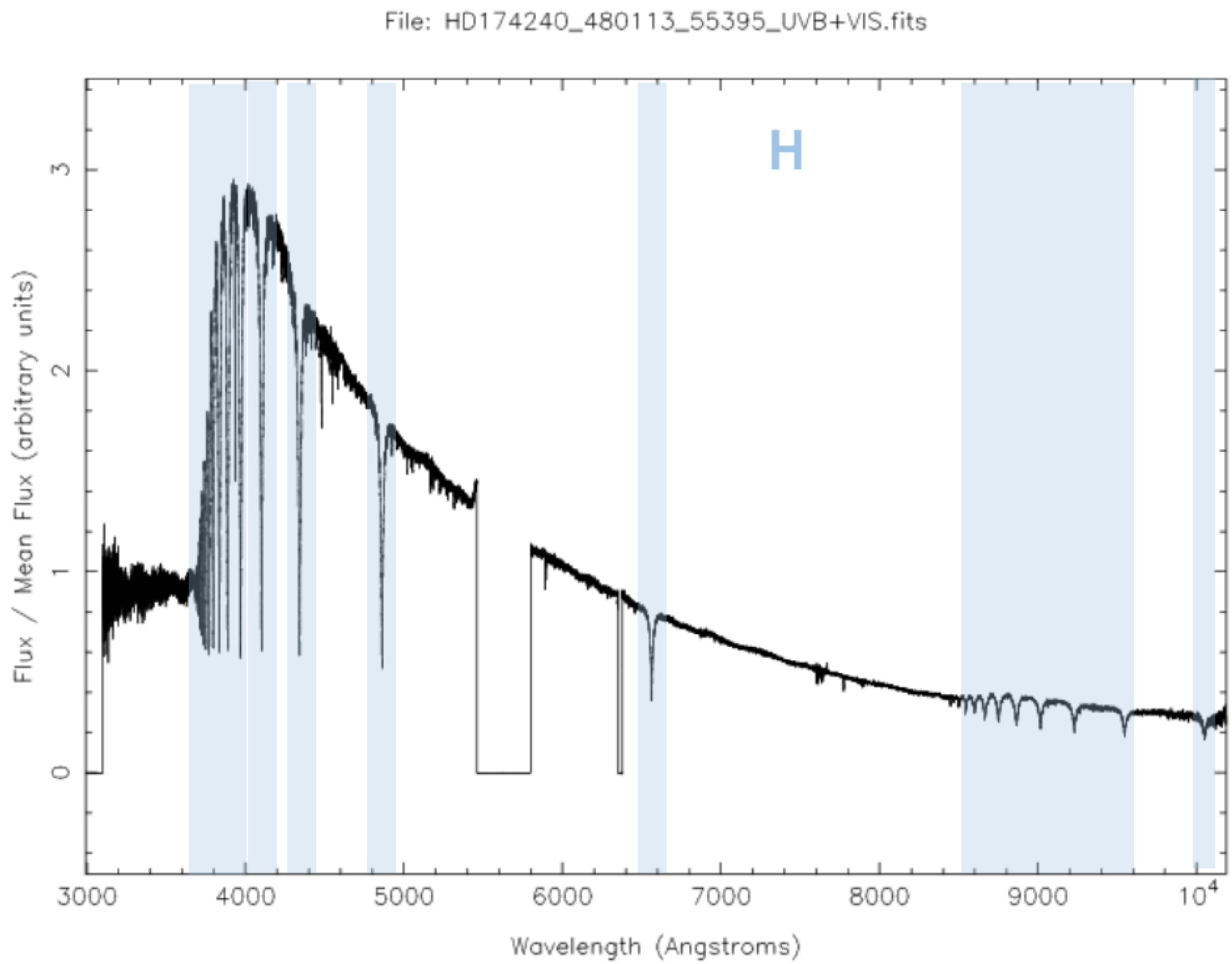

X-Shooter spectral library, `http://xsl.u-strasbg.fr/`

Spectral-type A

$T_{\mathrm{eff}} = 7500 - 10000\,\mathrm{K}$

Zero-Age Main Sequence (ZAMS)

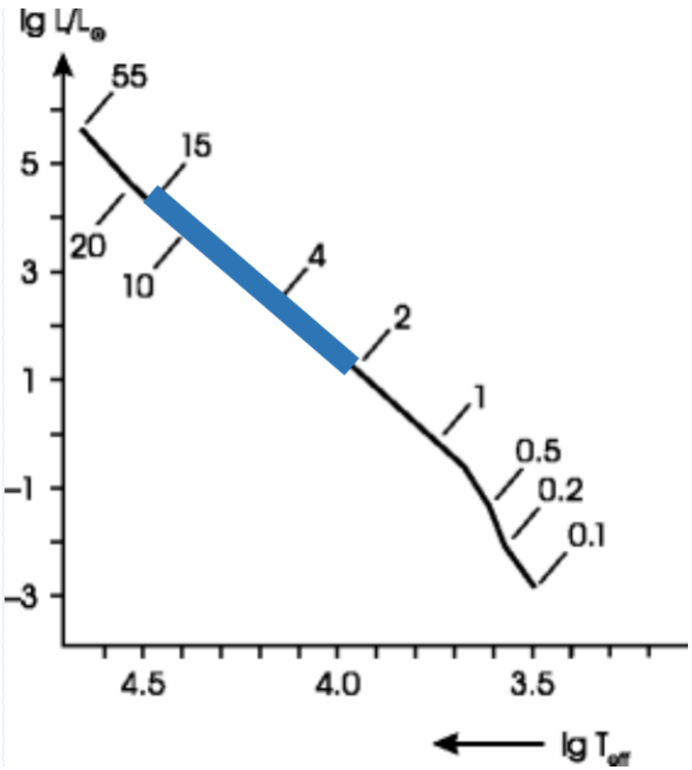

Kippenhahn, Weigert & Weiss 2012

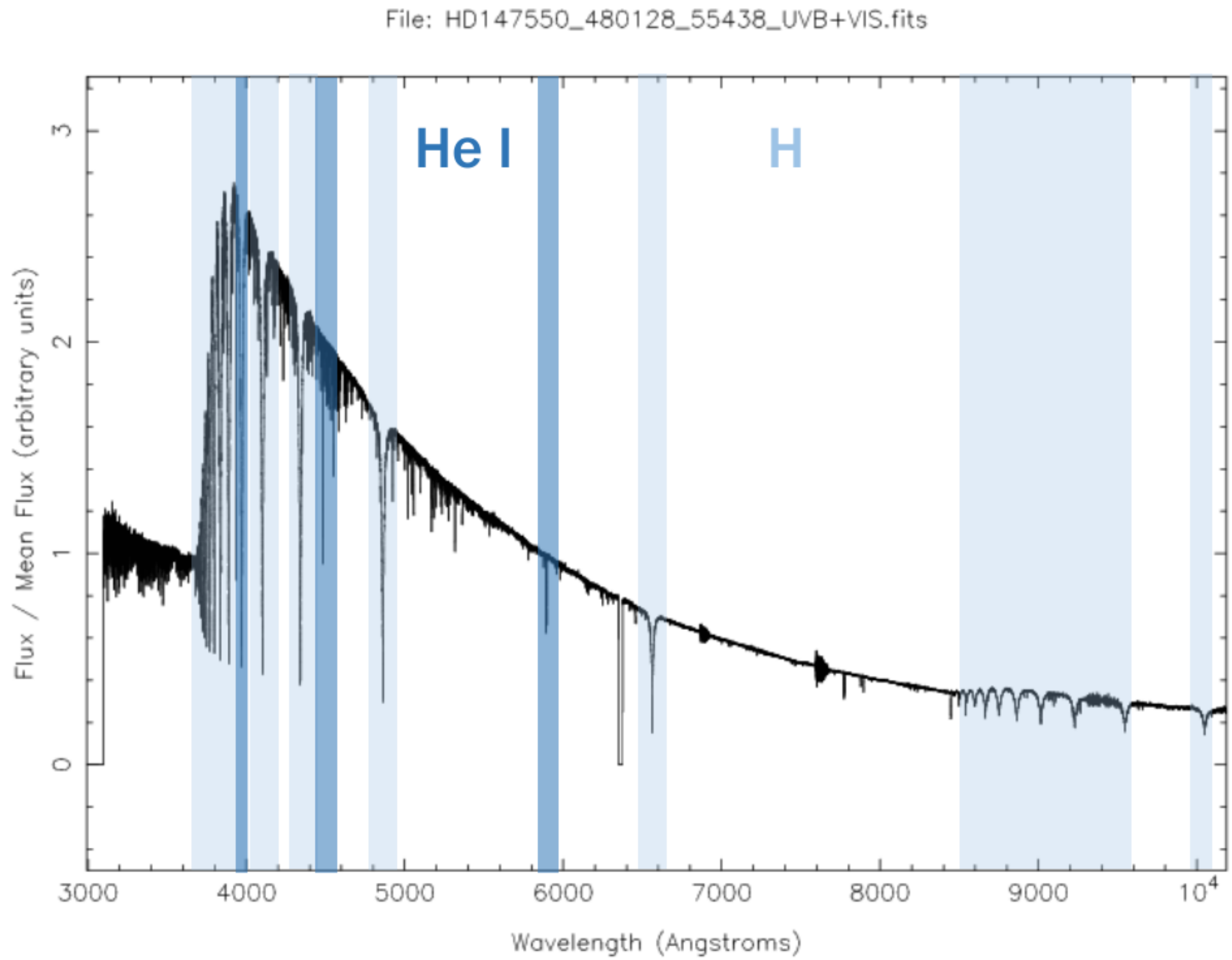

X-Shooter spectral library, `http://xsl.u-strasbg.fr/`

Spectral-type B

$T_{\mathrm{eff}} = 10000 - 30000\,\mathrm{K}$

Zero-Age Main Sequence (ZAMS)

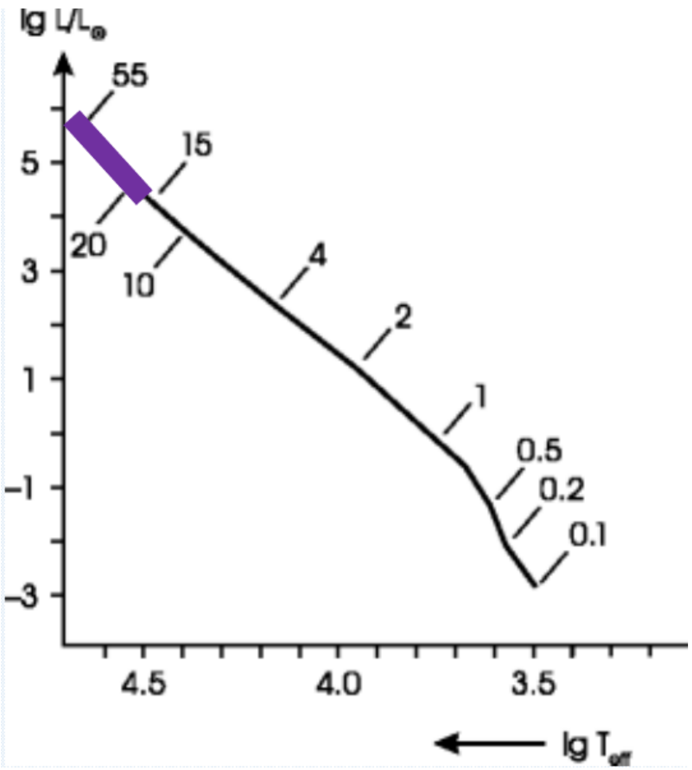

Kippenhahn, Weigert & Weiss 2012

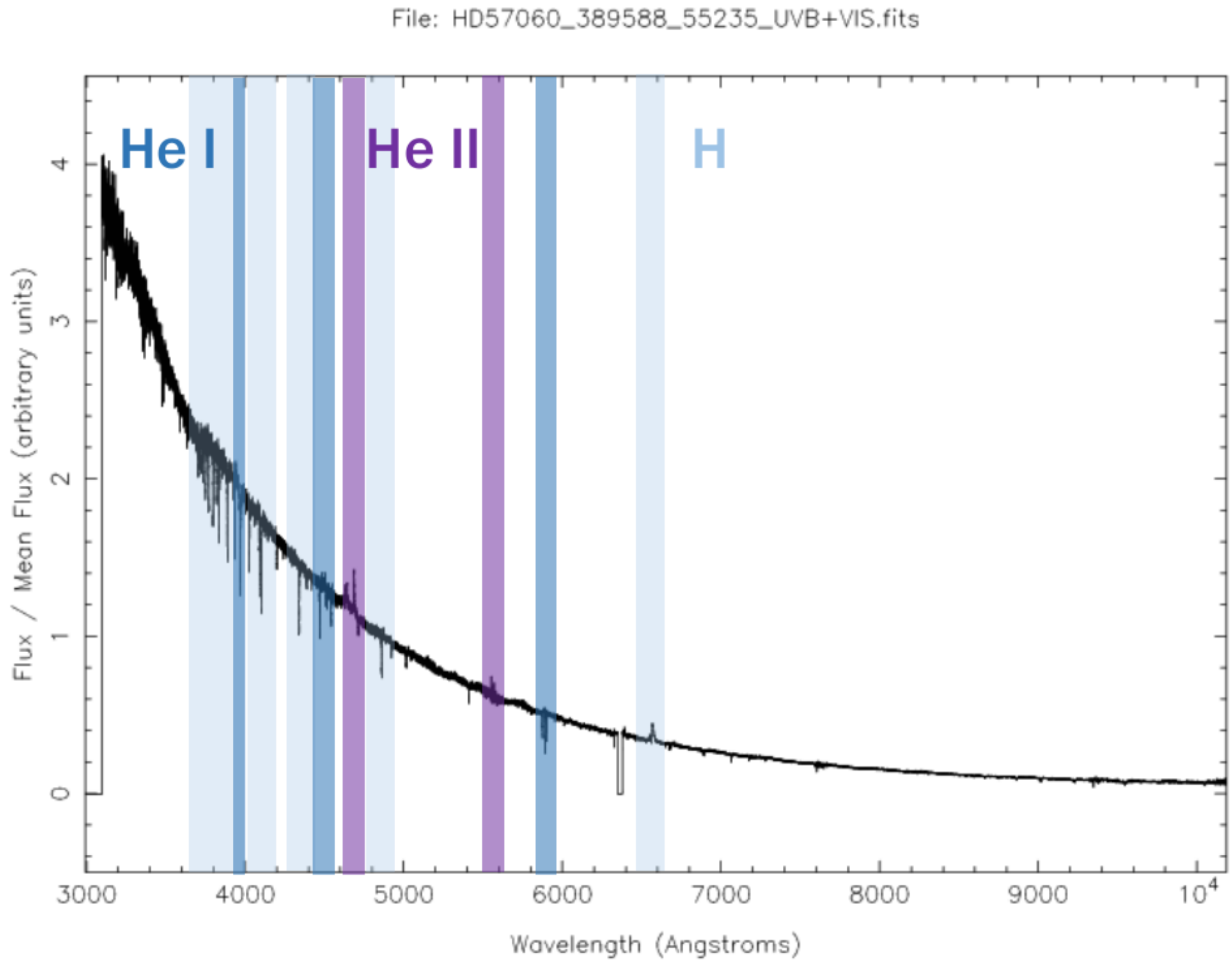

X-Shooter spectral library, `http://xsl.u-strasbg.fr/`

Spectral-type O

$T_{\rm eff} = 30000 - 50000\,\rm K$

Zero-Age Main Sequence (ZAMS)

Mass-radius relation

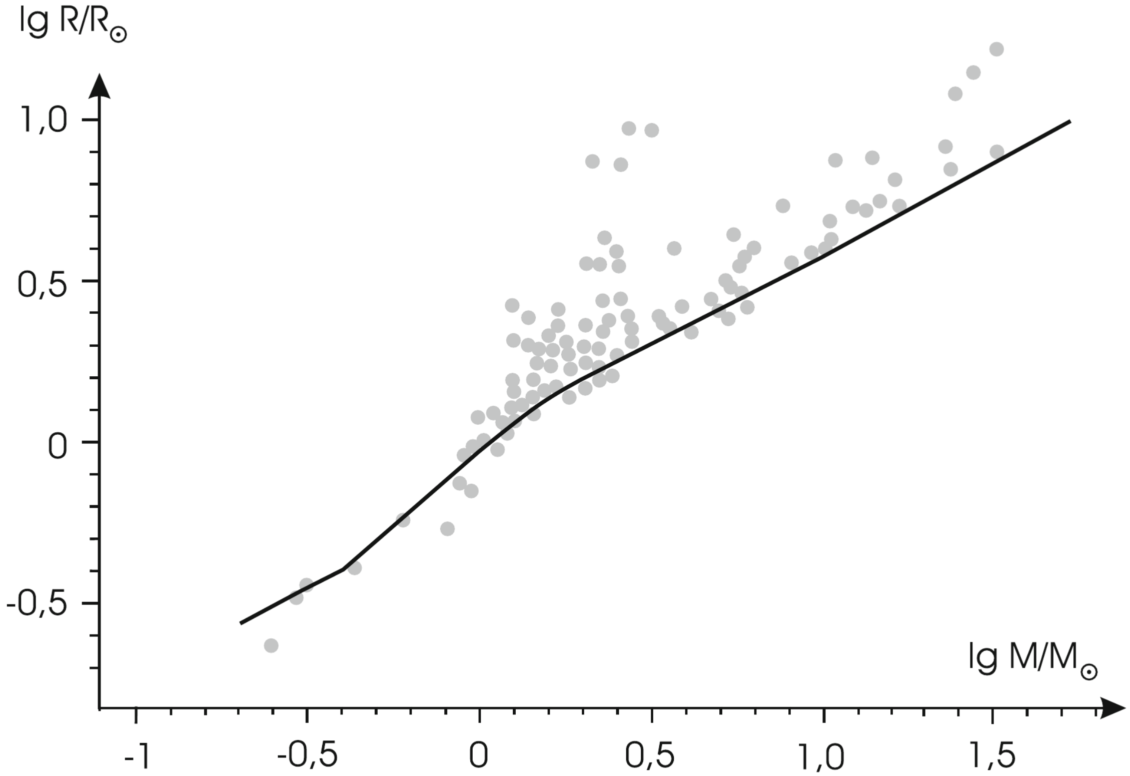

Kippenhahn, Weigert & Weiss 2012

Mass-luminosity relation

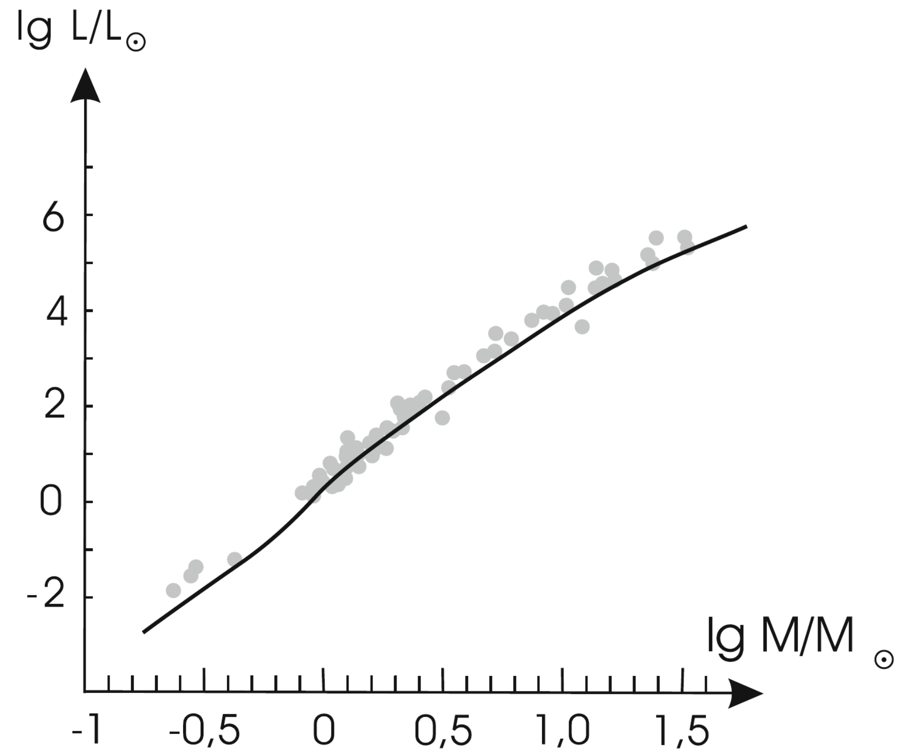

$$R \sim M^{0.56...0.79}$$

$$L \sim M^{3.89...3.35}$$

Interior structure of ZAMS stars

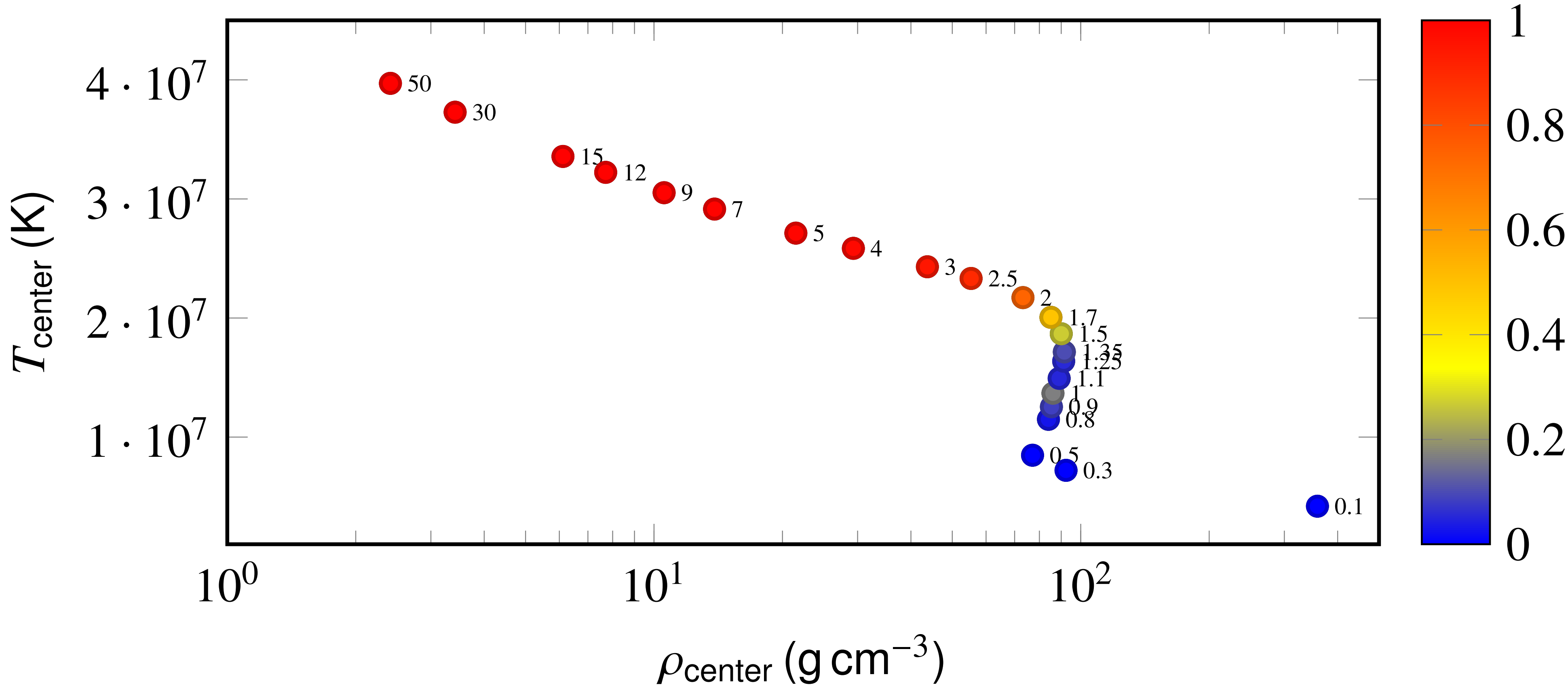

Central temperature versus central density for zero-age main sequence stars (based on EZ-models with X = 0.73 and Y = 0.26); color codes the fractional contribution of the CN-cycle to the total thermal energy generation

Jump due to **change from p-pchain to CNO-cycle**

Interior structure of ZAMS stars

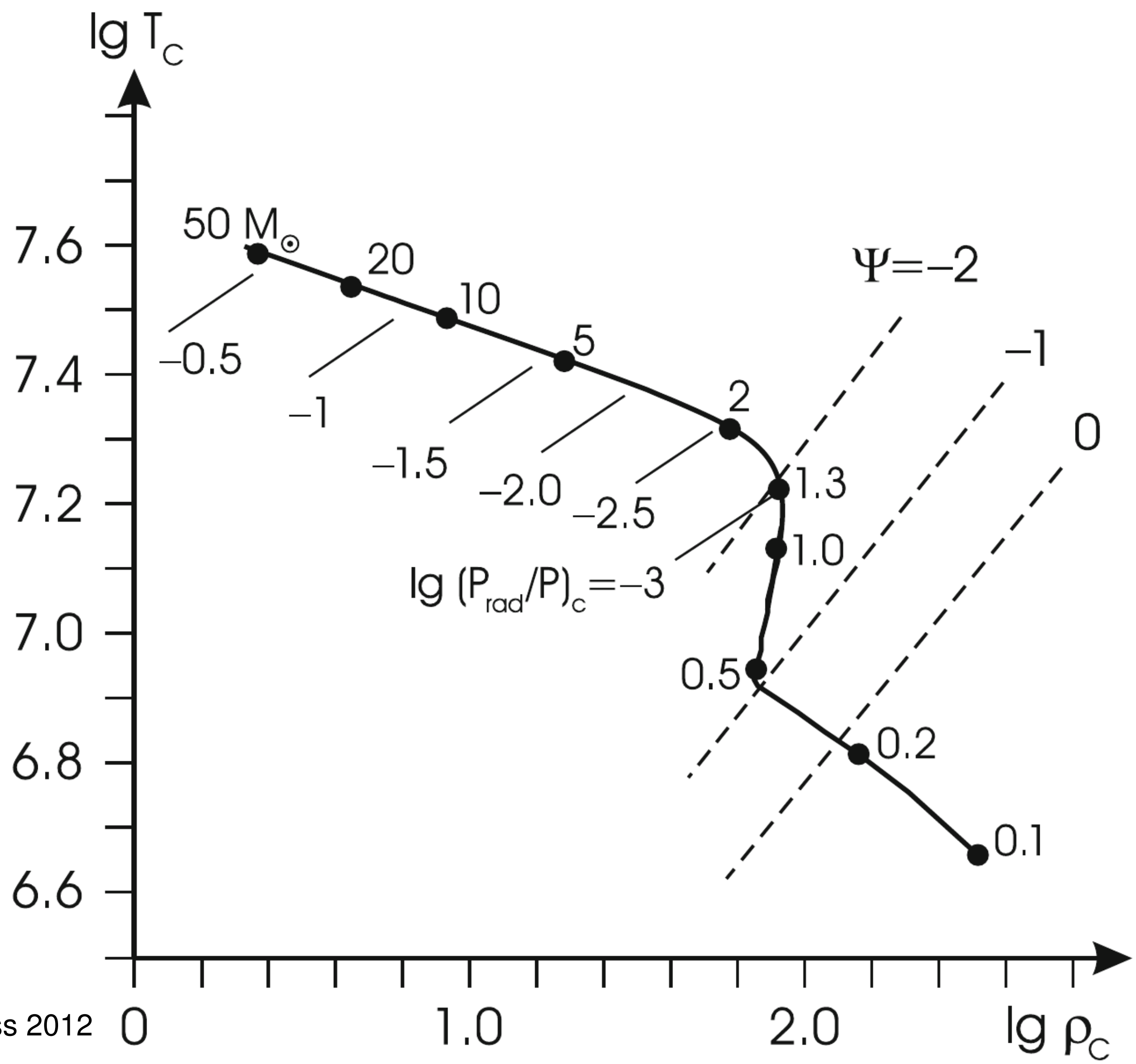

Kippenhahn, Weigert & Weiss 2012

$\rightarrow$ For lower masses, the core becomes partly degenerate

$\rightarrow$ For high masses, radiation pressure becomes significant

Interior structure of ZAMS stars

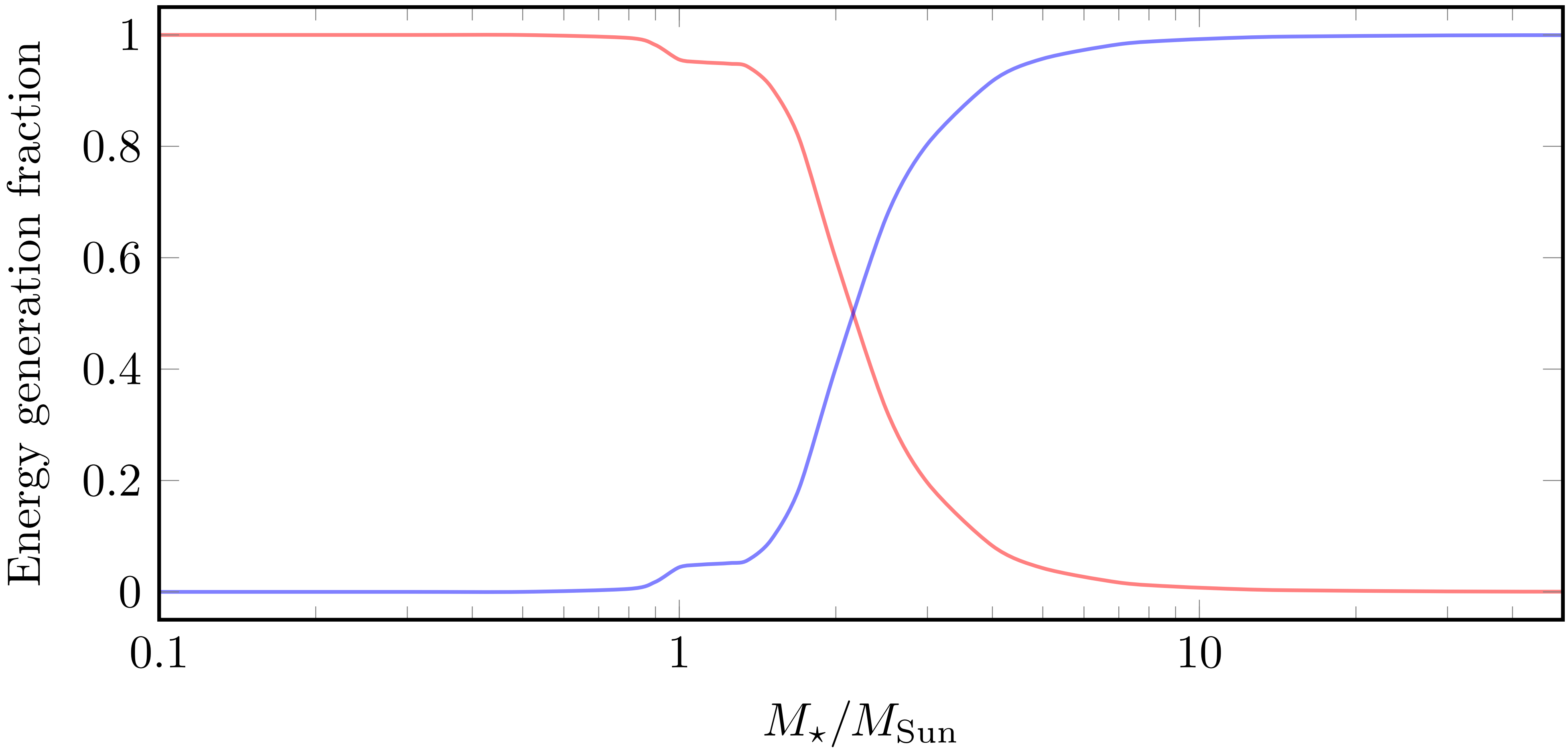

Fractional contribution of the proton-proton chain (red lines) and the CN-cycle (blue lines) to the total thermal energy generation as function of stellar mass

Interior structure of ZAMS stars

Temperature and pressure for a 1 $M_\odot$ ZAMS star

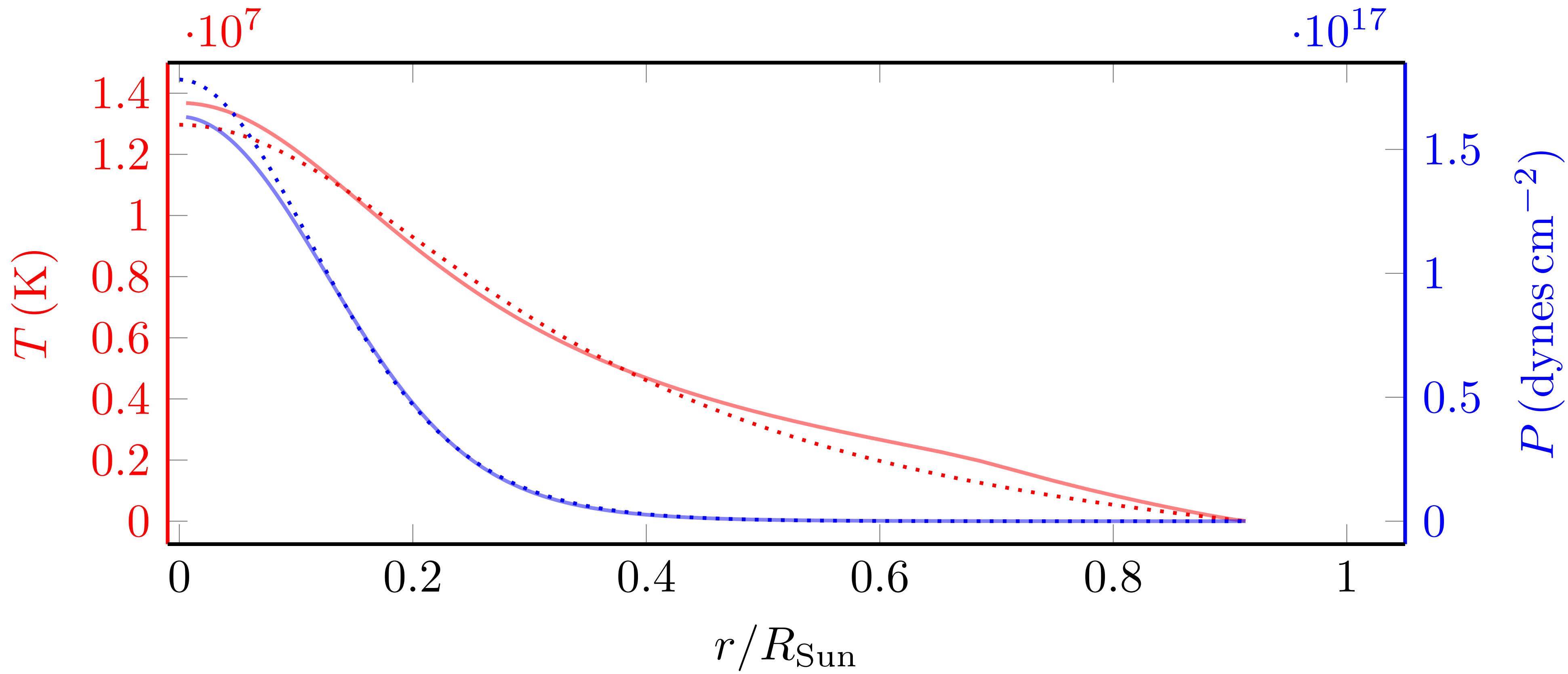

solid: *EZ*-model; dotted: polytropic standard model with radius according to *EZ*-model)

Interior structure of ZAMS stars

Temperature and pressure for a $1.35\,\mathrm{M}_\odot$ ZAMS star

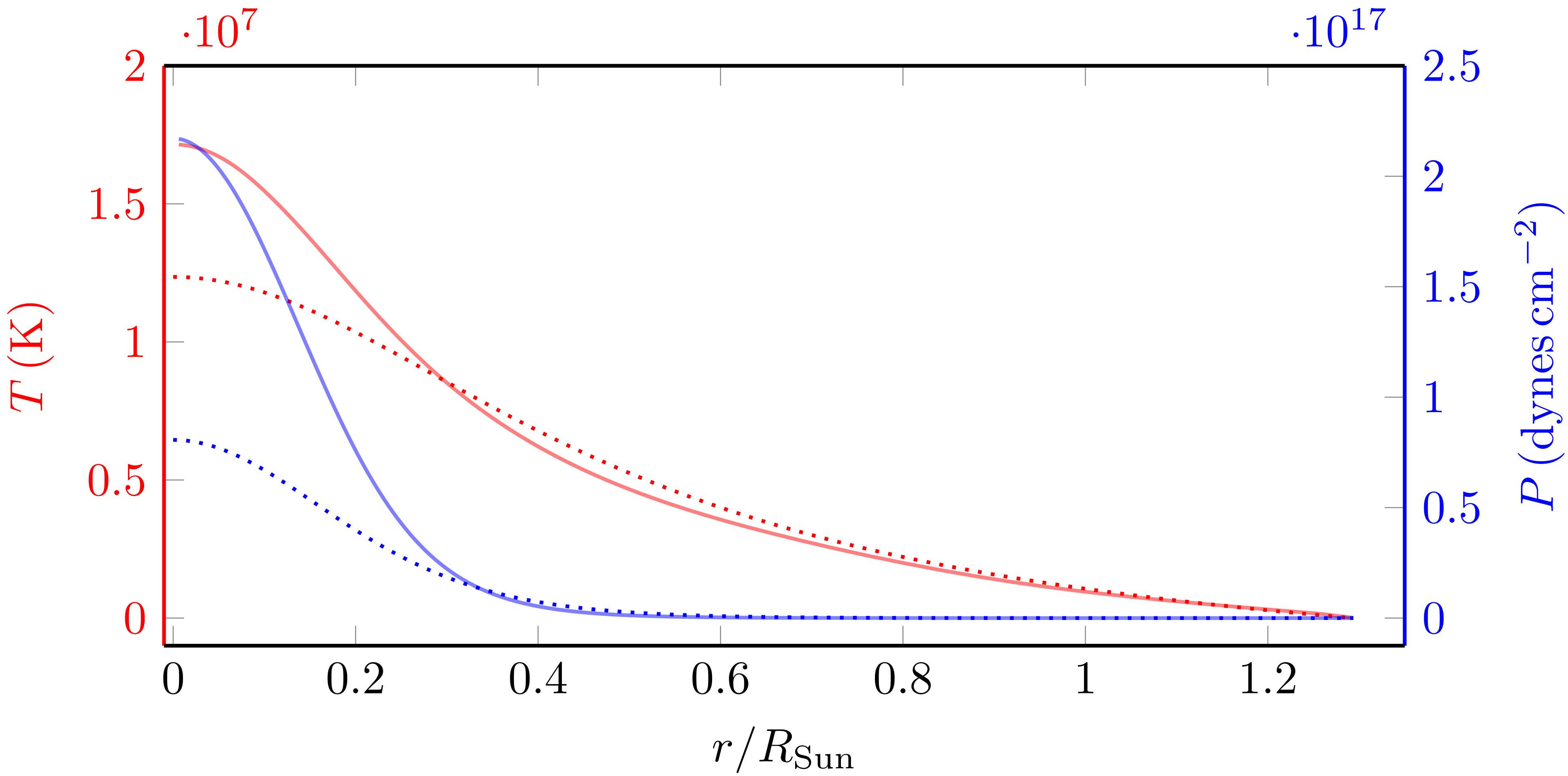

Interior structure of ZAMS stars

Temperature and pressure for a $3\,M_\odot$ ZAMS star

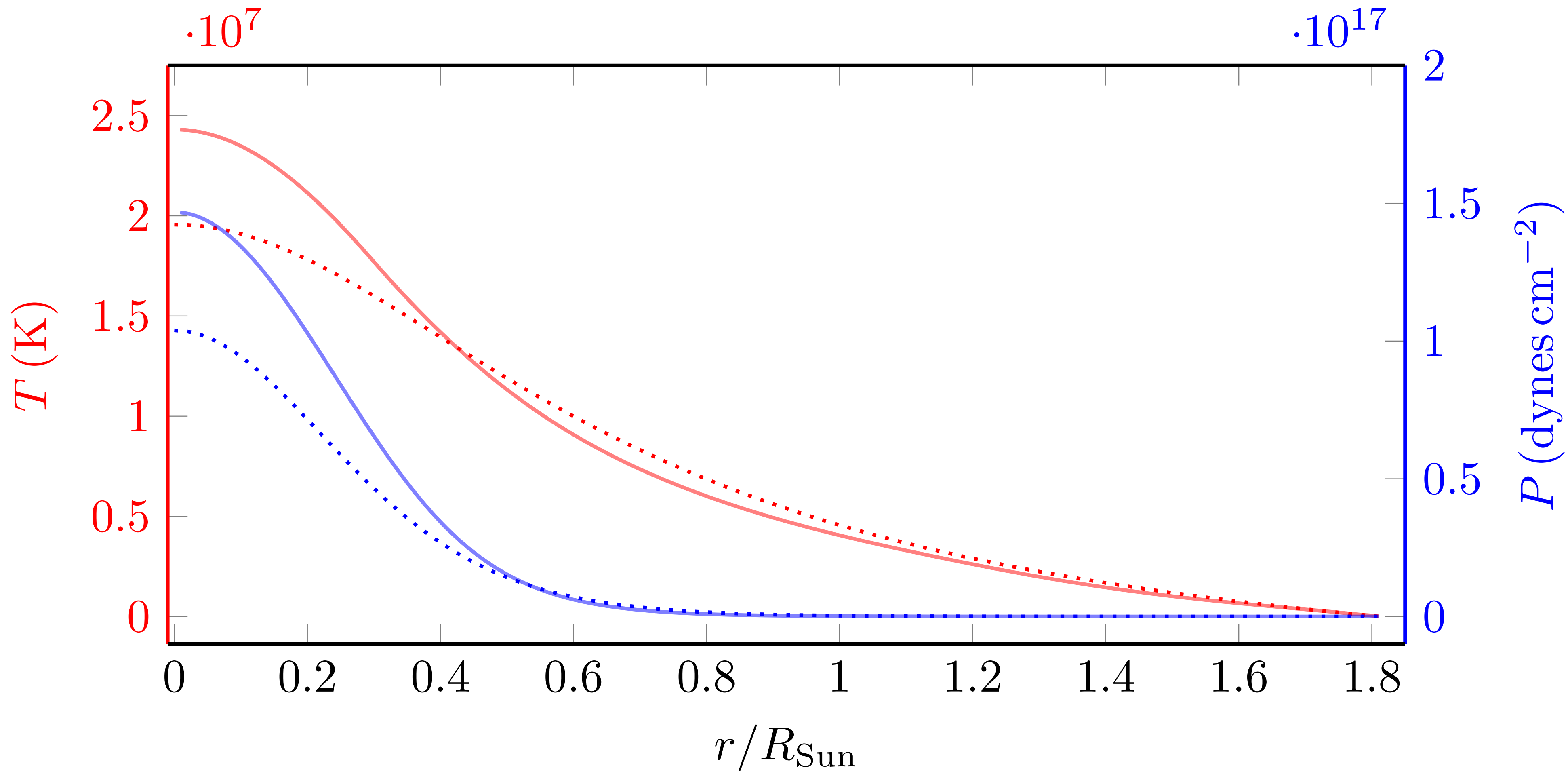

Interior structure of ZAMS stars

Temperature and pressure for a $7\,M_\odot$ ZAMS star

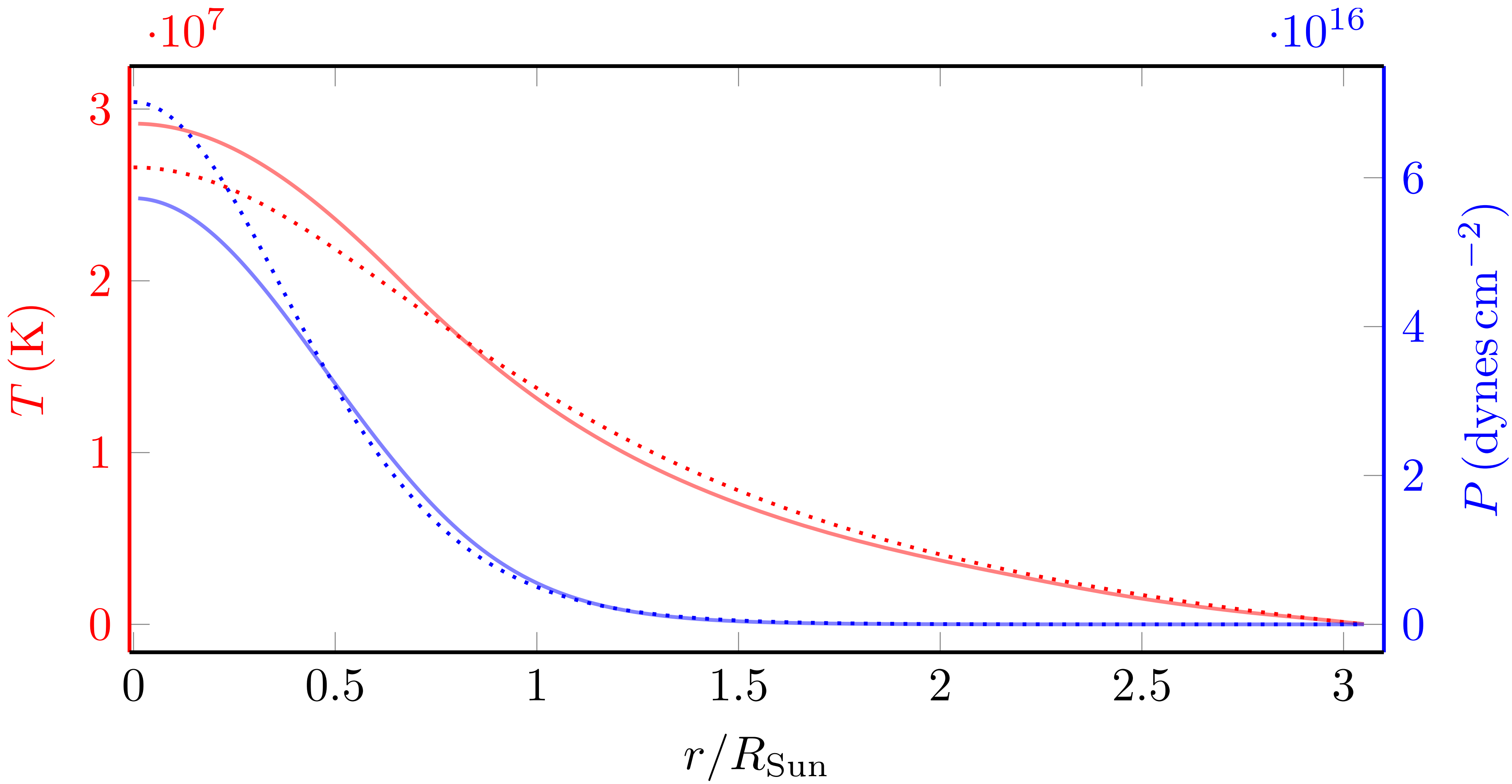

Interior structure of ZAMS stars

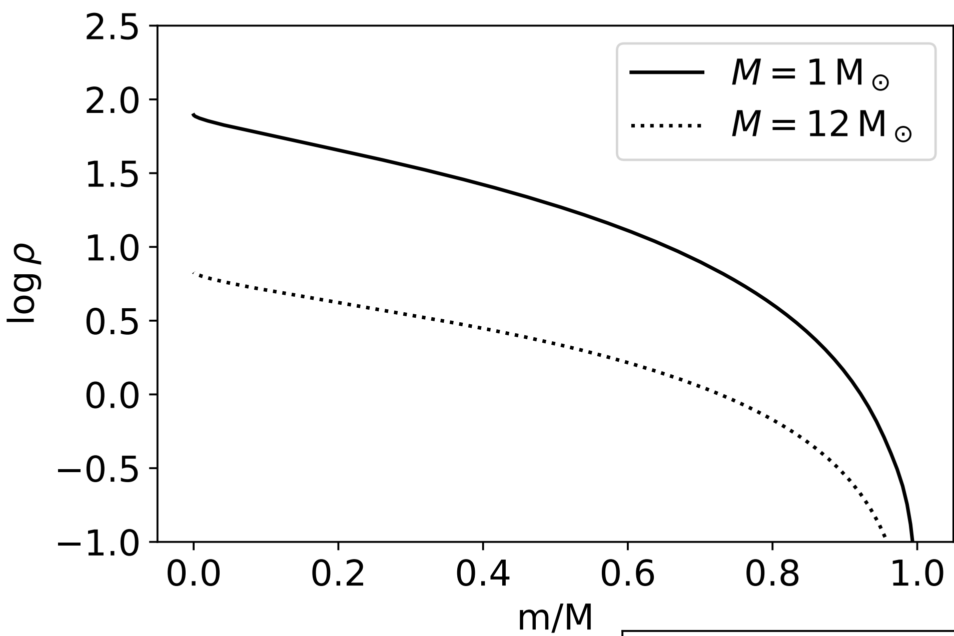

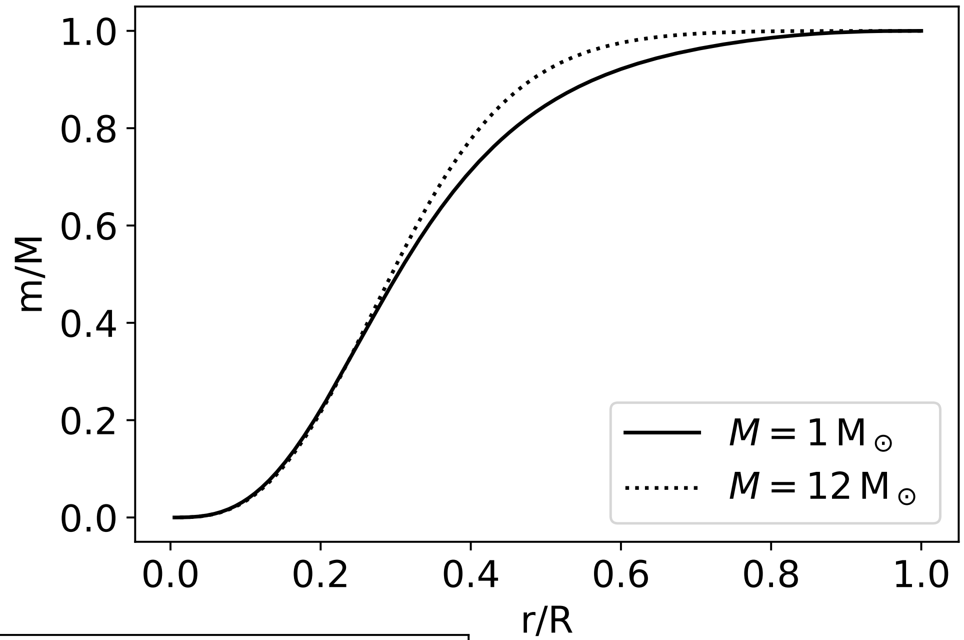

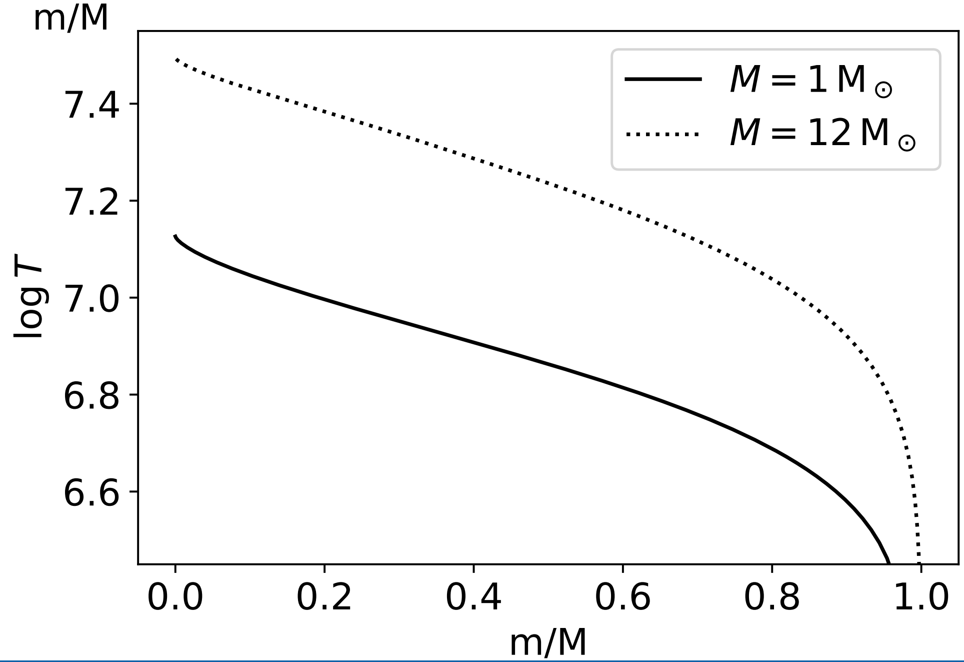

Interior structure of ZAMS stars

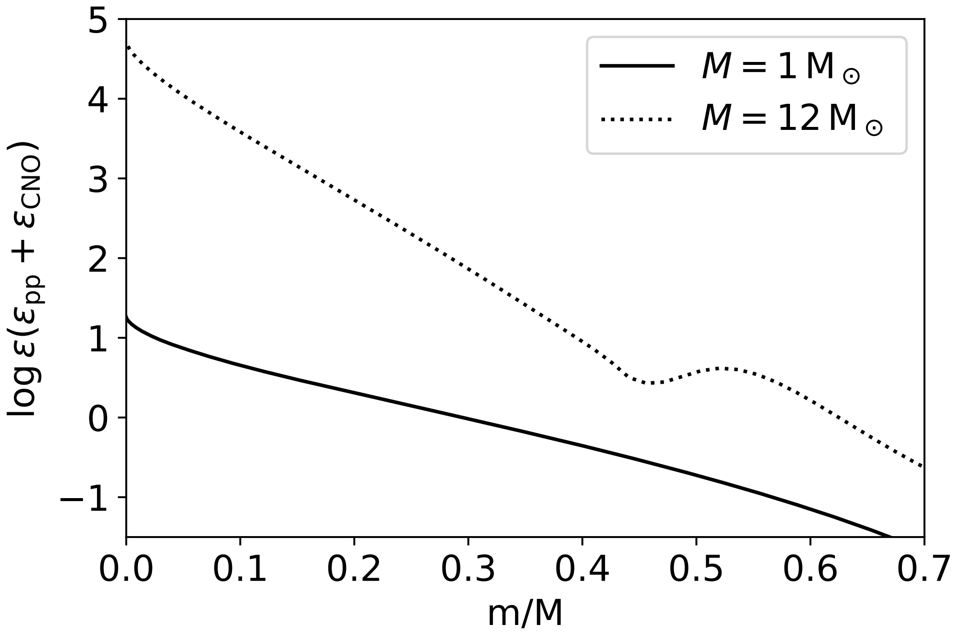

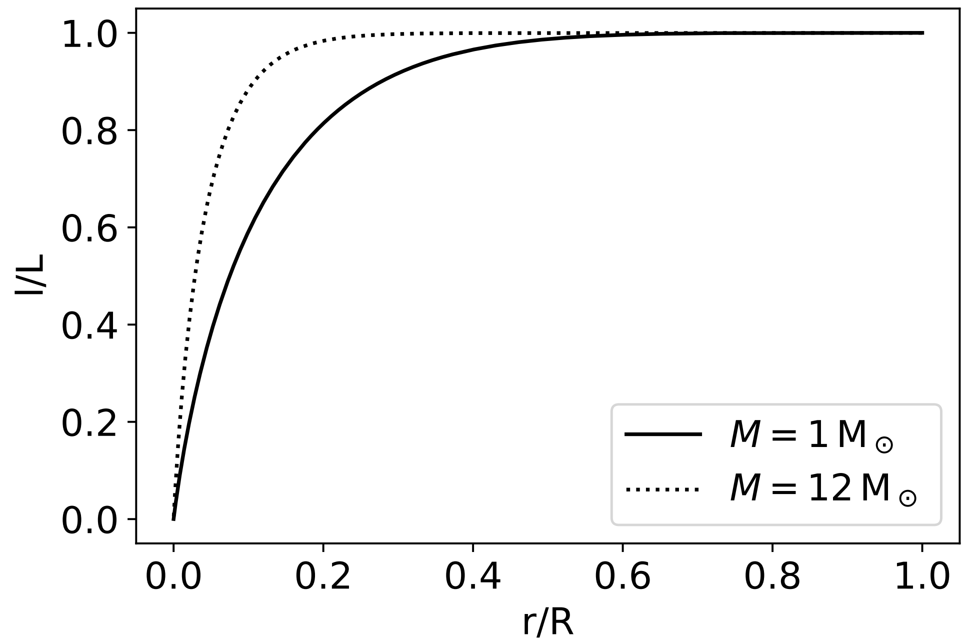

Differences mostly due to **change from p-p-chain to CNO-cycle**

Radial extension of convection zones for ZAMS stars

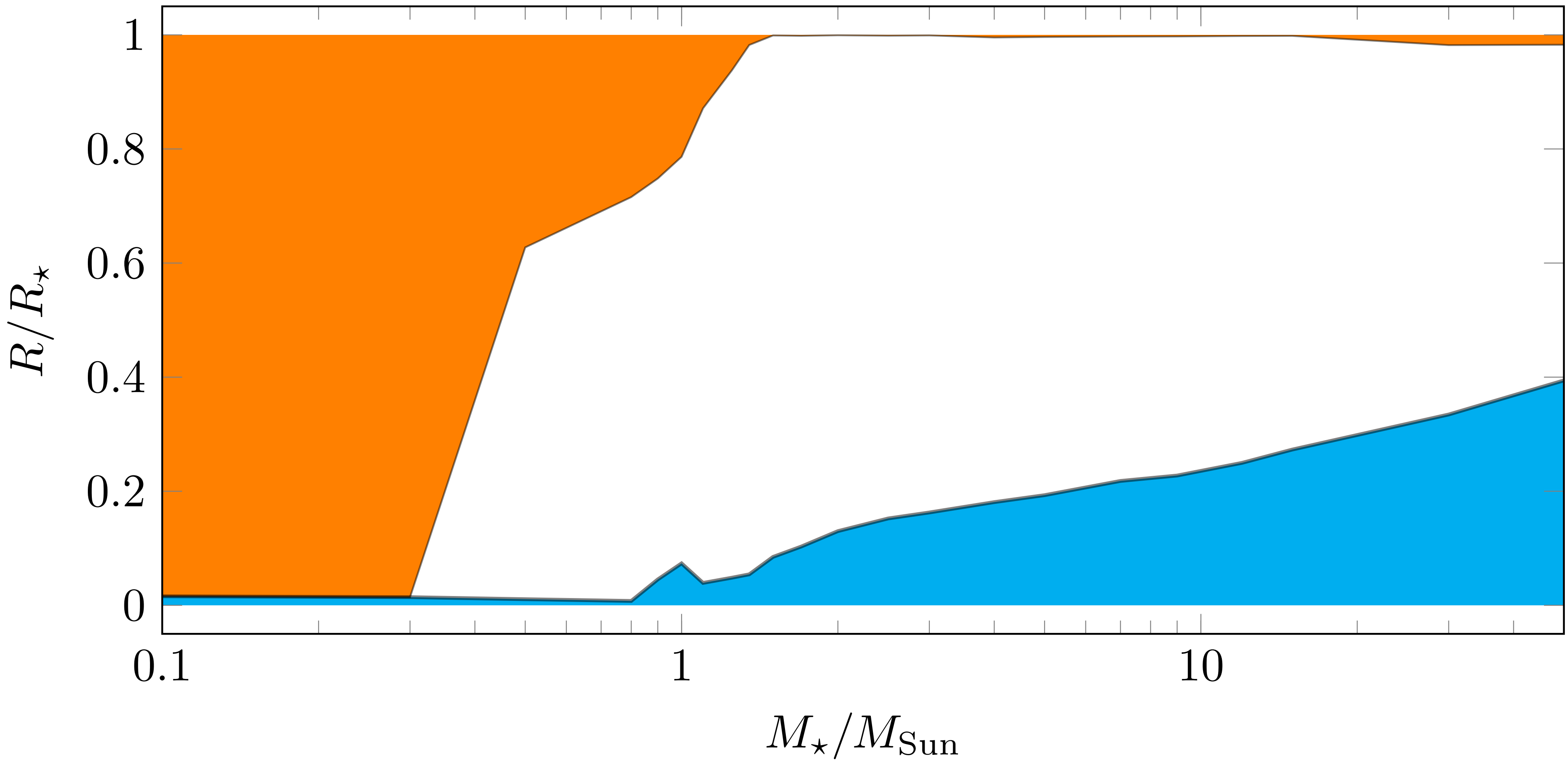

convection zone at the surface/center is shaded in orange/cyan. The surface convection zone increases with decreasing stellar mass while the opposite is true for the central convection zone

Radial extension of convection zones for ZAMS stars

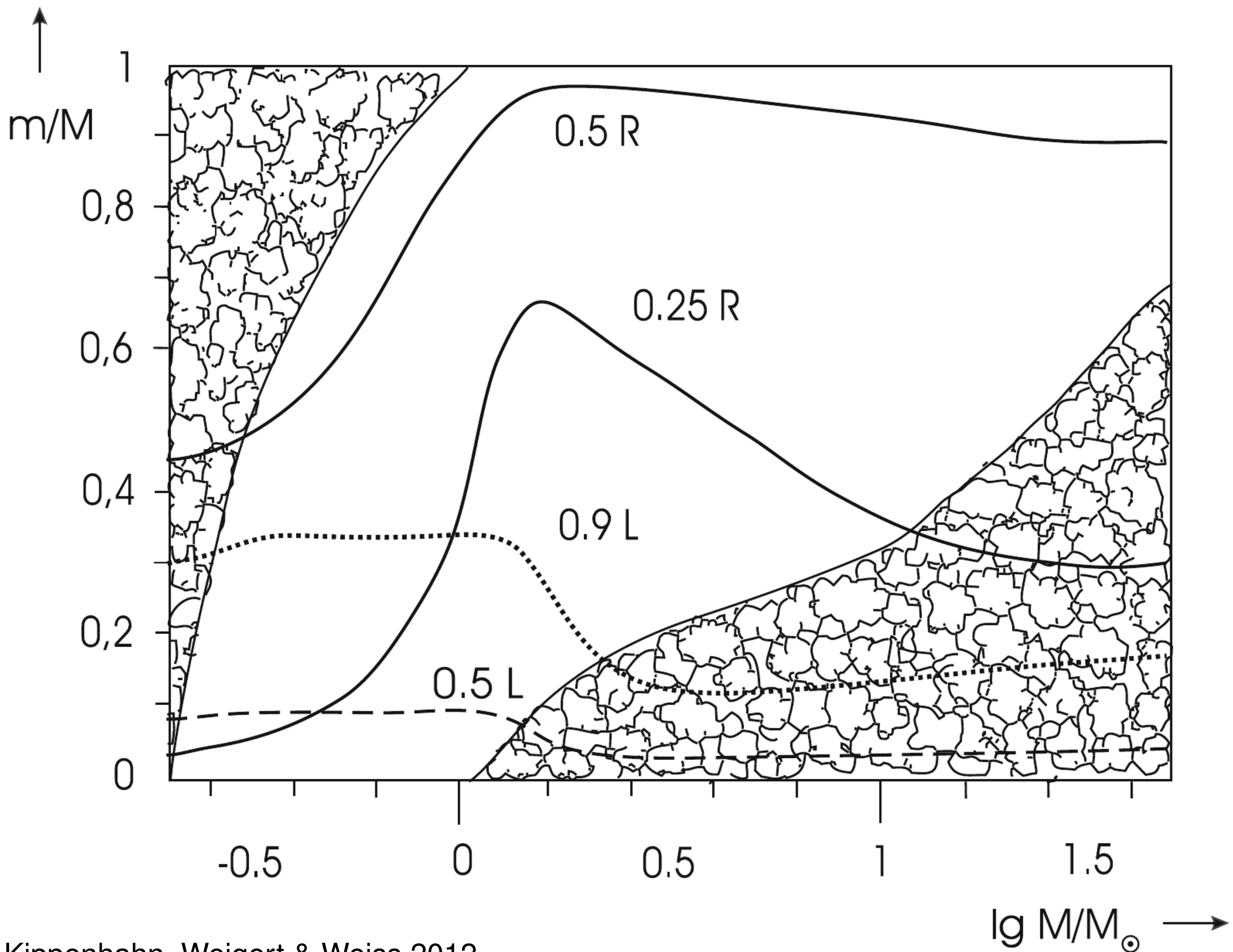

Kippenhahn, Weigert & Weiss 2012

Upper main sequence

$M \gtrsim 1\,\mathrm{M}_\odot$

$\rightarrow$ CNO cycle leads to high temperature gradient in the core

$\rightarrow$ **Convective core + radiative envelope**

Lower main sequence

$M \lesssim 1\,\mathrm{M}_\odot$

$\rightarrow$ Low temperature at the surface and high opacity

$\rightarrow$ **Radiative core + convective envelope**

$M \lesssim 0.25\,\mathrm{M}_\odot \rightarrow$ Fully convective

Zero-Age Main Sequence

Minimum mass $M \simeq 0.08\,\mathrm{M}_\odot$

$\rightarrow$ Hydrogen-burning limit

Substellar objects with masses $0.01 - 0.08\,\mathrm{M}_\odot$ are called brown dwarfs

$\rightarrow$ After a short phase of deuterium burning, they continue to cool down with τ_{KH}

$\rightarrow$ Discovered in 1995

$\rightarrow$ New spectral types L, T and Y have been introduced

$\rightarrow$ Objects with low luminosities and SEDs peaking in the infrared

Maximum mass $M \simeq 60 - 100\,\mathrm{M}_\odot$

$\rightarrow$ limited by **vibrational instability** and **radiation pressure**

At the upper end of the main sequence, radiation pressure becomes so high that the star becomes unbound ($g_\mathrm{rad} = -\frac{1}{\rho}\frac{\mathrm{d}P_\mathrm{rad}}{\mathrm{d}r} > g$)

$\rightarrow$ The critical luminosity is called **Eddington luminosity** L_E

$$\frac{L_\mathrm{E}}{L_\odot} = \frac{4\pi c G M}{\kappa} = 1.3 \times 10^4 \frac{1}{\kappa}\frac{M}{M_\odot}$$

Since $L \sim M^3$ this leads to a limiting mass dependent on metallicity

Zero-Age Main Sequence

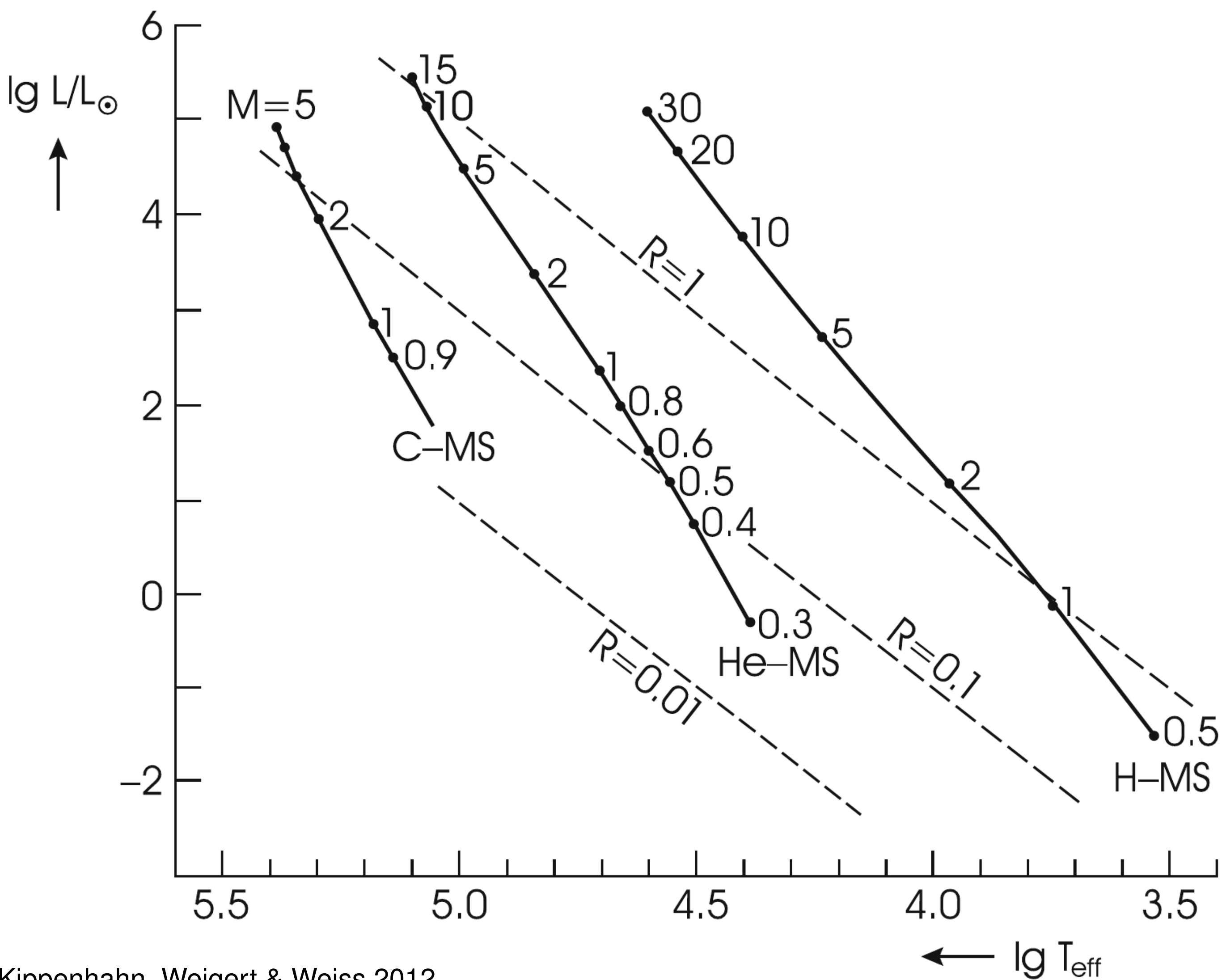

Kippenhahn, Weigert & Weiss 2012

Other main sequences can be constructed for **different compositions**

Relevant for later stages of stellar evolution are the **He-MS** and the **C-MS**

Main Sequence Evolution of a 1 $M_\odot$ star

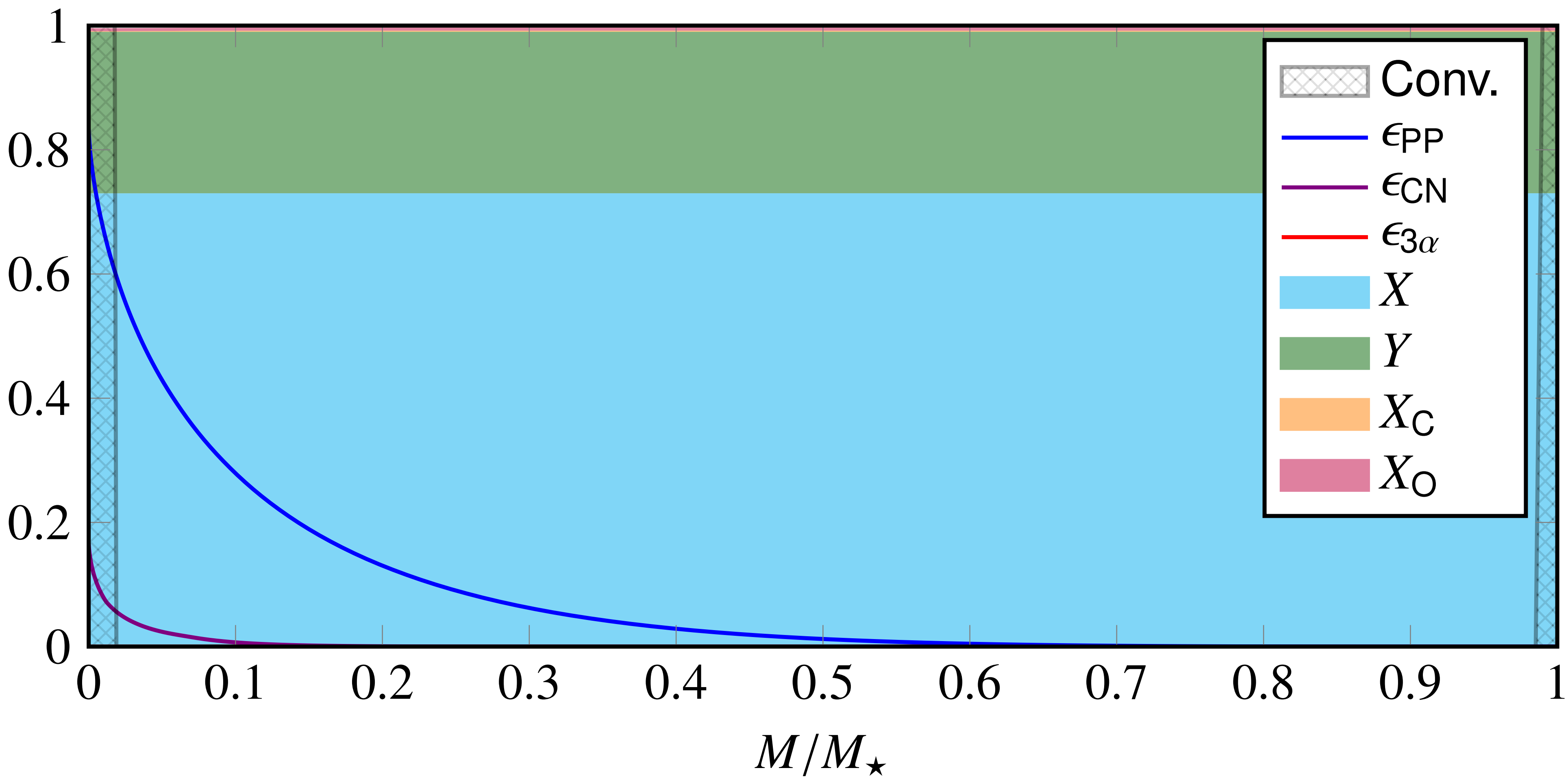

Occurrence of convection, chemical composition, energy generation as function of fractional mass coordinate for a 1 $M_\odot$ ZAMS star (based on EZ-models with $X = 0.73$, $Y = 0.26$)

Main Sequence Evolution of a 1 $M_\odot$ star

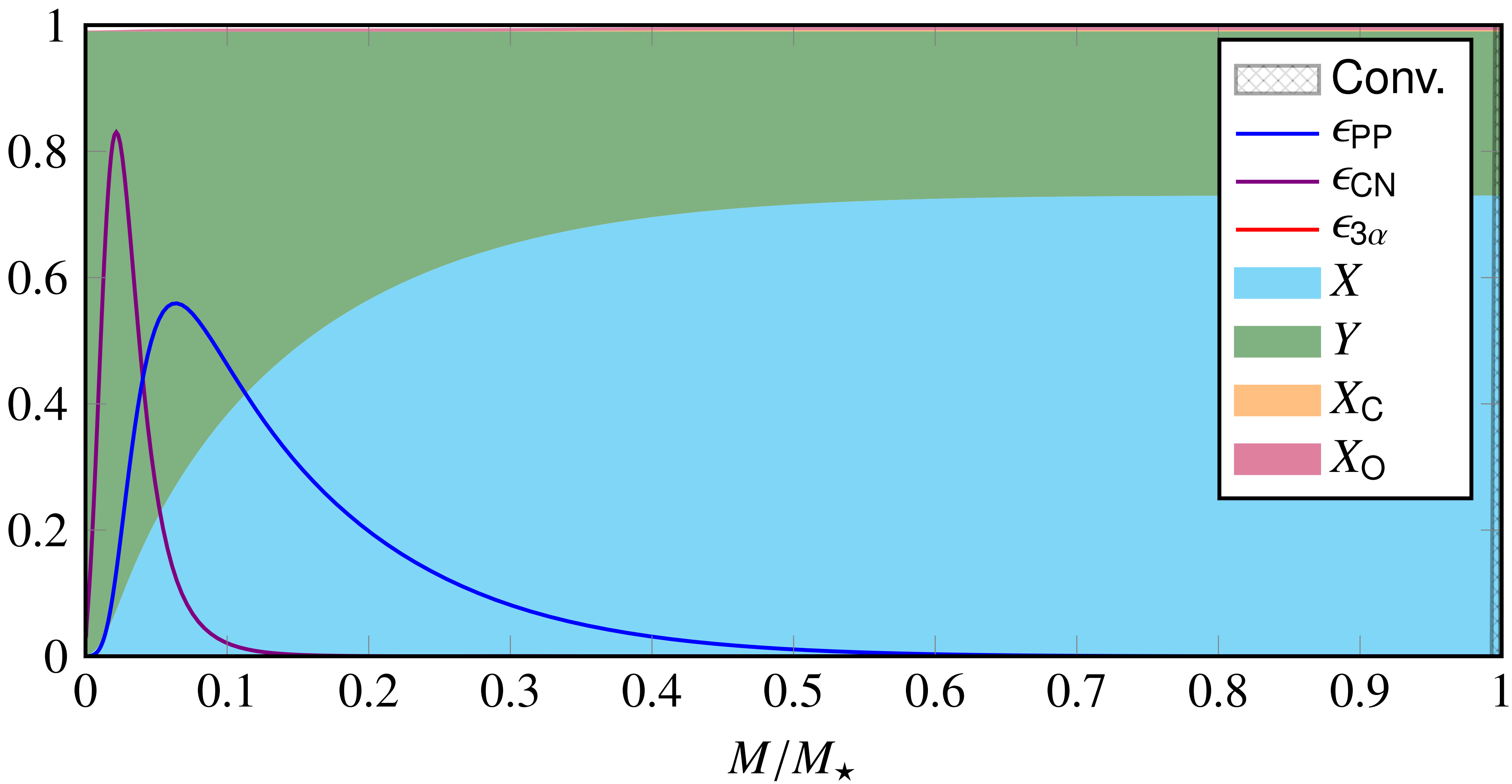

Occurrence of convection, chemical composition, energy generation as function of fractional mass coordinate for a 1 $M_\odot$ terminal-age main sequence (TAMS) star (based on EZ-models with $X = 0.73$, $Y = 0.26$)

Main Sequence Evolution of a 1 $M_\odot$ star

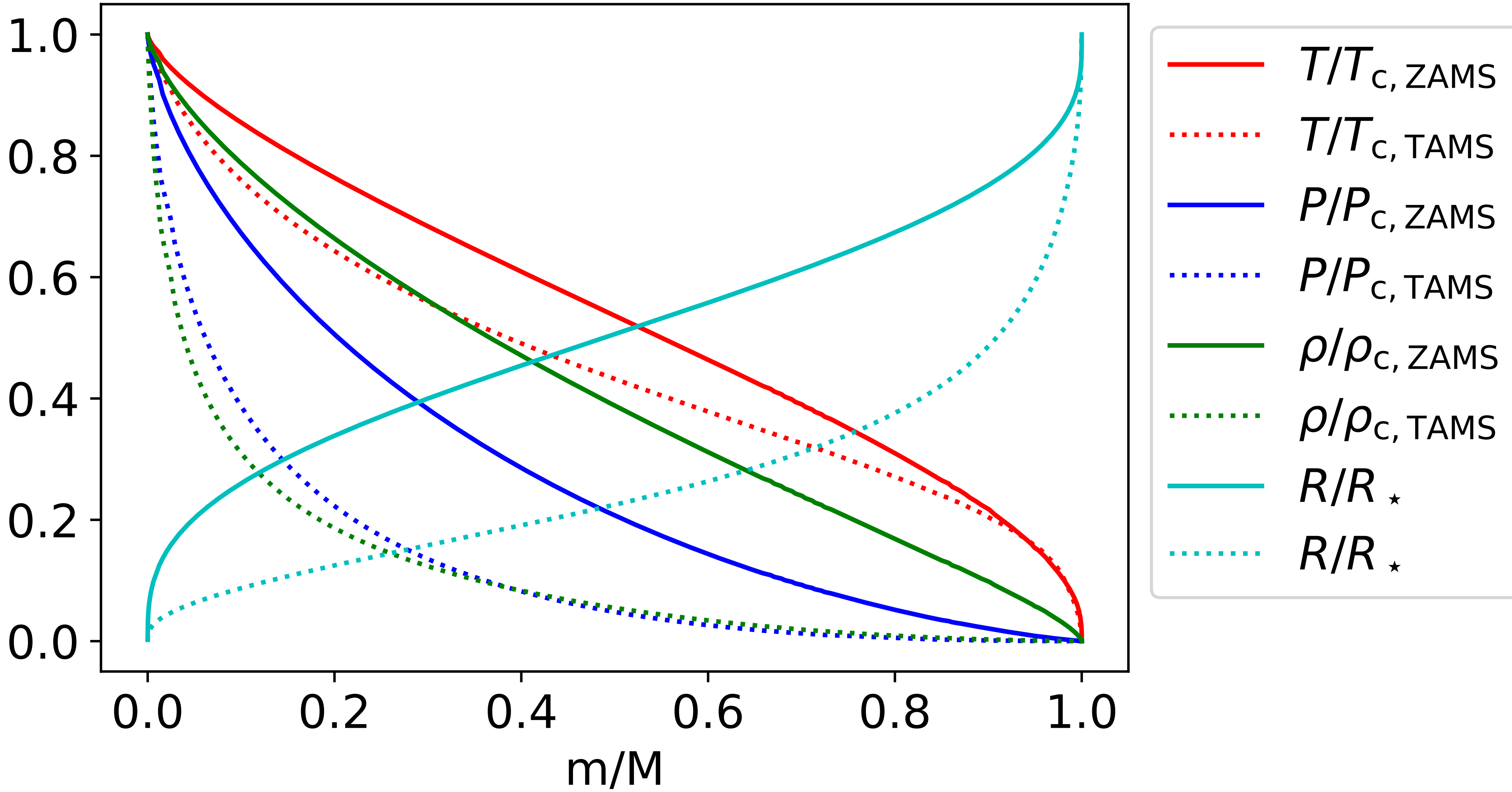

ZAMS and TAMS model (based on MESA-models: `http://www.astro.wisc.edu/~townsend/static.php?ref=mesa-web`) with X = 0.7, Y = 0.28).

Main Sequence Evolution of a 1 $M_\odot$ star

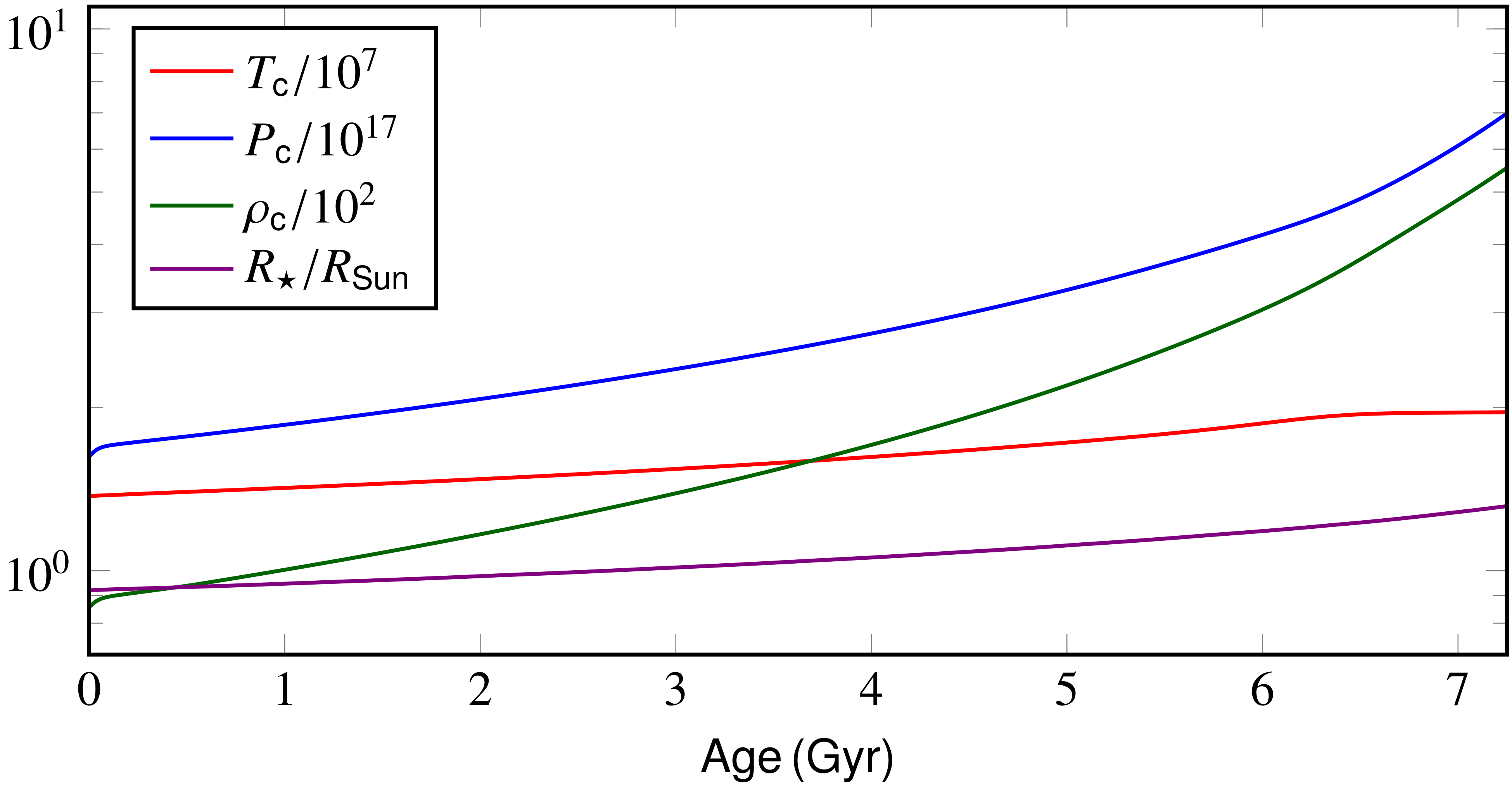

Temporal changes of central temperature T_c, pressure P_c, density ρ_c (all in cgs units), and stellar radius R (based on EZ-models with $X = 0.73$, $Y = 0.26$).

Main Sequence Evolution of a 1 $M_\odot$ star (MESA model)

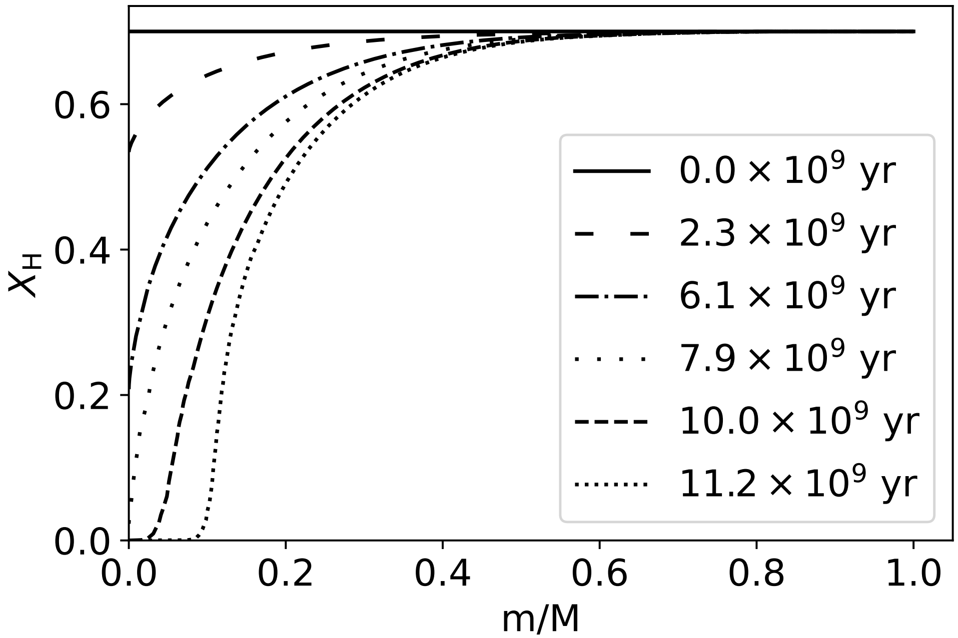

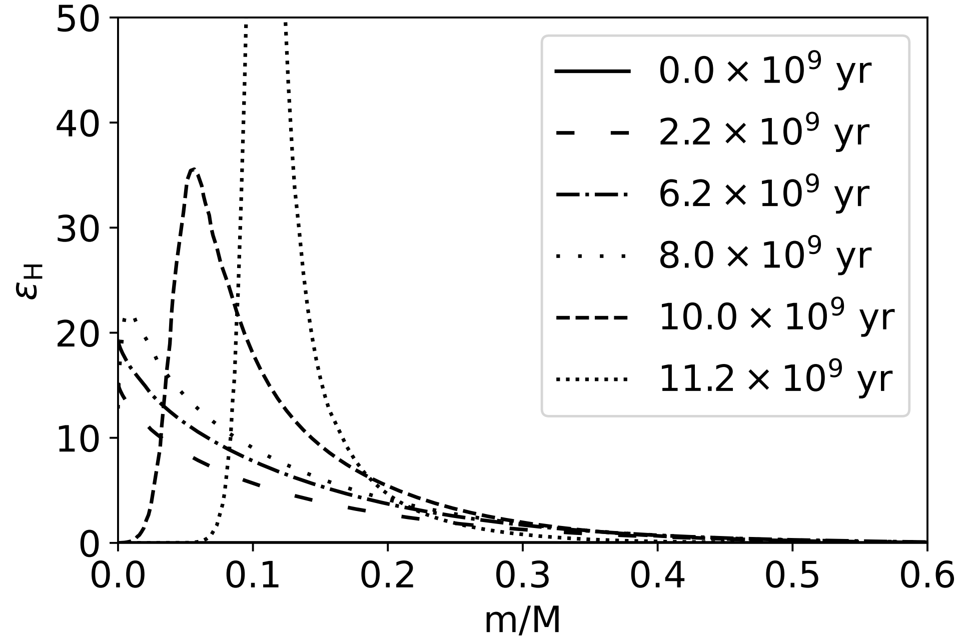

exhaustion of H in the core, H-burning develops in a shell around the He-rich core

$\rightarrow$ shell moves outward

$\rightarrow$ radiative core

$\rightarrow$ more massive stars have convective cores

MS Evolution of a $1\,M_\odot$ (radiative core) vs $5\,M_\odot$ (convective) star

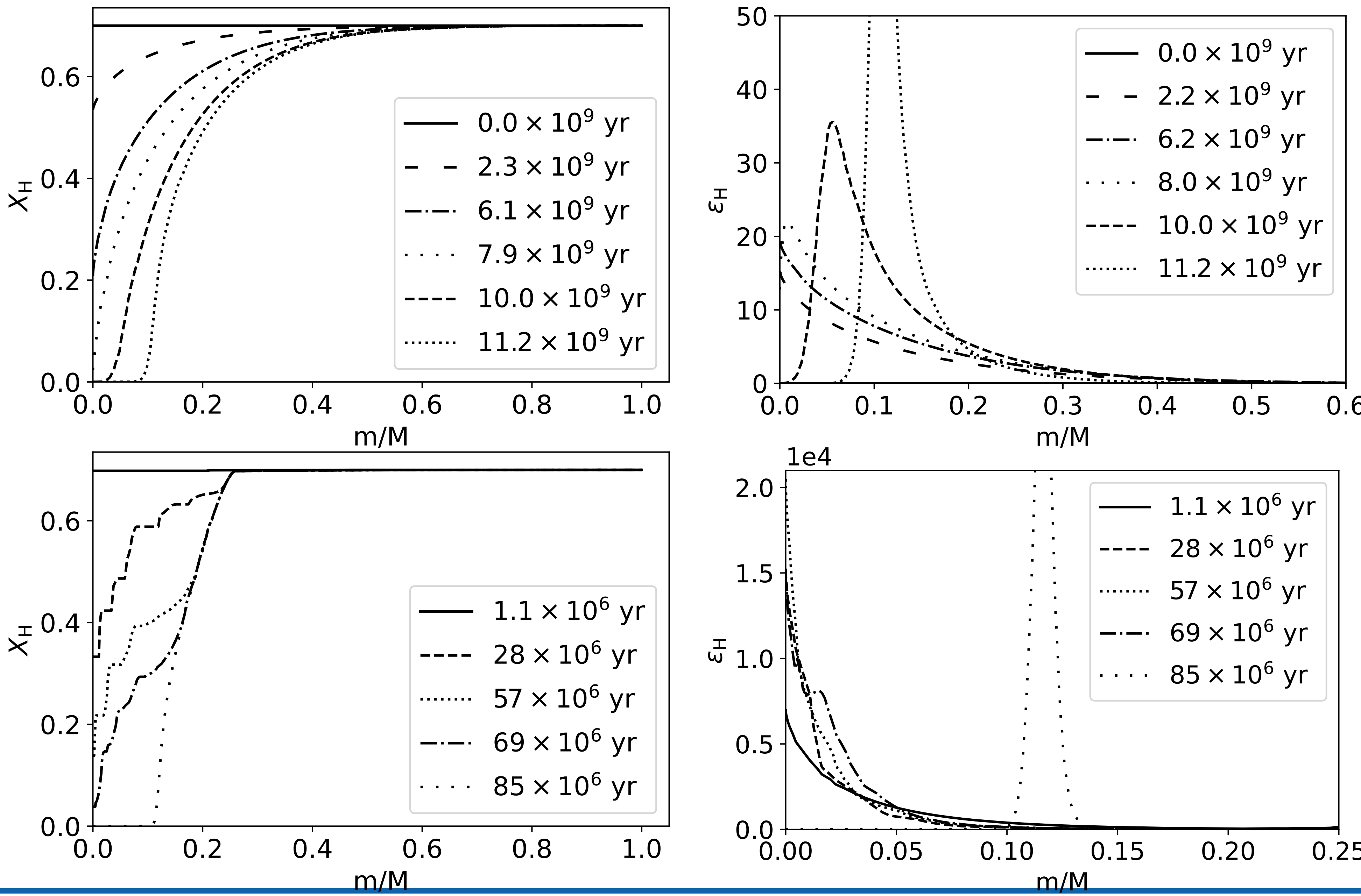

Main Sequence Evolution of a $7\,M_\odot$ star (EZ model)

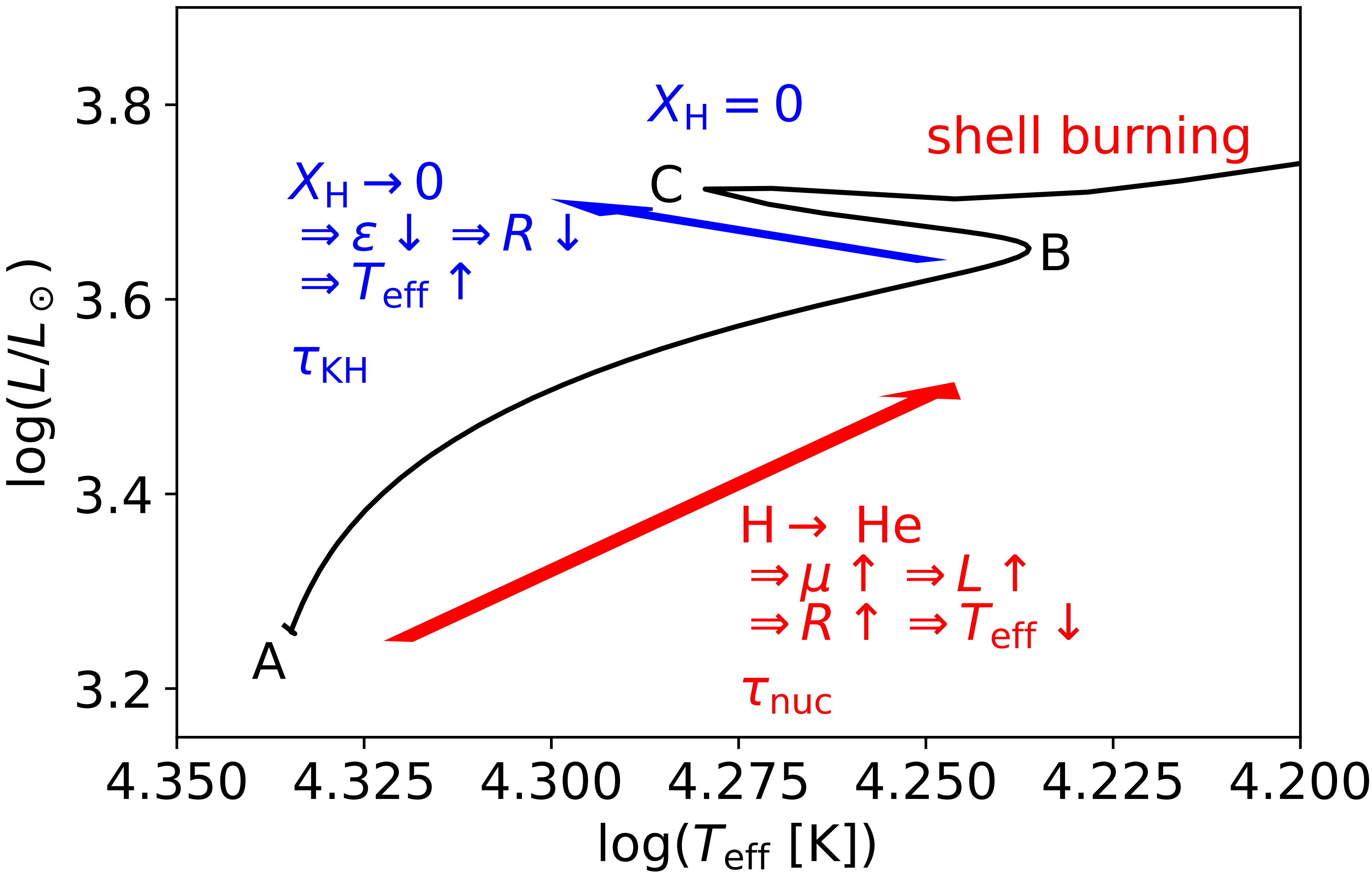

Main Sequence Evolution in the HRD

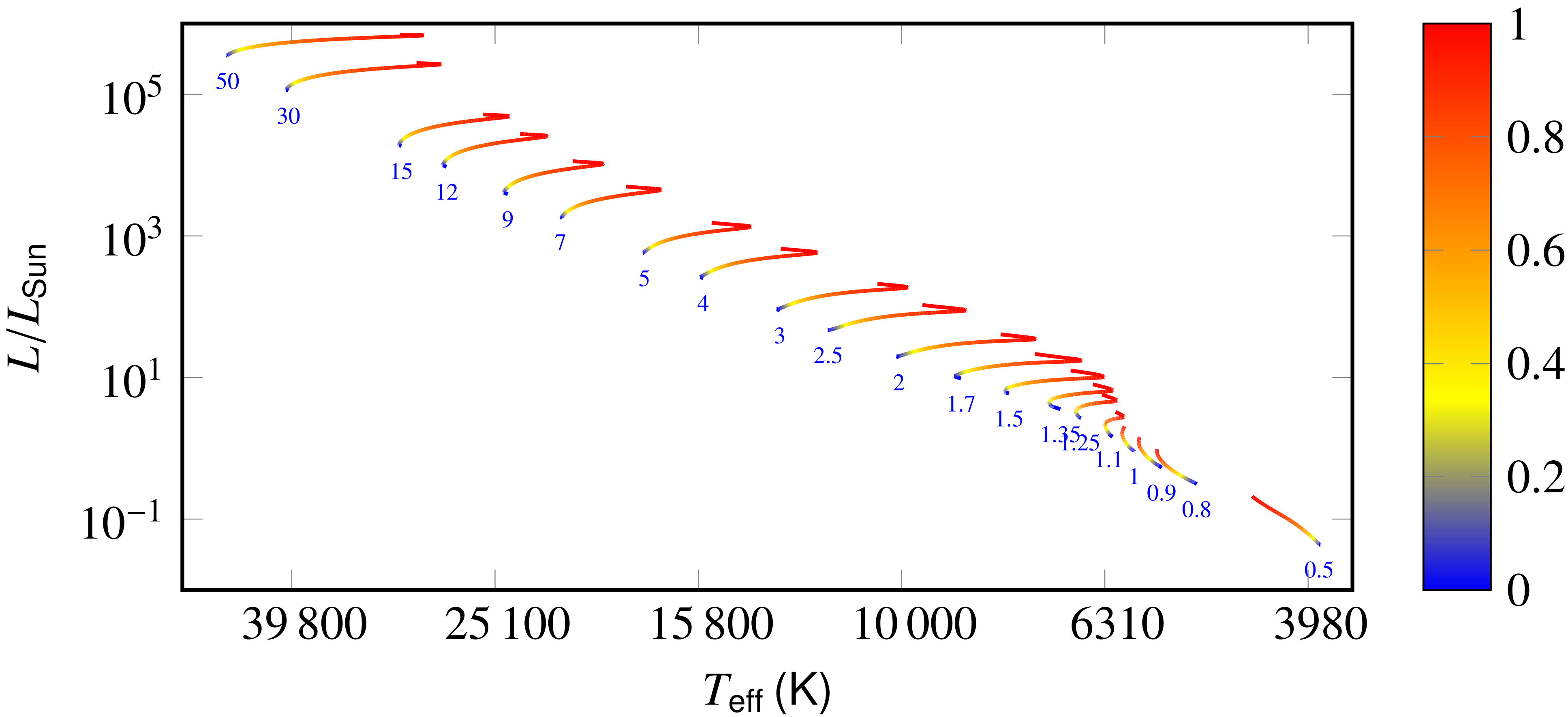

Theoretical Hertzsprung-Russell diagram showing the evolution during the main sequence phase (based on EZ-models with X = 0.73, Y = 0.26), the color codes the fractional age ranging from the ZAMS (blue) to the TAMS (red)

Nuclear time scale

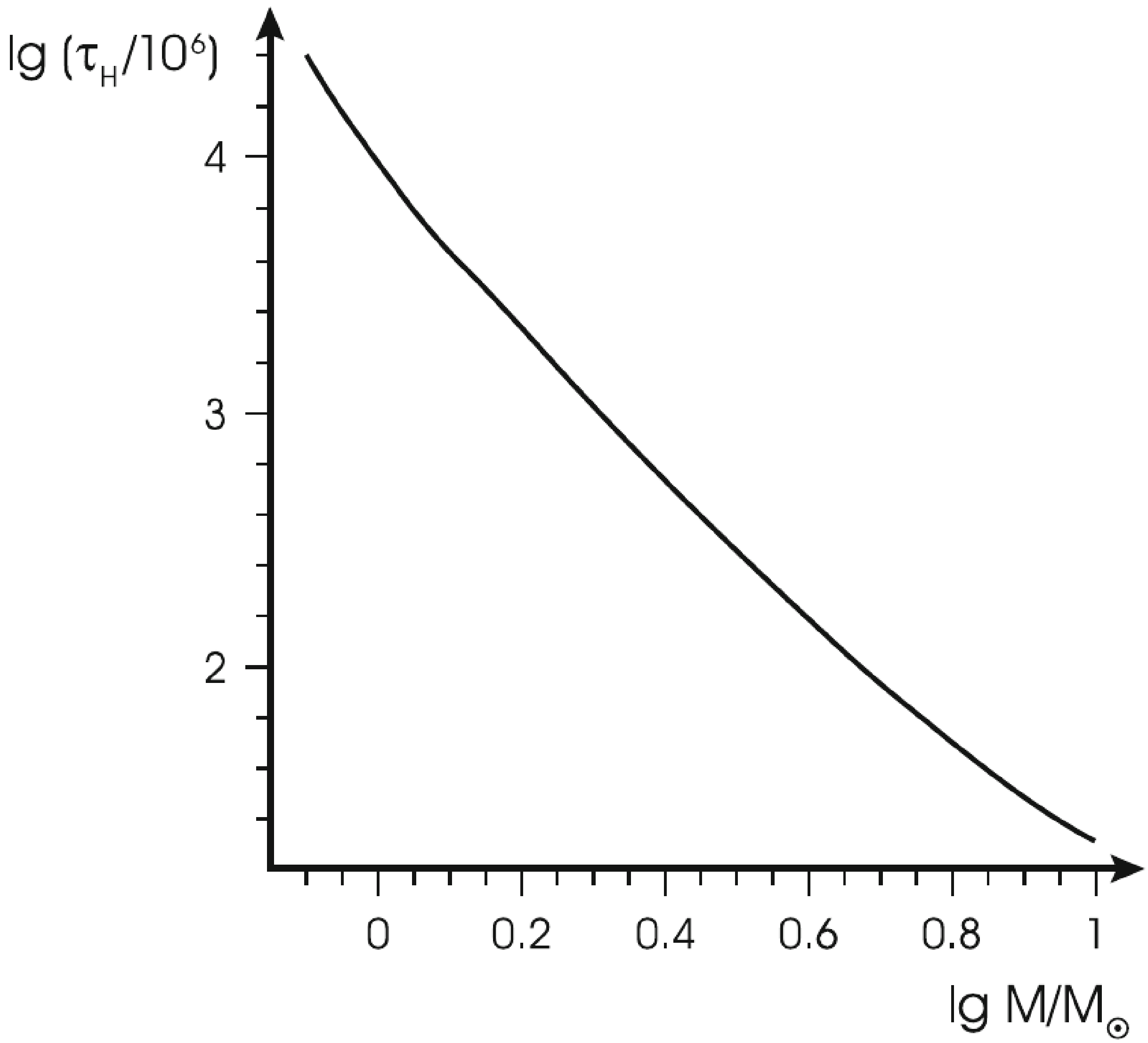

Kippenhahn, Weigert & Weiss 2012

The nuclear lifetime on the main sequence is a strong function of L and therefore M

$$\tau_H \sim M^{-2.5}$$

It ranges from several million years to more than the age of the Universe for $M < 0.8\,\mathrm{M}_\odot$

Evolution of a star with convective core

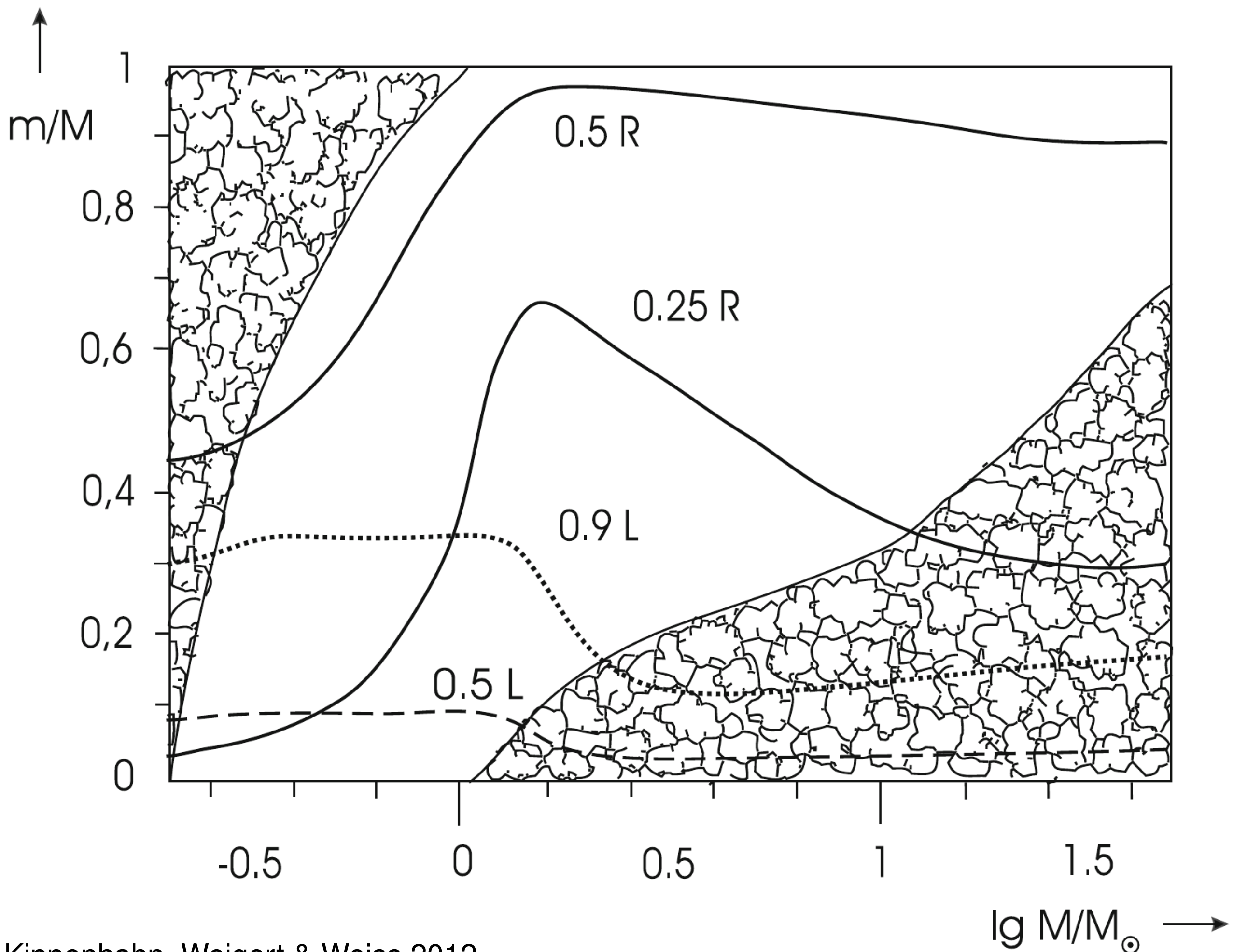

Kippenhahn, Weigert & Weiss 2012

seemingly nice and clear picture of the main-sequence phase

$\rightarrow$ notorious problem of convection

$\rightarrow$ precise determination of those regions in the deep interior in which convective motions occur and the extent to which the chemical elements are mixed

$\rightarrow$ mixing influences the later evolution, since the chemical profile, which is established and left behind, is a long-lasting memory

Convective Overshooting

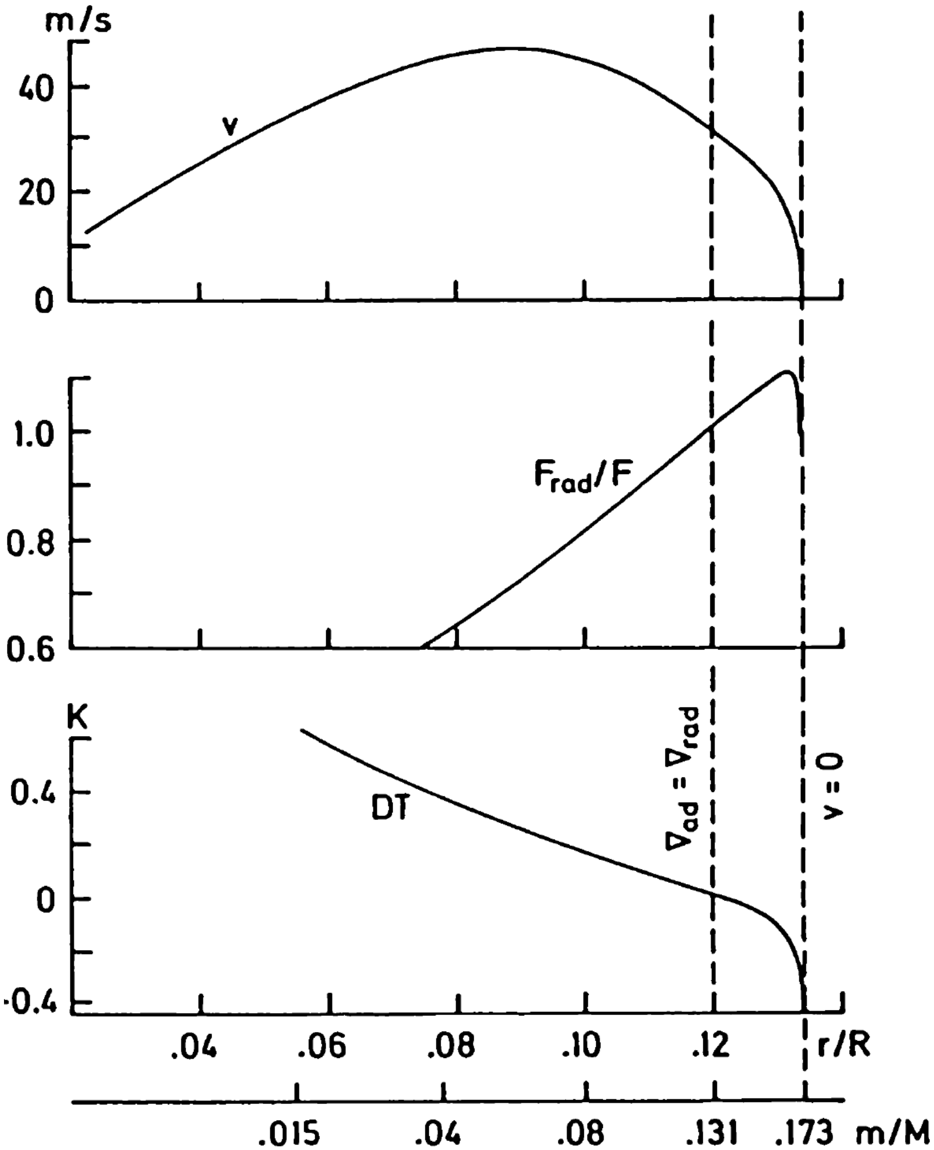

Kippenhahn, Weigert & Weiss 2012

At border between convective core and radiative envelope

$$\nabla_{\rm rad} = \nabla_{\rm ad}$$

$\rightarrow$ regimes in which convective motions are present ($v > 0$) and absent ($v = 0$)

$\rightarrow$ Inertia of the moving material

$\rightarrow$ Penetration into the radiative region

$\rightarrow$ **Convective overshooting**

$\rightarrow$ mixing-length parameter $\alpha = l_{\rm m}/H_p$

$\rightarrow$ $F = F_{\rm conv} + F_{\rm rad} = \frac{l}{4\pi r^2}$

$\rightarrow$ overshooting ($\alpha > 0$) brings more hydrogen in the core

Convective Overshooting

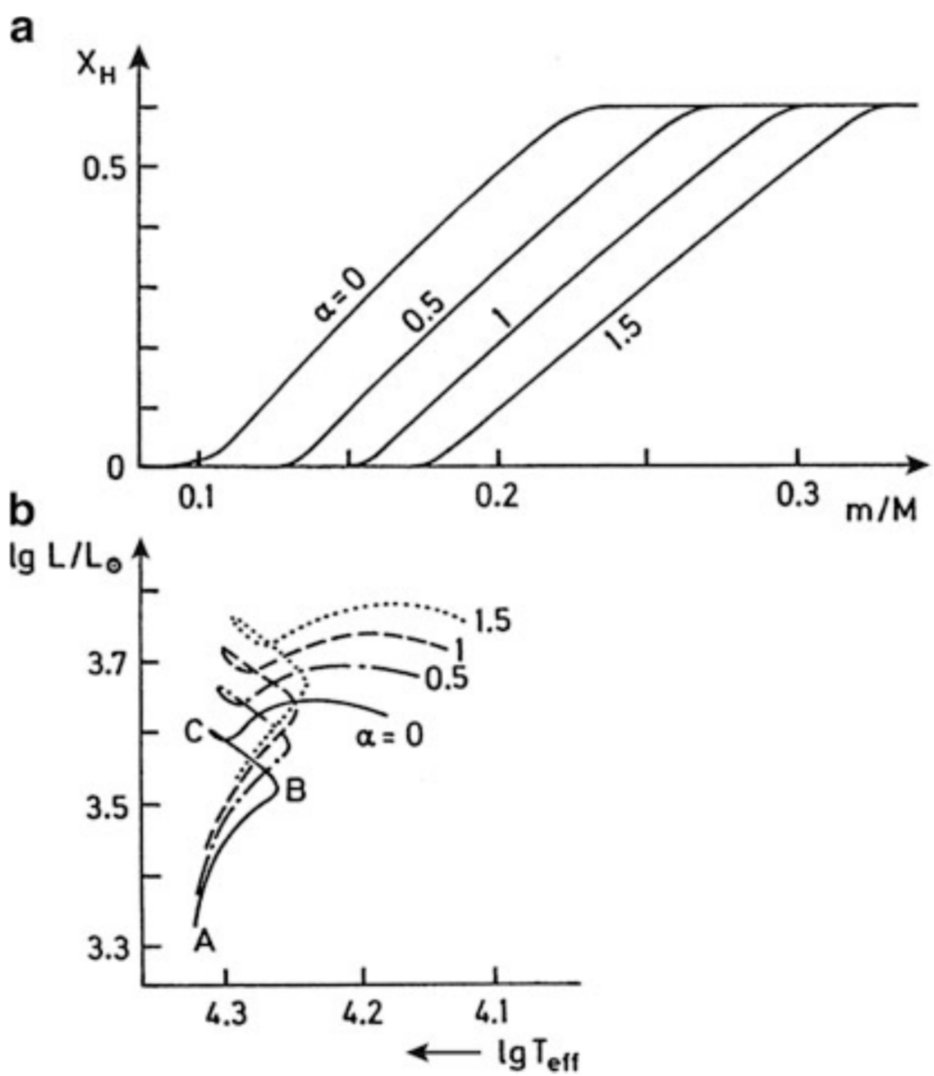

Kippenhahn, Weigert & Weiss 2012

overshooting ($\alpha > 0$) brings more hydrogen in the core

$\rightarrow$ Helium core becomes larger

$\rightarrow$ Main-sequence age increases

$\rightarrow$ Broader main sequence

Open issue in stellar evolution theory

Semiconvection

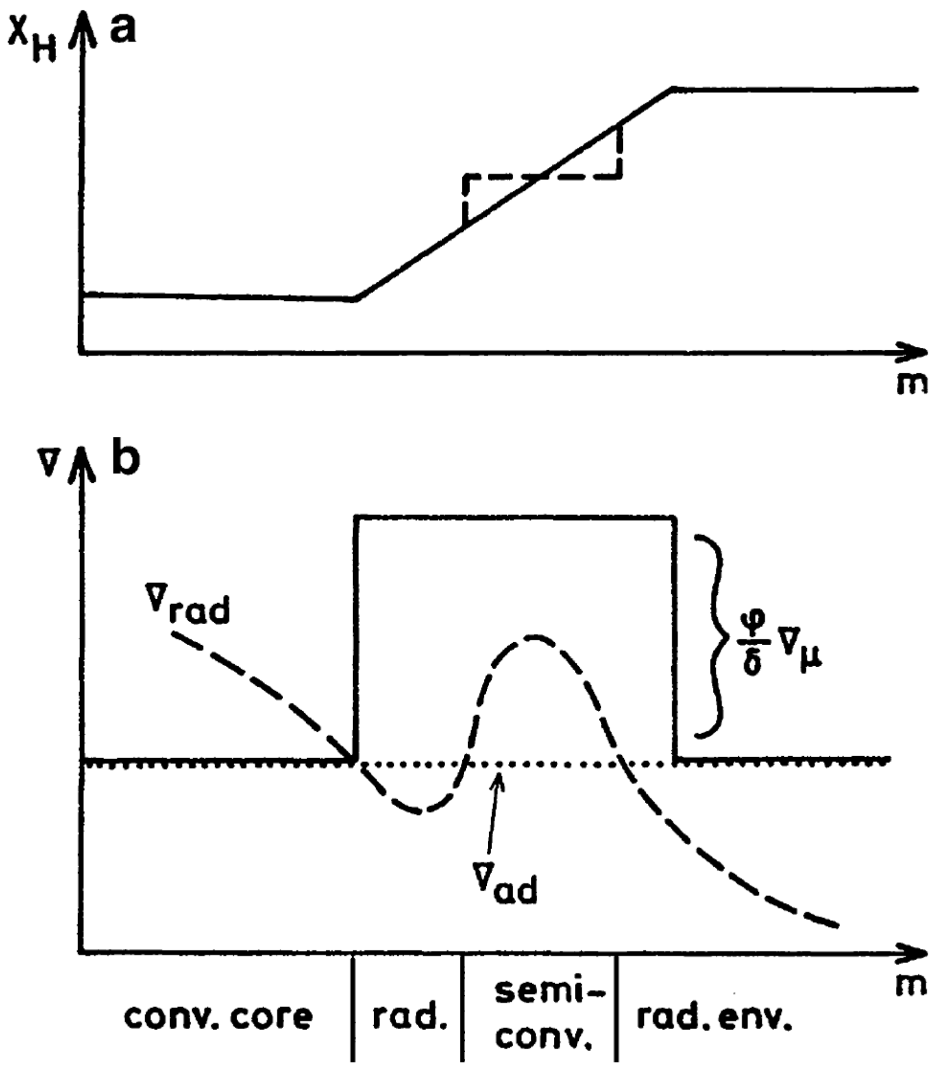

Kippenhahn, Weigert & Weiss 2012

semiconvection: slow mixing

massive stars $M \gtrsim 10\,\mathrm{M}_\odot$

- during central hydrogen burning the convective core retreats, leaving a certain hydrogen profile behind
- radiative gradient ∇_{rad} outside the core starts to rise and soon exceeds the adiabatic gradient ∇_{ad}
- dynamically stable due to Ledoux criterion

$$\nabla_{\mathrm{ad}} < \nabla_{\mathrm{rad}} < \nabla_{\mathrm{ad}} + \frac{\phi}{\delta}\nabla_\mu$$

- slightly displaced mass element starts to oscillate with slowly growing amplitude, penetrates more and more into regions of different chemical composition

Schönberg-Chandrasekhar Limit (SC-Limit)

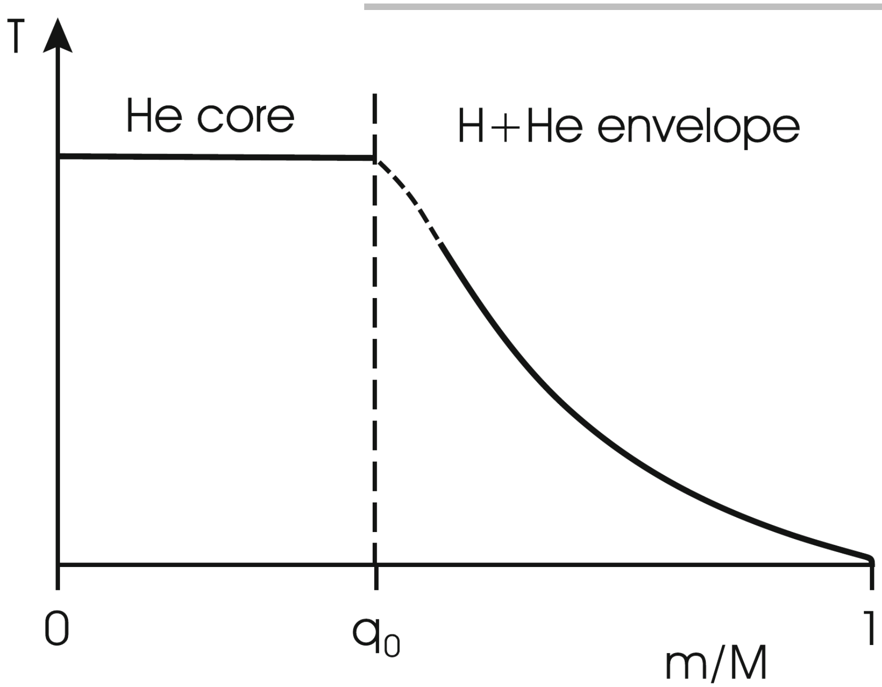

- at end of central H-burning, H-burning moves outward in a shell
- No energy produced in the He-core

$\rightarrow$ Isothermmal T_c = const

- Core grows in mass

How long can this last?

Kippenhahn, Weigert & Weiss 2012

Virial theorem for separate core and envelope:

$$P_0 = P_{\text{gas}} - P_{\text{grav}} = \frac{3}{4\pi}\frac{\mathcal{R}}{\mu_c}\frac{T_0 M_c}{R_c^3} - \frac{\theta G M_c^2}{4\pi R_c^4}$$

Maximum value $P_{0,\text{max}}$ at the radius $R_{c,\text{max}}$

$$\frac{dP_0}{dR_c} = 0 \Rightarrow R_{c,\text{max}} = \frac{4\theta G}{9\mathcal{R}}\frac{M_c \mu_c}{T_c} \Rightarrow P_{0,\text{max}} = C\frac{T_c^4}{\mu_c^4 M_c^2}$$

Schönberg-Chandrasekhar Limit (SC-Limit)

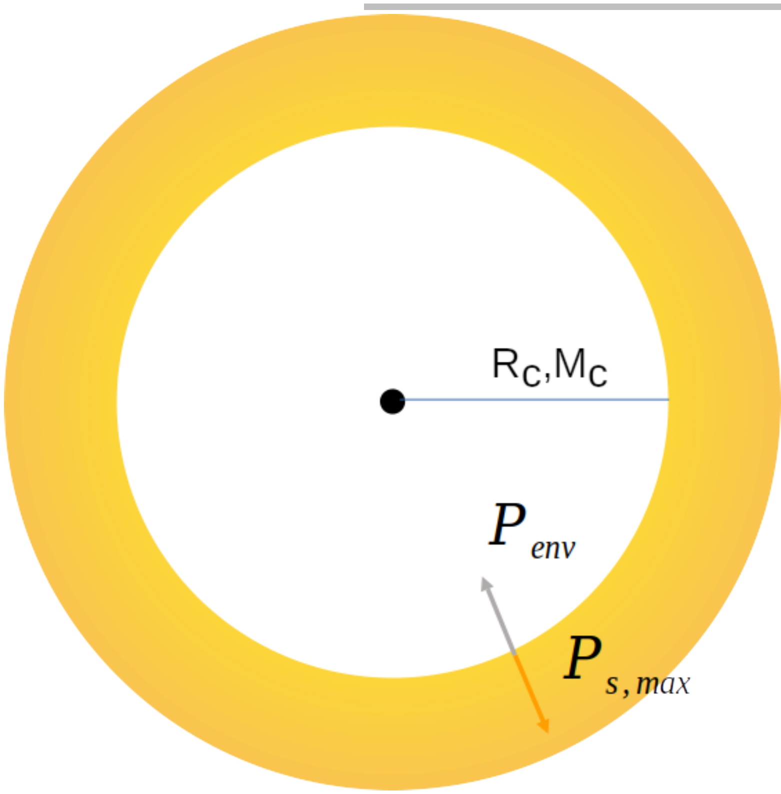

- $P_{0,\mathrm{max}}$ must balance the pressure exerted by the envelope P_{env}
- Assuming the core to be a point mass and hydrostatic equilibrium
  $\rightarrow P_{\mathrm{env}}$ equals the central pressure P_{c}

$$\Rightarrow C\frac{T_{\mathrm{c}}^4}{\mu_{\mathrm{c}}^4 M_{\mathrm{c}}^2} \geq \frac{GM^2}{8\pi R^4}$$

- Homology relation

$$T_{\mathrm{c}} \simeq \mu_{\mathrm{env}} M/R$$

$$\Rightarrow \frac{M_{\mathrm{c}}}{M} \leq \text{constant}\left(\frac{\mu_{\mathrm{env}}}{\mu_{\mathrm{c}}}\right)^2 \approx 0.37\left(\frac{\mu_{\mathrm{env}}}{\mu_{\mathrm{c}}}\right)^2 \approx 0.1 \tag{9.2}$$

Stars with mass $M > 2\,\mathrm{M}_\odot$: when mass of the He-core exceeds the SC-limit, the core starts to contract rapidly and the star leaves the main sequence.

For smaller stars: gas in the He-core partially degenerate before the star reaches the SC-limit (not T depended, hydrostatic equilibrium with higher P).

Schönberg-Chandrasekhar Limit (SC-Limit)

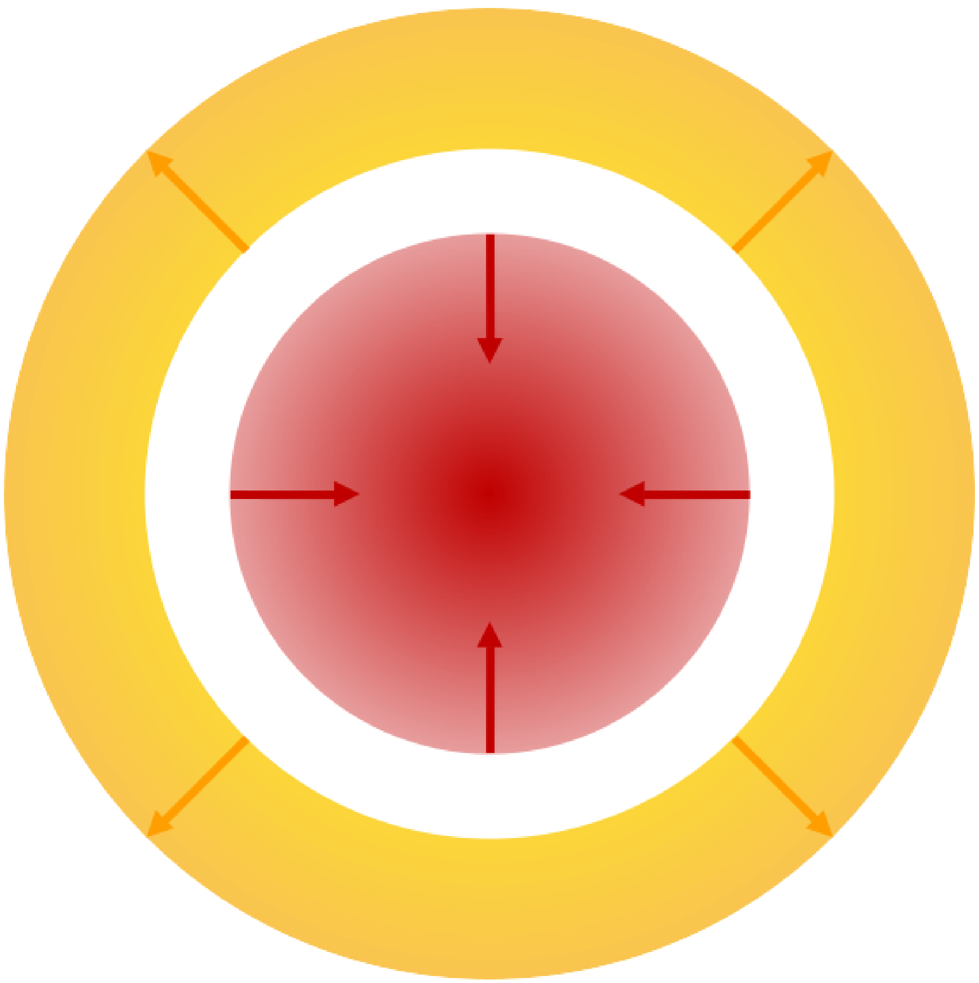

- **Contraction** of the He-core leads to **heating** of the core on the Kelvin-Helmholtz timescale (much shorter than nuclear timescale)
- As the core contracts, it generates energy, which flows outward

$\rightarrow$ The envelope expands

$\rightarrow$ The star moves to the red giant branch

The details of the further evolution strongly depend on stellar mass.

- **Low-mass stars** ($< 2.5\,\mathrm{M}_\odot$)
- **Intermediate-mass stars** ($2.5 - 8\,\mathrm{M}_\odot$)
- **Massive stars** ($> 8\,\mathrm{M}_\odot$)

Post-main sequence evolution

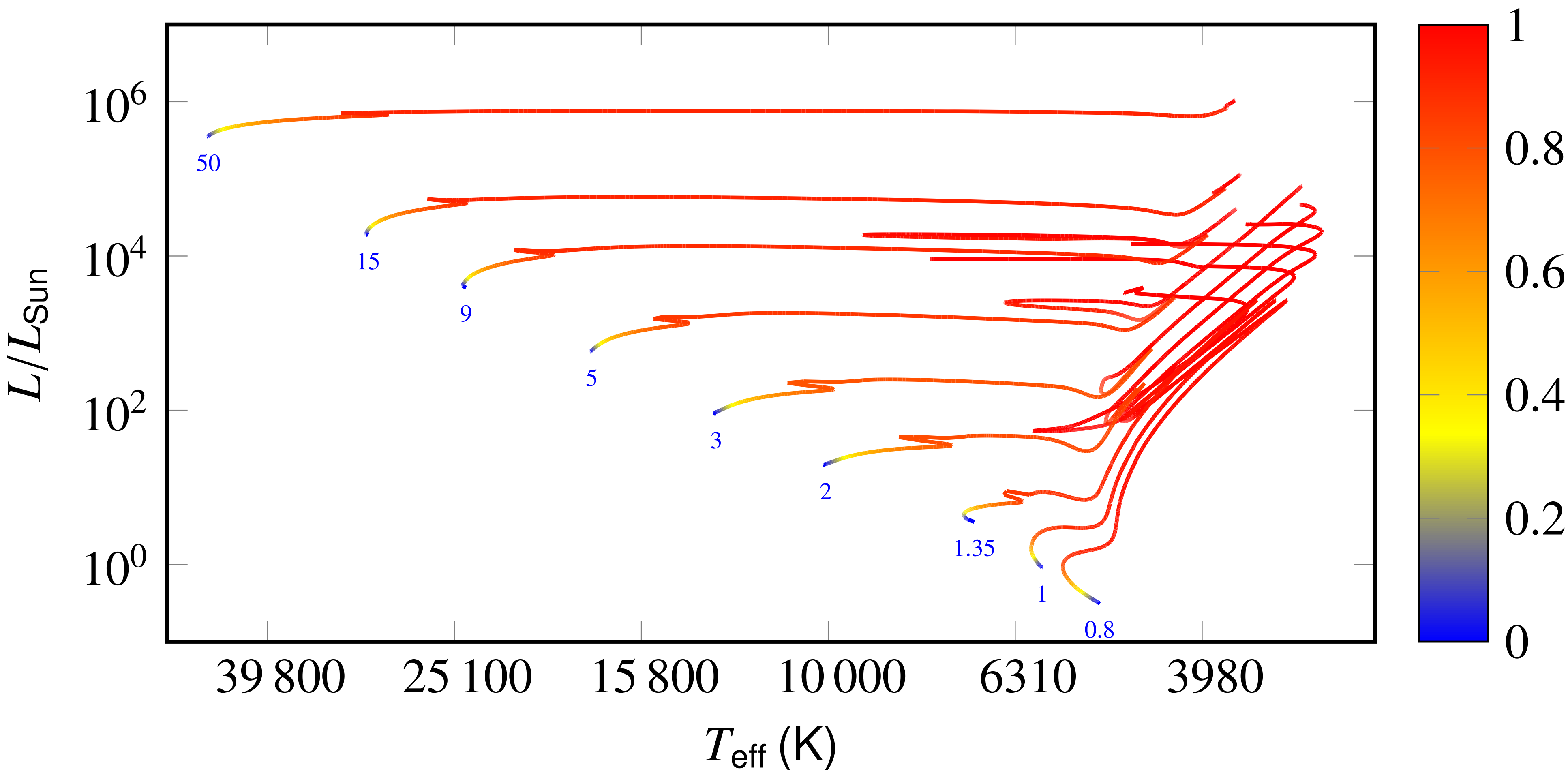

Theoretical Hertzsprung-Russell diagram (based on EZ-models with $X = 0.73$, $Y = 0.26$). The blue numbers indicate the mass in $M_\odot$. The color codes the fractional age on the displayed portion of the track.

Kippenhahn diagram

Kippenhahn diagram shows internal structure of star

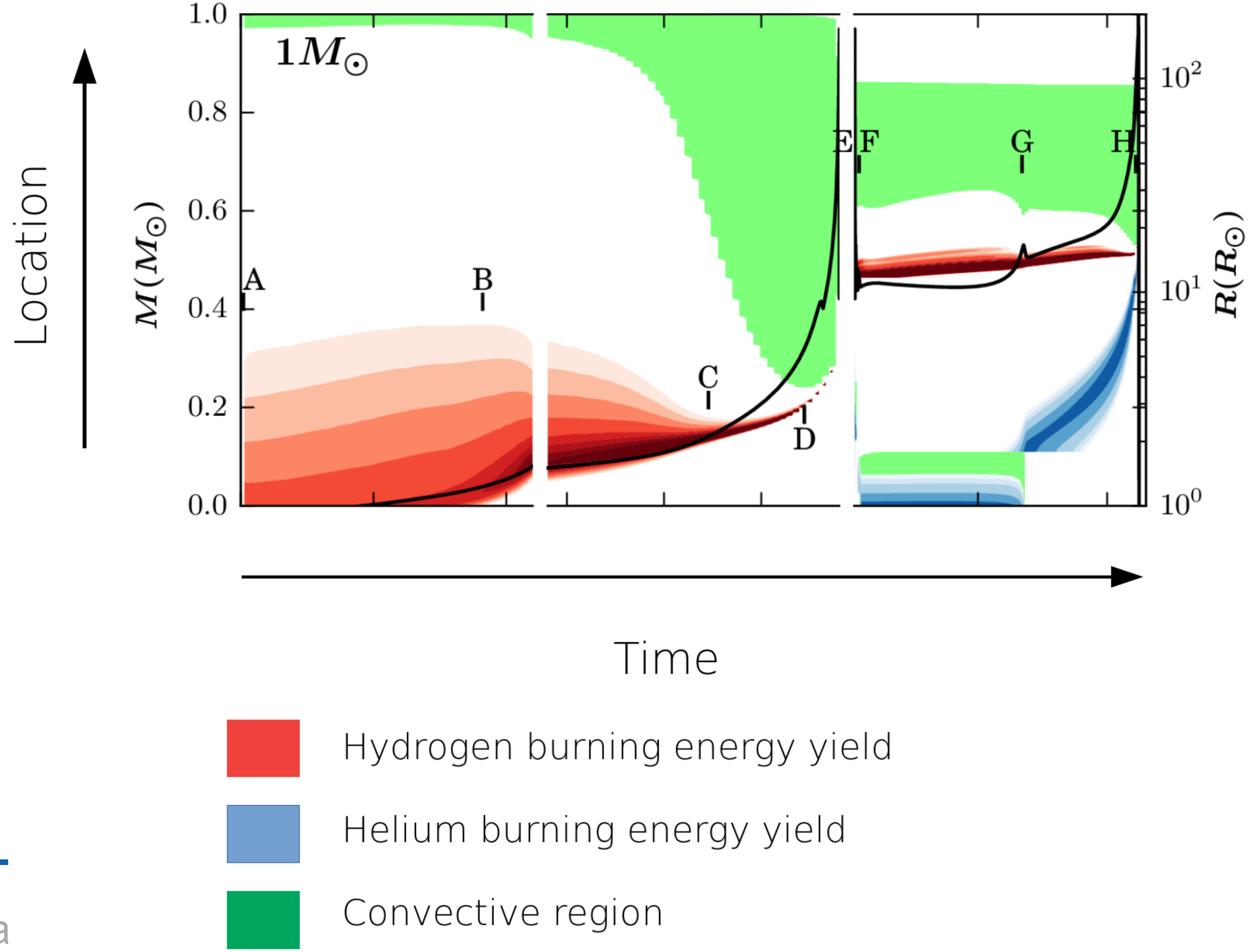

Intermediate stars im HRD (EZ model for a $5\,M_\odot$ star)

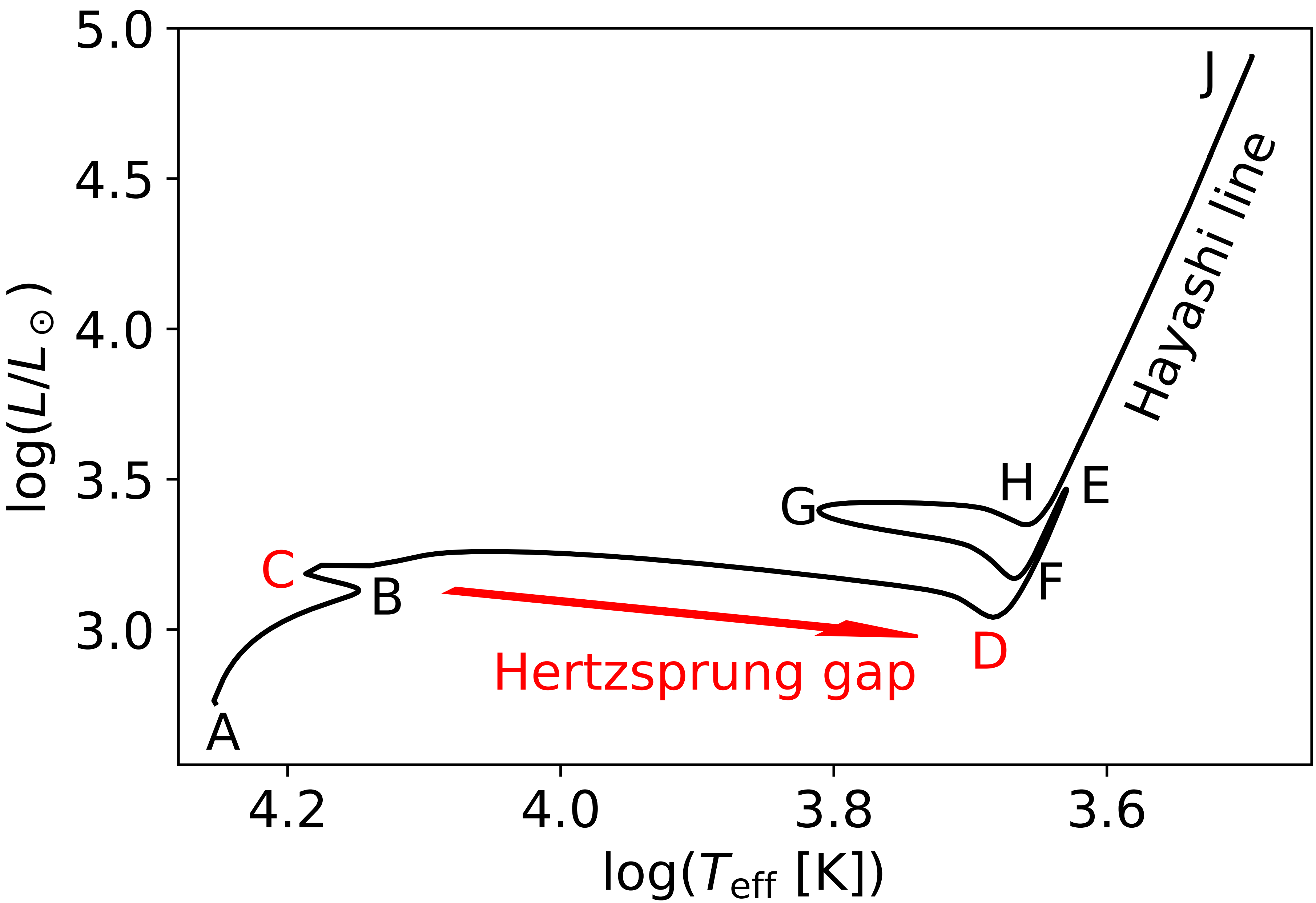

Post-main sequence evolution – Intermediate stars

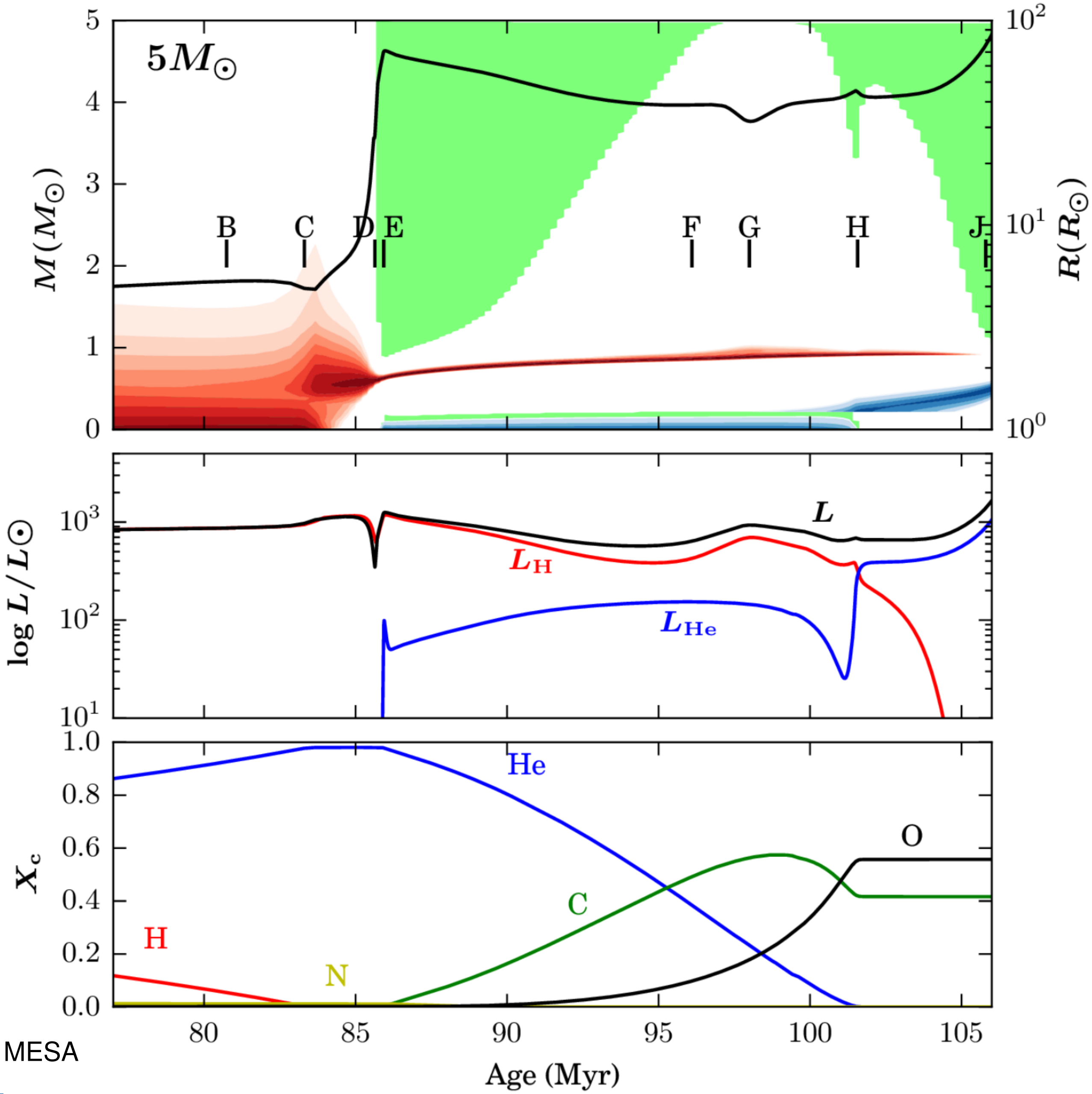

Main sequence (A-B)

- main energy production is H-burning due to CNO cycle
- stronger temperature dependence as PP cycle → star will expand more during the MS than a lower mass star

Main sequence (B-C)

- At point B the central H is getting depleted and the core starts contracting
- At C, all H in the core is used up.

Post-main sequence evolution – Intermediate stars

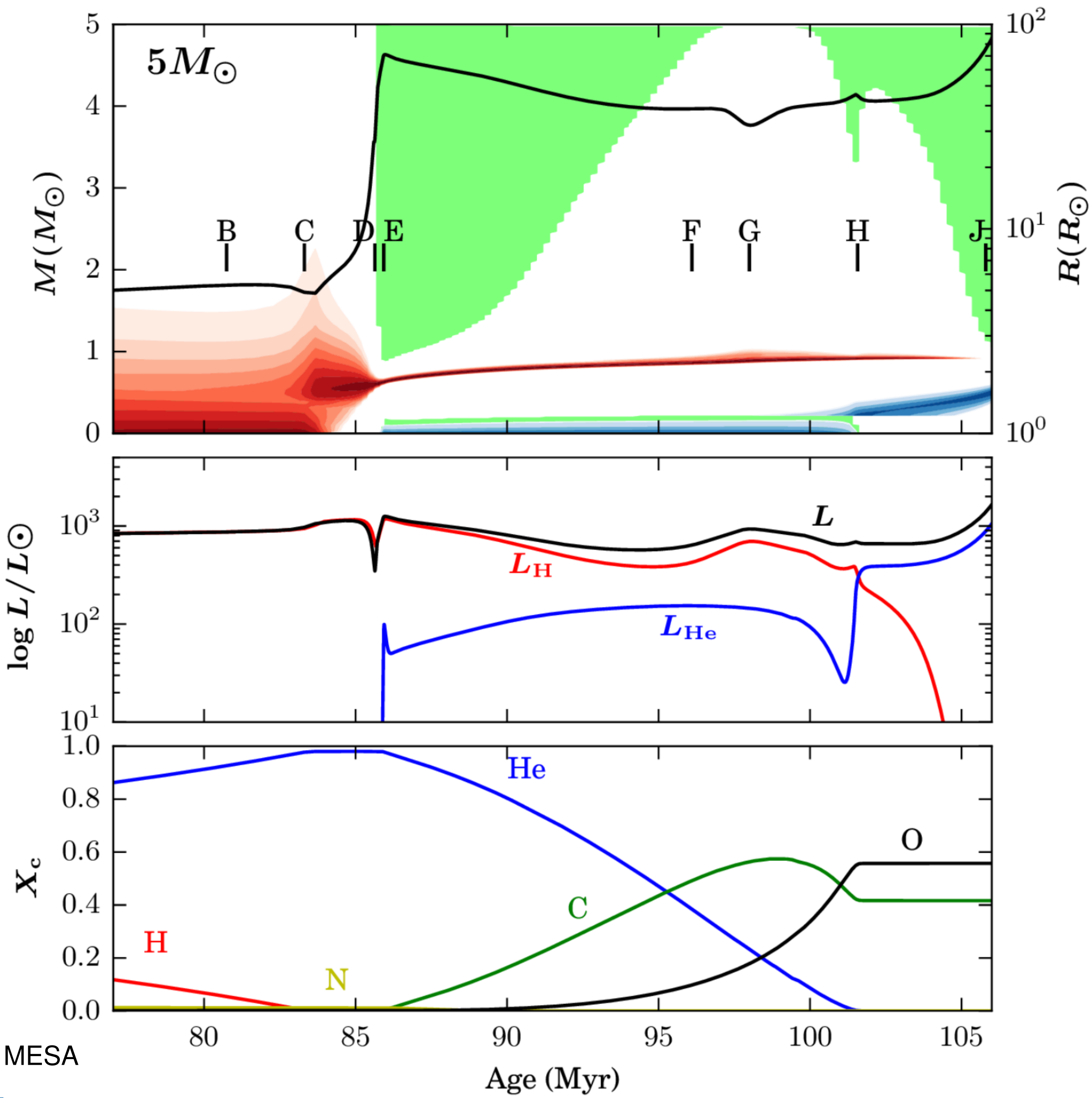

MESA

Thick shell burning (C-D)

- When the core H is exhausted, quick transition to H shell burning.
- Temperature gradient is small because the outer layers haven't puffed up much yet.

$\rightarrow$ H shell takes place in a thick shell.

- core keeps growing in mass

Post-main sequence evolution – Intermediate stars

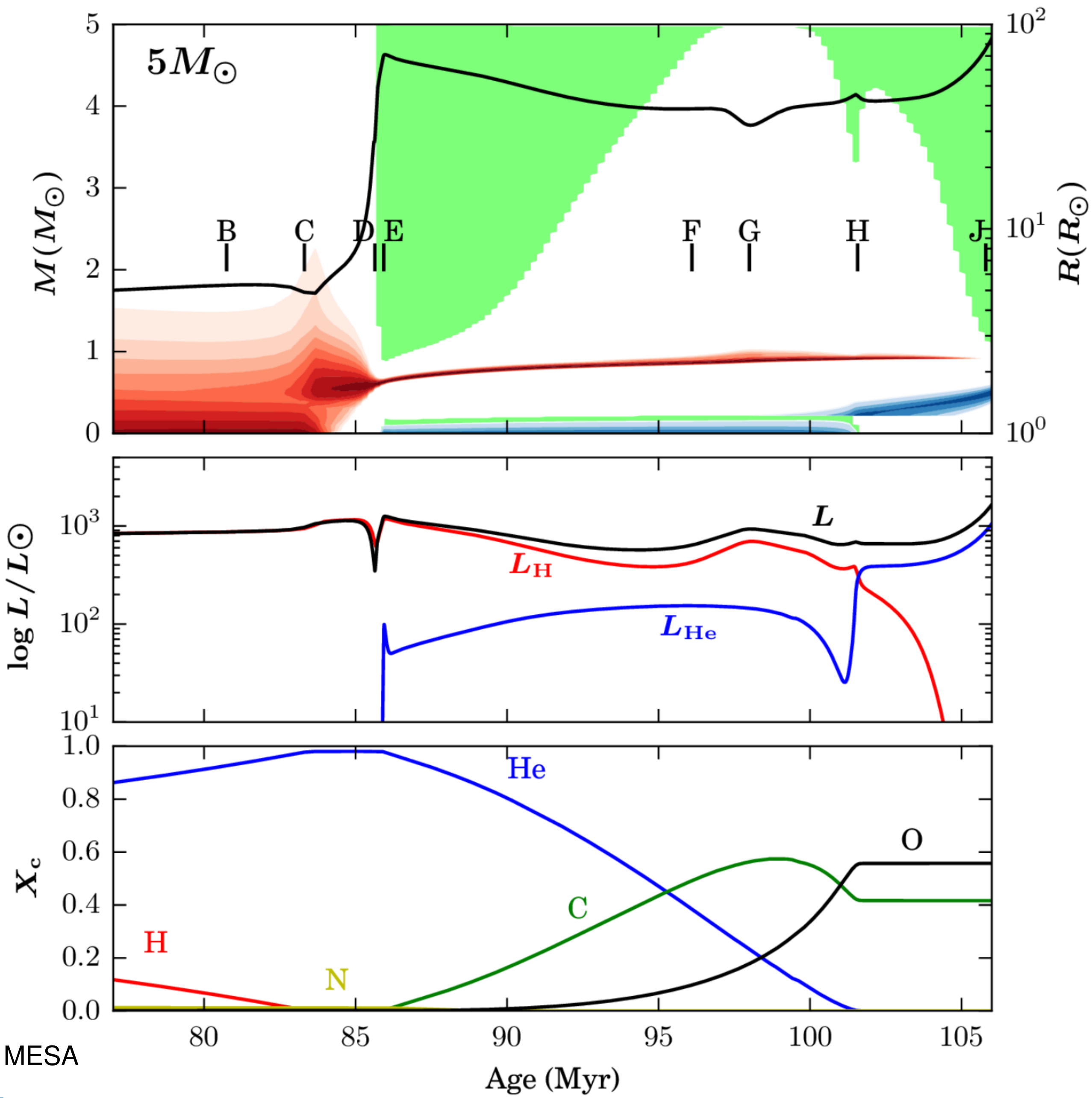

MESA

Thick shell burning (C-D)

- Fast evolution on Kelvin-Helmholtz timescale $\sim 10^7$ yr
- Not many stars in observed HRDs $\rightarrow$ **Hertzsprung gap**
- Luminosity and $T_{\rm eff}$ drops by a factor of ~ 3
- Radius increases by a factor of ~ 5
- at D core exceeds Schönberg-Chandrasekhar limit $\rightarrow$ envelope pushed out

Post-main sequence evolution – Intermediate stars

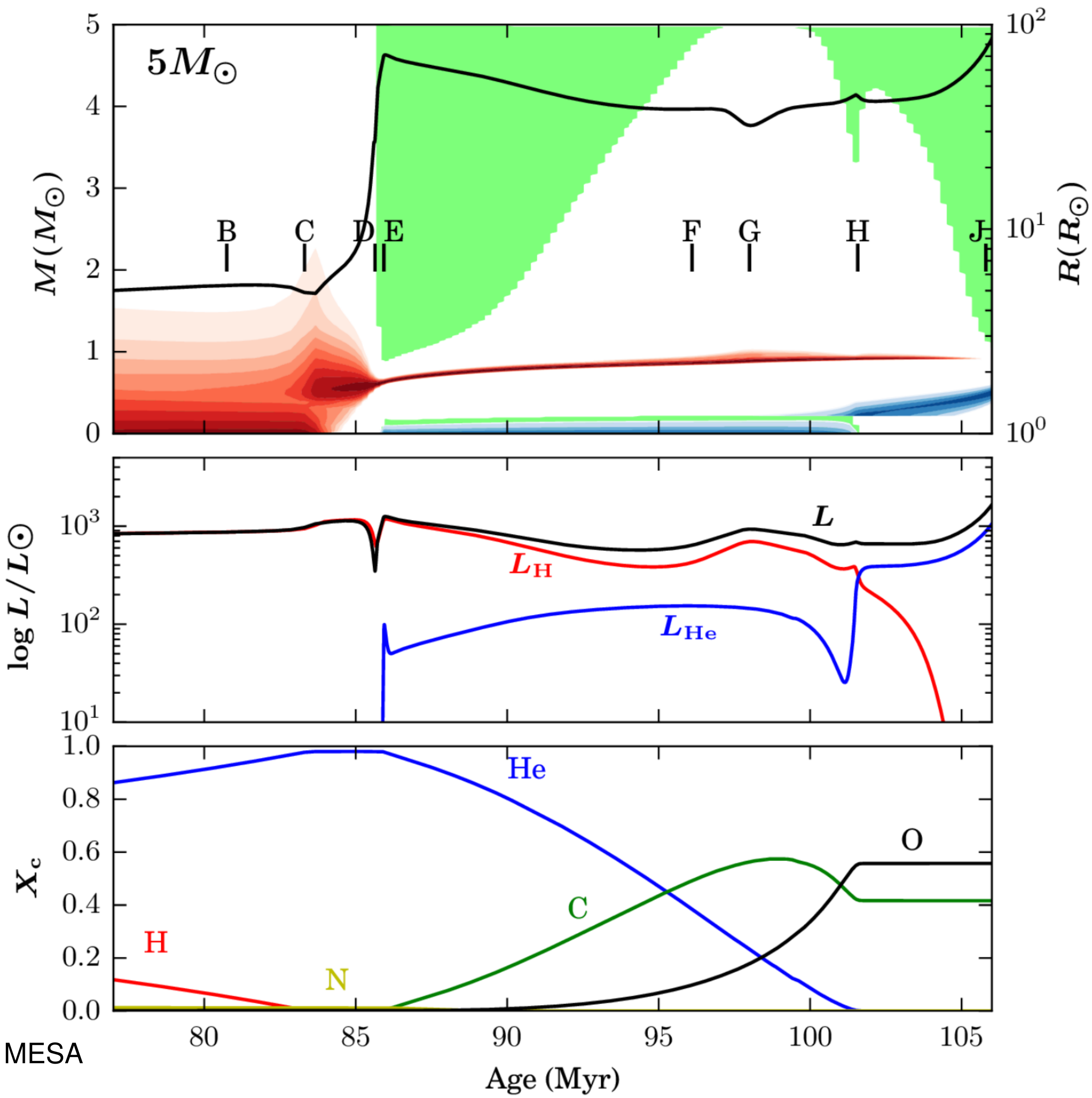

MESA

Red giant branch (RGB, D-E)

- expansion of the outer layers causes the T gradient to become steeper, and the H burning shell becomes much thinner
- envelope is fully convective: star is on the RGB
- Convection reaches into regions with nuclear processed material
- **First dredge-up** of processed material to the surface

$\rightarrow$ Red giant – Luminosity class III – $T \sim 4000 - 5000$ K

Post-main sequence evolution – Intermediate stars

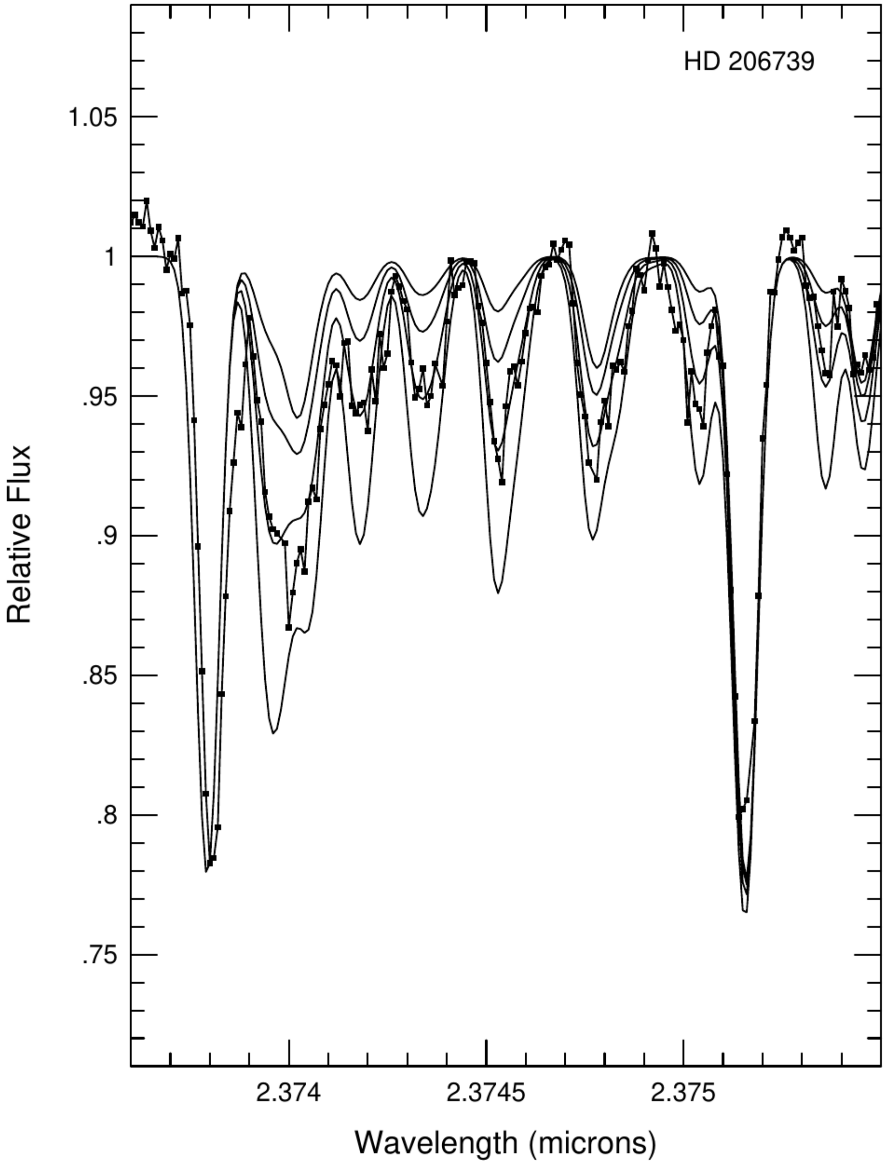

Keller, Pilachowski & Sneden 2001, AJ, 122, 2554

First dredge-up

- primordial ratio of the carbon isotopes $^{12}\mathrm{C}/^{13}\mathrm{C} \simeq 90$ is reduced due to CNO-processing
- first dredge-up brings material to the surface
- Molecular bands of CO in IR-spectra can be used to determine this ratio (10 ± 1)

$\rightarrow$ **Evidence** for the **first dredge-up** has been found

Post-main sequence evolution – Intermediate stars

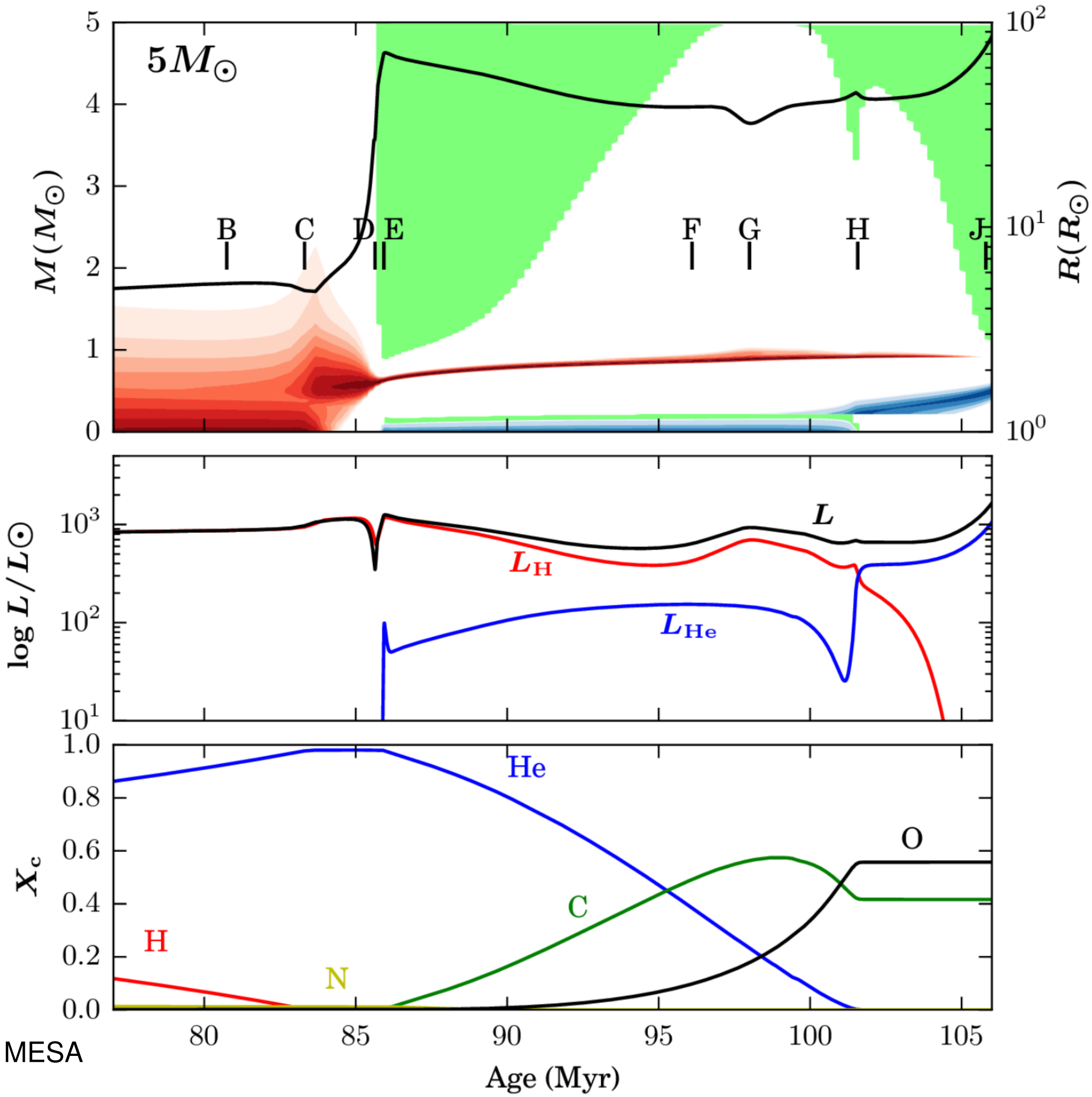

He ignition (E)

- When the core of the star reaches $T \sim 10^8$ K, it ignites Helium under non-degenerate conditions.
- He burning starts 'gently'
- reaction $3\,\alpha \longrightarrow {}^{12}$C, later ^{12}C + $\alpha \longrightarrow {}^{16}$O
- eventually ${}^{16}\mathrm{O}/{}^{12}\mathrm{C} \approx 0.5$

Blue loop (E-F-G-H)

- Star becomes smaller and hotter
- During core He burning, the star goes through the blue loop.

Post-main sequence evolution – Intermediate stars

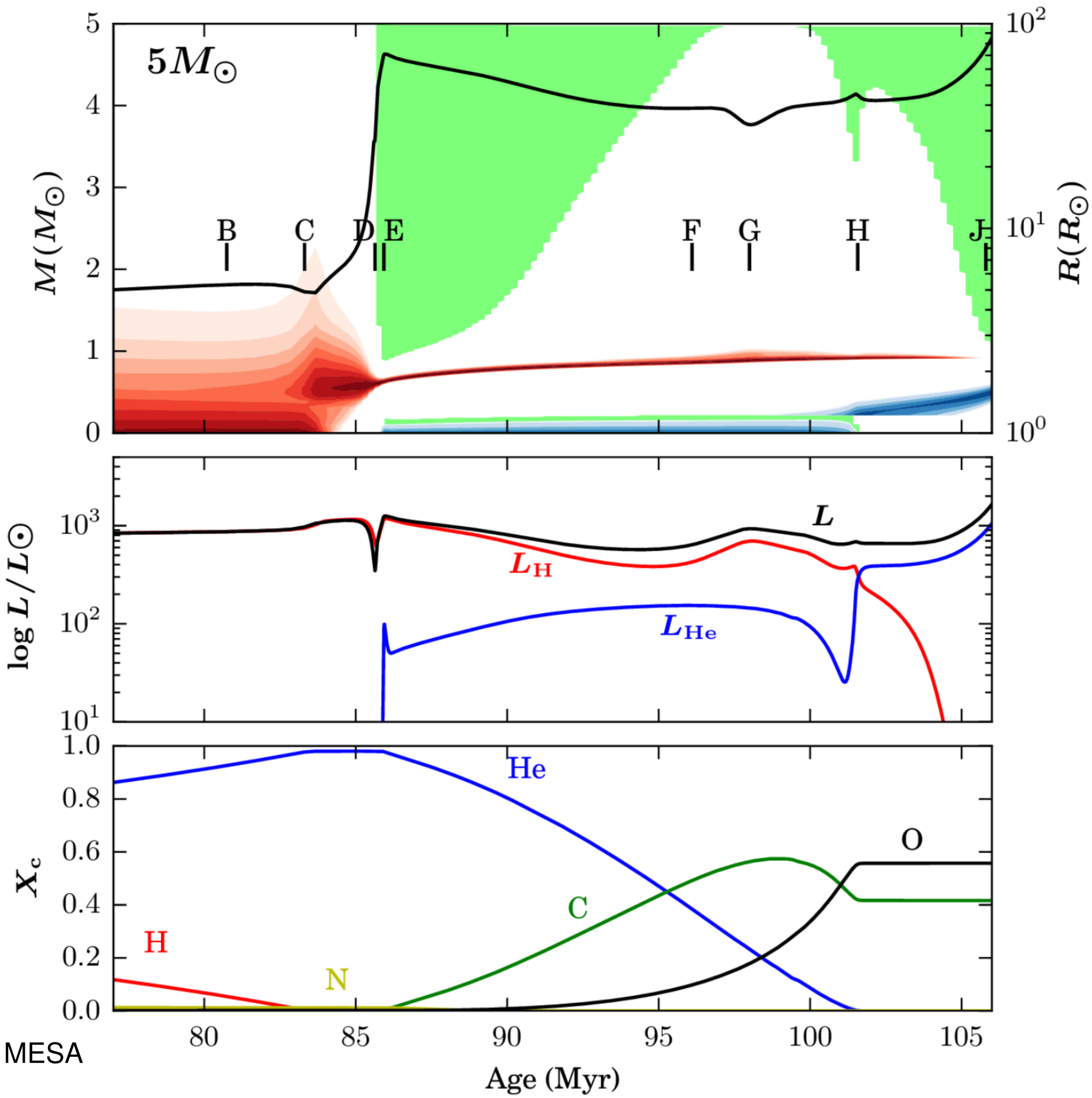

MESA

Blue loop (E-F-G-H)

- blueward direction: H-burning shell maintains an even level of efficiency and He-burning core increases
- redward: core starts to decrease in luminosity as He is running low
- important to explain Cepheid stars, when crossing the instability strip
- Details depend on composition, mixing and mass-loss
- Core helium burning stops, when helium is completely processed

Post-main sequence evolution – Intermediate stars

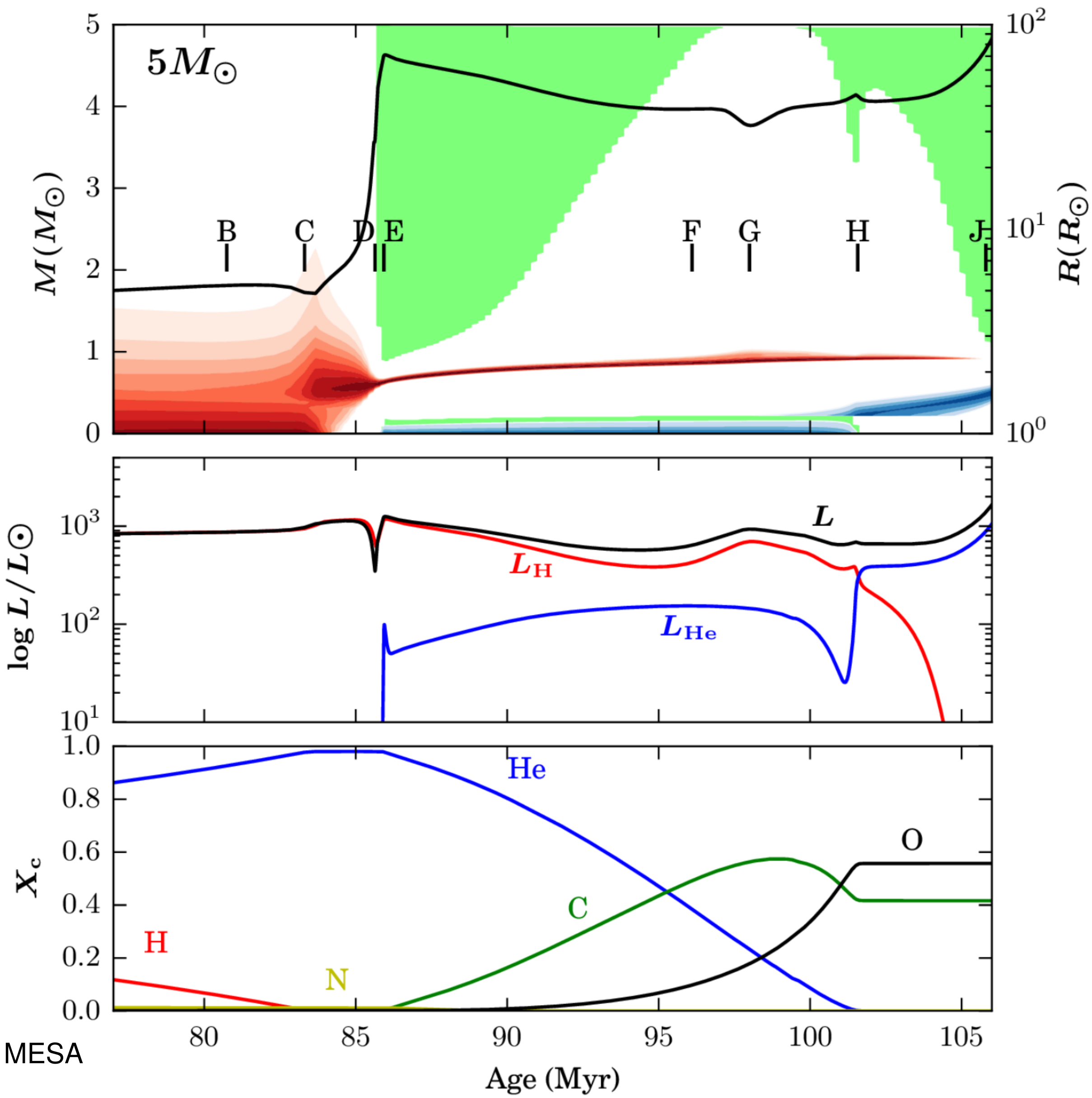

MESA

Asymptotic giant branch

(AGB, H-J)

- C/O core grows in mass and contracts, H and He-shell burning
- star reaches the AGB
- He-burning shell moves outward
- As the stars expands, the temperature in the H-shell drops
- H-shell burning ceases
- Convection reaches (again) into the core region

Post-main sequence evolution – Intermediate stars

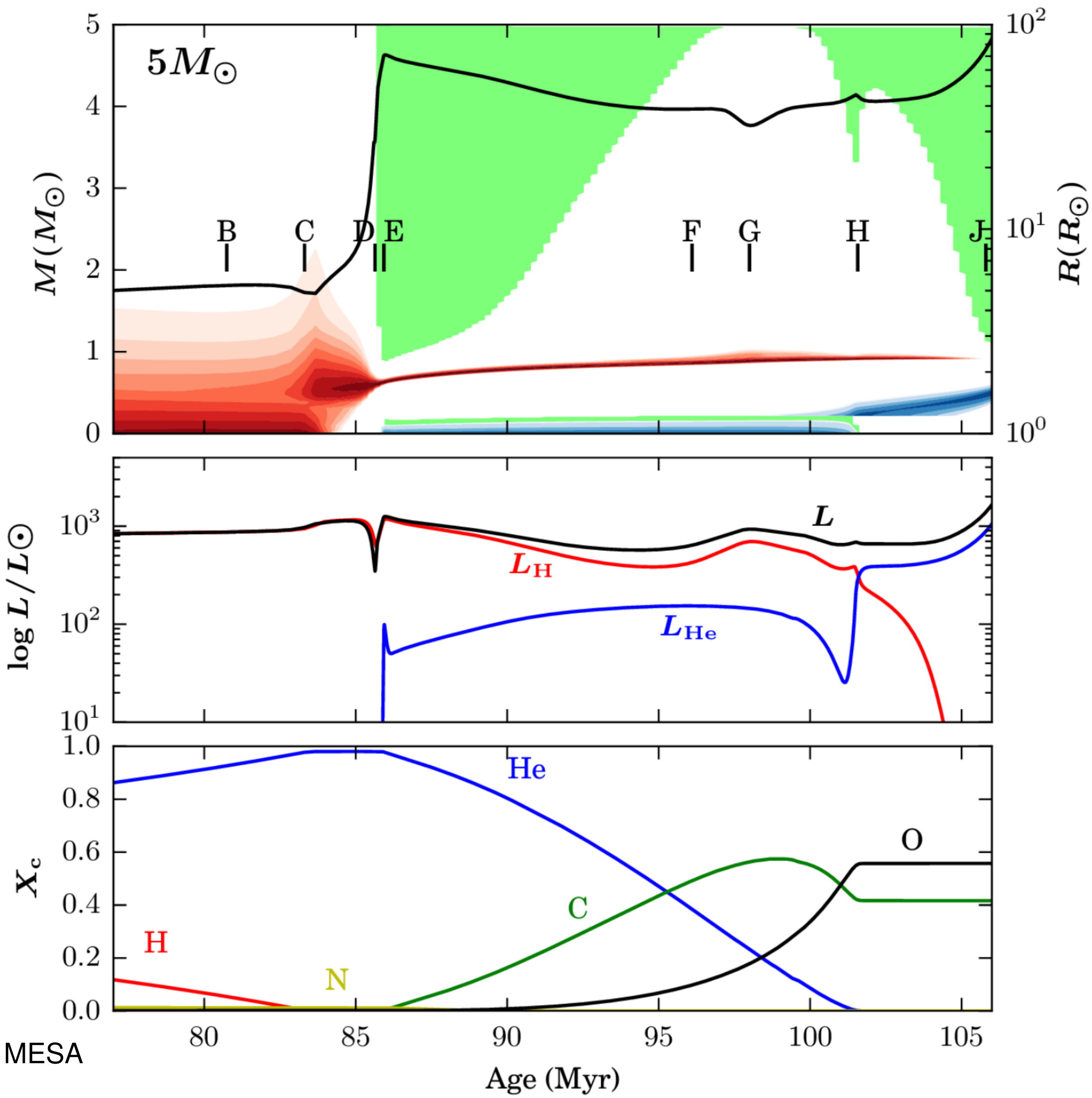

MESA

Asymptotic giant branch (AGB, H-J)

- **Second dredge-up** of H-processed material (He,N) to the surface
- C/O core grows further in mass
- Outward moving He-burning shell reignites H-burning shell

Post-main sequence evolution – Intermediate stars

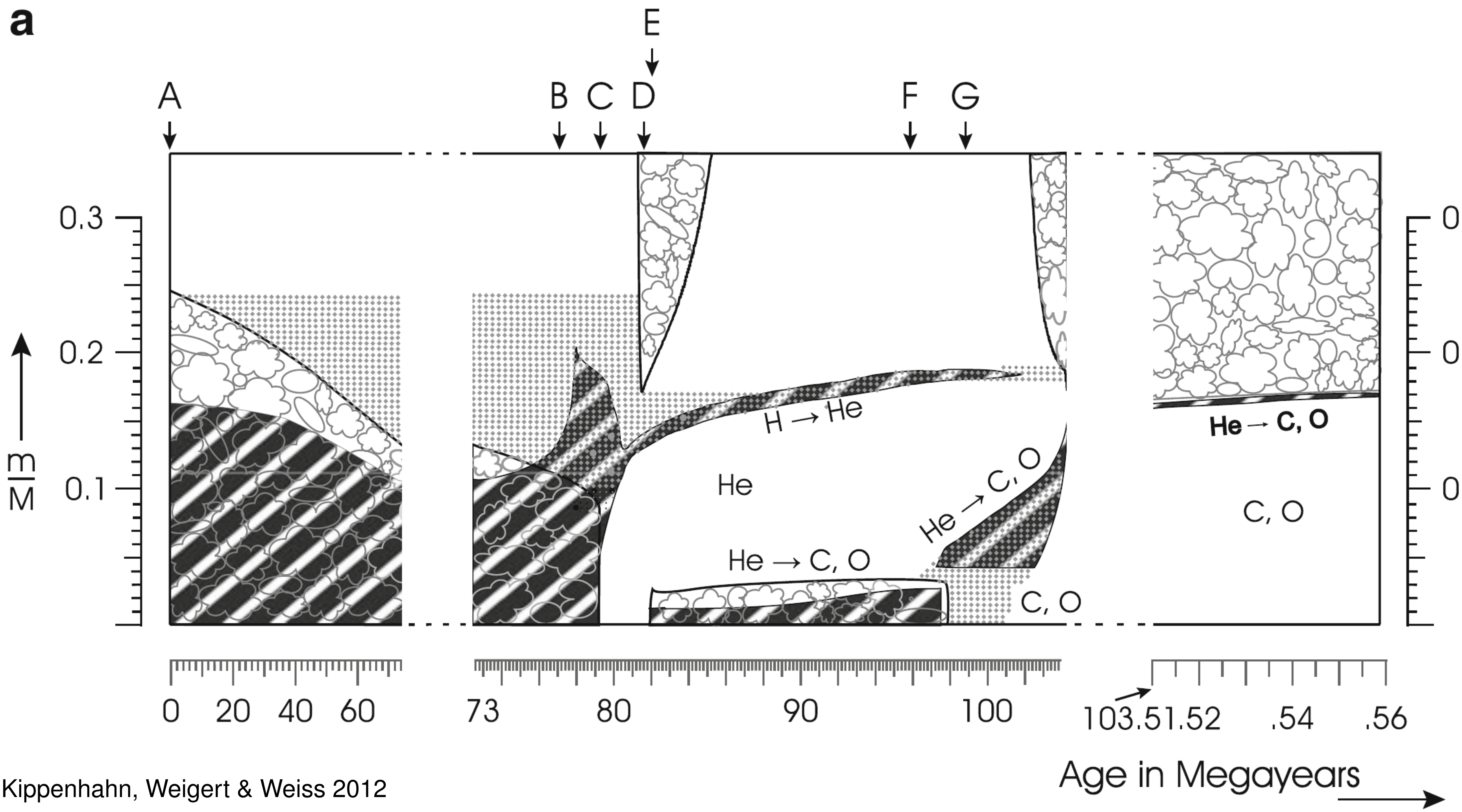

Kippenhahn, Weigert & Weiss 2012

"Cloudy" regions indicate convective areas. Heavily hatched regions indicate where the nuclear energy generation (H or He) exceeds $10^2\,\mathrm{erg\,g^{-1}\,s^{-1}}$. Regions of mixed chemical composition are dotted.

Post-main sequence evolution – Intermediate stars

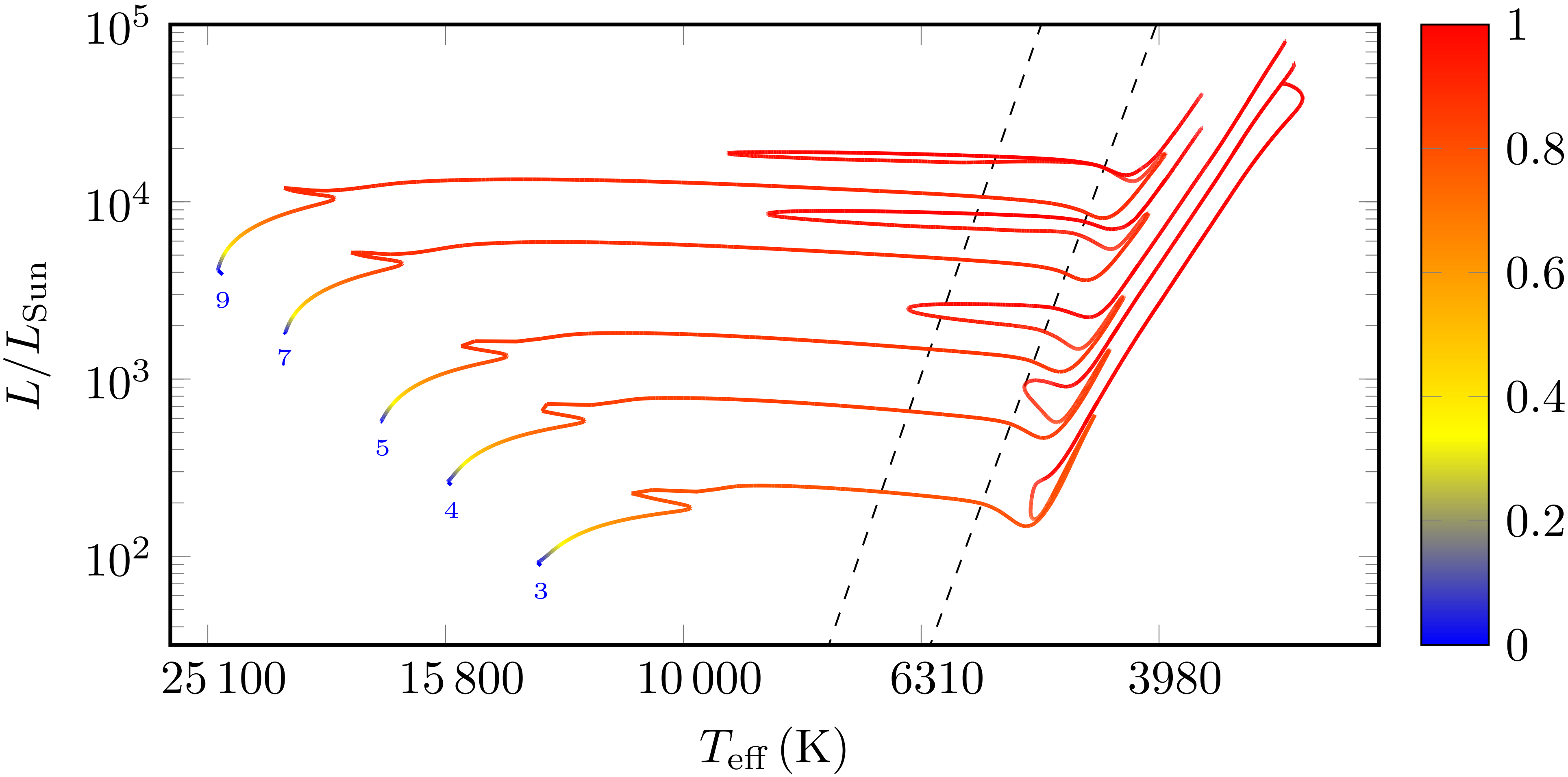

Evolution similar for different intermediate masses

dotted lines: instability strip

Post-main sequence evolution – Massive stars

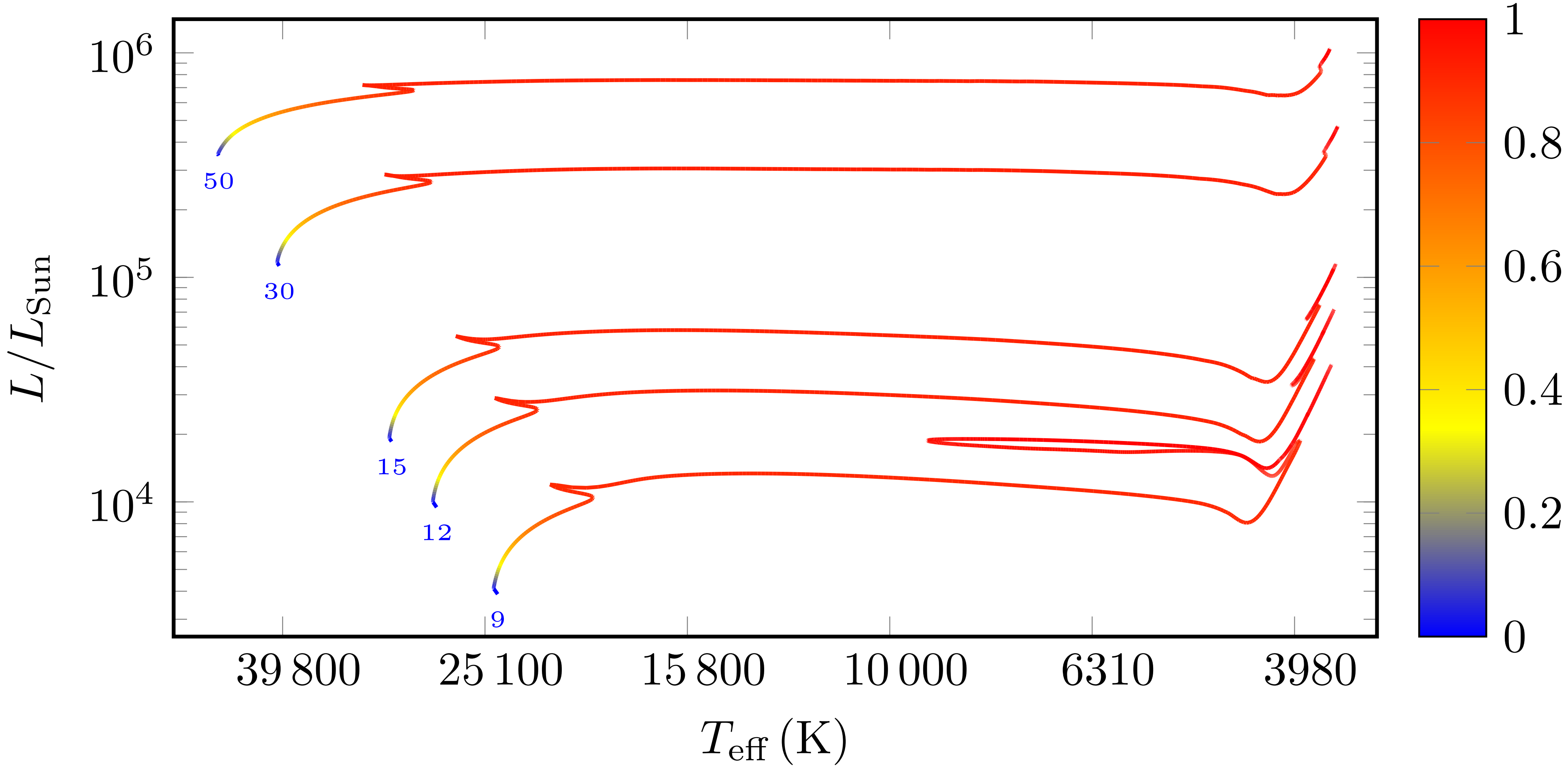

Post-main sequence evolution – Massive stars

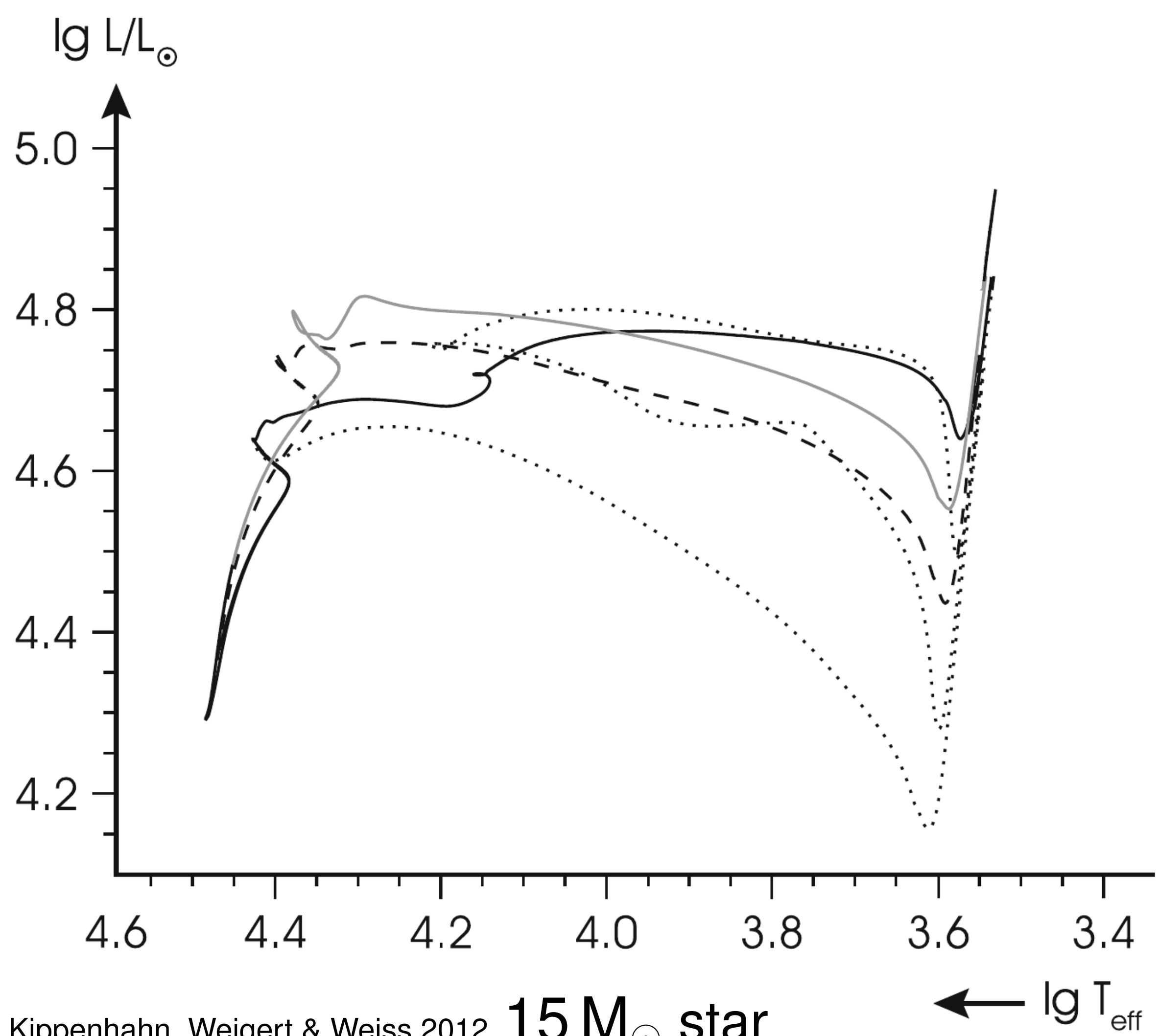

Kippenhahn, Weigert & Weiss 2012 15 M$_\odot$ star

Evolution of high-mass stars depends on uncertain physics

- convective core
  $\rightarrow$ Ledoux or Schwarzschild criterion
- Convective mixing
  - Overshooting
  - Semiconvection
- Rotational mixing
- Mass loss:
  15 M$_\odot$
  $\rightarrow \dot{M} = 1 - 2 \times 10^{-8} M_\odot/\mathrm{yr}$
  $\approx$ 1.15 M$_\odot$ at end of helium burning

grey: with mass loss and overshooting; dotted: Ledoux criterion (semi-convection); black/dashed : Schwarzschild criterion without/with overshooting

Post-main sequence evolution – Massive stars

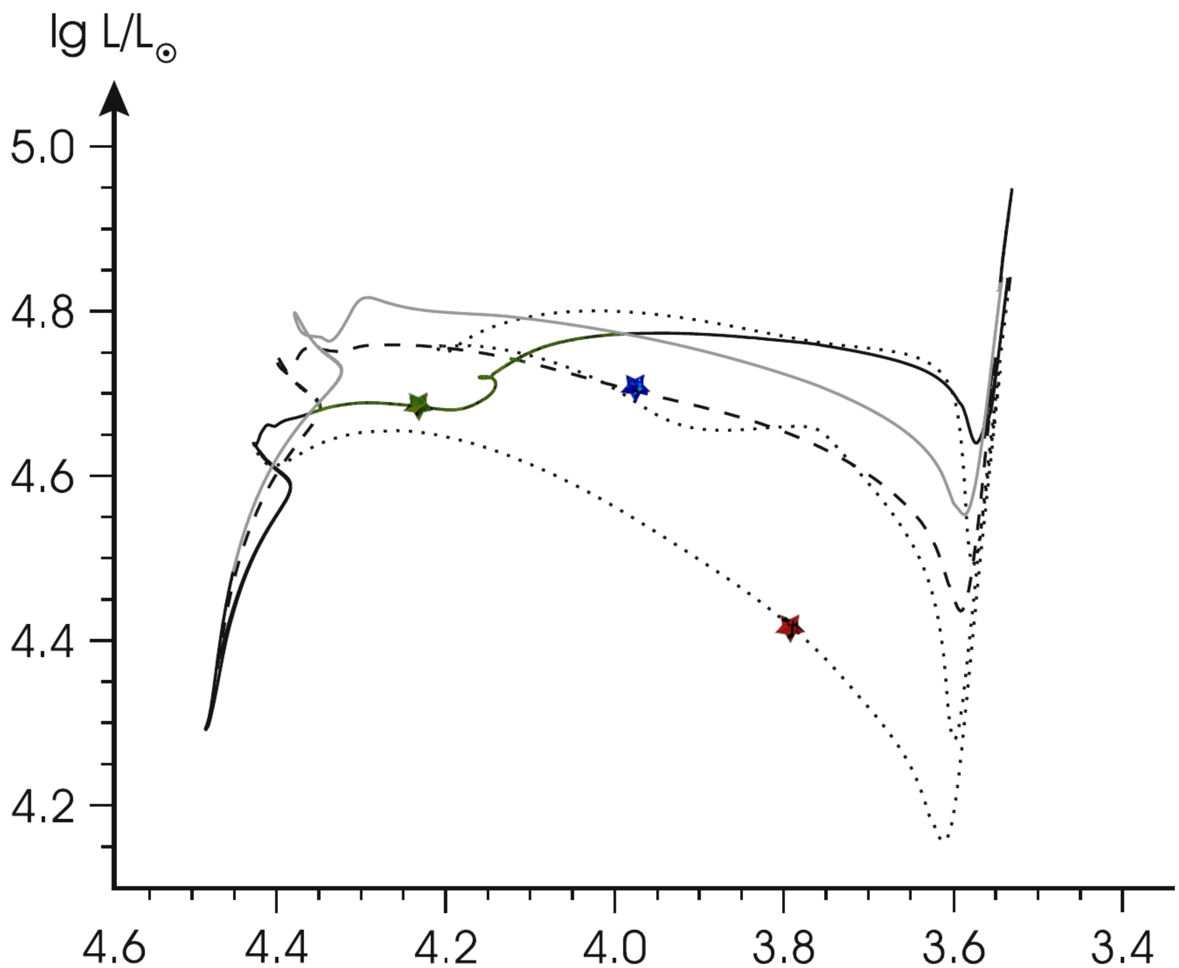

Kippenhahn, Weigert & Weiss 2012 15 $M_\odot$ star

Evolution of high-mass stars

Start of He-core burning ($\sim 10^6$ yr) highly model-dependent

- Schwarzschild criterion: layers become convective more easily and earlier in the evolution, He burning at an age of 9.35 Myr
- Semiconvection: region of varying chemical composition around the convective core $\rightarrow$ longer H-fusion, blue loop
- Overshooting: creating a smooth chemical profile, enlarges the convective helium-burning core, higher luminosity, reduced duration of nuclear phase

Post-main sequence evolution – Massive stars

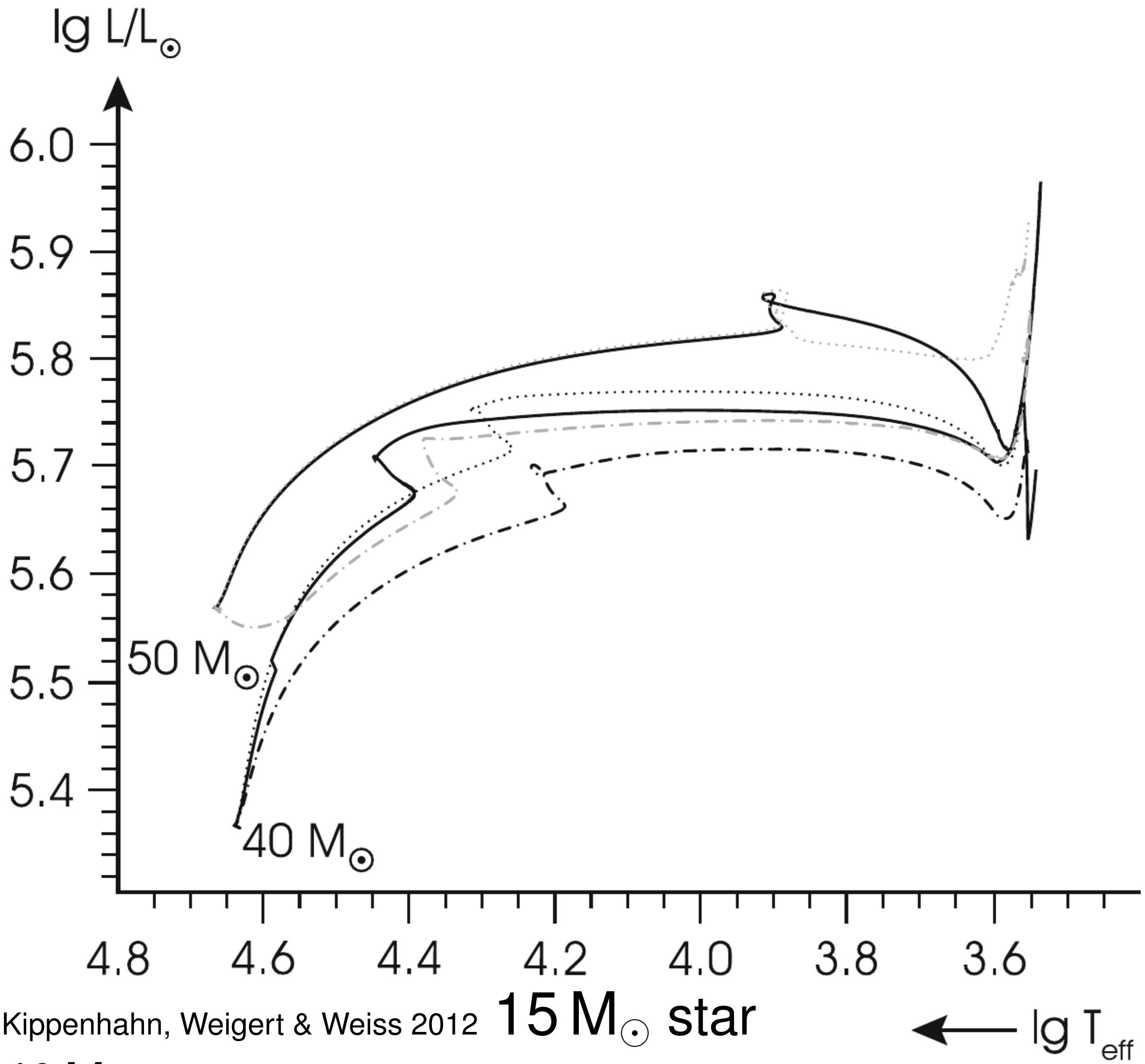

Kippenhahn, Weigert & Weiss 2012 15 $M_\odot$ star

Evolution of very high-mass stars

evolution highly model-dependent

- mass loss: $\sim 10^{-6} M_\odot/\mathrm{yr}$
  $\rightarrow$ timescale much longer than nuclear timescale
  $\rightarrow$ MS lifetime 4.5 Myr
  $\rightarrow$ star can adjust to the reduced mass and evolves similar to star of constant mass $\rightarrow$ (3 times) higher mass-loss: perturbation

40 $M_\odot$ star: Schwarzschild crit. (solid), overshooting (dotted), additional mass loss (dot dashed); 50 $M_\odot$ star: Ledoux criterion (solid), Schwarzschild criterion (grey dotted line), significantly enhanced mass loss (grey dash-dotted)

Post-main sequence evolution – Massive stars

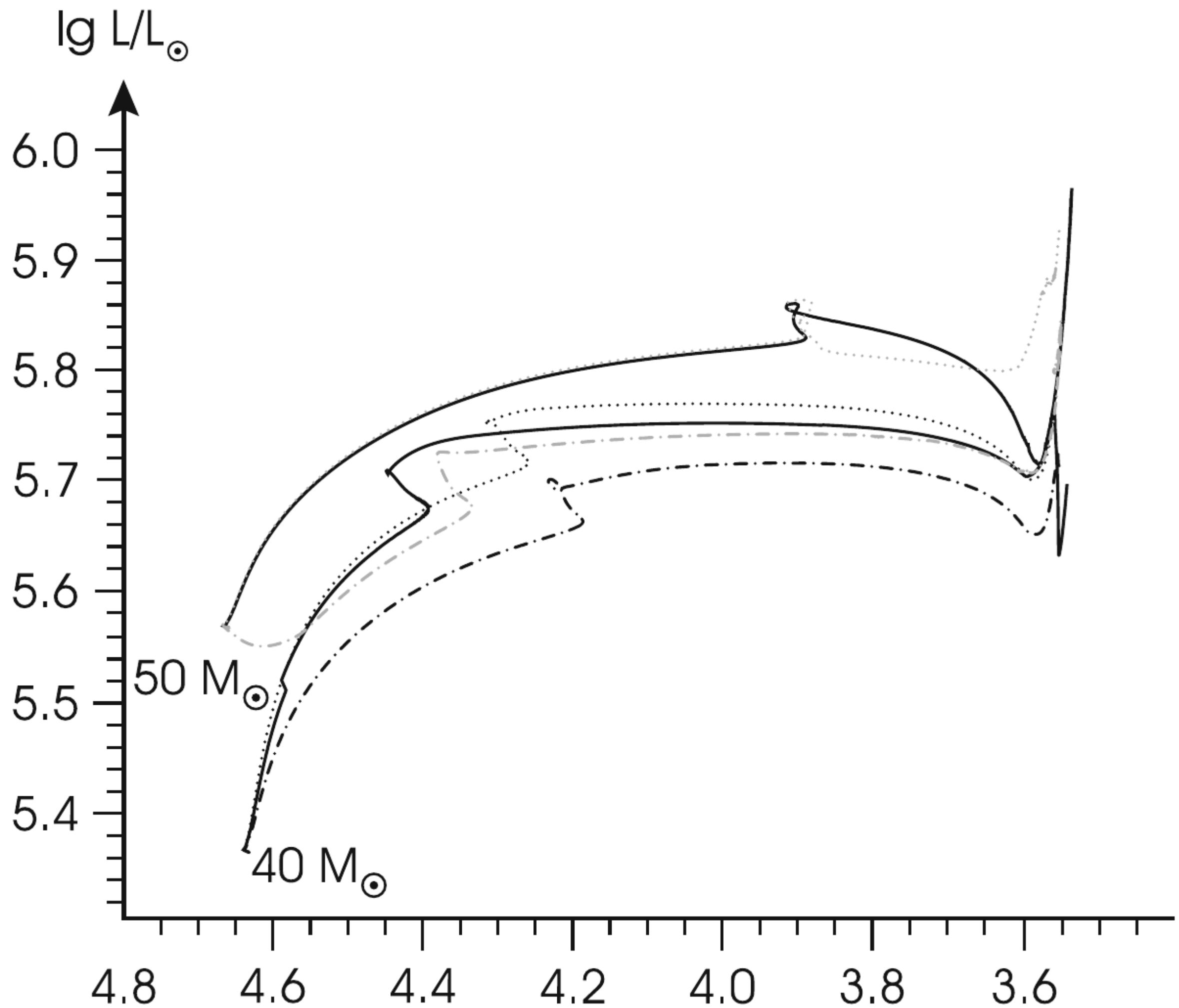

Kippenhahn, Weigert & Weiss 2012 $15\,M_\odot$ star ← lg $T_{\rm eff}$

Evolution of very high-mass stars

mass loss: $10^{-(4-6)} M_\odot/\mathrm{yr}$ caused by strong stellar winds, significant changes of the mass during stellar evolution up to several tens of $M_\odot$

most extreme cases: removal of the entire envelope, leaving behind the extremely hot $(30000 - 120000\,\mathrm{K})$ and still massive ($< 10\,M_\odot$) core surrounded by nebula and called Wolf-Rayet stars

Post-main sequence evolution – Massive stars

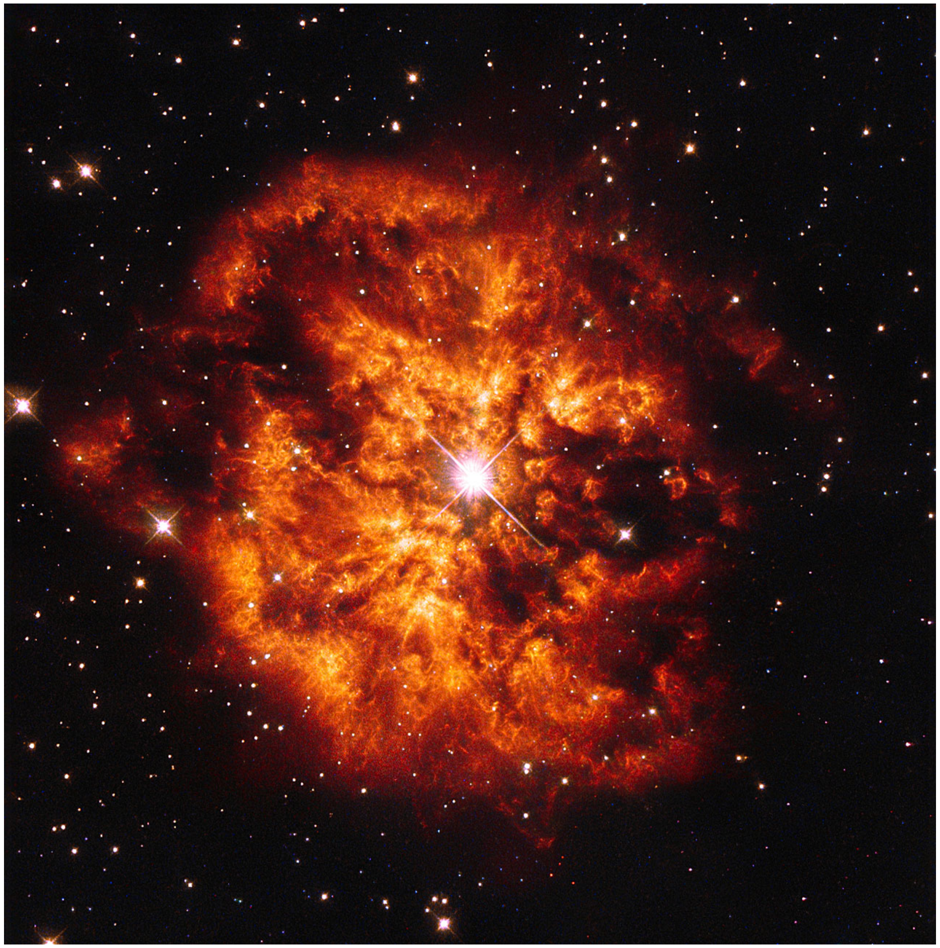

Hubble Legacy Archive

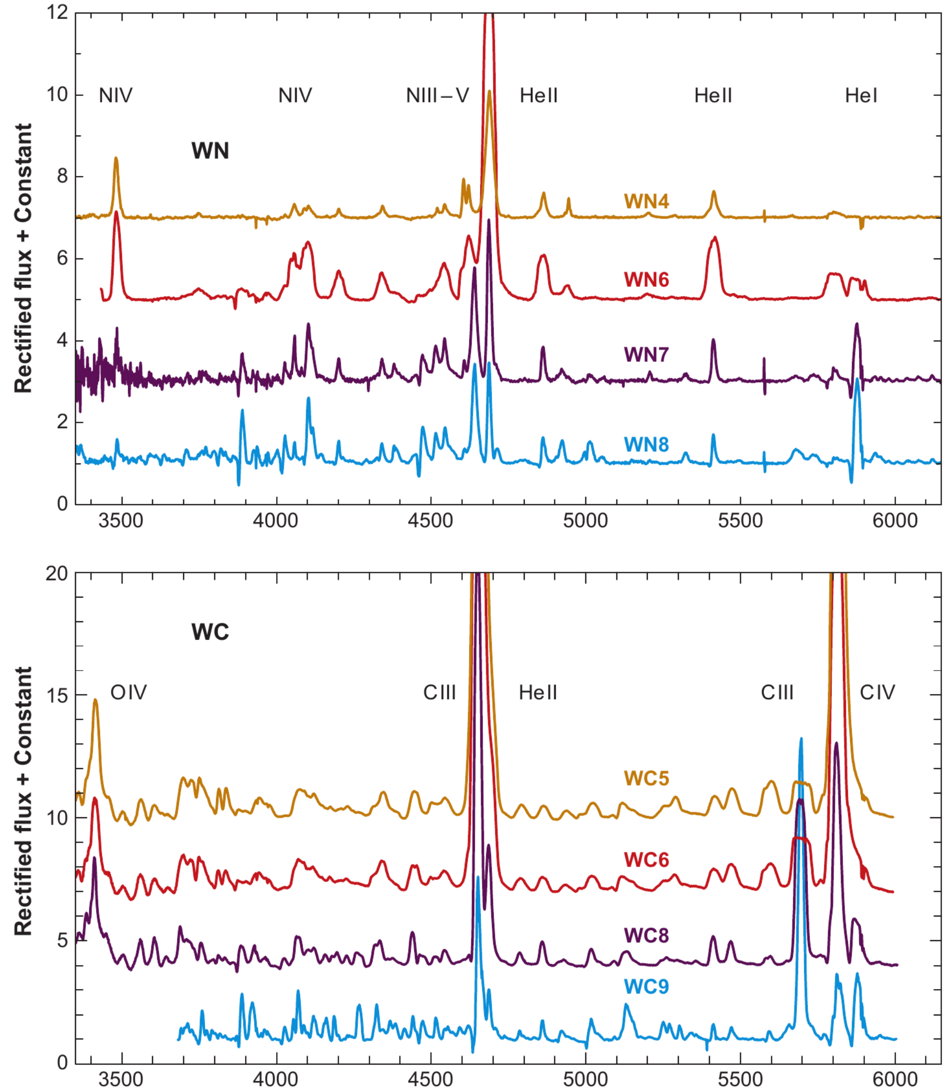

Crowther 2007, ARA&A, 45, 177

Spectra show lines of nuclear processed elements in emission

Classification based on most prominent elements: WN, WC, WO

Post-main sequence evolution – Massive stars

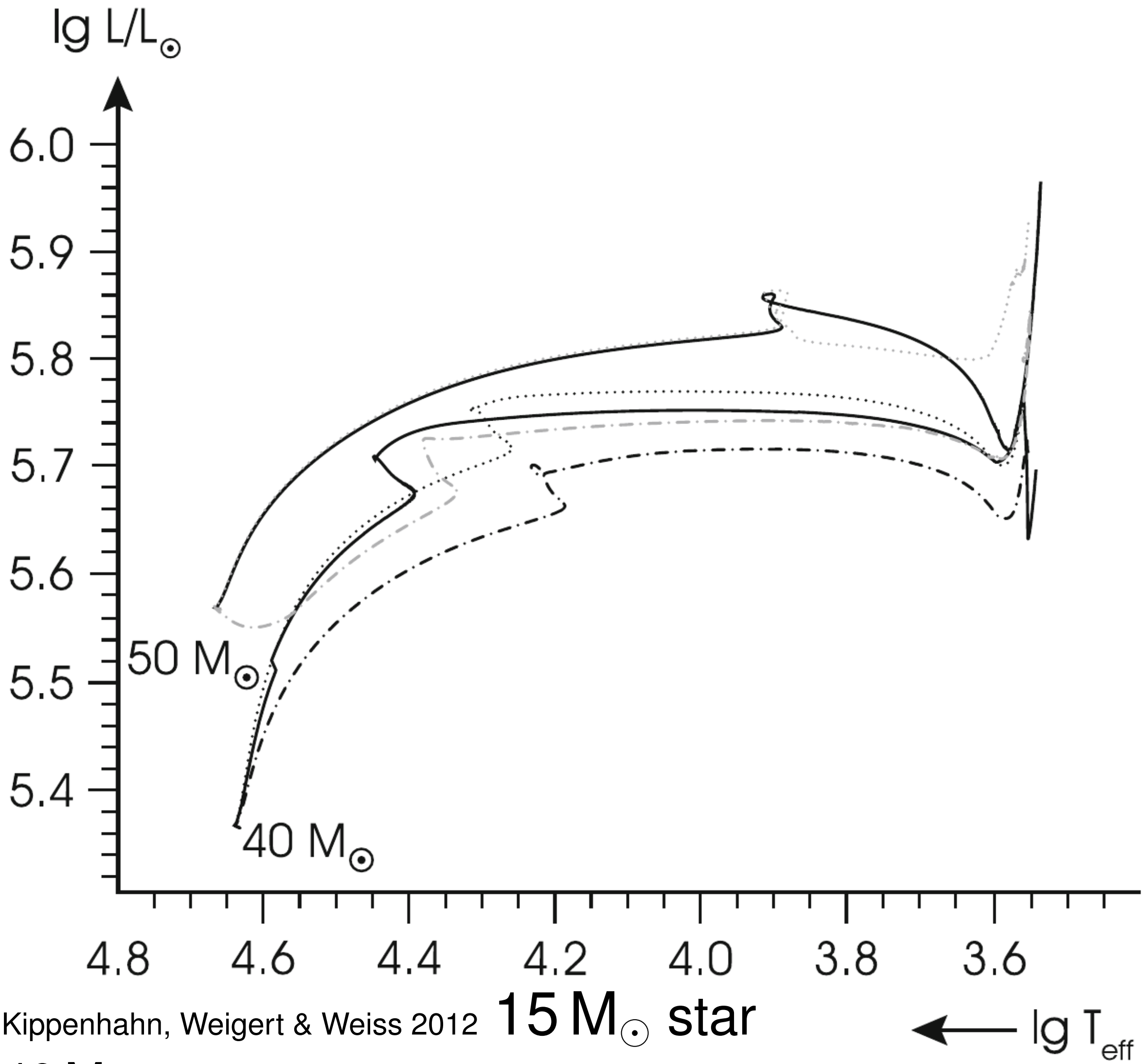

Kippenhahn, Weigert & Weiss 2012 $15\,M_\odot$ star

Evolution of very high-mass stars

- $L \approx 10^{5.6} - 10^{6}\,L_\odot$
- $T_{\mathrm{eff}} \approx 3000 - 25000$ K

$\rightarrow R \approx 40 - 4000\,R_\odot$

Blue, Yellow and Red Supergiants

- Most luminous stars, observable in other galaxies
- Red Supergiant Luminosity class I

$40\,M_\odot$ star: Schwarzschild crit. (solid), overshooting (dotted), additional mass loss (dot dashed); $50\,M_\odot$ star: Ledoux criterion (solid), Schwarzschild criterion (grey dotted line), significantly enhanced mass loss (grey dash-dotted)

Low mass stars in the HRD (EZ model for a $1\,M_\odot$ star)

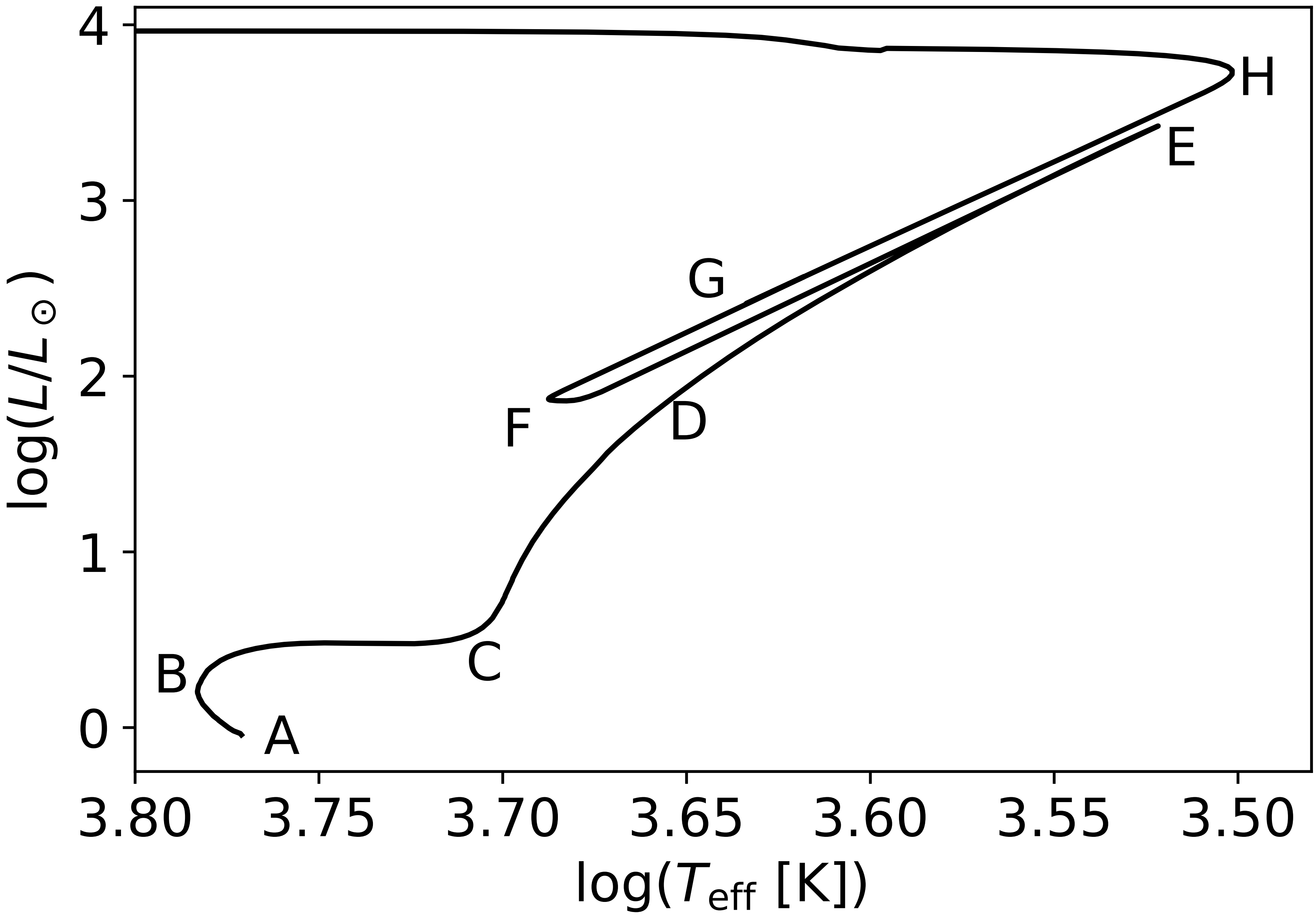

Post-main sequence evolution – Low mass stars

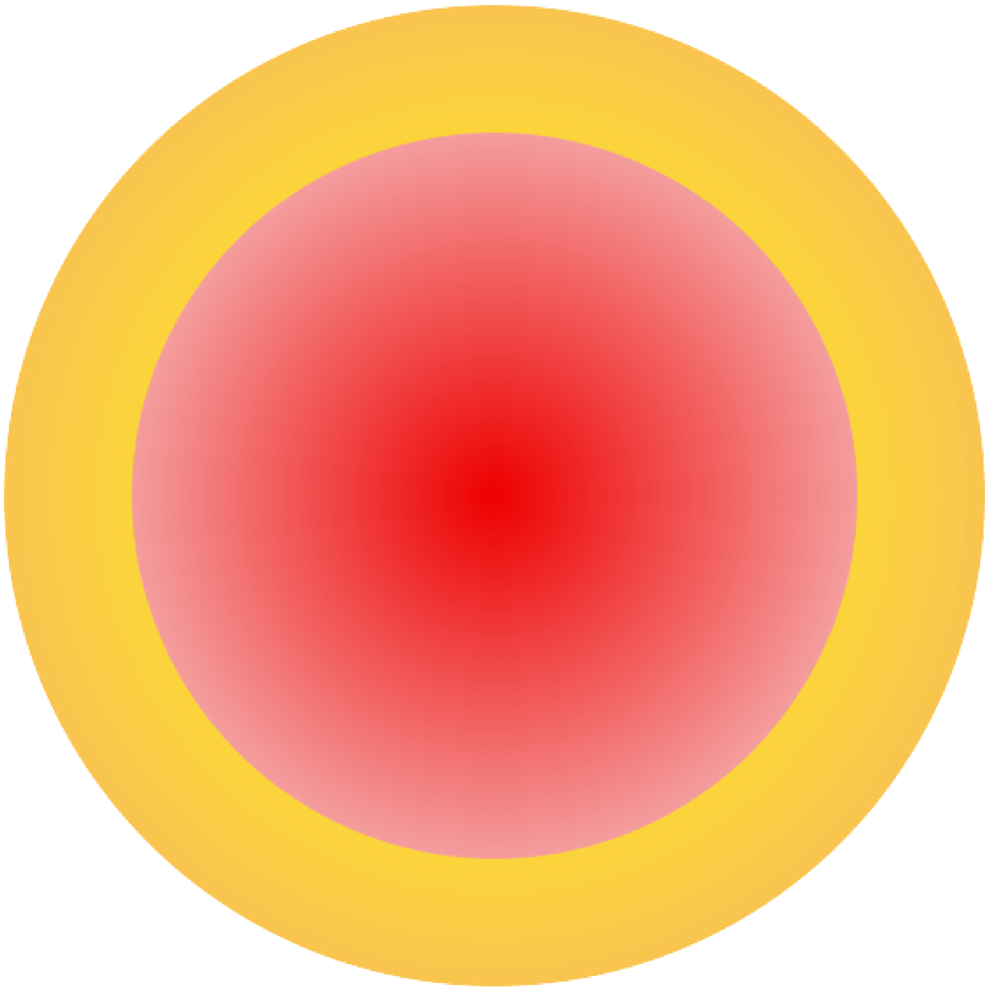

In **low-mass stars** the core is **radiative**

- No efficient mixing in the core
- Hydrogen is consumed starting in the center
- Smooth transition to shell burning

Post-main sequence evolution – Low mass stars

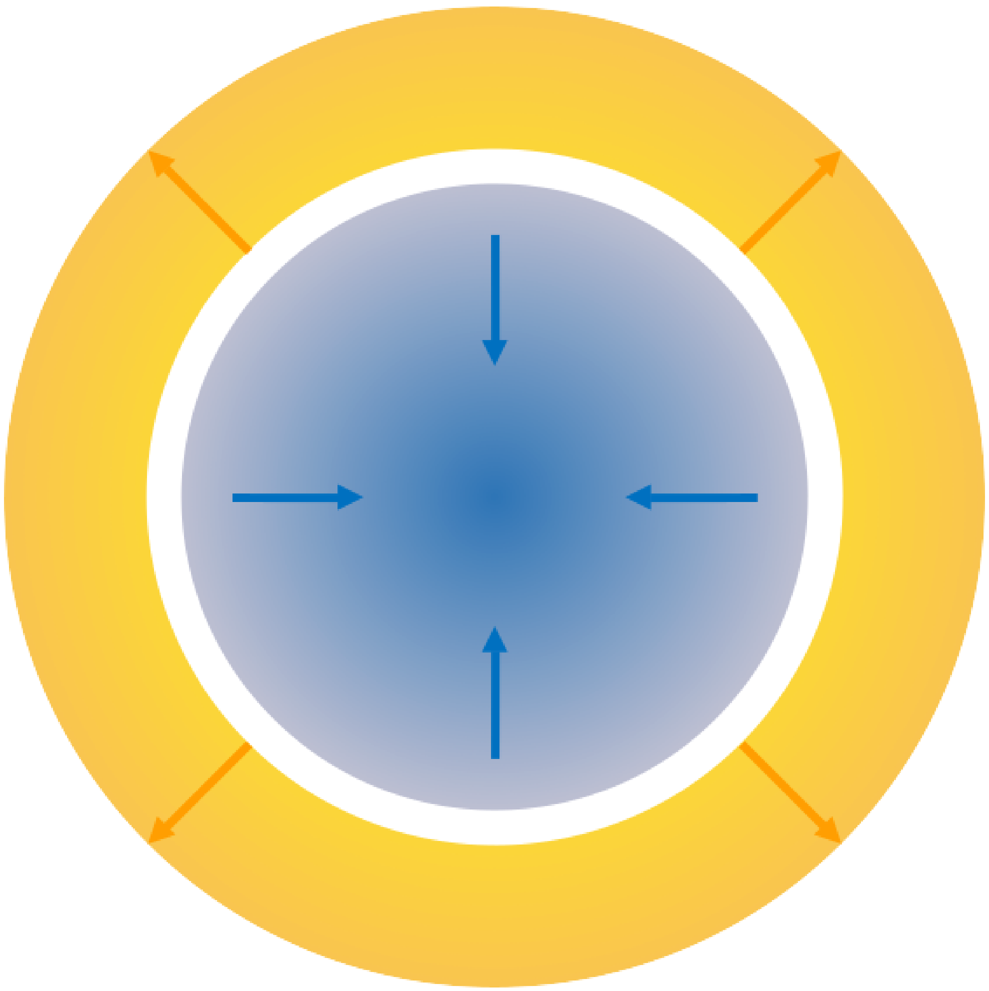

Due to the high density in the core, the electron gas becomes **degenerate**

- Isothermal, degenerate core is stable
- Schönberg-Chandrasekhar limit is not important
- Core can grow in mass

No rapid contraction of the core

- No Hertzsprung gap
- No heating during core contraction due to equation of state

$$P_e = 1.0036 \times 10^{13} \left(\frac{\rho}{\mu_e}\right)^{5/3}$$

Low mass stars in the HRD (EZ model for a 1 $M_\odot$ star)

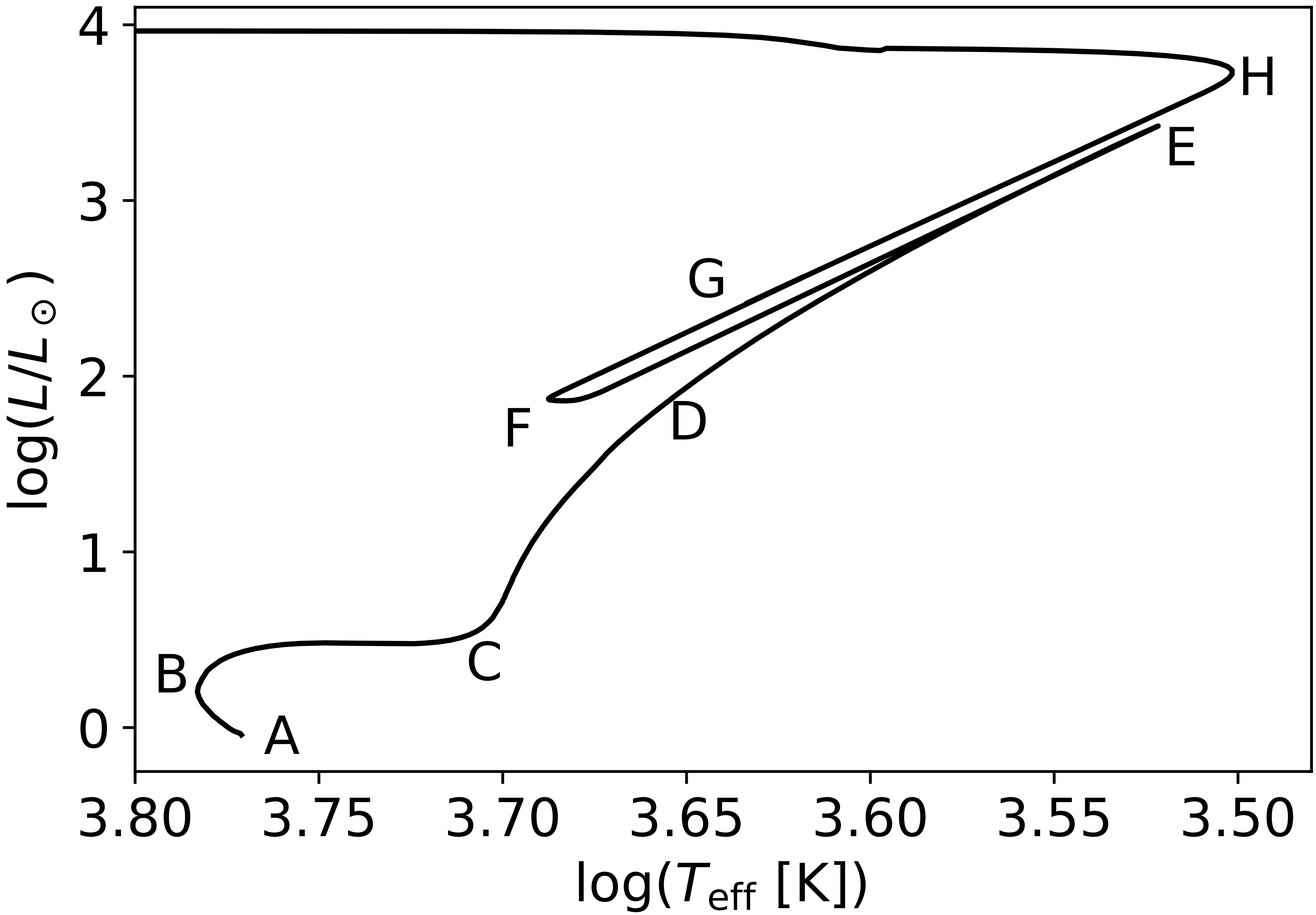

Post-main sequence evolution – Low mass stars

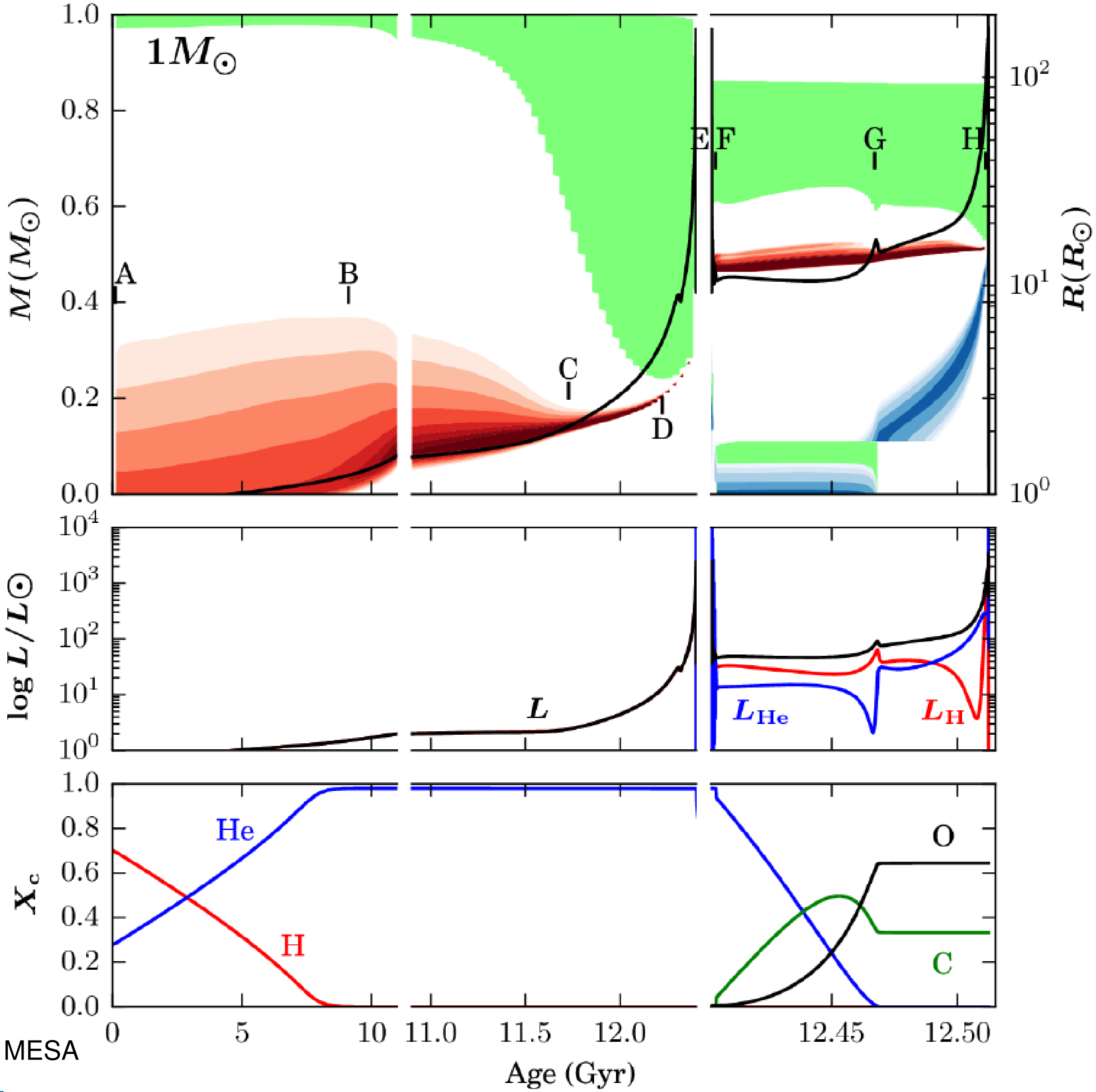

Main sequence (A-B)

- Slow fusion of hydrogen in the core of the star
- Time on MS depends on mass: $10^6 - 10^9$ yr
- Star evolves from the ZAMS towards higher luminosity and larger radii

Post-main sequence evolution – Low mass stars

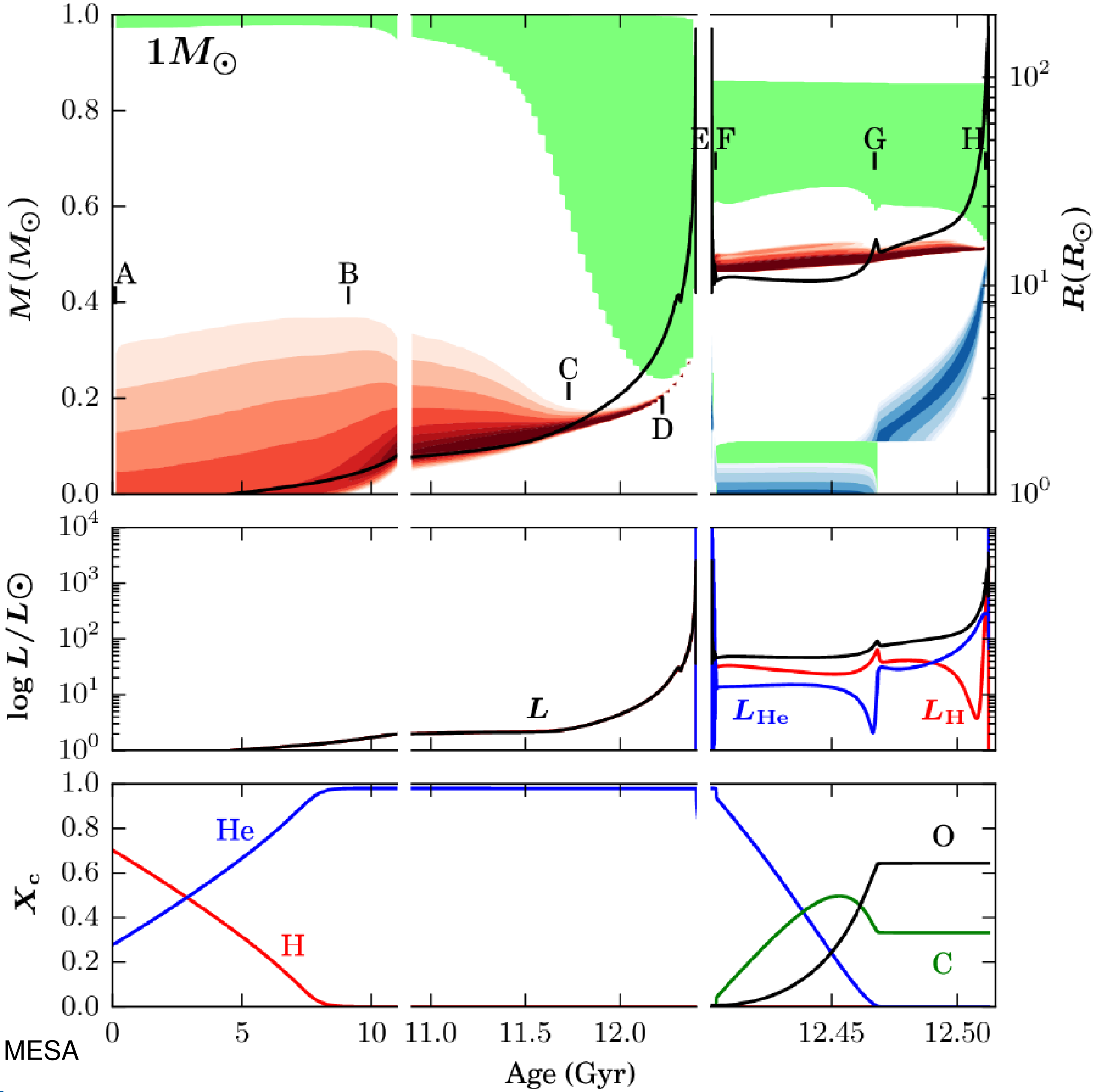

MESA

Sub giant branch (B-C)

- H runs out in the core at point B ($H_c < 0.001$)
- H-fusion moves to a shell around the core
- Core keeps growing in mass and contracts due to shell burning
- at C, He core becomes degenerate
- Core contracts, envelope expands

Post-main sequence evolution – Low mass stars

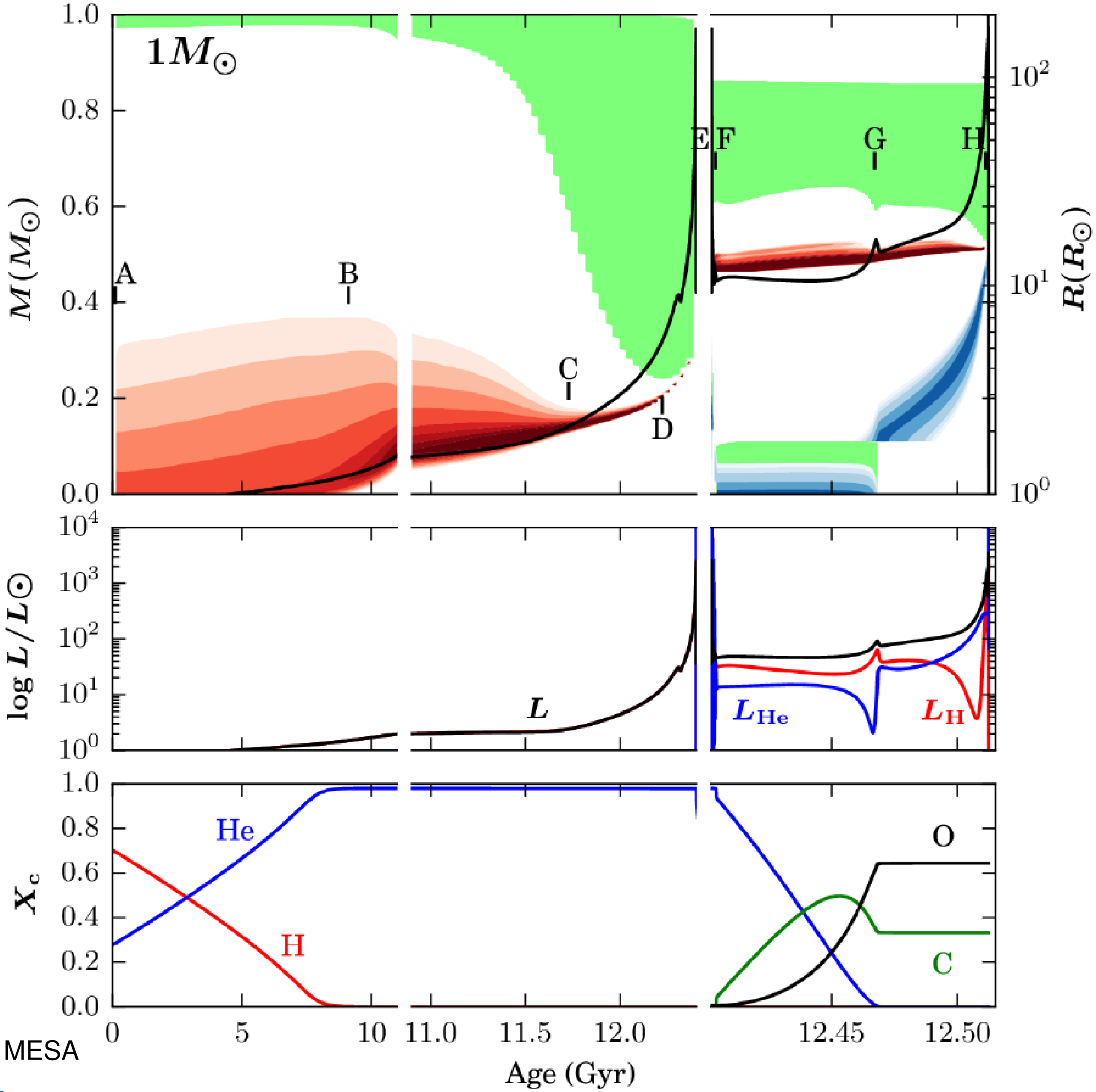

MESA

First dredge up (D)

- convective envelope is at it's deepest point and reaches into layers that were processed by H-burning
- Processed material is transported to the surface and changes the observed abundances of the star

Post-main sequence evolution – Low mass stars

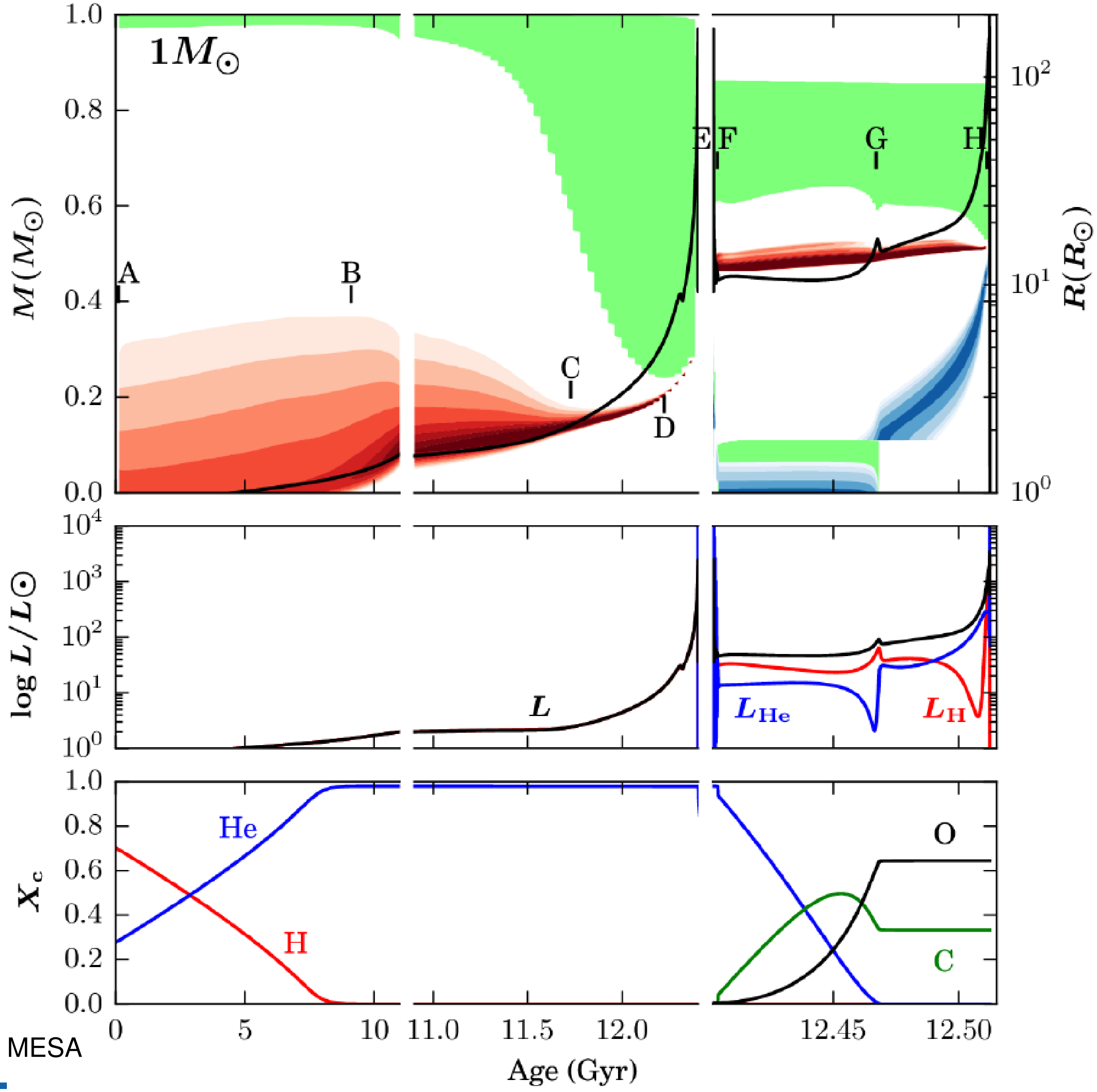

to tip of the **RGB** (D-E)

- Between D and E, the outer layers of the star become less bound, and a stellar wind will remove part of the envelope
- Due to the high concentration of mass in the core $L \sim M_{\rm core}$
- Temperature of the core increases
  $\rightarrow$Increase of T in the H-burning shell
  $\rightarrow$ Core contraction heats transition layer between core and shell

He flash

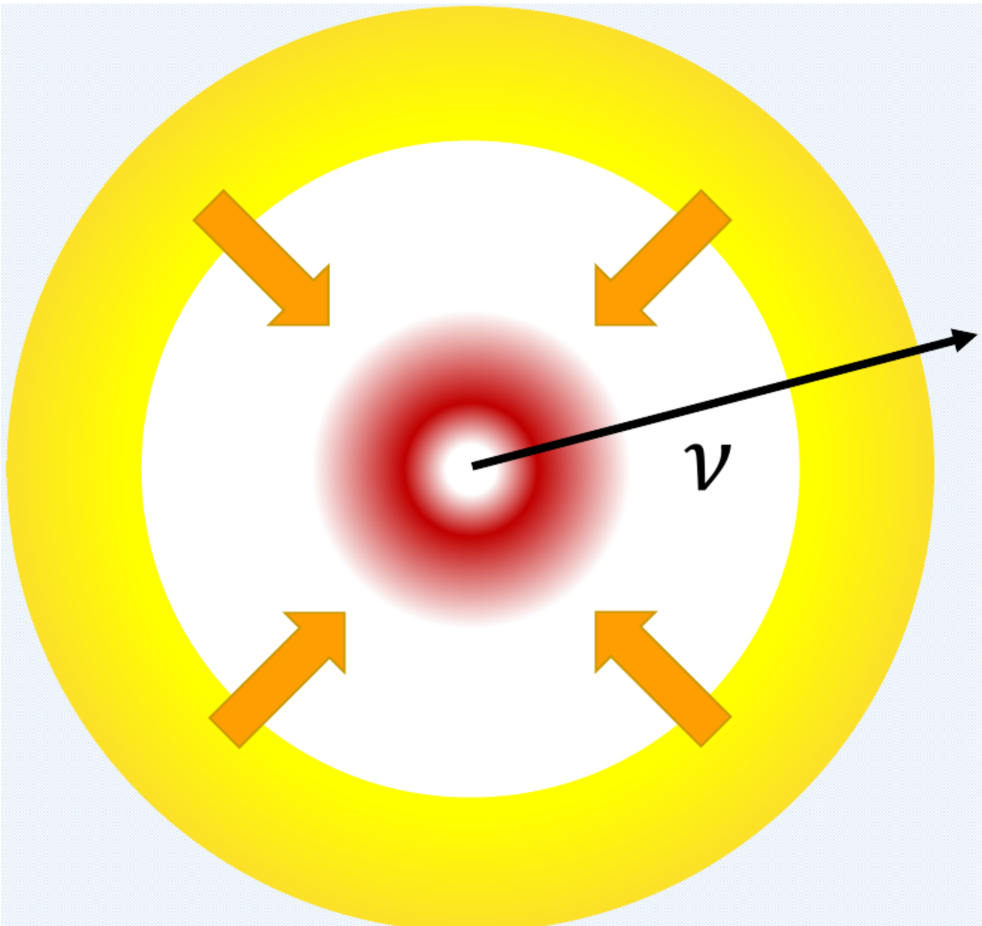

He-flash (E)

- At point E, the tip of the RGB, the core of the star has reached the critical temperature ($\sim 10^8$ K) at the necessary mass to ignite He
- Due to the degeneracy of the core, the actual core ignition mass is independent of the star mass ($M \sim 0.47\,M_\odot$)
- Due to **energy losses via neutrinos** leading to cooling in the center, helium is ignited in a shell

Due to the high temperature dependency of the 3α reaction $\langle\sigma v\rangle \sim \rho T^{40}$ nuclear energy is released fast and increases the core temperature but degenerate gas cannot expand with increasing temperature $\rightarrow$ fast increasing T_c

$\rightarrow$ Runaway burning of helium: **Helium flash**

He flash

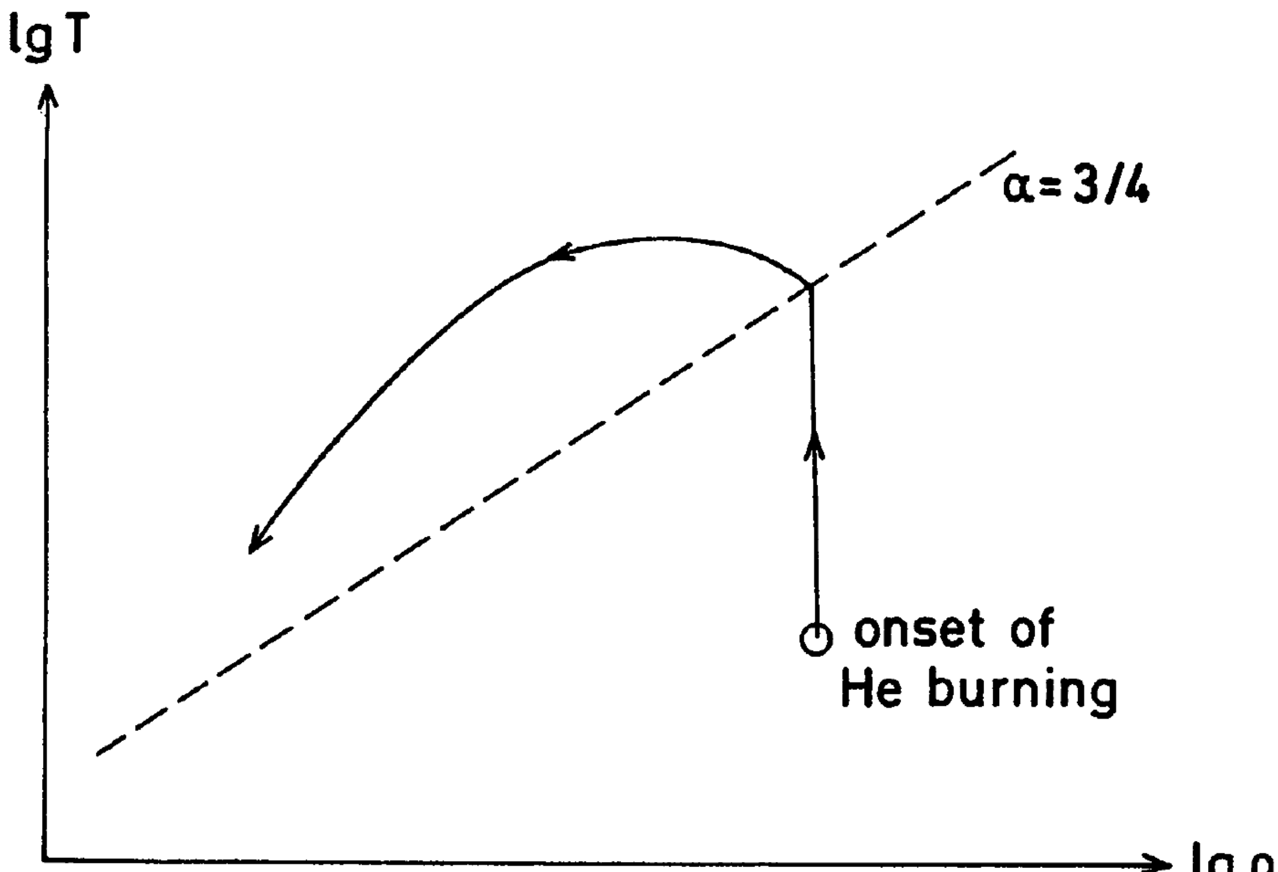

Kippenhahn, Weigert & Weiss 2012

Runaway burning of helium under degenerate conditions

- Luminosity during He flash reaches $\sim 10^{10}\,L_\odot$, small galaxy
- energy is used to expand the envelope, and is thus not visible

- Degeneracy is lifted
- Core expands, density drops
- Stable He-core burning

$\rightarrow$ Flash starts off center due to neutrino cooling

He flash

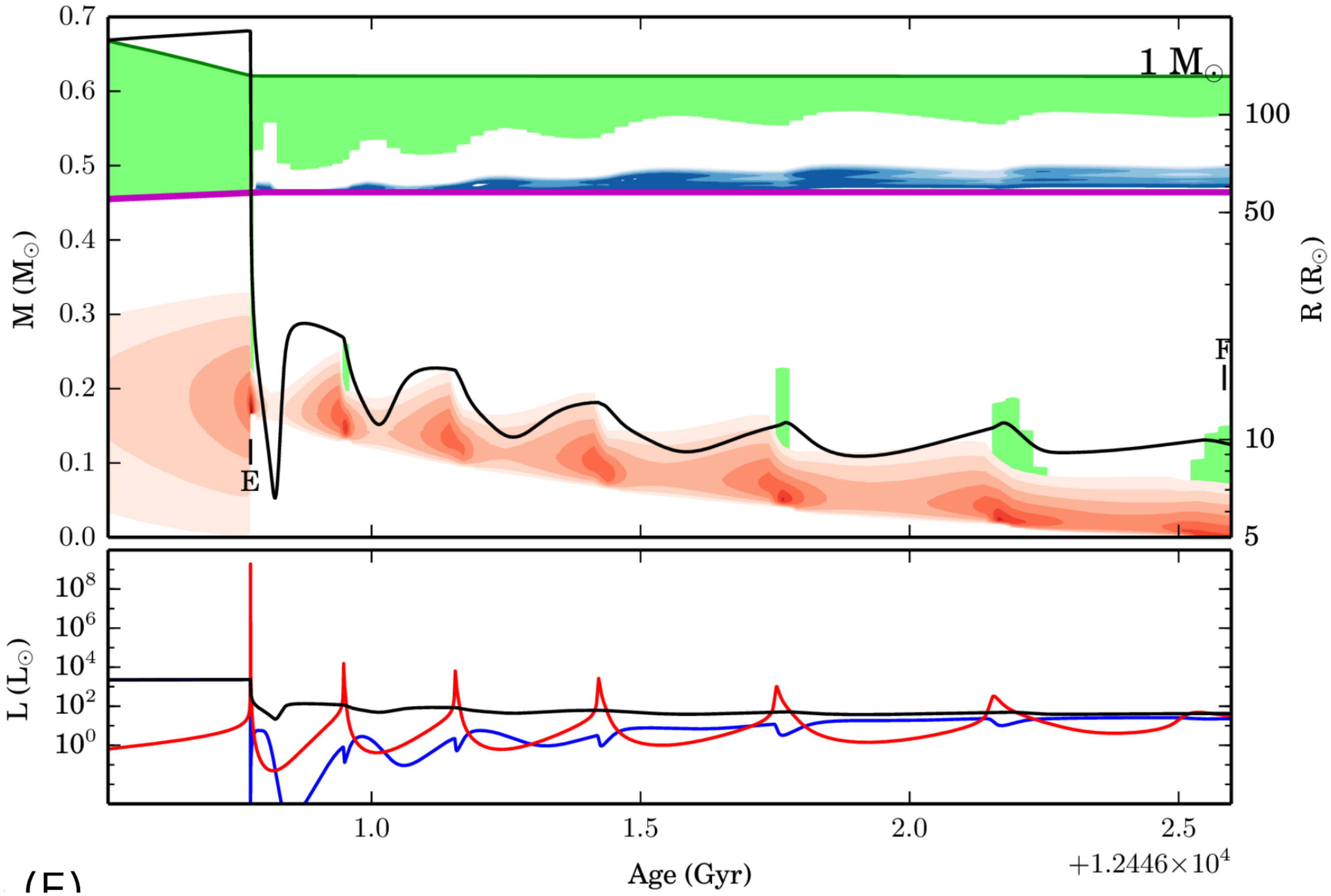

Subflashes when the burning moves from the shell towards the center

- He-flash is highly dynamic and not well understood
- Detailed hydrodynamical models necessary

He flash

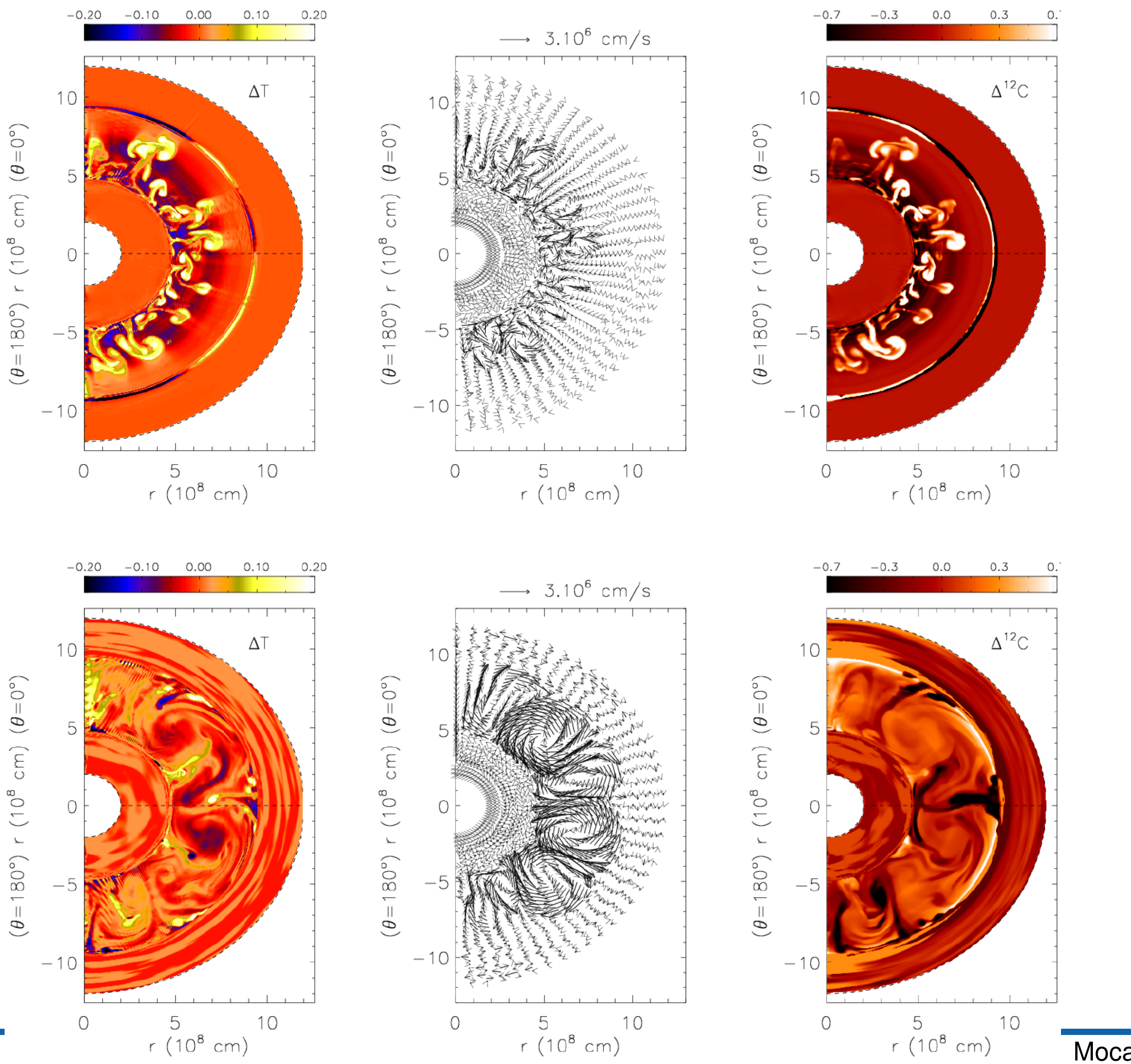

Mocak et al. 2008, A&A, 490, 265

Horizontal branch (EZ model for a $0.8\,M_\odot$ star)

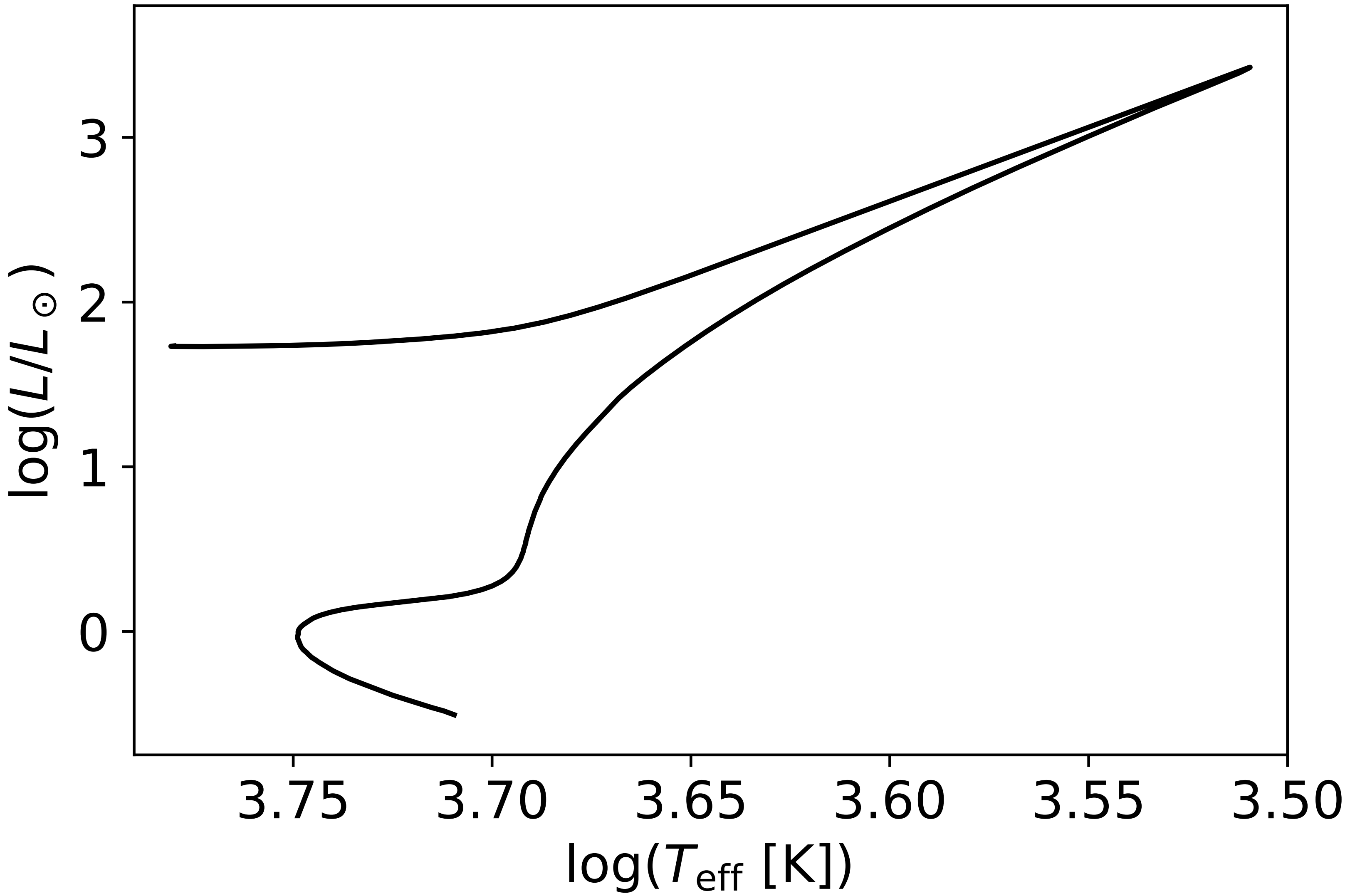

Phase of stable He-core and H-shell burning

$\rightarrow$ Stars occupy a region of (about) constant luminosity: **Horizontal branch**

Horizontal branch (HB)

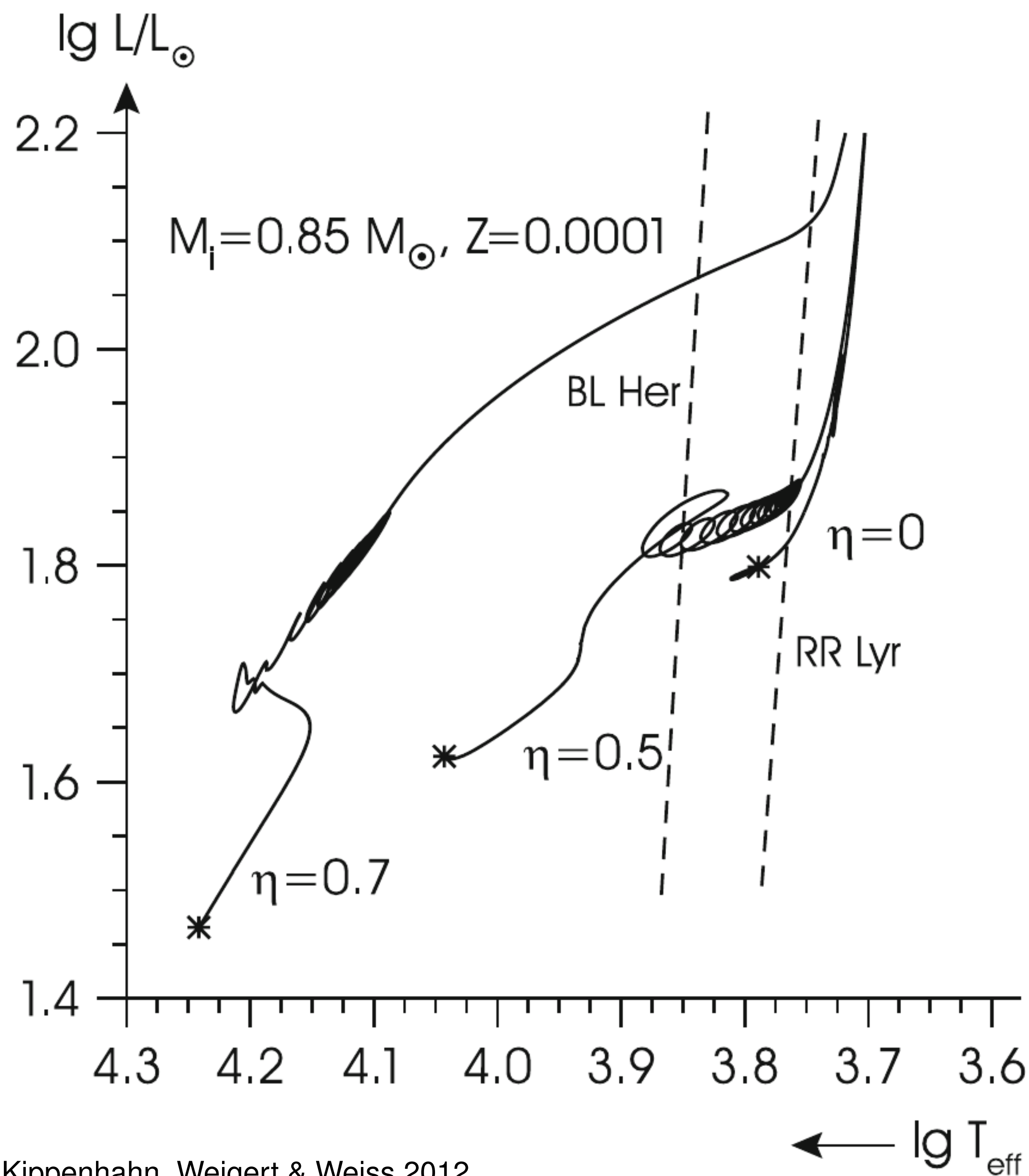

Kippenhahn, Weigert & Weiss 2012

Horizontal Branch stars

- Different mass loss η on the RGB leads to **different thickness of the hydrogen envelopes**
- Mass of the He-core is constant ($\sim 0.47\,M_\odot$)
- Diverse types of HB stars
- The thinner the hydrogen envelope, the bluer the HB star
- Morphology of HB depends on metallicity and age
- Luminosity during He burning is determined by core mass, which is similar for all low mass stars

Horizontal branch (HB)

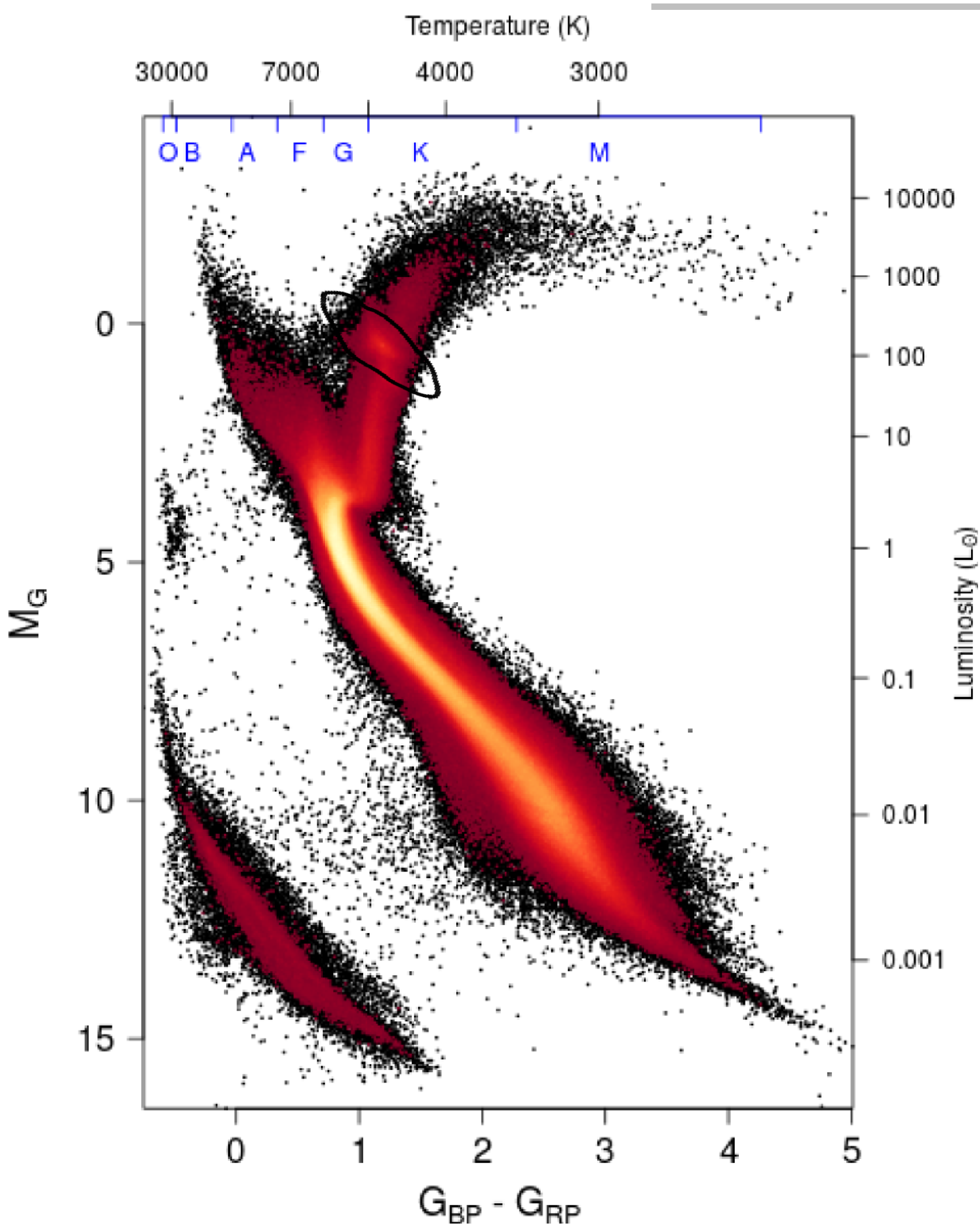

Gaia collaboration 2018, A&A 616, 10

Red clump (RC) stars

- red, close to RGB
- low-mass stars in their stage of central He-burning
- sizable convective envelopes result from either a moderately high metallicity or buffer of mass above the H-burning shell
- young population
- far more abundant than HB stars (1/3 of all red giants)
- RC stars can be used as standard candles

Horizontal branch (HB)

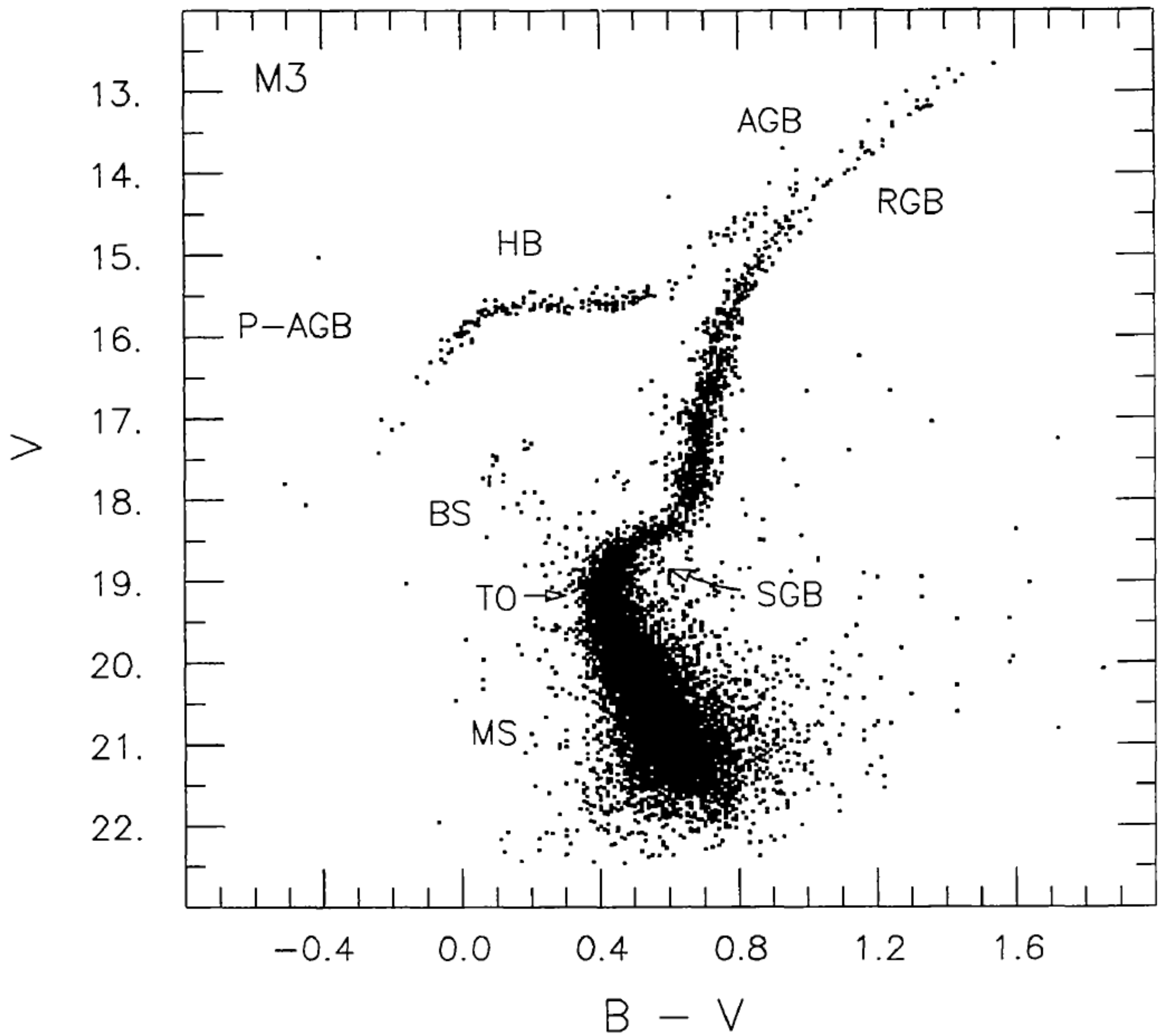

Renzini & Fusi Pecci 1988, ARA&A, 26, 199

Red Horizontal Branch (RHB) stars

- Redward of the MS
- (Sub-)giants
- Spectral types K, G
- metal-poor, old population

RR Lyr stars

- (Sub-)giants
- Spectral types F
- metal-poor, old population
- pulsators

Horizontal branch (HB)

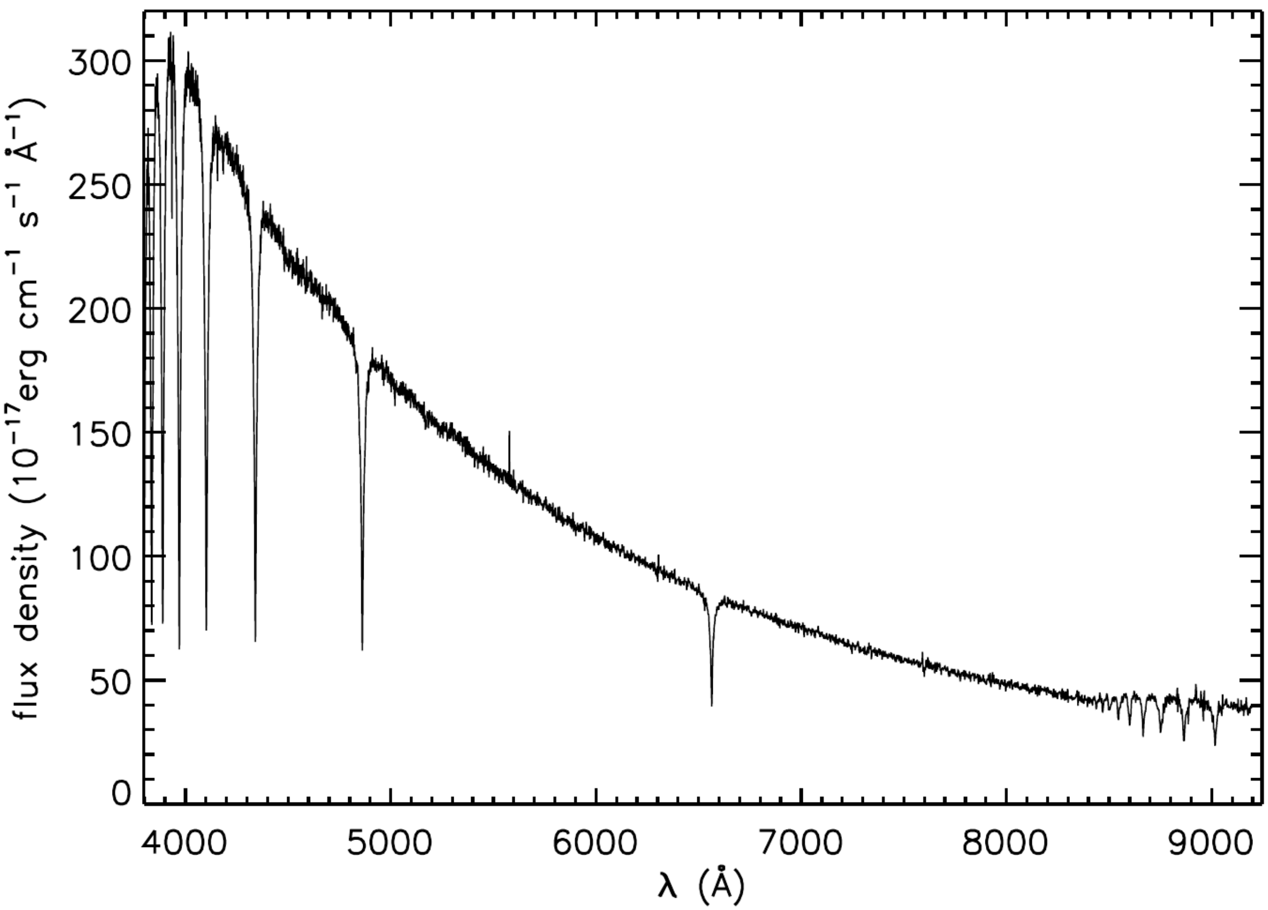

Xue et al. 2008, ApJ, 684, 1143

Blue Horizontal Branch (BHB) stars

- Blueward of the MS
- (Sub-)dwarfs
- Spectral types A,B (HBA, HBB)
- chemically peculiar

$\rightarrow$ low helium content
HBB $>$ 11500 K

$\rightarrow$ Light elements depleted, heavy elements enriched

$\rightarrow$ Slow rotation

Extreme Horizontal branch (EHB)

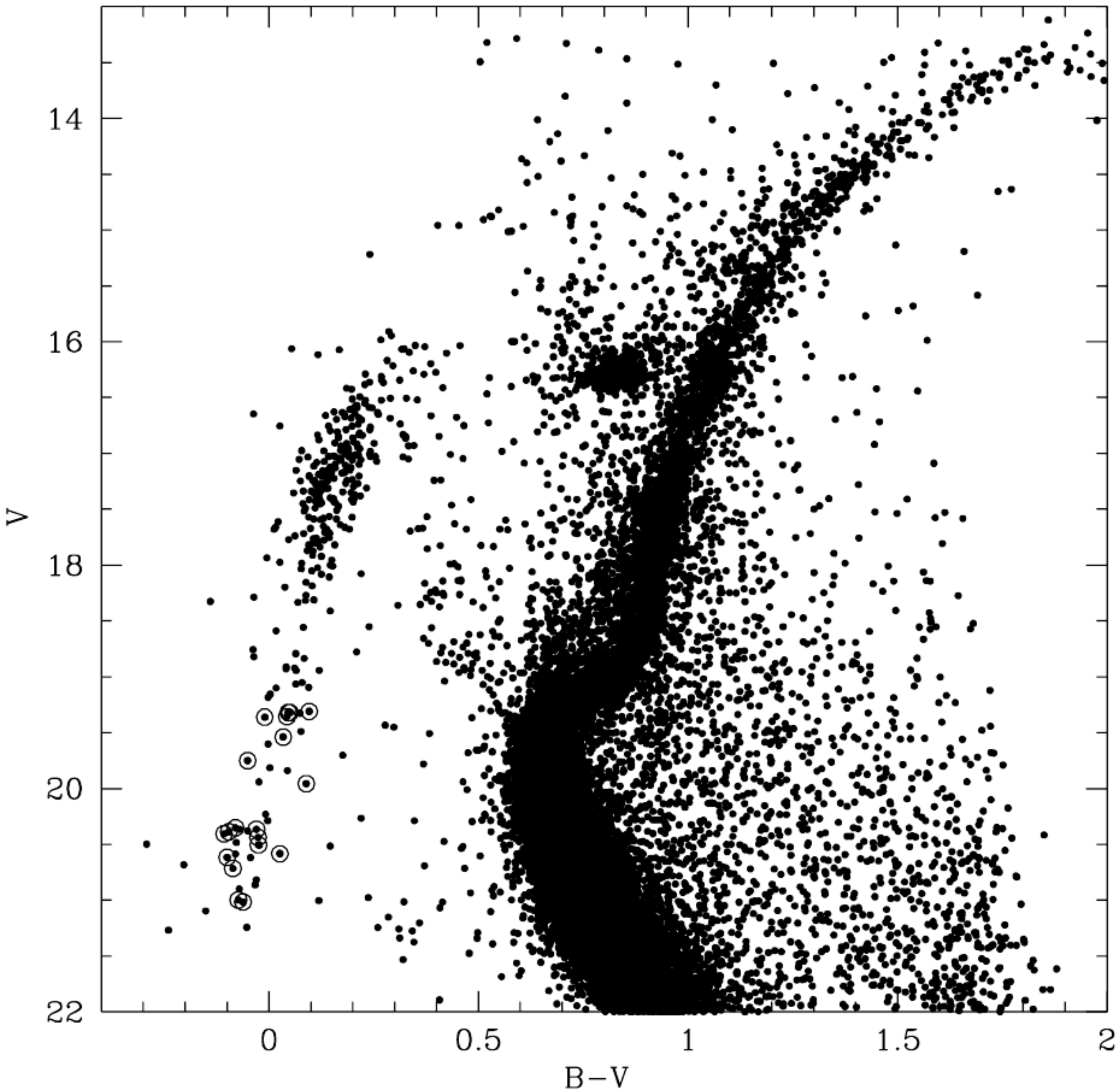

Moehler et al. 2004, A&A, 415, 313

Extreme Horizontal Branch (EHB) stars

- Subdwarfs
- Spectral types O, B (sdO, sdB)
- Extremely thin hydrogen envelopes, **no H-shell burning**
- mass close to He-core mass necessary for He-burning ($0.47\,M_\odot$)

Extreme Horizontal branch (EHB)

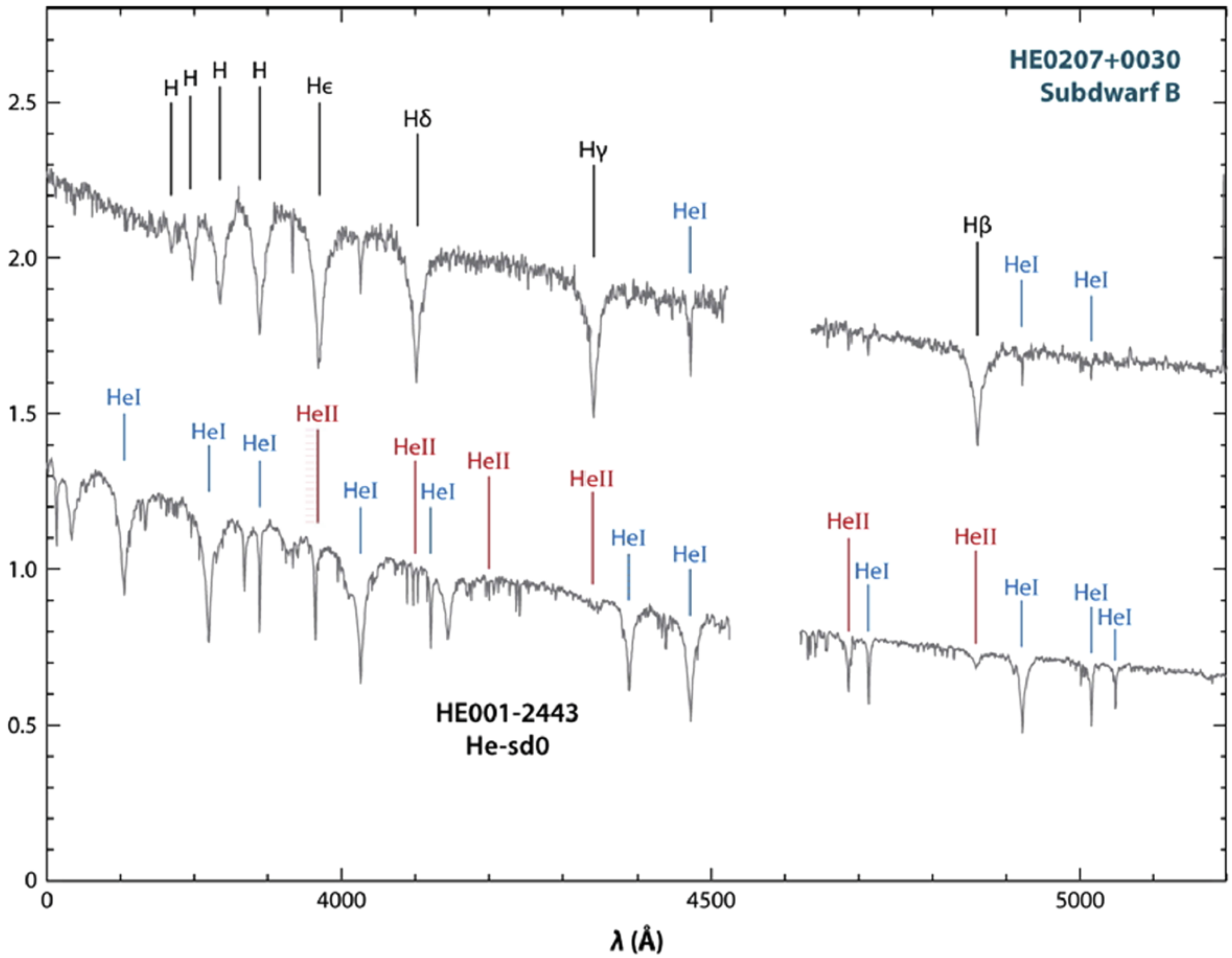

Heber 2016, PASP, 128, 966

Hydrogen-rich sdBs

- very low to solar helium content
- Light elements depleted, heavy elements enriched
- High binary fraction

Helium-rich sdO/Bs

- very high helium abundance
- Enrichment in carbon and/or nitrogen
- Single stars

Extreme Horizontal branch (EHB)

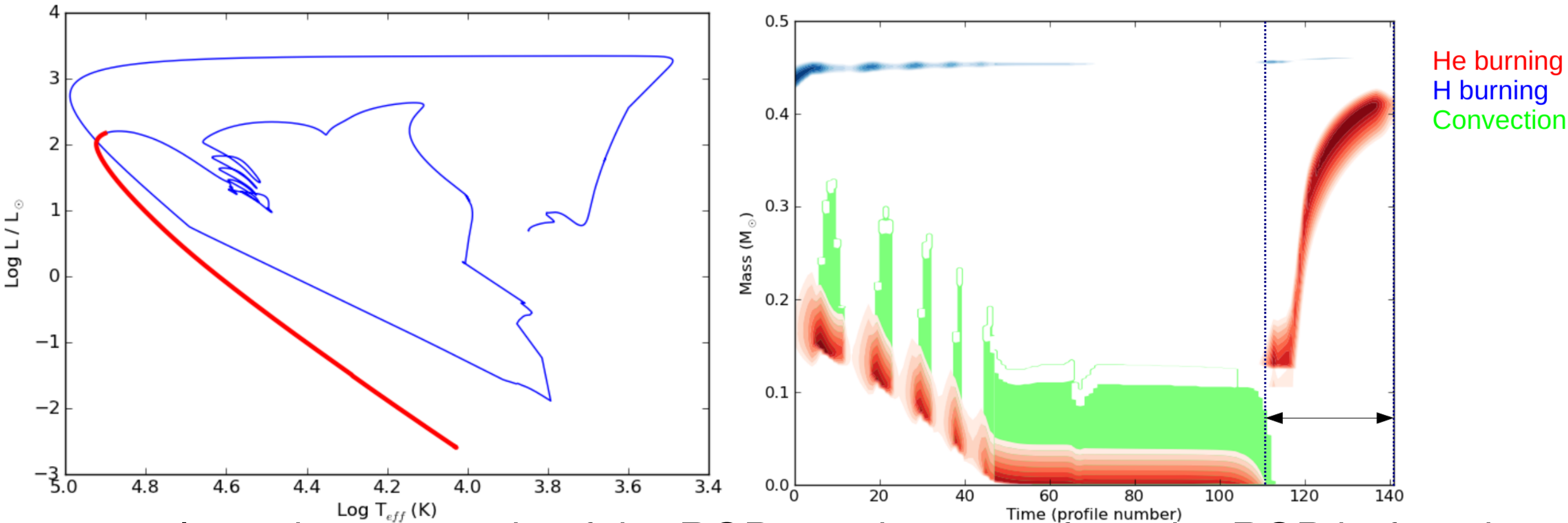

- mass-loss phase near tip of the RGB, moving away from the RGB before the core ignites
- Resettling/contraction of the sdB progenitor
- He flashes
- time about 2 Myr
- He-core burning ($\sim$ 100 Myr)
- He-shell burning
- white dwarf cooling track

Extreme Horizontal branch (EHB)

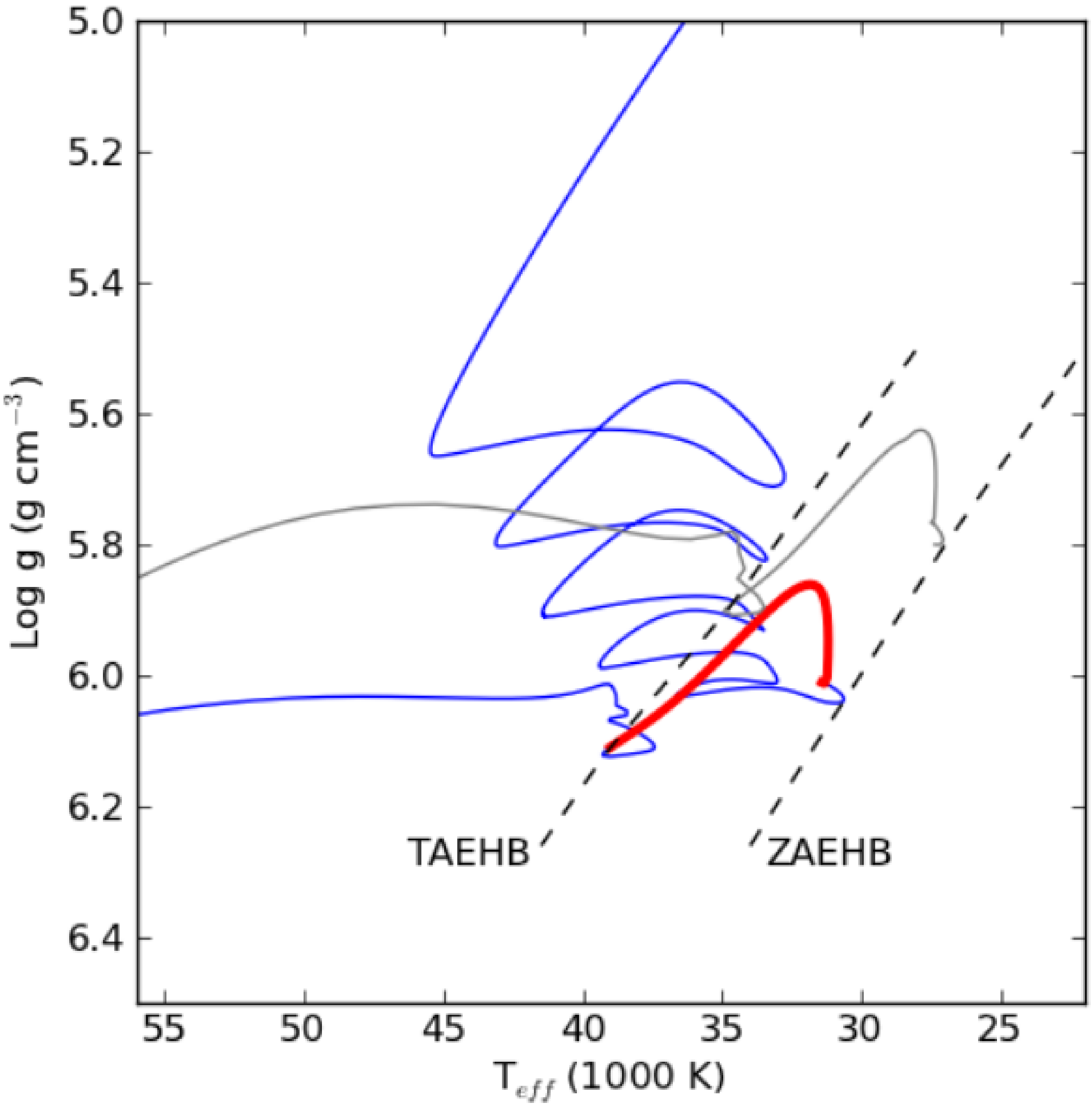

- He-core burning from the Zero Age Extreme Horizontal branch (ZA-EHB) to the Terminal Age Extreme Horizontal Branch (TAEHB)
- lifetime on the EHB $\sim$ 100 Myr

Extreme Horizontal branch (EHB)

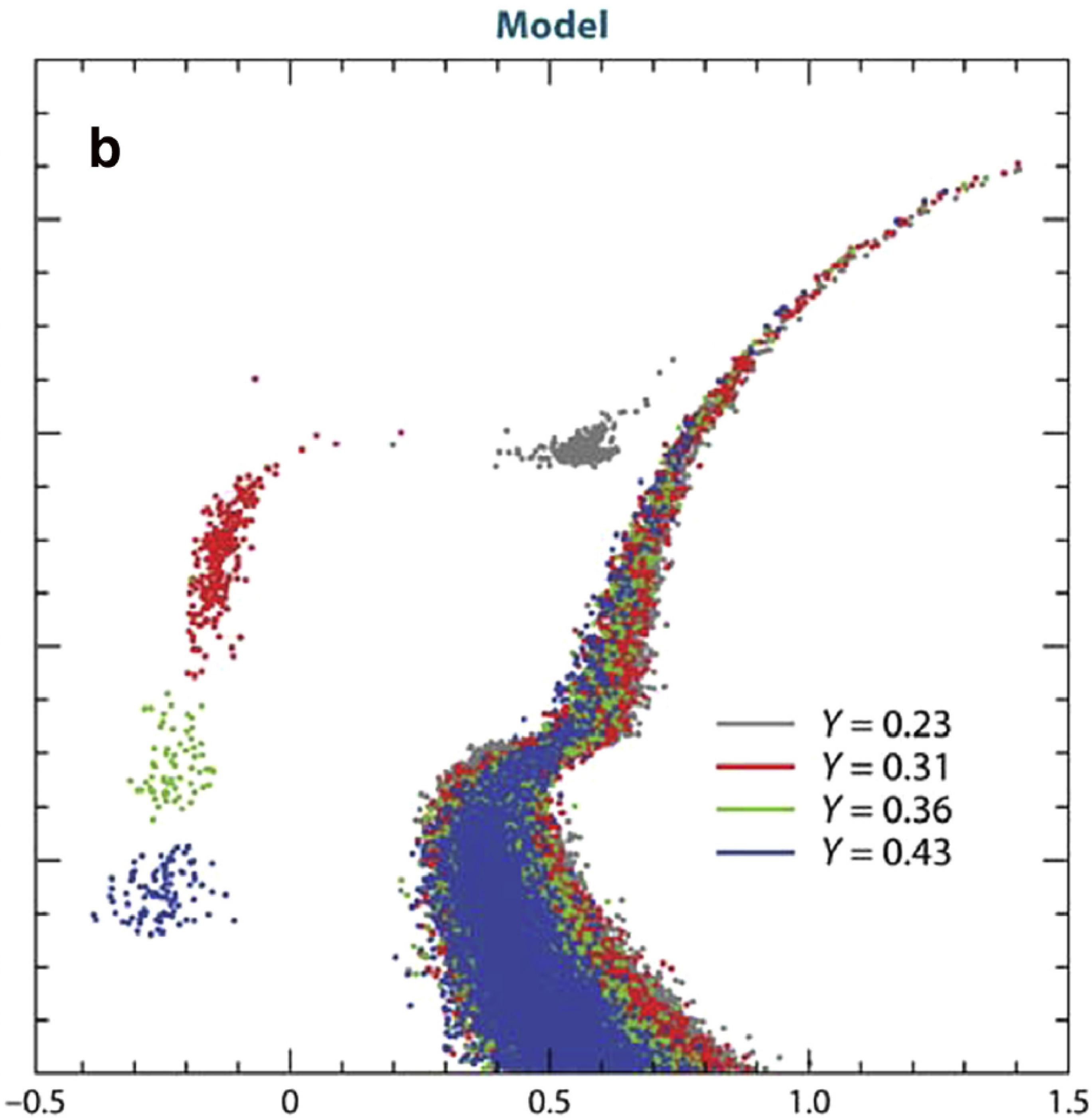

Alternative formation

- Helium enriched populations
- Due to previous episodes of star formation?
- Composition changes luminosity and temperature

Extreme Horizontal branch (EHB)

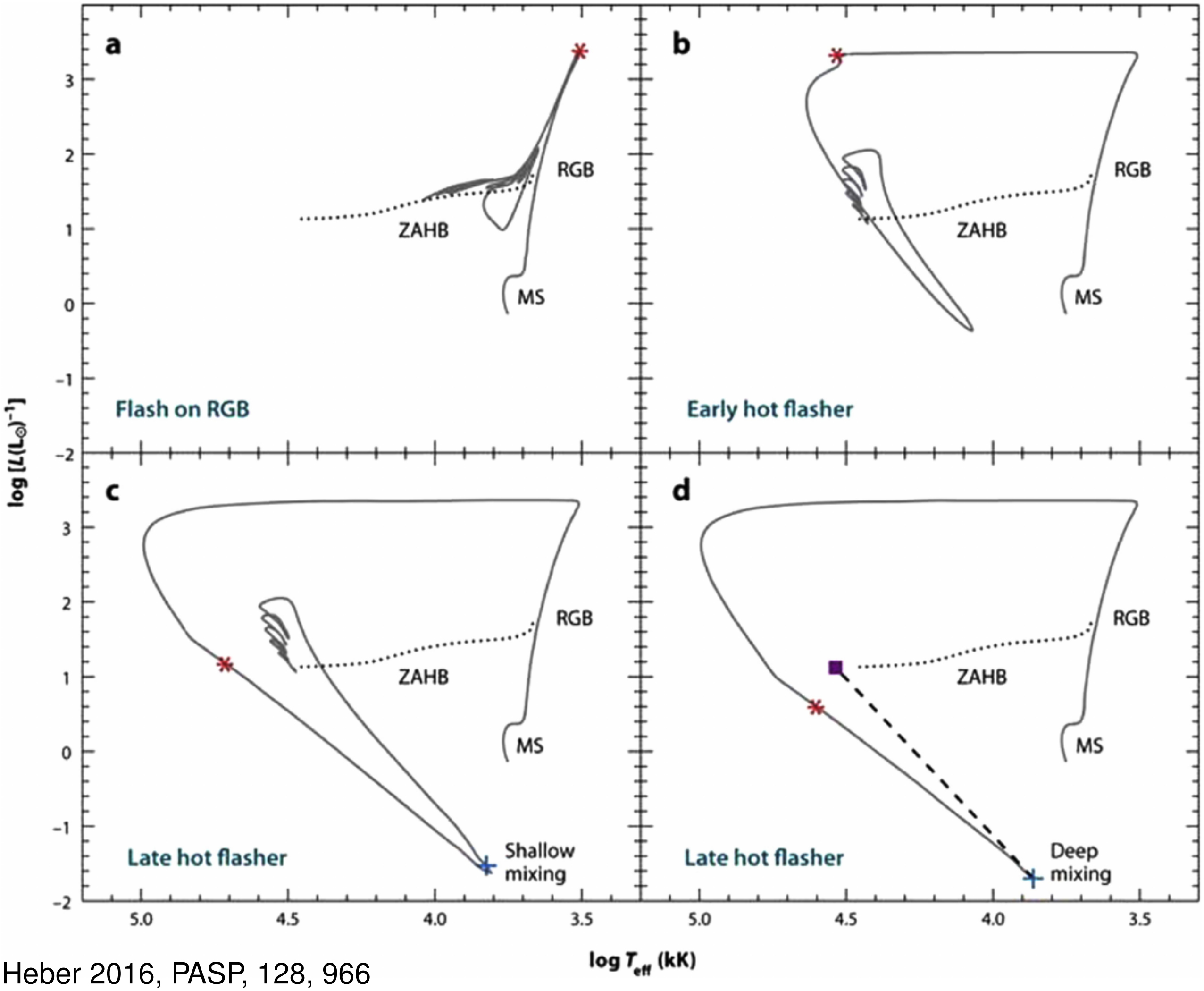

Heber 2016, PASP, 128, 966

Alternative formation

- Late hot helium flash
- After RGB phase
- Mixing of processed material (C,N)
- Dependent on evolution-ary phase

Extreme Horizontal branch (EHB)

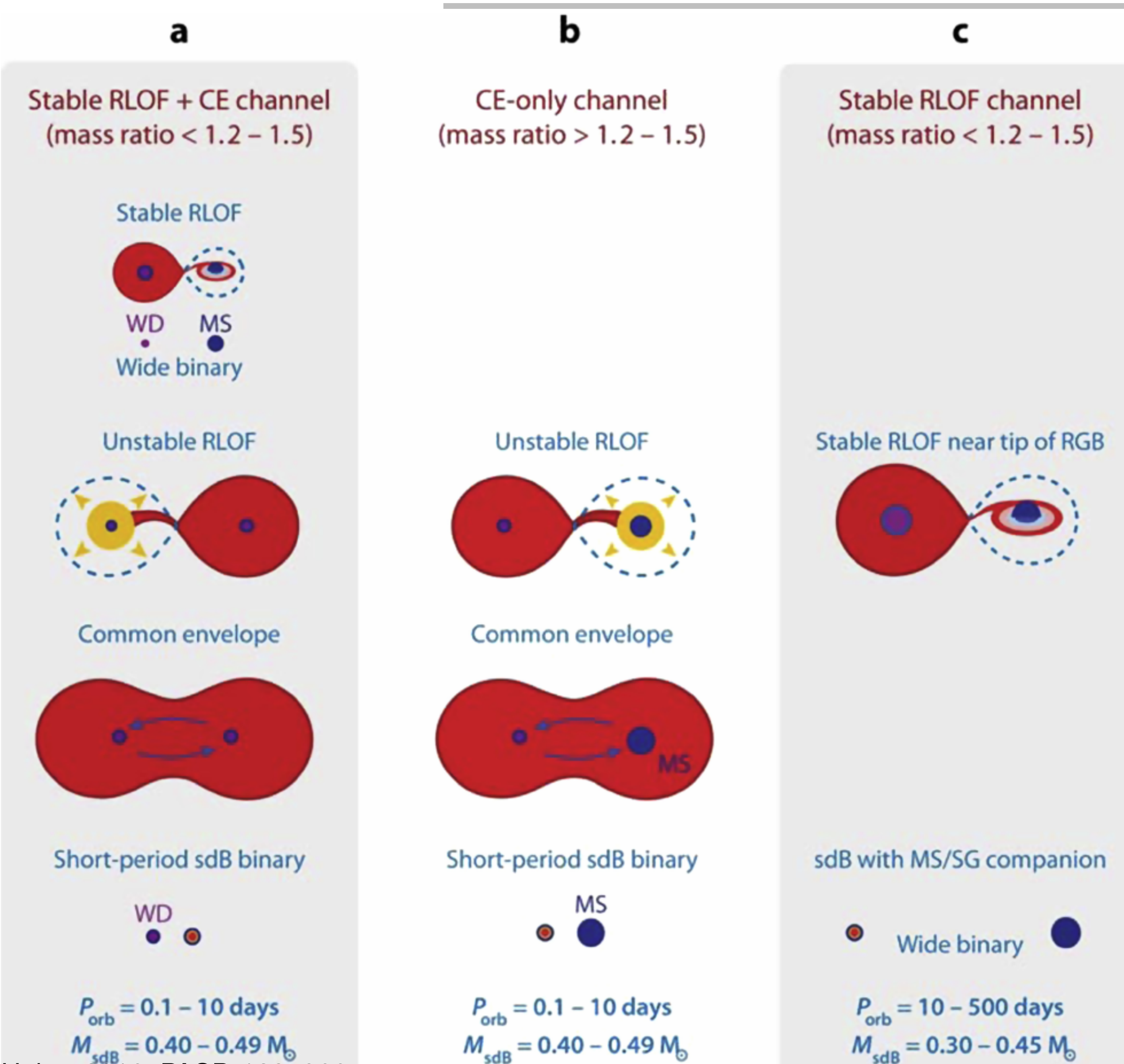

Heber 2016, PASP, 128, 966

Alternative formation

- Close binary evolution
- Helium-burning core of the red giant stripped by binary interaction
- Binary sdB stars

Extreme Horizontal branch (EHB)

Extreme Horizontal branch (EHB)

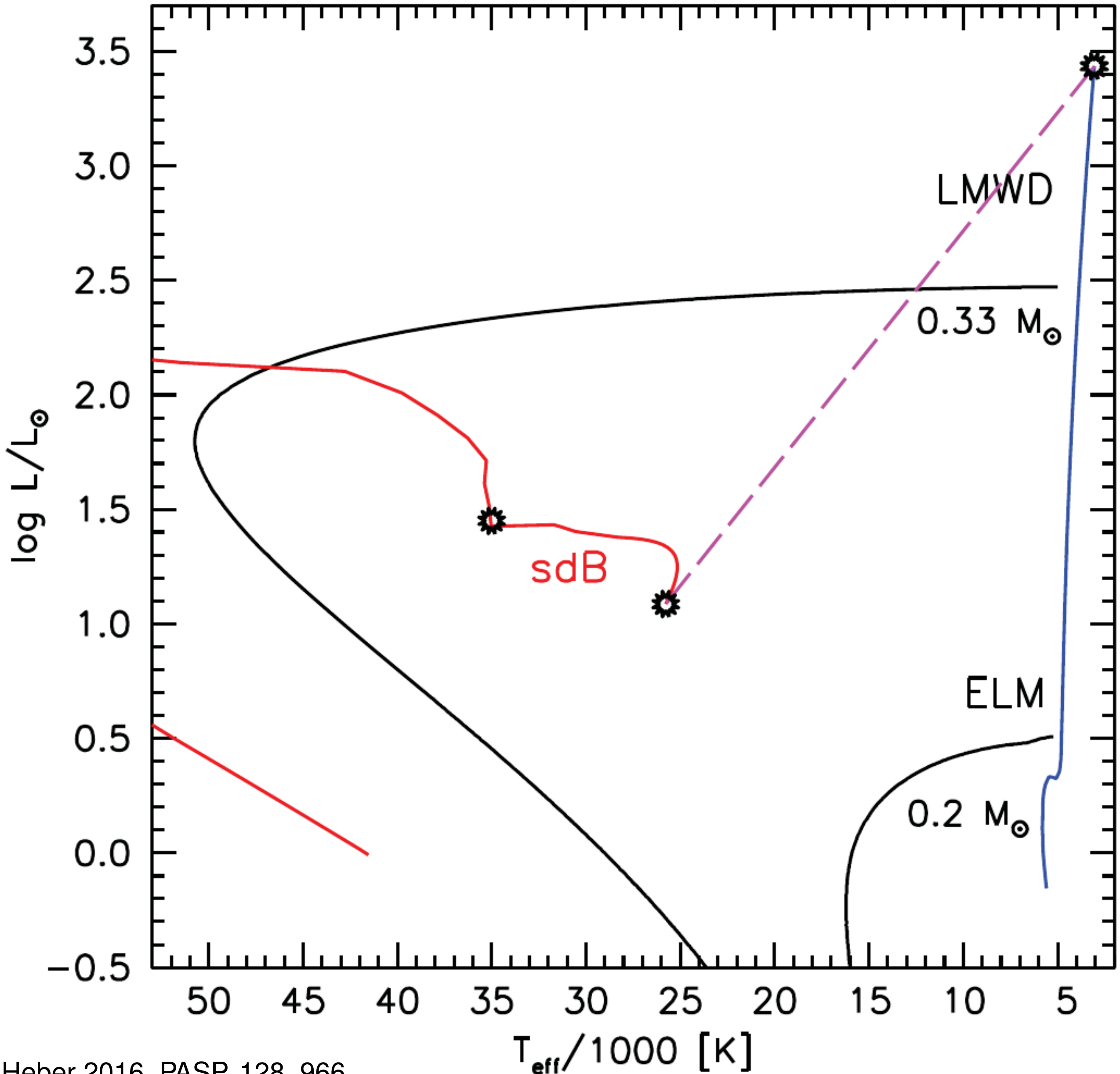

Heber 2016, PASP, 128, 966

Alternative formation

- Close binary evolution
- Star stripped before ignition of helium burning
- Evolutionary cooling timescales $10^6 - 10^8$ yr

Extreme Horizontal branch (EHB)

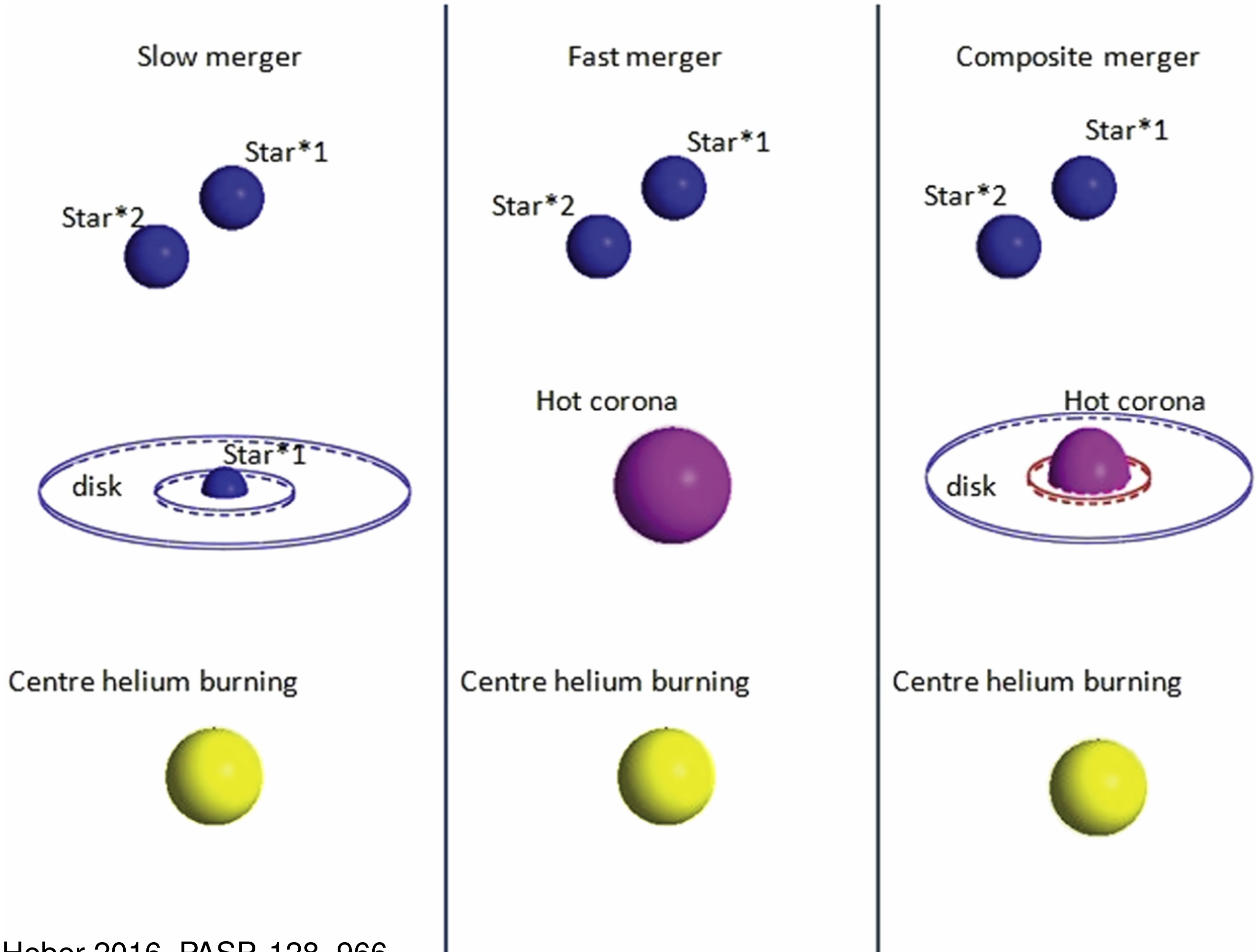

Heber 2016, PASP, 128, 966

Alternative formation

- Close binary evolution
- Merger of two white dwarfs of pure helium composition
- Single He-sdO/B stars

Horizontal Branch (HB)

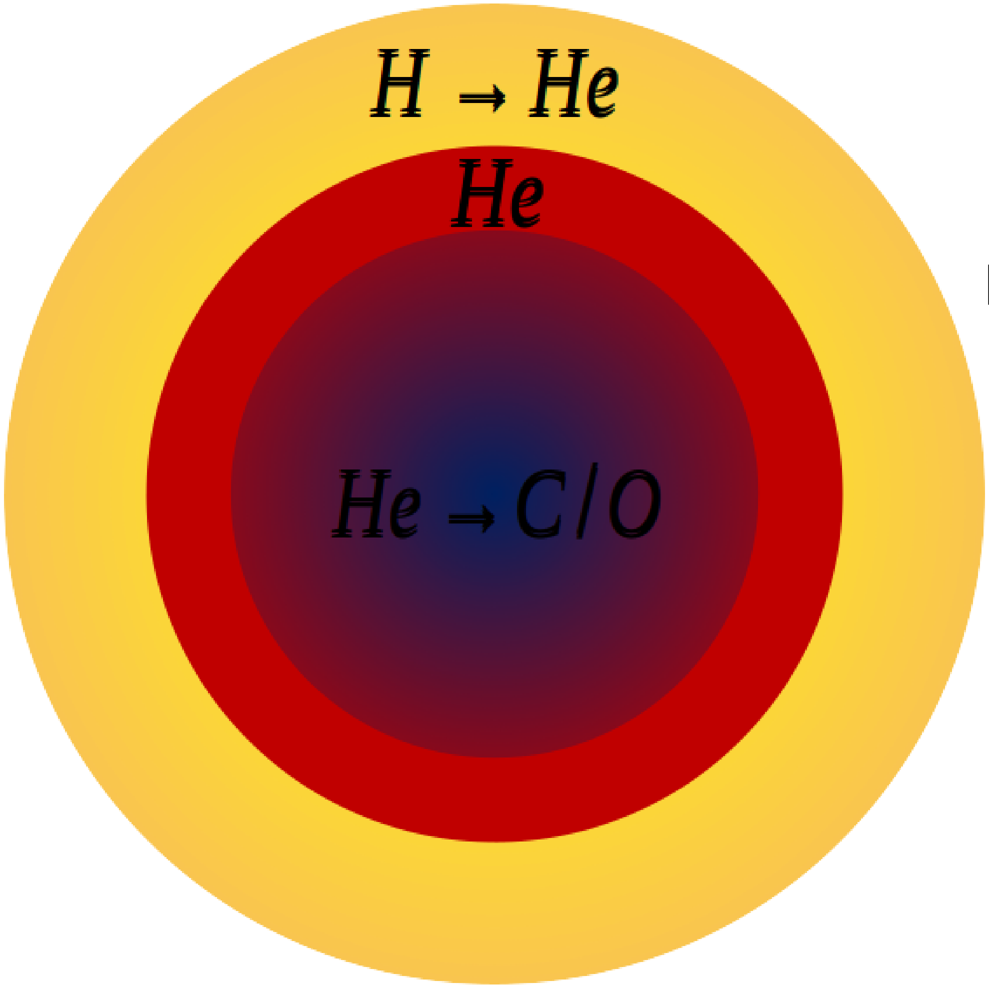

HB evolution (F-G)

- Stable He-burning in the convective core and H-burning in a shell
- lifetime $\sim 10^8$ yr
- Core grows through shell burning
- C/O becomes enriched in the core

Low mass stars in the HRD (EZ model for a $1\,M_\odot$ star)

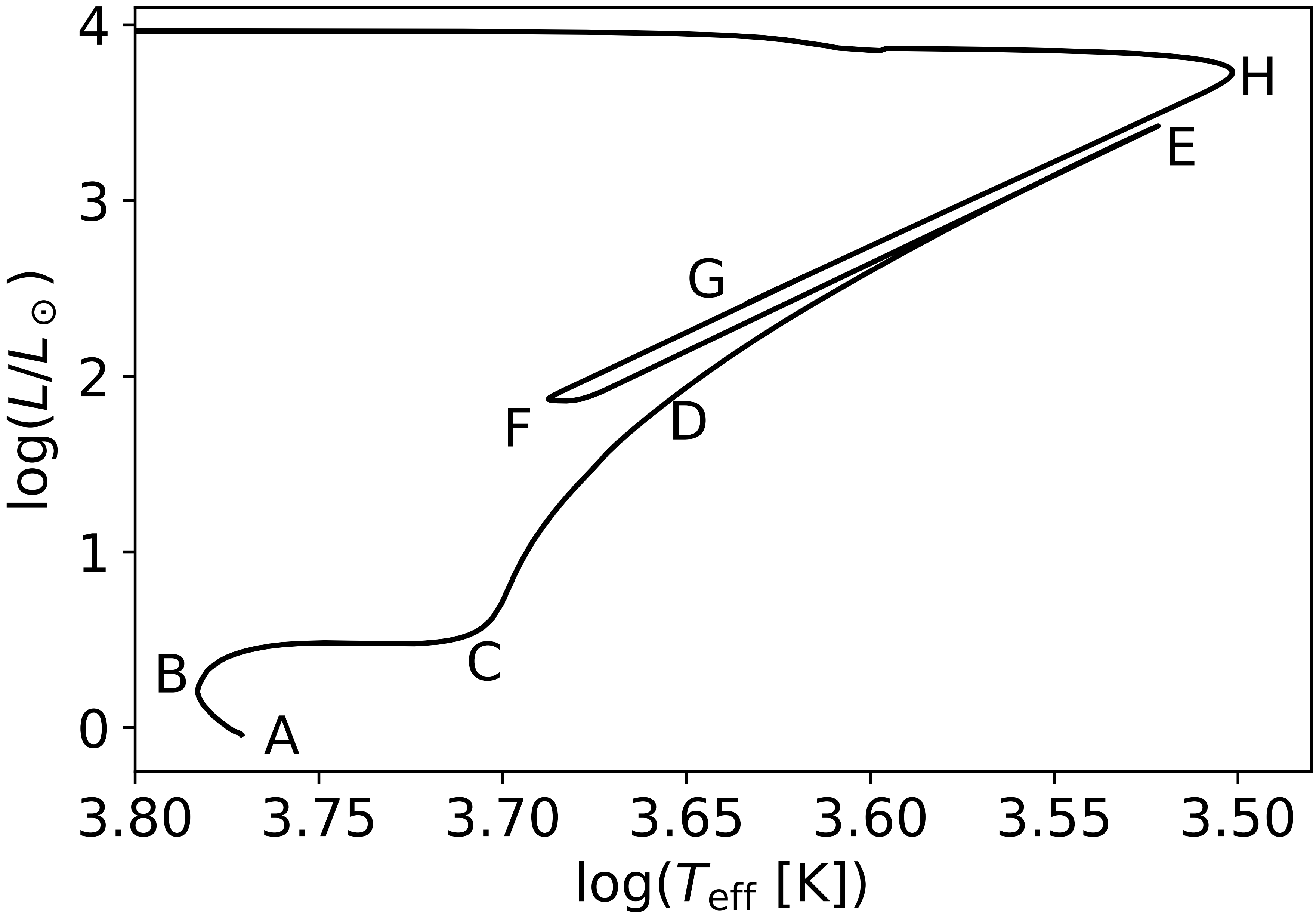

Intermediate mass stars in the HRD (EZ model for a $5\,M_\odot$ star)

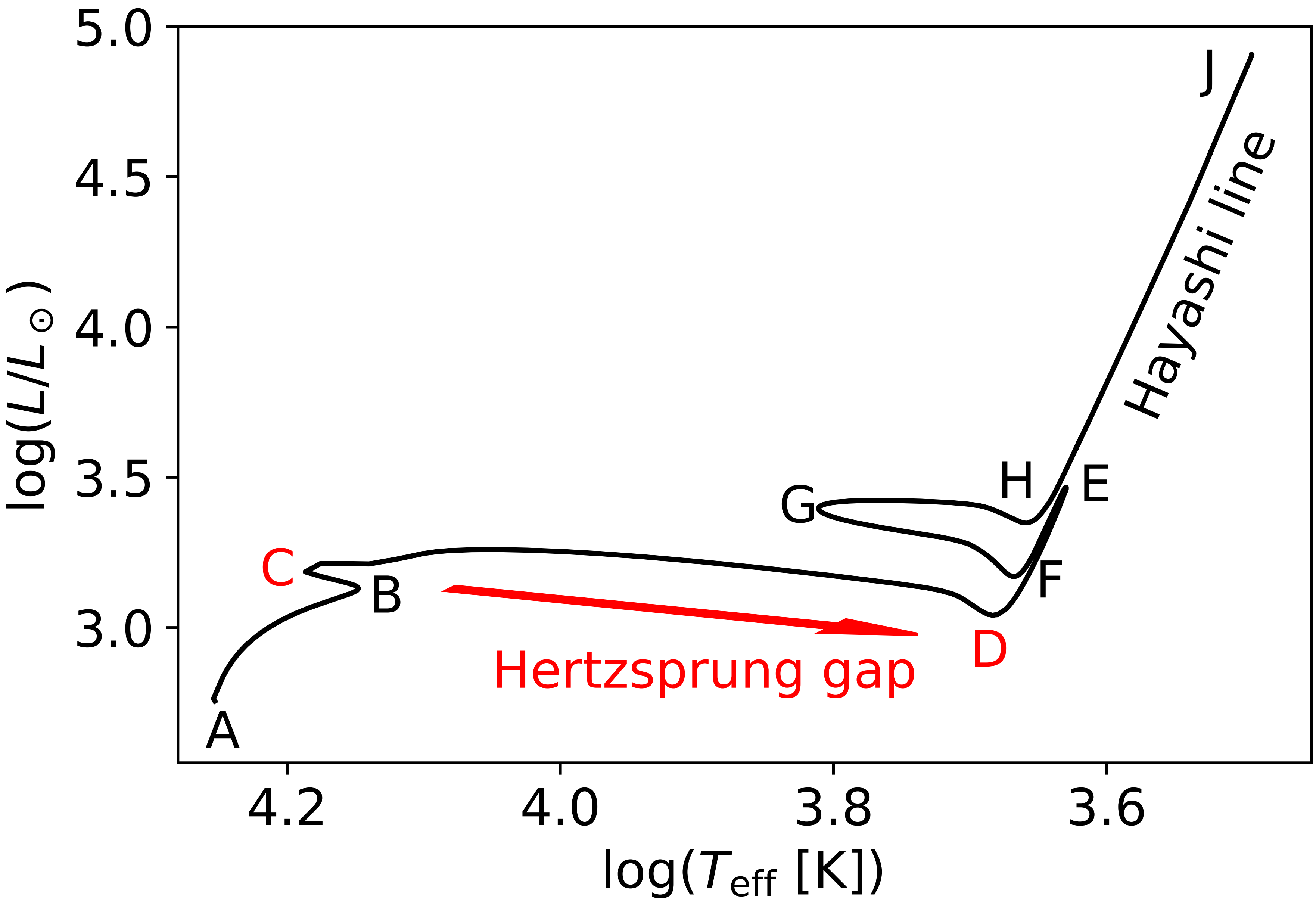

Evolution on the Asymptotic Giant Branch – Low/intermediate mass stars

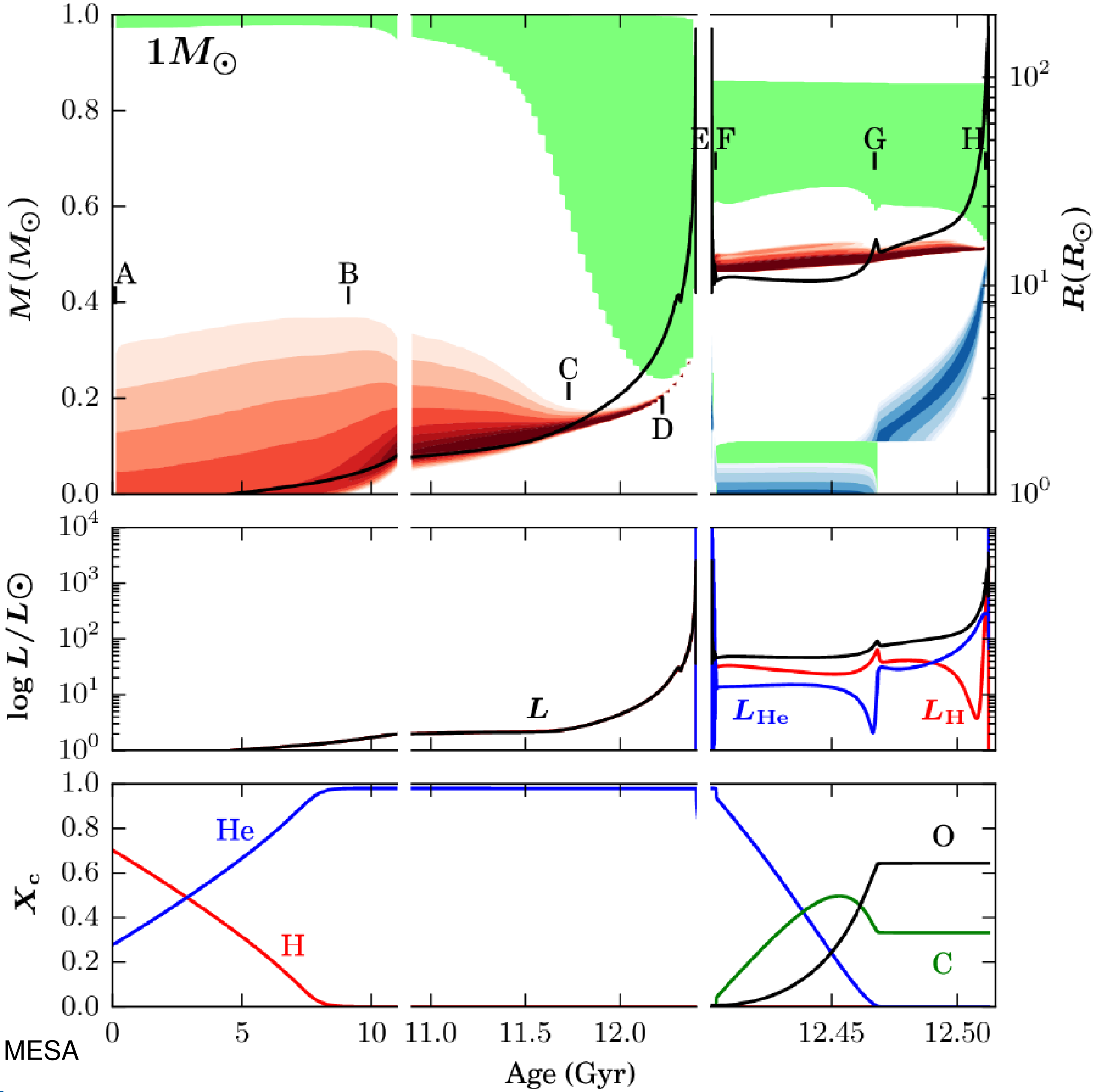

AGB (G-H)

- After central He is exhausted the CO core contracts. He shell burning starts and the star reaches the AGB
- Star has CO core, He burning shell, H burning shell and large H envelope
- Star can undergo thermal pulses when the ashes of H burning shell increase the mass of the He burning shell

Evolution on the Asymptotic Giant Branch – Low/intermediate mass stars

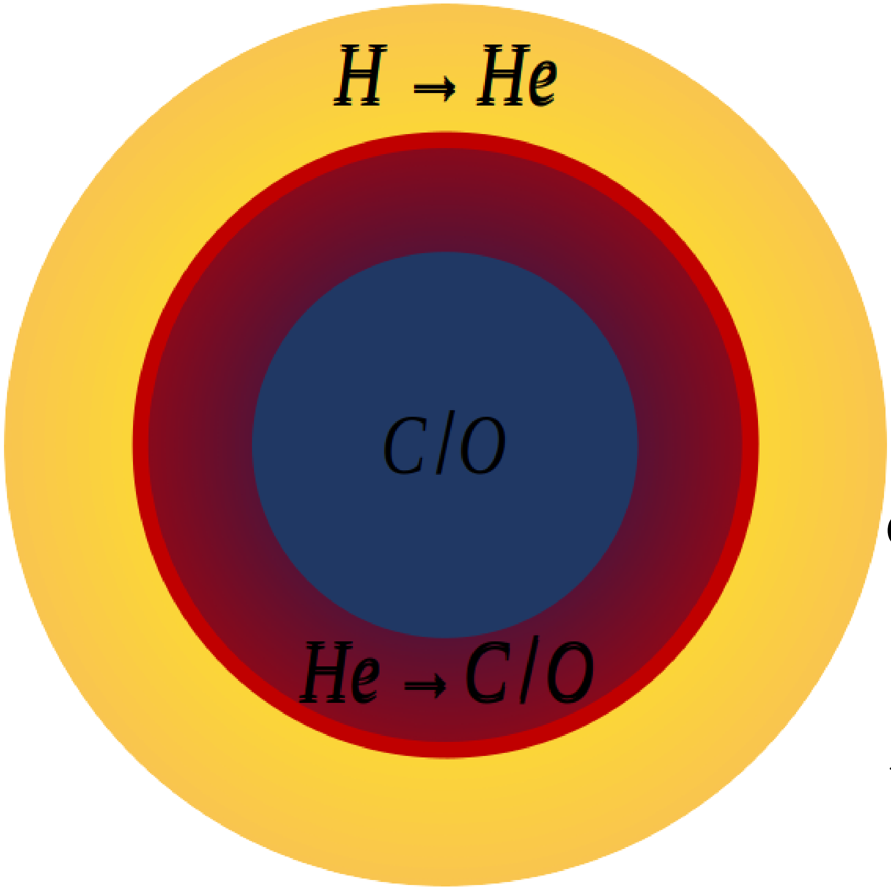

- He-shell burning phase
- gradually adds mass to the growing CO core, which becomes degenerate due to its increasing density

- AGB phase starts at the exhaustion of helium in the center
- low-mass stars: AGB at similar luminosities but higher $T_{\rm eff}$ than preceding RGB phase, stars $M > 2.5\,\mathrm{M}_\odot$: at higher luminosities than the RGB

early AGB phase

- CO core contracts
- two active burning (H,He) shells

$\rightarrow$ He-rich layers above core expand, outer envelope starts contracting

- due to expansion of the He-rich zone, the temperature in the H-shell decreases and the H-burning shell is extinguished

$\rightarrow$ He-rich layer plus H-rich outer envelope expanding in response to core contraction

Evolution on the Asymptotic Giant Branch – Low/intermediate mass stars

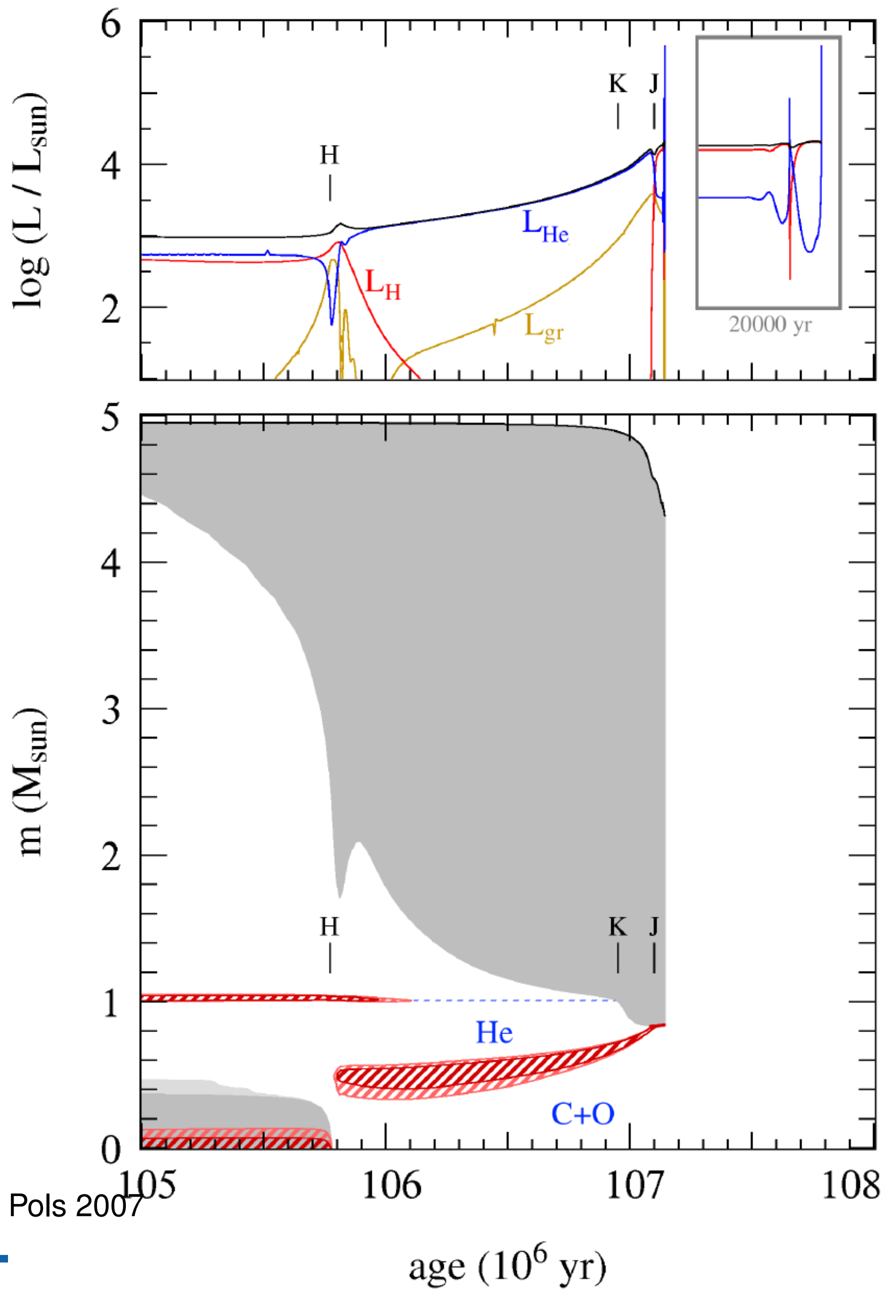

Pols 2007

Second dredge-up

- expanding envelope cools, convective envelope penetrates deeper until it reaches the composition discontinuity left by the extinct H-shell at K
- For stars $> 4\,M_\odot \rightarrow$ Second dredge-up
- lower-mass stars the H-burning shell remains active at a low level, which prevents the convective envelope from penetrating deeper into the star
- material that is dredged up $(0.2 - 1 M_\odot)$: hydrogen has been burned into helium, ^{12}C and ^{16}O almost completely converted into ^{14}N by CNO-cycle
- much more dramatic effect than first dredge-up om RGB

Evolution on the Asymptotic Giant Branch – Low/intermediate mass stars

- As the He-burning shell approaches the H-He discontinuity, its luminosity decreases as it runs out of fuel
- layers above contract, heating the extinguished H-burning shell until it is re-ignited

$\rightarrow$ Helium shell source much hotter than H-burning limit

- neighbouring shell sources can influence each other
- each type of burning requires a separate range of temperature
- Enormous increase in H-burning, when He shell approaches a H-rich layer
- relative motion of H and He shell (X_i mass concentration of reacting element)

$$\frac{\dot{m}_{\mathrm{H}}}{\dot{m}_{\mathrm{He}}} = \frac{L_{\mathrm{H}}}{L_{\mathrm{He}}} \frac{q_{\mathrm{H}}}{q_{\mathrm{He}}} \frac{X_{\mathrm{H}}}{X_{\mathrm{He}}} \qquad \overset{\text{stationary}}{\Rightarrow} \quad L_{\mathrm{H}} \approx 7 L_{\mathrm{He}}$$

Nuclear burning in the He-shell concentrated towards the outer edge

$\rightarrow$ Thin layer of thickness l and mass Δm

$$l = r - r_0 \ll R \qquad \Delta m = 4\pi r_0^2 l \rho \qquad \overset{r_0=\mathrm{const},\mathrm{d}m=0}{\longrightarrow} \frac{\mathrm{d}\rho}{\rho} = -\frac{\mathrm{d}l}{l} \overset{\mathrm{d}r=\mathrm{d}l}{=} -\frac{r}{l}\frac{\mathrm{d}r}{r}$$

Evolution on the Asymptotic Giant Branch – Low/intermediate mass stars

Shell expands as reaction to nuclear energy generation

$\rightarrow$ homology relation $$\frac{dP}{P} = -4\frac{dr}{r} \qquad \rightarrow \frac{dP}{P} = 4\frac{l}{r}\frac{d\rho}{\rho}$$

General equation of state

$$\frac{d\rho}{\rho} = \alpha\frac{dP}{P} - \delta\frac{dT}{T} = \alpha 4\frac{l}{r}\frac{d\rho}{\rho} - \delta\frac{dT}{T} \quad \overset{l/r\Rightarrow 0}{\longrightarrow} \quad \frac{d\rho}{\rho} = -\delta\frac{dT}{T}$$

expansion of a thin shell $\frac{d\rho}{\rho} < 0$ leads to an increase of the temperature $\frac{dT}{T} > 0$

- Higher temperature leads to higher nuclear enery production
- Runaway process: Thin shell instability of He-shell

Instability of the He-shell leads to thermal runaway until the shell has expanded enough to stop it

- He-shell extinguishes and contracts
- He-shell reignites
- Thermal pulses (TP-AGB)

Evolution on the Asymptotic Giant Branch – Low/intermediate mass stars

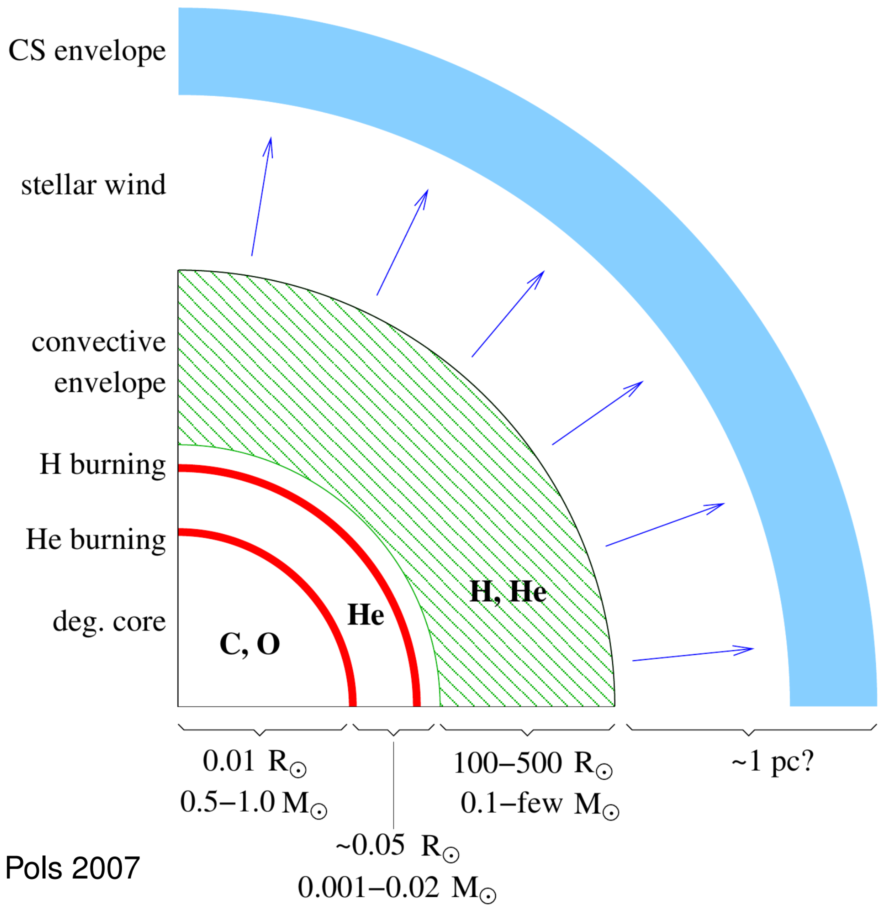

Pols 2007

thermally pulsing AGB phase

- phase of double shell burning
- most of the time, the He-burning shell is inactive
- H-burning shell adds mass to the He-rich region between the burning shells
- increases the pressure and temperature at the bottom of this region
- mass of the intershell region reaches a critical value $\rightarrow$ helium shell flash
- energy release by He-shell flash goes into expansion of the intershell
- phase of stable He- shell burning
- expansion and cooling of the intershell region after the He-shell flash, H-burning shell extinguishes

Evolution on the Asymptotic Giant Branch – Low/intermediate mass stars

thermally pulsing AGB phase

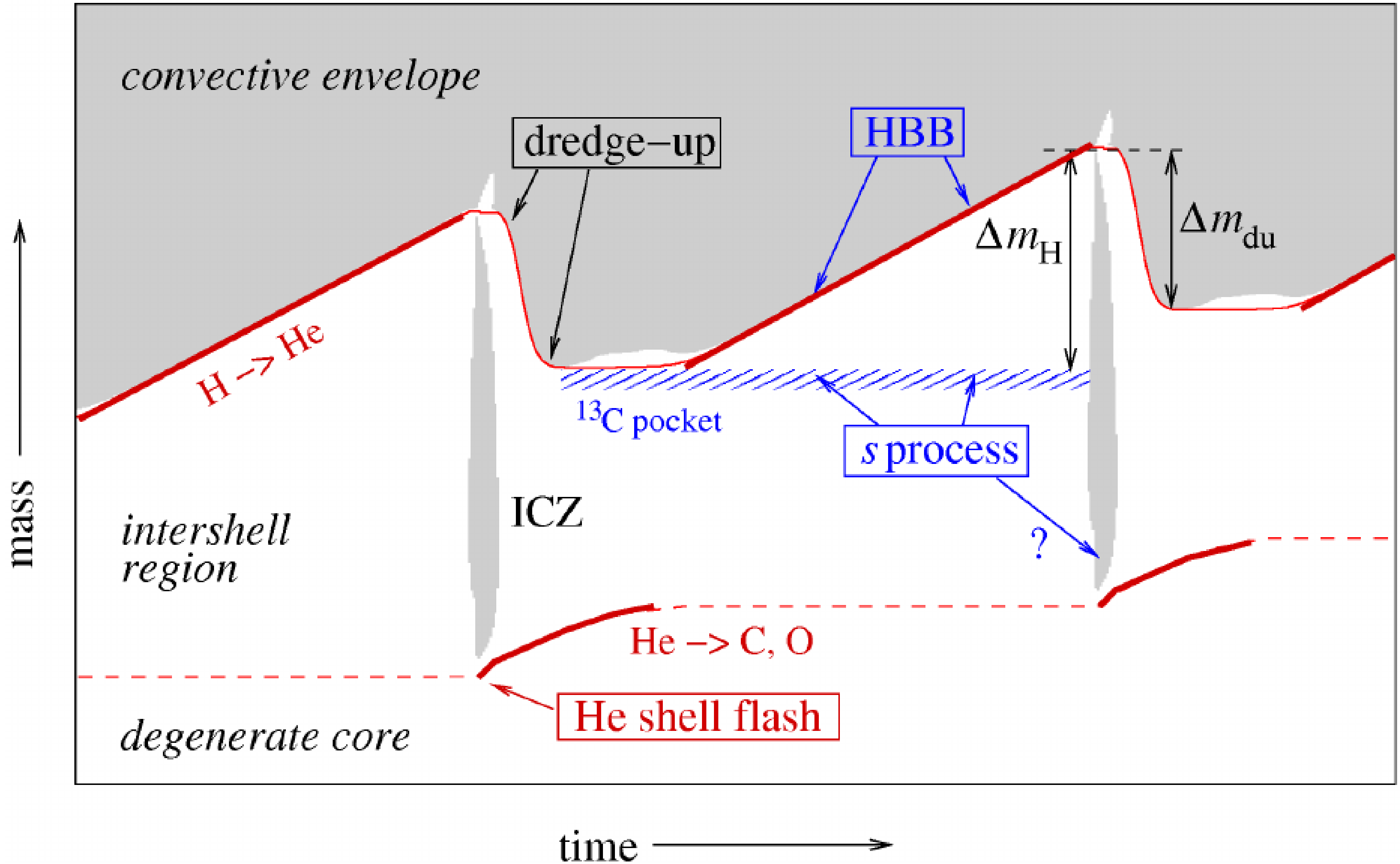

Evolution on the Asymptotic Giant Branch – Low/intermediate mass stars

Third dredge-up

- Expansion and cooling of the intershell region lead to a deeper penetration of the outer convective envelope beyond the now extinct H-burning shell
- material from the intershell region is mixed into the outer envelope $\rightarrow$ third dredge-up
- He, and He-burning products (^{12}C) can appear at the surface

$\rightarrow$ leads to important nucleosynthesis of ^{12}C, ^{14}N and elements heavier than iron

$\rightarrow$ makes the stellar envelope and atmosphere more carbon-rich

- H-burning shell is reignited $\rightarrow$ stable H-shell burning
- mass of the intershell region grows until the next thermal pulse occurs
- interpulse period depends on the core mass, lasting between $50,000$ yrs (for low-mass AGB stars with CO cores of $\sim 0.5\,M_\odot$) to < 1000 yrs for the most massive AGB stars.

Evolution on the Asymptotic Giant Branch – Low/intermediate mass stars

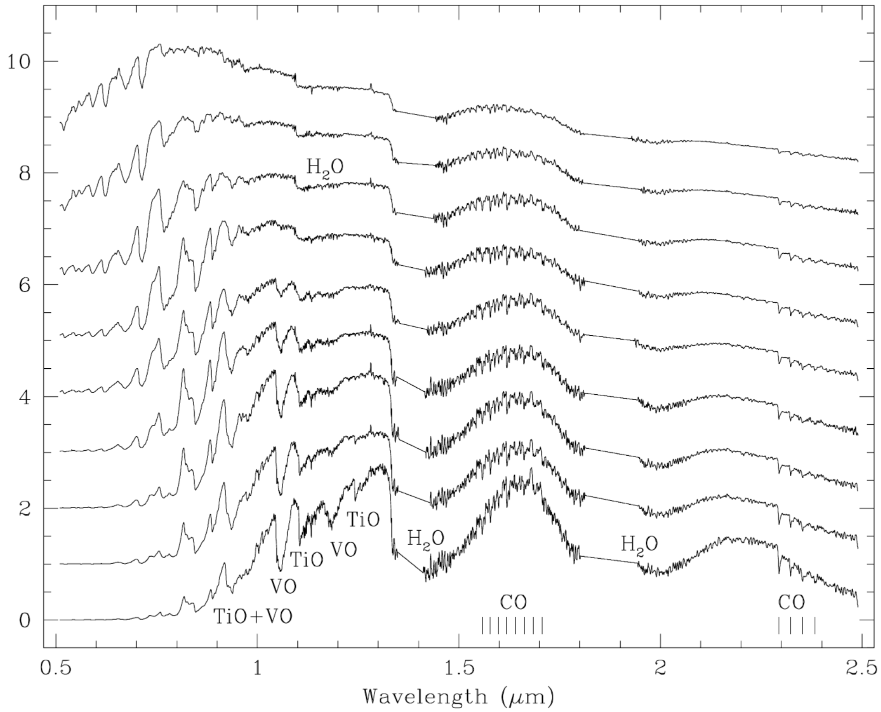

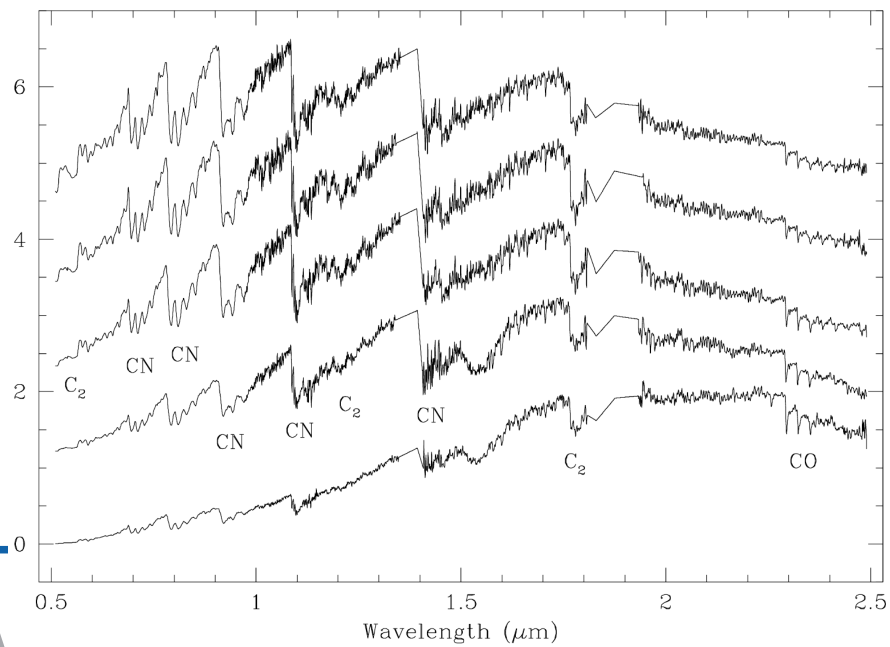

Lançon et al. 2002, A&A 393, 167

Abundance changes on the AGB

- appearance of helium-burning products at the surface $\rightarrow$ ^{12}C abundance increases after every dredge-up episode
- low temperatures in the stellar atmosphere C and O atoms bound into CO
- if $C/O < 1$: oxygen rich AGB stars (TiO, H_2O)
- after repeated dredge-ups $C/O > 1$: C forms carbon-rich molecules e.g. C_2, CN: carbon stars
- Formation of dust
- chemically peculiar; e.g. ^{19}F and ^{99}Tc

Red (super-)giants: Luminosity class III-I

Evolution on the Asymptotic Giant Branch – Low/intermediate mass stars

Nucleosynthesis on the AGB

- enriched in elements heavier than iron, such as Zr, Y, Sr, Tc, Ba, La and Pb
  $\rightarrow$ Trans-iron elements are produced via the s-process
- source of free neutrons produced in He-burning in the He-rich intershell region: $^{13}\mathrm{C}(\alpha,\mathrm{n})^{16}\mathrm{O}$, $^{22}\mathrm{Ne}(\alpha,\mathrm{n})^{25}\mathrm{Mg}$ (He-flash in massive AGB stars)
- ^{22}Ne abundant in the intershell region, because ^{14}N left by the CNO-cycle converted to ^{22}Ne by He-burning: $^{14}\mathrm{N}(\alpha,\gamma)^{18}\mathrm{F}(\beta^{+})^{18}\mathrm{O}(\alpha,\gamma)^{22}\mathrm{Ne}$
- main neutron source in low-mass stars: $^{13}\mathrm{C}(\alpha,\mathrm{n})^{16}\mathrm{O}$:
  thin shell or 'pocket' of ^{13}C formed by partial mixing of protons and ^{12}C at interface between the H-rich envelope and the C-rich intershell region, reacts with He when $T > 10^{8}\,\mathrm{K}$
- s-enriched pocket is ingested into the intershell convection zone during the next pulse, and mixed throughout the intershell region, together with carbon produced by He burning
- carbon and s-process material from the intershell region is subsequently mixed to the surface in the next dredge-up phase

Evolution on the Asymptotic Giant Branch – Low/intermediate mass stars

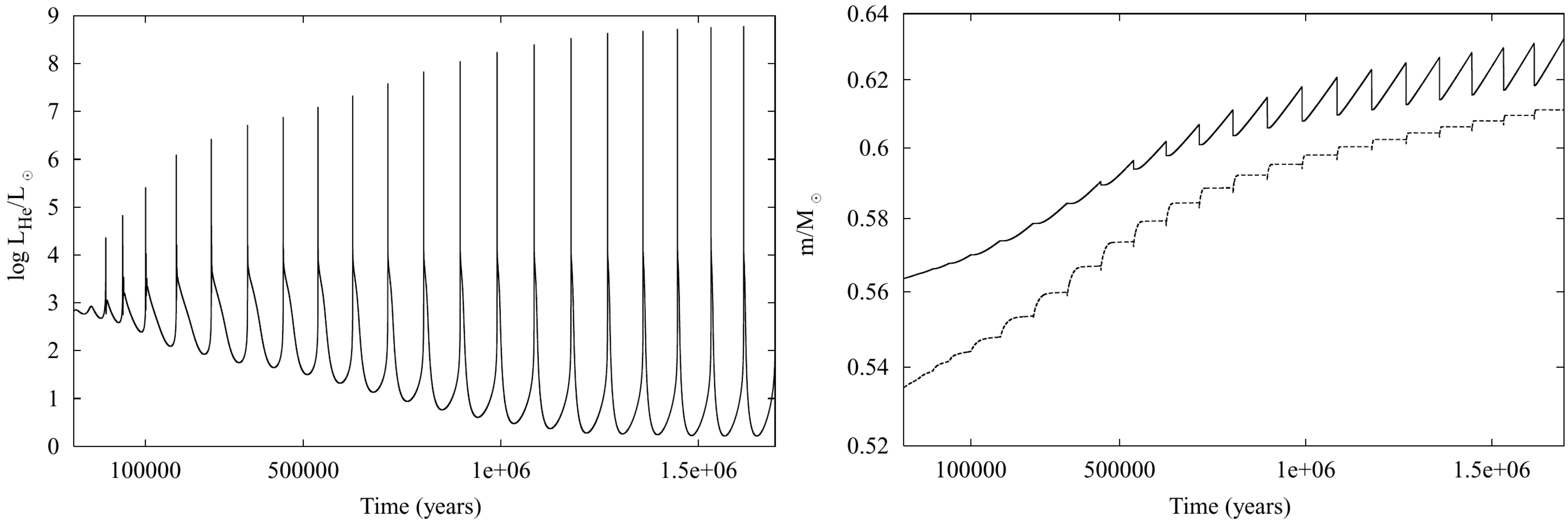

Stancliffe et al. 2004, MNRAS 352, 984

- Change in surface luminosity dependent on the stellar mass
- If the shells reach close to the surface, jumps in the HRD on short timescales ($\sim 10^4$ yr) are possible
- Luminosity depends on the core mass

$$\frac{L}{L_\odot} = 5.92 \times 10^4 \left(\frac{M_c}{M_\odot} - 0.52 \right)$$

Evolution on the Asymptotic Giant Branch – Low/intermediate mass stars

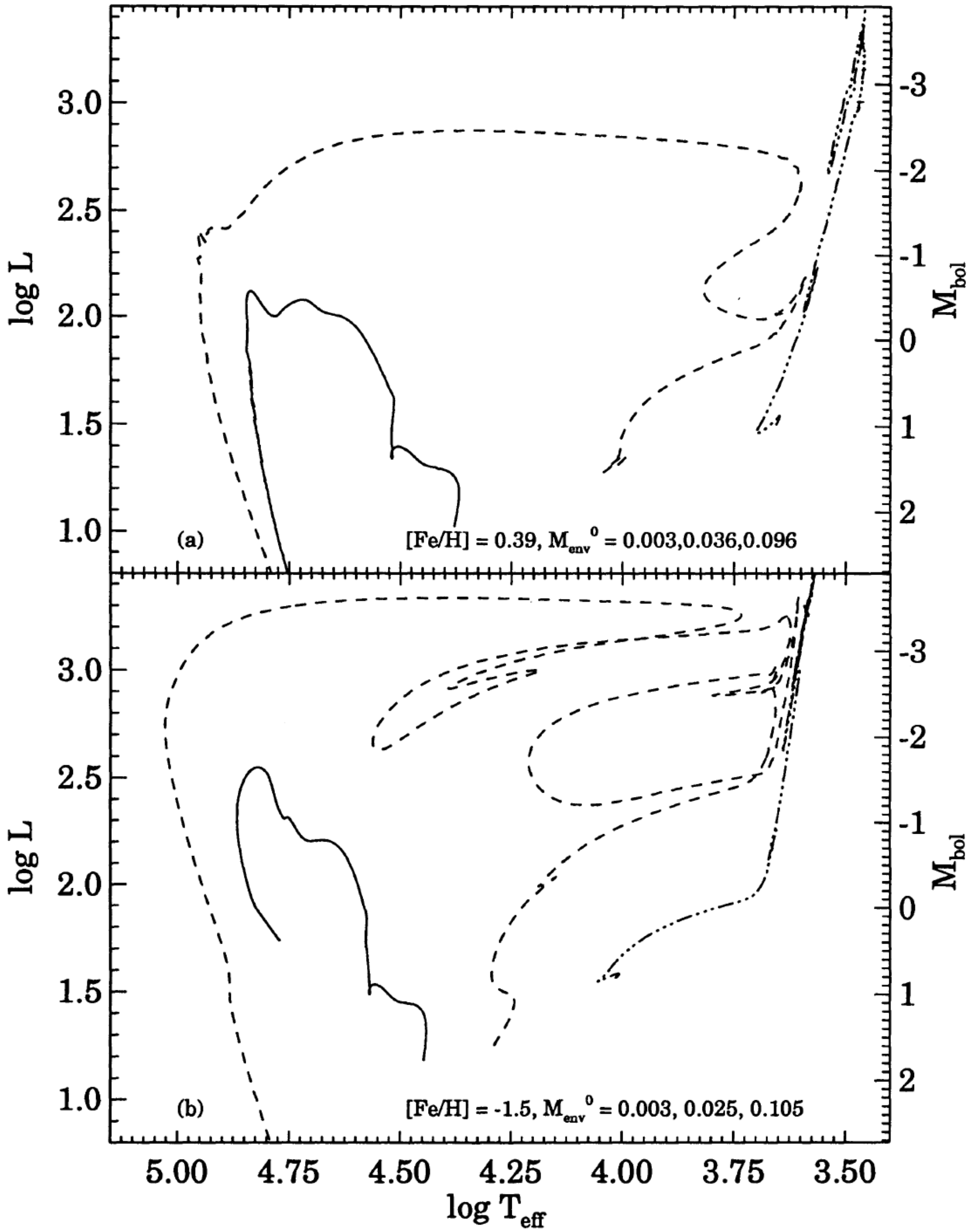

AGB-evolution depends also on the mass of the H-shell after the HB phase and the metallicity

- sdO/B stars do not reach the AGB phase
- AGB-manque (failed AGB)
- After He-shell burning they cool down to become low-mass C/O WDs ($\sim 0.3 - 0.47\,M_\odot$)
- Stars without He-core burning evolve to become low-mass or extremely low-mass (ELM) He WDs ($\sim 0.1 - 0.4\,M_\odot$)

Dorman et al. 1993, ApJ, 419, 596

Evolution on the Asymptotic Giant Branch – Low/intermediate mass stars

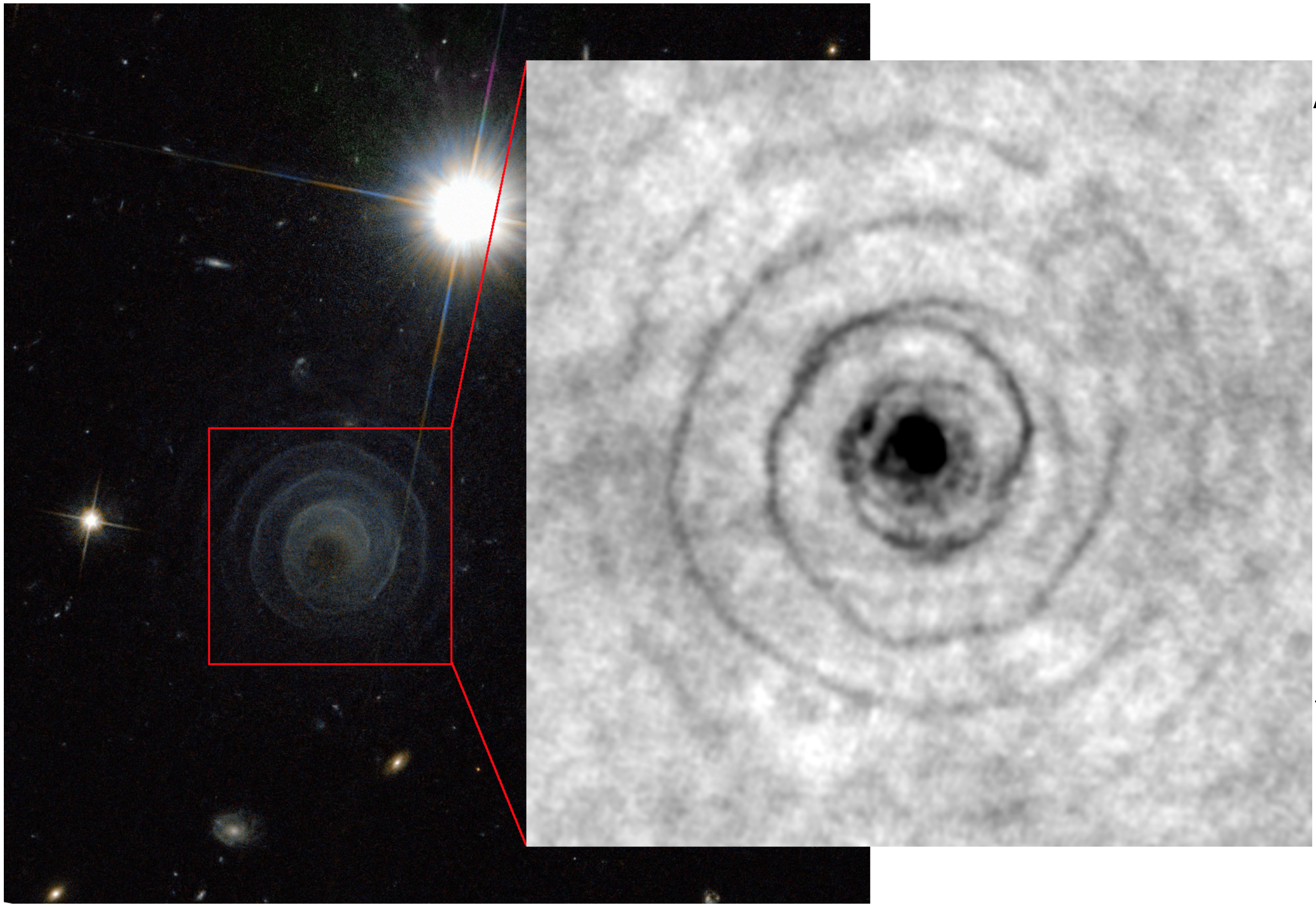

ESA/NASA & R. Sahai, ALMA, Hyosun Kim, et al.

AGB stars

- Strong mass loss (10^{-7}–$10^{-4}\,M_\odot/\mathrm{yr}$) driven by Mira pulsations and radiation pressure on dust particles formed in the cool atmosphere

$\rightarrow$ superwinds

Red (super-)giants: Luminosity class III-I

Evolution on the Asymptotic Giant Branch – Low/intermediate mass stars

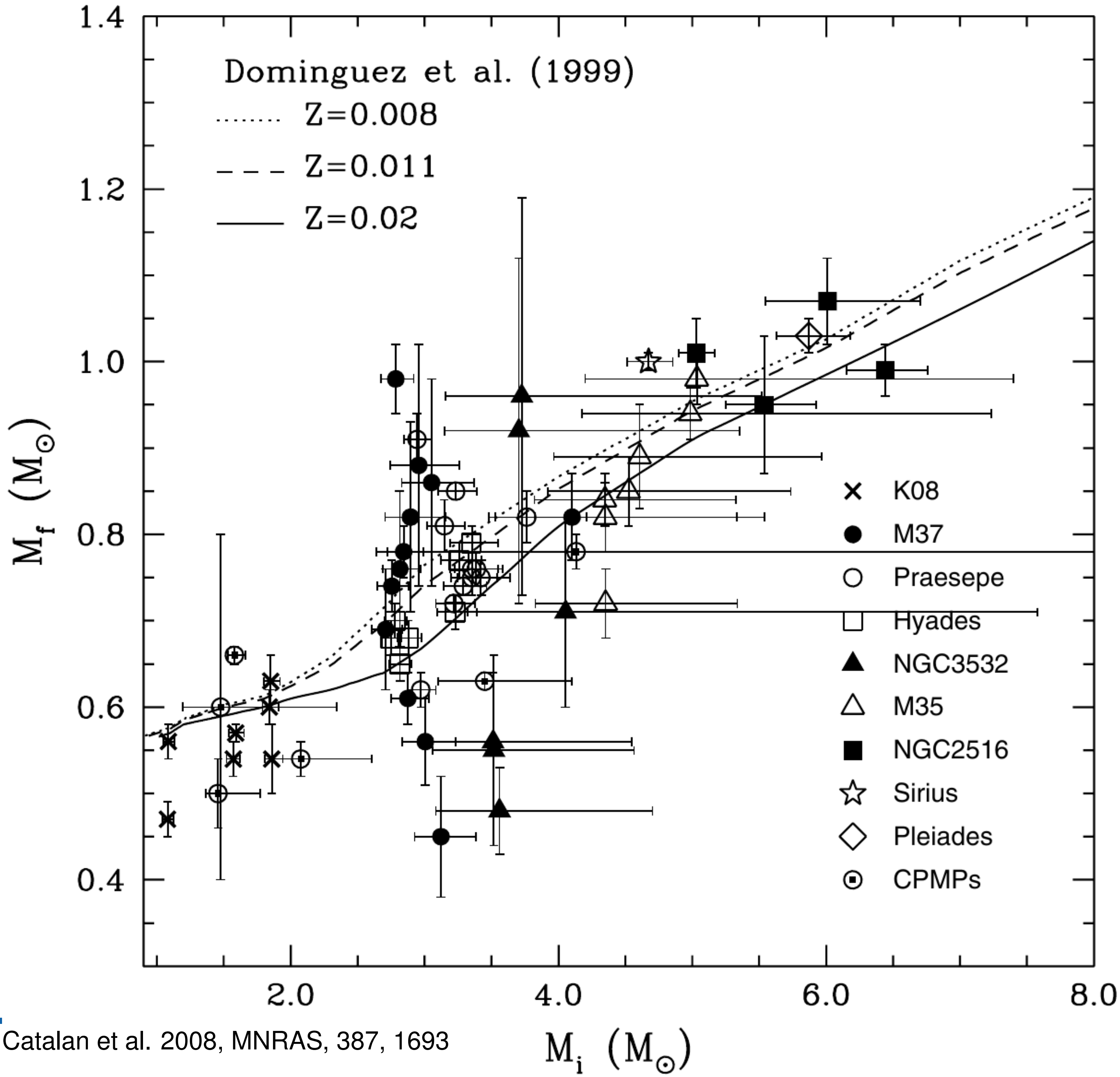

Catalan et al. 2008, MNRAS, 387, 1693

AGB stars

- Strong mass loss (10^{-7}–$10^{-4}\,M_\odot$/yr) driven by Mira pulsations and radiation pressure on dust particles formed in the cool atmosphere

$\rightarrow$ superwinds

Evolution on the Asymptotic Giant Branch – Low/intermediate mass stars

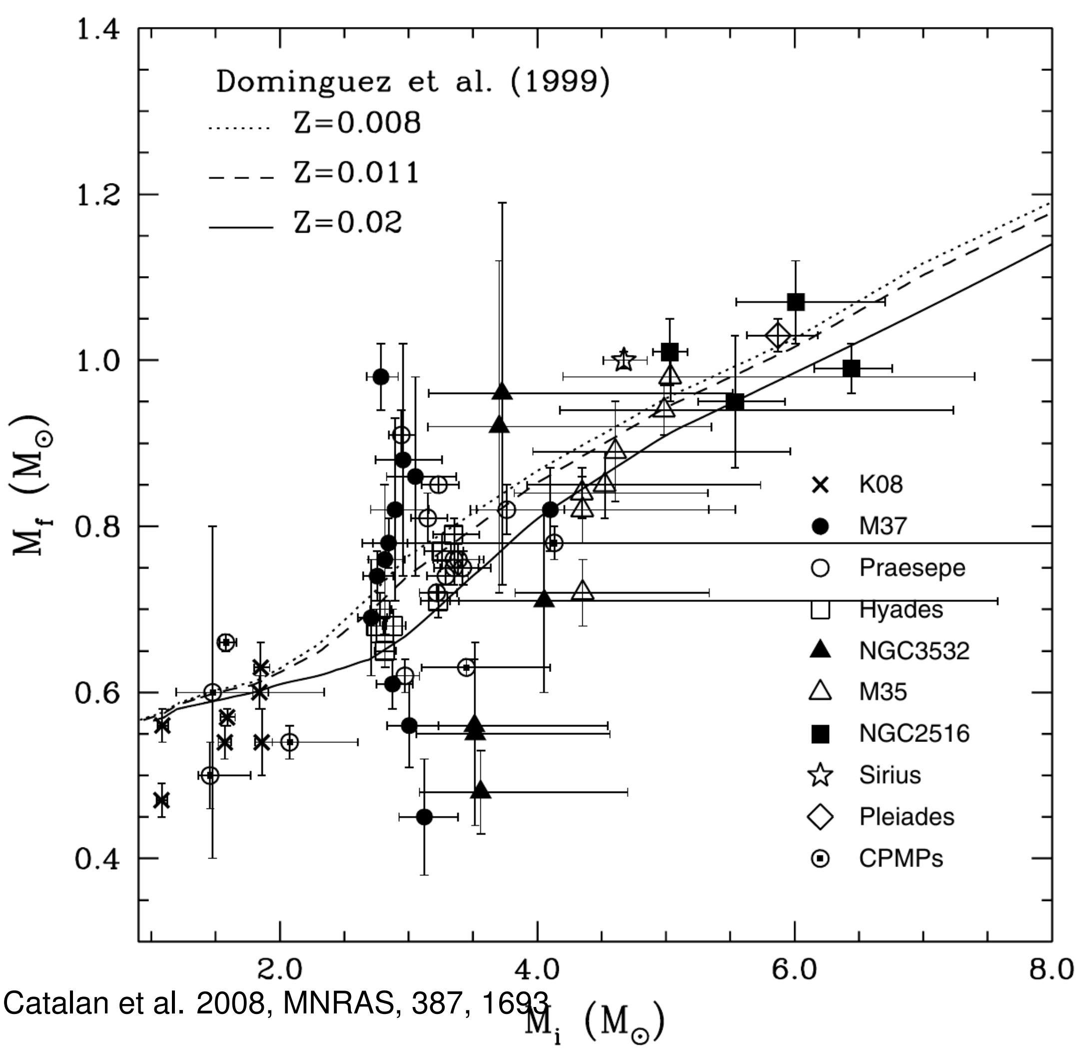

Catalan et al. 2008, MNRAS, 387, 1693

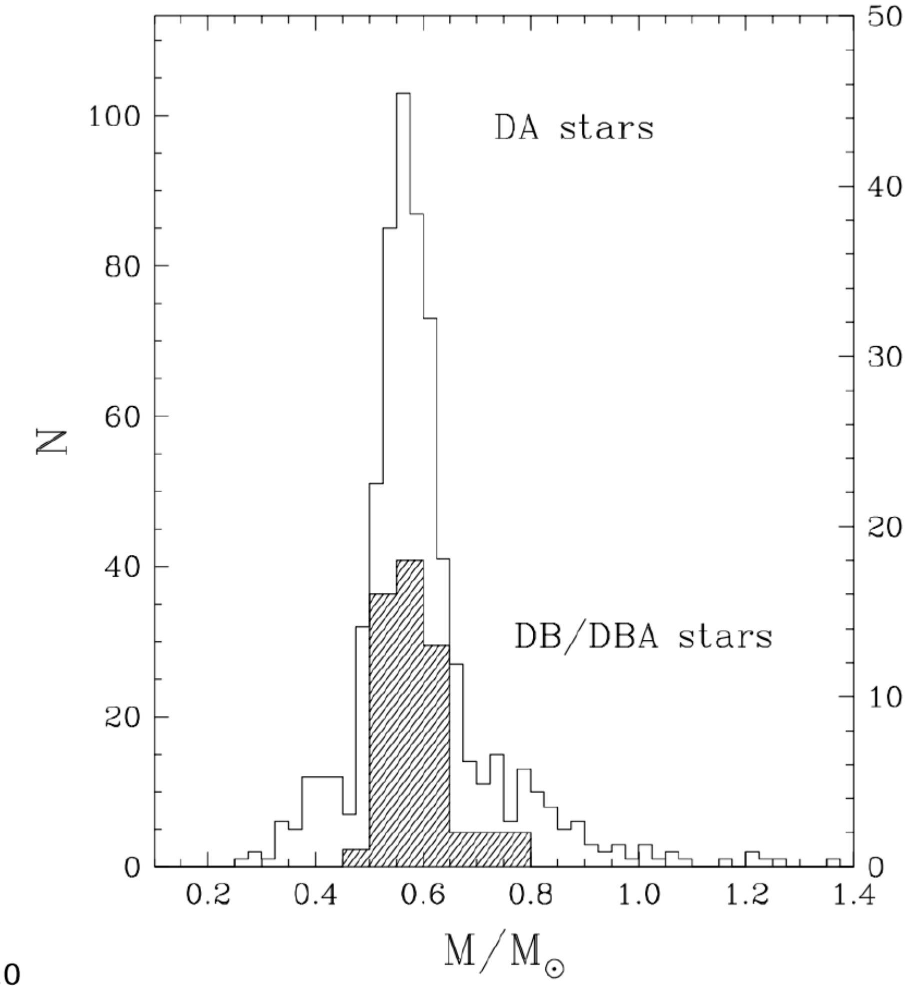

Bergeron et al. 2007, ASPC, 372, 29

Evolution beyond the Asymptotic Giant Branch

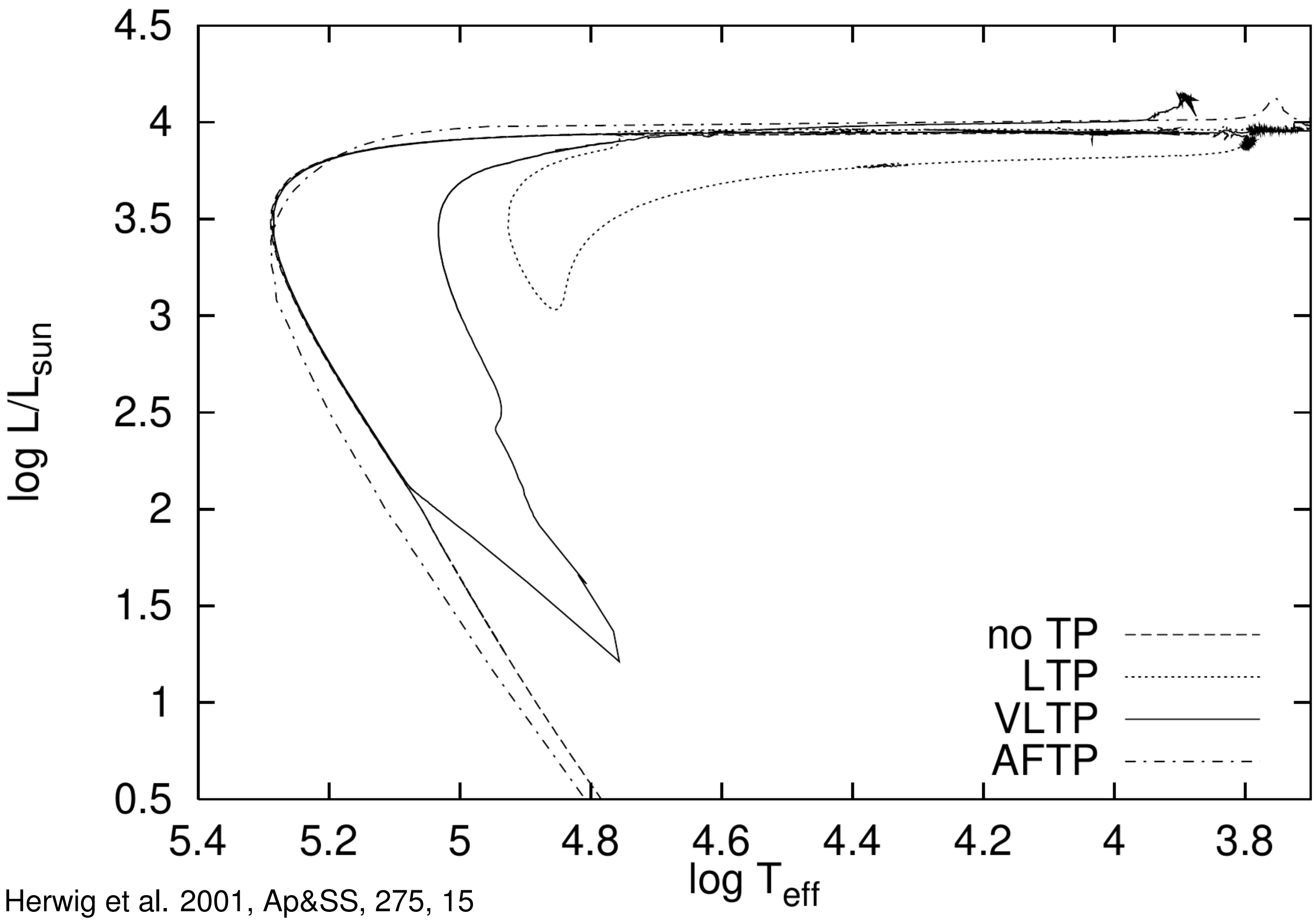

Herwig et al. 2001, Ap&SS, 275, 15

post-AGB evolution

- During the last pulses most of the stellar envelope is expelled
- Core is exposed and star heats up extremely ($T_{\mathrm{eff}} \sim 10^5\,\mathrm{K}$)

Evolution beyond the Asymptotic Giant Branch

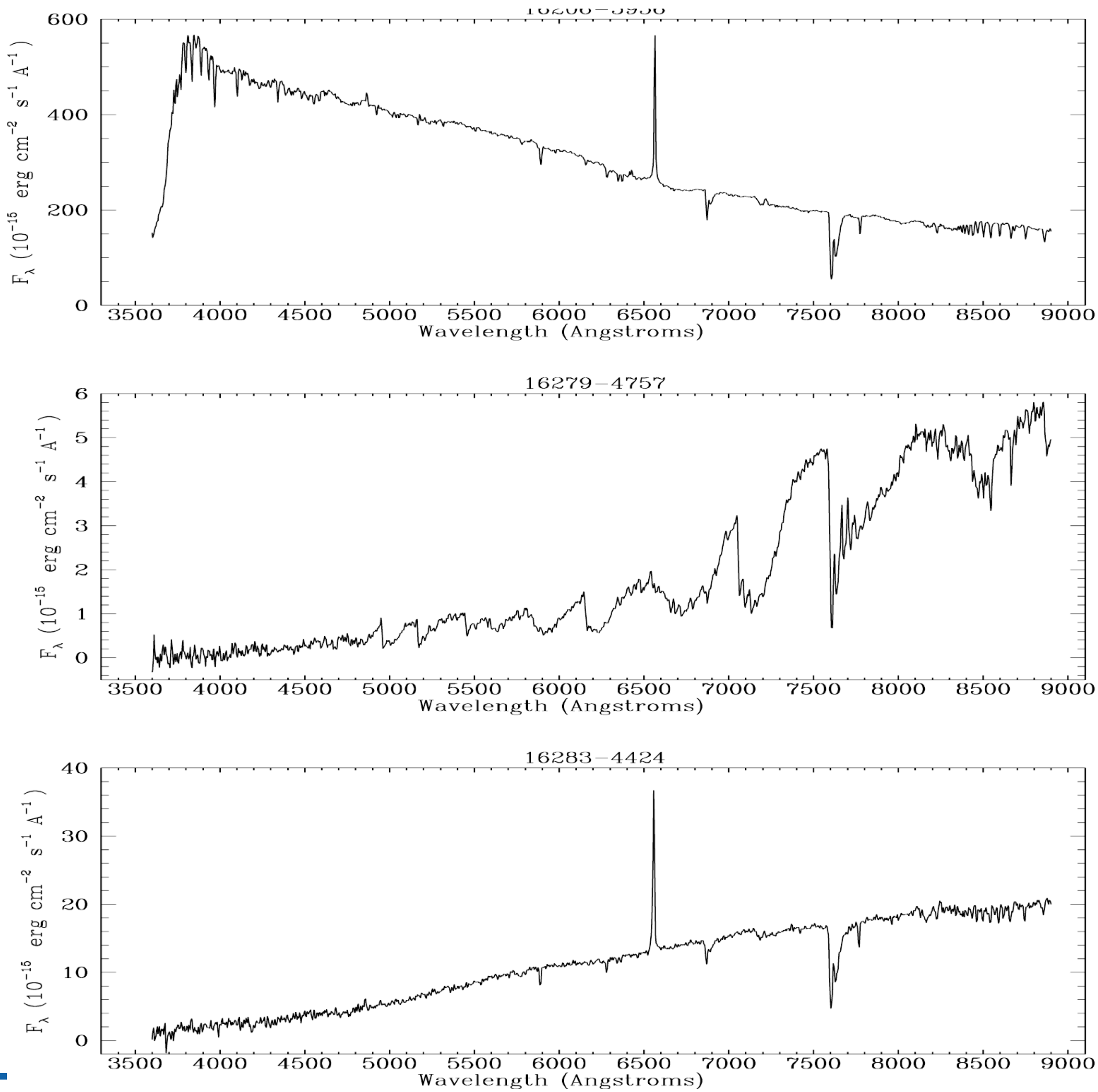

Suarez et al. 2006, A&A, 458, 173

post-AGB evolution

- Diverse spectral types from M to F/A
- (Super-)giants
- Reddening through dust and expelled material
- Emission of expelled material

Evolution beyond the Asymptotic Giant Branch

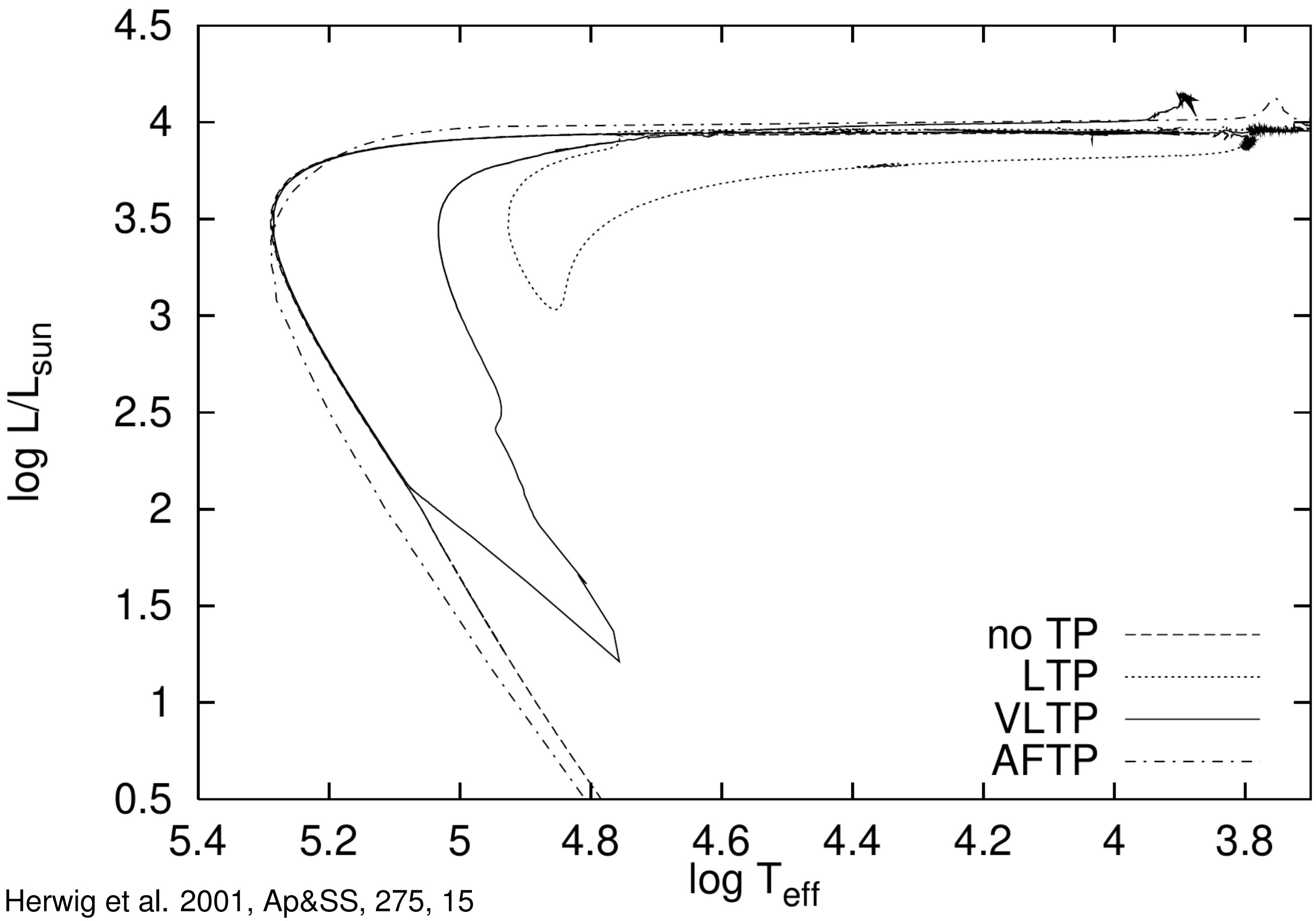

Herwig et al. 2001, Ap&SS, 275, 15

post-AGB evolution

- $T_{\mathrm{eff}} > 3 \times 10^4\,\mathrm{K}$
- Circumstellar matter becomes ionized
- **planetary nebula**
- Central stars of planetary nebula (CSPN)

Evolution beyond the Asymptotic Giant Branch

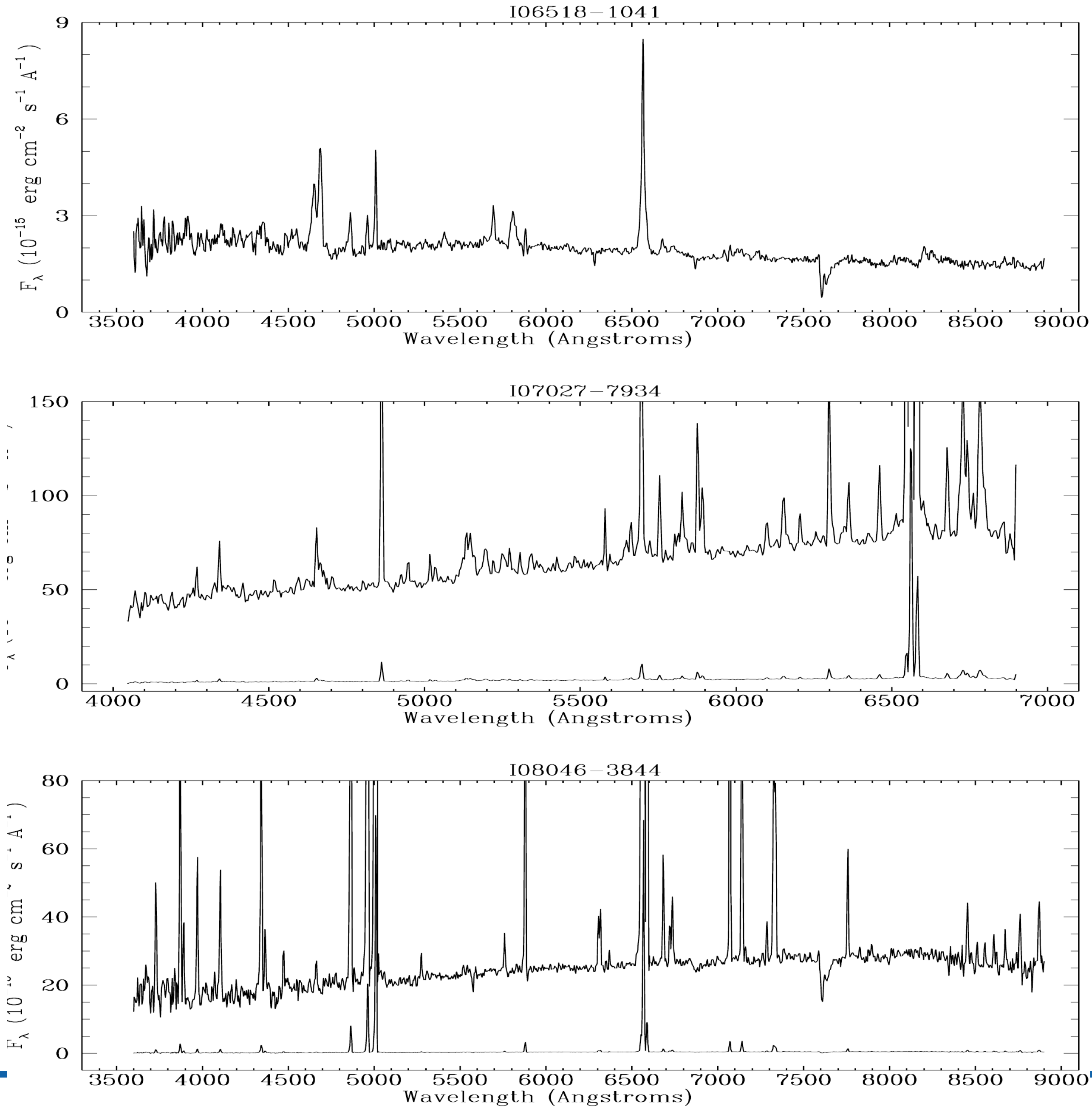

Suarez et al. 2006, A&A, 458, 173

post-AGB evolution

- CSPN spectra dominated by nebular emission lines
- Stellar wind and emission features
- H-rich types have spectral type B and O
- He-rich classes similar to massive WR-stars
- Spectral classes: [WN],[WC],[WO]

Evolution beyond the Asymptotic Giant Branch

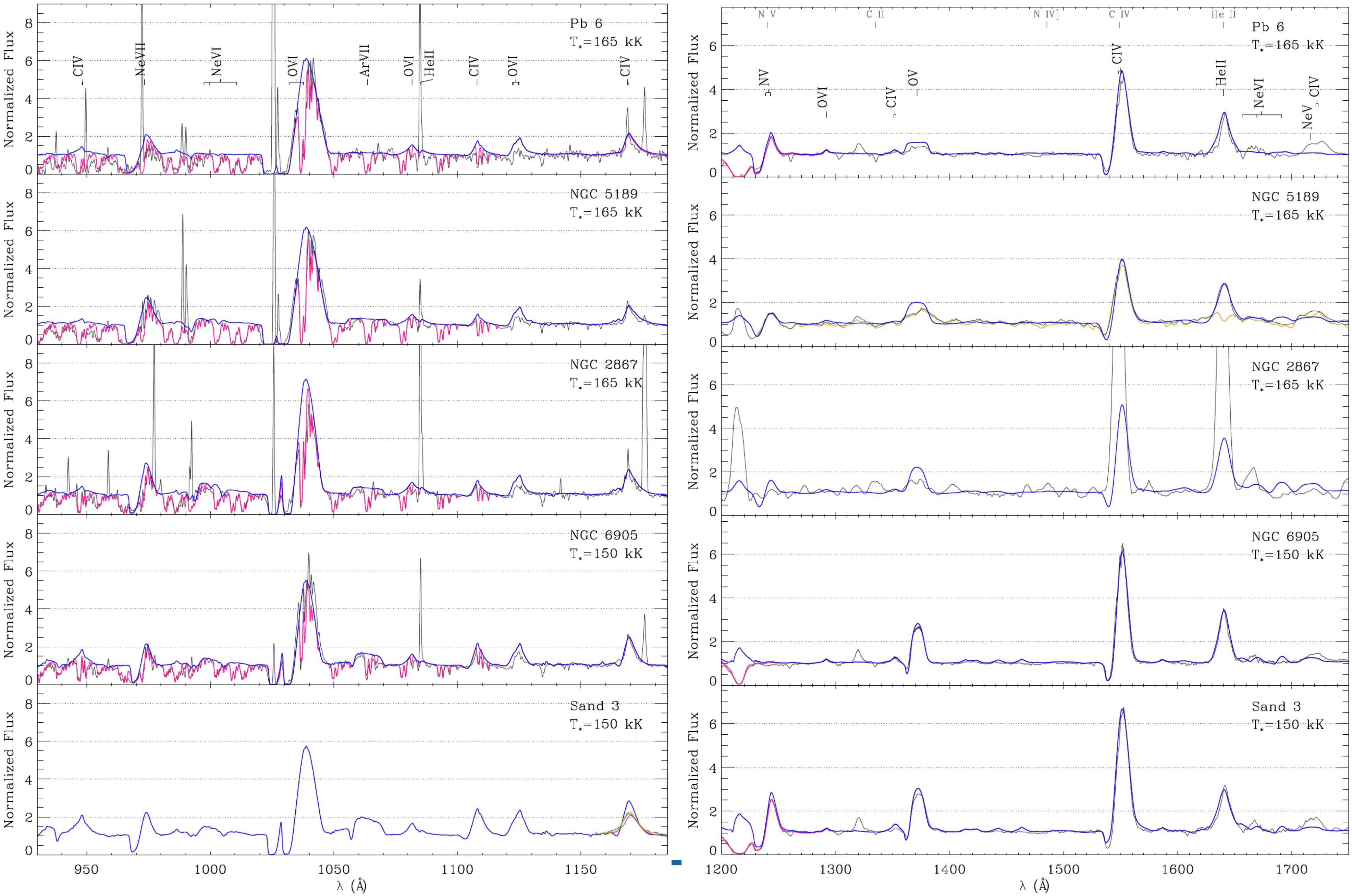

Keller et al. 2014, MNRAS, 442, 1379

Evolution beyond the Asymptotic Giant Branch

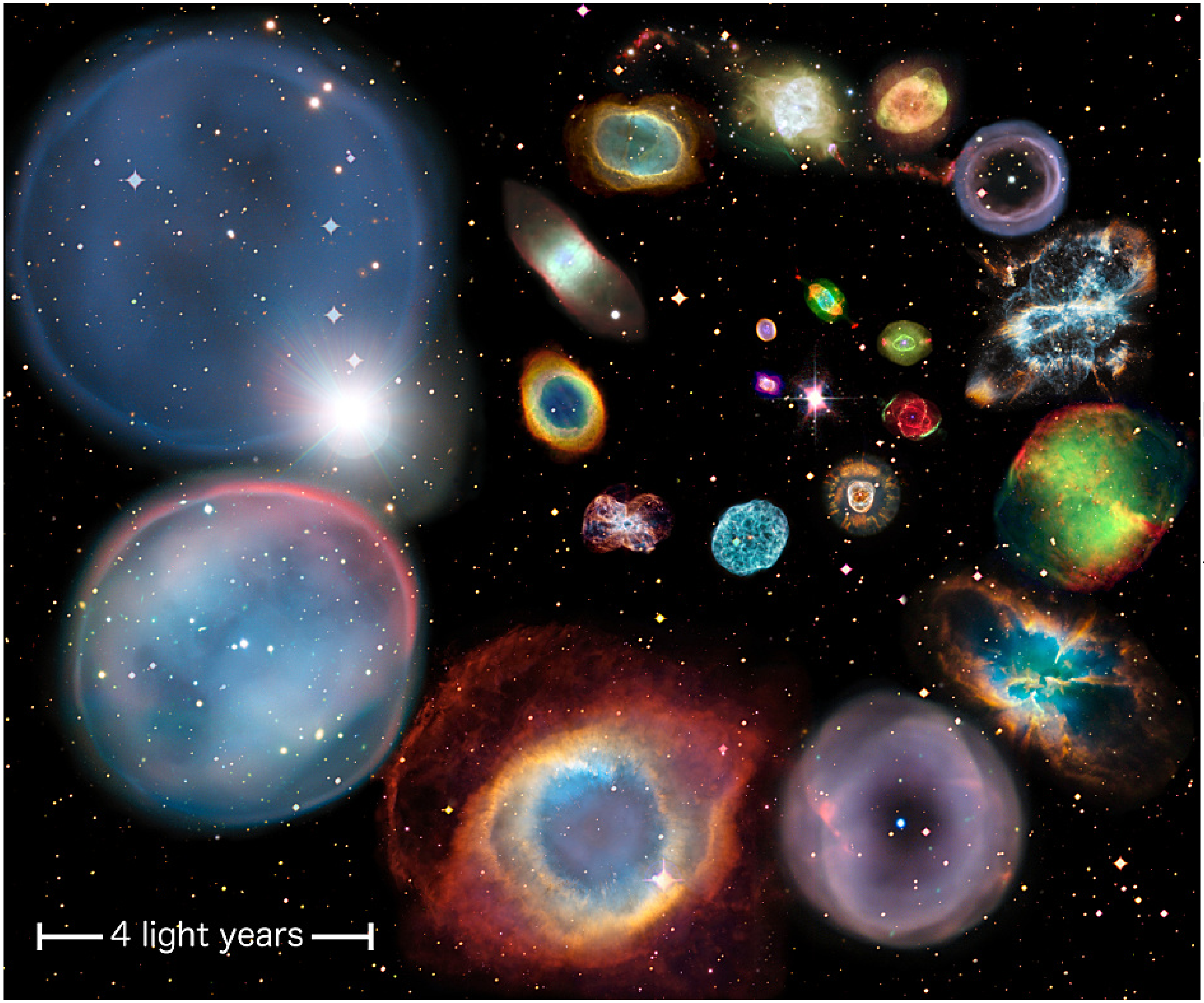

ESA/Hubble & NASA, ESO, Ivan Bojicic, David Frew, Quentin Parker

Planetary nebula

- Different shapes

$\rightarrow$ Binary evolution

- Lifetime $\sim 10^4$ yr

Evolution beyond the Asymptotic Giant Branch

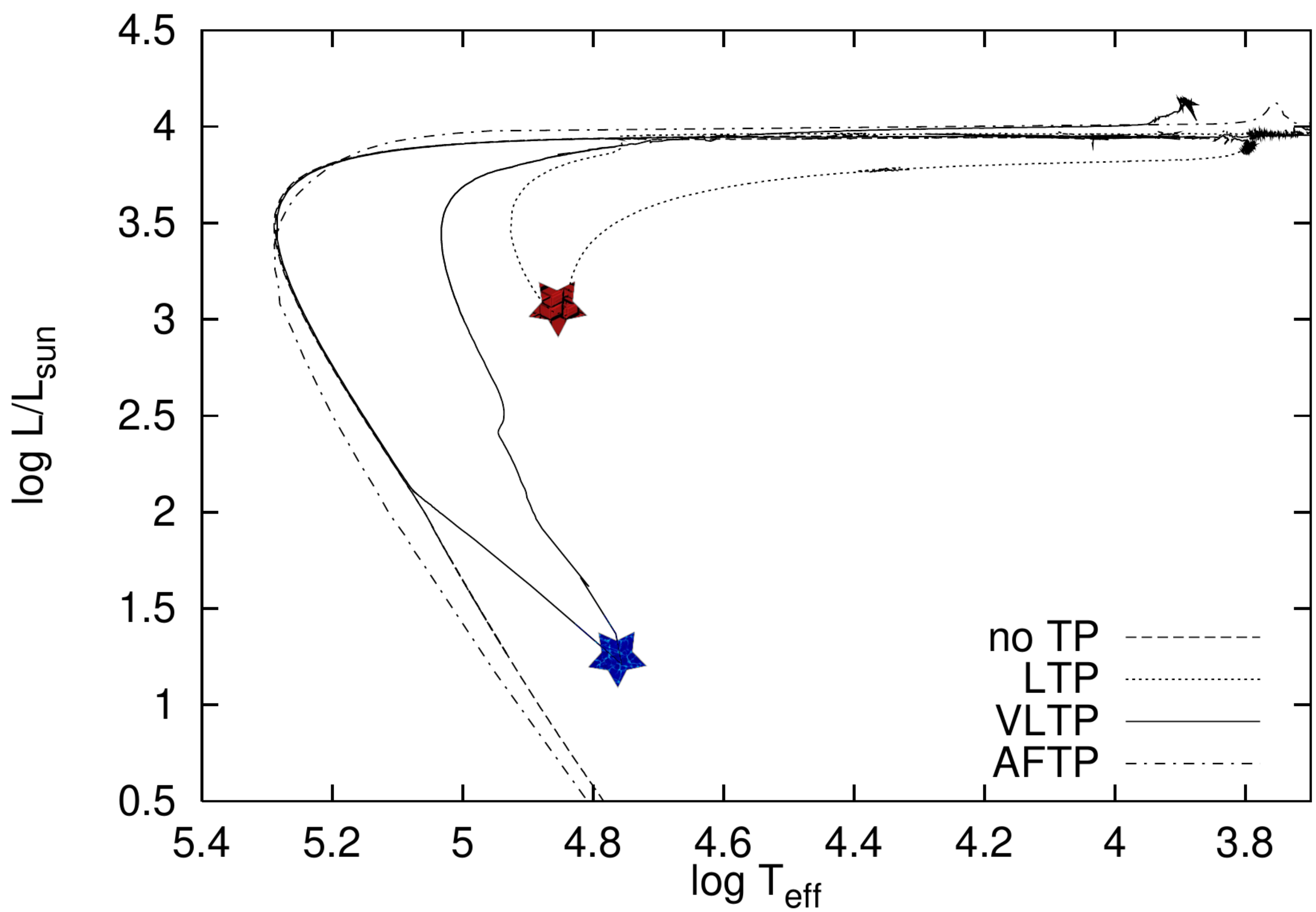

Herwig et al. 2001, Ap&SS, 275, 15

post-AGB evolution

- Thermal pulses can still happen at later stages
- Late thermal pulse (LTP)
- Very late thermal pulse (VLTP)
- Very short loops back to the red giant phase $\sim 10^1 - 10^3$ yr
- Stellar evolution can be seen in real-time

- Several objects known! (e.g. V4334 Sg, FG Sge) **"born-again" objects**

Evolution beyond the Asymptotic Giant Branch

Reindl et al. 2017, MNRAS, 464, 51; Youtube

Evolution beyond the Asymptotic Giant Branch

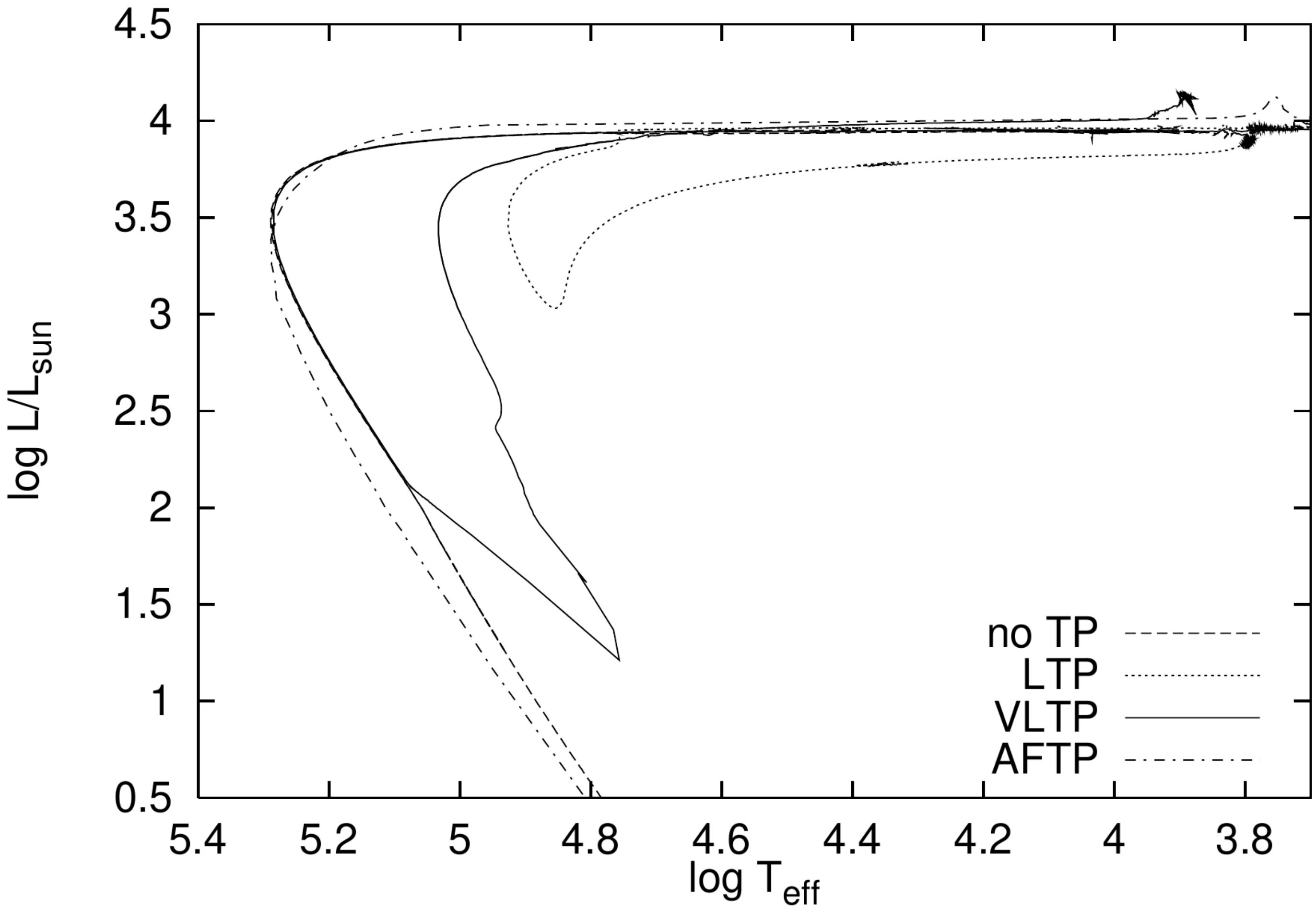

Herwig et al. 2001, Ap&SS, 275, 15

post-AGB evolution

- Finally, the core cools down and becomes a C/O white dwarf (WD)
- Depending on the details of evolution, the surface can be H- or He-rich
- Intermediate mass (Super-)AGB stars ($8 - 10\,M_\odot$) might ignite C/O burning
- Massive Ne/O WDs ($\sim 1.4\,M_\odot$)

Late massive core evolution

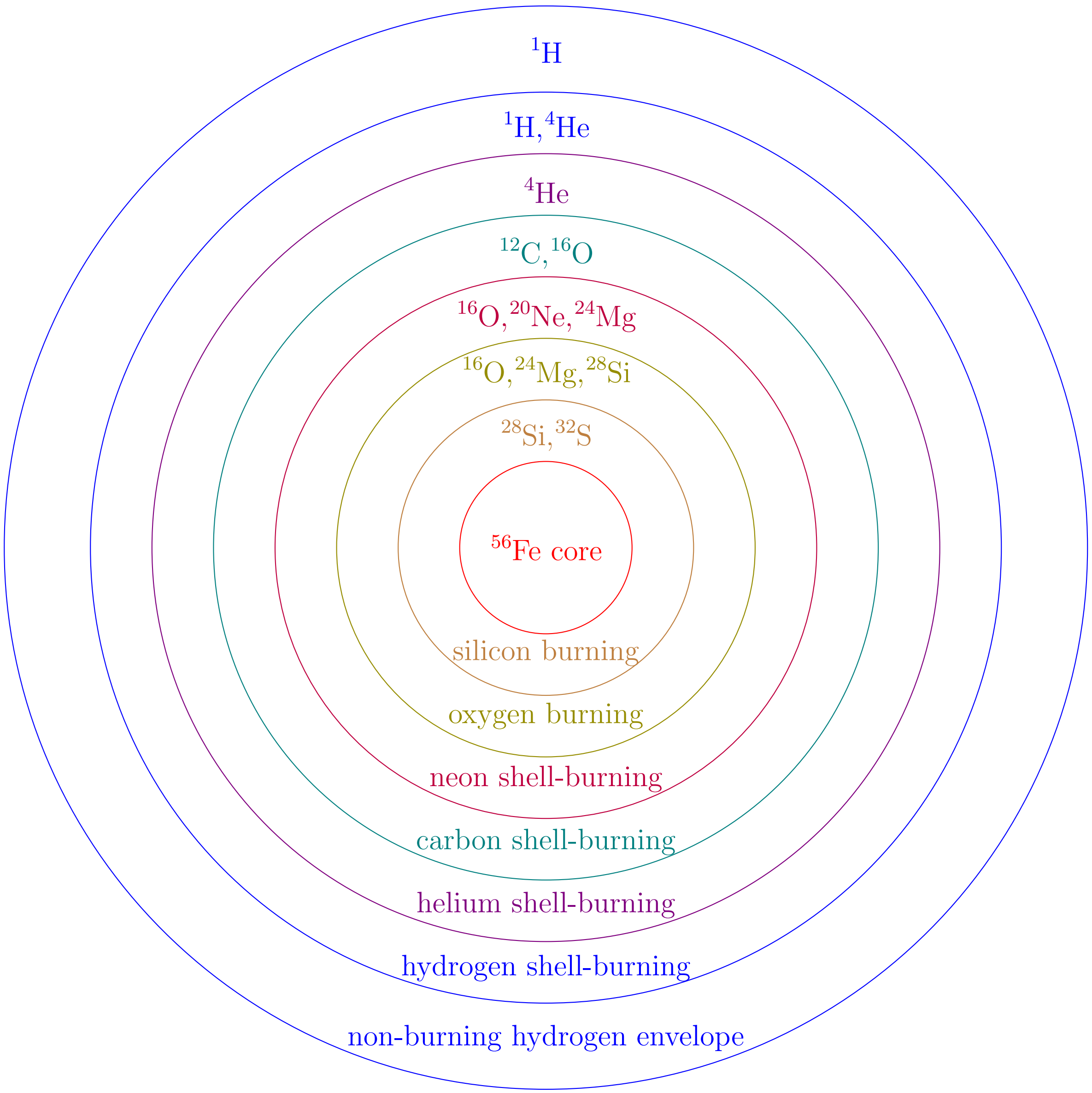

Massive stars with $M \gtrsim 10\,\mathrm{M}_\odot$ ignite successively burning of heavier elements

Core described by onion-skin model

- Each shell represents a nuclear burning stage that was originally located at the center of the star
- After depletion of the central fuel, the burning continued as shell burning in adjacent, heated layers and gradually moved outwards

Late massive core evolution

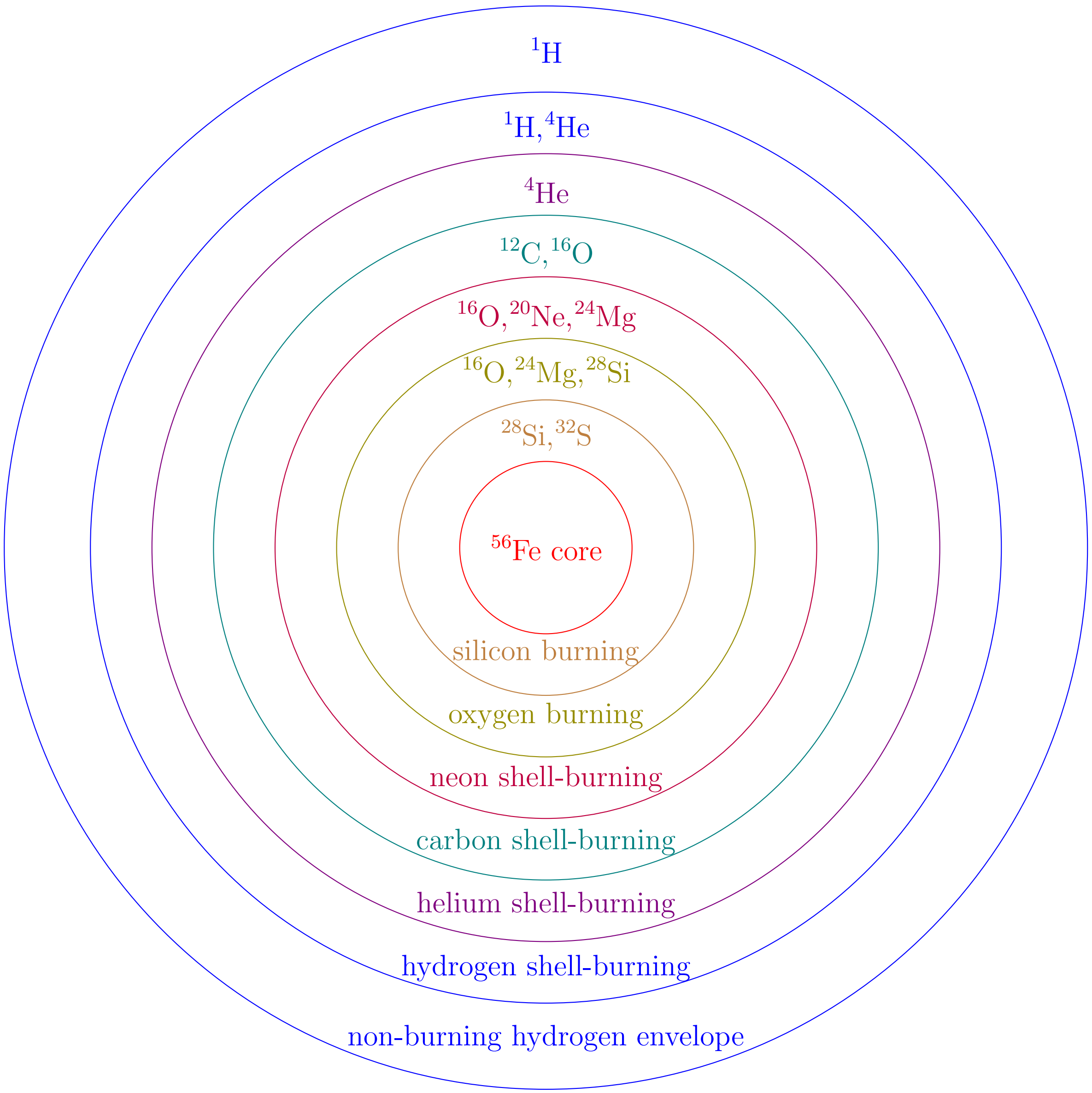

Core described by onion-skin model

Nuclear burning
↓
Exhaustion of fuel
↓
Core contraction
↓
Core heating
↓
Nuclear burning
…

Late massive core evolution

Due to the strongly declining energy released per nucleon
$\rightarrow$ Burning stages become shorter and shorter

Example $M = 40\,\mathrm{M}_\odot$:

H-burning:	5×10^6 yr
He-burning:	4×10^5 yr
C-burning:	200 yr
O-burning:	60 d
Ne-burning:	50 d
Si-burning:	13 h

Burning episodes stop in the iron core $\rightarrow$ No energy released

Late massive core evolution

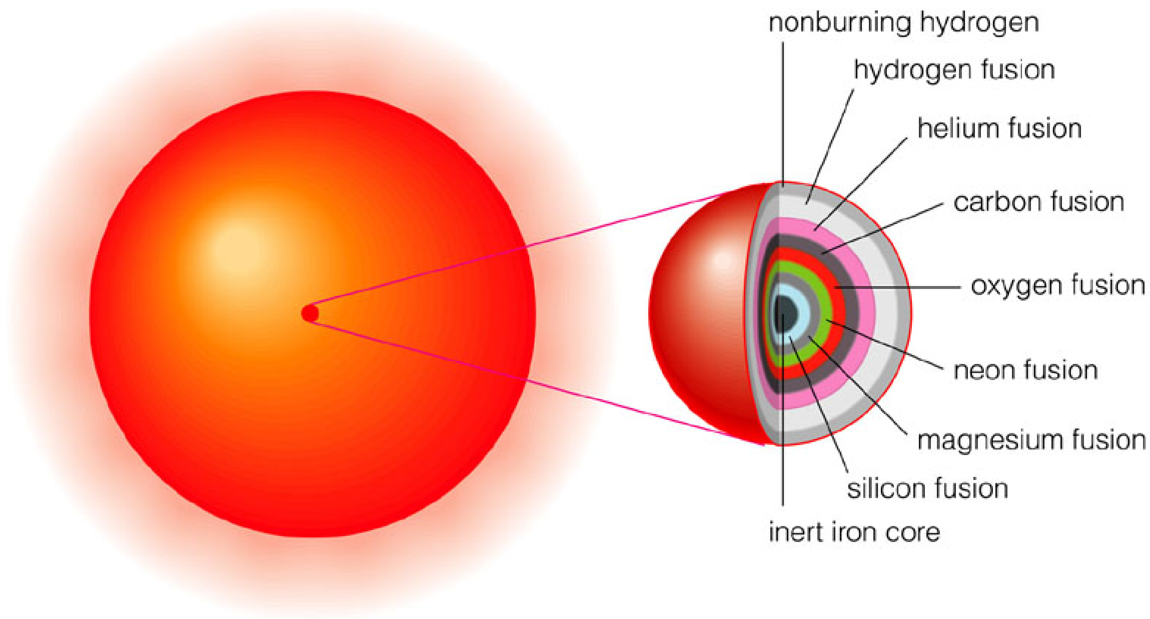

Real evolution quite complicated and uncertain

- Level of degeneracy
- Shell interactions
- Neutrino losses $L_\nu \sim 10^6\, L$

Final evolution not visible in the HRD

Final stages of stellar evolution

For stars with masses of less than $< 8 - 10\,\mathrm{M}_\odot$ (97% of all stars) mass is lost in the post-AGB phase and the core grows until shell-burning stops completely

$\rightarrow$ core cools, contracts and becomes fully degenerate

Objects in this final stage of stellar evolution are called **White Dwarfs** (WD)

From polytropic models for the non-relativistic fully degenerate electron gas follows the **mass-radius relation**

$$R \sim M^{-1/3}$$

$\rightarrow$ The higher the mass, the smaller the radius

At high densities, the equation of state changes and for the extreme relativistic degenerate electron gas follows the maximum **Chandrasekhar mass**

$$M_{\mathrm{Ch}} = \frac{5.836}{\mu_{\mathrm{e}}^2}\,\mathrm{M}_\odot = \left(\frac{2}{\mu_{\mathrm{e}}}\right)^2 \times 1.459\,\mathrm{M}_\odot$$

Final stages of stellar evolution

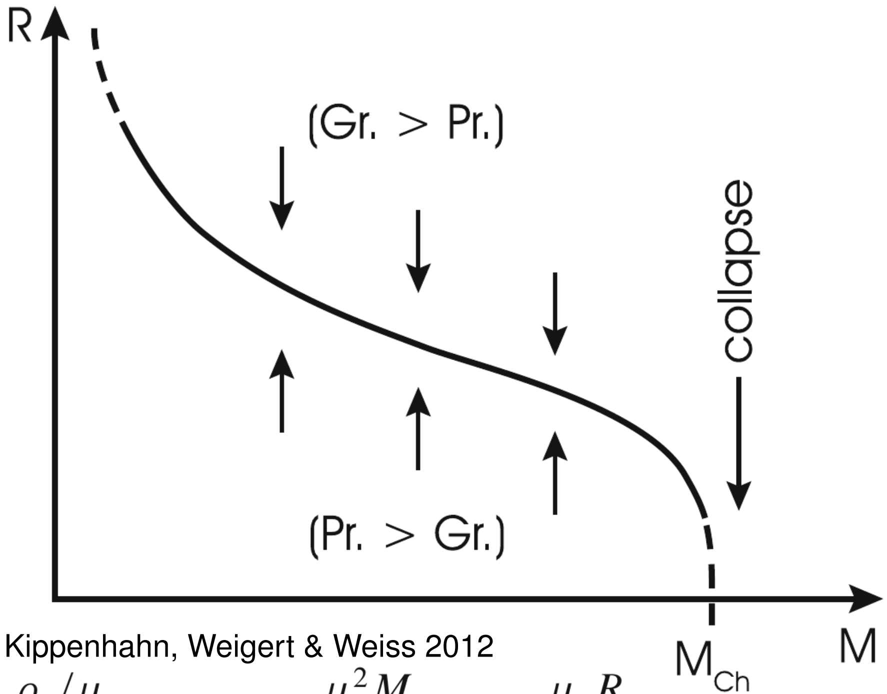

Kippenhahn, Weigert & Weiss 2012

ϱ_c/μ_e (g cm^{-3})	$\mu_e^2 M$ ($M_\odot$)	$\mu_e R$ (km)
∞	5.84	0
9.48×10^8	5.60	4.170
3.31×10^8	5.41	5.500
7.98×10^7	4.95	7.760
2.59×10^7	4.40	10.000
7.70×10^6	3.60	13.000
3.43×10^6	2.99	16.000
9.63×10^5	2.04	19.500
1.21×10^5	0.89	28.200
0	0	∞

Realistic WD models have to be calculated numerically
$\rightarrow$ Chandrasekhars theory
no longer polytrop, electrons fully degenerate, but degree of relativity $x = p_F/m_e c$

$$P = C_1 f(x),\ \rho = C_2 x^3;\ x = p_F/m_e c$$

Mass-radius relation depends on the **chemical composition** and the importance of **relativistic effects**

For low temperatures, crystallization due to electrostatic interactions sets in and changes the mechanical and chemical structure (phase separation)

Final stages of stellar evolution

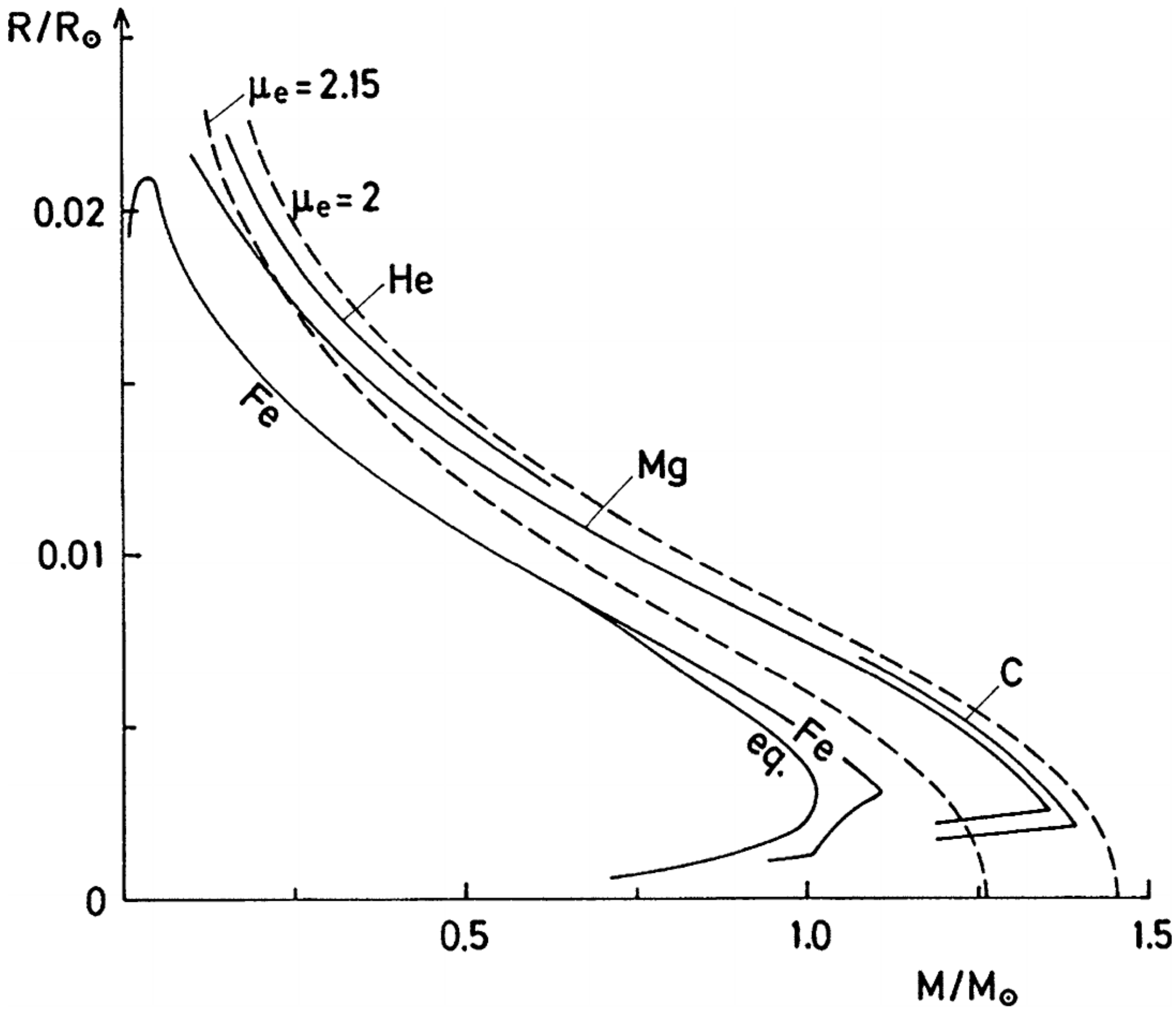

- Mass-radius relations for different compositions
- Solid lines include Coulomb interactions and phase transitions

If the radius is known, the mass of a WD can be calculated

- Radii are of the order of the radius of Earth

$$R_{\mathrm{WD}} \approx 0.01\,\mathrm{R}_\odot$$

- densities are

$$\rho_{\mathrm{WD}} \approx 10^6 \rho_\odot$$

Final stages of stellar evolution

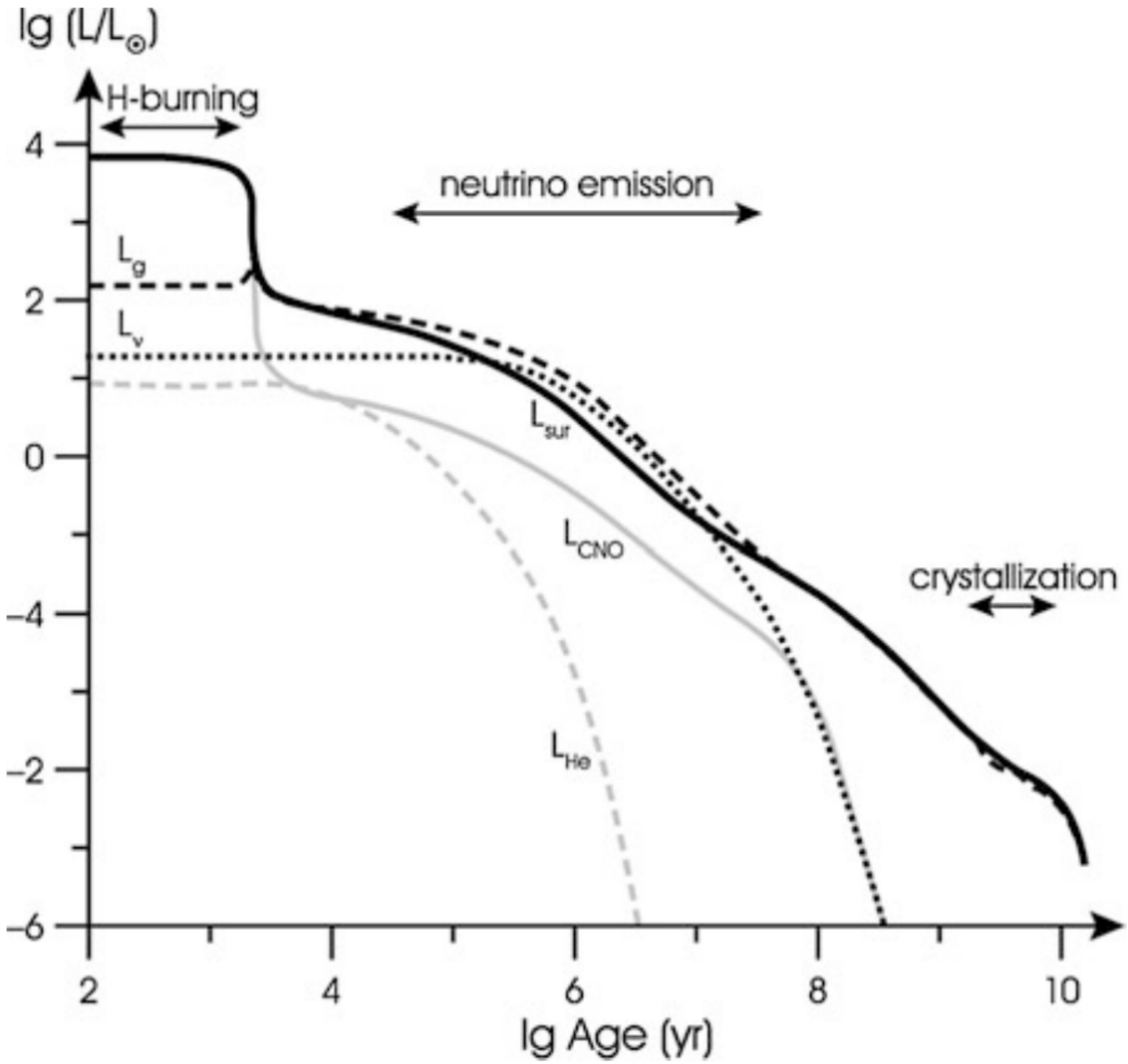

Kippenhahn, Weigert & Weiss 2012

After a short phase of H-shell burning WDs are cooling

Cooling time τ

$$\tau \approx \frac{4.7 \times 10^7}{A} \left(\frac{M/M_\odot}{L/L_\odot} \right)^{5/7} \text{yr}$$

Typically $\tau \approx 10^9$ yr
$\rightarrow$ Long evolutionary stage

Cooling mechanisms

- Neutrino emission
- Gravothermal energy

Core crystallization releases a considerable amount of latent heat and delays the cooling by about one billion years

Final stages of stellar evolution

Gaia reveals crystallization for the first time!

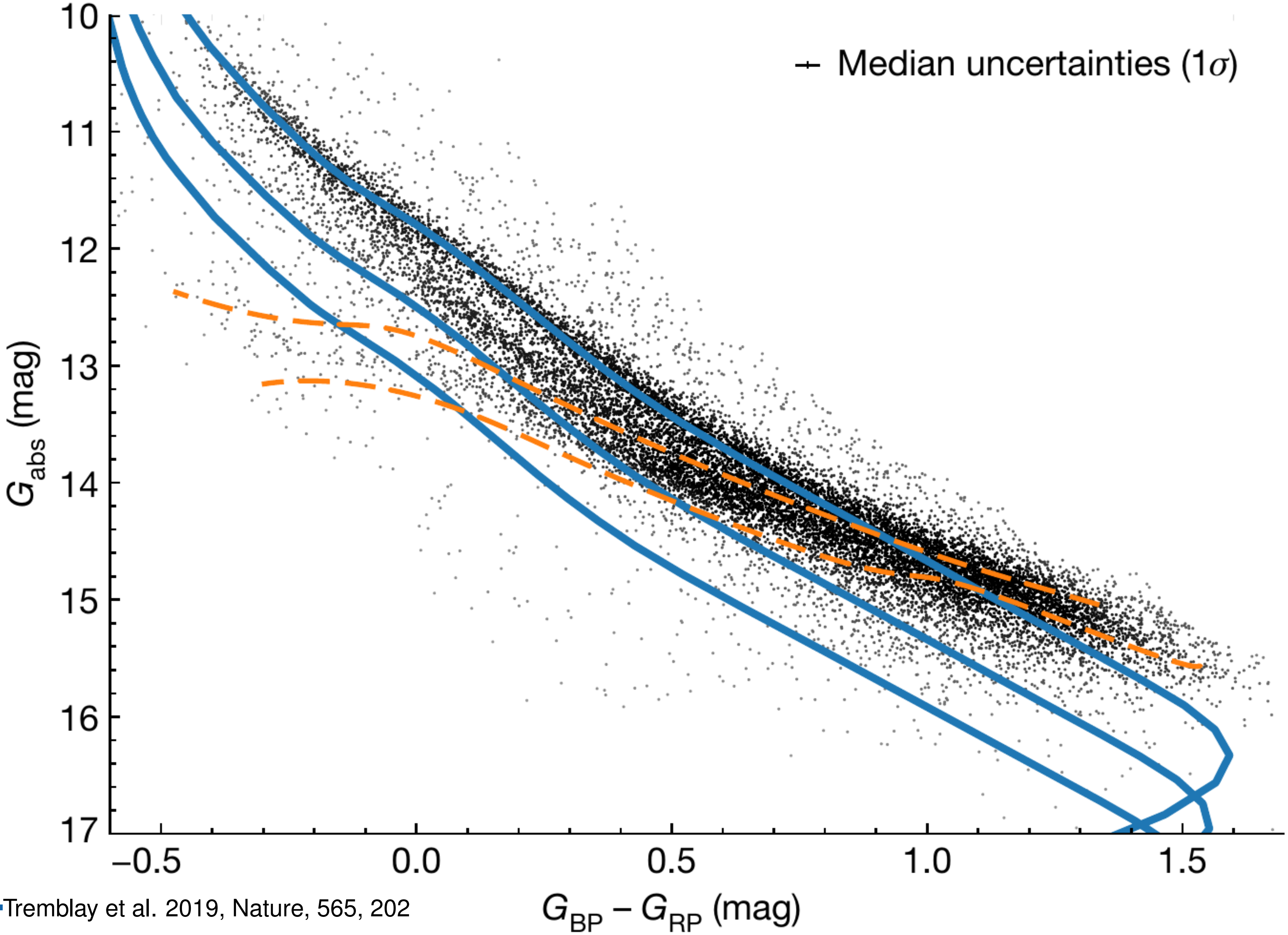

Tremblay et al. 2019, Nature, 565, 202

Final stages of stellar evolution

Gaia reveals crystallization for the first time!

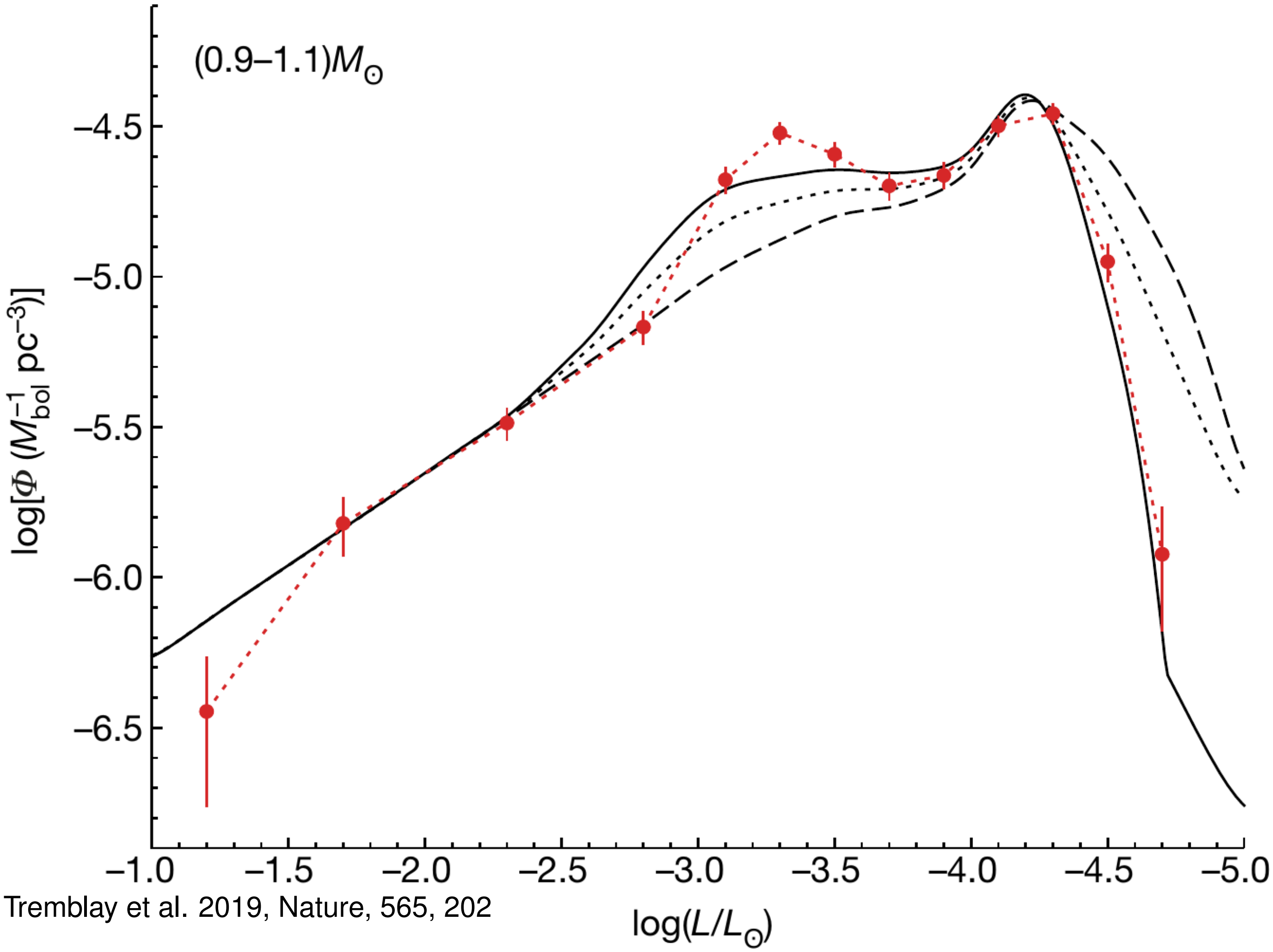

Tremblay et al. 2019, Nature, 565, 202

Luminosity function of WDs

$\rightarrow$ Can be used to measure the age of stellar populations

$\rightarrow$ Single-star evolution cannot have formed WDs with masses $\lesssim 0.5\,M_\odot$ because $\tau > t_{\rm Hubble}$

Final stages of stellar evolution

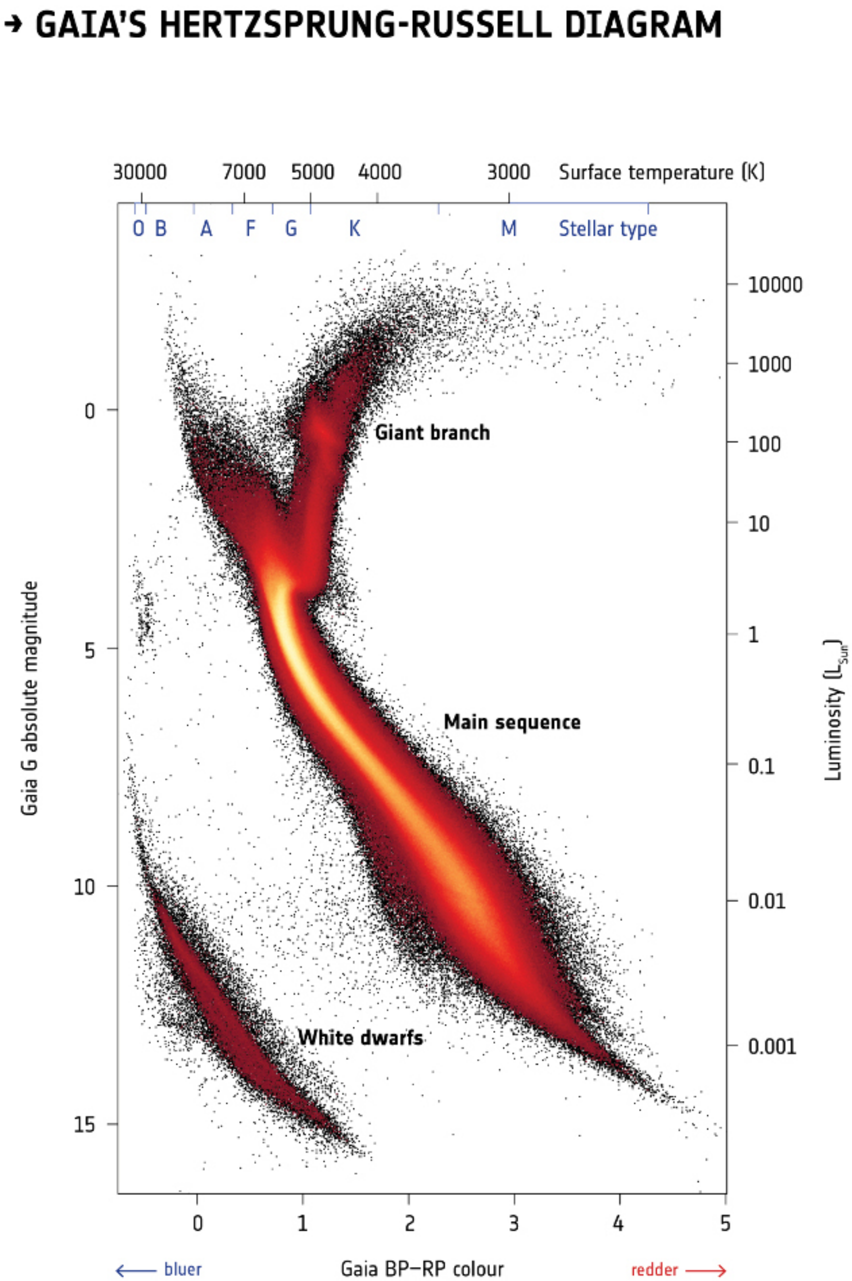

Gaia collaboration 2018, A&A, 616, 10

WDs form a well separated sequence in the observed HRD

$\rightarrow$ Luminosities depend on age, but are in general much smaller than for other stars ($\sim 10^{-4}\,L_\odot$)

White dwarf structure

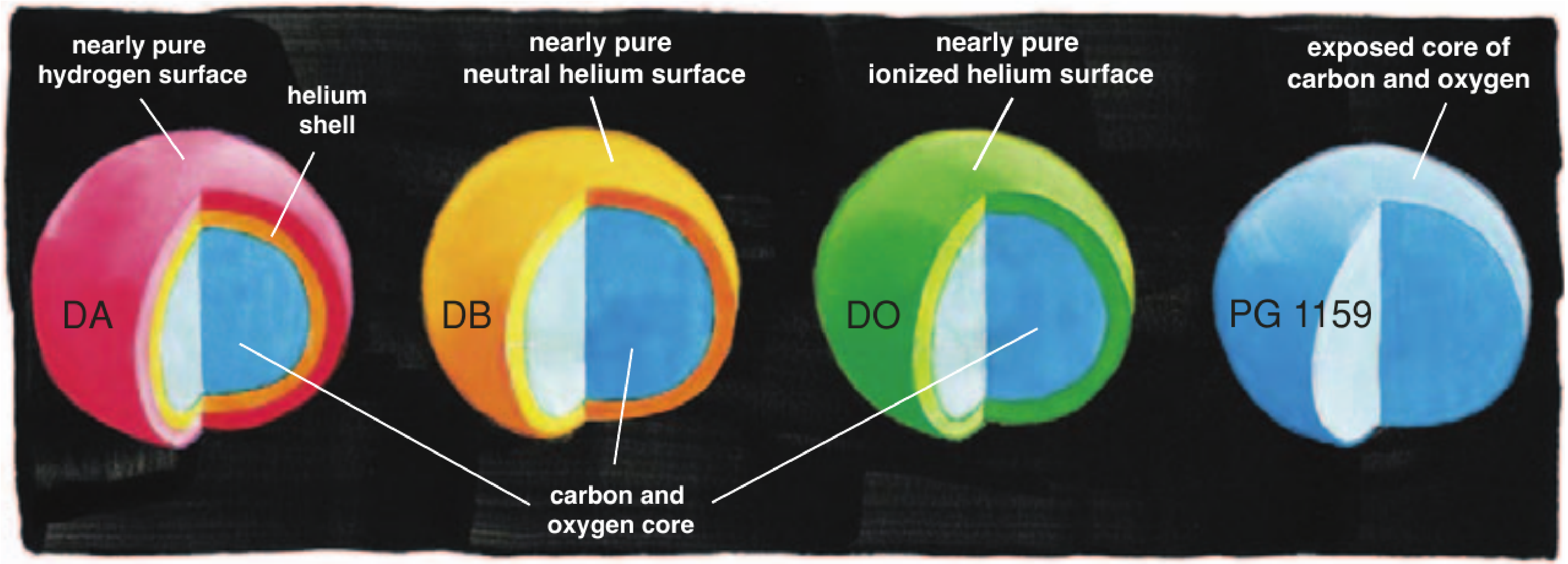

Spectral types of White Dwarfs

- DA: H lines present; subtype DAB
- DB: He I lines; subtype DBA
- DC: continuous spectrum, no lines
- DO: He II lines; subtype DAO, DOA
- DZ: Metal lines
- DQ: Carbon lines

- X: unclassifiable, peculiar spectrum
- P: magnetic WD with detectable polarization
- H: magnetic WD without polarization
- E: emission lines present
- V: variable WD
- ?: uncertain classification

White dwarf structure

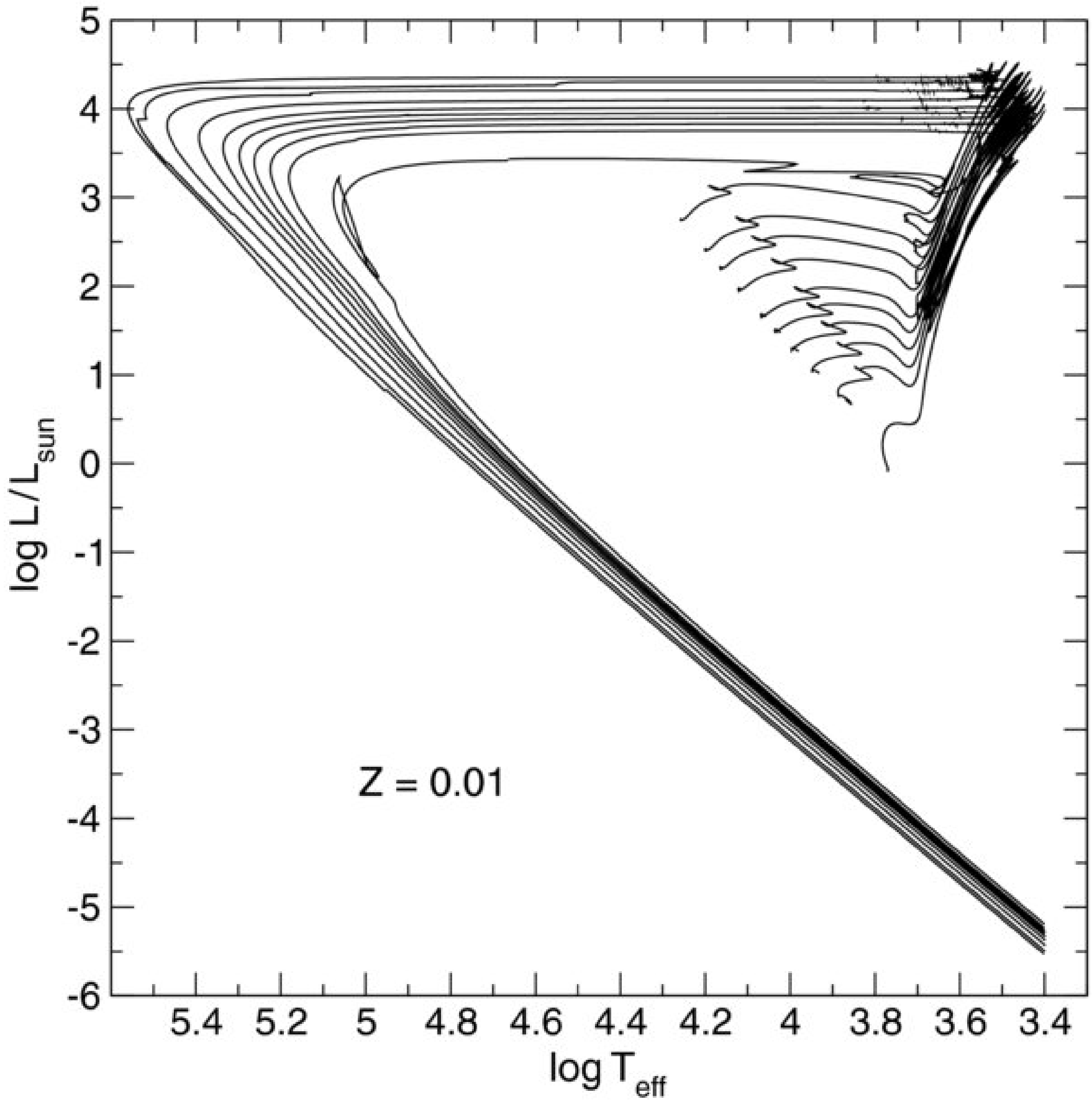

WDs of diverse compositions cool down and change their spectral types

- DA $\rightarrow$ cooler DA
- PG1159 $\rightarrow$ DO $\rightarrow$ DB $\rightarrow$ DC $\rightarrow$ DQ

Final stage: Black dwarf

- Not observed
- Universe is too young!

White dwarf structure

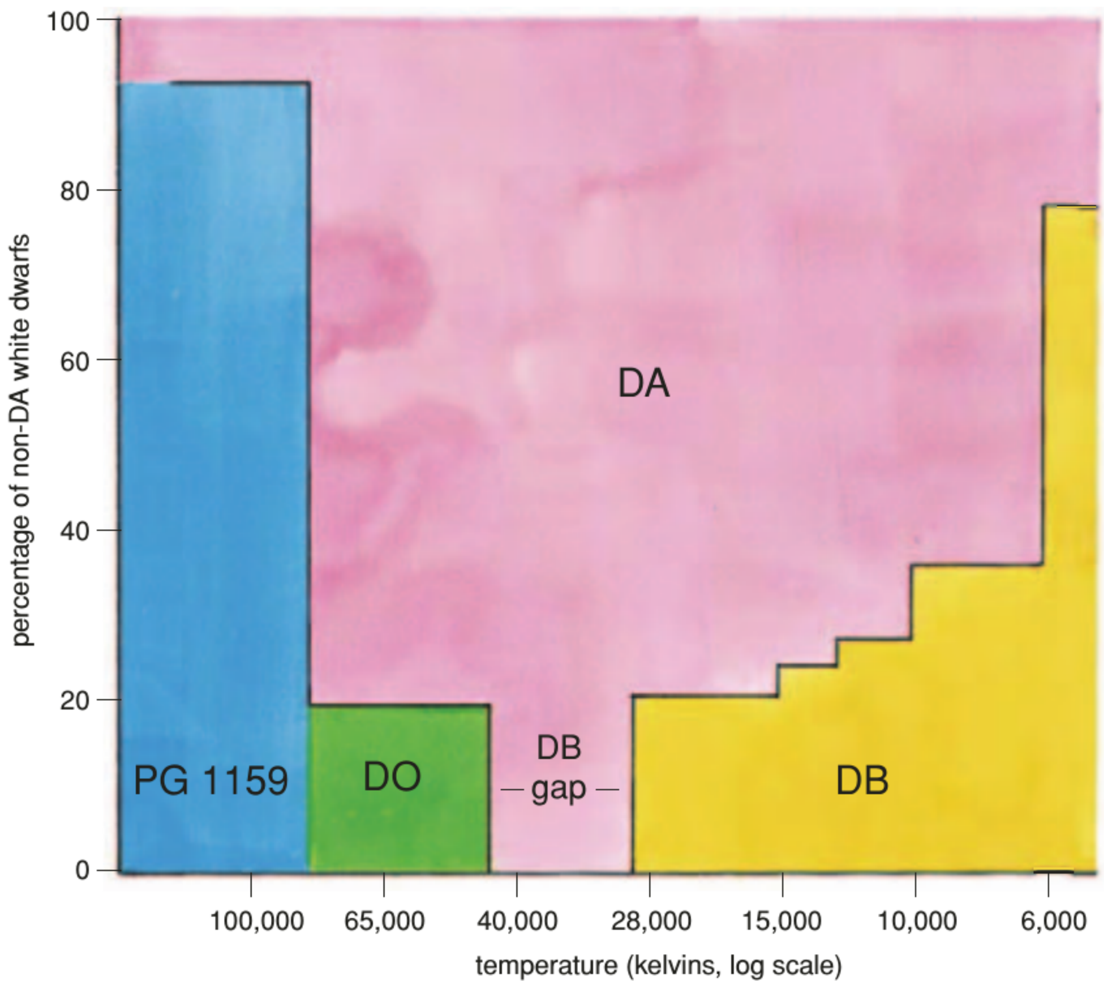

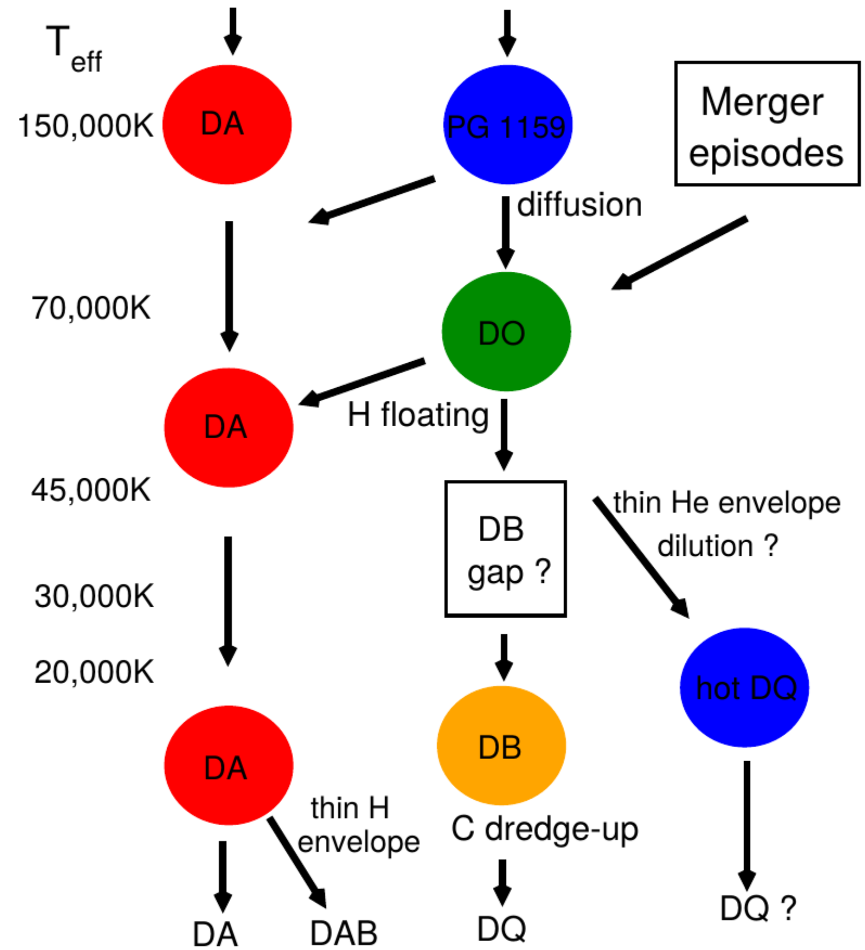

Structure of WDs depends on earlier phases of stellar evolution

- Mass-loss or mixing processes due to late thermal pulses remove H-rich and/or He-rich layers

White dwarf structure

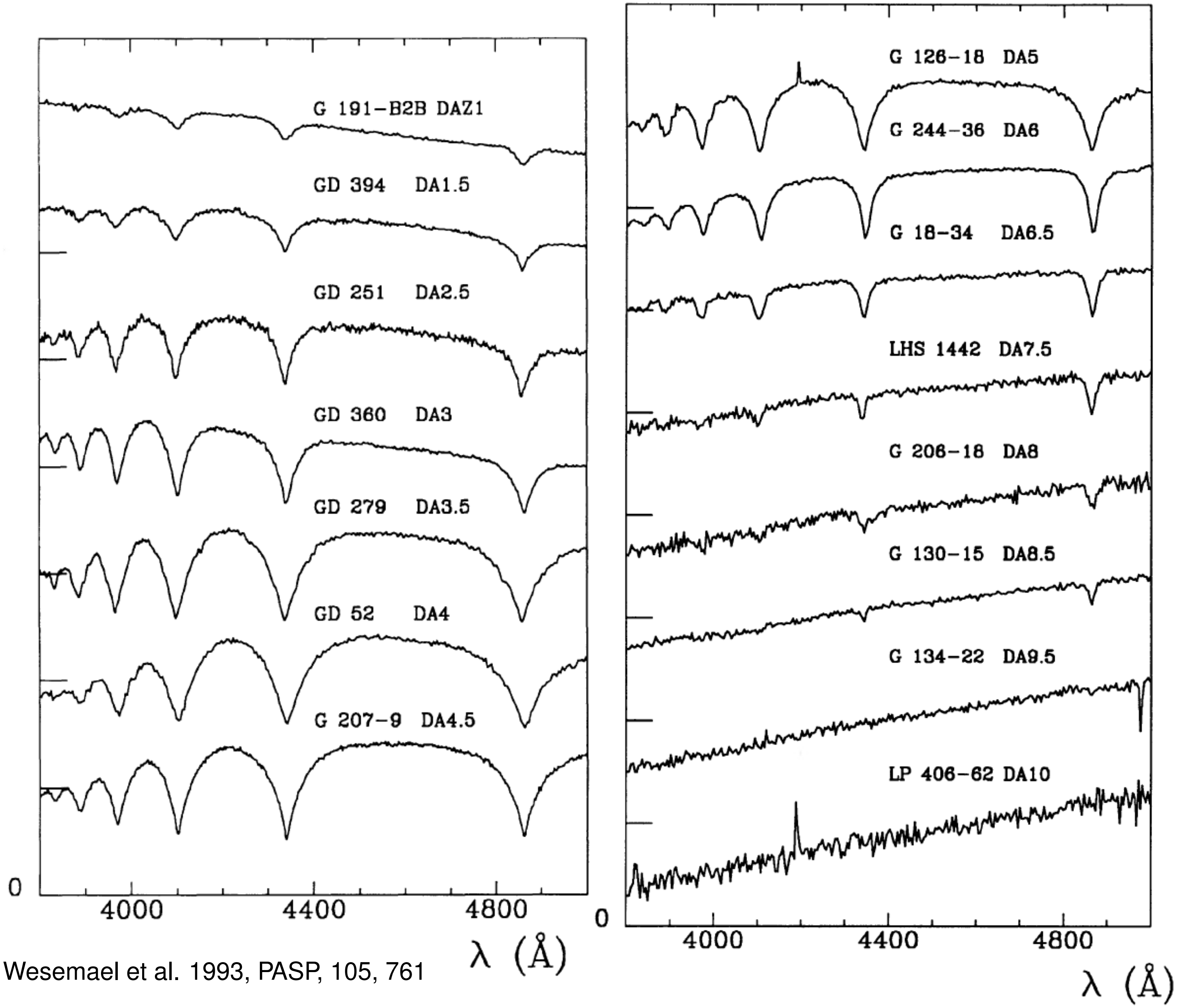

Wesemael et al. 1993, PASP, 105, 761

White dwarf Luminosity class VII

- H-rich: DA
- He-rich: PG1159, DO, DB, DC, DQ

White dwarf structure

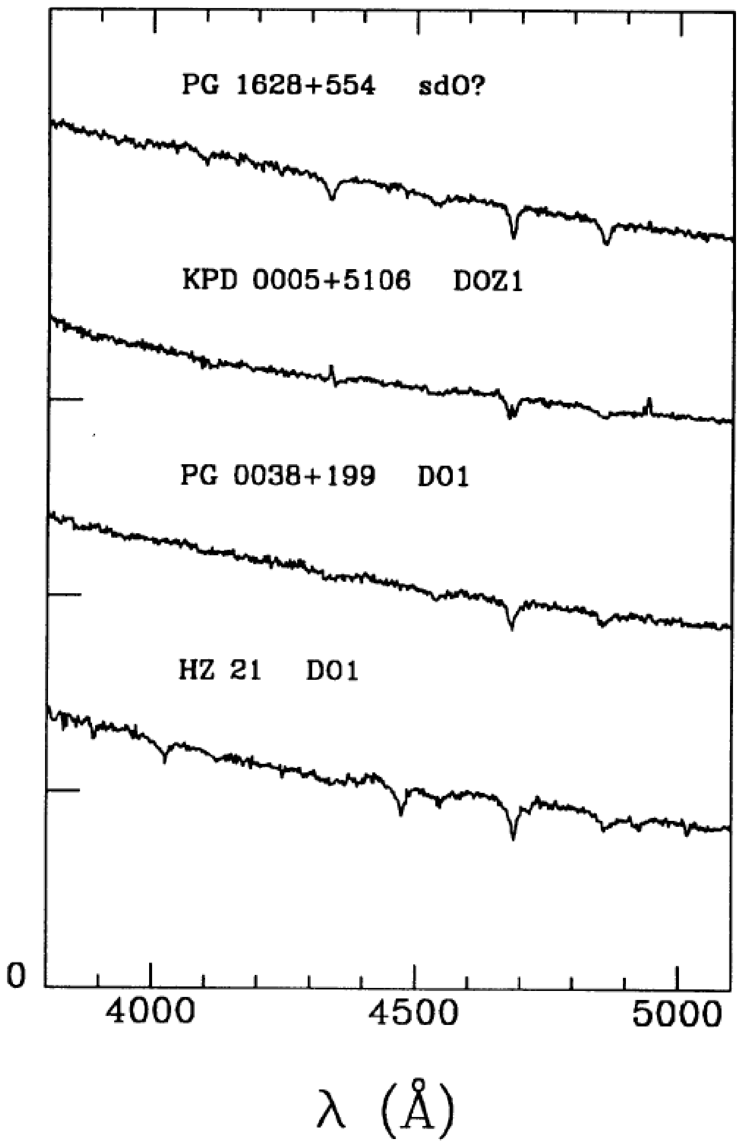

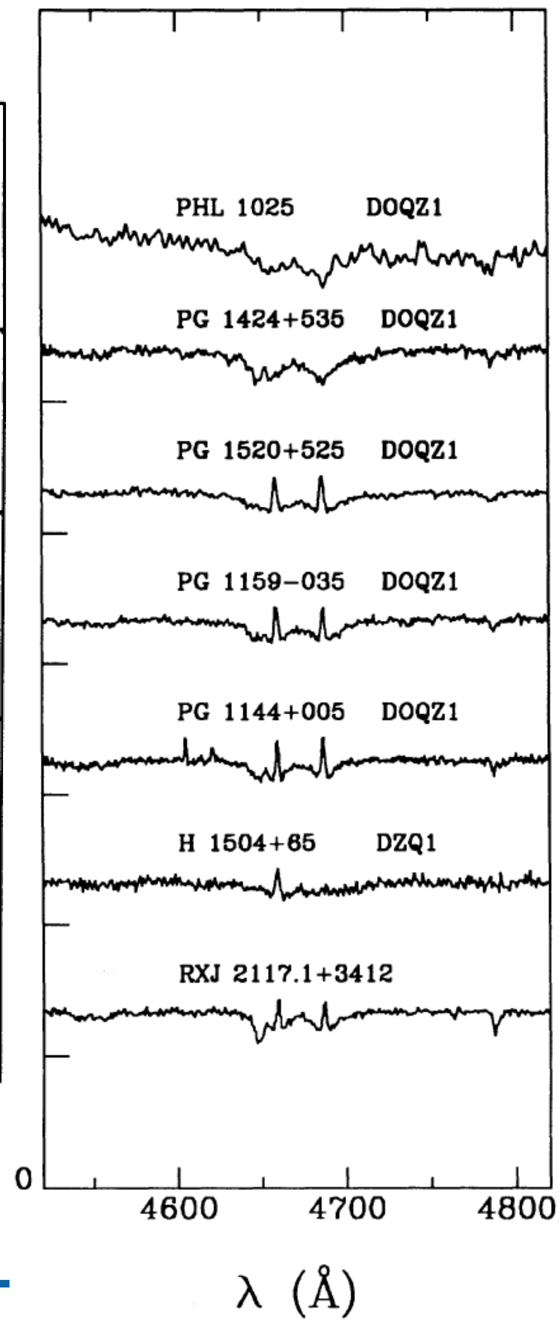

Wesemael et al. 1993, PASP, 105, 761

White dwarf Luminosity class VII

- H-rich: DA
- He-rich: PG1159, DO, DB, DC, DQ
- metal-rich: DZ

White dwarf structure

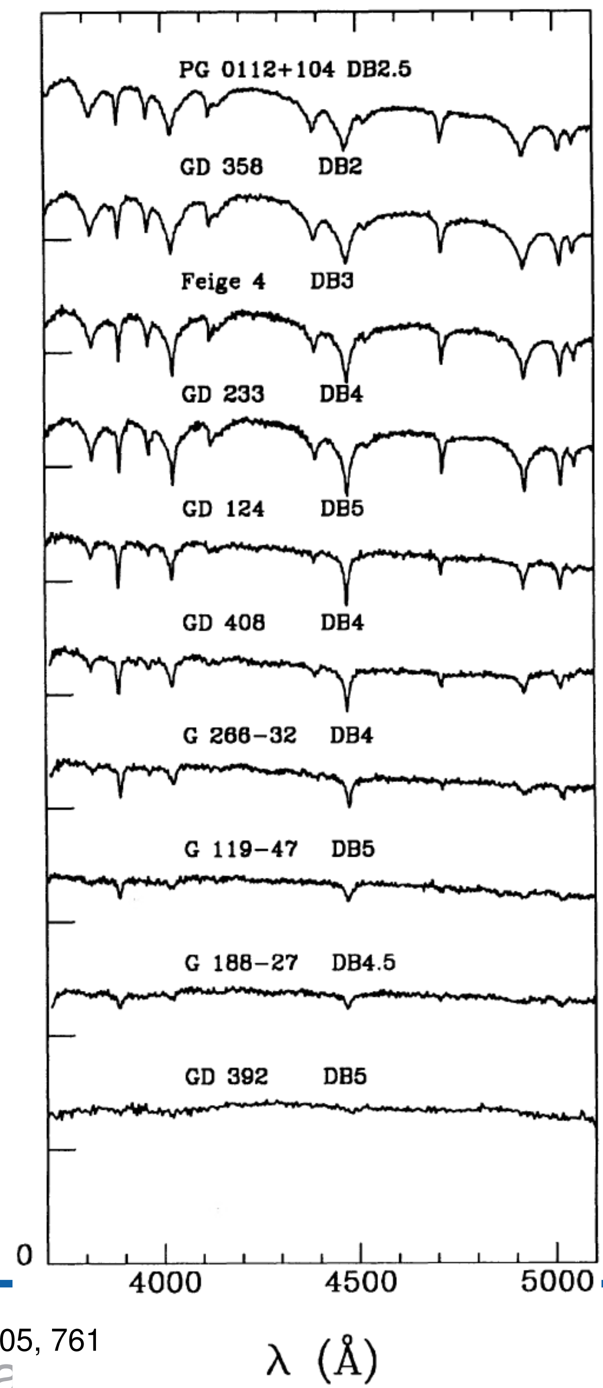

White dwarf Luminosity class VII

- H-rich: DA
- He-rich: PG1159, DO, DB, DC, DQ

Wesemael et al. 1993, PASP, 105, 761

White dwarf structure

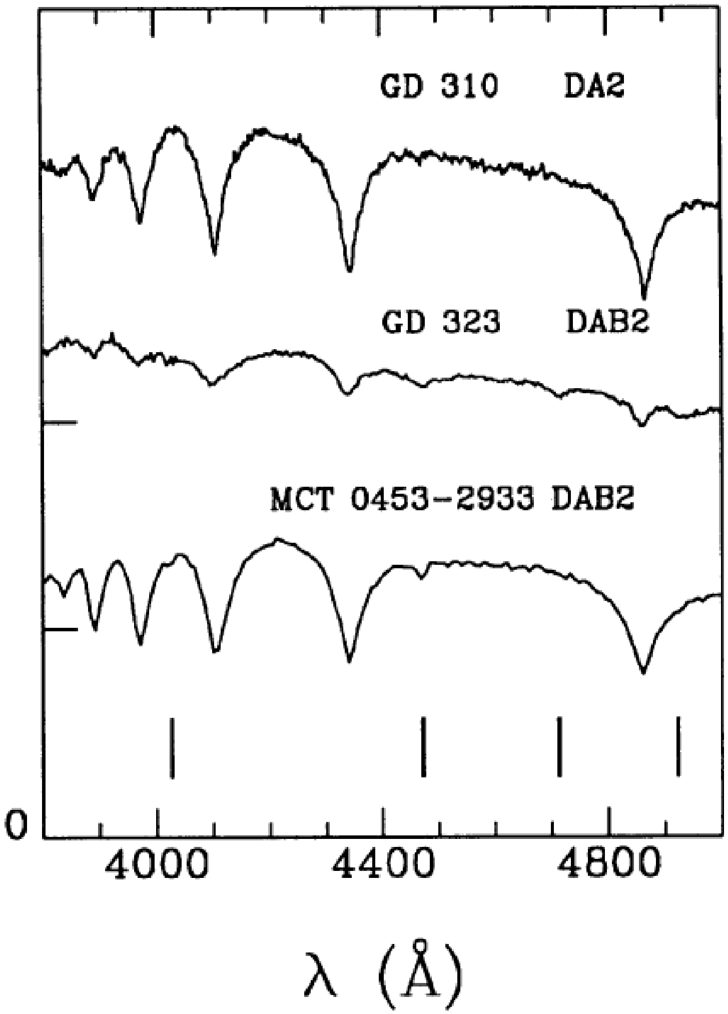

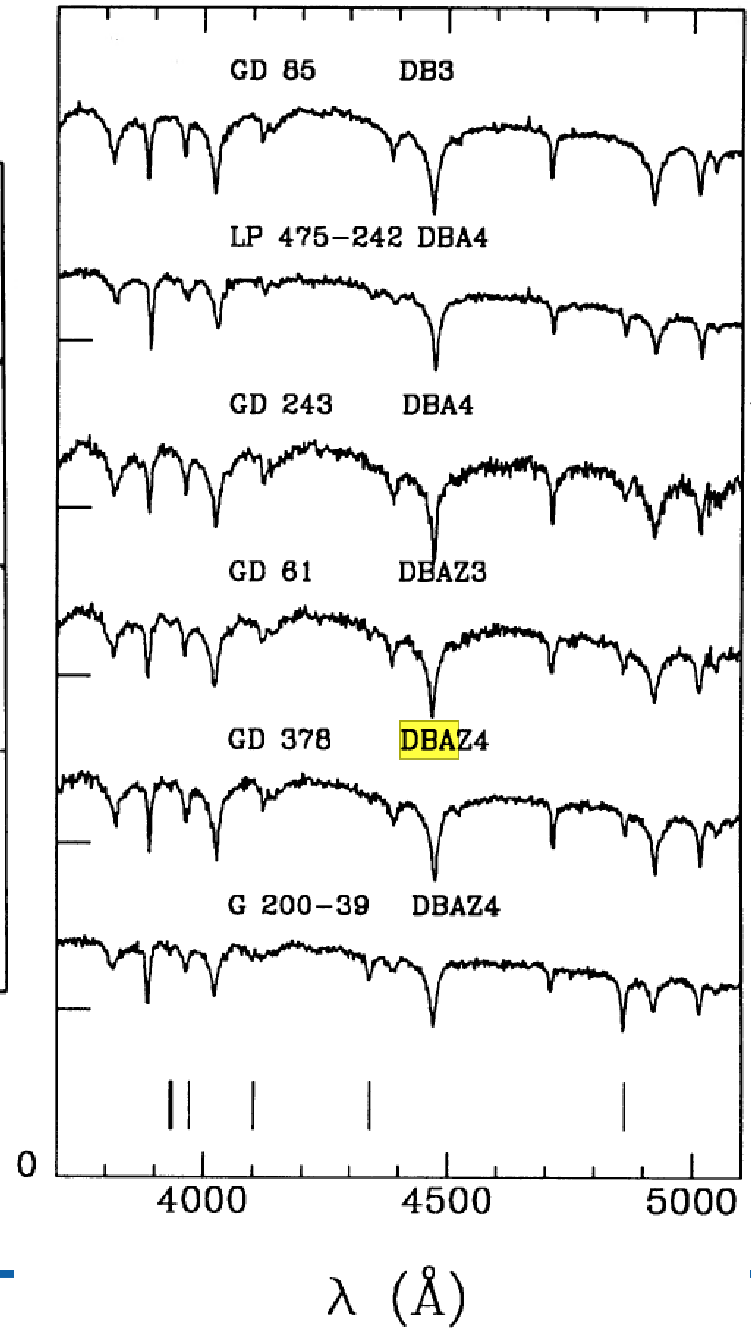

White dwarf Luminosity class VII

- H-rich: DA
- He-rich: PG1159, DO, DB, DC, DQ
- metal-rich: DZ

Wesemael et al. 1993, PASP, 105, 761

White dwarf structure

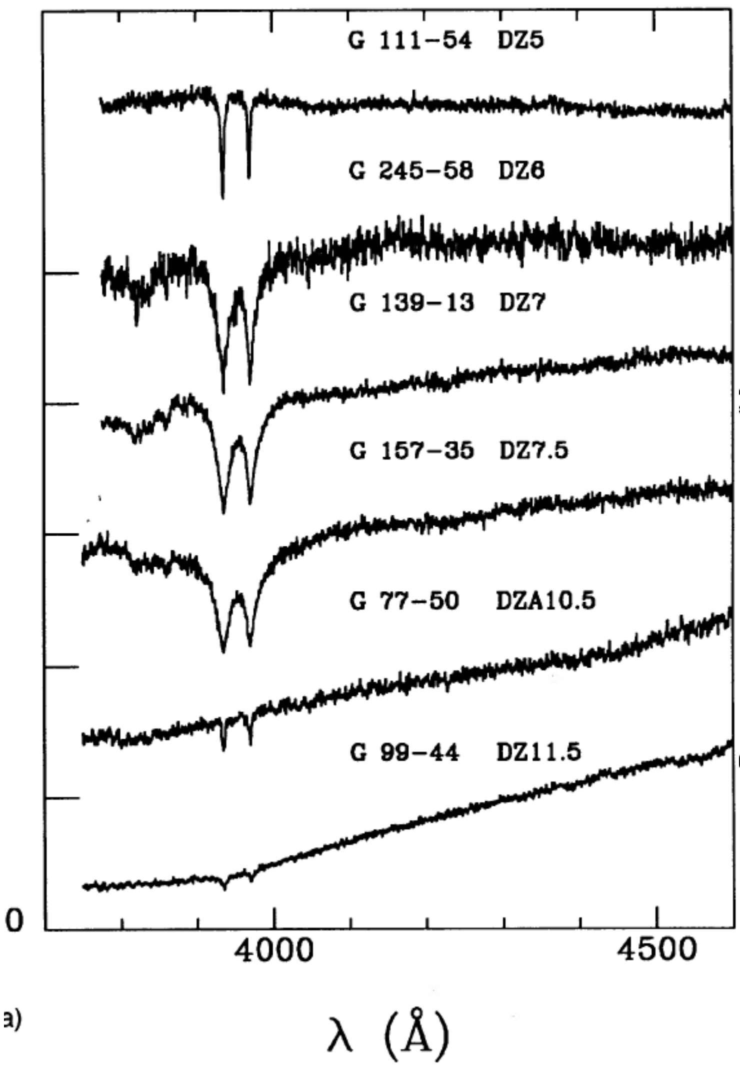

Wesemael et al. 1993, PASP, 105, 761

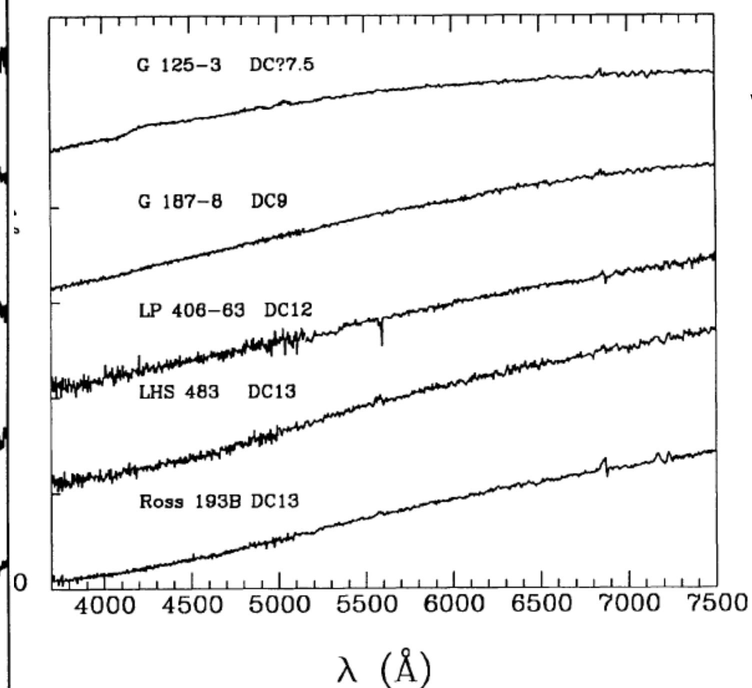

White dwarf Luminosity class VII

- H-rich: DA
- He-rich: PG1159, DO, DB, DC, DQ
- metal-rich: DZ

Seeing with sounds

- observations of the atmosphere by spectra
- how can we look into the interior?
- sound wave is a pressure wave:

$$c = \sqrt{\Gamma_1 p/\rho}$$

Γ_1 adiabatic coefficient

- ideal gas:

$$p = \rho k_\mathrm{B} T/\mu m_\mathrm{u}$$

μ mean molecular weight, m_u atomic mass unit

- sound speed depends on pressure, density, temperature and composition of the gas
- sounds tell us internal structure

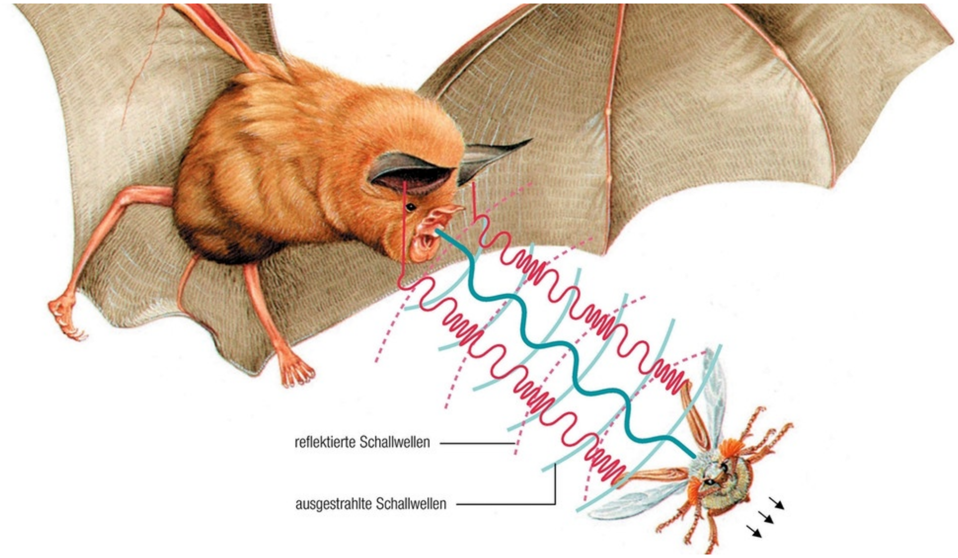

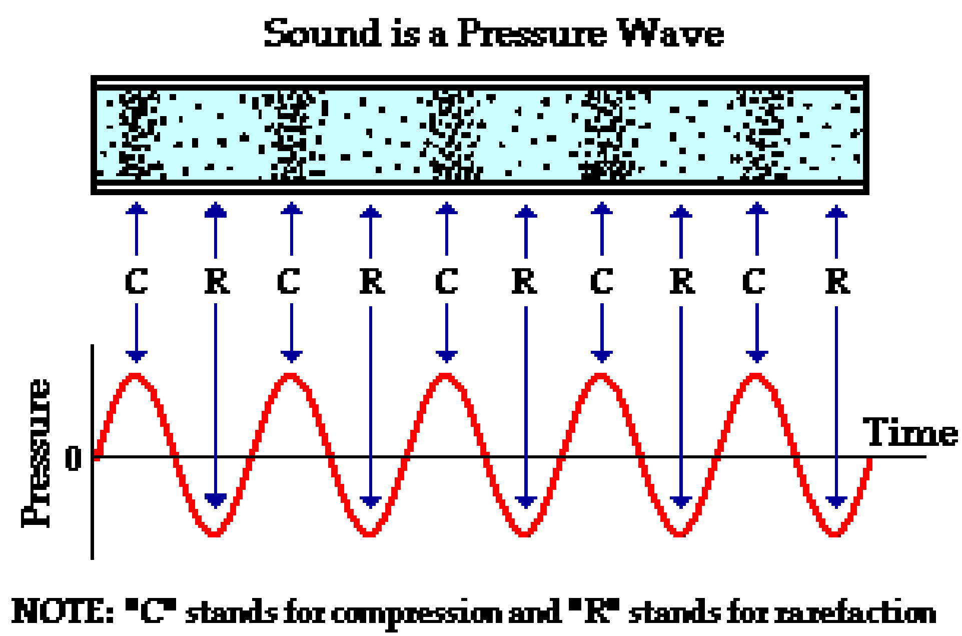

1-D oscillations

- everything has natural frequencies of pulsation
- obvious mode for a gas sphere (a star): star remains spherical and simply changes its volume (radial pulsations)
- pulsations in stars analogue to an open-at-one-end organ pipe
- A node (no movement) at the centre of the star, an antinode (maximum movement) at the surface
- radial pulsations can be fundamental, first overtone, second overtone, etc. all of these modes of variation can be excited at the same time

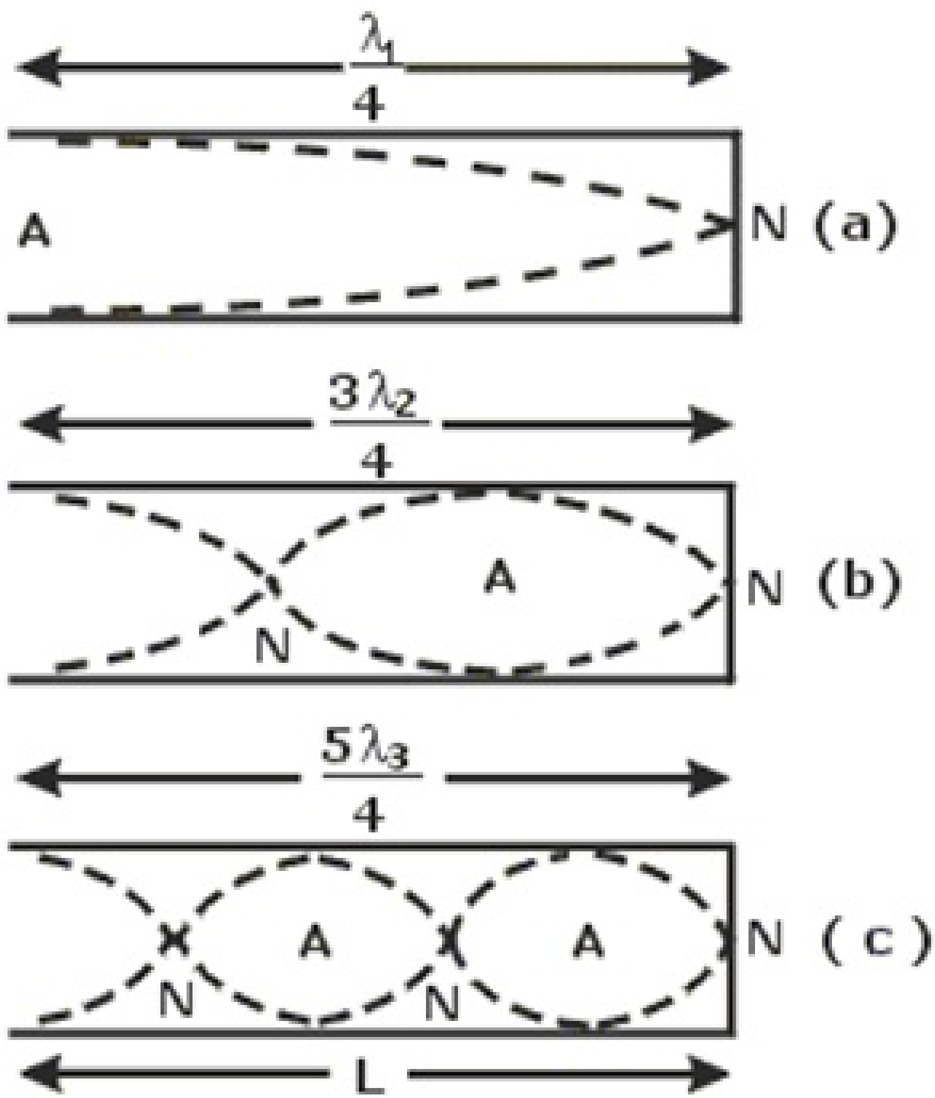

3-D oscillations

Stars are 3D, so natural oscillations have nodes in all 3 orthogonal directions

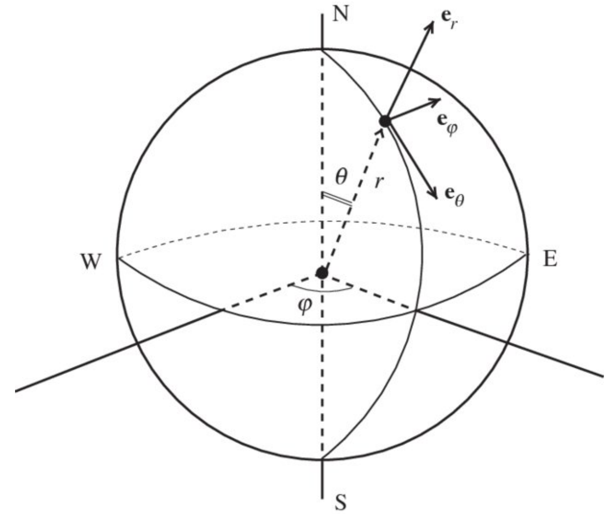

- spherical symmetric described by r, θ, ϕ
- nodes are concentric shells at constant r, cones of constant θ and planes of constant ϕ
- solutions to equation of motion have displacements in (r, θ, ϕ)

$$\xi_r(r,\theta,\phi,t) = a(r)\,Y_l^m(\theta,\phi)\exp(-i2\pi\nu t) \quad (9.3)$$

$$\xi_\theta(r,\theta,\phi,t) = b(r)\frac{\partial Y_l^m(\theta,\phi)}{\partial\theta}\exp(-i2\pi\nu t) \quad (9.4)$$

$$\xi_\phi(r,\theta,\phi,t) = \frac{b(r)}{\sin\theta}\frac{\partial Y_l^m(\theta,\phi)}{\partial\phi}\exp(-i2\pi\nu t) \quad (9.5)$$

amplitudes $a(r)$, $b(r)$, oscillation frequency ν

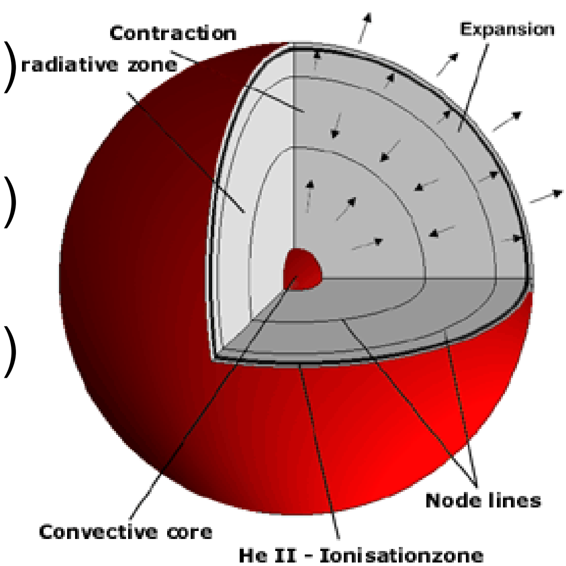

Zima 1999

Spherical harmonics

Solution to Laplace's equation: $\nabla^2 T(r,\theta,\phi) = 0$, $T(r,\theta,\phi) = R(r)\Theta(\theta)\Phi(\phi)$

Laplacian in spherical coordinates

$$\nabla^2 = \frac{1}{r^2}\frac{\partial}{\partial r}\left(r^2\frac{\partial}{\partial r}\right) + \frac{1}{r^2\sin^2\theta}\frac{\partial}{\partial\theta}\left(\sin\theta\frac{\partial}{\partial\theta}\right) + \frac{1}{r^2\sin^2\theta}\frac{\partial^2}{\partial\phi^2}$$

$$\Phi(\phi) = \begin{cases} \exp(im\phi) \\ \exp(-im\phi) \end{cases} \qquad \text{for } m = 0, 1, 2, 3, ... \tag{9.6}$$

$$R(r) = \begin{cases} r^l \\ r^{-l-1} \end{cases} \tag{9.7}$$

Legendre polynomials

$$\Theta(\theta) = P_l^m(x = \cos\theta) = \frac{1}{2^l l!}(1 - x^2)^{m/2}\frac{d^{l+m}}{dx^{l+m}}(x^2 - 1)^l \tag{9.8}$$

$l = 0, 1, 2, 3, ...$ and $m = -l, -l + 1, ..., l - 1, l$

$$T(r,\theta,\phi) = \begin{cases} r^l \\ r^{-l-1} \end{cases} P_l^m(\cos\theta) \begin{cases} \exp(im\phi) \\ \exp(-im\phi) \end{cases} \tag{9.9}$$

Spherical harmonics

spherical harmonics $Y_l^m(\theta\phi)$

$$Y_l^m(\theta,\phi) = (-1)^m\sqrt{\frac{(2l+1)}{4\pi}\frac{(l-m)!}{(l+m)!}}P_l^m(\cos\theta)e^{im\phi} \tag{9.10}$$

$$T(r,\theta,\phi) = \sum_{l=0}^{\infty}\sum_{m=-l}^{l}(a_{lm}r^l + b_{lm}r^{-l-1})Y_l^m(\theta,\phi) \tag{9.11}$$

Modes specified by three quantum numbers:

- n overtone: Number of radial nodes
- l degree: number of surface nodes present
  $\rightarrow$ $l = 0$ radial mode, $l = 1$ dipole, ..
- m azimuthal order: $|m|$ How many of the surface nodes are lines of longitude
  $\rightarrow$ m ranges from $-l$ to l.

3-D oscillations $l = 3$

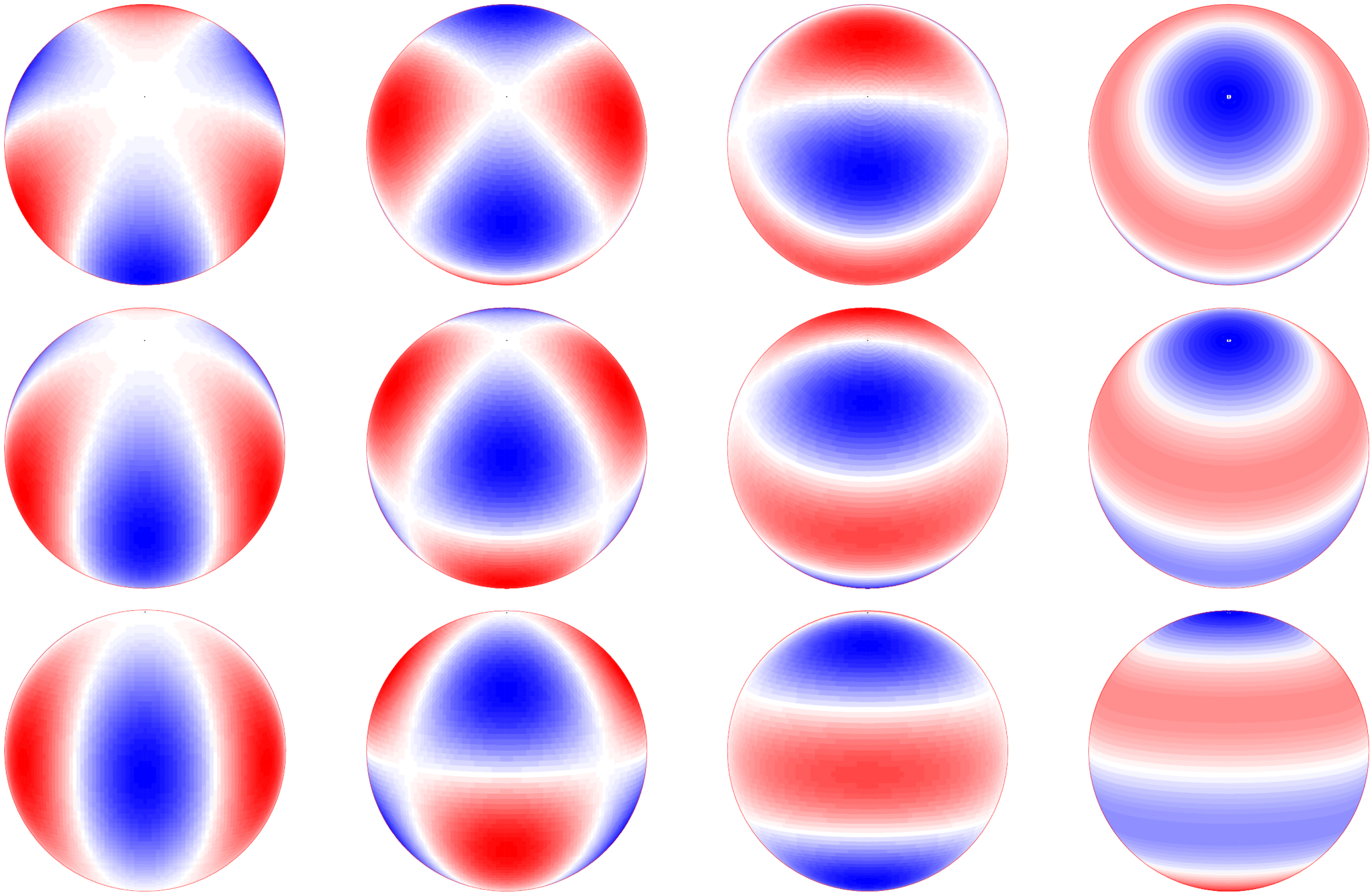

3-D oscillations

$l = 1, m = 0$ $l = 1, m = 1$ $l = 2, m = 1$ $l = 2, m = 2$

$l = 3, m = 0$ $l = 3, m = 1$ $l = 3, m = 2$ $l = 3, m = 3$

`http://www.physics.usyd.edu.au/~bedding/animations/visual.html`

nice program to simulate a pulsating star: `http://userpages.irap.omp.eu/~scharpinet/glpulse3d/`

3-D oscillations

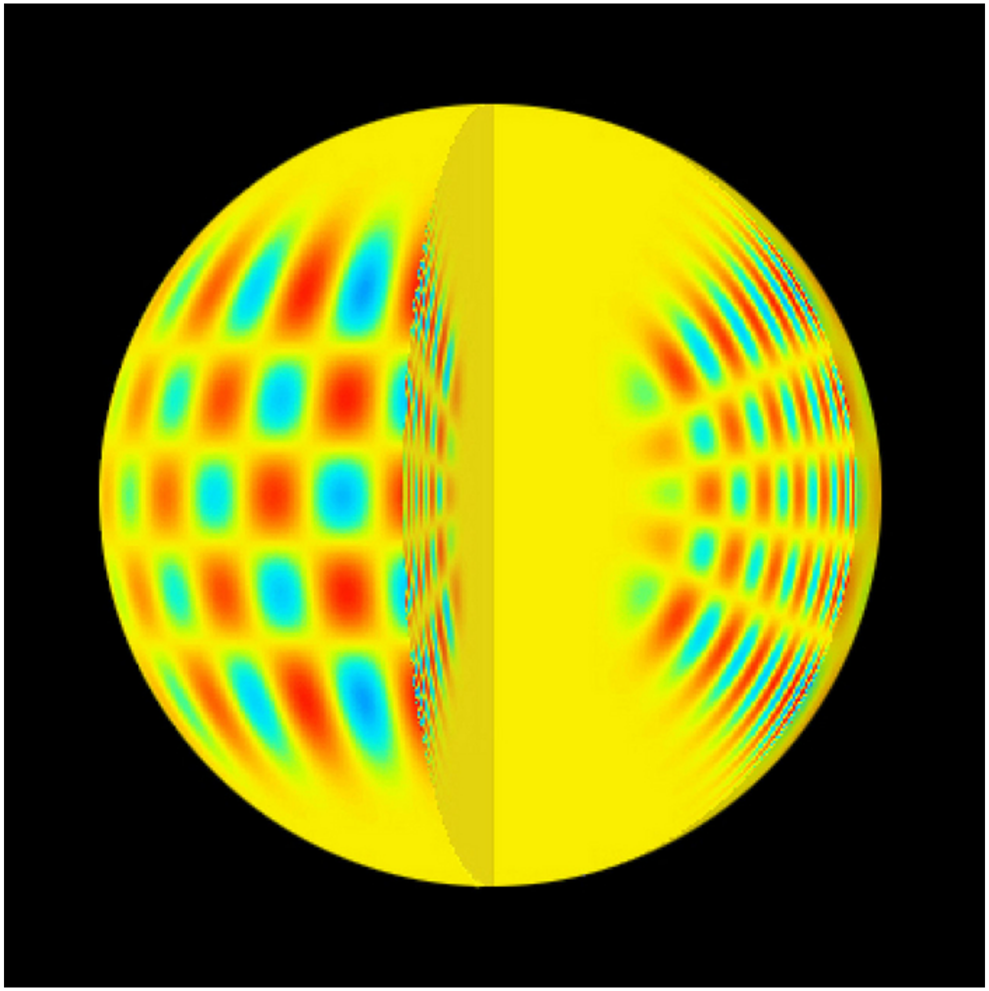


representation of high order (n) and high degree (l) non-radial mode. The different colours represent the surface rising/falling – alternatively cooling/heating.

Lightcurves of pulsating stars

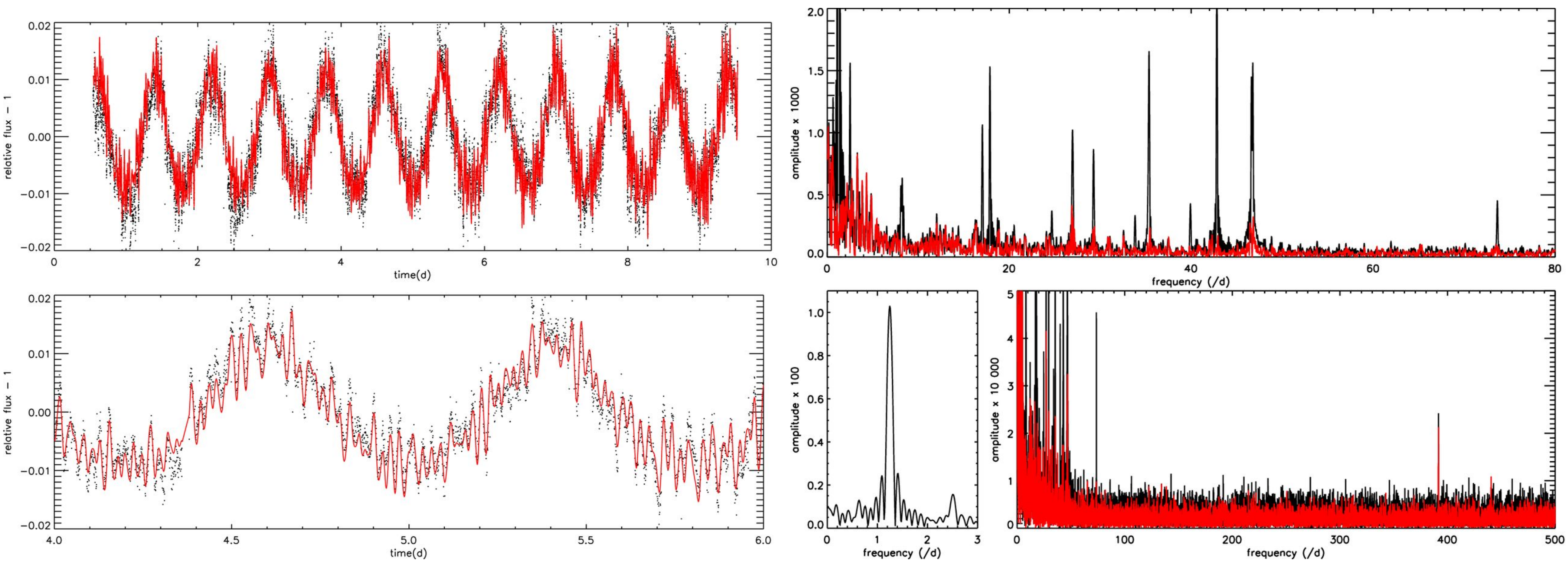

Jeffery & Ramsay 2014

- Light curve is the variation of the integrated light over the stellar surface over time
- Fourier transformation gives you the oscillation frequencies of the underlying pulsations
- Radial velocity variations can also be used to measure pulsations

Driving mechanism of pulsations

- During each pulsation cycle, energy is lost $\rightarrow$ Damping
- To maintain pulsations for a long time, a driving mechanism is needed
- Radial layer, which gains heat during the compression part of the pulsation cycle drives the pulsations

$\rightarrow$ Heat-engine mechanism

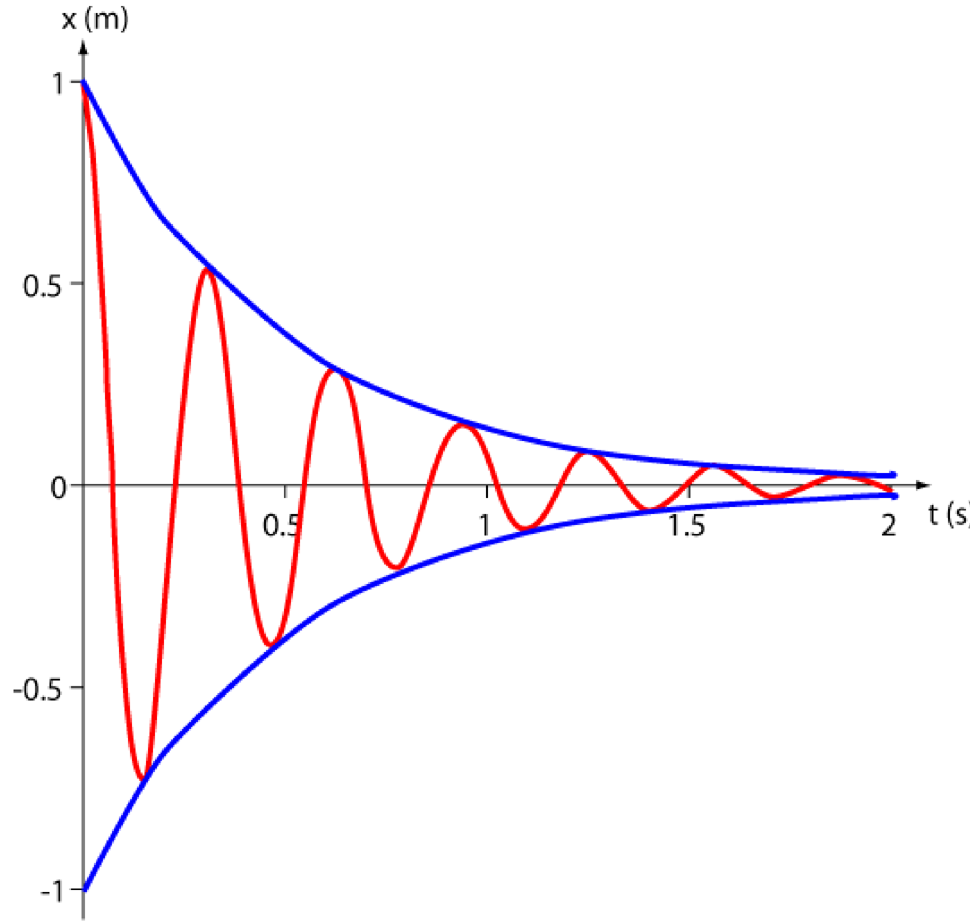

κ mechnism

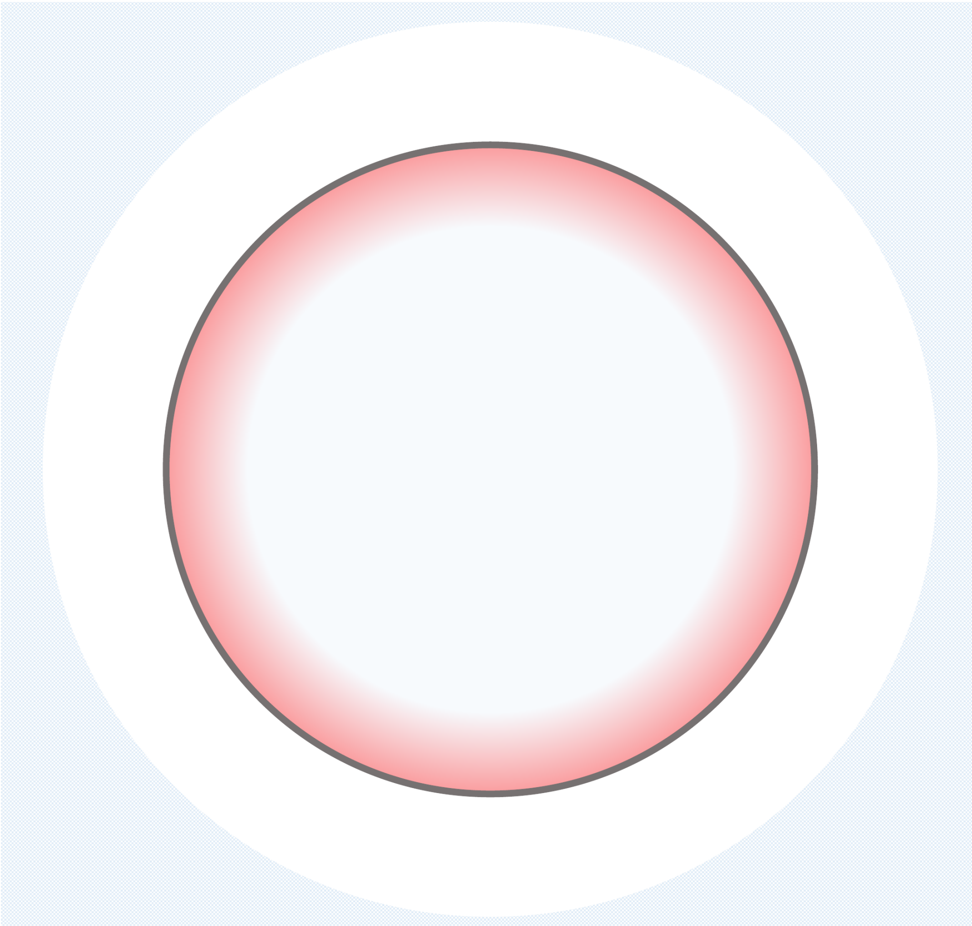

- according to Kramer's Law:
  - $\kappa \sim \frac{\rho}{T^{3.5}}$
- Ionized matter contains free electrons and – at the temperatures inside a star – electron scattering and free-free absorption will dominate the opacity κ
- in partial ionized layers energy released during a layer's compression can be used for further ionisation, instead of temperature increase of the gas

opacity κ builds up in ionization layer (H, He, Fe)

- radiation is blocked
- gas heats
- pressure increases

κ mechnism

Stars expand

- recombination lowers opacity
- radiation flows
- gas cools, pressure drops

κ mechnism

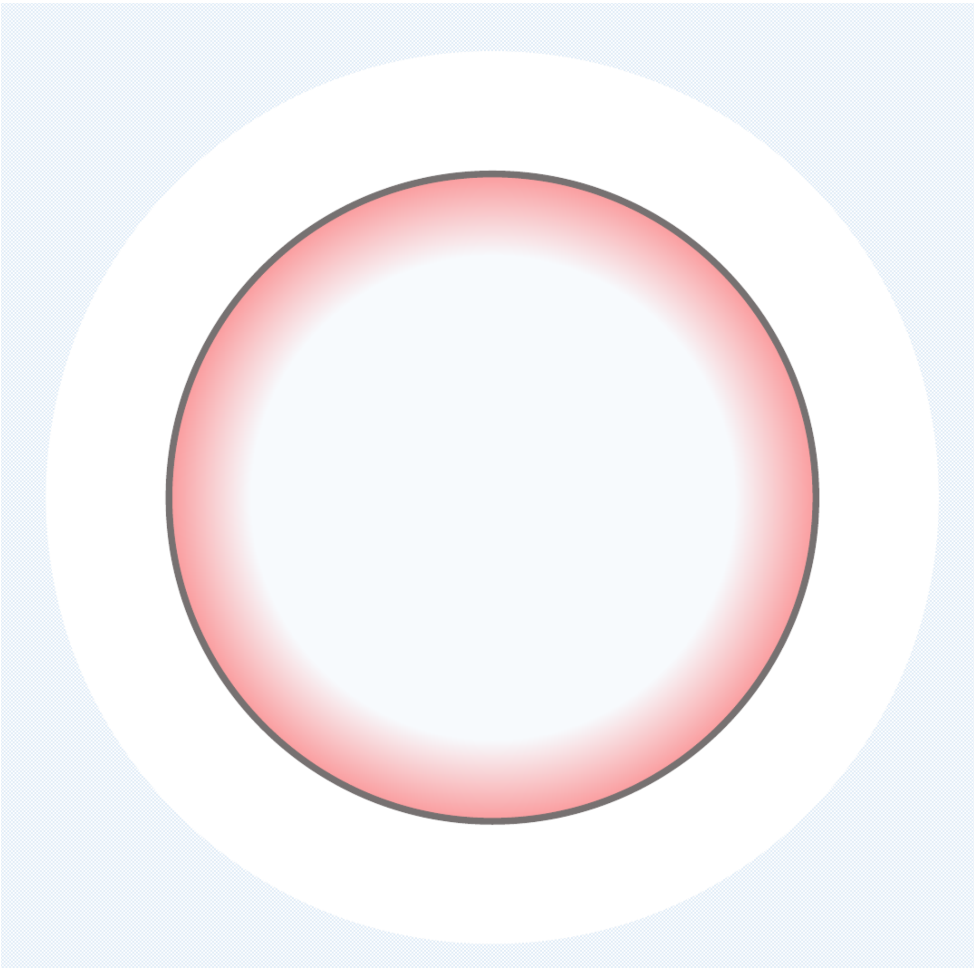

star contracts

- ionization increases opacity again
- next pulsation cycle begins

$\rightarrow$ increased ability of layers to participate in κ mechanism to gain heat during compression (adiabatic coefficient) is called γ mechanism
$\rightarrow$ κ and γmechanism work together

Oscillations can only be excited when a suitable combination of stellar luminosity, temperature, and chemical composition occurs. For this reason, non-radial oscillations are excited in so-called instability strips in the Hertzsprung-Russell diagram

ϵ mechanism

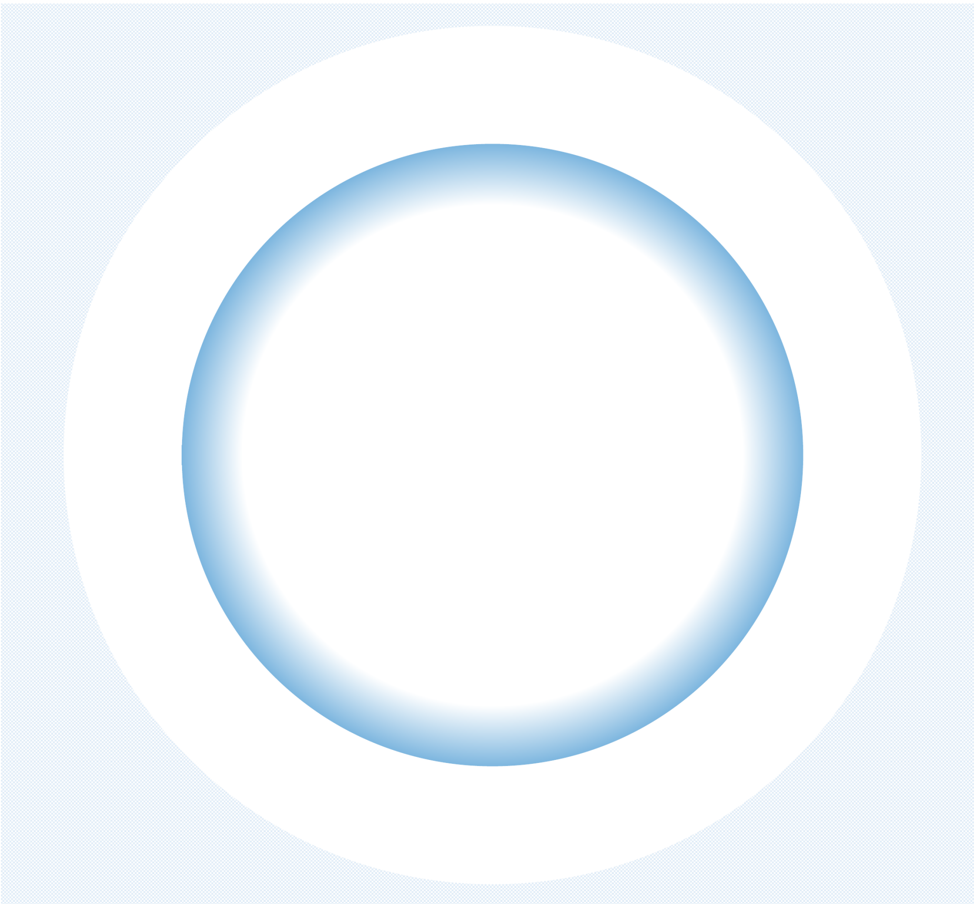

- energy generation rate ϵ in the stellar core
- energy generation is dependent on high powers of the temperature, it might be supposed that small variations, even statistical fluctuations, could lead to variations in energy generation rates which might be self-sustaining
- e.g., He-shell sub-flashes, fluctuations in nuclear burning rate
- proposed for fully-convective stars – such as the coolest M dwarfs – and in the most massive stars – perhaps with $M > 60\,\mathrm{M}_\odot$
- not observationally confirmed

Stochastic oscillations

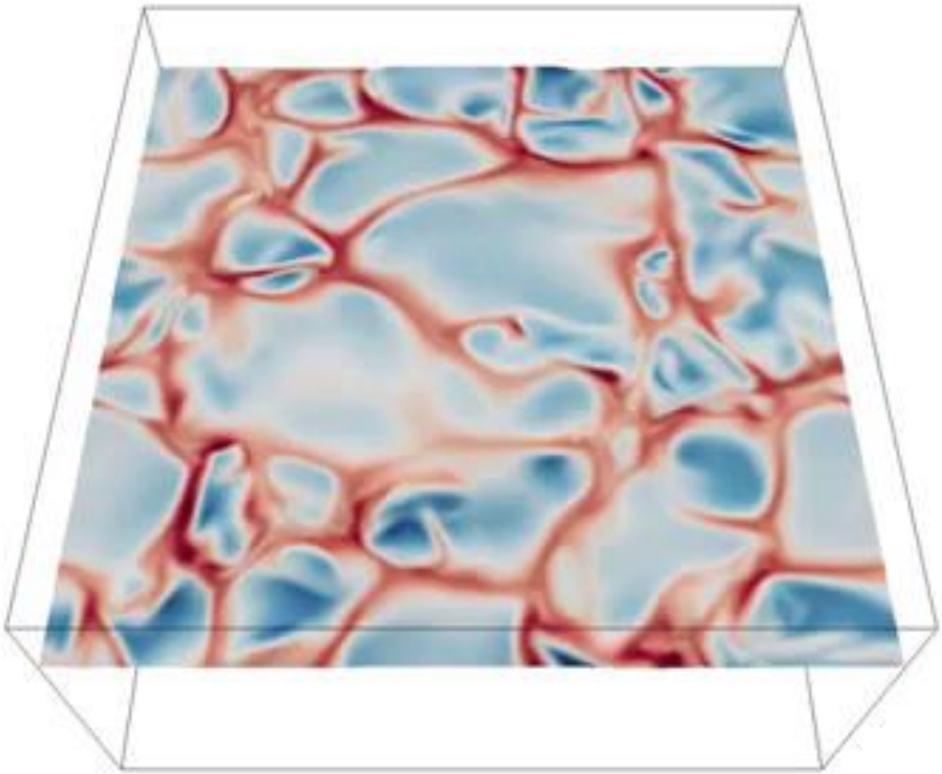

Outer convection zone can drive oscillations

- very small variations (typically at the micromagnitude level rather than the $>$ millimag level which is usually all we can observe in stars) are maintained by stochastic noise generated by convection near the surface
- observed in the sun and red-giants
- lifetimes of the order of days to weeks
- stochastically excited modes

Types of pulsations

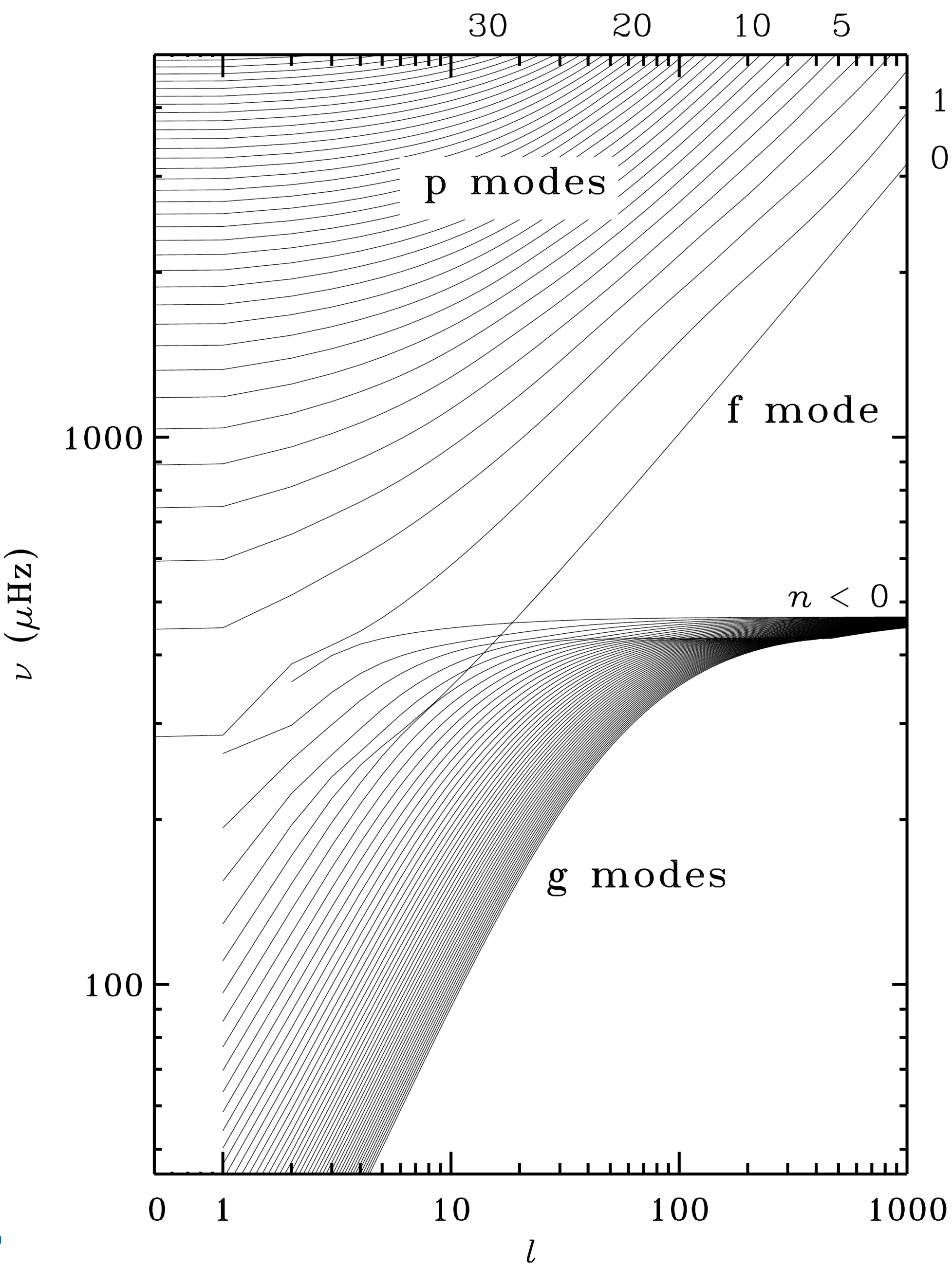

Kurtz 2006

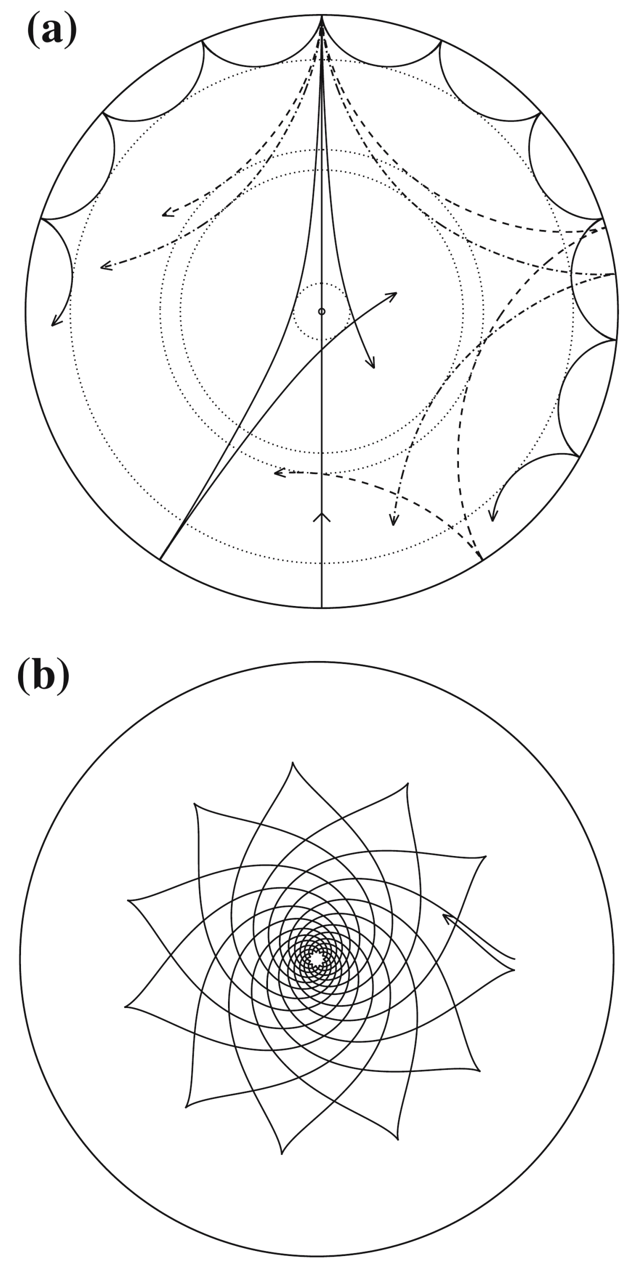

Cunha et al. 2007

two main sets of solutions of the equation of motion

p-mode: pressure is restoring force acoustic waves

g-mode: buoyancy is restoring force gas motion primarily horizontal

Equations of stellar oscillations

characteristic acoustic frequency S_l with $S_l^2 = \frac{l(l+1)c^2}{r^2} = \frac{L^2c^2}{r^2} = k_\mathrm{h}^2 c^2$, $c^2 = \Gamma_1 p/\rho$

oscillation equations for nonradial, adiabatic oscillations

$$\frac{\mathrm{d}\xi_r}{\mathrm{d}r} = -\left(\frac{2}{r} + \frac{1}{\Gamma_1 p}\frac{\mathrm{d}p}{\mathrm{d}r}\right)\xi_r + \frac{1}{\rho c^2}\left(\frac{S_l^2}{\omega^2} - 1\right)p' + \frac{l(l+1)}{\omega^2 r^2}\Phi' \tag{9.12}$$

$$\frac{\mathrm{d}p'}{\mathrm{d}r} = \rho(\omega^2 - N^2)\xi_r + \frac{1}{\Gamma_1 p}\frac{\mathrm{d}p}{\mathrm{d}r}p' - \rho\frac{\mathrm{d}\Phi'}{\mathrm{d}r}, \;\; N^2 = g\left(\frac{1}{\Gamma_1 p}\frac{\mathrm{d}p}{\mathrm{d}r} - \frac{1}{\rho}\frac{\mathrm{d}\rho}{\mathrm{d}r}\right) \tag{9.13}$$

with N the buoyancy frequency

$$\frac{1}{r^2}\frac{\mathrm{d}}{\mathrm{d}r}\left(r^2\frac{\mathrm{d}\Phi'}{\mathrm{d}r}\right) = 4\pi G\left(\frac{p'}{c^2} + \frac{\rho\xi_r}{g}N^2\right) + \frac{l(l+1)}{r^2}\Phi' \tag{9.14}$$

fourth-order system of ordinary differential equations for the four dependent variables ξ_r, p', Φ' and $\mathrm{d}\Phi'/\mathrm{d}r$

Asymptotic equation of stellar oscillations

Cowling Approximation:

Eulerian perturbation of the gravitational potential is neglected: $\Phi' = 0$, valid when density small or l is large or radial mode $|n|$ is large

$$\frac{d\xi_r}{dr} = -\left(\frac{2}{r} - \frac{1}{\Gamma_1}H_p^{-1}\right)\xi_r + \frac{1}{\rho c^2}\left(\frac{S_l^2}{\omega^2} - 1\right)p' \quad (9.15)$$

$$\frac{dp'}{dr} = \rho(\omega^2 - N^2)\xi_r - \frac{1}{\Gamma_1}H_p^{-1}p', \quad H_p^{-1} = -\frac{d\ln p}{dr} \quad (9.16)$$

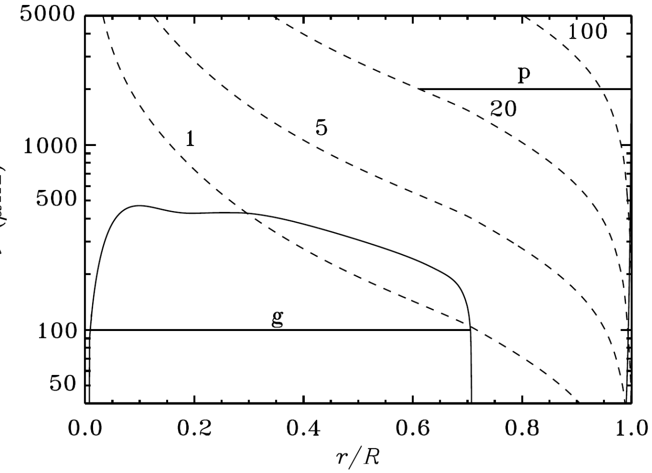

H_p is the pressure scale height For oscillations of high radial order this simplifies to

$$\frac{d^2\xi_r}{dr^2} = \frac{\omega^2}{c^2}\left(1 - \frac{N^2}{\omega^2}\right)\left(\frac{S_l^2}{\omega^2} - 1\right)\xi_r = -K_s(r)\xi_r \quad (9.17)$$

ξ_r oscillates if $K_s > 0$

o1) $|\omega| > |N|$ and $|\omega| > S_l$: p mode

o2) $|\omega| < |N|$ and $|\omega| < S_l$: g mode

Stellar timescales

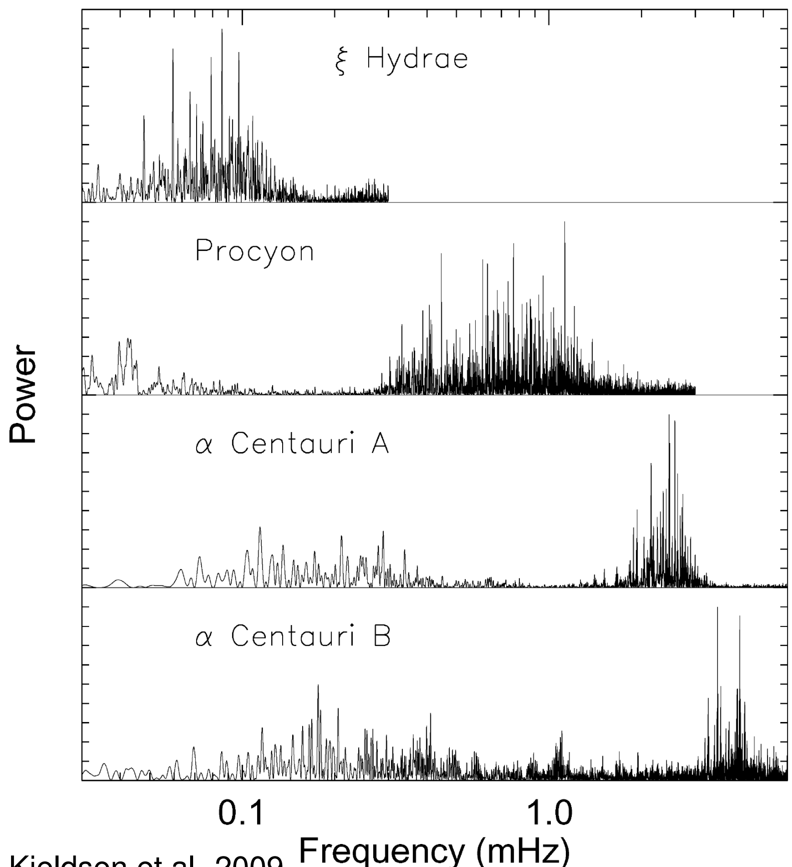

Kjeldsen et al. 2009

- Kelvin-Helmholtz (thermal) time scale

$$\tau_{\mathrm{th}} = \frac{GM^2}{RL} \backsimeq \frac{\langle c_p T\rangle M}{L} \qquad (9.18)$$

time a star can shine with gravity as only energy source

- longest timescale: nuclear time scale

$$\tau_{\mathrm{nuc}} = \frac{\epsilon q M c^2}{L} \qquad (9.19)$$

time a star can shine with nuclear fusion as energy source

- shortest timescale: dynamical time scale

$$\tau_{\mathrm{dyn}} = \sqrt{\frac{R^3}{GM}} \backsimeq \sqrt{\frac{1}{G\bar{\rho}}} \qquad (9.20)$$

time the star needs to return to hydrostatic equilibrium after disturbance by dynamical process

Pulsation periods

radial oscillations as standing acoustic waves: characteristic period

$$\Pi = 2\int_0^R \frac{\mathrm{d}r}{c(r)} \sim \frac{R}{\langle c\rangle} \tag{9.21}$$

mean sound speed $\langle c\rangle = \sqrt{\Gamma_1 p/\rho}$ mean density and pressure given by hydrostatic equilibrium

$$\rho \simeq \frac{M}{R^3}, \; p \simeq \frac{GM^2}{R^4} \tag{9.22}$$

so we can calculate the characteristic period of radial oscillations

$$\Pi = \sqrt{\frac{3\pi}{2\Gamma_1 G\langle\rho\rangle}} \sim \left(\frac{R^3}{GM}\right)^{1/2} = t_{\mathrm{dyn}} \tag{9.23}$$

Pulsation periods and ampliudes depend on equilibrium stellar structure (ρ, p, Γ_1, g, composition as functions of r) $\rightarrow$ Frequency of pulsation mode at the surface depends on the sound travel time along its ray path

$\Rightarrow$ probing the structure of stars: Asteroseismology

Asteroseismology

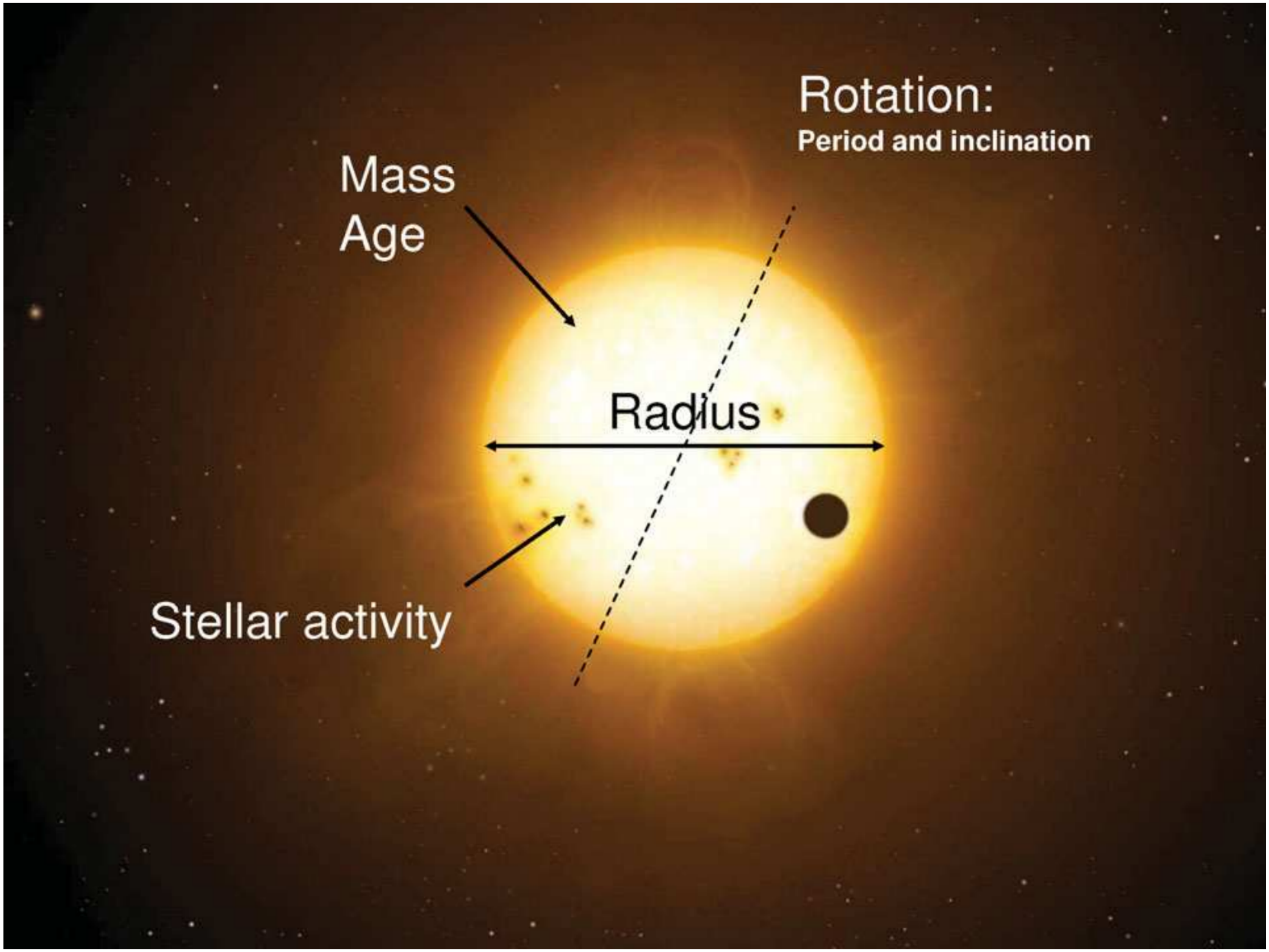

Kjeldsen et al. 2009, IAU Symp. 253, 309

Pulsation modes

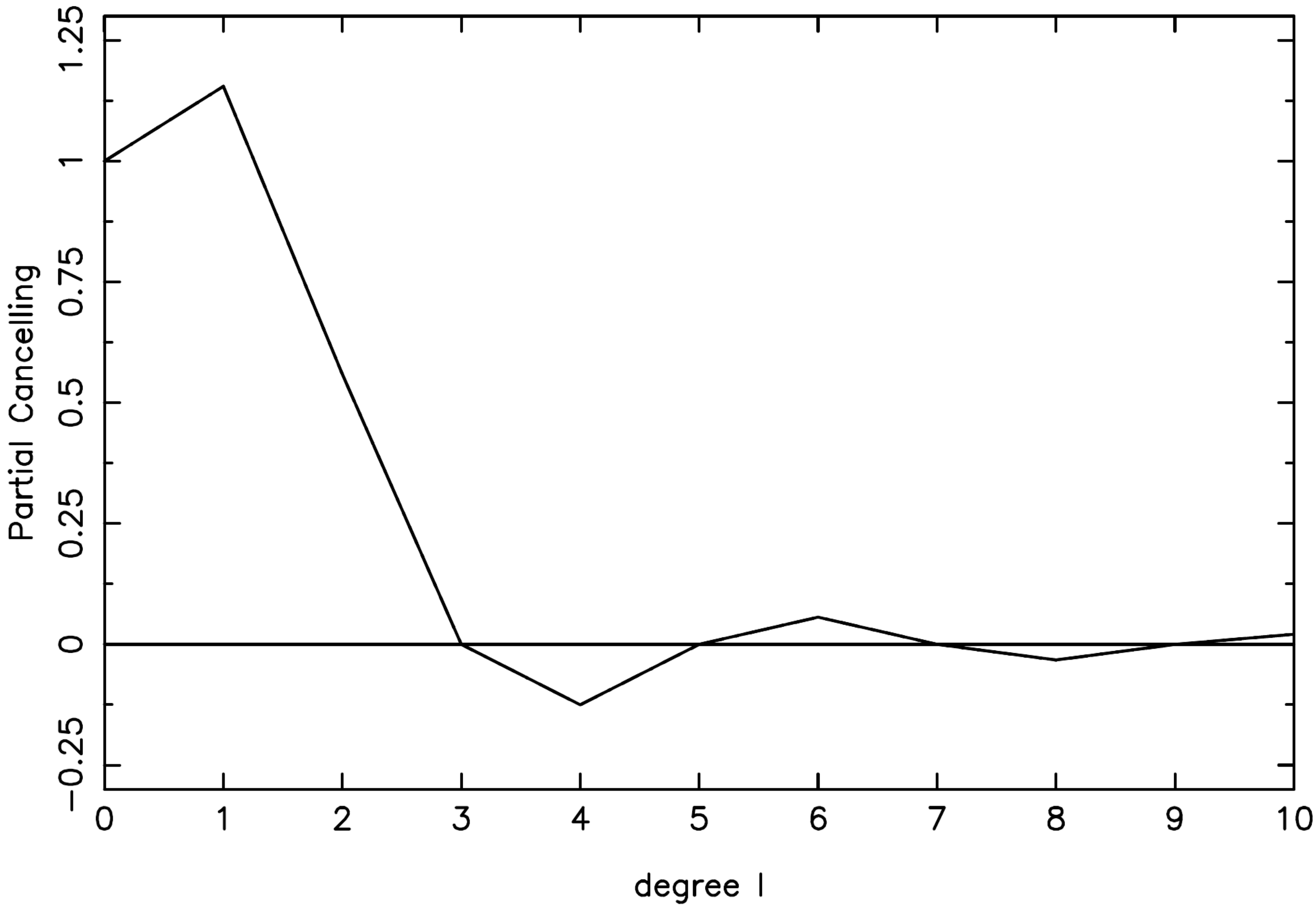

Limitation → High order modes cancel in integrated light

Pulsating stars

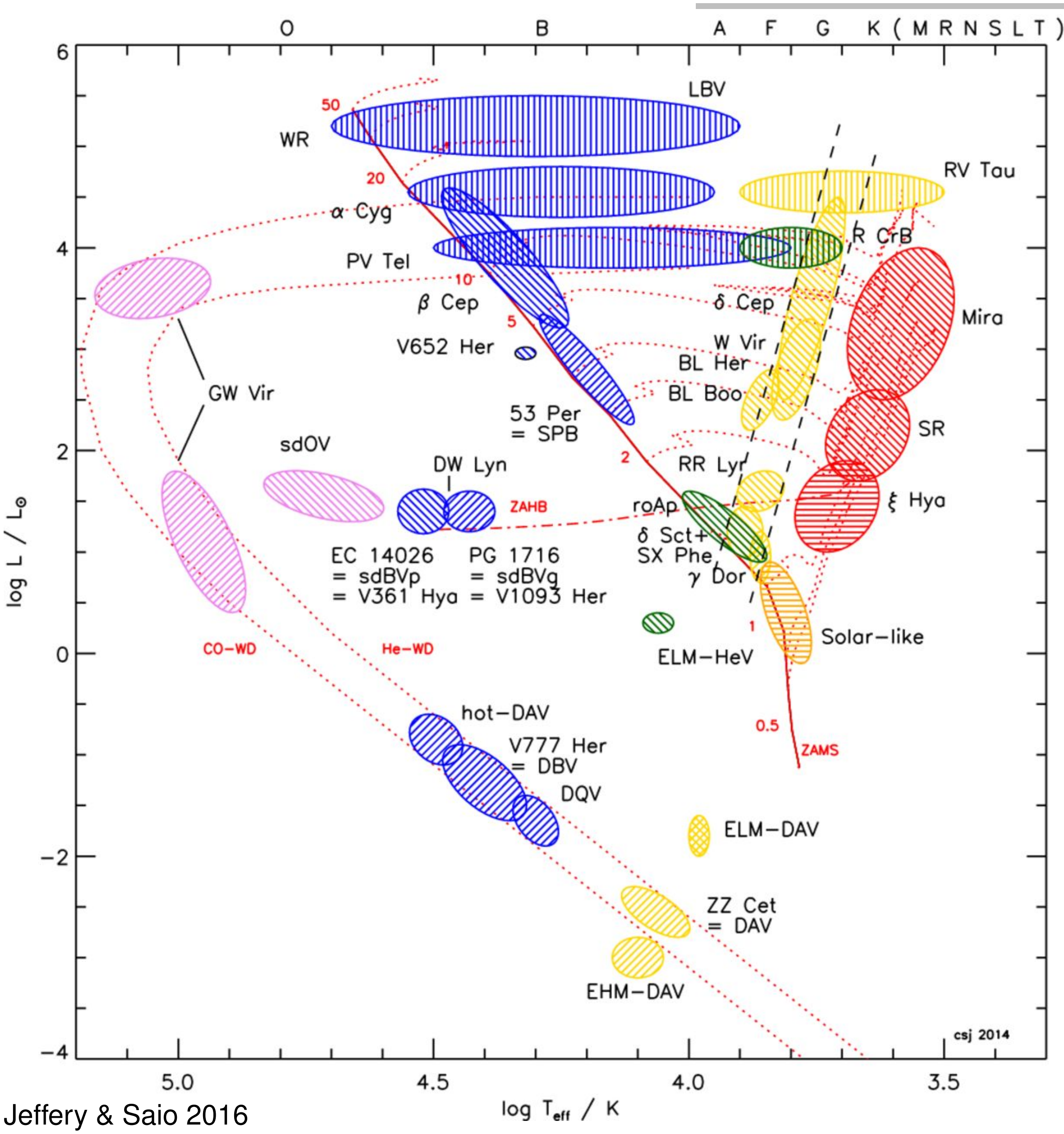

Jeffery & Saio 2016

Pulsating stars are found all over the HRD (and new ones discovered constantly)

- Driving mechanisms require special conditions (ionization zones, surface convection, etc.)
- **Instability strips**

Solar oscillations

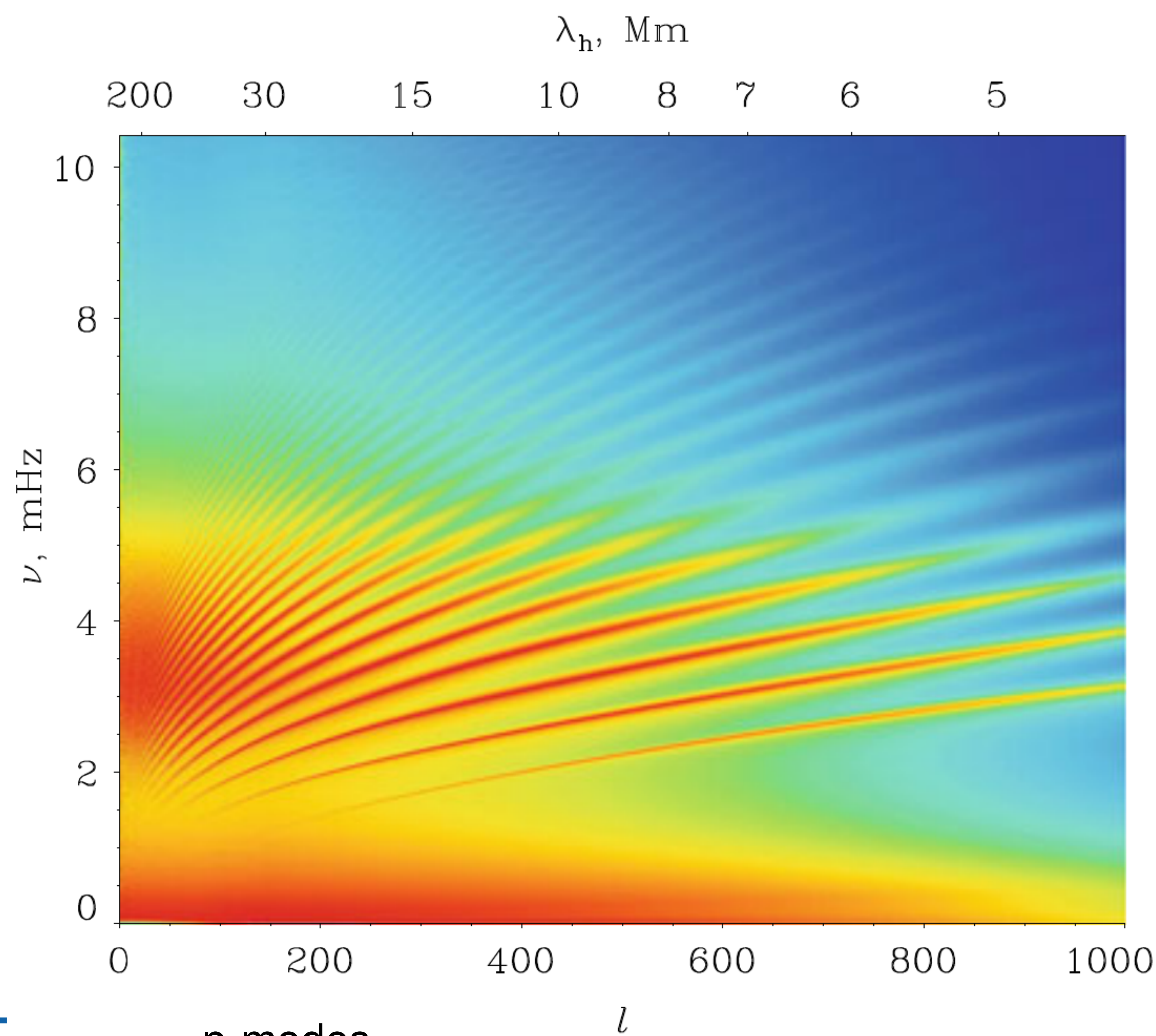

Rozelot & Neiner 2011

p-modes

Periodogram of the sun observed by GOLF/SOHO

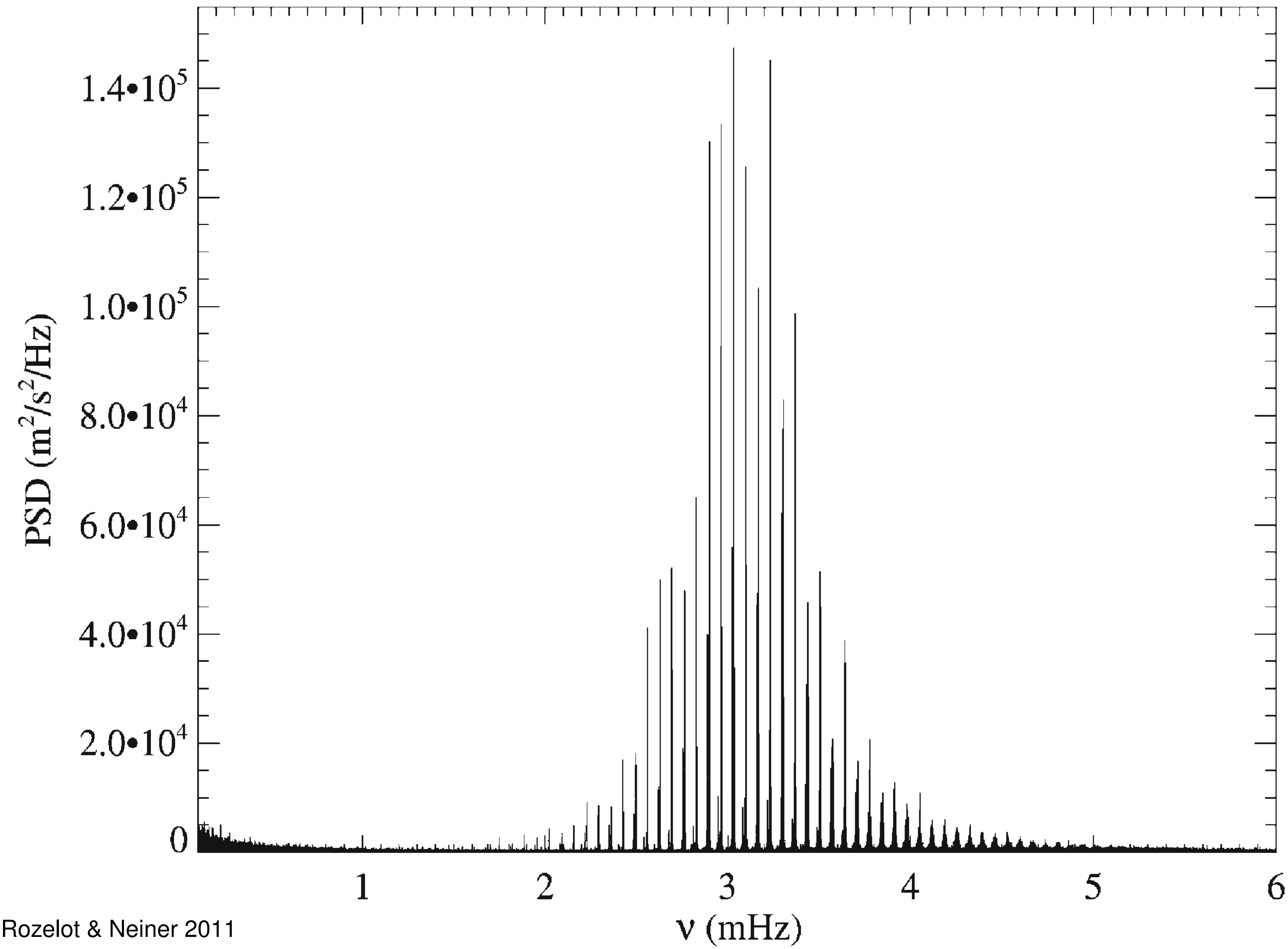

Rozelot & Neiner 2011

Periodogram of the sun observed by GOLF/SOHO

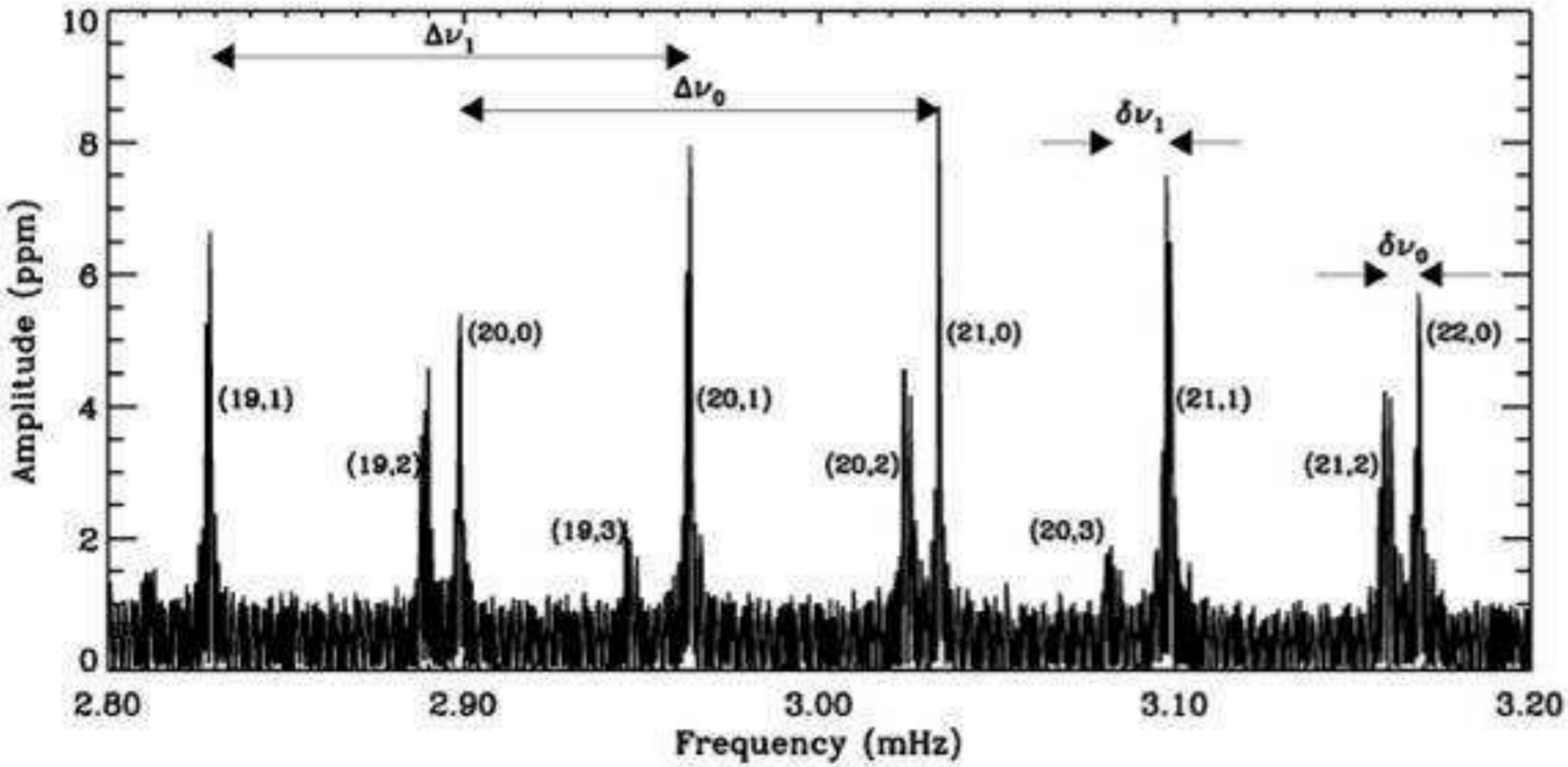

Rozelot & Neiner 2011

90% of the solar interior known!

large frequency separation $\Delta\nu = \nu_{n+1\,l} - \nu_{nl} = \left(2\int_0^R \frac{\mathrm{d}r}{c}\right)^{-1} \sim \sqrt{\langle\rho\rangle}$

small separation $\delta_\nu \equiv \nu_{nl} - \nu_{n-1\,l+2} \simeq -(4l+6)\frac{\Delta\nu}{4\pi^2\nu_{nl}}\int_0^R \frac{\mathrm{d}c}{\mathrm{d}r}\frac{\mathrm{d}r}{r}$

Solar-like pulsators

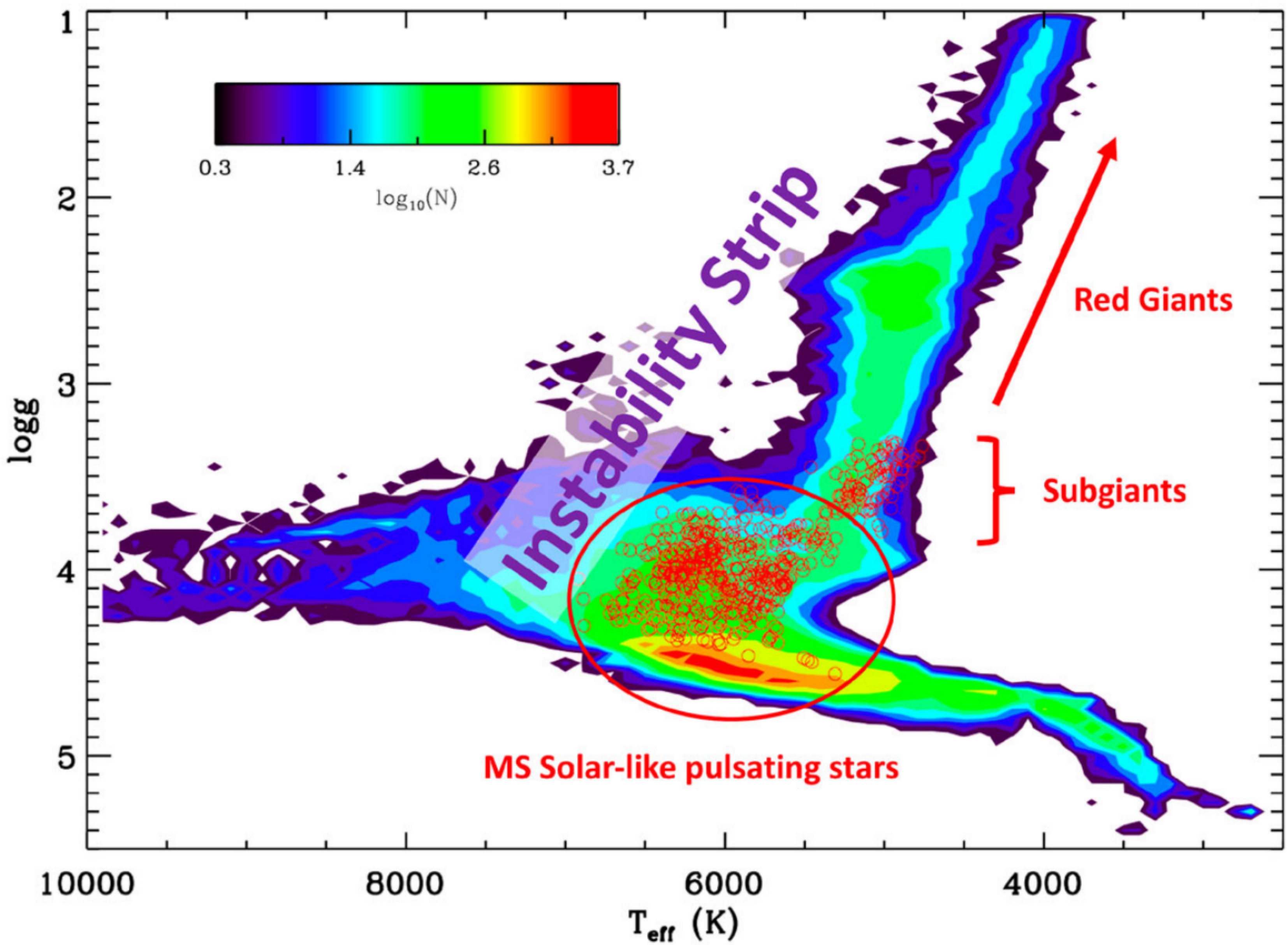

Garcia & Ballot

Mira variables

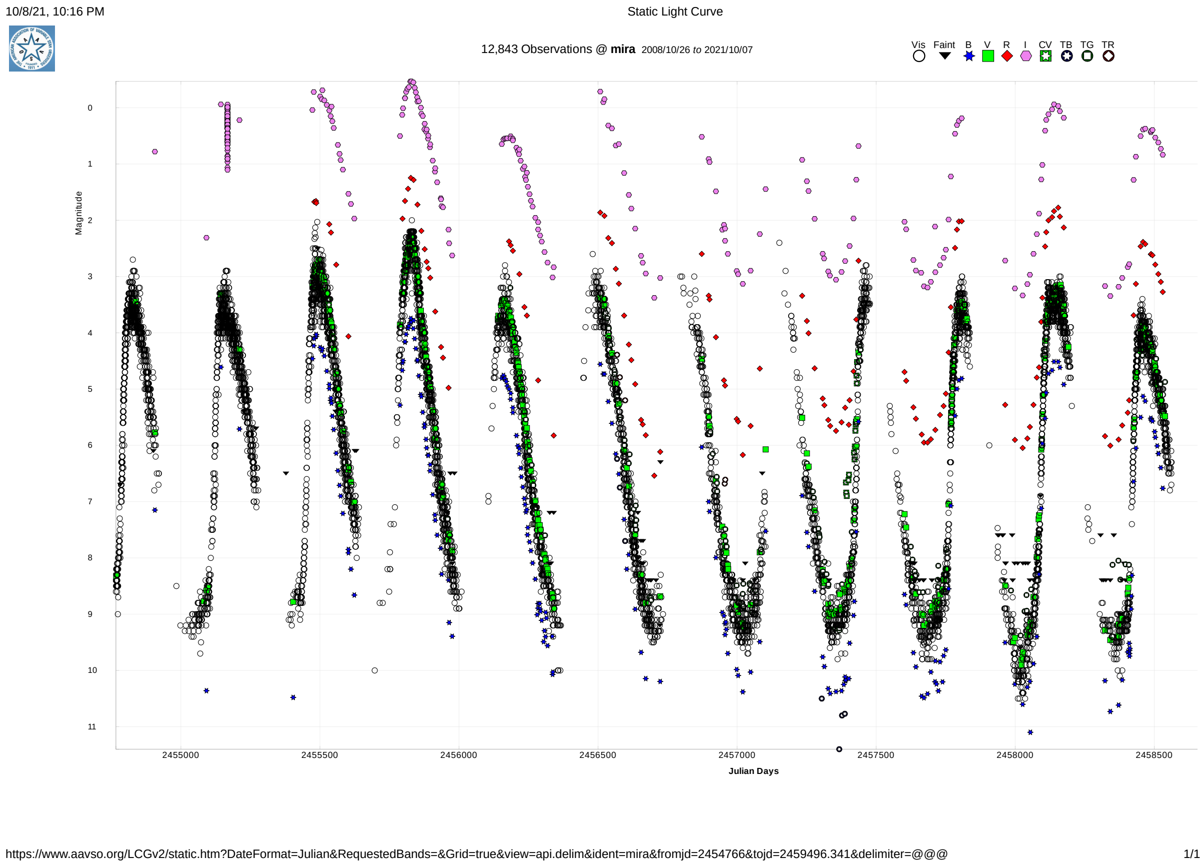

- have periods from 80 to 1000 h d with visual amplitudes > 2.5 mag
- giant stars with effective temperature near 3000 K near the tip of the AGB

$\rightarrow$ cool giant stars with very large radii powered by fusion from a hydrogen and a helium burning-shell

$\rightarrow$ very low average density, significant mass loss

$\rightarrow$ less massive then on the main sequence

RR Lyrae

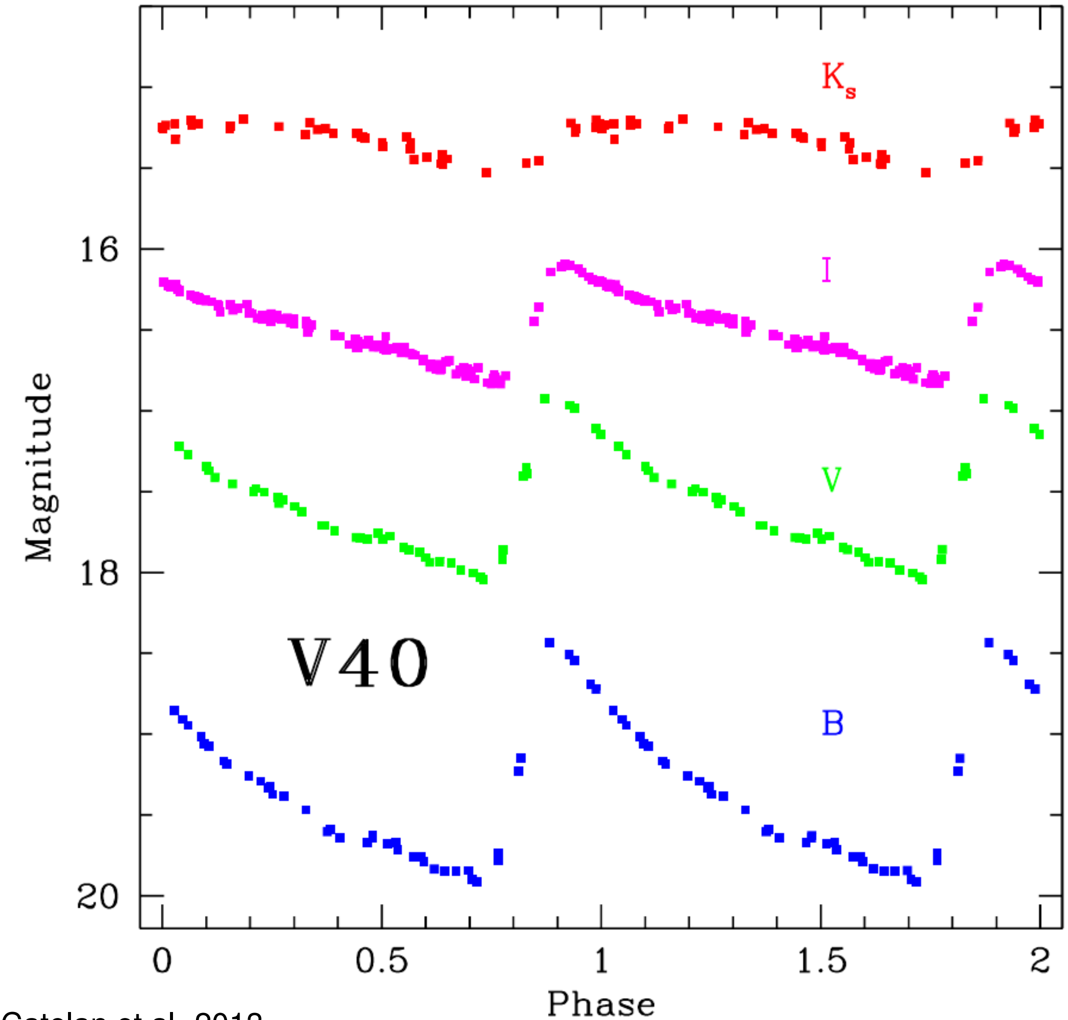

Catelan et al. 2013

- RR Lyrae stars are low-mass ($\approx$ $0.6 - 0.8\,M_\odot$) horizontal branch stars falling within the instability strip

- periods between 0.2 and 1.0 d
- amplitudes $\Delta m \sim 0.2 - 2$ mag
- three classes: a (largest amplitude, steepest rise to maximum), b (smaller amplitude and longer periods), c (shorter periods, lower amplitudes, more symmetric)
- found in the instability strip near absolute magnitude of +0.6 mag
- temperatures between 6000 and 7250 K
- only found in populations older than 10 Gy
- amplitude of the light curves increase from the infrared to the UV

RR Lyrae as standard candles

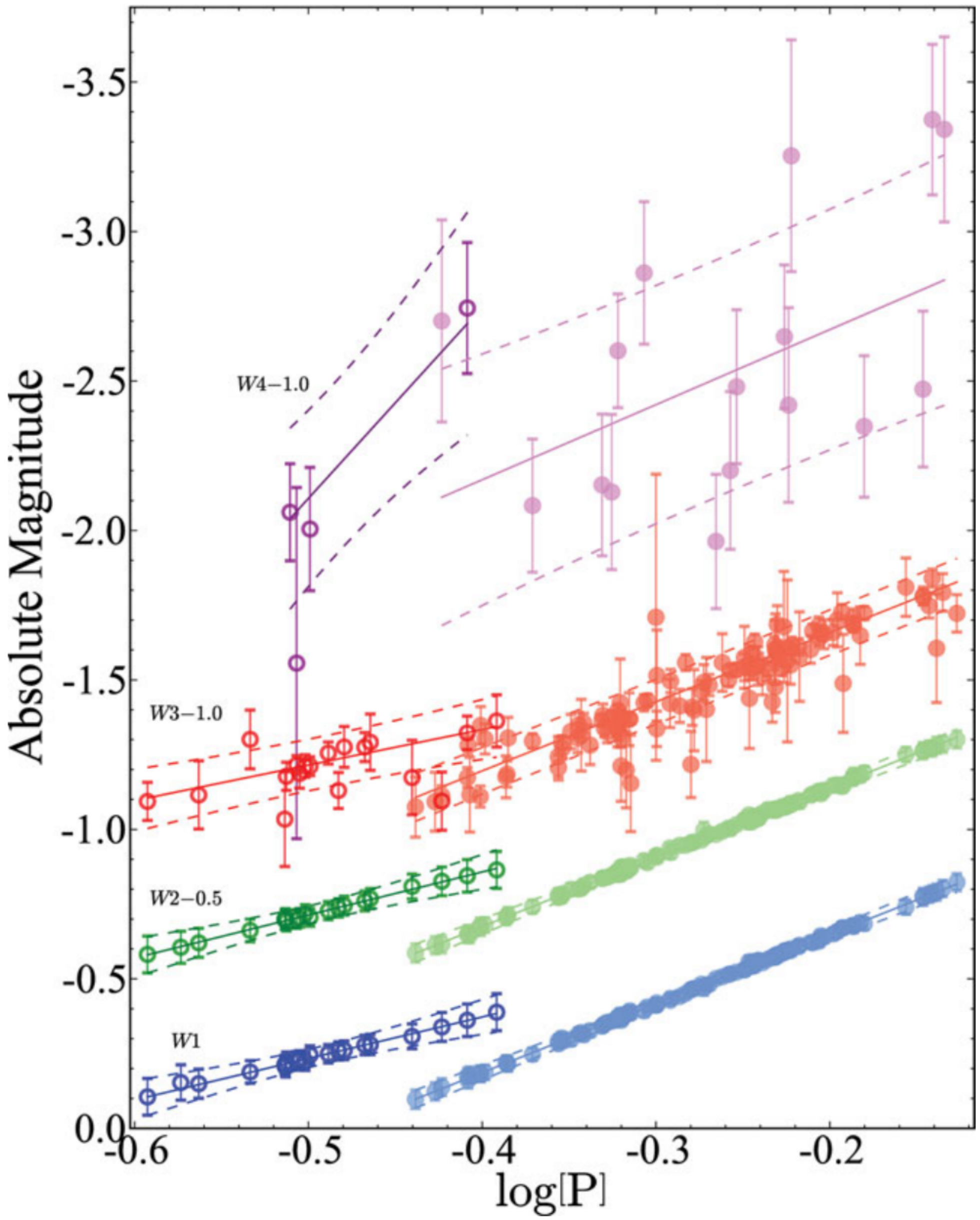

Ngeow et al. 2013

- measuring distances to systems containing old stellar populations
- located on horizontal branch $\rightarrow$ horizontal in V
- in other filters period-luminosity relation (Infrared)
- radial pulsations on dynamical timescales $\rightarrow P\sqrt{\rho}$ = const
- absolute magnitude also depends on metallicity $\langle M_V \rangle = a + b\,[\mathrm{Fe/H}]$
- zero-point calibration for using period-luminosity relation in the Infrared

Classical Cepheids

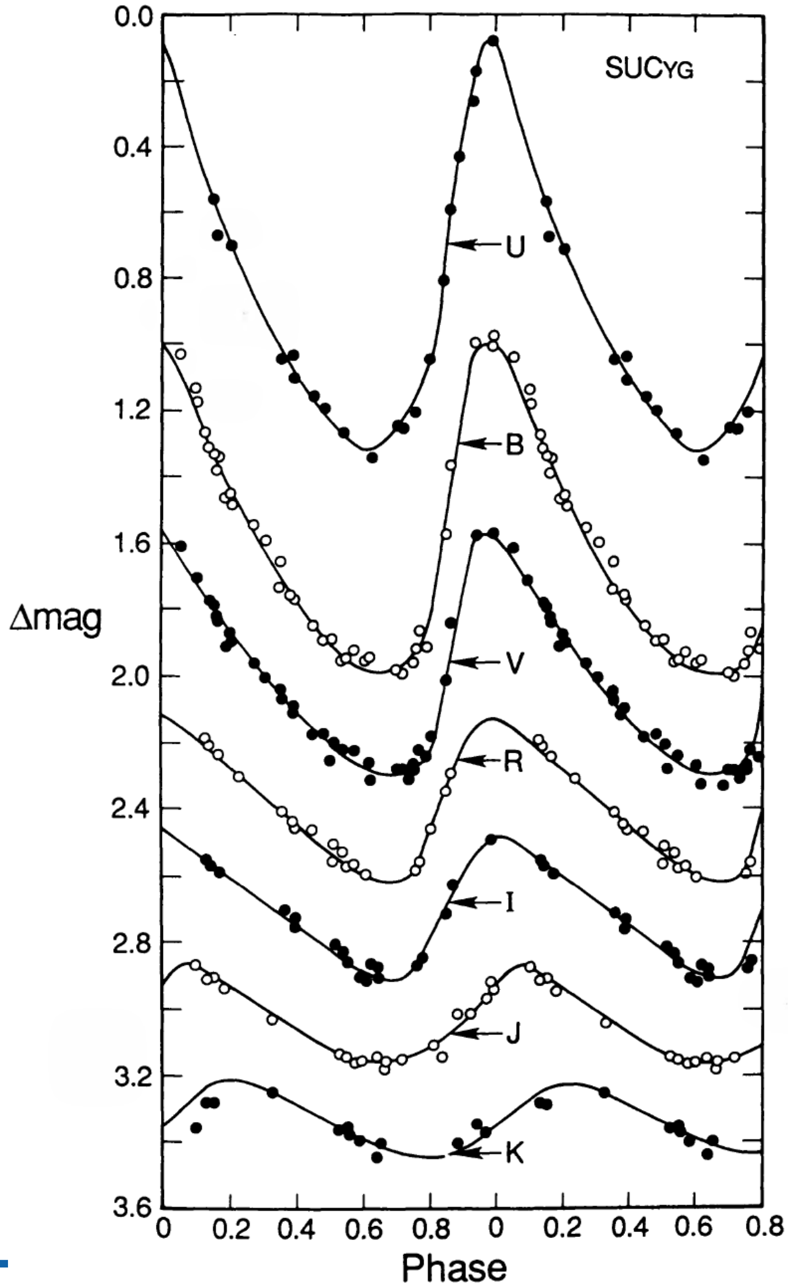

- evolved, radially pulsating stars in the instability strip, more luminous than RR Lyrae
- classical Cepheids (δ Cepheids or type I Cepheids): from F-type ($M_V = -2$) to G or K type ($M_V = -6$)
- pulsation periods mostly from 1 to 100 d
- pulsation excited by κ and γ mechanism
- more massive than sun, have evolved from $2 - 20\,M_\odot$ main-sequence stars, many from $4 - 9\,M_\odot$ stars
- cross instability strip on the way to the RGB and on the blue loop during He burning
- young stars from 10^7 the brightest to 10^8 years the faintest
- found in regions of recent star formation, in the Milky Way in the disk

Classical Cepheids

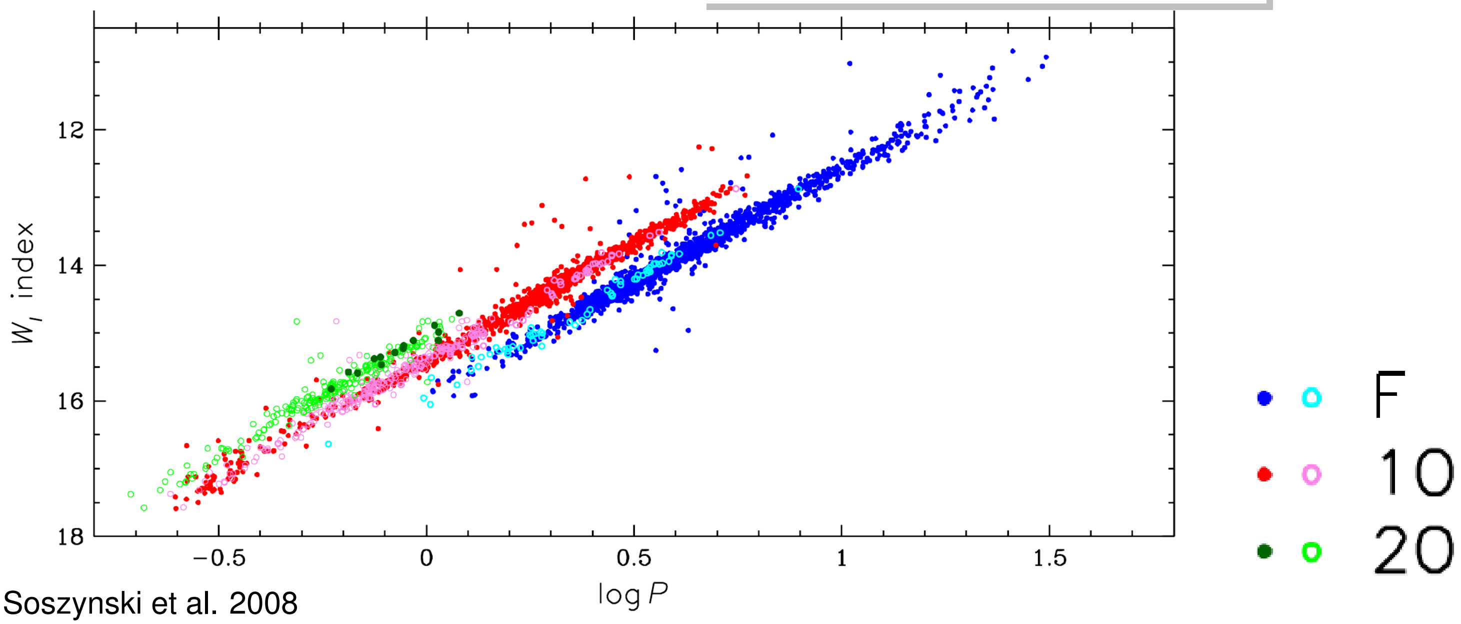

Soszynski et al. 2008

Relation between L and P expected

$$M_{\rm bol} = -5\log(R) - 10\log(T_{\rm eff}) + \text{const},\ P\sqrt{\langle\rho\rangle} = \text{const},\ \langle\rho\rangle = \frac{\text{M}}{4/3\pi\text{R}^3}$$

$$\Rightarrow \log(P) + 0.5\log(M) + 0.3M_{\rm bol} + 3\log(T_{\rm eff}) = \text{const}$$

Mass-luminosity relation (compare MS stars): $M_{\rm bol} = -8\log(M) + \text{const}$

$$\log(P) = -0.24M_{\rm bol} - 3\log(T_{\rm eff}) + \text{const}$$

$$\Rightarrow M_V = \alpha\log P + \beta(B-V)_0 + \gamma \tag{9.24}$$

$$M_V = -(2.77\pm0.08)(\log P - 1) - (4.08\pm0.04) \tag{9.25}$$

Type II Cepheids

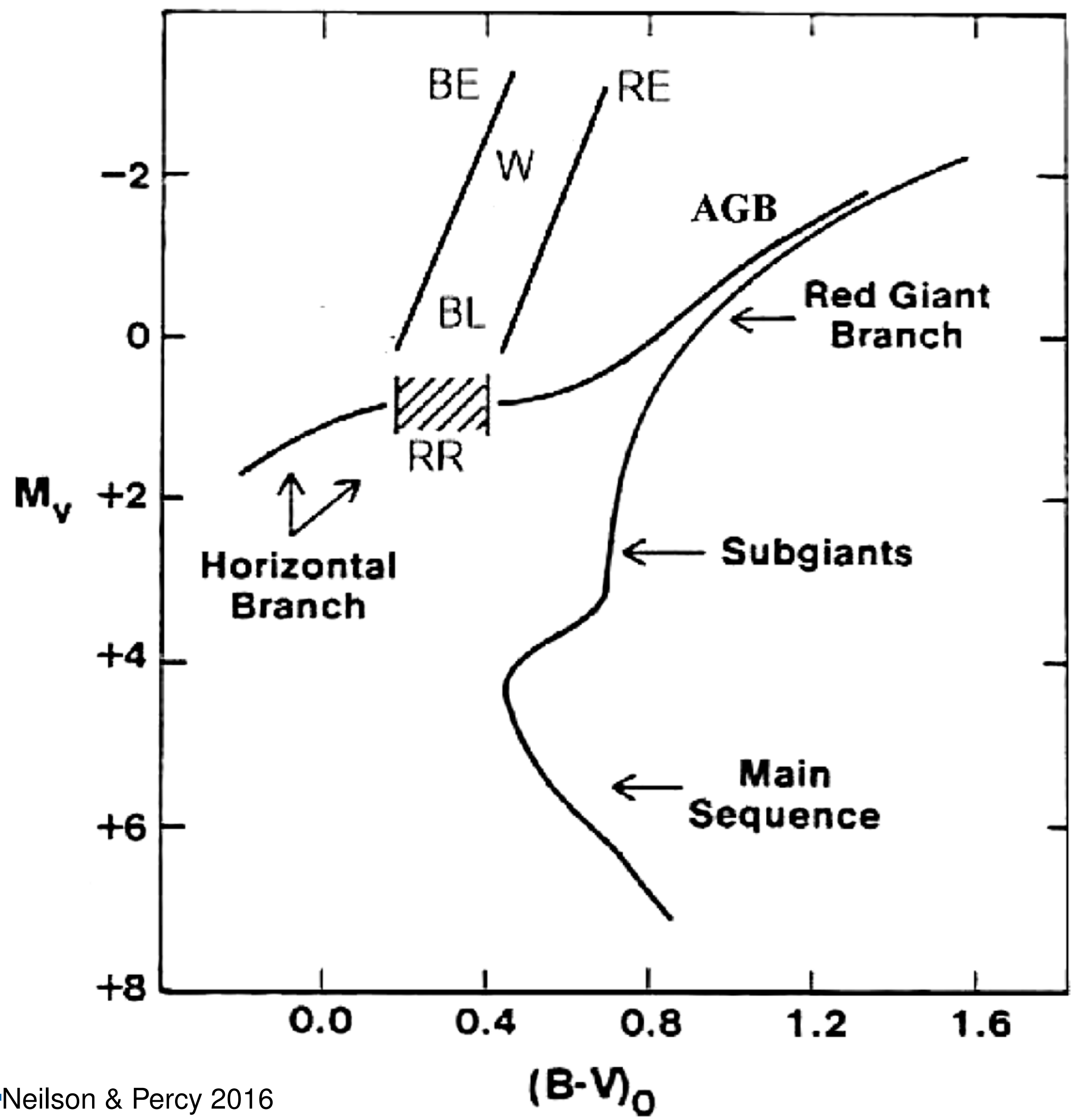

Neilson & Percy 2016

- Hubble used Cepheids to measure distances to nearby Galaxies
- Cepheid with emission lines found $\rightarrow$ different type with different luminosity
- old, evolved stars of low mass ($\sim 0.5 - 0.6\,M_\odot$)
- found in globular clusters, halo, bulge, old disk populations, Magellanic clouds, some Local Group galaxies
- rarer than RR Lyrae
- luminosities larger than horizontal branch, smaller than Classical Cepheids
- shell-burning

Type II Cepheids

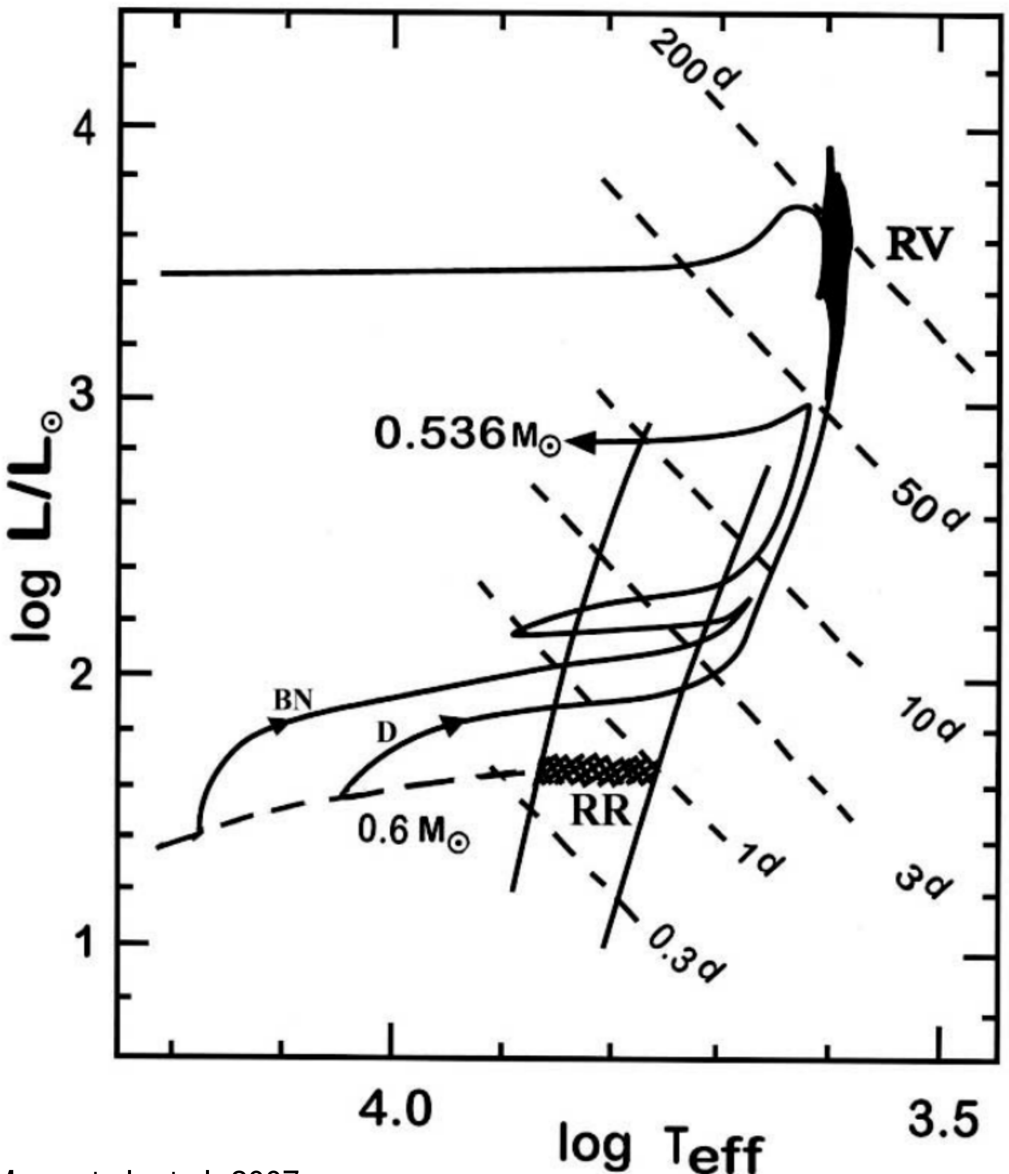

Maas et al. et al. 2007

- BL Her stars: blue HB star moves quite fast from HB to AGB crossing instability strip, increasing periods
- W Vir stars: He-shell flashes on AGB $\rightarrow$ more common in more metal-rich clusters, low envelope masses, period decrease or increase
- even bluer, lower-mass HB stars with masses as small as $0.52\,M_\odot$ cross the instability strip several times moving to the AGB
- metal-rich HB stars are found on the red HB never crossing the instability strip, few solar-metallicity Type II Cepheids had large mass-loss on the RGB

Pulsating stars close to the lower main sequence in the HRD

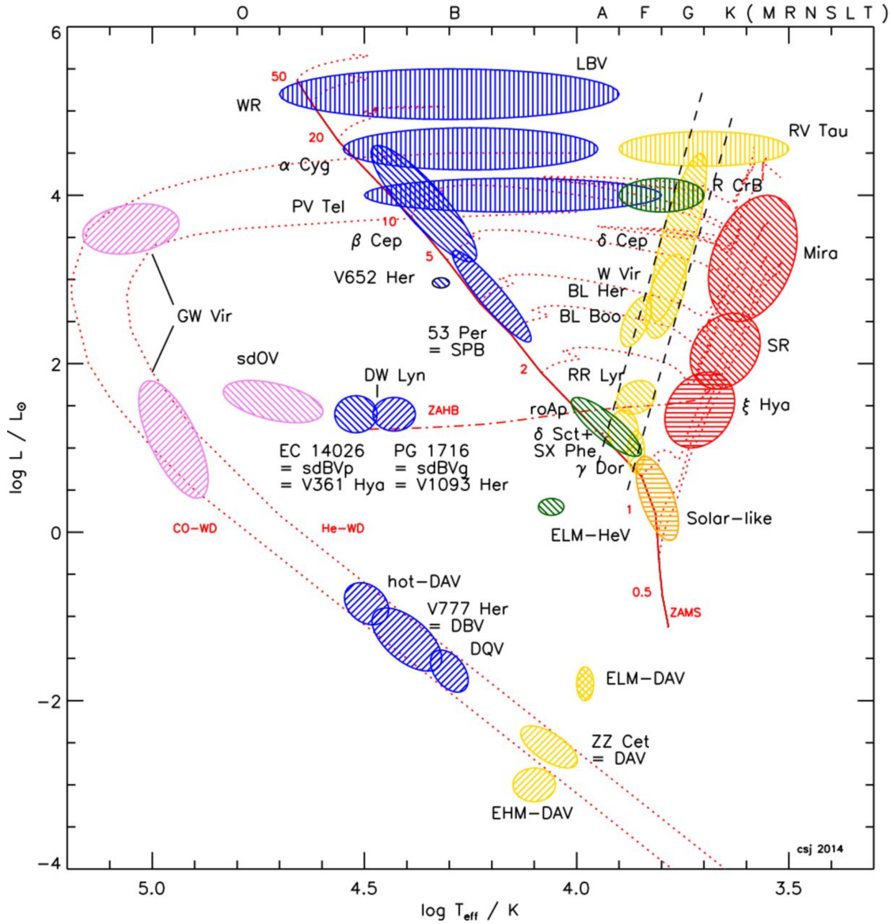

Jeffery & Saio 2016

type	P(d)	A_V(mag)	modes	Z
δ Scuti	0.008-0.42	0.001-1.7	R+NR(p, low order)	$\approx$ solar
SX Phoenicis	0.01-0.4	0.002-1	R+NR(p, low order)	$<$ to $\ll$ solar
γ Doradus	0.3-3	<0.1	NR (g)	$\approx$ solar
roAp	0.002-0.016	<0.012	NR (p, high-order)	$\sim$ solar, but peculiar

Pulsating stars close to the upper main sequence in the HRD

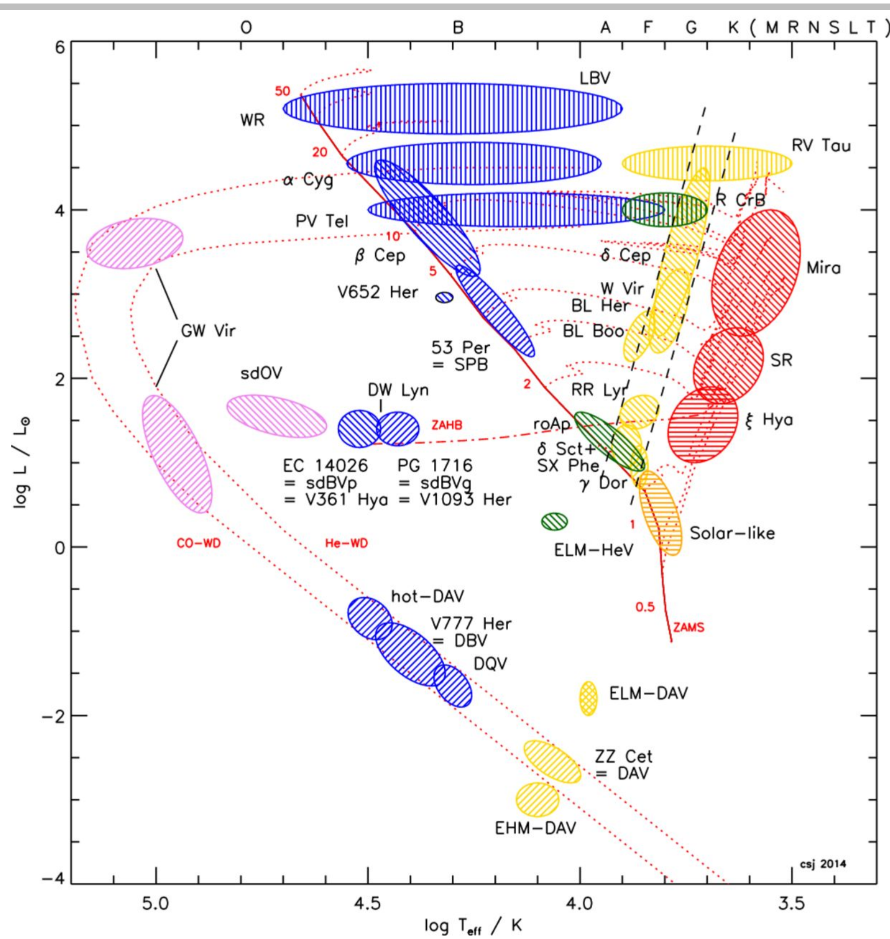

Jeffery & Saio 2016

type	P(d)	A_V(mag)	modes
β Cephei	0.1-0.6	0.01-0.32	NR(p)
Slowly Pulsating B stars (SPB)	0.4-6	<0.03	NR(g)

Pulsating Supergiant Stars

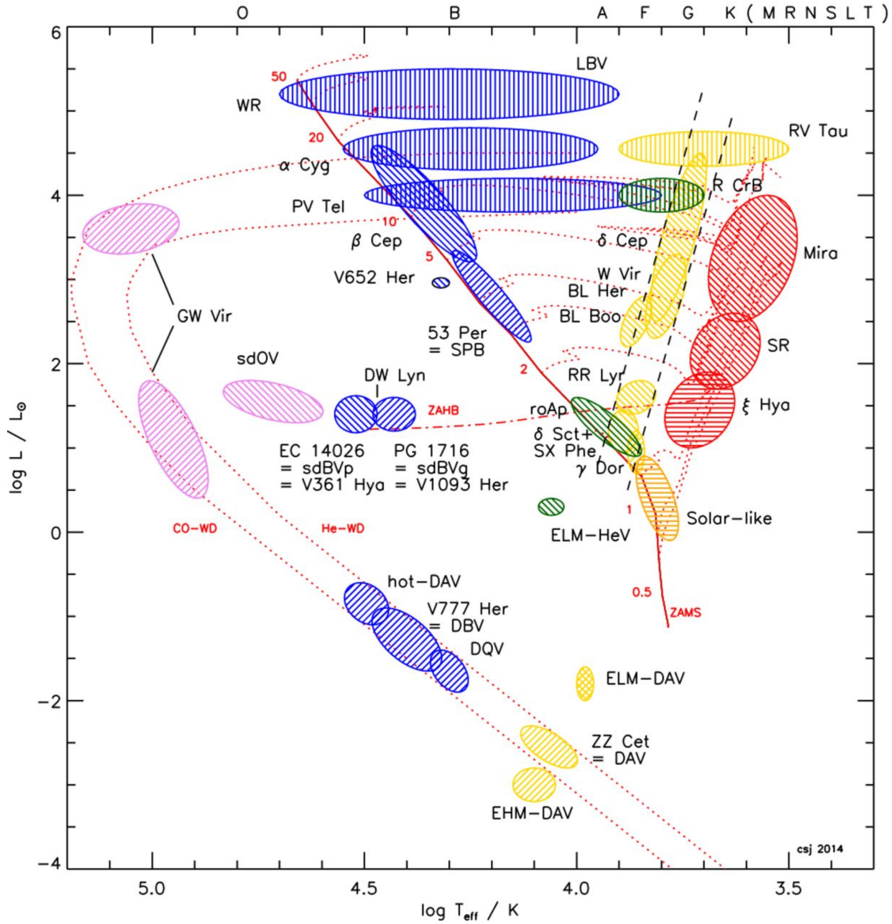

Jeffery & Saio 2016

type	SPBsg	α Cygni	PV Tel I	PV Tel II	PV Tel III	V652 Her
P (d)	0.35-47	1.2-100	5-30	0.5-5	30-100	≈ 0.1
A_V (mag)	$\lesssim 0.004$	0.01-0.1	'low'	'low'	'low'	≈ 0.1
Modes	NR(g,p)	NR(g,SM)	R(SM)	NR(g,SM)	R	R

Hot Subdwarf Pulsators

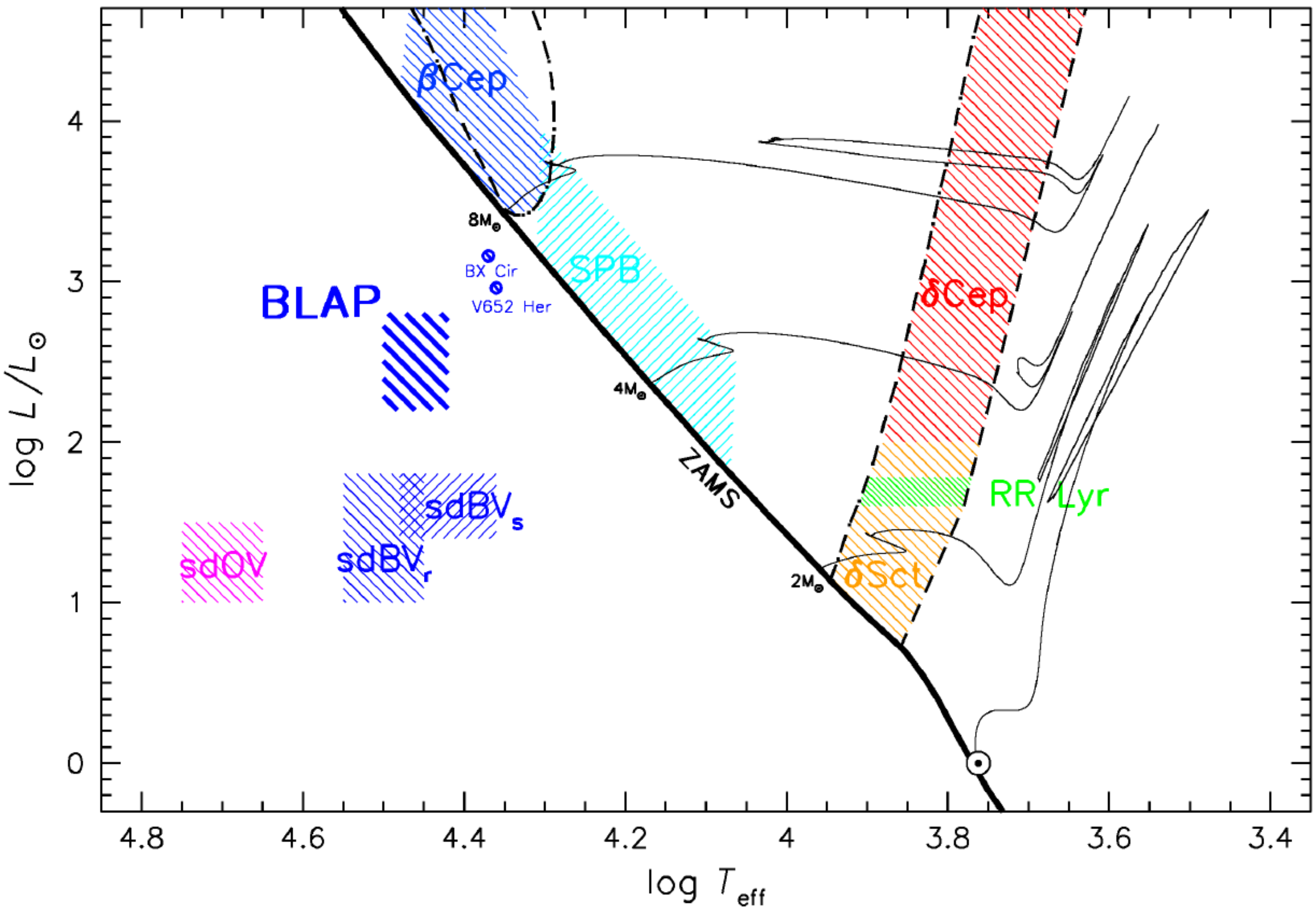

Pietrukowicz et al. 2017

type	EC 14026	PG 1716+426	sdOV	He-sdBV	BLAP	high-gravity BLAP
P (s)	64-573	1000-14 600	60-120	1950-5080	1300-2400	200-475
A_V (mmag)	1-300	0.4-41	1.3-40	1.0-2.7	200-400	50-200
Modes	R+NR(p)	NR(g)	NR(p)	NR(g)	R(p) or NR(g)	low-order R(p)?

Hot Subdwarf Pulsators

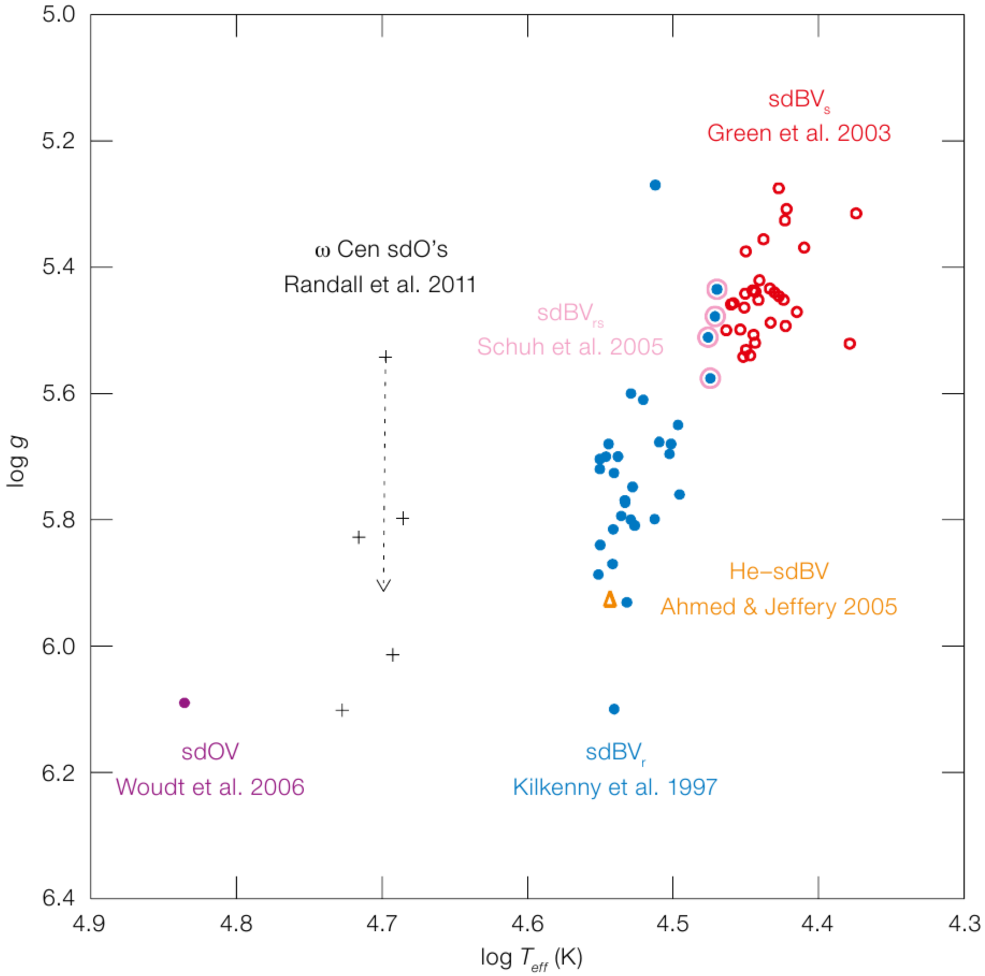

Randall et al. 2016

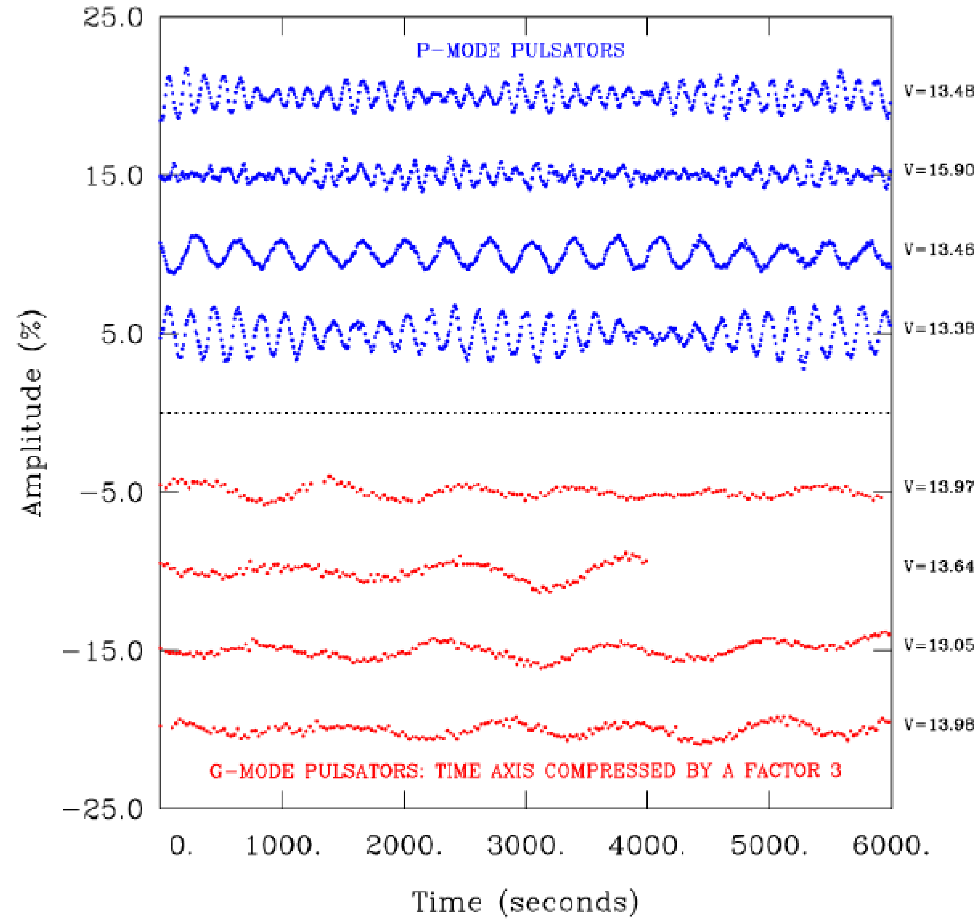

Charpinet et al. 2009, AIP Conf. Proc., 1170, 585

Pulsating White Dwarfs and Pre-White Dwarfs

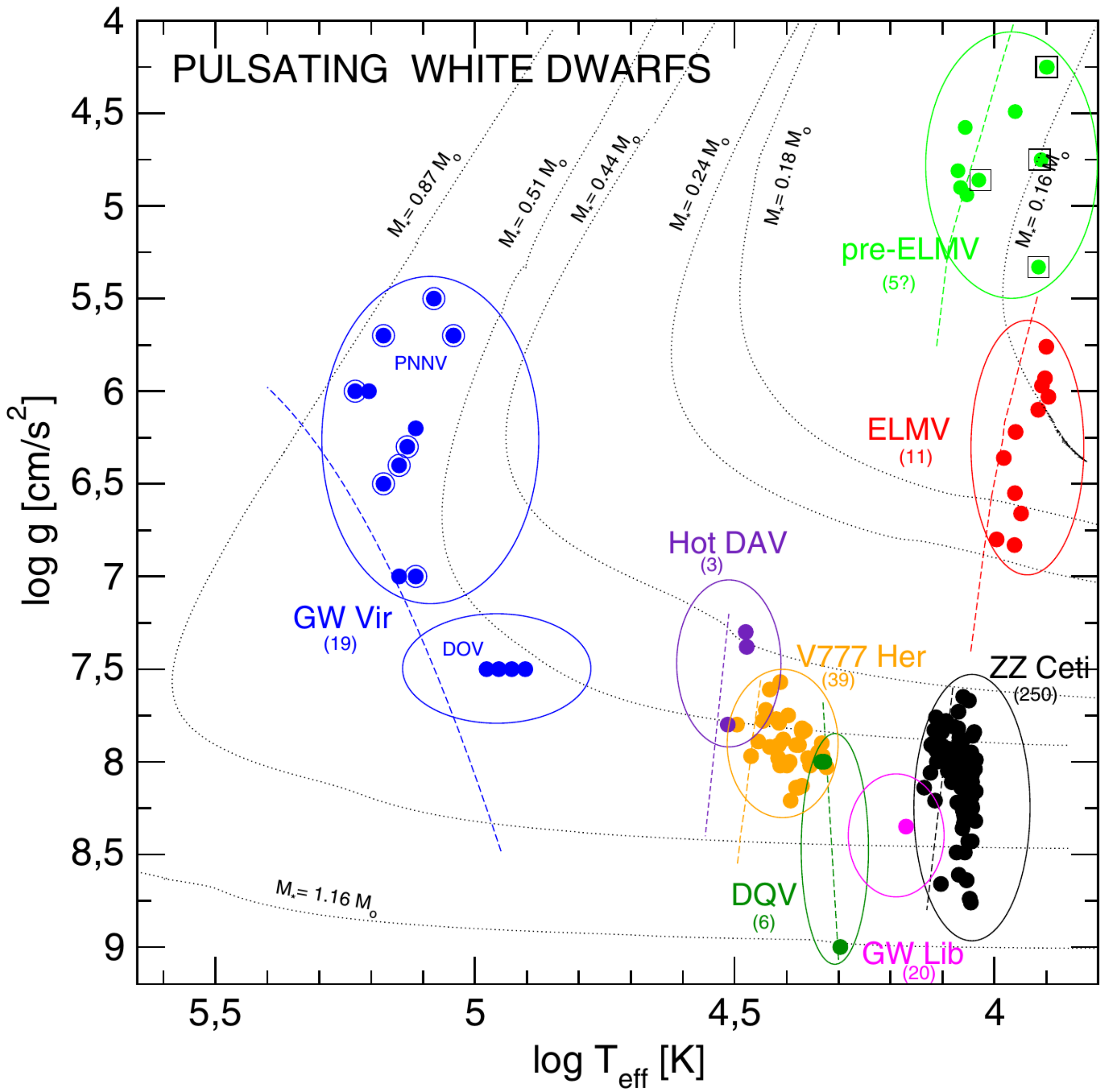

Corsico et al. 2019

Properties of pulsating White Dwarfs

type	P(min)	A_V(mag)	T_{eff}(kK)	Modes	driving zone
GW Vir	5-101	0.01-0.15	80-170	NR(g)	C V-VI, O VII-VIII
Hot DAV	2.7-11.8	0.0010-0.0014	29.9-32.6	NR(g)	μ gradient
DBV	2-18	0.001-0.3	22.4-29.2	NR(g)	He I-II
DQV	2.7-18	0.004-0.016	19.8-21.7	NR(g)	C III-VI, He II
DAV	1.6-23.9	0.01-0.3	10.4-12.9	NR(g)	H I
pre-ELMV	5-83	0.001-0.05	8-13	R+NR(p,mixed)	He I-II
ELM-DAV	19.4-103.9	0.0015-0.041	7.80-9.9	NR(g,p?)	H I
GW Lib	3.5-21.5	0.007-0.07	10.5-16	NR(g)	H I,He I-II

ZZ Ceti (DAV) Stars

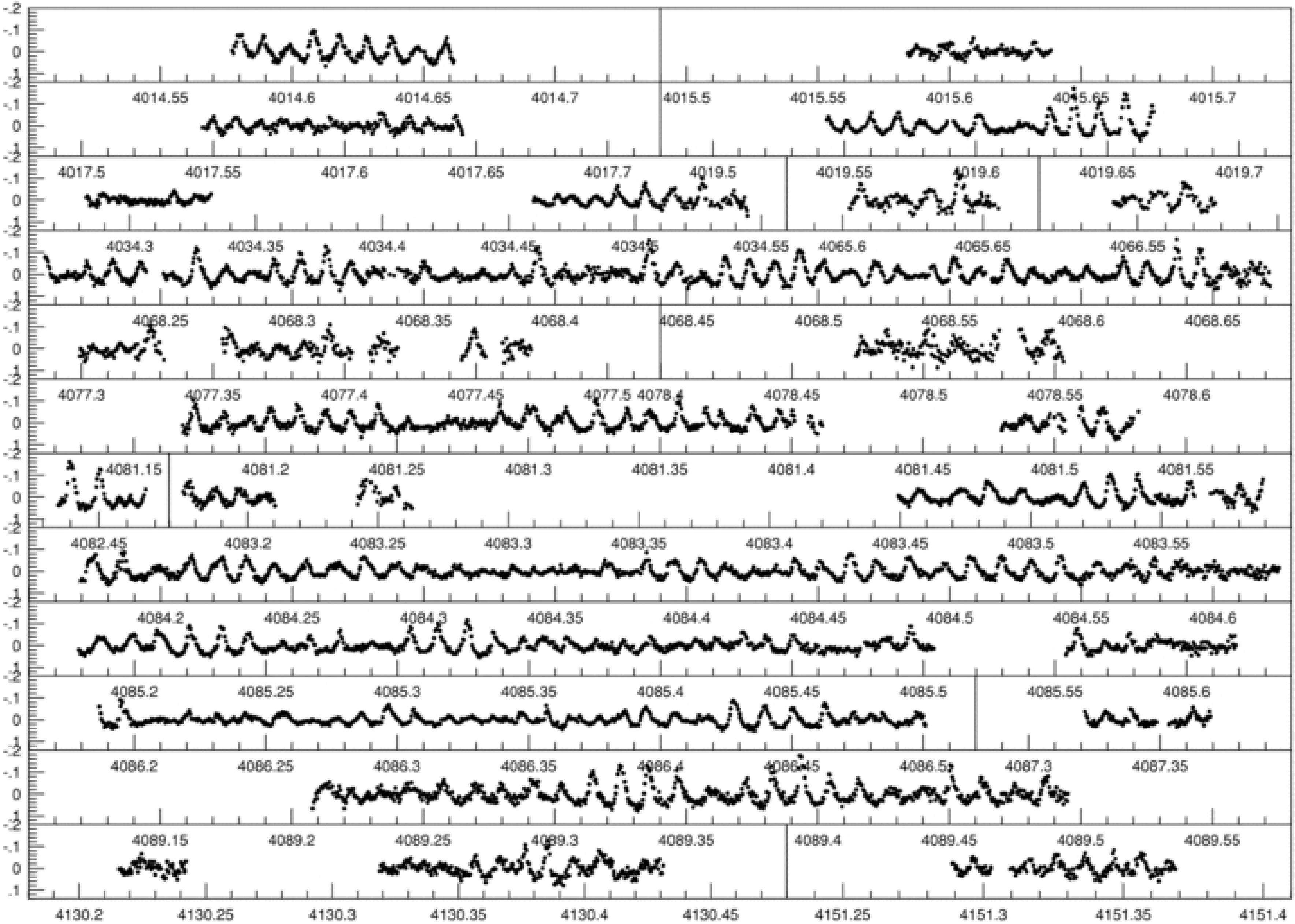

Bognar et al. 2009

Final stages of stellar evolution

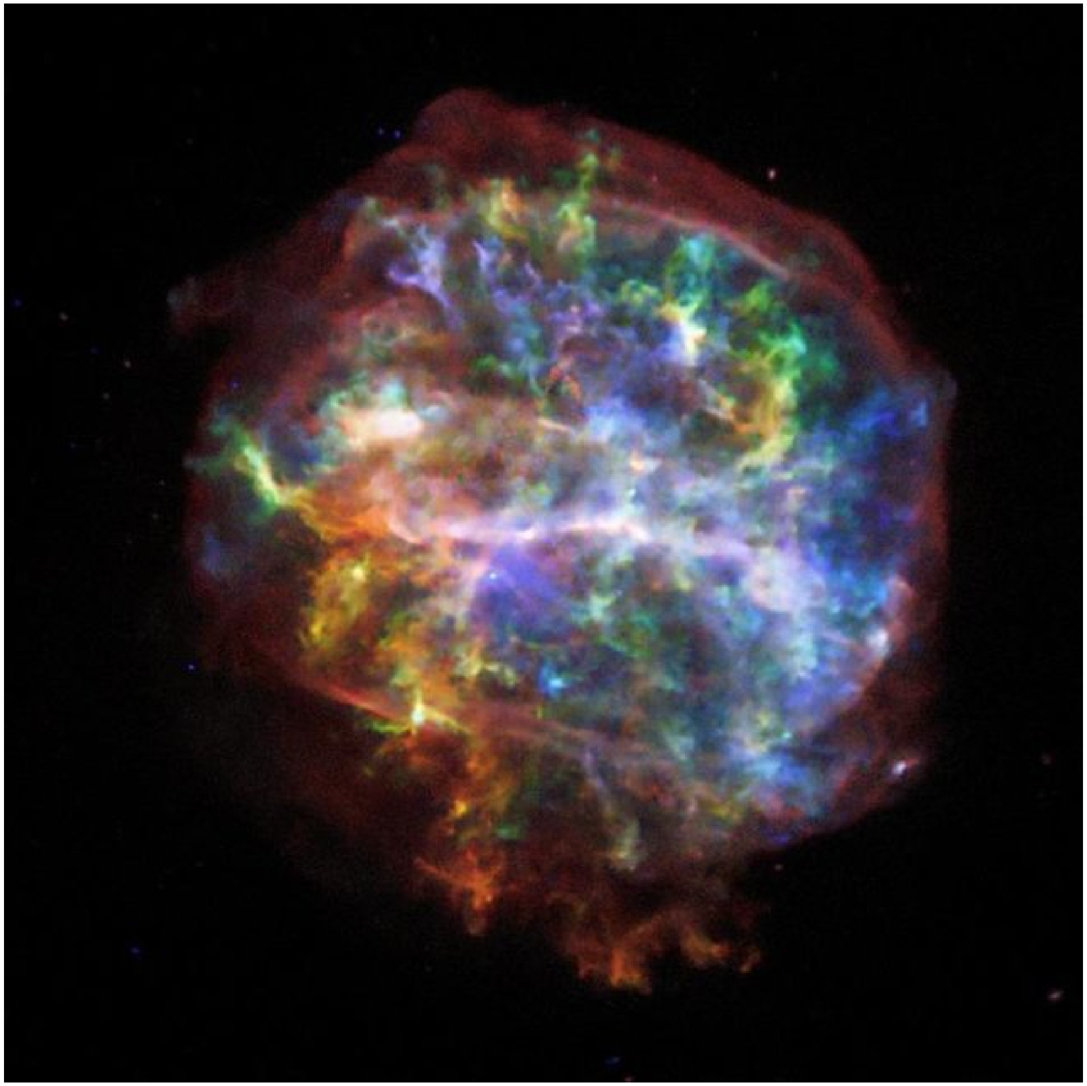

Core-collapse supernova: rapid collapse and violent explosion of a massive star

Final stages of stellar evolution

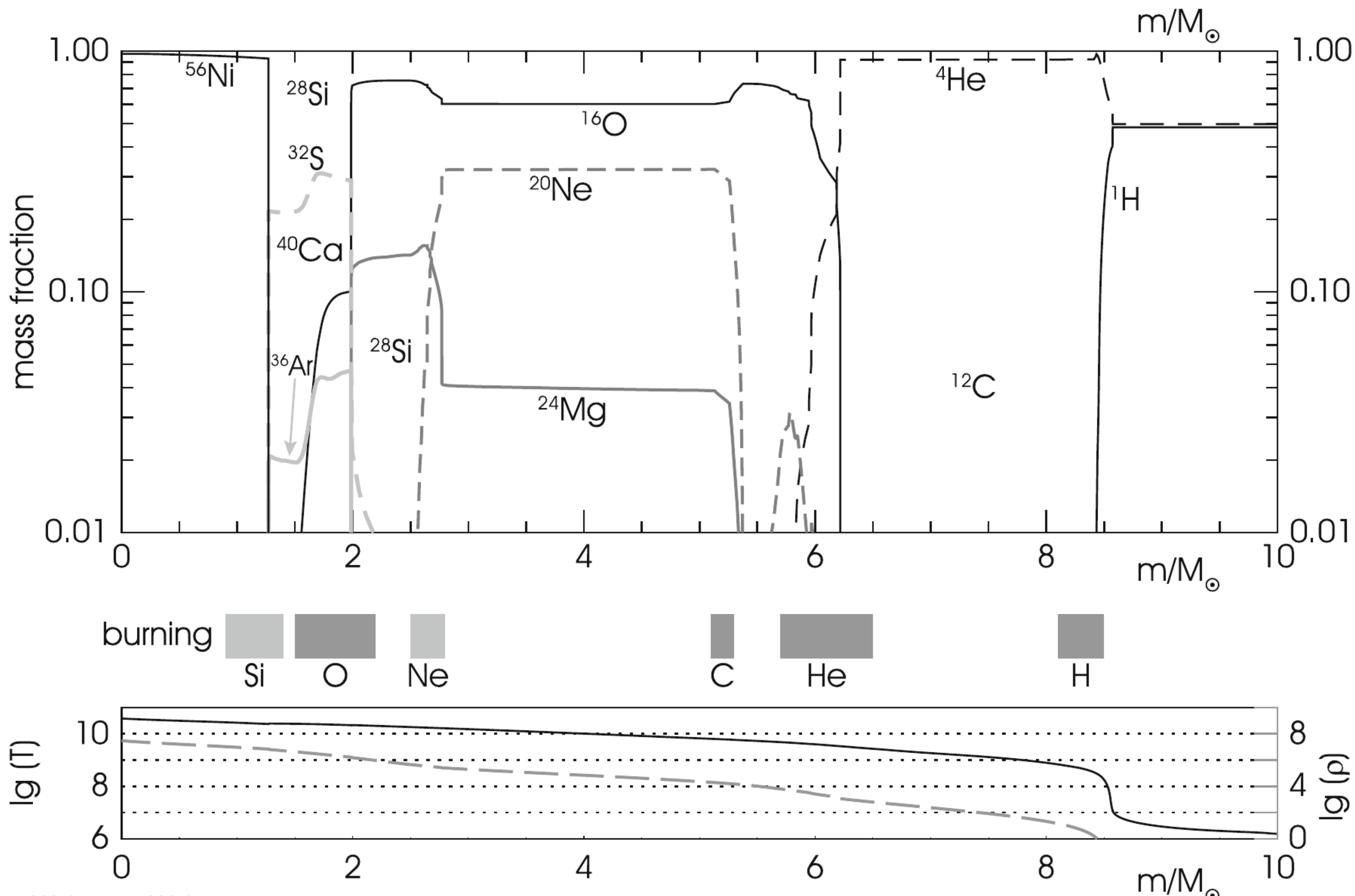

Kippenhahn, Weigert & Weiss 2012

chemical composition of interior of 25 $M_\odot$ star

Final stages of stellar evolution

Onion-shell structure of pre-collapse star

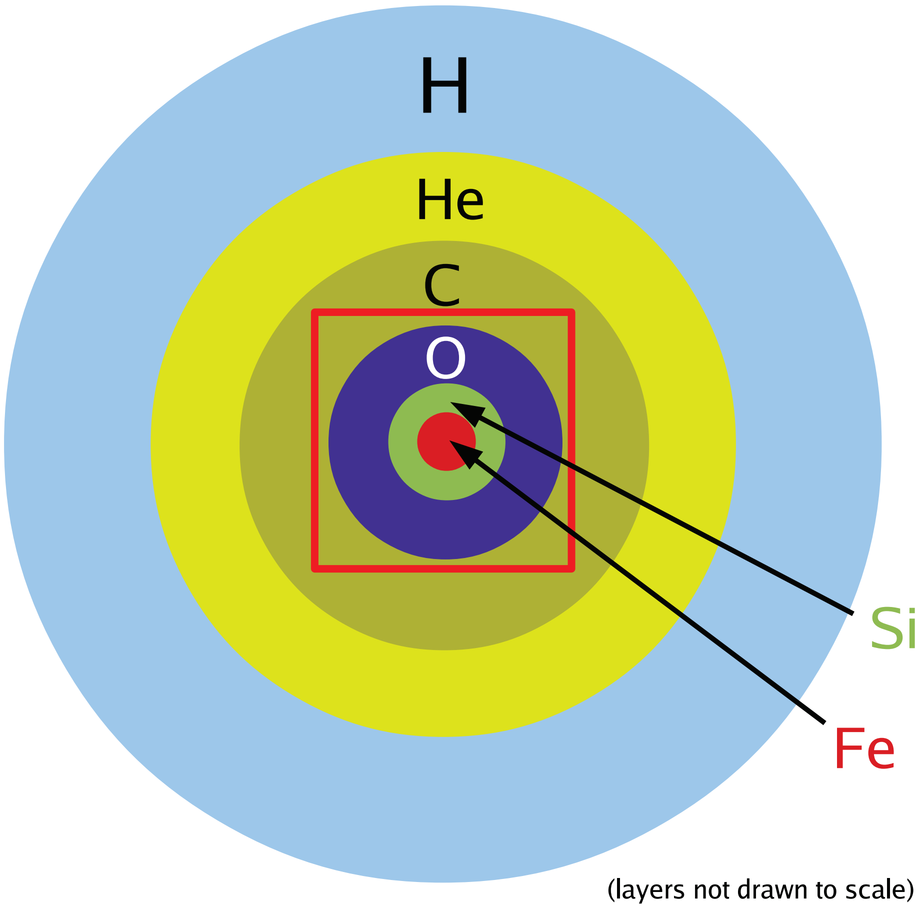

For stars with masses of more than $> 8 - 10\,M_\odot$ (3% of all stars)

Iron core develops, which does not have fusion in the core anymore

Janka et al. 2012

Final stages of stellar evolution

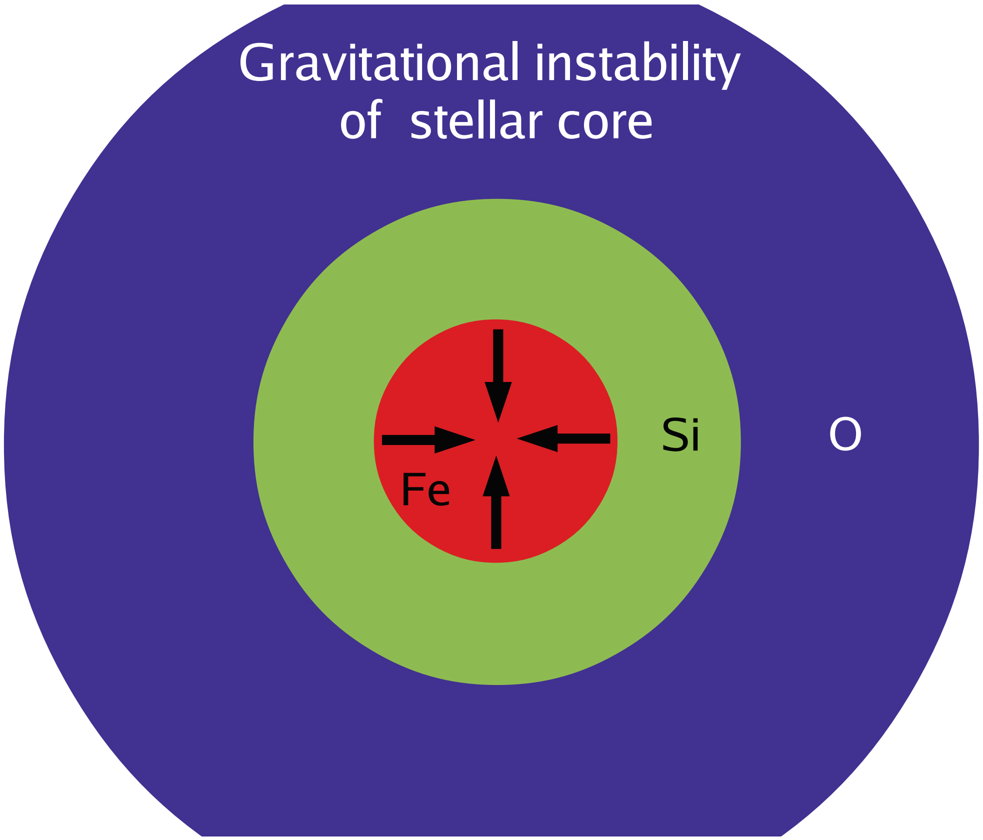

Janka et al. 2012

Core contracts and heats up
$T \simeq 10^{10}$ K
$\rightarrow$ photo-disintegration:

$$^{56}\mathrm{Fe} + \gamma \rightarrow 13\,^{4}\mathrm{He} + 4n$$

$$\gamma + {}^{4}\mathrm{He} \rightarrow 2p + 2n$$

$\rightarrow$ Electron captures by heavy nuclei reduce pressure

$$\mathrm{p} + \mathrm{e}^{-} \longrightarrow \mathrm{n} + \nu_{\mathrm{e}}$$

Neutronisation

$\rightarrow$ **Core collapse** ($\tau_{\mathrm{ff}} \sim$ ms)

$\rightarrow$ inert core exceeds the Chandrasekhar limit of about 1.4 $\mathrm{M}_{\odot}$, electron degeneracy is no longer sufficient to counter the gravitational compression

Final stages of stellar evolution

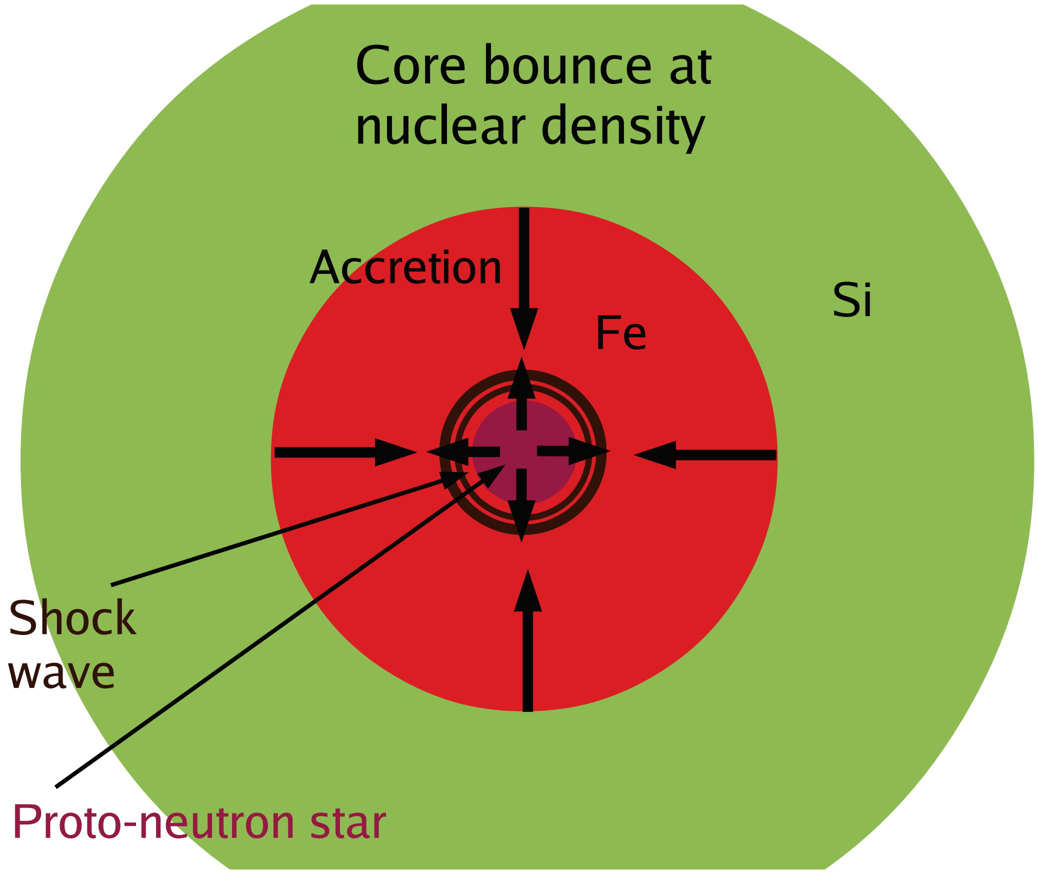

Janka et al. 2012

Collapse stops as soon as the core reaches $\rho \sim 10^{14}\,\mathrm{g\,cm^{-3}}$: density of atomic nuclei

$\rightarrow$ Neutron gas becomes **degenerate**

$\rightarrow$ Degeneracy pressure stabilizes the core

Collapsing material reflected back

$\rightarrow$ Shock wave moves outward

Final stages of stellar evolution

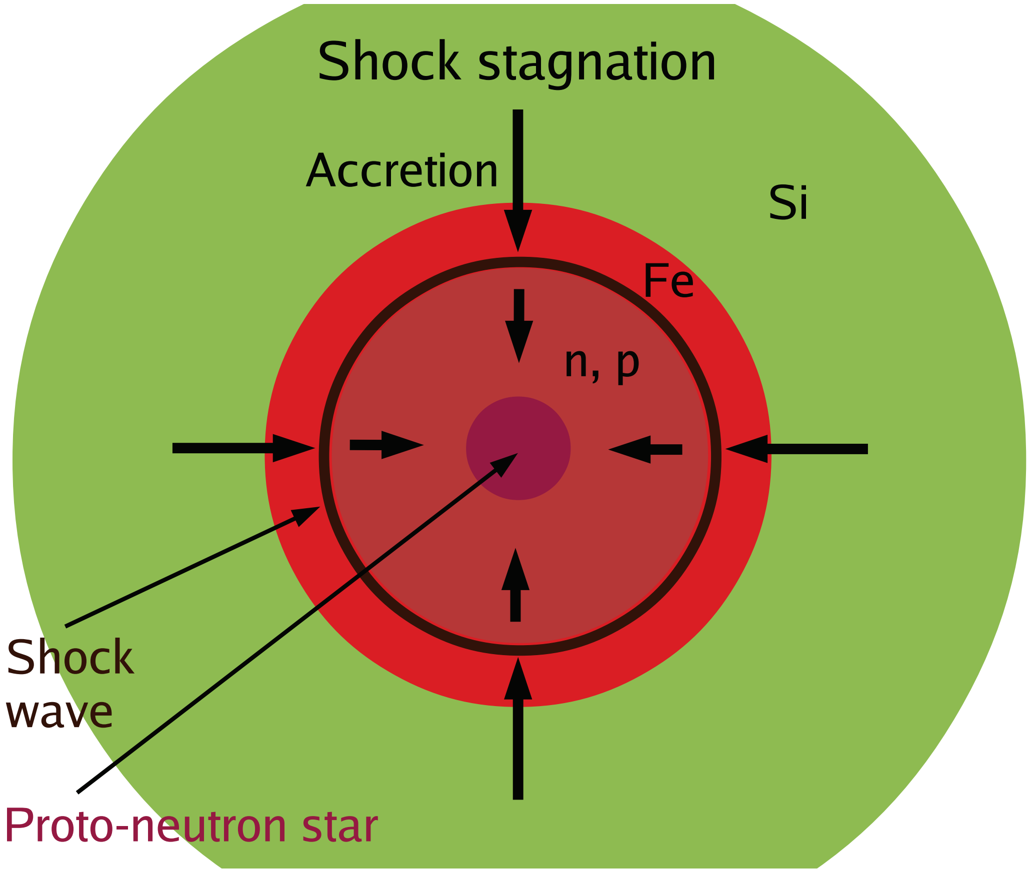

Janka et al. 2012

Energy released during the final collapse

- Core radius before the collapse: $\sim R_{\mathrm{WD}} \sim 10^4\,\mathrm{km}$
- Core radius after the collapse: $R_{\mathrm{n}} \sim 10\,\mathrm{km}$

$$E \approx GM_{\mathrm{c}}^2 \left(\frac{1}{R_{\mathrm{n}}} - \frac{1}{R_{\mathrm{WD}}}\right)$$

$$\approx \frac{GM_{\mathrm{c}}^2}{R_{\mathrm{n}}} \approx 3 \times 10^{53}\,\mathrm{erg}$$

Final stages of stellar evolution

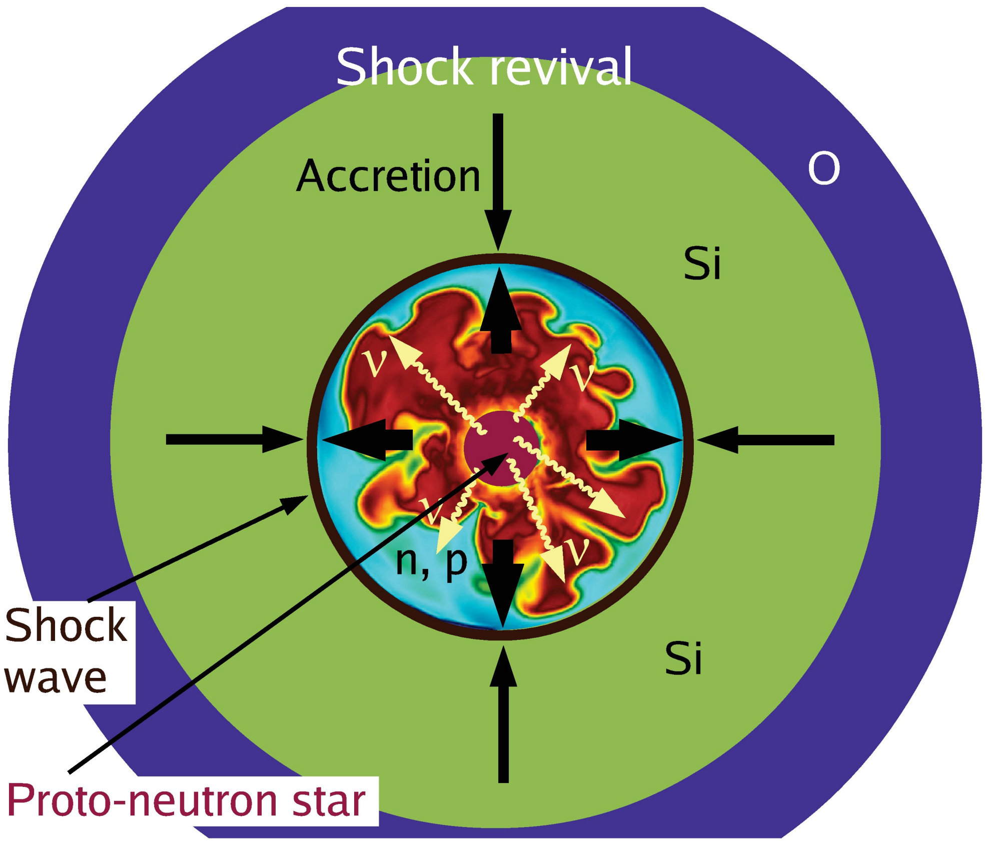

Janka et al. 2012

Energy needed to unbind the envelope

$$E_e = \int_{M_{WD}}^{M} \frac{Gm\mathrm{d}m}{r} \approx 3 \times 10^{52}\,\mathrm{erg}$$

Star explodes, ultracompact remnant remains?

However, most of this energy cannot be transformed to kinetic energy

$\rightarrow$ Photodisintegration of in-falling iron

$\rightarrow$ Neutrino emission $\sim 10^{53}$ erg

No explosion possible?

Final stages of stellar evolution

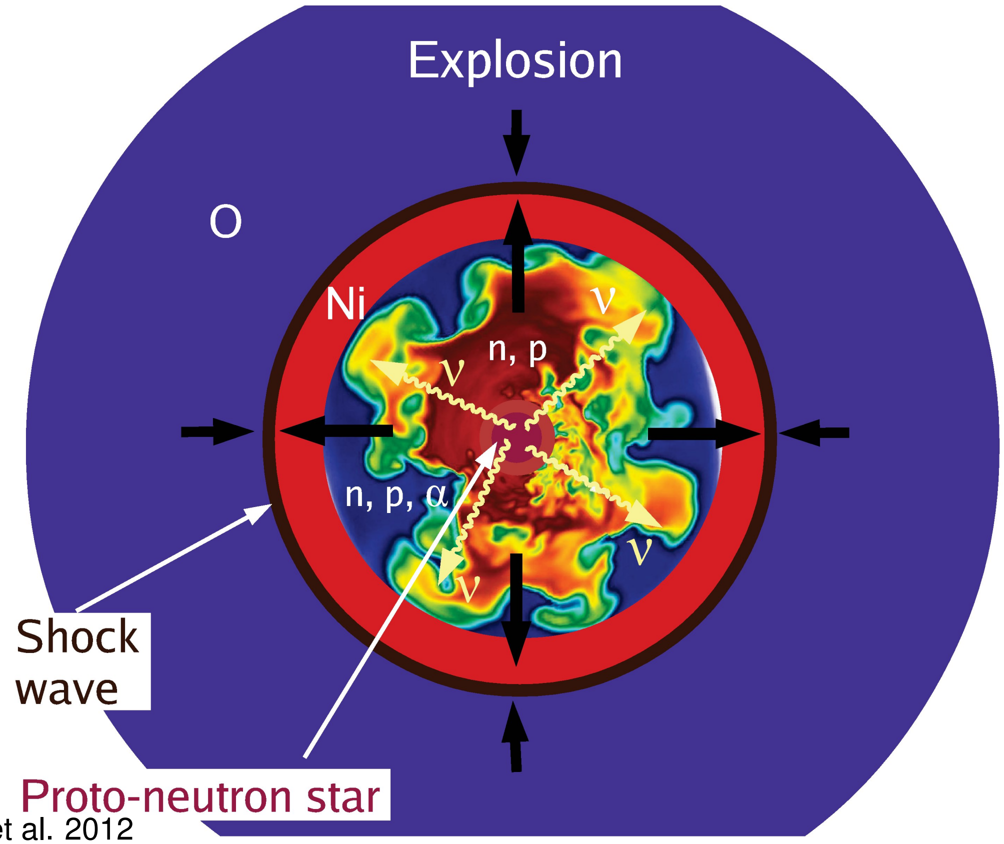

Janka et al. 2012

Neutrinos behave differently under the extreme conditions in the core

Energy of the order of the relativistic Fermi energy of the electrons

$$\frac{E_\nu}{m_e c^2} \approx \frac{E_F}{m_e c^2}$$

$$\frac{E_F}{m_e c^2} = x = \frac{p_F}{m_e c} = \left(\frac{3}{8\pi m_u}\right)^{1/3} \frac{h}{m_e c} \left(\frac{\rho}{\mu_e}\right)^{1/3} \approx 10^{-2} \left(\frac{\rho}{\mu_e}\right)^{1/3}$$

Neutrinos can react with heavy nuclei by scattering and transfer kinetic energy

$$\nu + (Z, A) \longrightarrow (Z, A) + \nu$$

Final stages of stellar evolution

How often does that happen? Is the mean free path l_ν in collapsing core small enough?

$$\sigma_\nu \approx 10^{-45}\left(\frac{E_\nu}{m_e c^2}\right)^2 A^2\,[\mathrm{cm}^2]$$

$$\frac{E_\nu}{m_e c^2} \approx 10^{-2}\left(\frac{\rho}{\mu_e}\right)^{1/3}$$

$$\sigma_\nu \approx 10^{-49} A^2 \left(\frac{\rho}{\mu_e}\right)^{2/3}\,[\mathrm{cm}^2]$$

Number density of nuclei $n = \rho/Am_u$

$$l_\nu \approx \frac{1}{n\sigma_\nu} = 1.7\times 10^{25}\frac{1}{\mu_e A}\left(\frac{\rho}{\mu_e}\right)^{-5/3}\,[\mathrm{cm}]$$

For $A = 100$, $\mu_e = 2$ and $\rho = 10^{10} - 10^{14}\,\mathrm{g\,cm^{-3}}$

$$l_\nu \approx 1 - 10^6\,\mathrm{cm}$$

Mean free path smaller than core size!

Final stages of stellar evolution

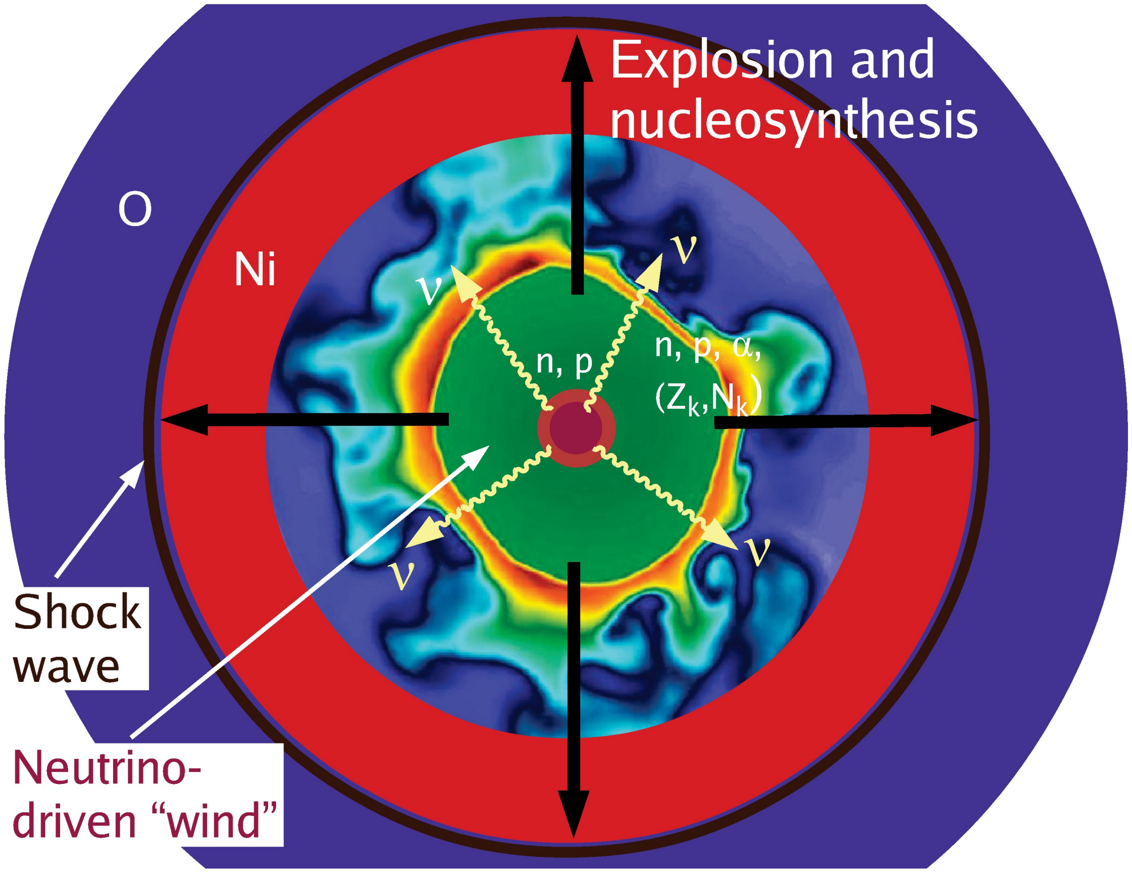

Neutrinos shock front transfers kinetic energy and helps to unbind the envelope

Only 1% of the total energy is kinetic energy $\sim 10^{51}$ erg

Hydrodynamical simulations are needed to study this in detail

Final stages of stellar evolution

SXS collaboration 2012, Youtube

Core-collapse supernova

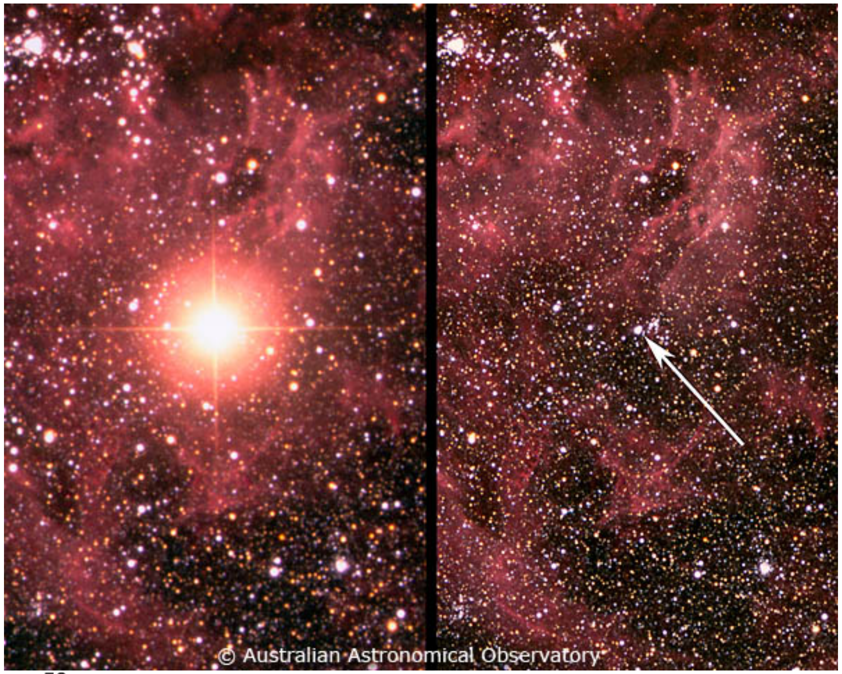

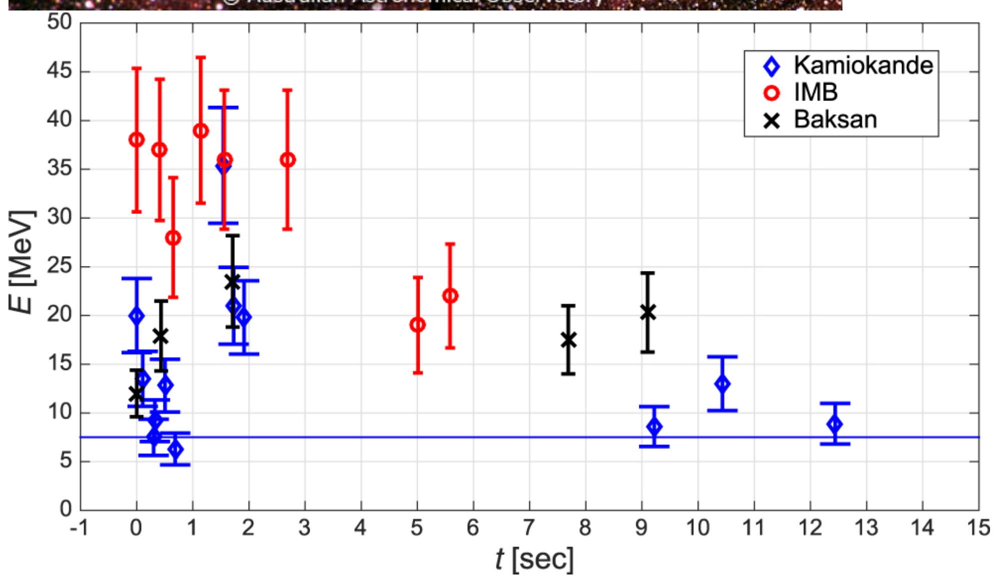

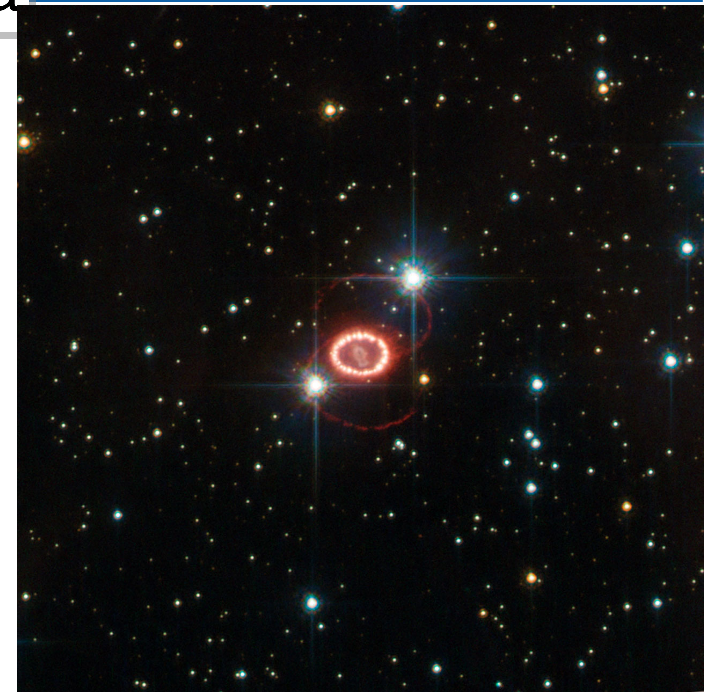

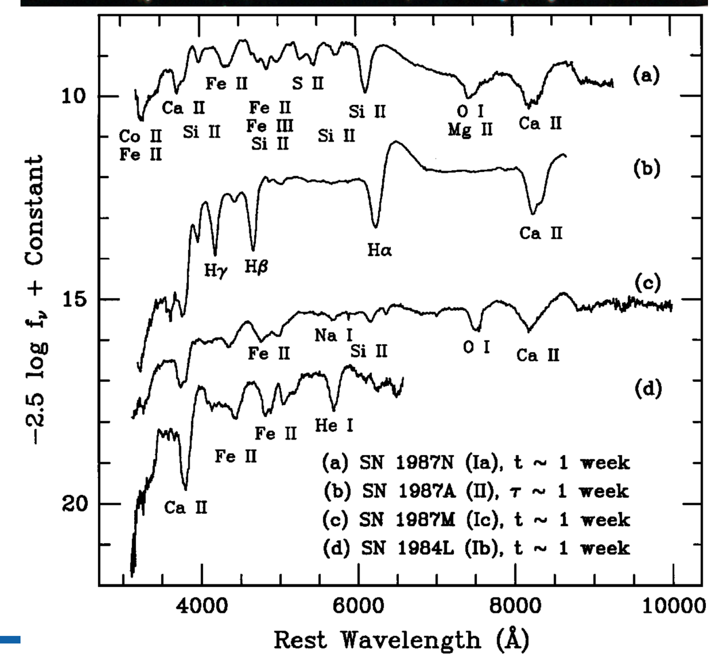

Blum et al. 2016, ApJ, 828, 31

Filippenko 1997, ARA&A, 35, 309

Light curves of core-collapse supernovae

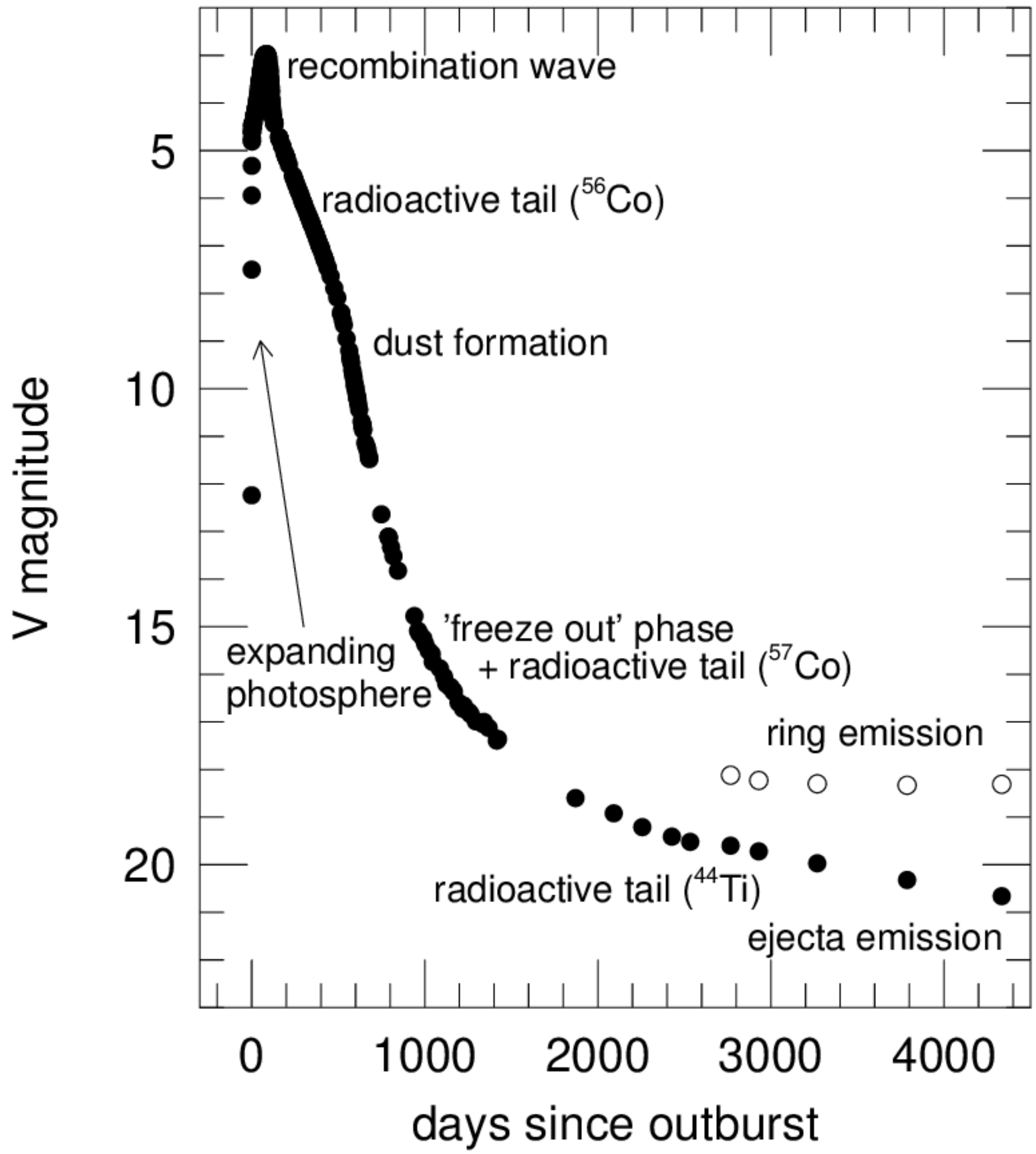

Leibundgut & Suntze

- brightness of the shock break out determined by the temperature in shock and size of the progenitor star (peak few h to couple of d)
- rapid, initial cooling
- large progenitors: plateau
- small stars: decline, before light curve brightens to plateau
- balance between receding photosphere in the expanding ejecta
- heating by radioactive decay
- masses of Ni
- 'freeze-out' from material which was ionized and recombines

Classification of supernovae

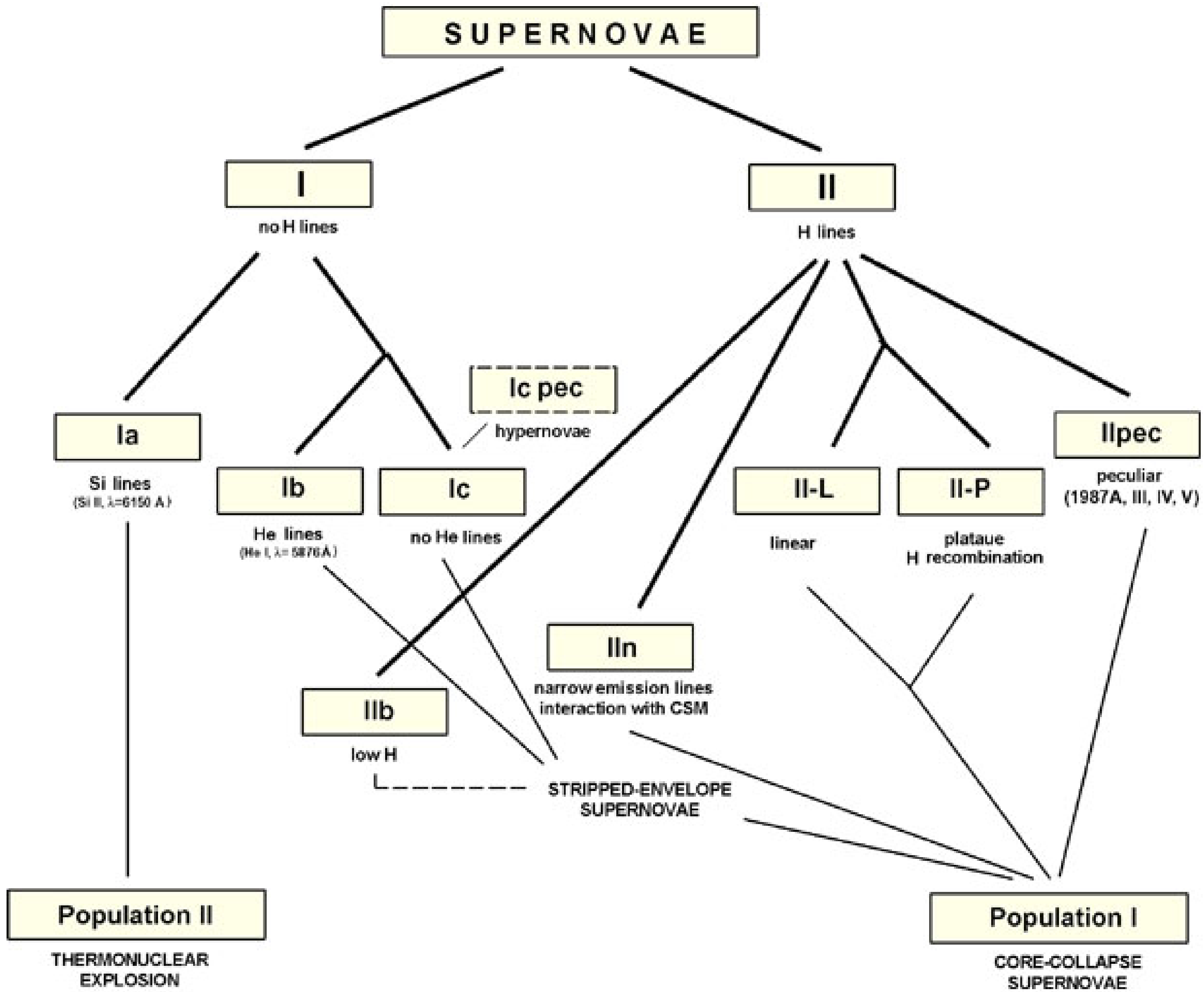

Types of light curves of supernovae

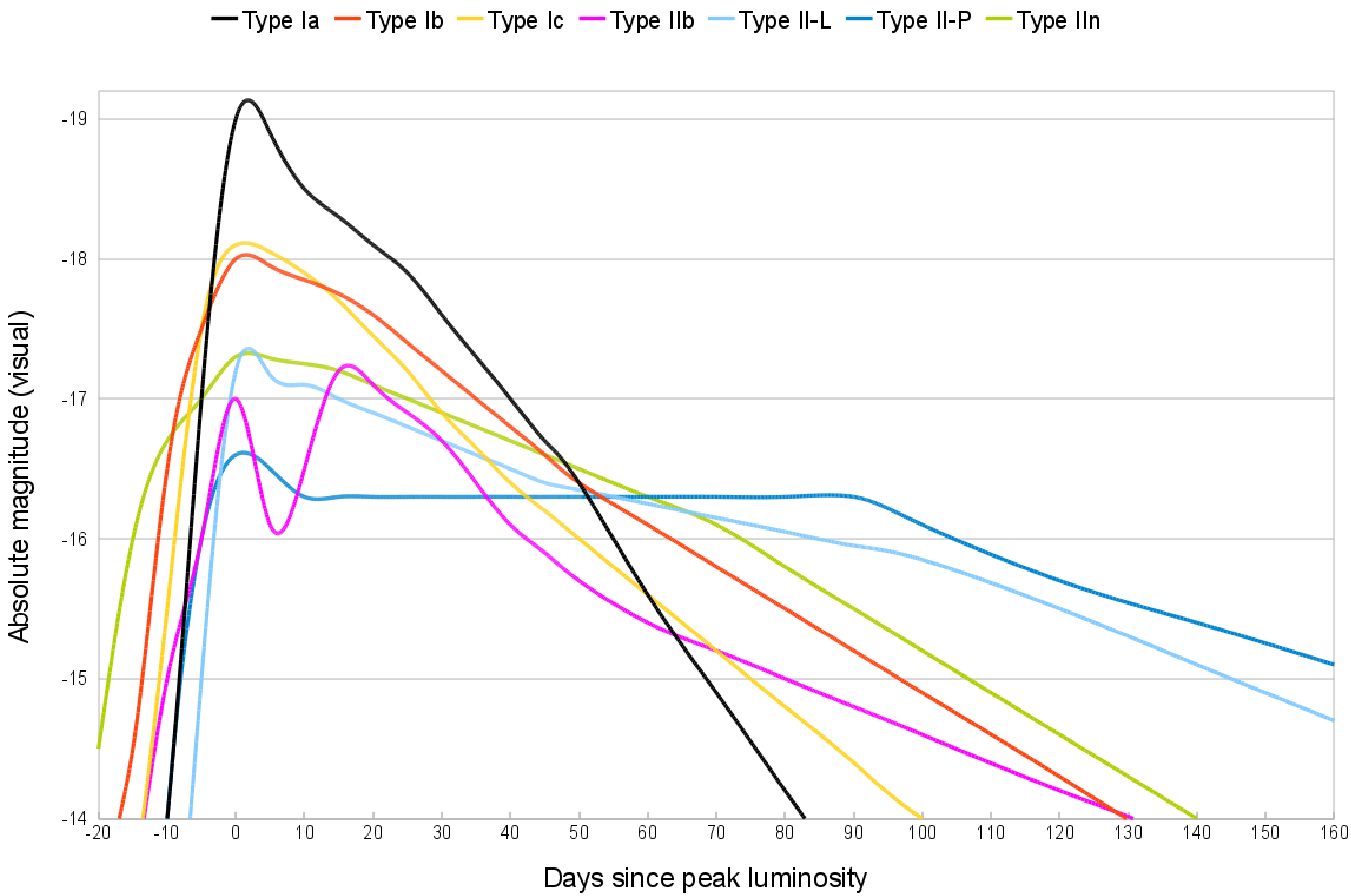

Final stages of stellar evolution

For very massive stars ($> 30\,M_\odot$) core collapses into a fast-rotating black hole and infalling matter assembles in an accretion disk around it.

Part of the binding or rotation energy might be ejected in collimated outflows (jets = beams of ionised matter accelerated close to the speed of light).

NASA **Collapsar model**

Final stages of stellar evolution

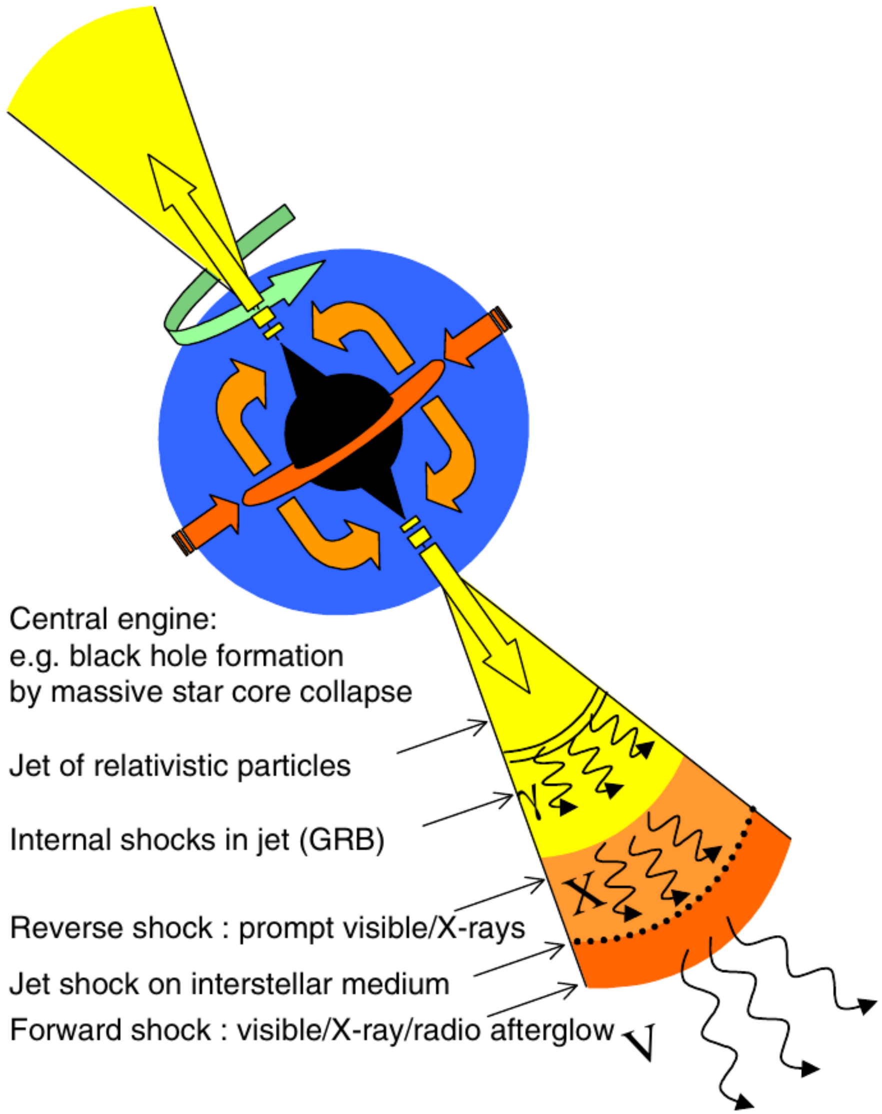

Schanne et al. 2005

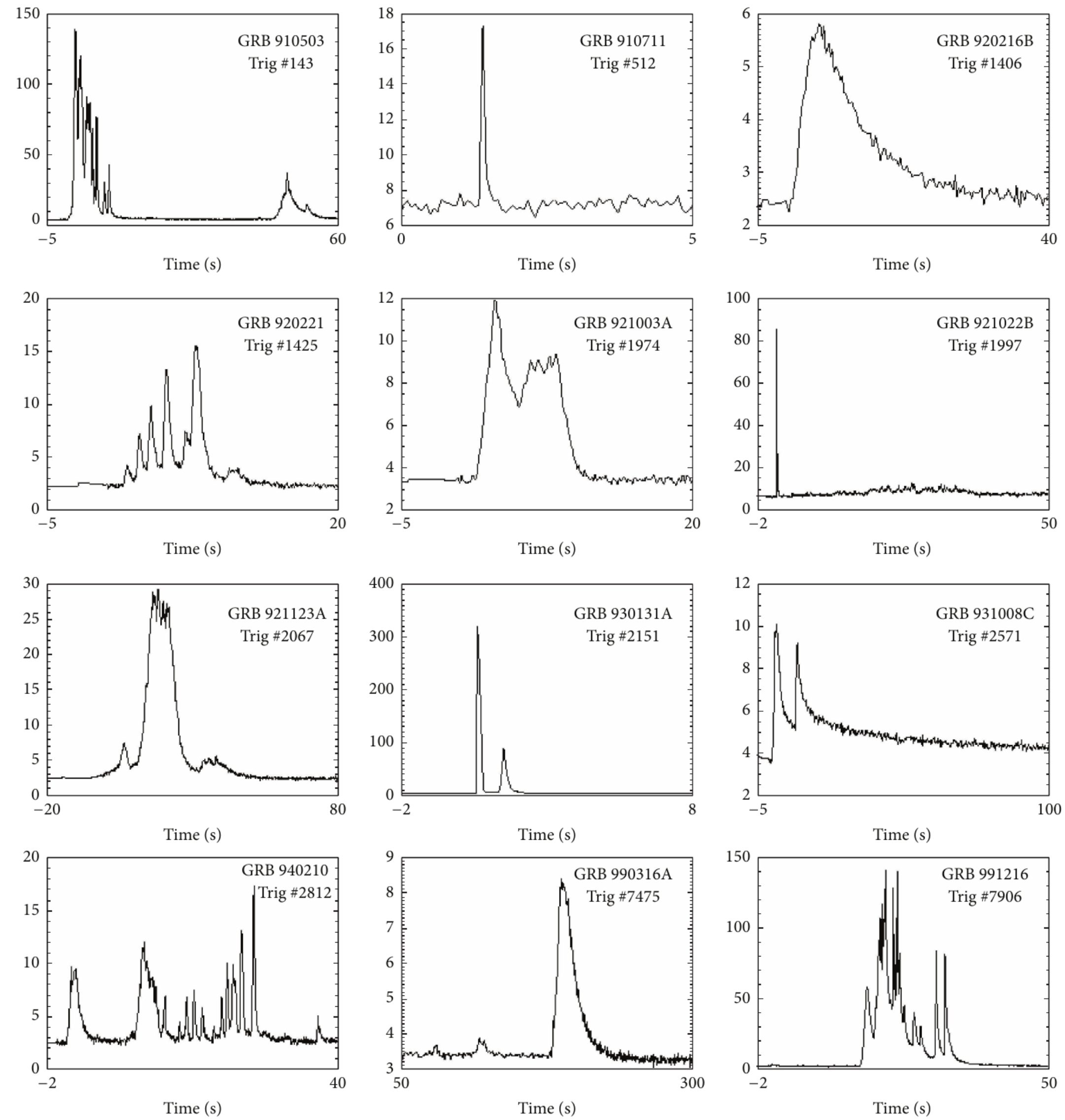

Pe'er 2014

Final stages of stellar evolution

M87

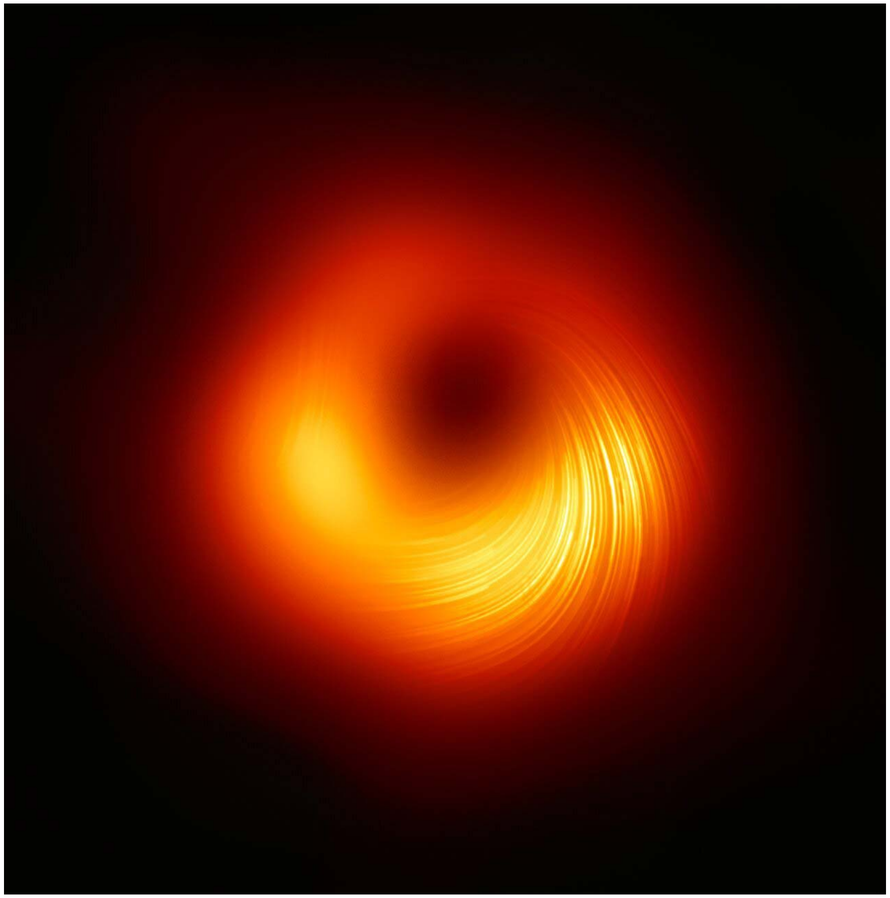

Andrew A. Chael, Youtube

EHT

As a spinning BH pulls in matter, it creates a rotating "accretion disc" of charged particles. The motion generates twisted magnetic fields that accelerate particles into two thin jets.

Final stages of stellar evolution

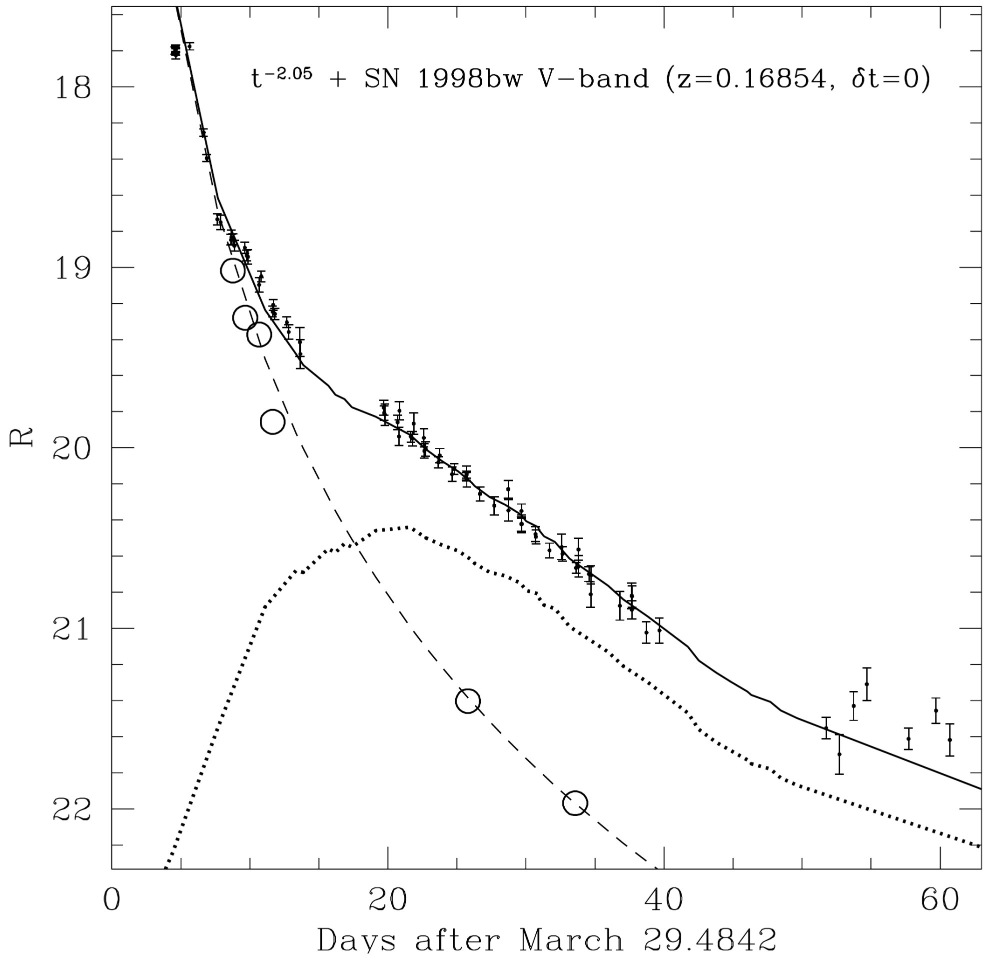

Matheson et al. 2003, ApJ, 599, 394

Long-duration **Gamma Ray Bursts** (GRB) connected to **SN Ib/c (Hypernovae)**

$\rightarrow$ power-law continuum of GRB + later SN light curve

Final stages of stellar evolution

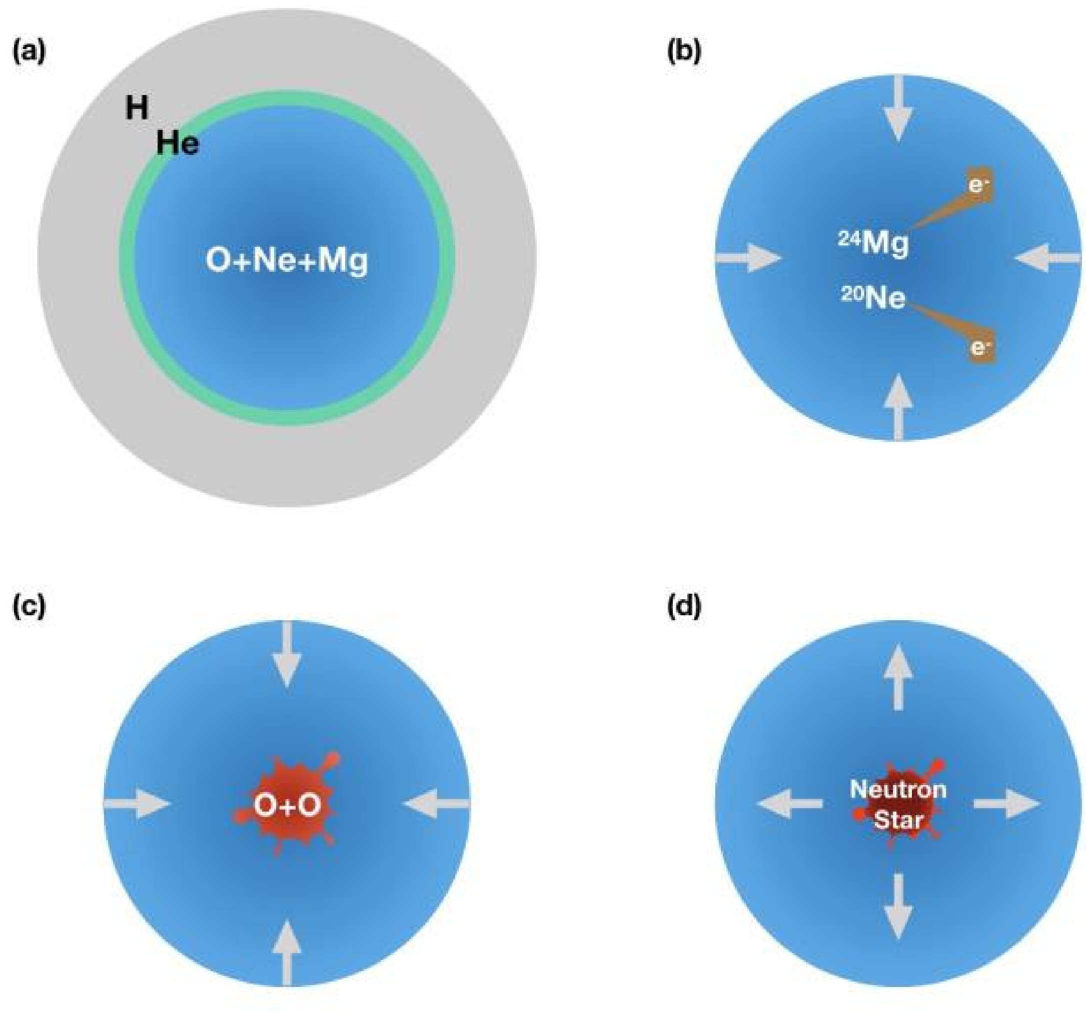

Zha et al. **Electron-capture supernova**

Collapse can start earlier, if a degenerate NeOMg core $\sim$ $1.37\,\mathrm{M}_\odot$ reaches a critical density (initial mass $\sim 9\,M_\odot$)

$\rightarrow$ **Electron-capture** on ^{24}Mg and ^{20}Ne leads to decrease in pressure and collapse

Lower energy SN expected $\sim 10^{50}\,$erg

Candidates are under debate

Final stages of stellar evolution

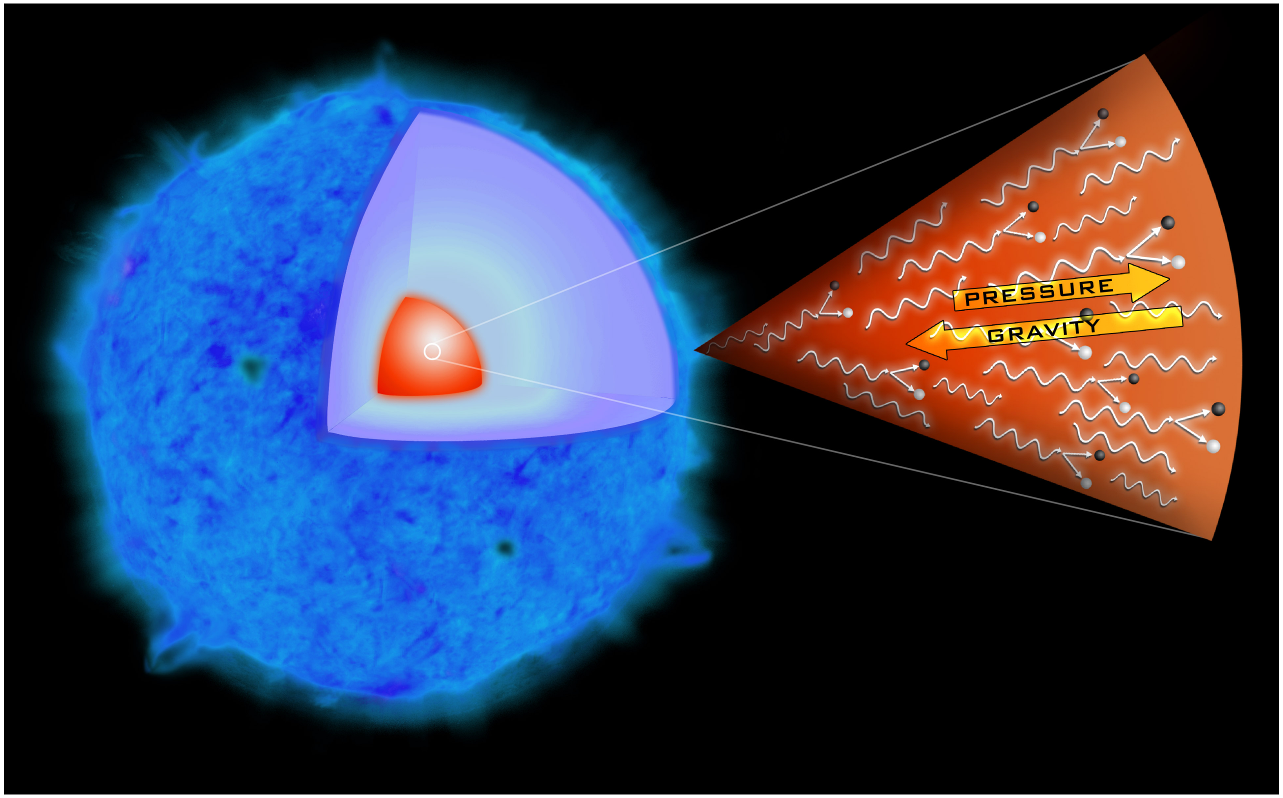

Wikipedia **Pair instability supernova**

For the most massive stars ($\sim 80 - 100\,\mathrm{M}_\odot$) energies in the cores can be high enough to create electron-positron pairs

$$\gamma + \gamma \longrightarrow e^- + e^+$$

$\rightarrow$ **Pair production** reduces the pressure and may lead to collapse

Candidates are under debate

Final stages of stellar evolution

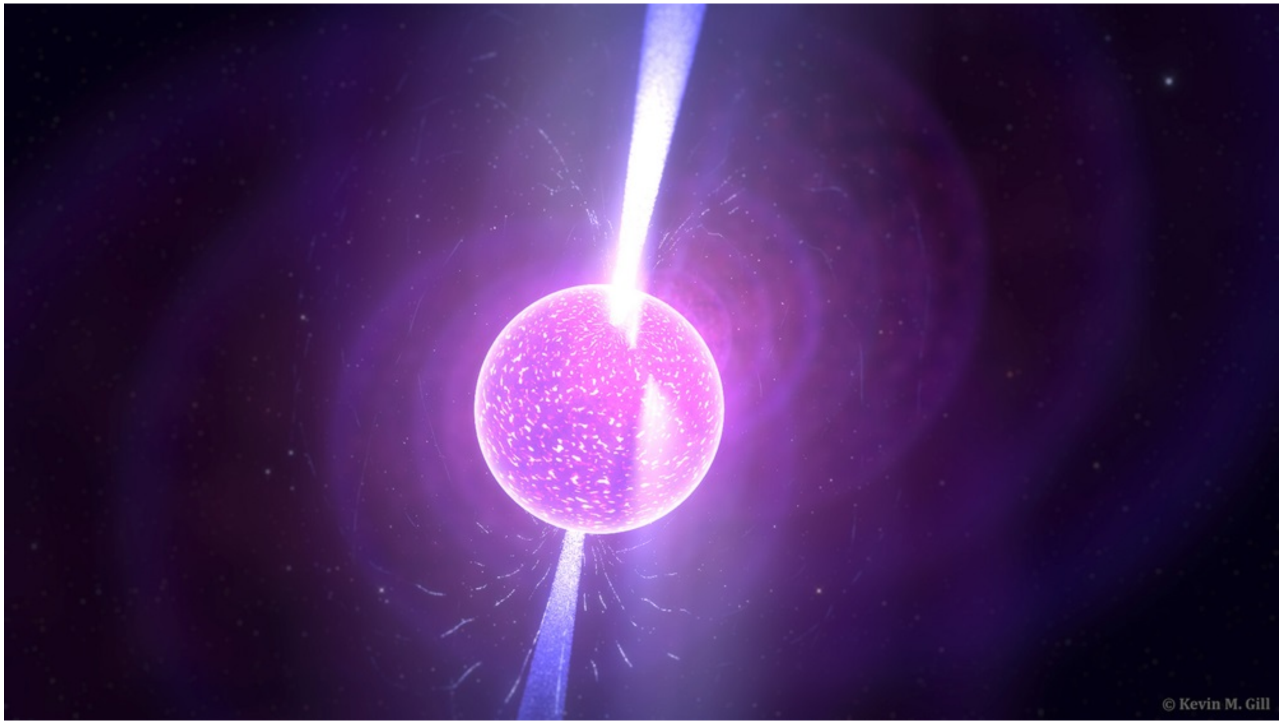

Astronomy.com/Kevin Gill

Remnant of core collapse is extremely dense $\bar{\rho} \simeq 10^{14}\,\mathrm{g\,cm^{-3}}$

Neutron star

$\rightarrow$ Radius $\sim$ 10 km

$\rightarrow$ Mass $\sim 1.4 - 3\,\mathrm{M}_\odot$

- Magnetic field $\sim 10^9 - 10^{15}$ gauss

Evolution

Temperature drops quickly from 10^{10} K to 10^8 K in $\sim$ 100 yr due to **neutrino emisision**

Contraction leads to increasing density

Final stages of stellar evolution

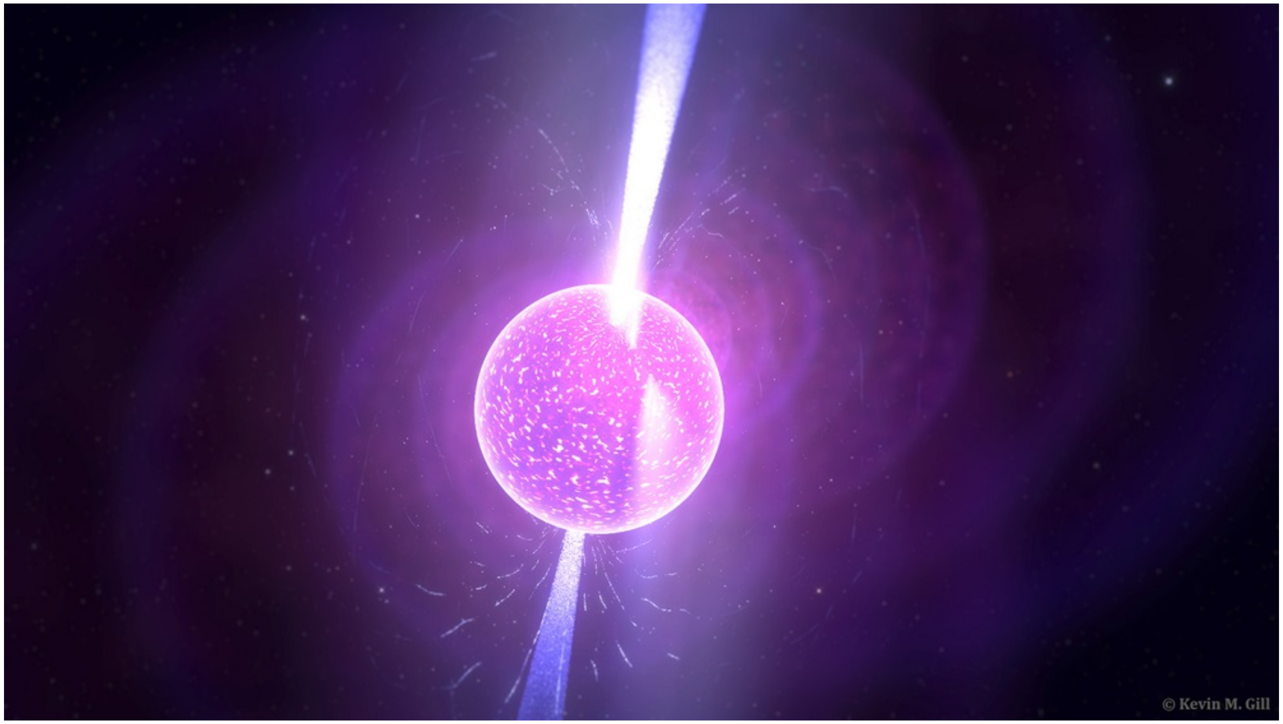

Astronomy.com/Kevin Gill

Matter consists initially of crystallized heavy nuclei, electrons and neutrons

$\rightarrow$ Neutron-rich nuclei release neutrons

$\rightarrow$ electron-capture of protons

$\rightarrow$ destroys nuclei

$\rightarrow$ Neutronisation

Pressure of the **non-relativistic degenerate neutrons** becomes dominant

$$P_\mathrm{n} = \frac{1}{20}\left(\frac{3}{\pi}\right)^{2/3}\frac{h^2}{m_\mathrm{n}^{8/3}}\rho_0^{5/3}$$

Neutron gas (or liquid) with some protons and electrons develops

Final stages of stellar evolution

For higher densities in the core ($\gg 6 \times 10^{15}\,\mathrm{g\,cm^{-3}}$), the situation becomes much more complicated

Energy density needs to be taken into account additional to rest-mass density ρ_0 (not necessary for electrons, because density determined by ions)

$$\rho = \rho_0 + u/c^2$$

Equation of state becomes **relativistic** $\rho_0 \ll u/c^2$

$$\rho \approx u/c^2 \Rightarrow u \approx \rho c^2$$

For relativistic particles

$$P = u/3 = \rho c^2/3$$

Interactions between nucleons become important

$\rightarrow$ Equation of state not "ideal" any more

Final stages of stellar evolution

For a given equation of state, the **equation for hydrostatic equilibrium in general relativity** (Tolman-Oppenheimer-Volkoff equation)

$$\frac{\mathrm{d}P}{\mathrm{d}r} = -\frac{Gm}{r^2}\rho\left(1+\frac{P}{\rho c^2}\right)\left(1+\frac{4\pi r^3 P}{mc^2}\right)\left(1-\frac{2Gm}{rc^2}\right)^{-1}$$

can be used to obtain **neutron star models**

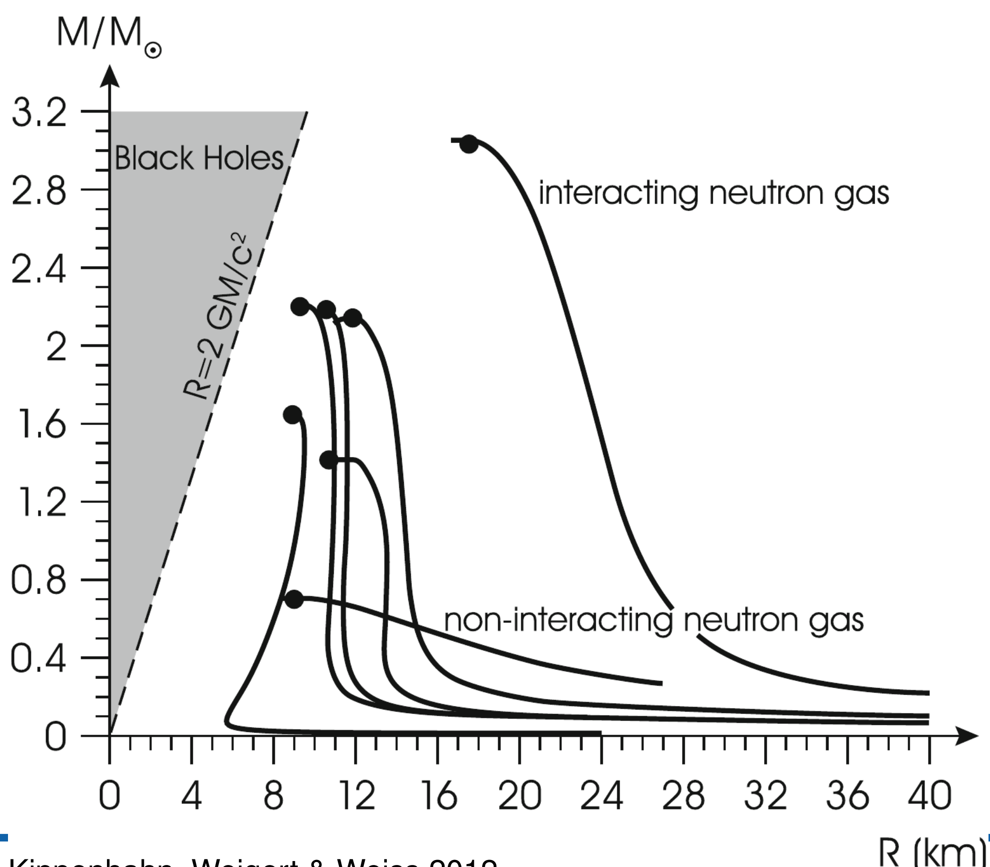

Kippenhahn, Weigert & Weiss 2012

Equation of state of neutron stars is not known. Different models have been proposed and are under debate

Models predict a **limiting mass** for neutron stars

$\rightarrow$ **Oppenheimer-Volkoff mass** $\sim 1.4 - 3.0\,M_\odot$

$\rightarrow$ For higher masses, the pressure of the degenerate neutron gas cannot compensate gravity any more

Neutron star becomes unstable and collapses

Final stages of stellar evolution

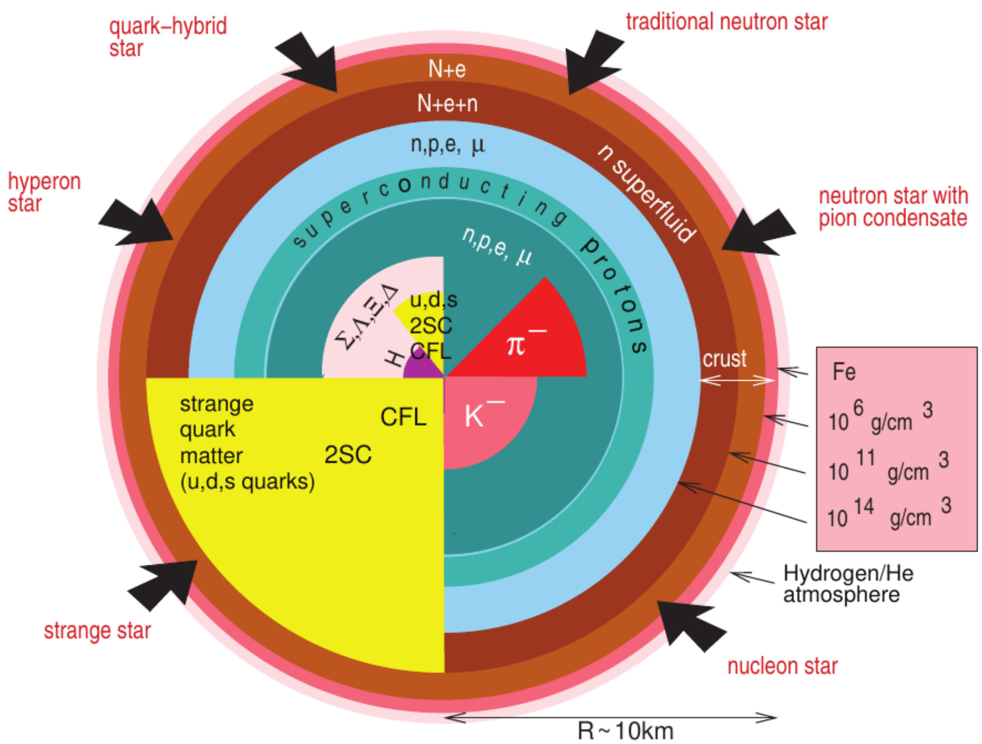

Weber et al. 2009

Fermi energies of nucleons reach rest masses of **hyperons** (baryon with strange quark) and potentially also **free quarks**

$\rightarrow$ Lowest mass hyperons (Λ, Σ, Δ, ...) contain one strange quark

$\rightarrow$ **Strange stars** and **quark stars** postulated

- Atmosphere very hot $\sim 10^6$ K and extremely compressed $\log g \sim 14$ (thickness: cm) $\rightarrow$ Spectral lines of heavy nuclei observed in X-rays
- Surface of WD like material $\rho \sim 10^6\,\mathrm{g\,cm^{-3}}$
- Solid crust of crystallized Fe nuclei and degenerate electrons
- Interior superfluid neutron liquid + solid core?

Final stages of stellar evolution

Light house model

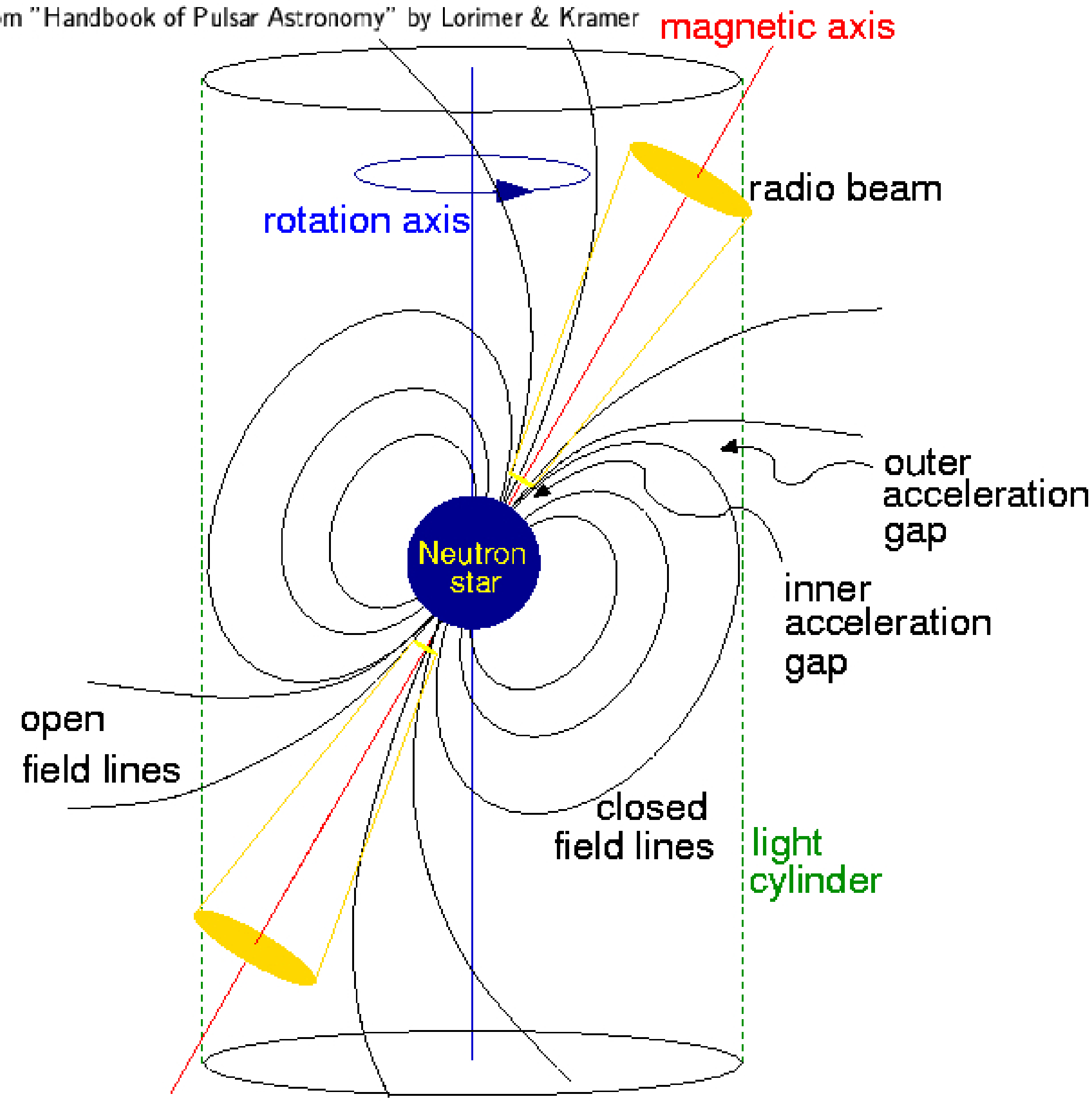

Neutron stars are observed as **pulsars**

$\rightarrow$ Radio observations allow to measure the pulses with extreme accuracy

- Accurate dynamical **masses** can be derived in **binary pulsars**

Final stages of stellar evolution

http://www.astron.nl/pulsars/animations/

Slowing down due to **magnetic dipole radiation**

magnet dipole radiation

$$\boxed{P_{\rm rad} \sim \frac{(BR^3 \sin\alpha)^2}{P^4}} = -\dot{E}_{\rm rot} \quad (9.26)$$

Energy loss

$$\boxed{\dot{E} = \frac{d}{dt}\left(\frac{2\pi^2 I}{P^2}\right) = -\frac{4\pi^2 I \dot{P}}{P^3}} \quad (9.27)$$

characteristic age

$$\boxed{\tau = \frac{P}{2\dot{P}}} \quad (9.28)$$

Final stages of stellar evolution

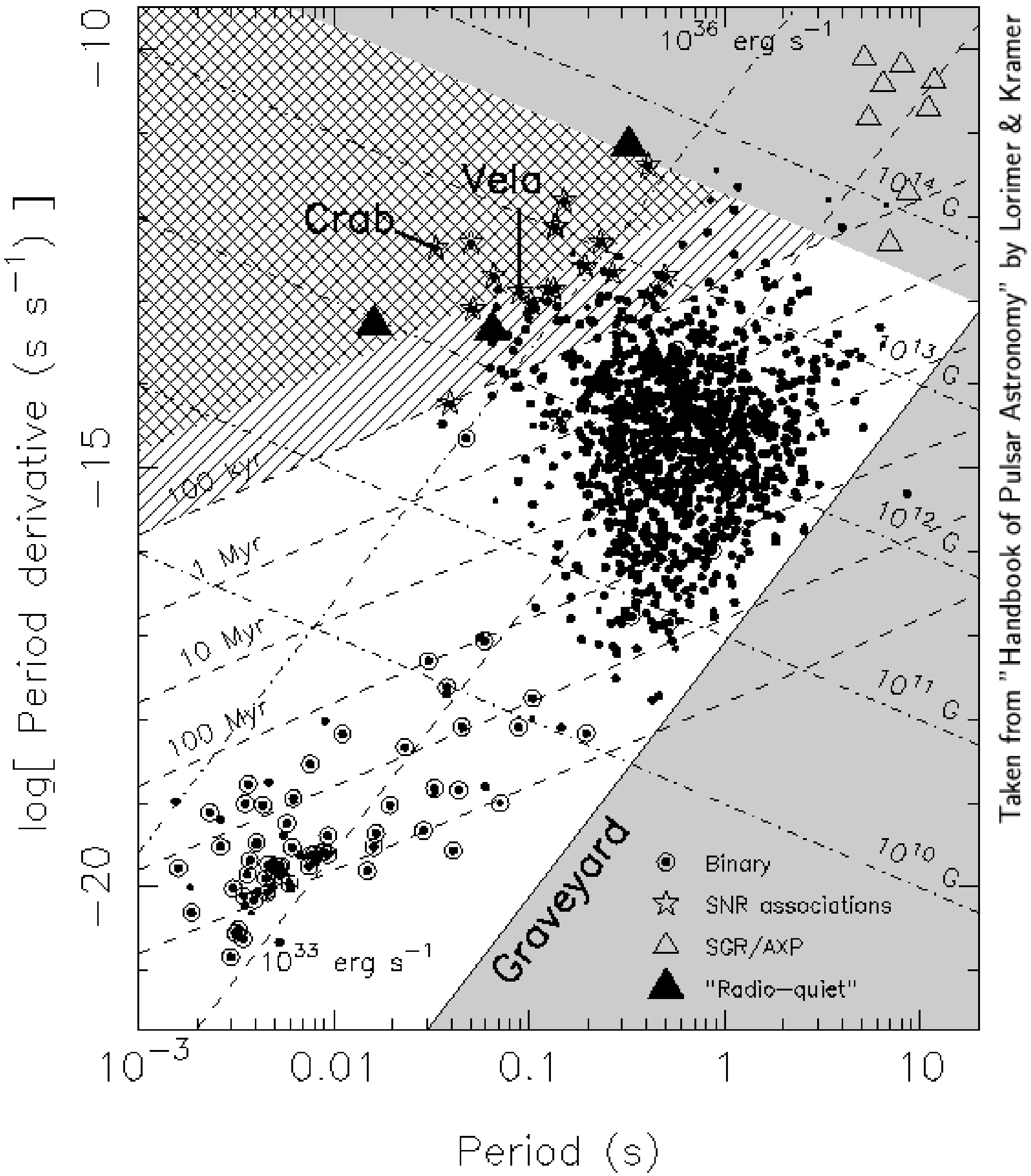

$$\tau = \frac{P}{2\dot{P}}$$

$$B \sim \sqrt{P\dot{P}}$$

Binary Pulsars

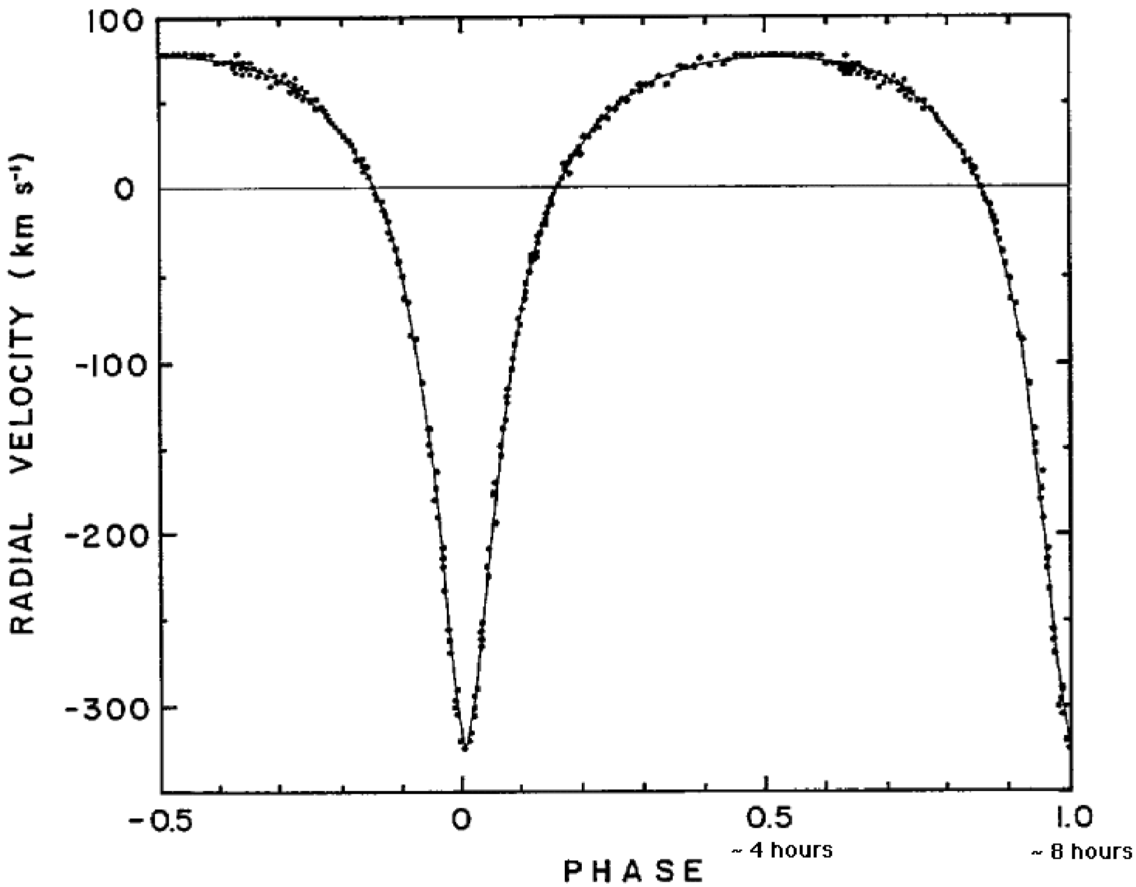

Hulse & Taylor 1975, ApJ 195, L51

PSRB1913+16:

- discovered by Hulse & Taylor (1975):
  ”attempts to measure its period to an accuracy of $\pm 1\mu$s were frustrated by changes in period of up to 80 μs from day to day”
- $\Rightarrow$ Binary Pulsar
- Orbital period:
  P = 7.751938773864 hr
- Eccentricity: 0.6171334
- Rotation period:
  59.02999792988 ms
- Note the number of significant digits!

Binary Pulsars

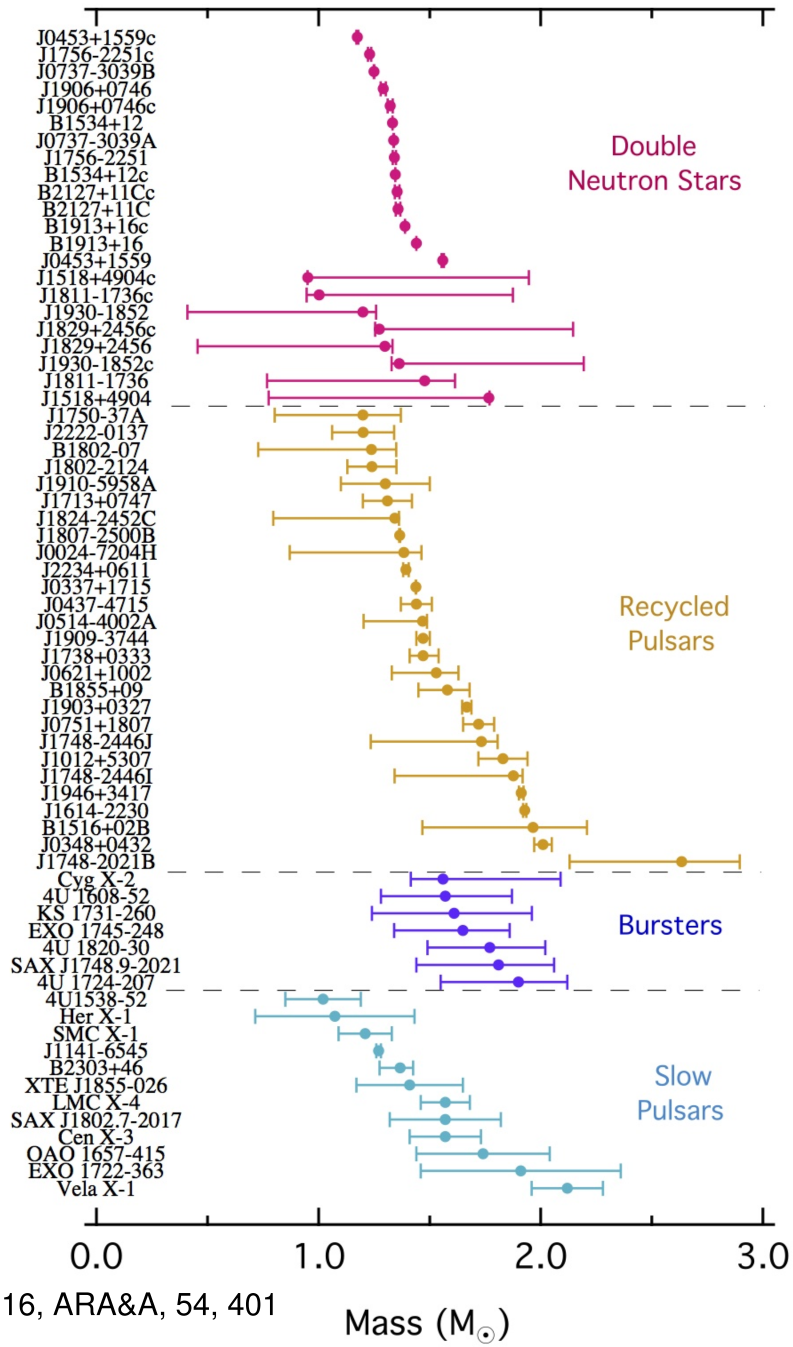

Neutron stars are observed as accreting objects in X-ray binaries

$\rightarrow$ Dynamical masses can be measured

$\rightarrow$ Masses and radii can be derived from the X-ray spectra:

$$L_X \sim R_{NS}^2 T_{\mathrm{eff,NS}}^4$$

Özel & Freire 2016, ARA&A, 54, 401

Final stages of stellar evolution

NASA

Merging neutron stars are observed with gravitational wave detectors (two so far)

$\rightarrow$ Masses and radii can be derived from the GW signal

$\rightarrow$ Short-duration gamma ray burst

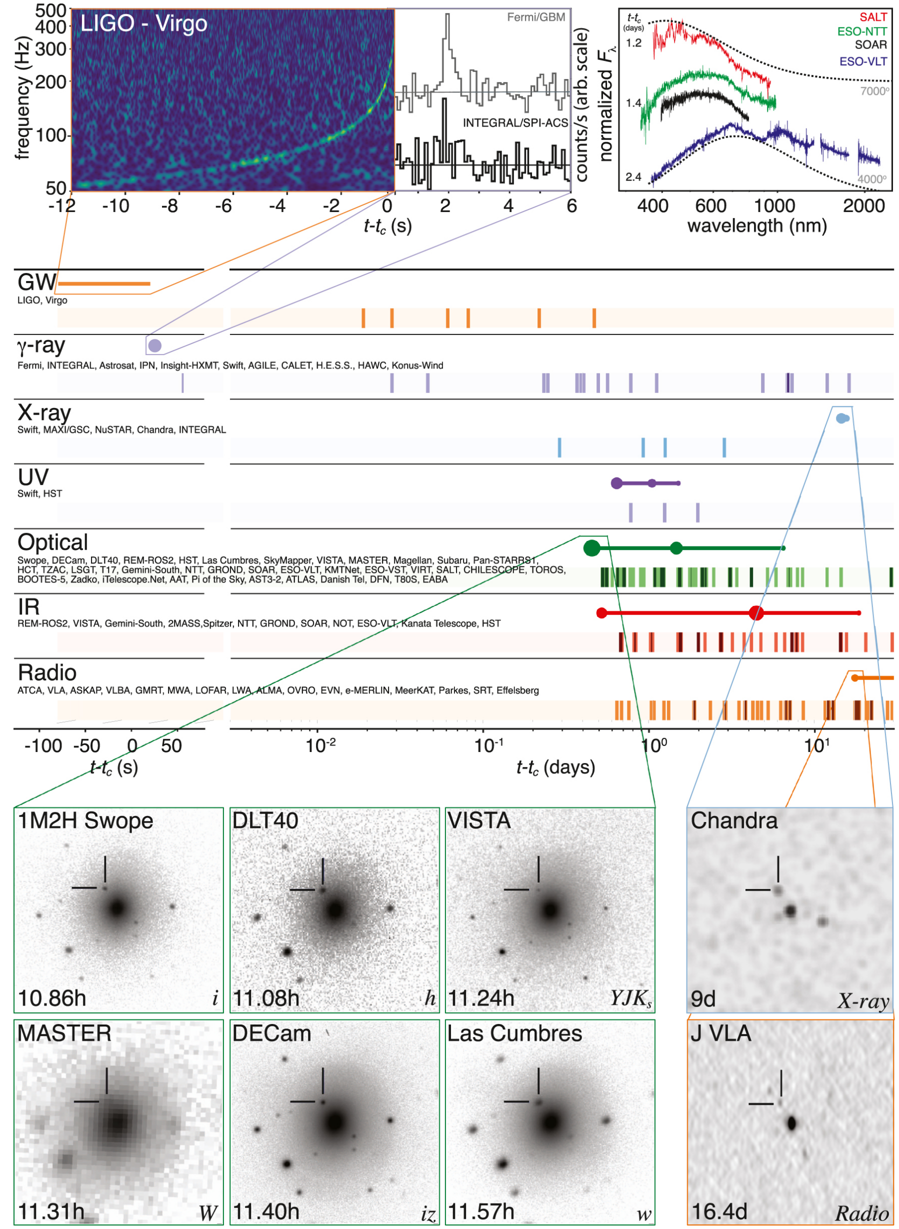

Abbott et al. 2017, ApJ, 848, L12

Final stages of stellar evolution

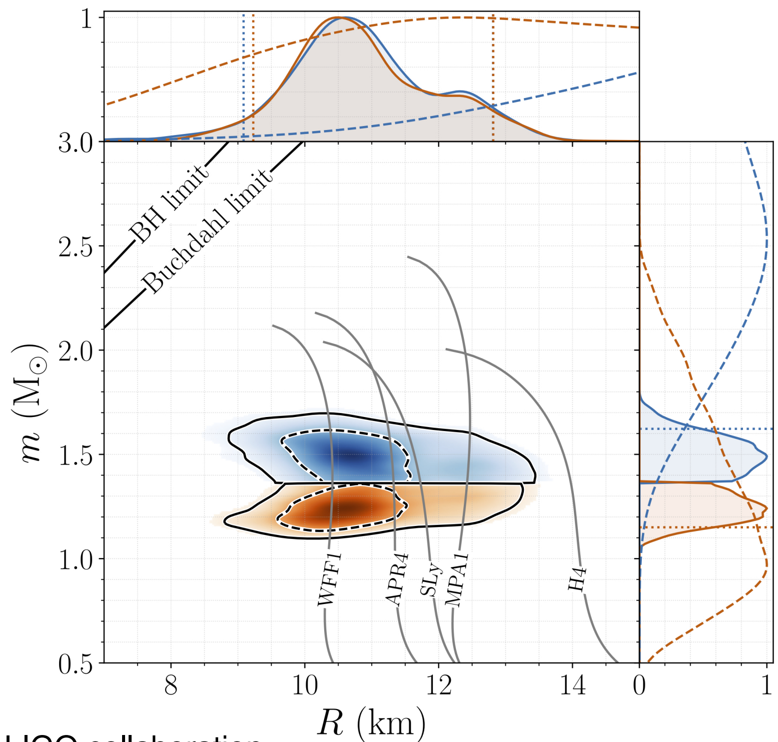

LIGO collaboration

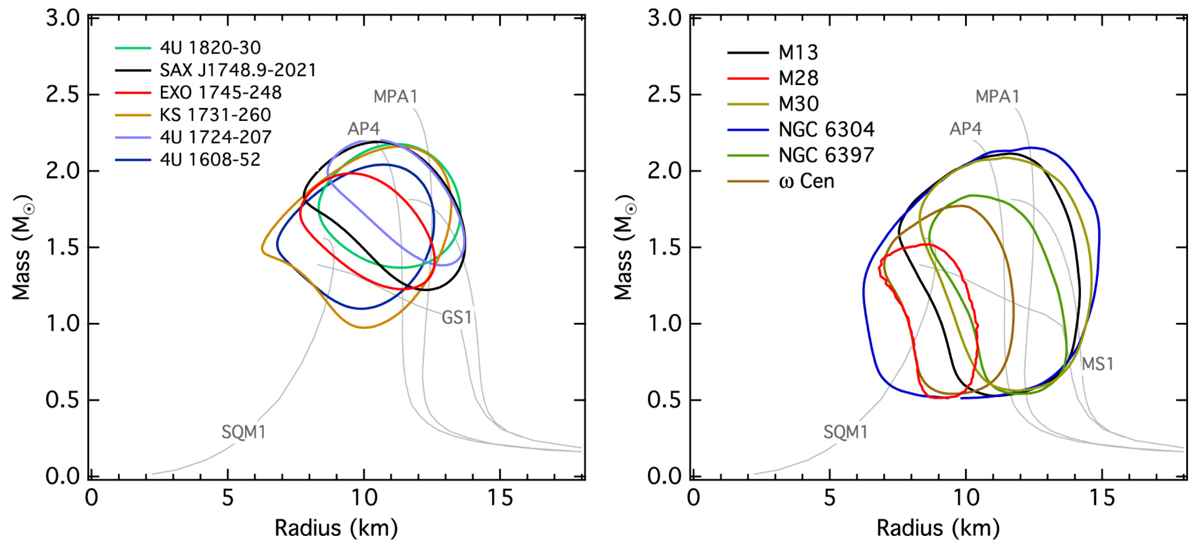

Özel et al. 2016, ApJ, 820, 28

Measurements used to constrain the equation of state

Final stages of stellar evolution

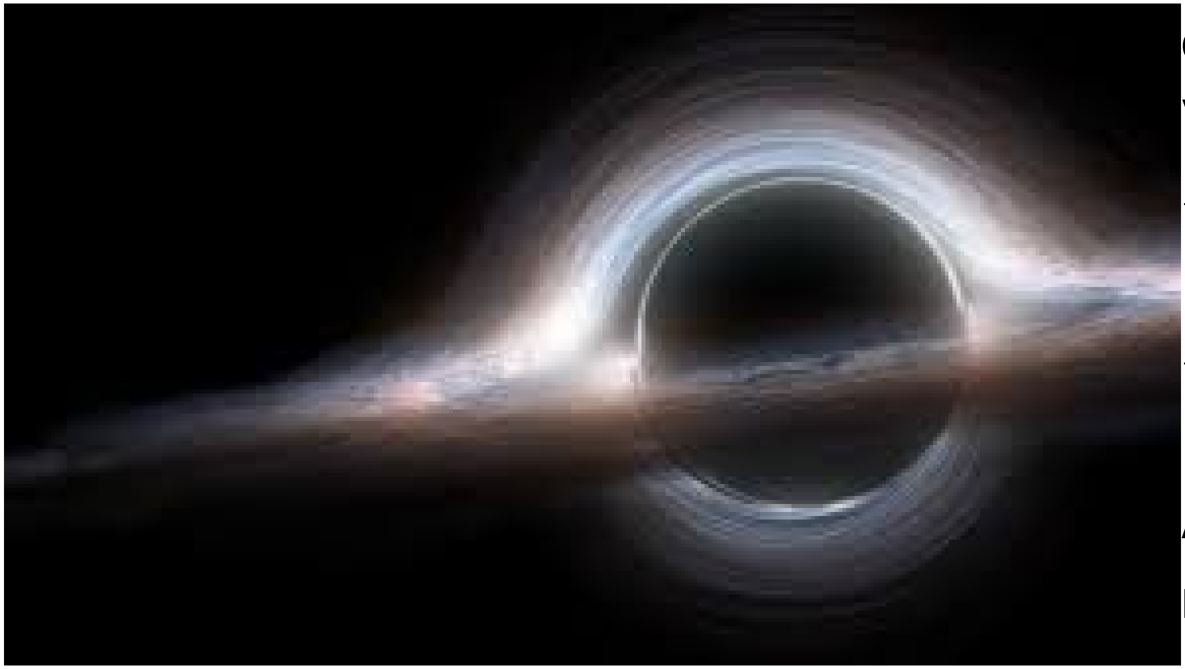

Interstellar

Fully characterized by mass, spin and charge

$\rightarrow$ Solutions for rotating (Kerr) and charged BHs are known

Stellar remnants with masses exceeding the Oppenheimer-Volkoff limit collapse further

$\rightarrow$ No denser state of matter is known

$\rightarrow$ No further pressure sources can counteract gravity

As soon as the Schwarzschild radius

$$R_S = \frac{2GM}{c^2} \tag{9.29}$$

is reached, radiation cannot escape any more (event horizon)

$\rightarrow$ Black hole is formed

Final stages of stellar evolution

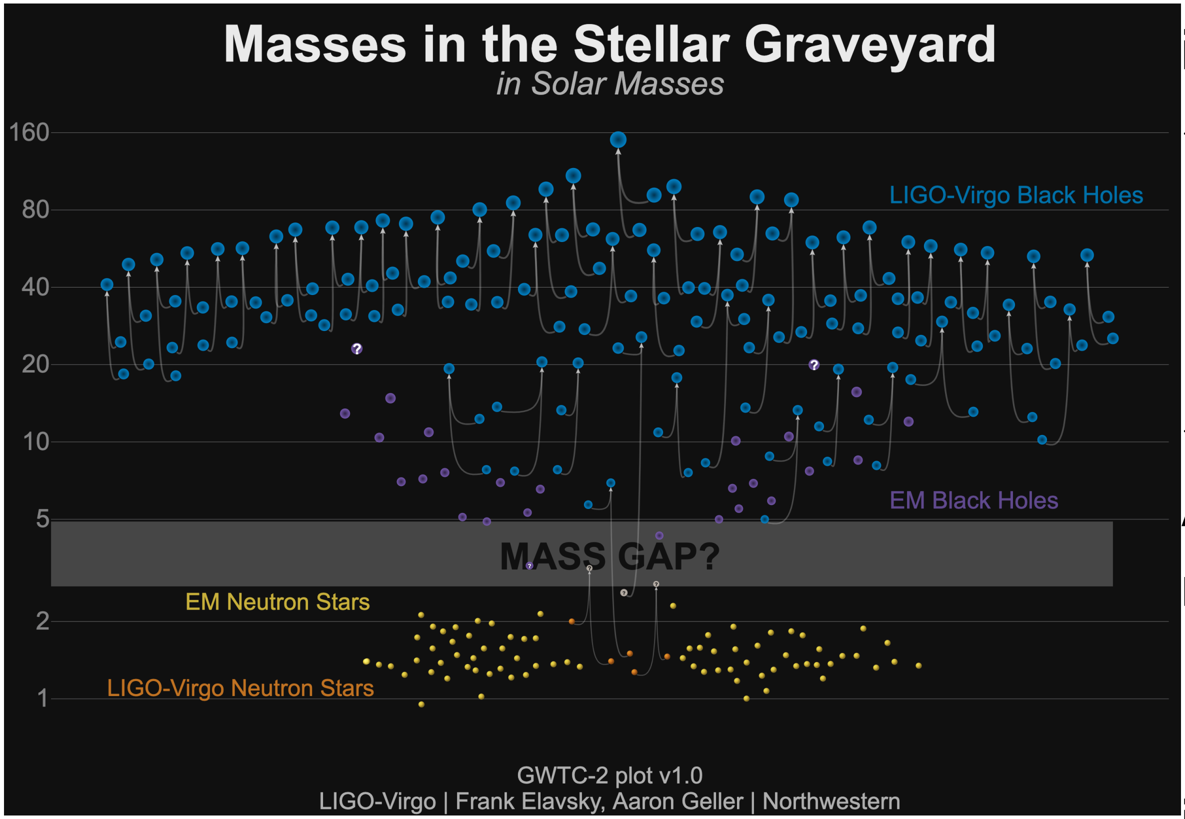

Ligo collaboration

Stellar mass black holes are observed as accreting objects in X-ray binaries

$\longrightarrow$ Dynamical masses can be measured

$$M_{\mathrm{BH,X-ray}} \approx 5 - 20\,\mathrm{M}_\odot$$

$\longrightarrow$ Consistent with predictions

As soon as the Schwarzschild radius

$$R_\mathrm{S} = \frac{2GM}{c^2} \tag{9.30}$$

is reached, radiation cannot escape any more (event horizon)

$\longrightarrow$ Black hole is formed

Final stages of stellar evolution

Merging black holes, neutron stars and BH-NS are observed with gravitational wave detectors

- more than 100 events so far
- 22 definitive binary merger events, 2 NS mergers, 3 NS-BH mergers, 18 BH mergers
- Masses and other properties can be derived from the GW signal

LIGO collaboration

- $M_{\text{BH,grav,wave}} \approx 5 - 80\,\mathrm{M}_{\odot}$
  $\rightarrow$ surprisingly many heavy BH (selection effect?)
- Most massive BHs hard to explain with stellar evolution

Final stages of stellar evolution

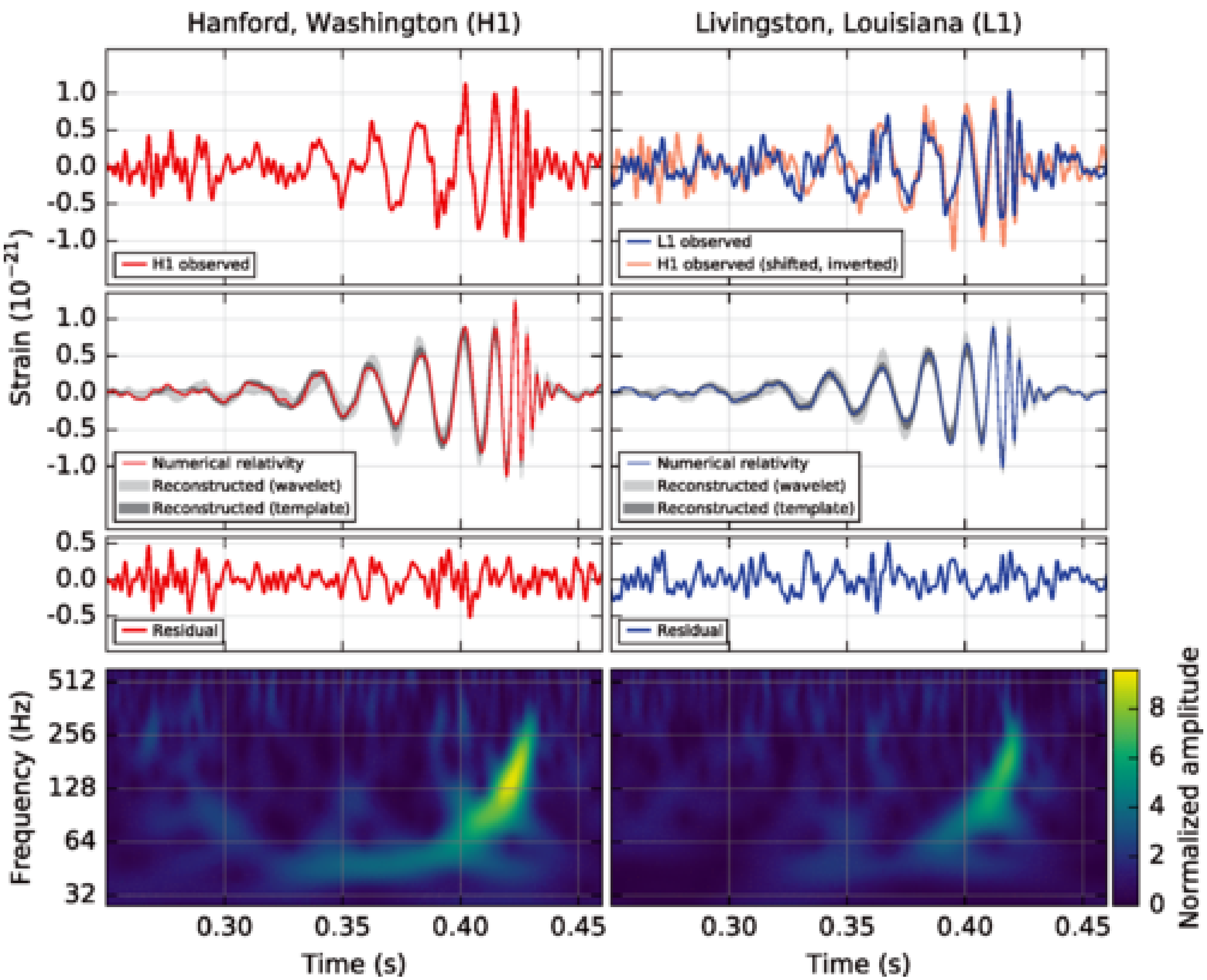

LIGO collaboration

Merging black holes observed with gravitational wave detectors

- 18 BH mergers $M_{\mathrm{BH,grav,wave}} \approx 5-80\,\mathrm{M}_\odot$
- Most massive BHs hard to explain with stellar evolution
- Merger of smaller BHs in cluster centers?
- Primordial BHs? Dark matter?
- Extremely massive and close binary as progenitor?

Stellar evolution of binaries

Stellar evolution of binaries

Most stars are not born alone

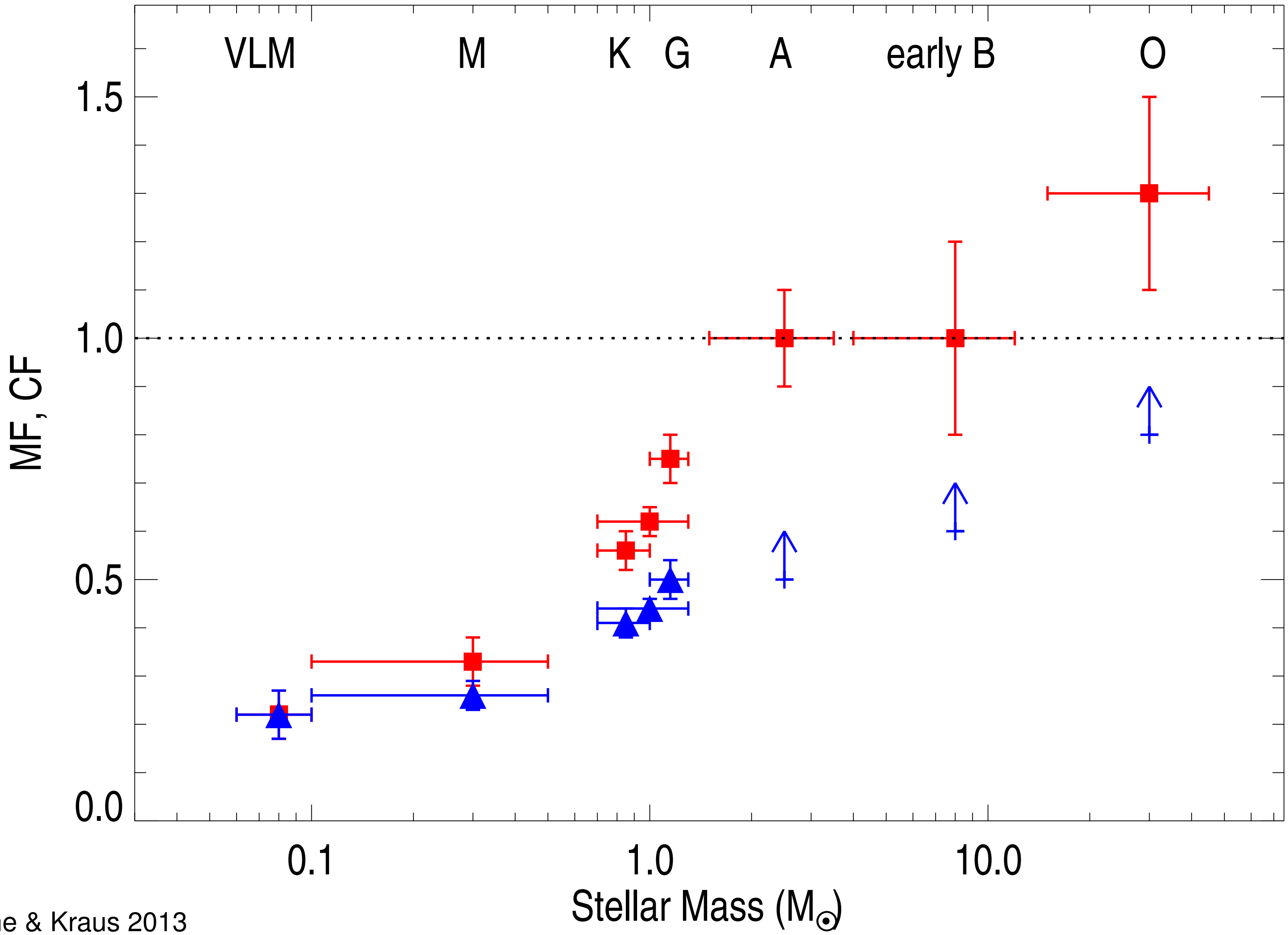

Duchene & Kraus 2013

→ stellar evolution cannot be understood without understanding binary evolution

Stellar evolution of binaries

Types of binaries

- **Visual binary**: double star system where you can see both stars and they appear to move around each other

Kruegar 60

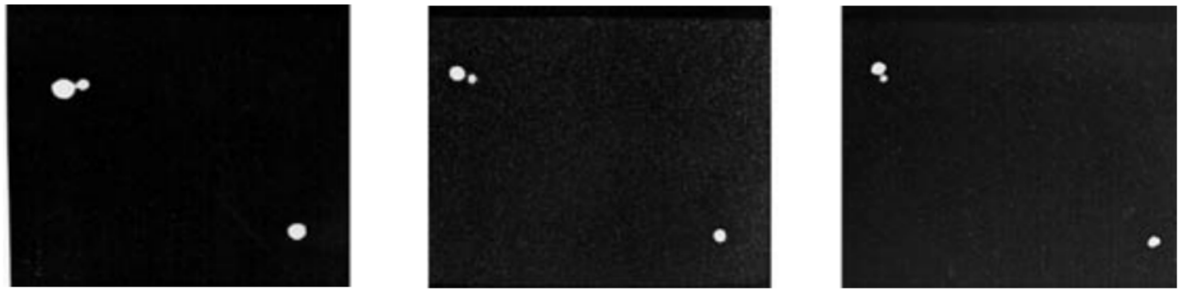

1908 1915 1920

70 Ophiuchi

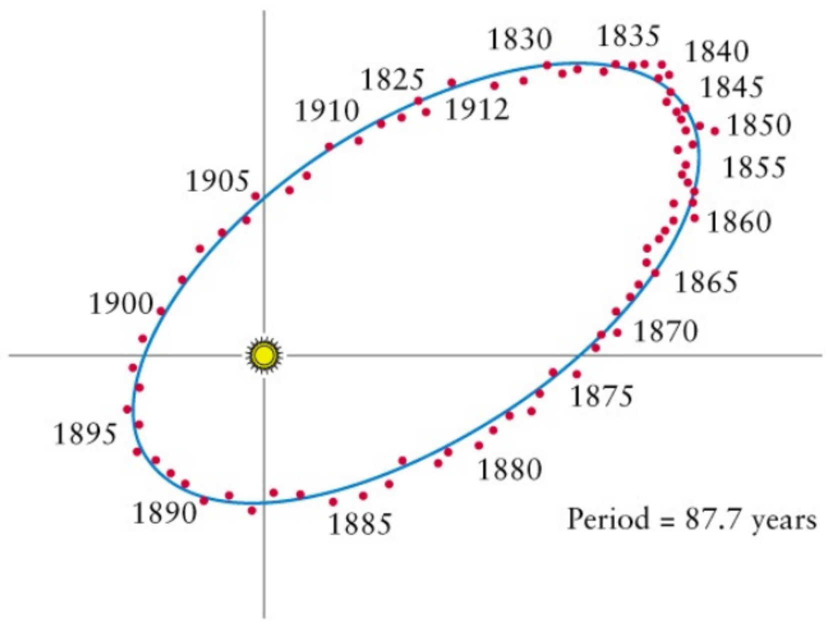

Types of binaries

- **Astrometric binary**: Similar to a visual binary, but only one component can be seen. The visible component will 'wobble' around the center of mass of the binary.

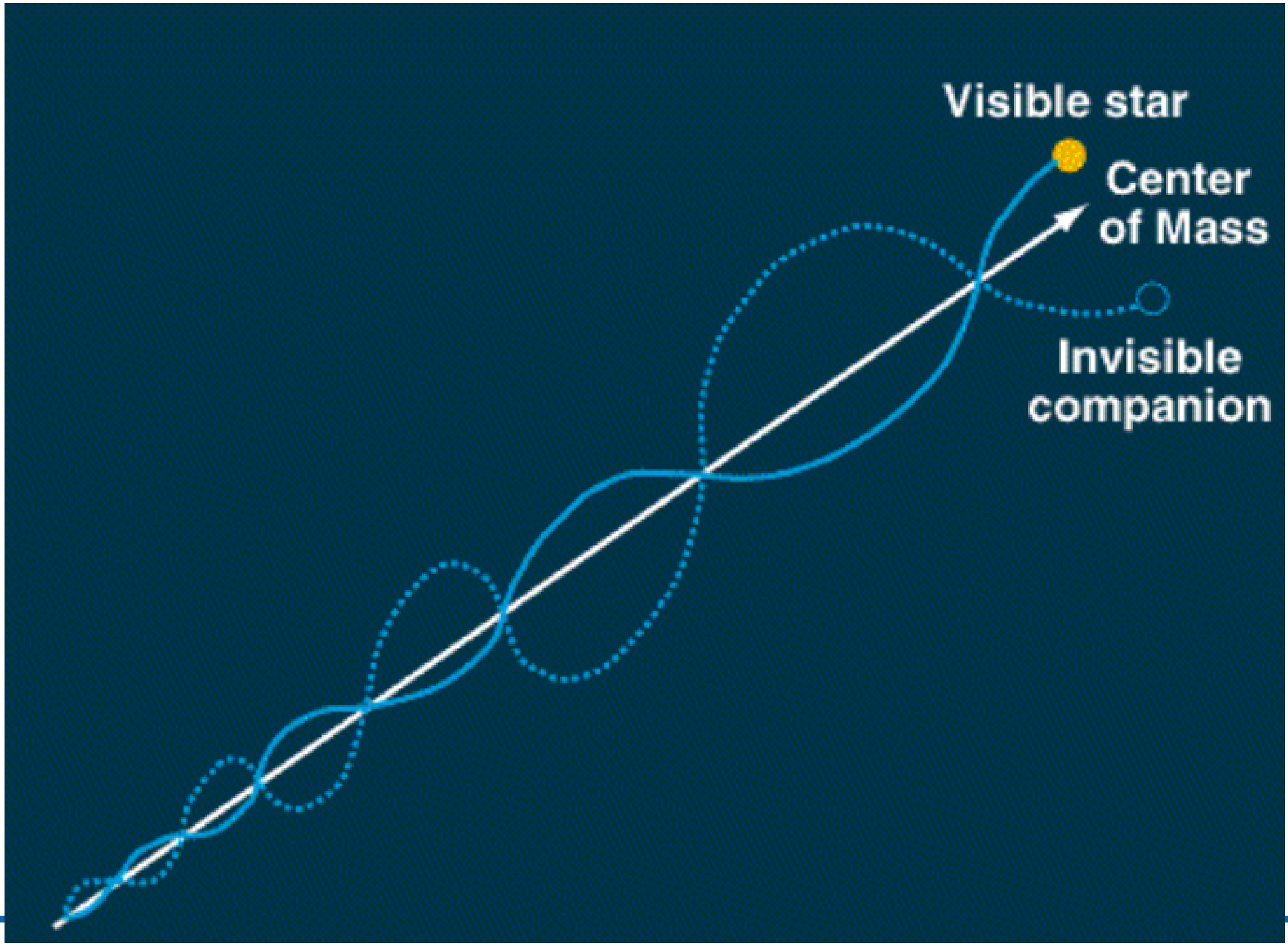

Stellar evolution of binaries

Types of binaries

- **Spectroscopic binary**: Components of the binary can not be distinguished visually. Spectrum of the star(s) shows a different Doppler shift at different times.

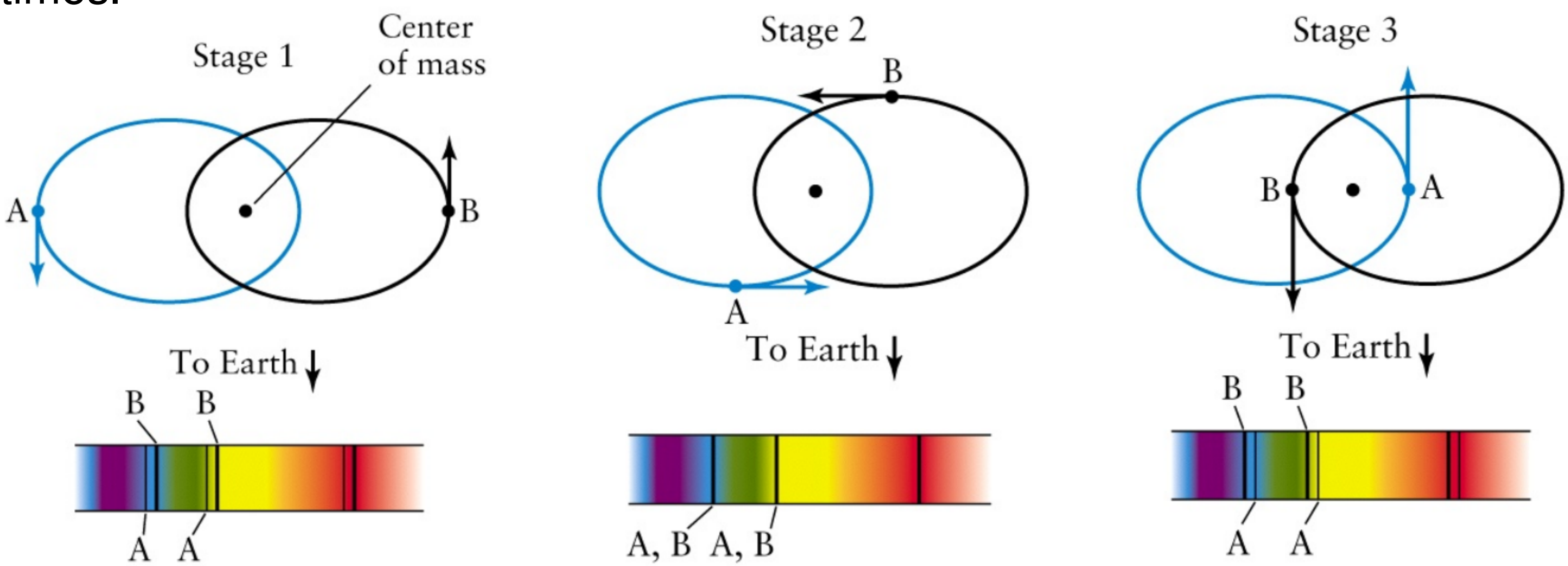

Stellar evolution of binaries

Types of binaries

- **Spectroscopic binary**: Doppler shift can be used to determine radial velocities of 1 or both stars. (in our line of sight)
  Single lined system: only one star is visible in the spectrum
  Double lines system: both stars are visible in the spectrum

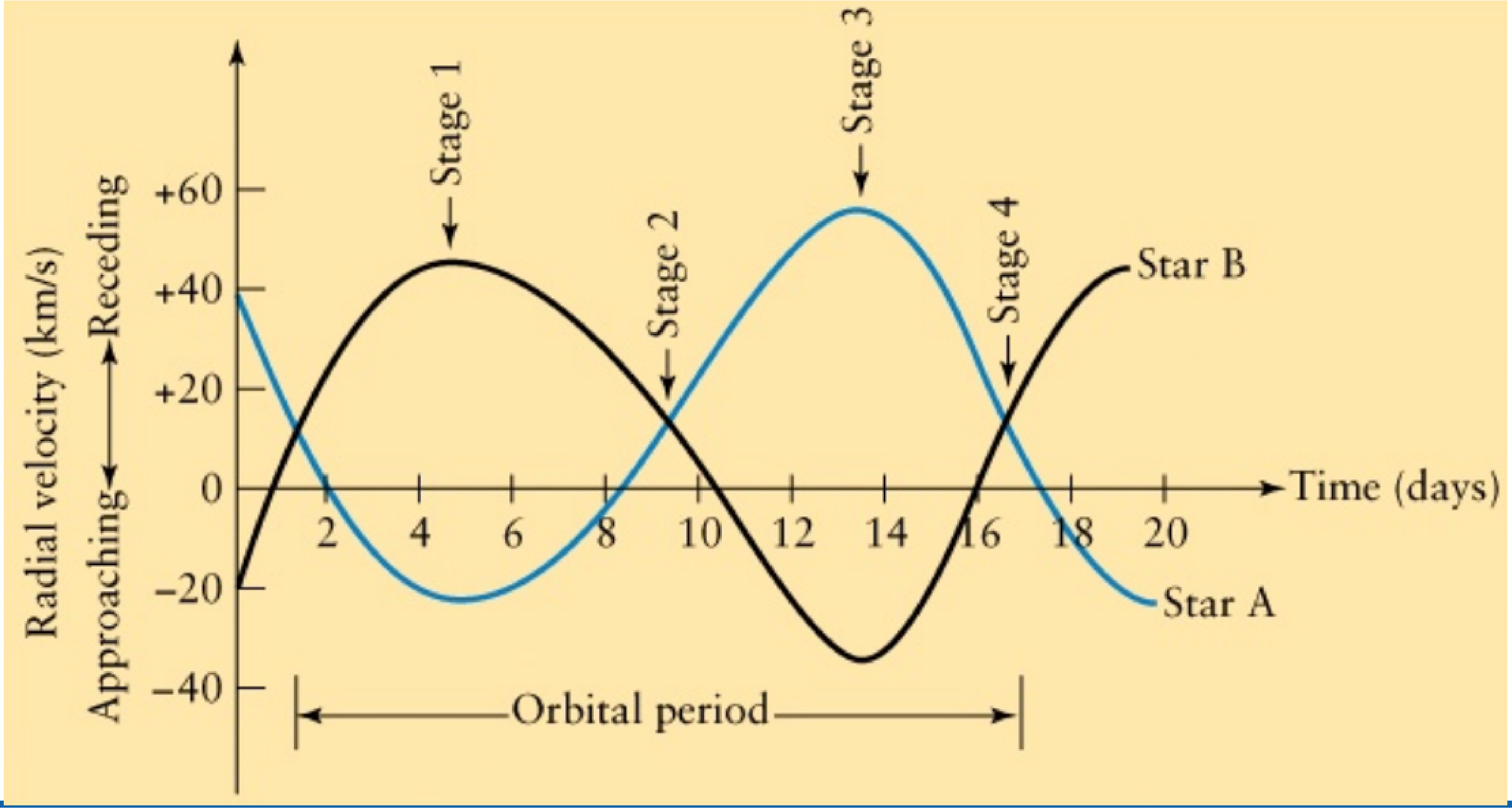

Stellar evolution of binaries

Types of binaries

Spectroscopic Binary: IM Mon, $P = 1.2$ days, $e = 0$

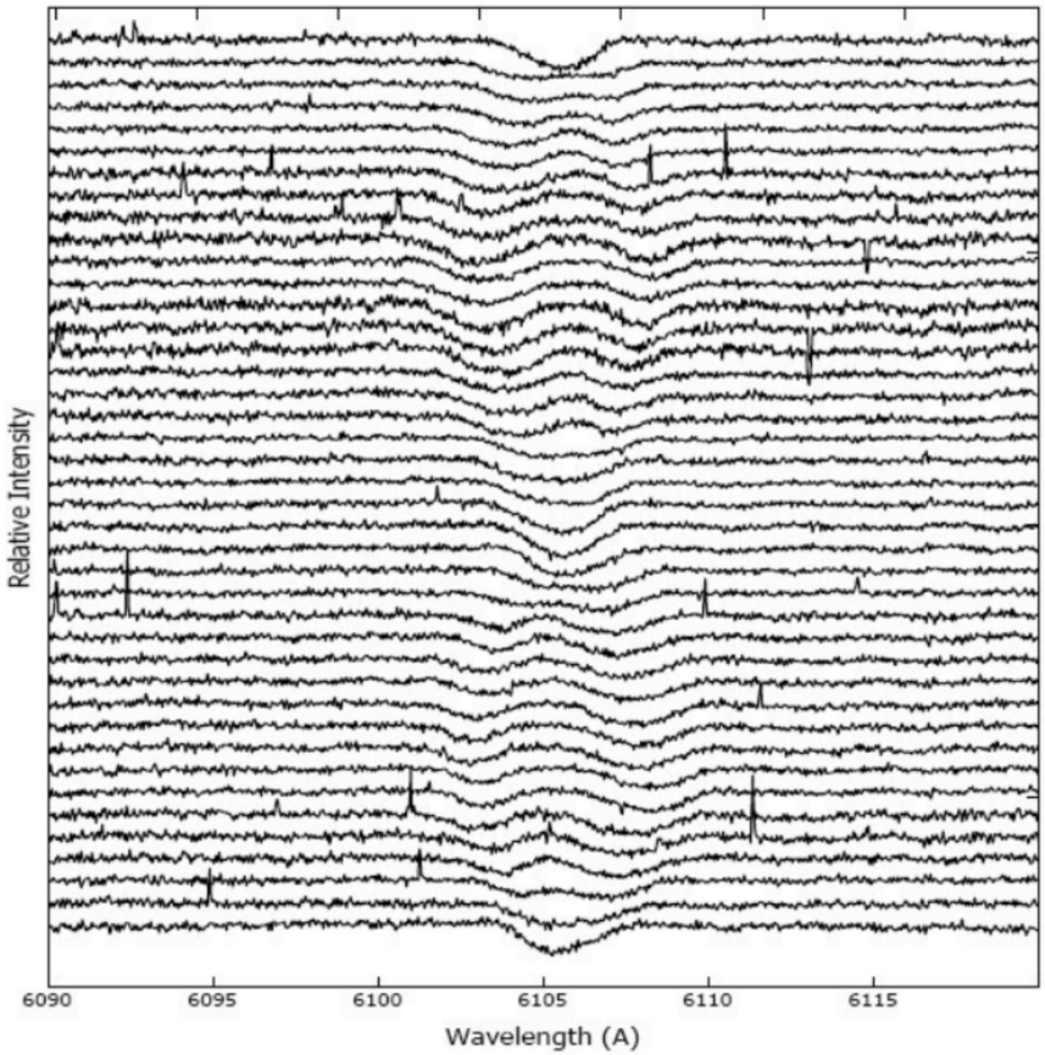

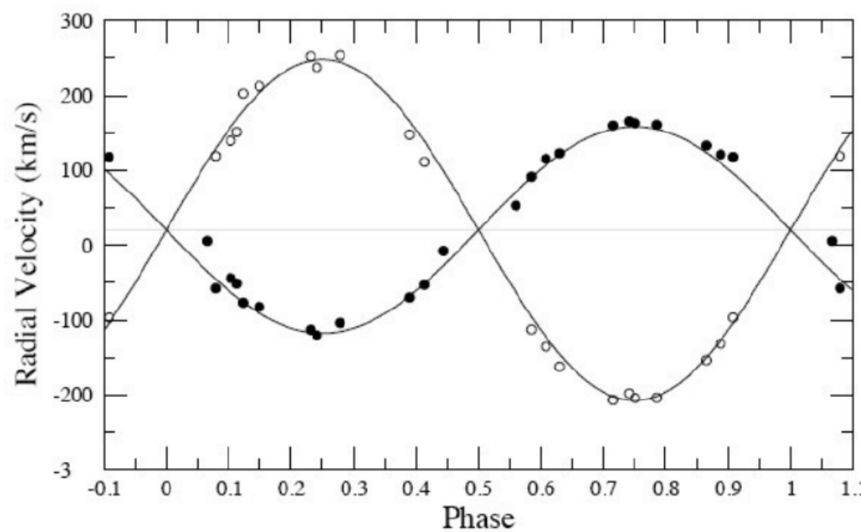

Stellar evolution of binaries

Types of binaries

- **Eclipsing binary**: Stars rotate in the same plane as our line of sight (or with very small inclination). Stars will pass in front of each other causing eclipses. Duration/depth of the eclipses can be used to calculate size of the stars.

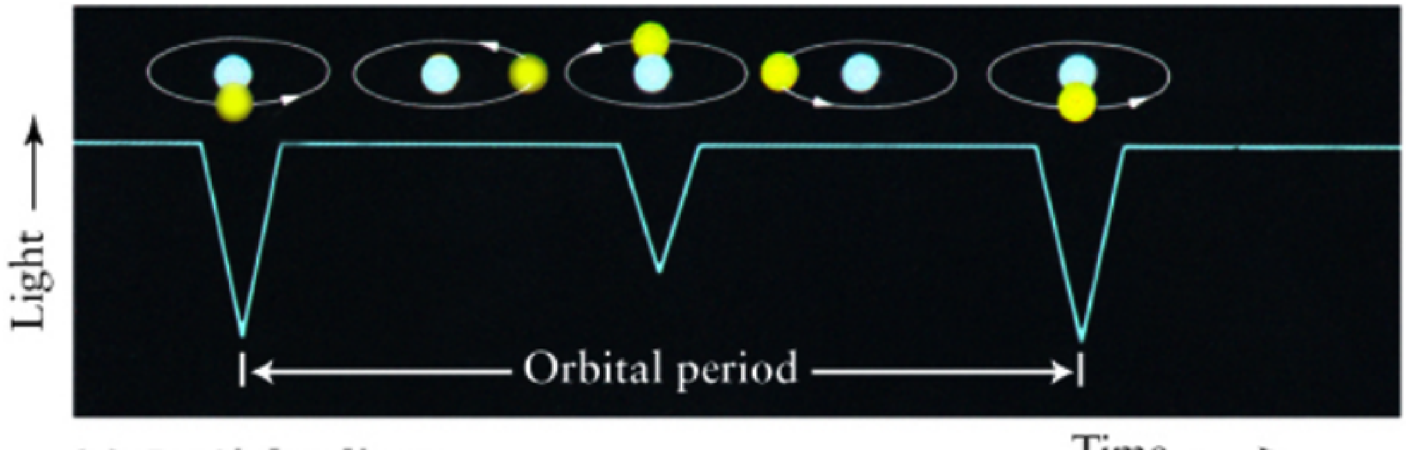

(a) Partial eclipse

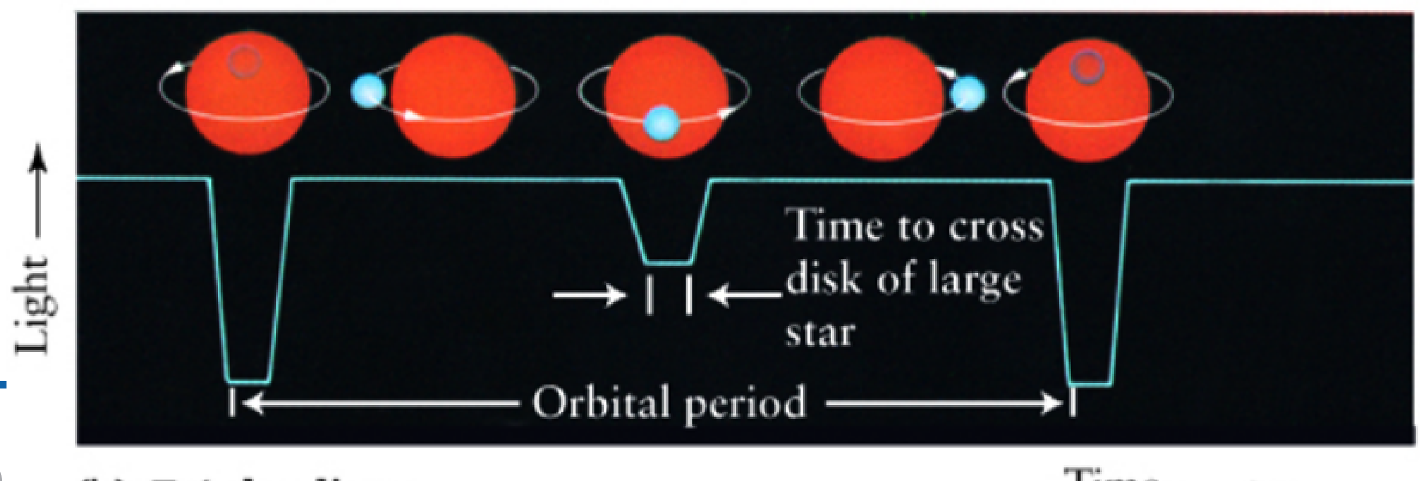

(b) Total eclipse

Stellar evolution of binaries

Multiple systems: common but harder to detect, Non hierarchical systems are always dynamical unstable

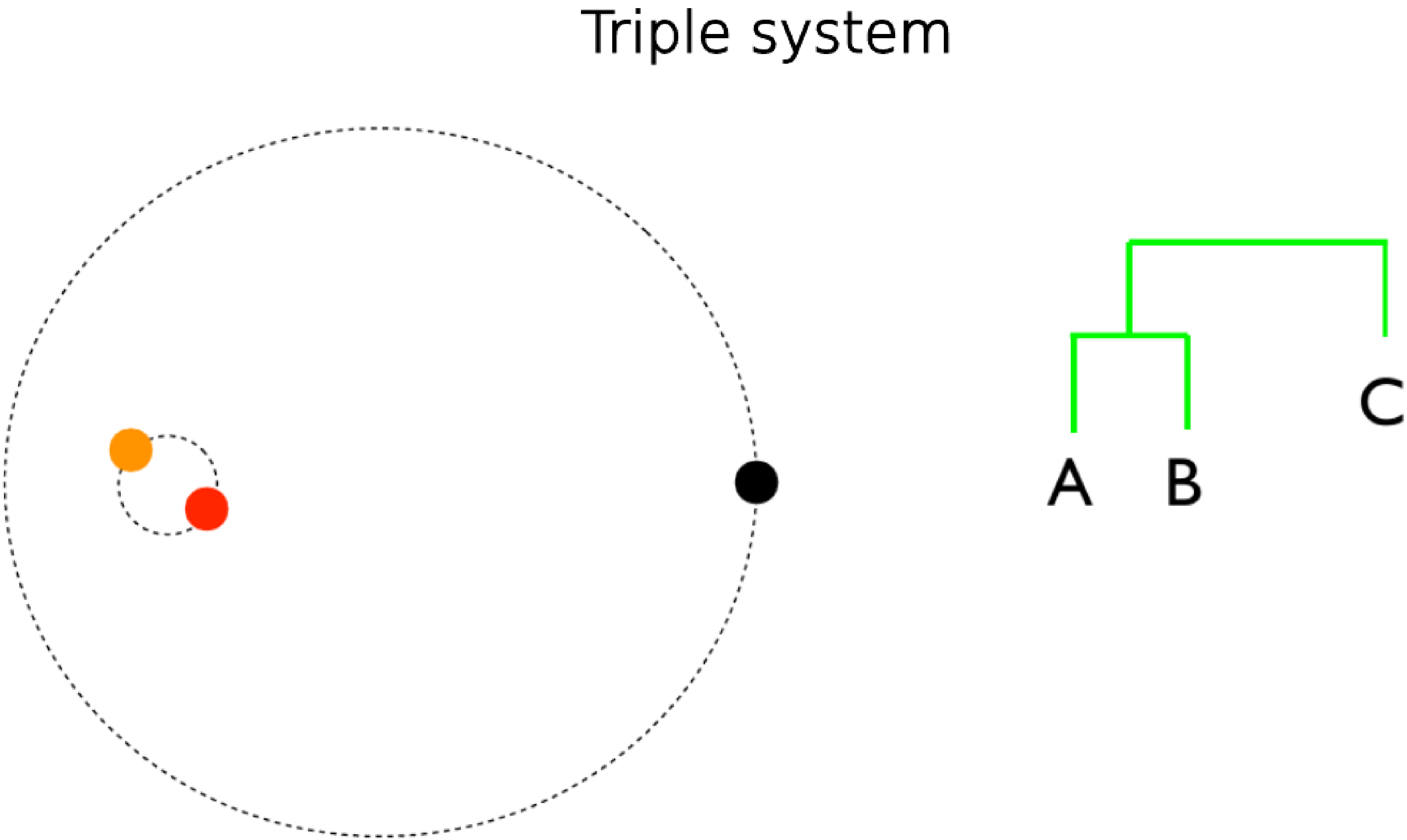

Stellar evolution of binaries

Multiple systems

Quadruple system

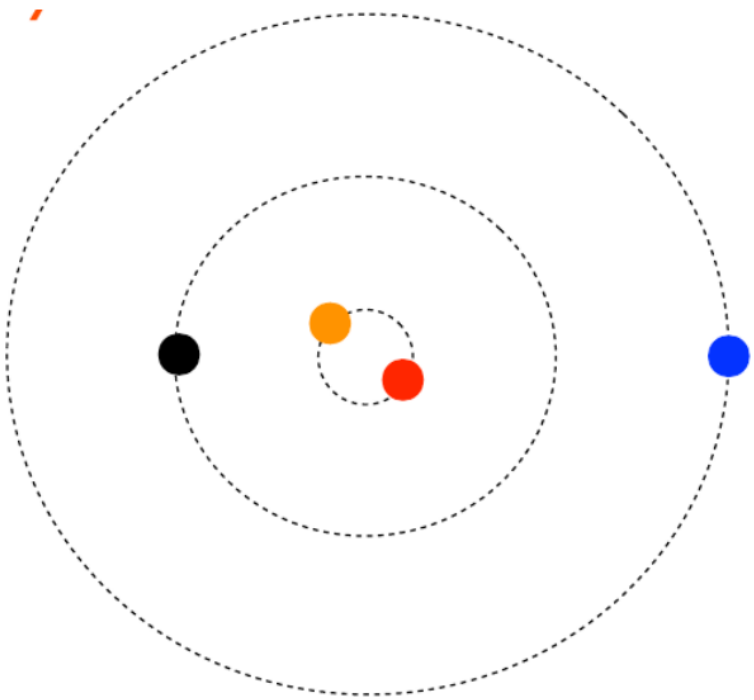

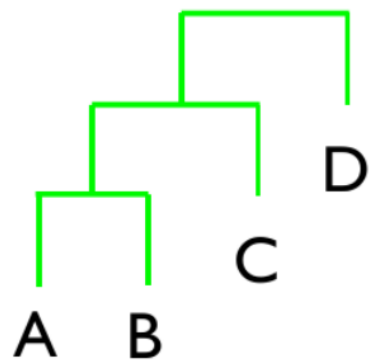

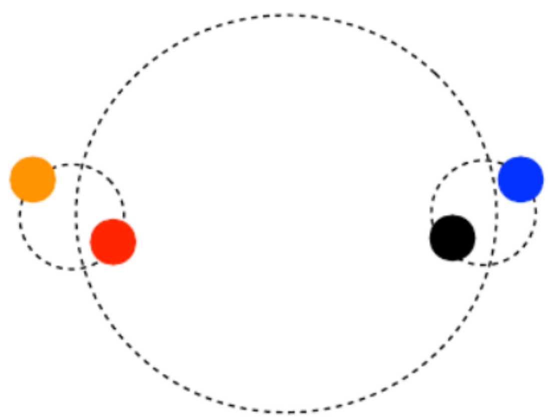

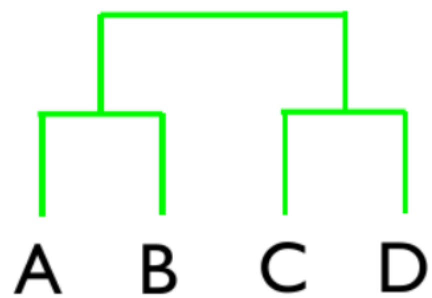

Multiple systems

Sextuple system (Castor)

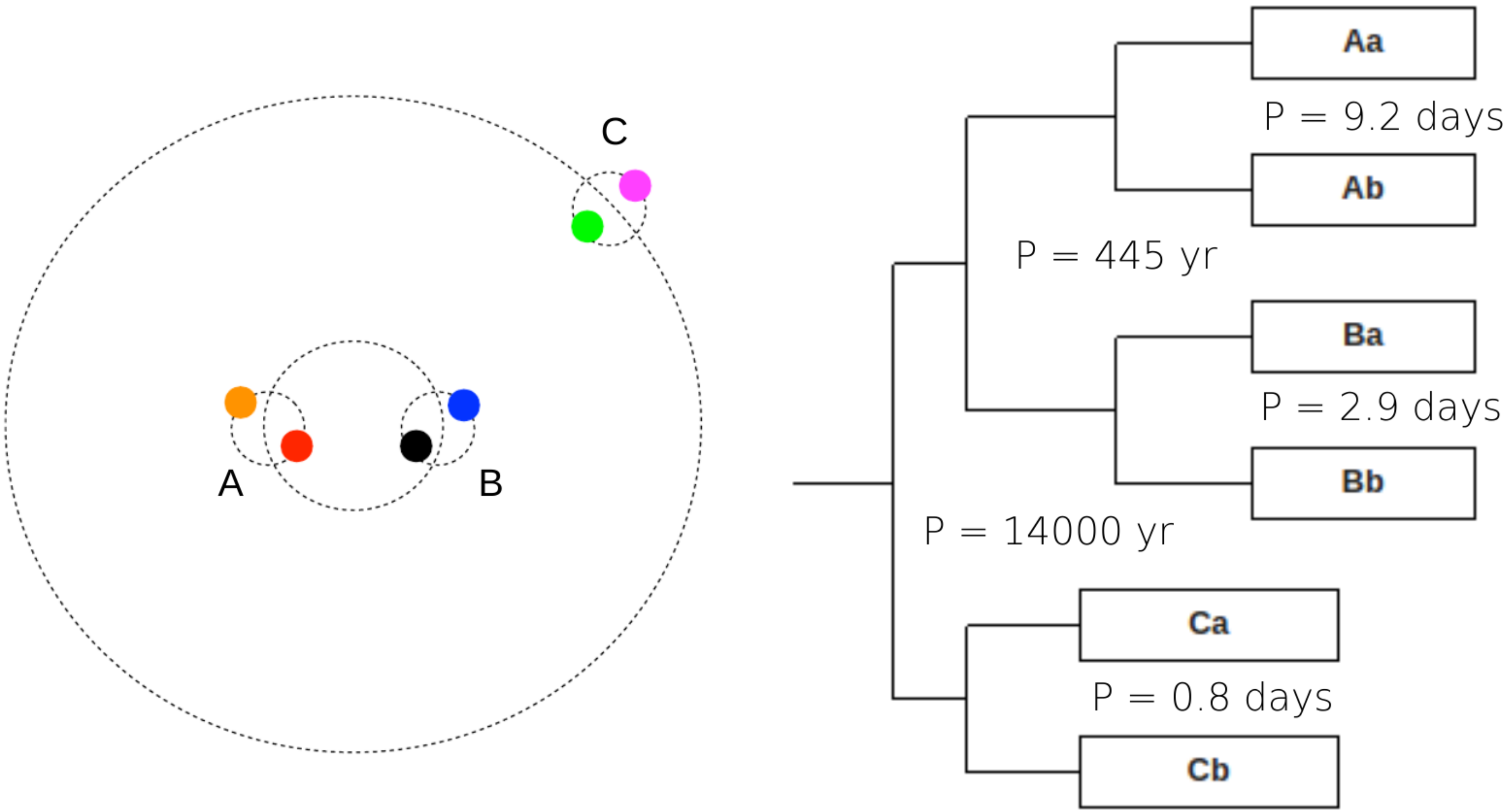

Stellar evolution of binaries

Potential wells

- **Detached binary**: Both stars are within their potential well, and are more or less undistorted (they can be approximated as being spherical).

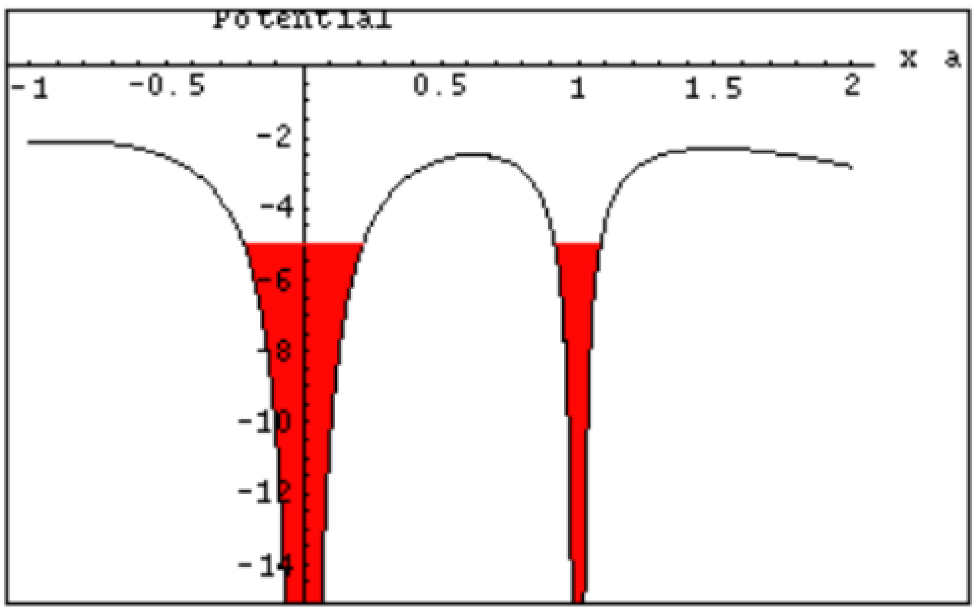

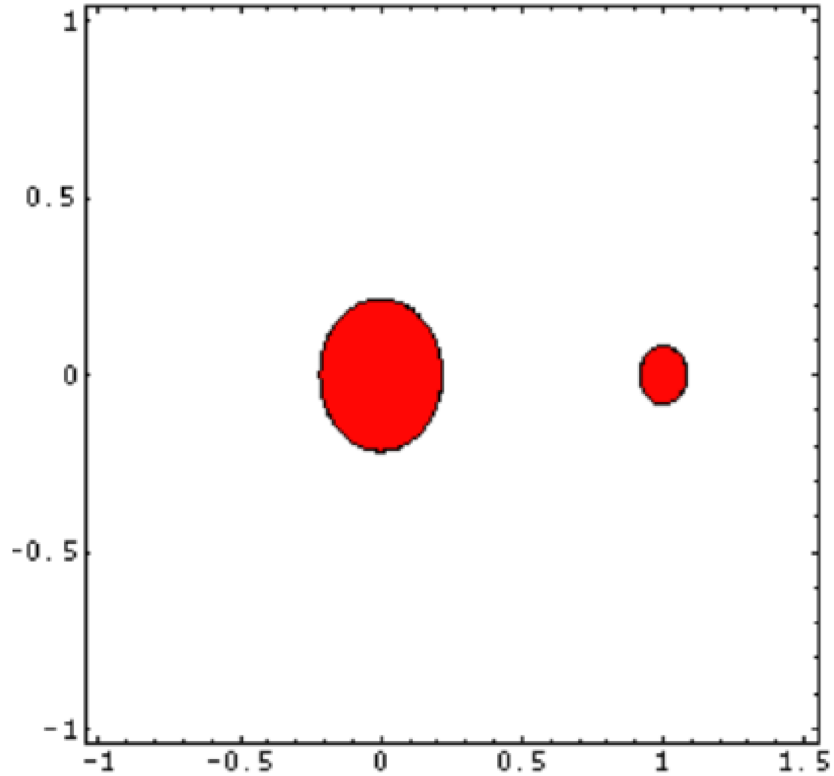

Stellar evolution of binaries

Potential wells

- **Semi-detached binary**: One of the stars has expanded to the point where it reached the saddle point (this star can not be considered spherical anymore).

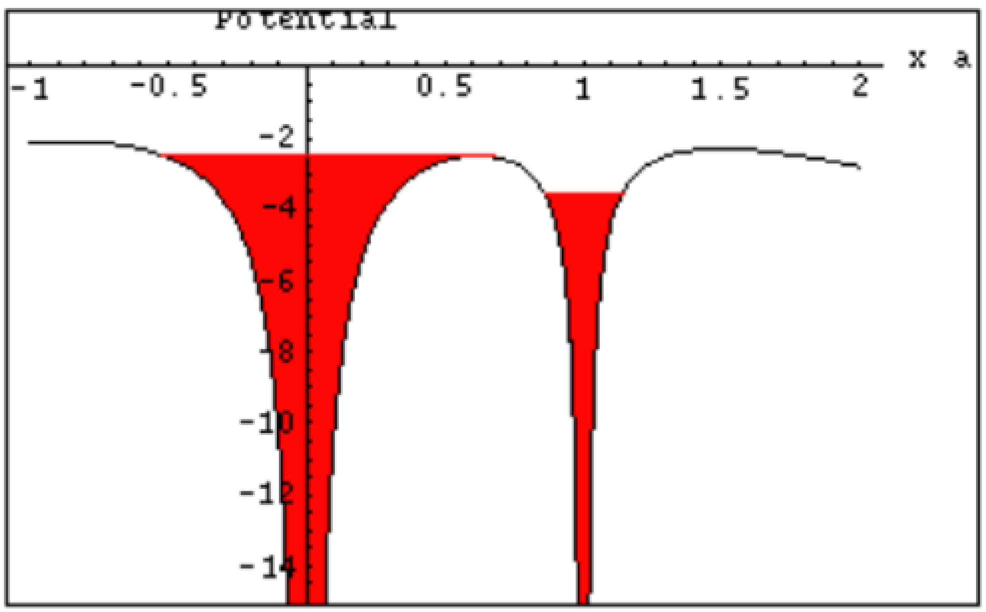

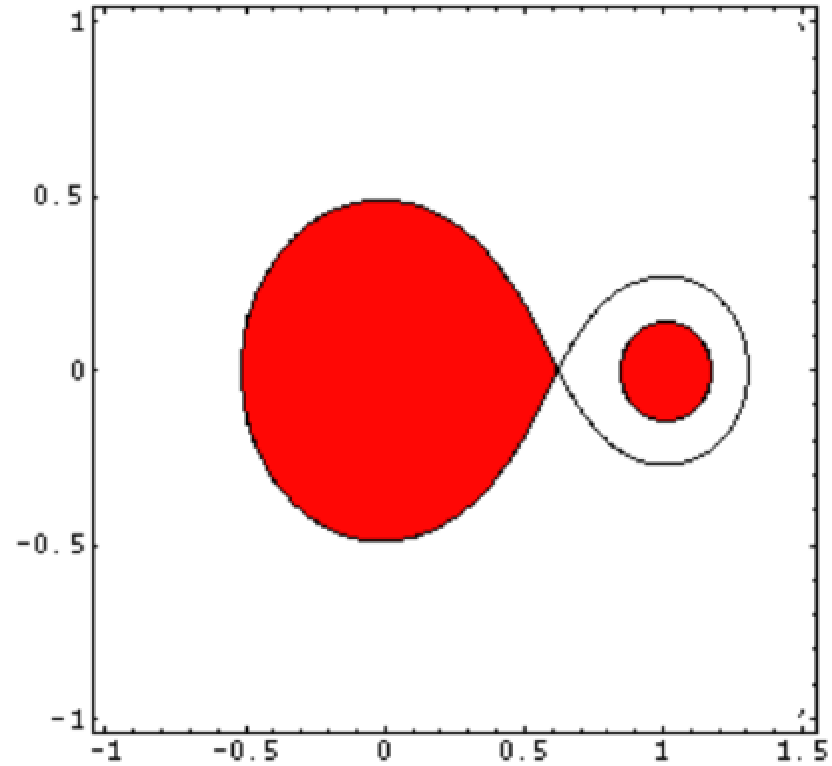

Stellar evolution of binaries

Potential wells

- **Contact binary**: Both stars are filling their potential well. This can occur because the mass that flows from the first star that fills it's well fills up the potential well of the secondary star. Or because both stars expand to fill their well.

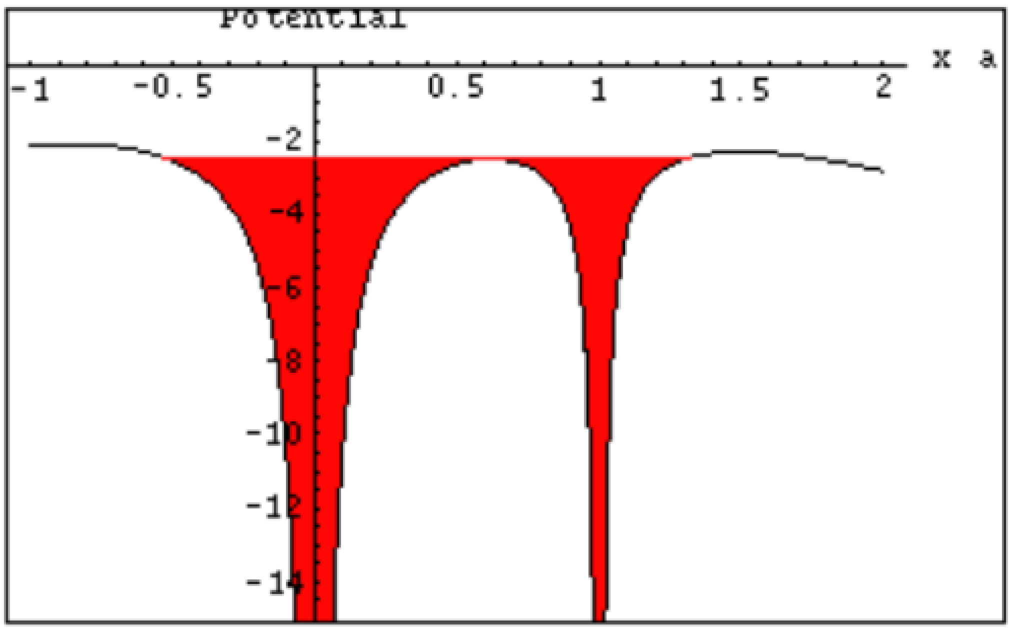

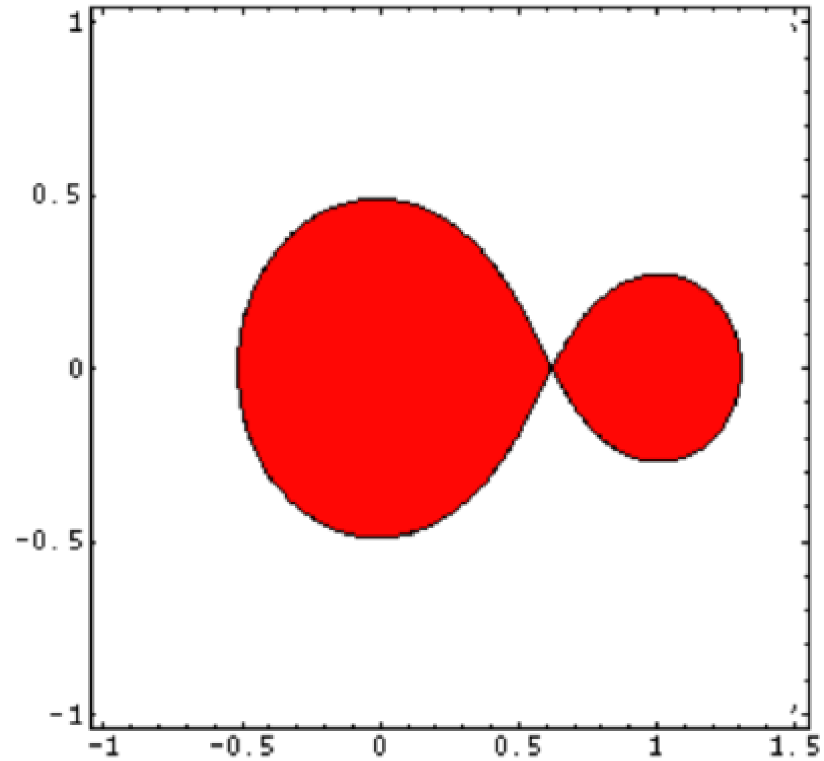

Stellar evolution of binaries

Potential wells

- **Overcontact binary**: Both stars are overfilling their potential well, so that there is only one common surface visible.

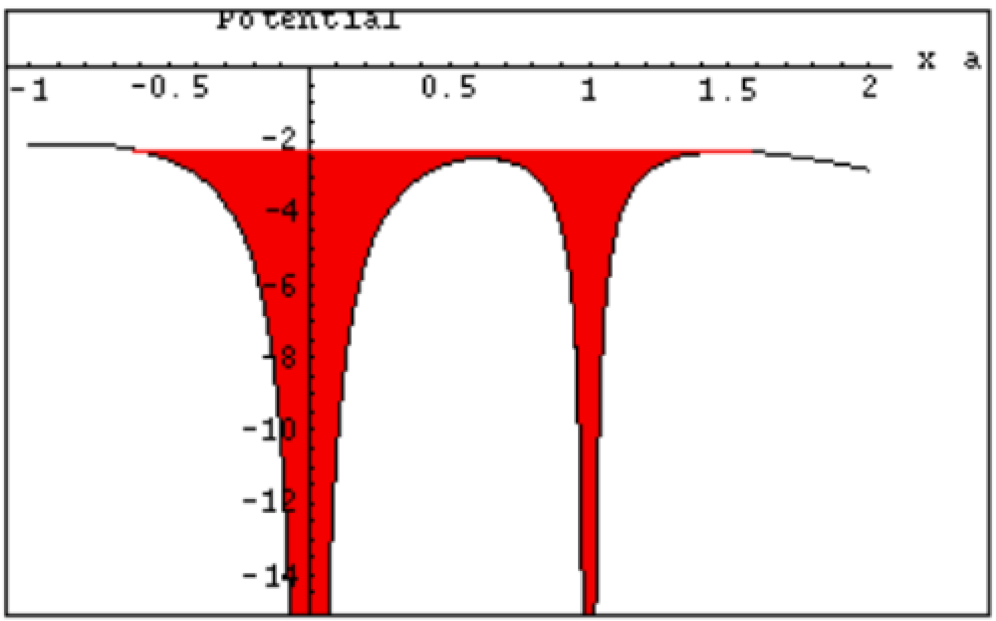

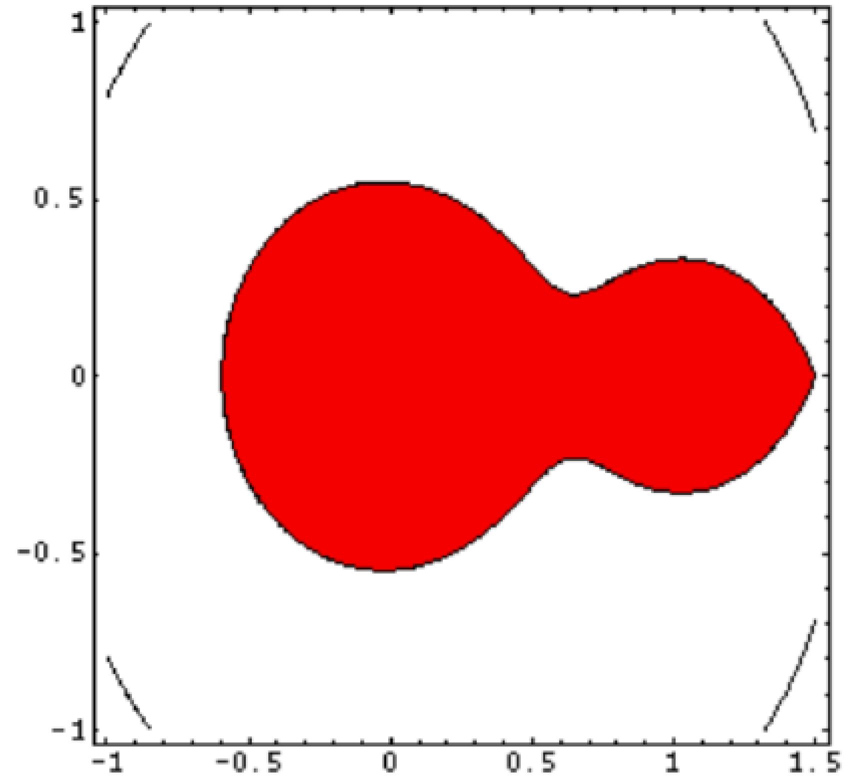

Stellar evolution of binaries

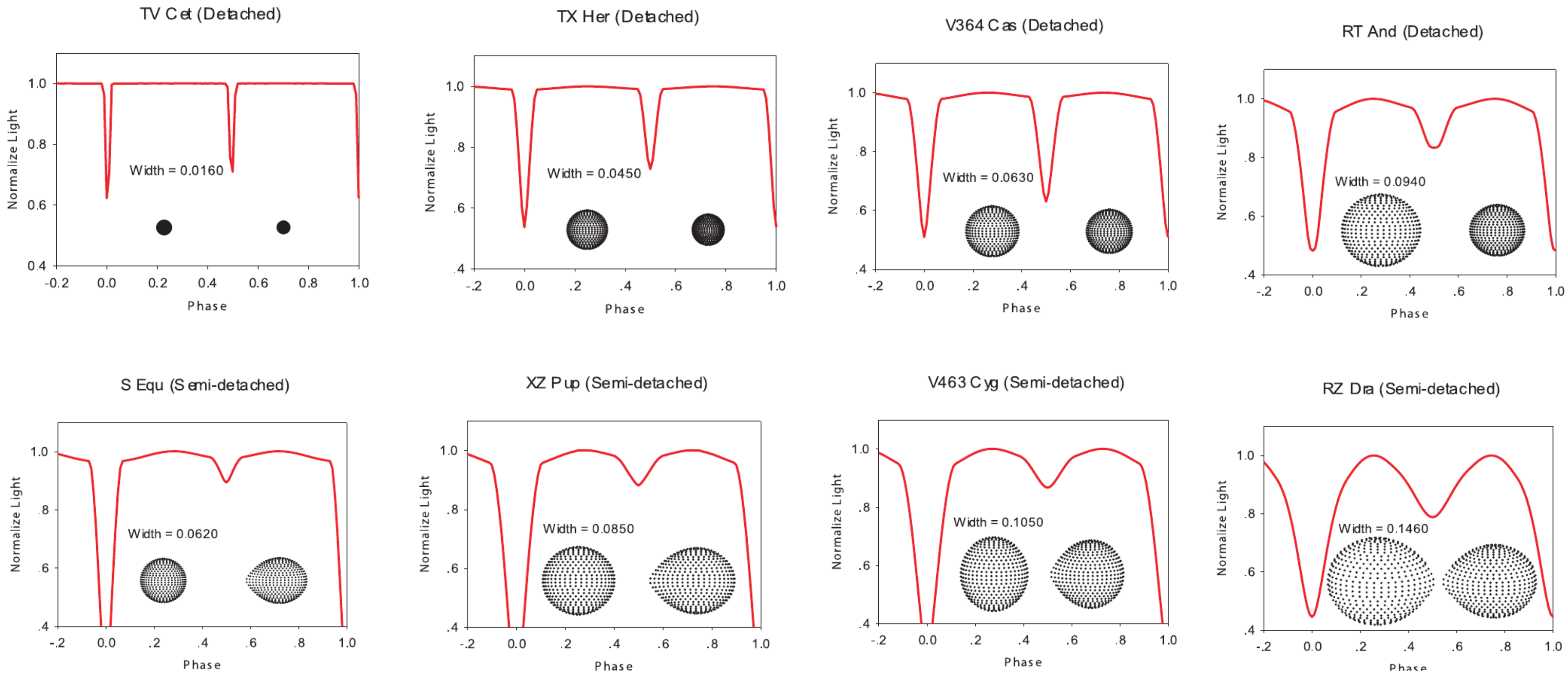

Kang 2010

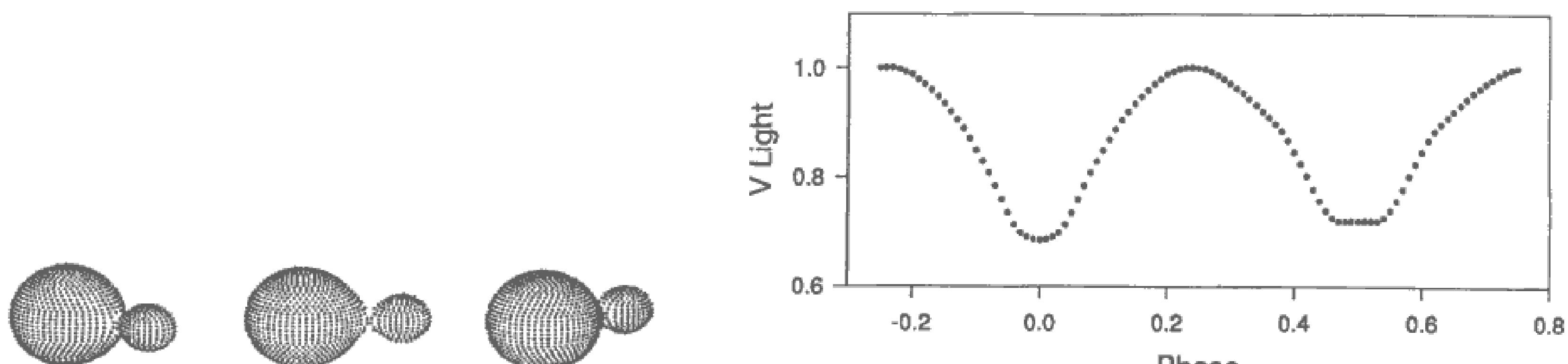

Wilson 1994

Roche formalism

potential wells can be depicted in a more mathematical way using the Roche formalism: Roche potential – shape of stars are given by equipotential surfaces

Roche lobes: equipotential surfaces through the L1 Lagrangian point: region within which orbiting material is gravitationally bound to that star.

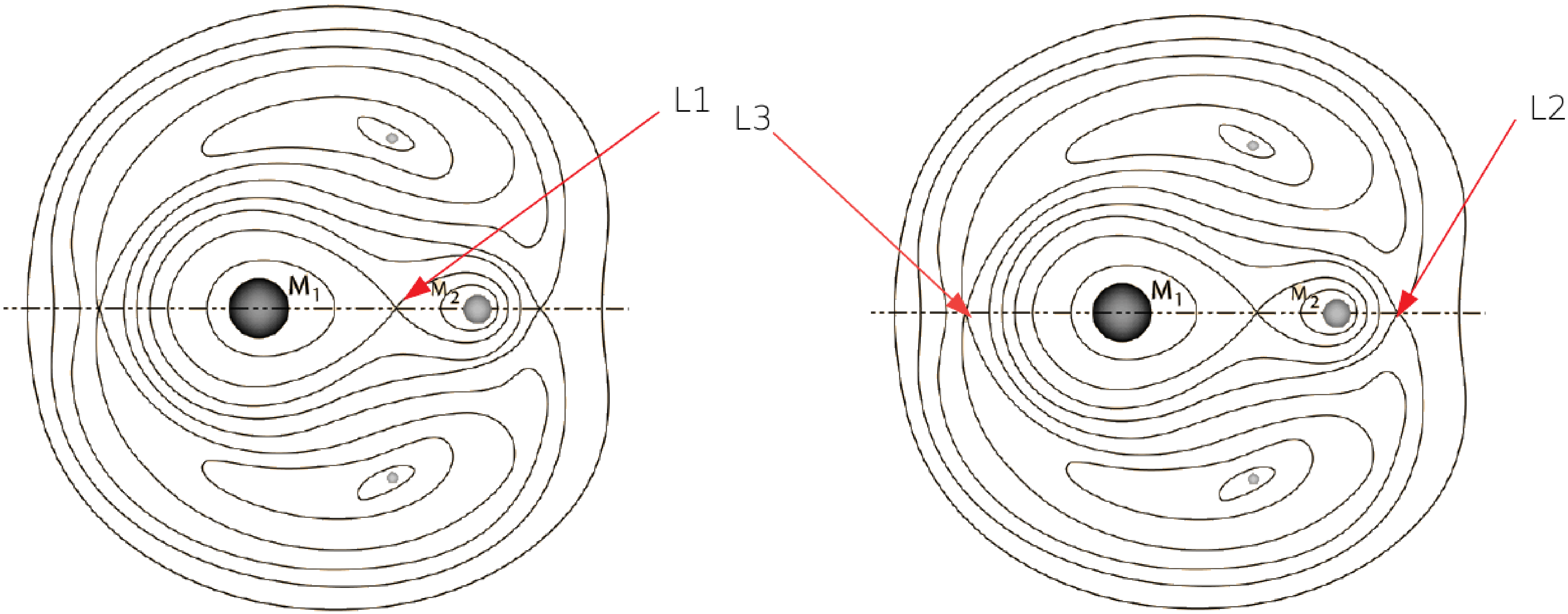

Stellar evolution of binaries

Roche formalism Roche lobes: equipotential surfaces through the L1 Lagrangian point: region within which orbiting material is gravitationally bound to that star.

relevant, if one or both of the stars radii start approaching it's Roche lobe.

When a star reaches it's Roche lobe it becomes an **interacting binary**. Mass can then start flowing from the Roche lobe filling star to it's companion.

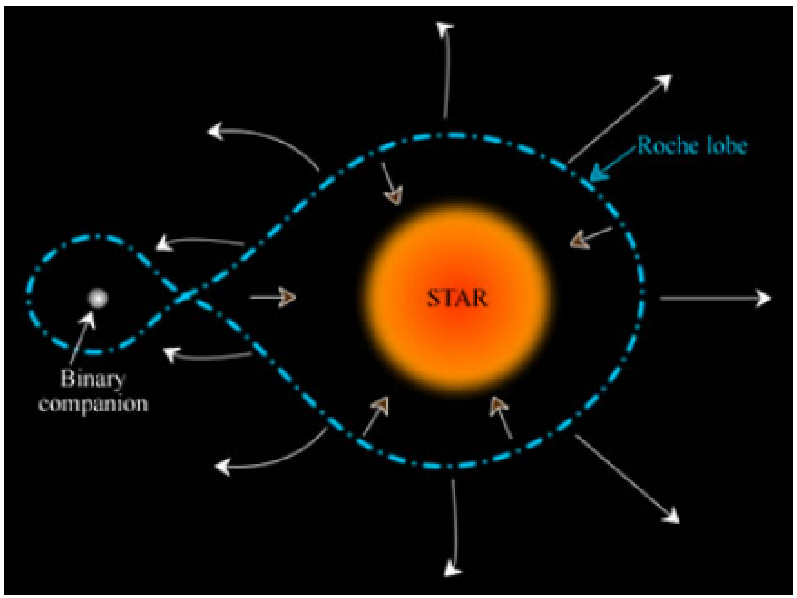

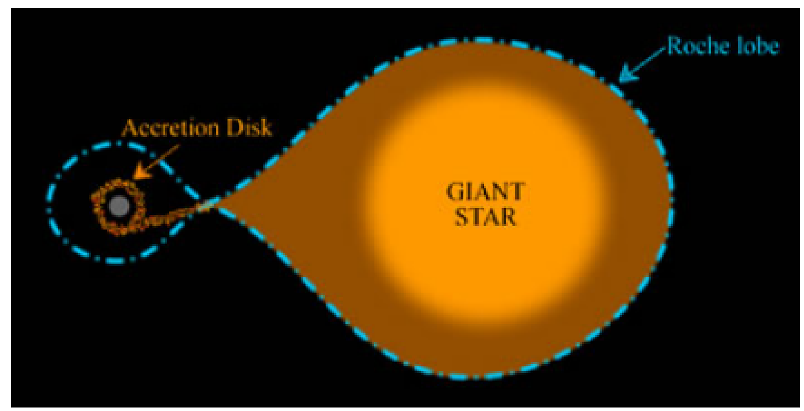

Stellar evolution of binaries

Mass transfer: can change stellar evolution

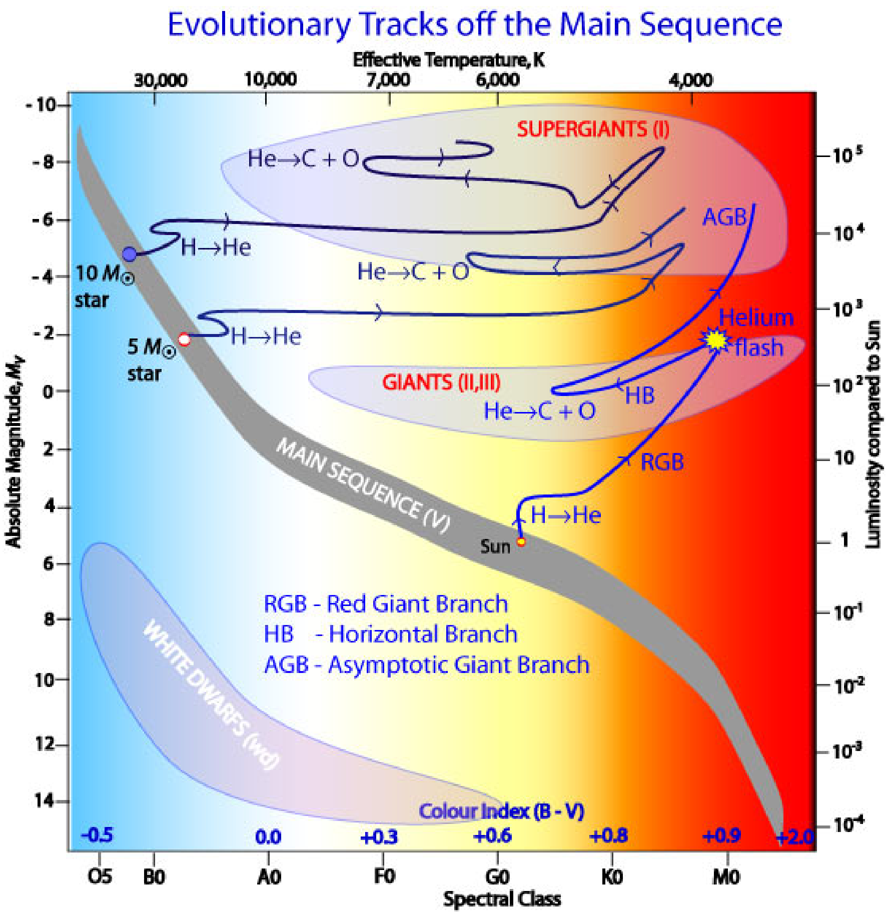

S. Cartwright, University of Sheffield

Close binary evolution: Evolution of both components linked by Roche Lobe Overflow (RLOF)

Three cases of mass transfer phases:

- Case A: RLOF at the core hydrogen burning phase ($P \approx 1 - 10$ d)
- Case B: RLOF at the hydrogen-shell burning phase (RGB) ($P \approx 10 - 100$ d)
- Case C: RLOF after core helium exhaustion phase (AGB) ($P \approx 100$ d)

Stellar evolution of binaries

ESO/L. Calçada/M. Kornmesser/S.E. de Mink

Influence on stellar evolution can be complicated: masses, size, shape and rotation changes

Stellar evolution of binaries

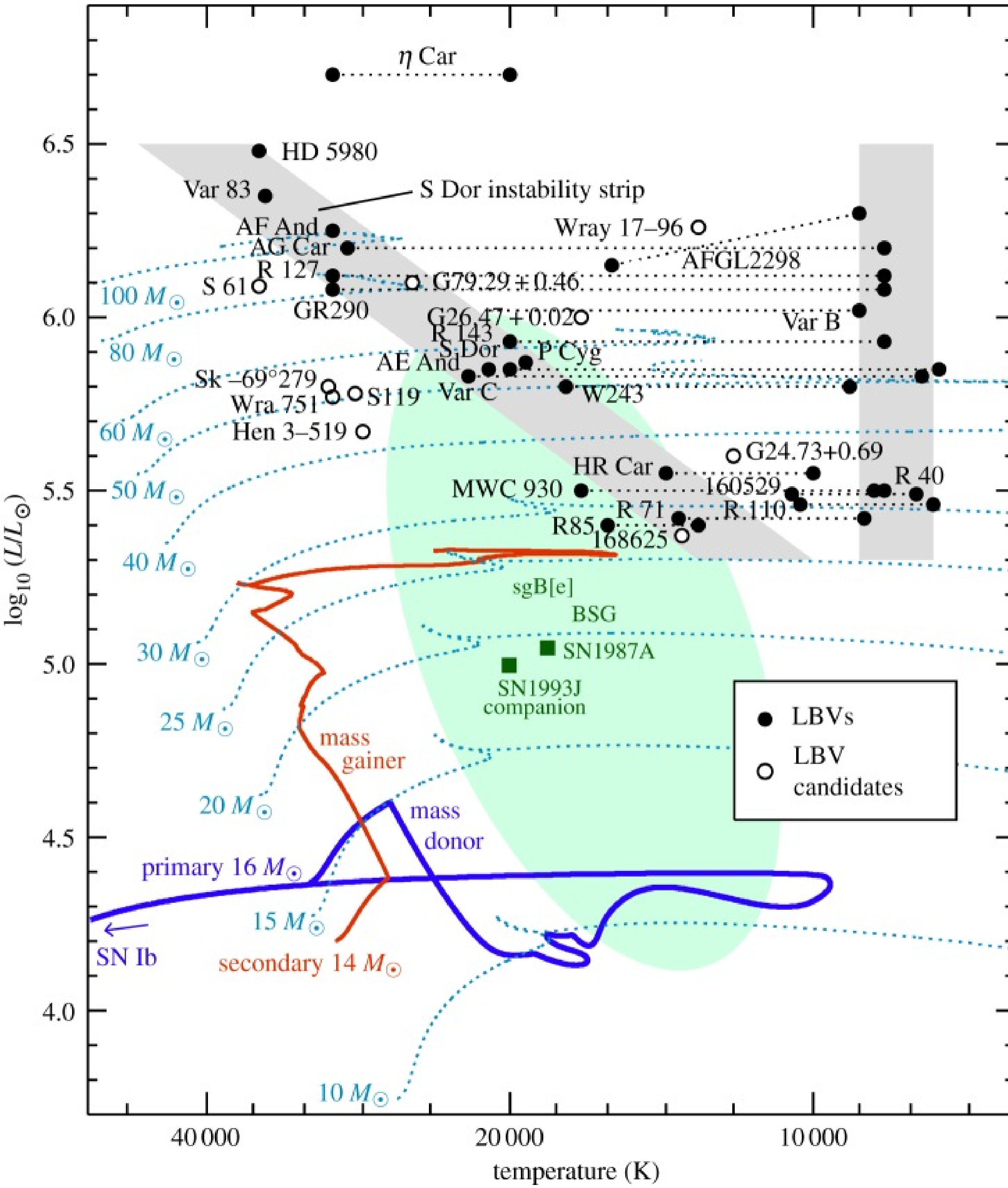

Smith 2017

Stellar evolution of binaries

Stable mass transfer: Roche lobe overflow

- **Direct impact**: If the secondary star is large, then the mass stream that enters from the L1 point can fall directly onto the star. Higher transfer of angular momentum.

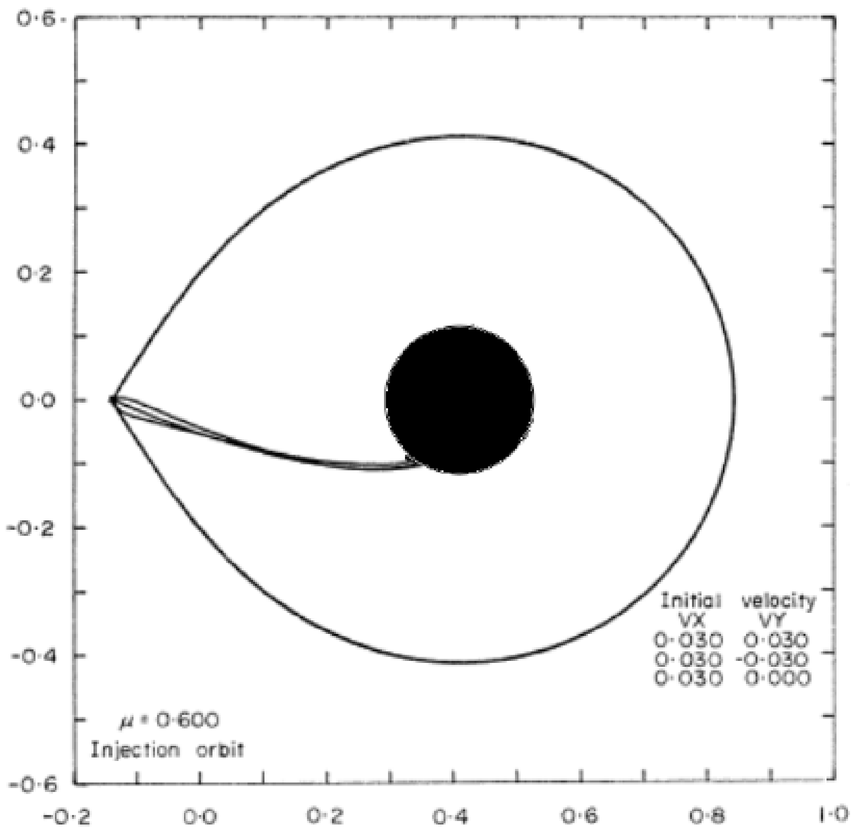

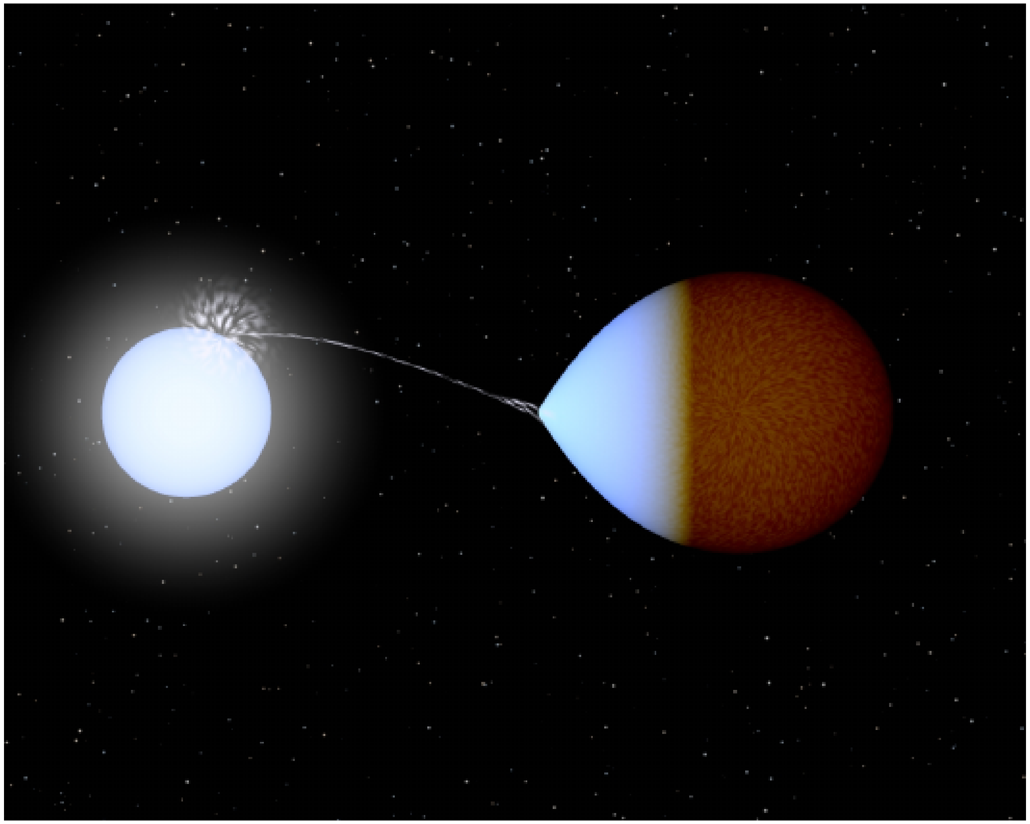

Stellar evolution of binaries

Stable mass transfer: Roche lobe overflow

- **Accretion disc**: If the secondary star is small, the mass stream will not hit the star, but curve around it until it folds back onto itself, spread out due to friction and forms an accretion disc. The disc will fill up until it reaches the secondary star, and then mass will be accreted onto the secondary. Angular momentum accretion is slower.

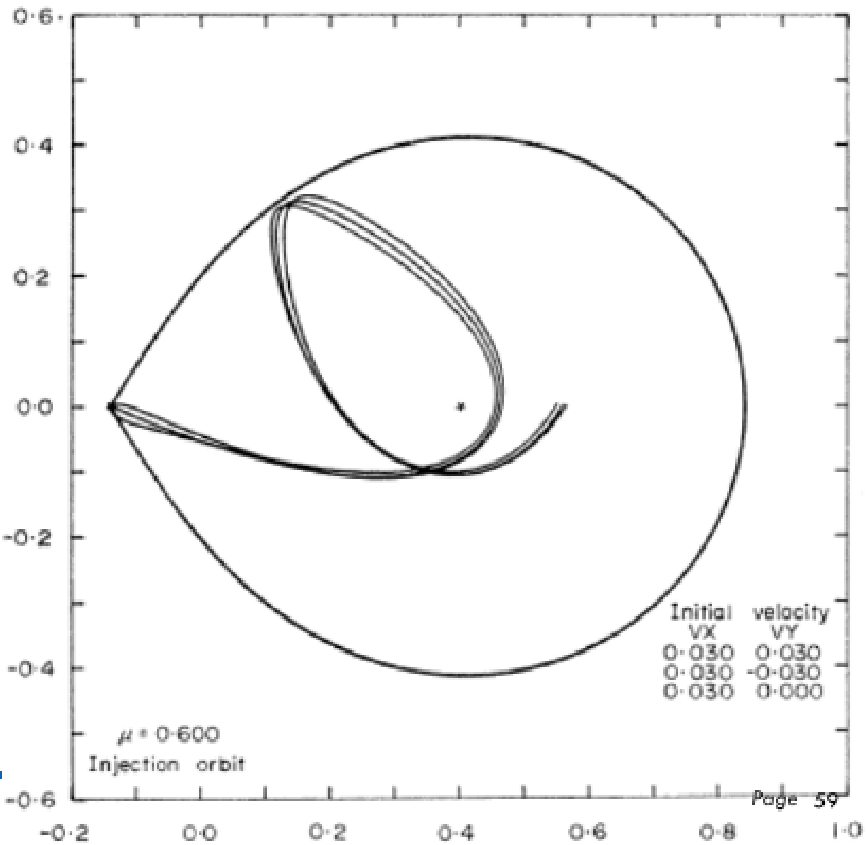

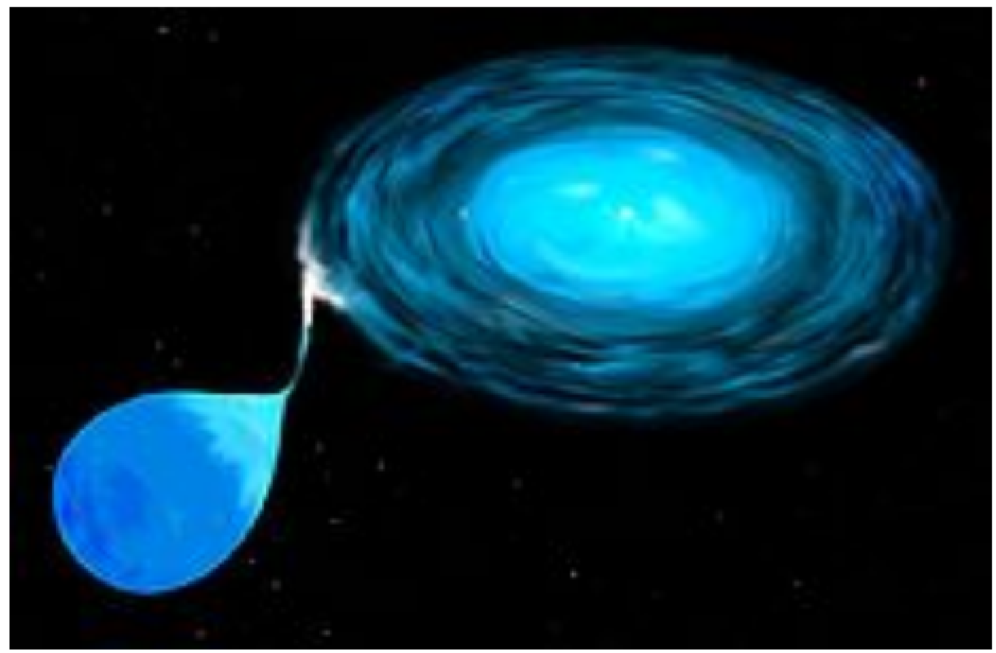

Stellar evolution of binaries

Stable mass transfer: Roche lobe overflow

secondary star can accrete all or part of the mass lost by the primary. This depends on what type of star the secondary is, and how fast the mass loss is.

- **Spin up:** if the secondary accretes mass, it also accretes angular momentum. This causes the star to spin up. When the star reaches breakup velocity any more mass that lands on the star is thrown off again.
- **Bloating:** Adding extra mass onto a star can cause it to expand rapidly due to the extra energy that is dumped in the atmosphere. The secondary will start to resemble a red giant, and can even fill its Roche lobe leading to a contact system
- **Eddington luminosity:** The maximum accretion rate that can be attained by a star is determined by the Eddington luminosity. Intuition: This is the point where the radiation pressure caused by the accreted matter equals the gravitational attraction. Any extra mass will be pushed away by radiation pressure.

Stellar evolution of binaries

Unstable mass transfer: common envelope evolution

Youtube/Thomas Reichardt

Binary merger

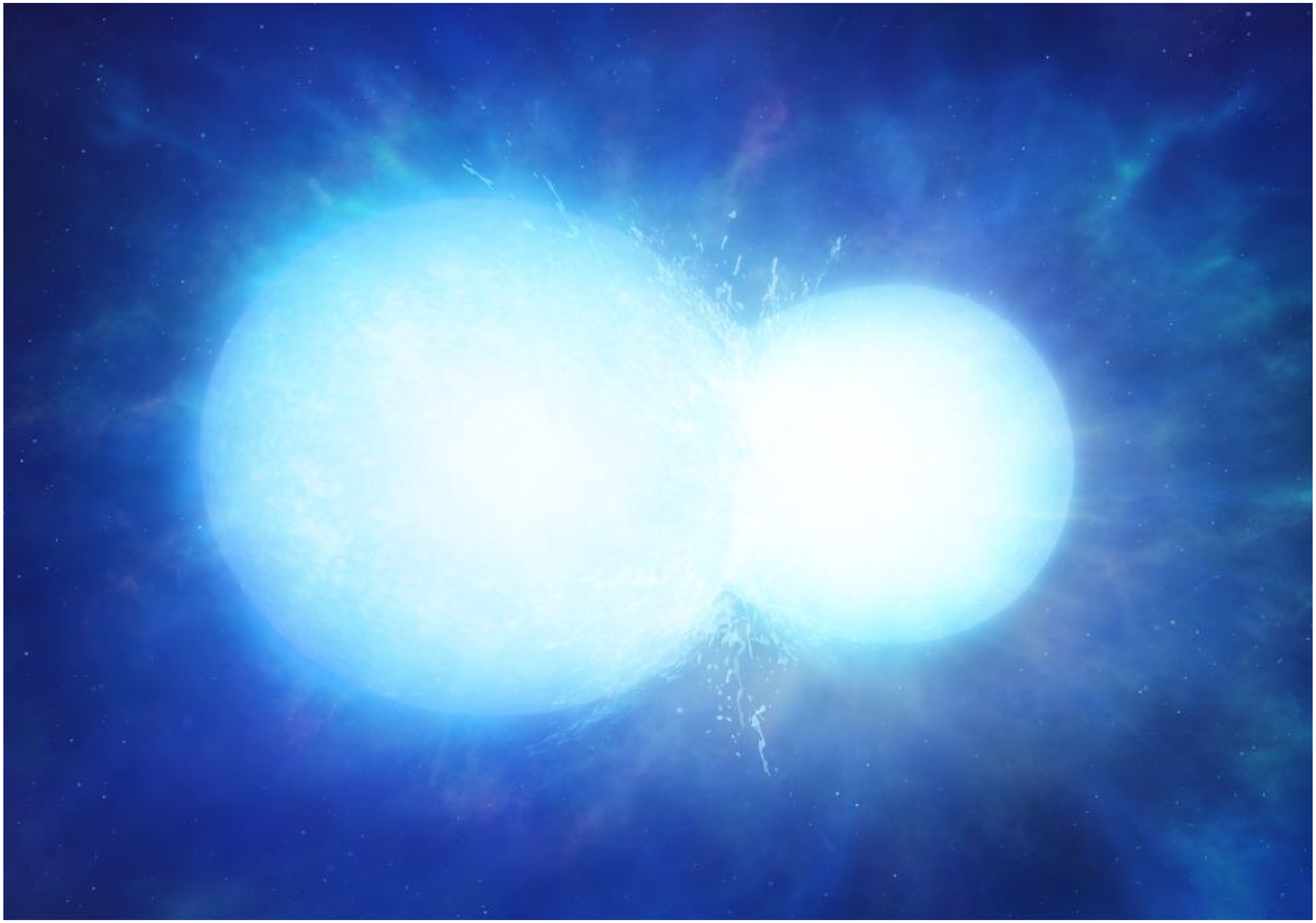

University of Warwick/Mark Garlick

Stellar evolution of binaries

Binary merger

Youtube/Mike Zingale

Stellar evolution of binaries

Barium stars, CH stars, G/K-giants

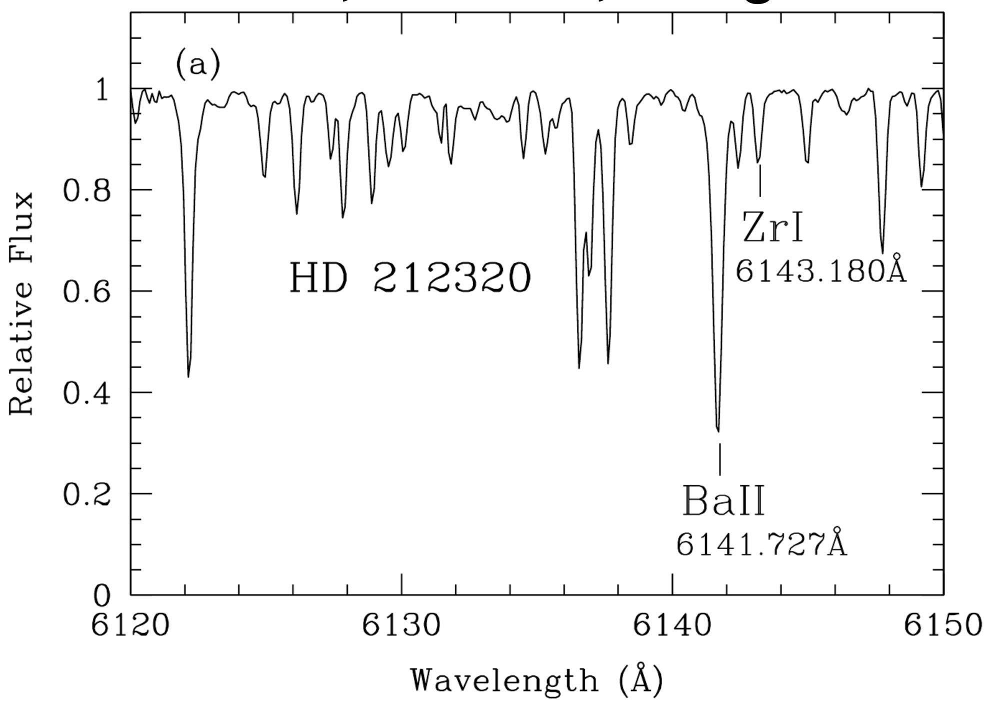

Yang et al. 2016, RAA, 16, 19

Pollution from evolved AGB companions in the past responsible for **weird enrichments of elements**

Dwarf carbon stars (dC) – M dwarfs

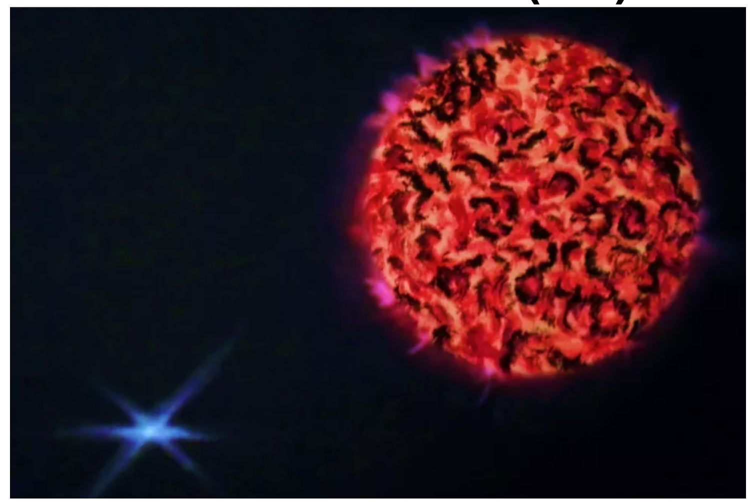

UCSC

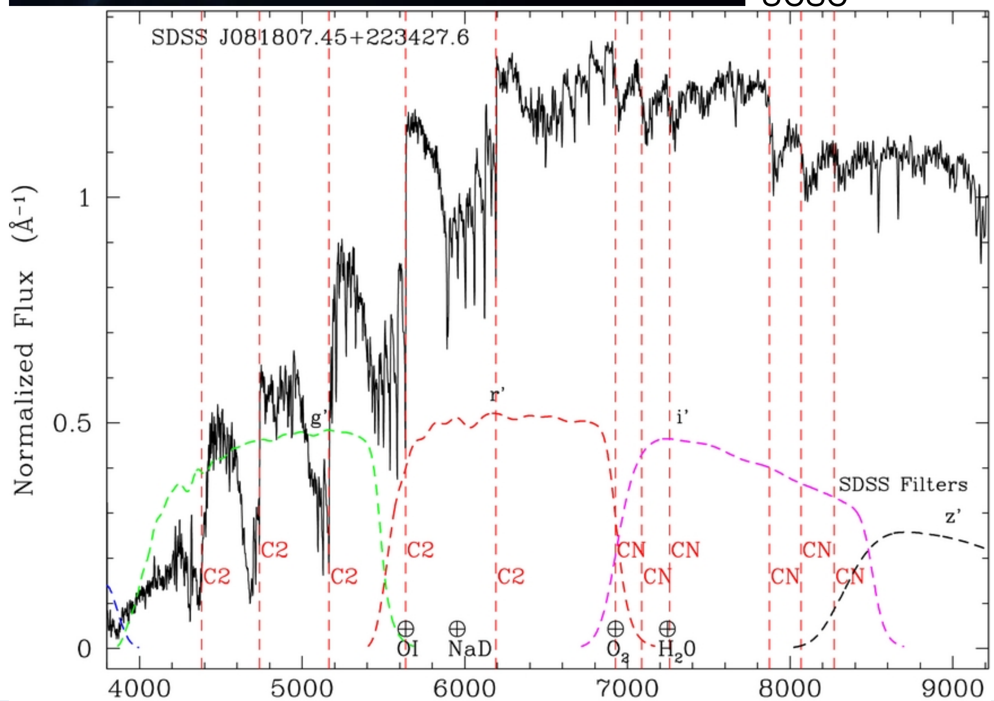

Green 2013, ApJ, 765, 12

Stellar evolution of binaries

Some star types are formed exclusively by binary interactions

Hot subdwarfs, low-mass He-WDs

- Stripped cores of red giants
- He-WD mergers

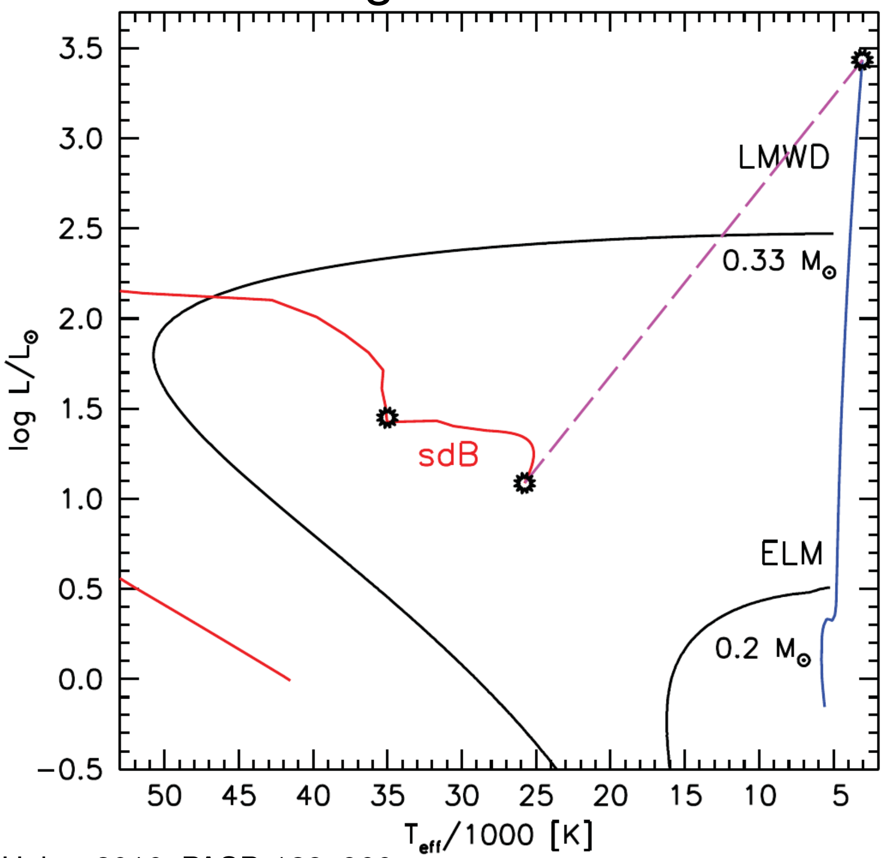

Heber 2016, PASP, 128, 966

R Coronae Borealis stars

C-rich yellow supergiant

- variable due to dust
- merger of CO- and He-WD

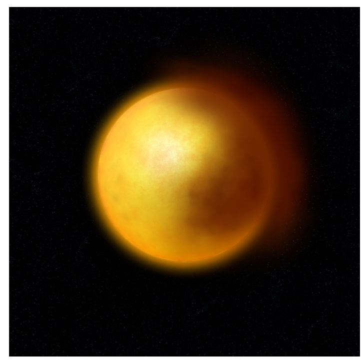

ESO

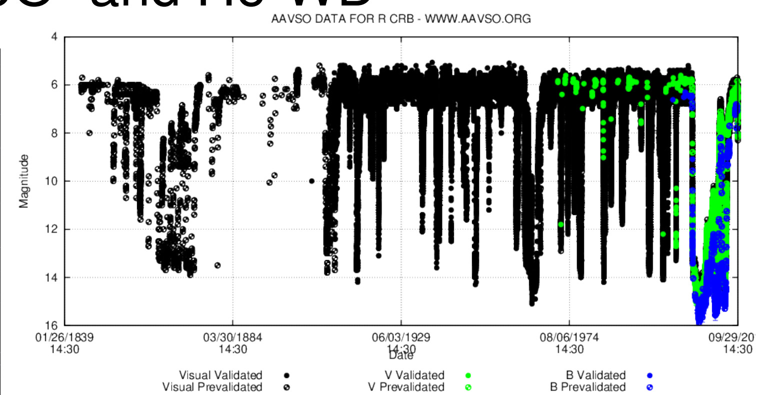

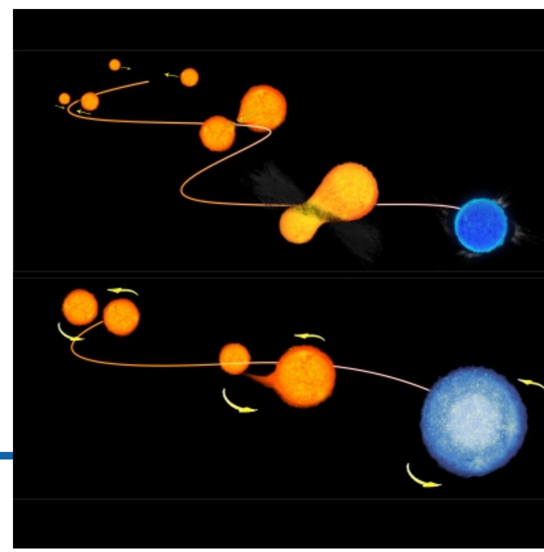

Blue stragglers

- MS-stars too massive for host clusters

$\rightarrow$ mass transfer

Interacting binaries with white dwarf stars – Cataclysmic variables

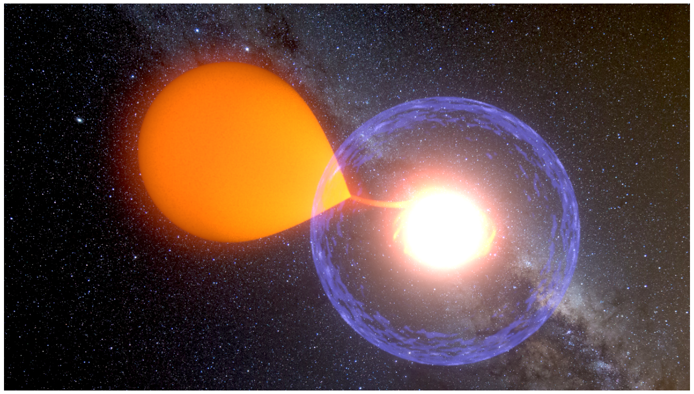

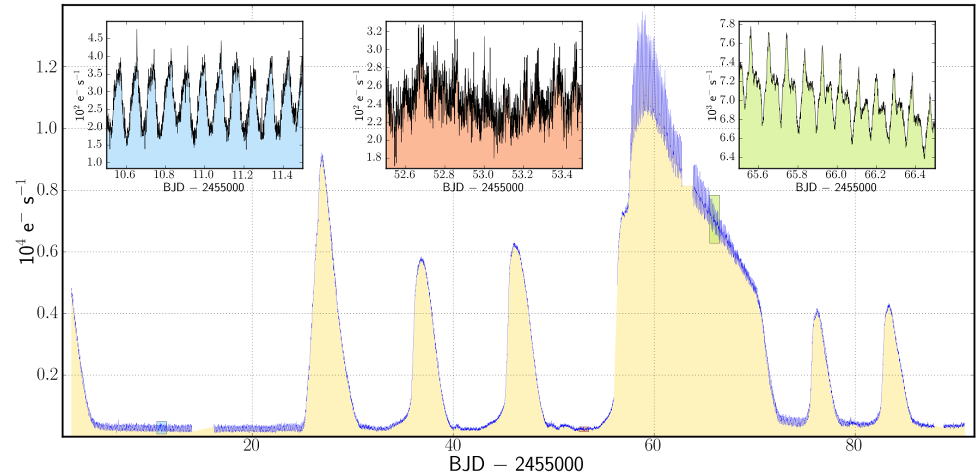

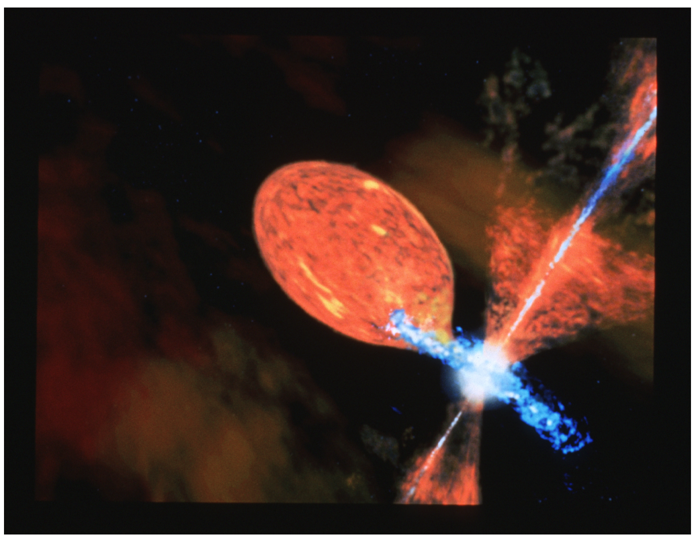

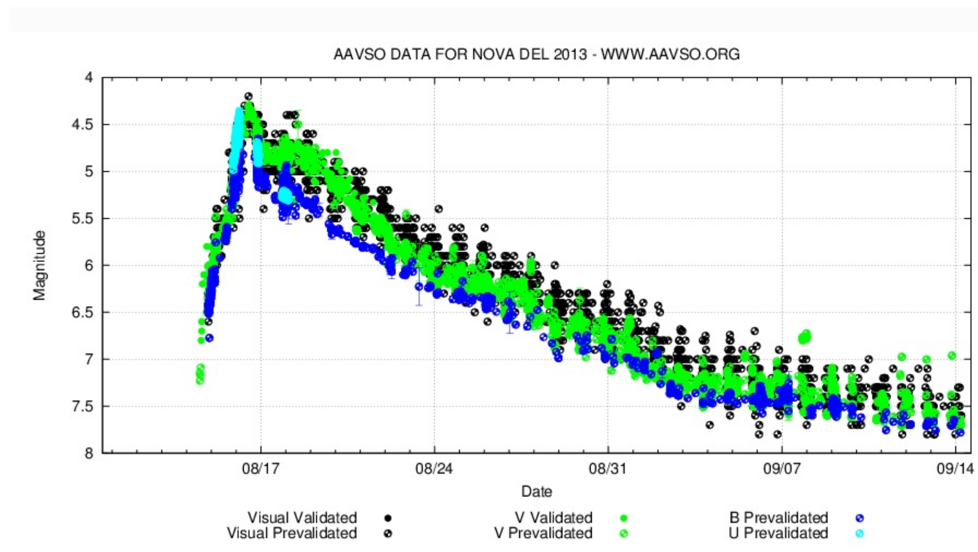

stable

mass transfer from MS or RG companion to white dwarf

→ Mass-transfer to a WD can lead to stable or runaway-H-burning on its surface

→ mass transfer in non-magnetic WD via accretion disc, which gets unstable

Stellar evolution of binaries

Supernova type Ia (SN Ia)

ESA/Hubble, NASA, P. Ruiz-Lapuente, S. Geier

→ Single-degenerate scenario: white dwarf accretes mass from main sequence star, red giant, or He star until Chandrasekhar mass is reached

ESO

→ Double-degenerate scenario: merger of two WD due to emission of gravitational waves, combined mass near Chandrasekhar limit

Mass-transfer to a CO-WD can lead to a C-flash in the degenerate core
→ **Thermonuclear Supernova type Ia (SN Ia)**

Stellar evolution of binaries

Hypervelocity stars:

James Josephides (Swinburne Astronomy Productions)

CAST group, YouTube

Interaction of close binaries with the super-massive black hole in the Galactic center
$\rightarrow$ **Ejection of hypervelocity stars**

encounters in star clusters can disrupt binaries
$\rightarrow$ **runaway stars**

NASA

Stellar evolution of binaries

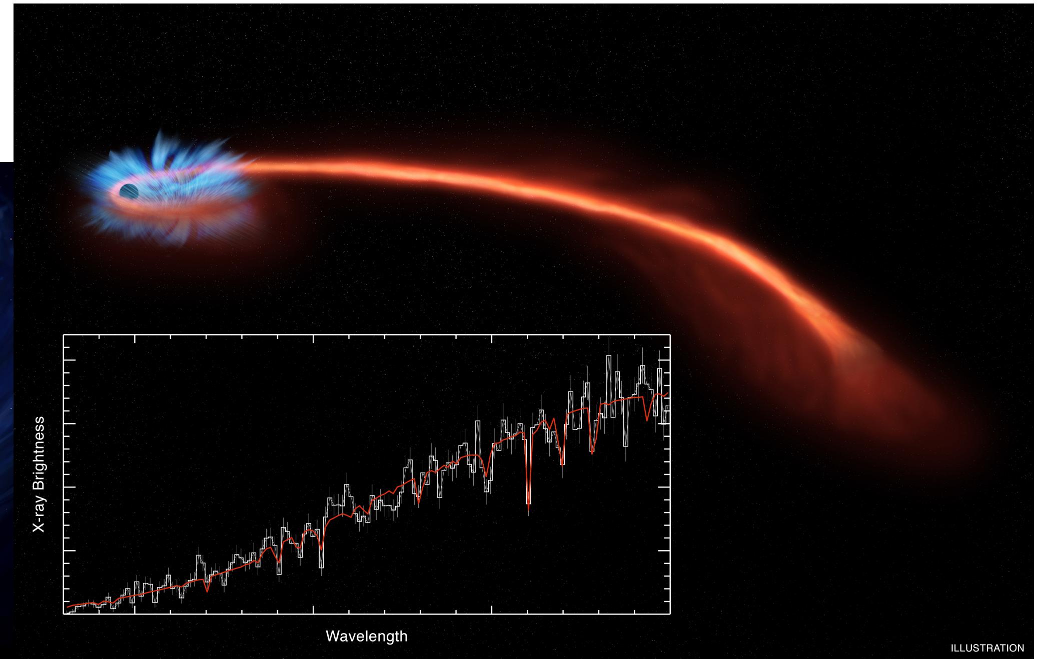

NASA/CXC/M. Weiss

Mark Garlick

Interaction stars with supermassive black holes can lead to the disruption of the star

⇒ **Tidal-disruption event**

DESY, Science Communication Lab